



ADVANCED COMPOSITE ELEVATOR FOR BOEING 727 AIRCRAFT VOLUME 2—FINAL REPORT

FEDD REMOVED PER NASA
LTR OTO 1-10-83,
S/J.G. ROSS

Boeing Commercial Airplane Company
P.O. Box 3707, Seattle, WA 98124

LIBRARY COPY

DEC 17 1980

CONTRACT NAS1-14952
NOVEMBER 1980

LANGLEY RESEARCH CENTER
LIBRARY, NASA
HAMPTON, VIRGINIA

~~FOR EARLY DOMESTIC DISSEMINATION~~

~~Because of its significant early commercial potential, this information, which has been developed under a U.S. Government program, is being disseminated within the United States in advance of general publication. This information may be duplicated and used by the recipient with the express limitation that it not be published. Release of this information to other domestic parties by the recipient shall be made subject to these limitations.~~

~~Foreign release may be made only with prior NASA approval and appropriate export licenses. This legend shall be marked on any reproduction of this information in whole or in part.~~

Review for general release November 1982.

NASA

National Aeronautics and
Space Administration

Langley Research Center
Hampton, Virginia 23665
AC 804 827-3966

FOREWORD

This Final Technical Report (Volume 2) and a Technical Summary (Volume 1) were prepared by the Boeing Commercial Airplane Company, Renton, Washington, under Contract NAS1-14952. They cover work performed between 24 May 1977 and 31 December 1979. The program was sponsored by the National Aeronautics and Space Administration, Langley Research Center (NASA-LRC). Dr. H. A. Leybold was the NASA project manager.

The following Boeing personnel were principal contributors to the program:

Design

C. R. Zehnder
G. N. Roe
W. C. Brown
H. Syder

Structural Analysis

G. G. Holland
R. D. Wilson
R. W. Johnson
J. E. McCarty

Weight and Balance Analysis

J. T. Parsons
R. E. Baum

Manufacturing Technology

M. C. Garvey
V. S. Thompson
D. Cantrell
E. S. Jamison

Production Manager

W. D. Grant

Technical Operations Manager

L. D. Pritchett

Business Management

D. Foster
C. M. Lytle
M. R. Wiebe
D. V. Chovil

SUMMARY

This is the final report for the advanced composite elevator program for the Boeing 727 commercial transport. It covers all work performed on the program from May 1977 through December 1979.

Program development and design activities were concentrated on providing an optimum elevator design and preparing an overall technical plan for development of an advanced composite elevator that would meet the same criteria as those for the existing metal elevator.

Preliminary design activity consisted of developing and analyzing alternate design concepts and selecting the optimum elevator configuration. This included trade studies in which durability, inspectability, producibility, repairability, and customer acceptance were evaluated. Preliminary development efforts consisted of evaluating and selecting material, identifying ancillary structural development test requirements, and defining full-scale ground and flight test requirements necessary to obtain Federal Aviation Administration (FAA) certification.

After selection of the optimum elevator configuration, detail design was begun and included basic configuration design improvements resulting from manufacturing verification hardware, the ancillary test program, weight analysis, and structural analysis. Detail and assembly tools were designed and fabricated to support a full-scope production program, rather than a limited run. The producibility development programs were used to verify tooling approaches, fabrication processes, and inspection methods for the production mode. Quality parts were readily fabricated and assembled with a minimum rejection rate, using prior inspection methods.

Basic program goals were: (1) make extensive and effective use of advanced composite material; (2) obtain a minimum weight reduction of the composite elevator over the metal elevator by 20% (27% was achieved); and (3) establish a cost data base in a production environment. All program goals were realized when the design met or exceeded all established design requirements, criteria, and objectives with an FAA certification in December 1979.

The five shipsets produced on the program are flying in routine airline service on United Airlines aircraft.

CONTENTS

	Page
1.0 INTRODUCTION	1
2.0 SYMBOLS AND ABBREVIATIONS	5
3.0 DESIGN	11
3.1 Concept Development	11
3.1.1 Design Criteria and Objectives	11
3.1.2 Design Trade Studies	11
3.1.3 Structure Common to Aluminum Elevator	19
3.2 Detail Design--Component Definition	20
3.2.1 Upper and Lower Skin Panels	20
3.2.2 Ribs	22
3.2.3 Front and Rear Spars	22
3.2.4 Elevator Assembly	26
3.2.5 Control Tab	27
3.2.6 Balance Weights	27
3.2.7 Thermal Considerations	27
3.2.8 Corrosion Protection System	30
3.2.9 Structural Repair Documentation	30
3.2.10 Maintenance and Inspection Documentation	30
4.0 ANALYSIS AND TEST	33
4.1 Analysis	33
4.1.1 Structural Criteria	33
4.1.2 External Loads Analysis	35
4.1.3 Stiffness Analysis	35
4.1.4 Sonic Analysis	38
4.1.5 Thermal Analysis	38
4.1.6 Moisture Analysis	40
4.1.7 Strength Analysis	42
4.1.8 Buckling Analysis	55
4.2 Ancillary Testing	64
4.2.1 Coupon Tests	64
4.2.2 Structural Element Tests	71
4.2.3 Subcomponent Tests	79
4.2.4 Production Hardware Verification Tests	103
4.2.5 Lightning Protection Panel Tests	106
4.2.6 Repair Tests	108
4.2.7 Real-Time Exposure Environmental Tests	109
4.3 Full-Scale Ground Test	114
4.3.1 Description of Test Setup	114
4.3.2 Static Loads	116
4.3.3 Test Results	118

	Page
4.4 Ground Vibration Test	127
4.5 Flight Tests	127
4.6 FAA Certification	127
4.7 Weights	129
4.7.1 Technical Approach	129
4.7.2 Analysis	130
4.7.3 Weight/Time History	130
4.7.4 Conclusions	131
5.0 OPERATIONS	135
5.1 Manufacturing Development	135
5.1.1 Producibility Studies	135
5.1.2 Ancillary Test Hardware Fabrication	144
5.2 Manufacturing Verification Hardware	158
5.3 Quality Assurance Standards and Nondestructive Test Development	164
5.3.1 Material Control	164
5.3.2 Process Control	164
5.3.3 Completed Part Inspection	164
5.3.4 Assembly Inspection	165
5.3.5 Repair Evaluation	165
5.3.6 Quality Assurance Records	166
5.3.7 Nondestructive Inspection Standards	169
5.3.8 Nondestructive Inspection Techniques	181
6.0 PRODUCTION	187
6.1 Detail Tooling	188
6.1.1 Front Spar	189
6.1.2 Rear Spar	189
6.1.3 Inboard Closure Rib	189
6.1.4 Outboard Closure Rib	192
6.1.5 Rib--Station 117.37	192
6.1.6 Rear-Spar Header	192
6.1.7 Actuator Fairing	195
6.1.8 Skin Panels	195
6.1.8 Control Tab	195
6.1.10 Control Tab Spar	198
6.2 Assembly Tooling	199
6.3 Component Manufacture	202
6.4 Assembly Operations	213
6.4.1 Part Fitup	213
6.4.2 Hole Preparation	220
6.4.3 Fastening Systems--Hi-Lok Bolt	223
6.4.4 Fastening Systems--Nutplates	226
6.4.5 Control Tab Assembly	226

	Page
7.0 COST ANALYSIS	229
7.1 Labor Costs	230
7.2 Usage Factors	236
7.3 Conclusions	239
8.0 CONCLUDING REMARKS	241
9.0 REFERENCES	243
APPENDIX A: MAINTENANCE PLANNING DATA--AIRCRAFT STRUCTURAL INSPECTION, COMPOSITE ELEVATOR	A-1
APPENDIX B: STRUCTURAL REPAIR MANUAL--727 GRAPHITE- EPOXY ELEVATOR	B-1
APPENDIX C: ANCILLARY TEST PROGRAM ORIGINAL COUPON TEST DATA	C-1

FIGURES

No.		Page
1	727 Elevator General Arrangement	2
2	Advanced Composites Elevator Program Schedule	3
3	Preliminary Composite Elevator Configuration--Concept 1	14
5	Preliminary Composite Elevator Configuration--Concept 2	14
4	Preliminary Bead-Stiffened Panel Composite Elevator Configuration--Concept 3	15
6	Preliminary Blade-Stiffened Panel Composite Elevator Configuration--Concept 4	16
7	727 Composite Elevator Structural Arrangement	18
8	Sliding Block Hinge Fitting	18
9	Rear-Spar Trailing Edge	19
10	Elevator Skin Panel	21
11	Lightning Protection System	23
12	Graphite-Epoxy Honeycomb Rib	24
13	Rib at Station 117.36	25
14	Front Spar	25
15	Rear Spar	26
16	Control Tab	28
17	Adjustable Seals and Piano Hinge	29
18	Corrosion Protection--Typical Graphite-Epoxy/Aluminum Interface	31
19	Lightning Strike Zones and Intensities	34
20	CAR 4b V-n Diagram	36
21	Critical Design Conditions	36
22	727 Elevator Spanwise Bending Stiffness	37
23	727 Elevator Torsional Stiffness	37
24	Production Aluminum Elevator	37

No.		Page
25	Graphite-Epoxy Composite Elevator	38
26	Maximum Overall Sound Pressure Level on 727 Horizontal Tail	39
27	727 Elevator Thermal Analysis Results	40
28	Exposure Time Versus Moisture Content for Laminates	41
29	Exposure Time Versus Moisture Content for Sandwich Skin Panel Face	41
30	Elevator/Stabilizer Finite Element Model	42
31	Detail Finite Element Analysis Areas	43
32	Front-Spar Chord Strains for Load Case 125	47
33	Rear-Spar Chord Strains for Load Case 125	47
34	Ultimate Skin Panel Strains, Load Case 125	48
35	Ultimate Skin Panel Strains, Load Case 125	49
36	Ultimate Skin Panel Strains, Load Case 125	50
37	Ultimate Skin Panel Strains, Load Case 125	51
38	Actuator Rib Strains for Load Case 125	52
39	Front-Spar Chord Thermal Strains at -59°C (-75°F)	52
40	Skin Panel Strains, Thermal Load Case $T = -81^{\circ}\text{C}$ (-145°F) ($T = -59^{\circ}\text{C}$ (-75°F))	53
41	Material Strength Correction Factors	54
42	Example Calculation of Design Value	54
43	Strength Analysis of Front-Spar Lower Chord--Station 97 for LC 125 at 82°C (180°F)	56
44	Design Value Compression Strain Versus Temperature	56
45	Strength Analysis of Skin Panel for LC 125 at 82°C (180°F)	57
46	Strength Analysis of Actuator Rib-to-Rear-Spar Attachment for LC 128 at 82°C (180°F)	58
47	Strength Analysis of Tab Skin at Actuator Fitting for LC 129 at 82°C (180°F)	59
48	Interaction Curves--Outboard Skin Panel	60
49	Interaction Curves--Skin Panel Between Actuator Rib and Transition Rib	61

No.		Page
50	Interaction Curves--Inboard Skin Panel	62
51	Shear Buckling Versus Plate Aspect Ratio--Laminate Material	63
52	Mechanical Properties Test Plan (NASA Test 1)	65
53	Basic Laminate Properties Test Plan (Boeing Funded)	66
54	Effect of Moisture, Temperature, and W/D on Tension Failure Strains of ± 45 -deg Fabric Laminate Coupons	67
55	Effect of Moisture, Temperature, and W/D on Tension Failure of $\pm 45/0/90$ -deg Fabric Laminate Coupons	67
56	Effect of Moisture, Temperature, and W/D on Compression Failure Strains of ± 45 -deg Fabric Laminate Coupons	68
57	Effect of Moisture, Temperature, and W/D on Compression Failure Strains of $\pm 45/0/90$ -deg Fabric Laminate Coupons	68
58	Effect of Moisture, Temperature, and Hole Diameter on Rail Shear Test Results for ± 45 -deg Fabric Laminate	69
59	Effect of Moisture, Temperature, and Hole Diameter on Rail Shear Test Results for $\pm 45/0/90$ -deg Fabric Laminate	69
60	Effect of Moisture and Impact on Tension Failure Strains of ± 45 -deg and $\pm 45/0/90$ -deg Fabric Laminate Coupons	70
61	Effect of Moisture and Impact on Compression Failure Strains of ± 45 -deg and $\pm 45/0/90$ -deg Fabric Laminate Coupons	70
62	Effect of Moisture and Delamination Size on Compression Failure Strains of ± 45 -deg and $\pm 45/0/90$ -deg Fabric Laminate Coupons	71
63	Effect of Temperature on Tensile Failure Strains of ± 45 -deg and $\pm 45/0/90$ -deg Fabric Laminate Coupons	72
64	Effect of Temperature on Compression Failure Strains of ± 45 -deg and $\pm 45/0/90$ -deg Fabric Laminate Coupons	72
65	Effect of Temperature and Moisture on Failure Strains of Four-Point Beam-Bending Specimens--Tool Surface in Compression	73
66	Effect of Temperature and Moisture on Failure Strains of Four-Point Beam-Bending Specimens--Tool Surface in Tension	74
67	Structural Elements Test Plan (Test 4)	75
68	Effect of Moisture and Temperature on Fastener Bearing Stress	76
69	Effect of Fastener Spacing (W/D) on Bearing Stress	76
70	Effect of Edge Margin (e/D) on Bearing Stress	77

No.		Page
71	Effect of W/D on Tension Failure Strain Values for Open and Filled Holes	78
72	Elevator Subcomponent Test Plan	80
73	Cover Panel Padup Specimen Geometry (Test 8)	81
74	Cover Panel Padup at Rib Test Setup	82
75	Cover Panel Padup Strain Calculation	82
76	Spar Web Shear Test Specimen (Test 9)	83
77	Spar Web Shear Test Setup	83
78	Typical Moire Fringe Pattern Prior to Failure for Spar Web Shear Test Panel	84
79	Honeycomb Skin Panel Compression Test Setup (Test 10)	84
80	Moire Fringe Pattern of Honeycomb Compression Panel at a Load of 40.03 kN (9000 lb)	85
81	Honeycomb Skin Panel Shear Test Setup (Test 10)	86
82	Moire Fringe Pattern of Honeycomb Shear Panel	87
83	Honeycomb Panel Shear Test Panel Modification	87
84	Panel Edge Shear and Bending Test Specimen Geometry (Test 12)	88
85	Panel Edge Shear and Bending Test Setup (Test 12)	89
86	Actuator Rib Test Setup Schematic (Test 14)	90
87	Actuator Support Rib Test	91
88	Actuator Rib Chord, Strain at Failure	91
89	Actuator Rib Chord, Predicted Failure Strain	92
90	Front-Spar Actuator Fitting Splice Test Schematic (Test 11)	93
91	Front-Spar Actuator Fitting Splice Environmental Control Chamber (Test 11)	93
92	Front-Spar Actuator Fitting Splice Test Specimen Failure (Test 11)	94
93	Front-Spar Actuator Fitting Splice Predicted Failure Load	95
94	Front-Spar Actuator Fitting Specimen Damage Areas	96
95	Front-Spar Actuator Fitting Specimen, Tension Chord Saw Cut	97

No.		Page
96	Front-Spar Actuator Fitting, Failed Durability Test Specimen	97
97	Front-Spar Actuator Fitting Specimen, Measured Vertical Deflections	98
98	Elevator Test Box Lower Surface (Test 17)	99
99	Elevator Test Box Upper Surface (Test 17)	99
100	Elevator Outboard Box Test Setup (Test 17)	100
101	Elevator Outboard Box Test Setup (Test 17)	100
102	Elevator Outboard Box Section--Finite Element Model	101
103	Elevator Outboard Box Section Test--Torsion Windup Test and Prediction Comparison	101
104	Elevator-Box Sonic Test Setup (Test 15)	102
105	Production Verification Hardware Test Coupons	103
106	Graphite-Epoxy Elevator Lightning Test Article	106
107	Lightning Laboratory Test Setup	107
108	Zone 1B Lightning Test Waveform and Test Values Used for Testing	107
109	727 Composite Elevator Test Article After Zone 1B Lightning Test	108
110	Honeycomb Repair Test Results	109
111	Environmental Test Plan	110
112	Outdoor Rooftop Specimen Rack	111
113	Environmental Chamber Cycle	112
114	Environmental Test Specimen Loading Device	112
115	Tension Coupon Environmental Exposure Test Results	113
116	Honeycomb Compression Coupon Environmental Exposure Test Results	113
117	Elevator Ground Test Setup	114
118	727 Composite Test Elevator Hinge Locations	115
119	Elevator Ground-Test Setup Showing Bonded Pads	115
120	Induced Deflections, Air Loads, and Panel Pressure Loads	117

No.		Page
121	Full-Scale Ground-Test Locations for Ultrasonic Inspection-- Upper and Lower Skin Panels	119
122	Full-Scale Ground-Test X-ray Inspection Locations--Upper and Lower Skin Panels	120
123	Skin Buckle Location	120
124	Elevator Nose Skin Structural Modification	121
125	Lower Skin Panel Outer Face Strain Comparisons--Predicted Versus Test	122
126	Spar and Rib Strain Comparisons--Predicted Versus Test	122
127	Hinge-Load Ultimate Loads--Predicted Versus Test	123
128	Elevator Rotation Comparison for Load Case 128	123
129	Full-Scale Test Elevator Upper Surface Failure at Station 172--Fail-Safe Test	124
130	Full-Scale Test Elevator Front-Spar Failure at Station 172-- Fail-Safe Test	124
131	Fail-Safe Loading Failure Analysis Location	125
132	Fail-Safe Loading Failure Analysis	126
133	Interaction Curve Bearing Stress Versus Tension Bypass Strain	126
134	Typical Ground Vibration Test Setup	128
135	Flight Flutter Altitude and Speed Test Conditions	129
136	Advanced-Composite Elevator System Predicted Weight/Time History	131
137	Elevator System Actual Weight and Balance Data (Elevator Surface, Control Tab, and Balance Panels)	133
138	Honeycomb Sandwich and Corrugated Laminate Ribs	135
139	Layup of Fabric Skin Panel	136
140	Layup of Preplied Tape Skin Panel	136
141	Graphite-Epoxy Feasibility for Skin Panel	137
142	Trailing-Edge Tolerance	138
143	Core Locating Method	138
144	Application of Trailing-Edge Sealant and Adhesive	139

No.		Page
145	Elevator Major Jig Position Showing Upper Skin Panel in Position During Sealant Cure	139
146	Lightning Strike Panel	140
147	Layup of Lightning Protection System	141
148	Lightning Strike Panel Showing Layup of Doublers and Outer Skin	141
149	Lightning Strike Panel Showing Core in Place on Outer Skin	142
150	Lightning Strike Panel Showing FM 300 Adhesive on Core	142
151	Lightning Strike Panel Showing Completed Layup Ready for Bagging	143
152	Lightning Strike Panel with Bonded Aluminum Strip	143
153	Lightning Strike Panel--Finished Part Ready for Test	144
154	Rear-Spar Feasibility Hardware	145
155	Rear-Spar Layup Material	145
156	Rear-Spar Test Part Showing Initial Ply Layup Before Precured Filler	146
157	Rear-Spar Test Part Showing Application of Adhesive for Precured Filler	146
158	Rear-Spar Test Part Showing Location of Precured Filler	147
159	Rear-Spar Test Part Showing Finished Part with Tooling	147
160	Panel-to-Rib Pad (Test 8) Showing Typical Test Specimen	149
161	Spar/Aluminum Splice (Test 11) Showing Test Part Being Assembled	149
162	Honeycomb Panel (Test 10) Showing Honeycomb Panel with Grips	150
163	Rib Verification (Test 14) Showing Rib Ready for Cure	150
164	Second Sonic Box (Test 18) Showing Skin Panel in Autoclave	151
165	Sonic Test Box (Test 15) Showing Test Box Being Assembled	151
166	Sonic Test Box (Test 15) Showing Assembled Test Box	151
167	10-ft Test Box (Test 17) Showing Completed Cover Panel	152
168	10-ft Test Box (Test 17) Showing Cover Panel Being Inspected by Through-Transmission Ultrasonic	152

No.		Page
169	Assembly of Test 17 Outboard Test Box, Showing Assembled Lower Skin, Ribs, and Rear Spar	152
170	Sonic Test Box (Test 15) Equipment Used in Repairing Damage to Test Box	154
171	Sonic Test Box (Test 15) Showing Start of Repair	154
172	Sonic Test Box (Test 15) Showing Adhesive, Precured Graphite-Epoxy, and Core for Repair	154
173	Sonic Test Box (Test 15) Showing Core in Place	154
174	Sonic Test Box (Test 15) Showing Precured Graphite-Epoxy Skins Being Positioned	154
175	Sonic Test Box (Test 15) Showing Repair Ready for Cure	155
176	Improved Flow Characteristics of Narmco 5208 Resin	156
177	Hand Drill (Right), Showing Standard Vacuum Unit and Modified Vacuum Unit (Left)	157
178	Drilling Attach Angles on Front Spar, Showing Interference Between Angle and Vacuum Collar	157
179	Vacuum Dust Collector Mounted on Standard Router	159
180	DOTCO Router Motor	159
181	Manufacturing Verification (Test 16) Showing Front Spar Being Laid Up	160
182	Manufacturing Verification (Test 16) Showing Completed Rear-Spar Header	160
183	Manufacturing Verification Hardware (Test 16 Skin Panel) Showing Doubler Being Laid Up	161
184	Manufacturing Verification Hardware (Test 16) Showing Skin Panel in TTU Inspection	161
185	Manufacturing Verification Hardware (Test 16) Showing Front Spar, Two Ribs, and Lower Skin Being Assembled	162
186	Manufacturing Verification Hardware (Test 16) Showing Aluminum Nose Ribs Being Attached to Front Spar	162
187	Manufacturing Verification Hardware (Test 16) Showing View of Completed Assembly	163
188	Manufacturing Verification Hardware (Test 16) Showing Rear View of Completed Assembly	163
189	Visually Acceptable Repair to Skin Panel	166

No.		Page
190	Fokker Bond Tester Inspection of Repair to Skin Panel	167
191	Examples of X-ray Examination of Repairs to Skin Panels	167
192	Rework and Scrap History	168
193	NDI Standards--Laminate and Honeycomb Panel	169
194	NDI Reference Standard--Graphite-Epoxy Laminate	170
195	NDI Reference Standard--Graphite-Epoxy Honeycomb	171
196	NDI Standard--Step Laminate	172
197	Laminate Step Standard	173
198	NDI Standard--Two Honeycomb Skin Panels	174
199	NDI Standard--Honeycomb Skin Panels Simulating Trailing-Edge Assembly	174
200	Skin Panel Standard	175
201	Taper Edge Standard	176
202	Front-Spar Chord Standard	177
203	Preliminary NDI Standard--Front-Spar Chord	178
204	727 Advanced Composite Elevator Skin-Panel Standard	179
205	727 Advanced Composite Elevator Trailing-Edge Assembly Standard	179
206	727 Advanced Composite Elevator Rear-Spar Standard	180
207	727 Advanced Composite Elevator Front-Spar Standard	180
208	727 Advanced Composite Elevator Rib Standard	181
209	Automated TTU Scanner	182
210	Graphite-Epoxy Test Panel Standard, Computerized C-Scan Recording	183
211	Semiportable TTU Scanner without C-Scan Capability	184
212	Portable TTU Scanner, Showing Inspection of Flange Area by Hand-Held TTU Unit	184
213	Sondicator Inspection of Configuration Not Suitable for TTU Scan	185
214	Fokker Bond Testing of Configuration Not Suitable for TTU Scan	185

No.		Page
215	Elevator/Tab/Balance Panel Assembly	187
216	Front Spar and Layup Mandrel	189
217	Front-Spar Assembly Tool with Outboard Spar Detail	190
218	Rear Spar and Layup Mandrel	190
219	Rear-Spar Detail on Layup Mandrel	191
220	Inboard Closure Rib and Layup Mandrel	191
221	Inboard Closure Rib Layup Tools	192
222	Outboard Closure Rib and Layup Mandrel	193
223	Rib--Station 117.37 and Layup Mandrel	193
224	Station 117.37 Rib Layup Tool	194
225	Rear-Spar Header Layup Mandrels	194
226	Actuator Fairing and Layup Mandrel	195
227	Skin Panel and Layup Mandrel	196
228	Skin Panel Layup Tool	196
229	Skin Panel Layup Tool Showing Outboard End and Forward Layup Areas	197
230	Control Tab Bonding Tool	197
231	Control Tab Spar	198
232	Control Tab Rear-Spar Layup Tool	198
233	Model 727 Metal Elevator Structure	199
234	Rear-Spar Assembly Tool	200
235	Front-Spar/Leading-Edge Assembly Tool	200
236	Elevator Major Jig	201
237	Elevator Assembly Showing Vacuum System Used for Dust Collection	201
238	Drilling Operation Using Index Holes Sized to Vacuum Nozzle	202
239	Typical Advanced Composite Fabrication Process	203
240	Growth Factors	204
241	Core Growth Test Panel	205

No.		Page
242	Core Setback on Elevator Skin Panels Prior to Cure	205
243	Layup of Skin Panel	206
244	Skin Panel with Outer Layup and Honeycomb Core in Place	206
245	Skin Panel Compaction with Vacuum	207
246	Application of FM 300 Adhesive to Core of Skin Panel	207
247	Application of Fiberglass Layer to Trailing Edge of Skin Panel	208
248	Upper Skin Panel Ready for Autoclave Cure	208
249	Upper Skin Panel After Autoclave Cure	209
250	Upper Skin Panel in TTU Inspection	209
251	Trim Tool for Upper Skin Panel	210
252	Upper Skin Panel Ready for Transport to Assembly Shop	210
253	Control Tab Bonding Sequence	211
254	Control Tab Second Stage Bond Showing Spar, Core, Toolside Skin, and Trailing-Edge Fillers	212
255	Inboard Closure Rib	212
256	Station 117.37 Rib	213
257	Elevator Assembly Breakdown	214
258	Rear-Spar Assembly	214
259	Front-Spar/Leading-Edge Assembly Buildup	215
260	Closeup View of Actuator Fitting in Front Spar	215
261	Front-Spar/Leading-Edge Assembly Located in Major Jig	216
262	Actuator Backup Rib Assembly	216
263	Elevator Major Assembly Tool	217
264	Lower Skin Panel in Place with Internal Structure of Elevator--Major Jig Position	217
265	Upper Skin Panel in Position in Major Jig	218
266	Completed Elevator Assembly	218
267	Front Spar Showing Warp Removed on Assembly	219
268	Front-Spar Rib Attach Angle	219

No.		Page
269	Rear-Spar Channel	220
270	Rear-Spar Channel Showing Trailing-Edge Gap	221
271	Lower Skin Panel Showing Warp at Inboard End	221
272	Upper Skin Panel Showing Warp at Outboard End	222
273	Modified Countersink Tool	223
274	Hi-Lok Fastener Hex-Drive Bolt and Collar Installation	224
275	High-Torque Bolt Installation	224
276	Torque-Set Bolt, 100-deg Flush-Reduced Head	225
277	Torque-Set Bolt Installation	225
278	Visu-Lock Blind Fastener	226
279	Installation Procedure of Monogram/Aerospace "Bigfoot" Fastening System	227
280	Elevator Trailing-Edge Rivet Installation	227
281	Total Recurring and Nonrecurring Production Costs by Major Element--5-1/2 Shipsets	230
282	Total Recurring and Nonrecurring Component Production Labor Hours--5-1/2 Shipsets	232
283	Total Recurring and Nonrecurring Fabrication Hours--5-1/2 Shipsets	232
284	Total Recurring and Nonrecurring Assembly Labor Hours-- 5-1/2 Shipsets	234
285	727 Composite Elevator--Graphite Components Percentage of Component Labor Recurring Costs--5-1/2 Shipsets	235
286	Fabrication and Assembly Recurring Costs Percentage of Labor Hours--5-1/2 Shipsets	236
287	Relative Elevator Cost Comparison (for Initial 200 Shipsets)	237
288	Relative Elevator Cost Trends (for Initial 200 Shipsets)	237

TABLES

No.		Page
1	Concept Comparison	17
2	Elevator Elements and Input Properties	44
3	Design Ultimate Loads	44
4	Elevator Pressures	45
5	Residual Strength Comparison of Fatigue-Conditioned Fastener Specimens	78
6	Honeycomb Skin Panel Compression Stability Test Results	85
7	Honeycomb Skin Panel Shear Test Results	87
8	Panel Edge Shear and Bending Test Results (Test 12)	89
9	Verification Hardware Coupon Test Results	104
10	Static Test Loads and Deflections	116
11	Full-Scale Ground-Test Inspection Schedule	118
12	Comparison of Ground Vibration Test and Analysis Natural Frequencies	128
13	Weight Comparison [kg (lb)/airplane]	132
14	Material Form and Finishing Cost Study	137
15	727 Elevator Quality History	168
16	Ground Test Labor Hours--727 Composite Elevator	229
17	Recurring Labor Hours, 5-1/2 Shipsets--727 Composite Elevator	231
18	Component Production Labor Expenditures--Total Recurring and Nonrecurring (Excludes Tooling)	233
19	Production Tooling--727 Elevator	234
20	Metal Elevator Versus Composite Elevator Cost Comparison Assumptions	238

1.0 INTRODUCTION

The escalation of jet fuel prices has caused a reassessment of technology concepts and trades used in designing and building commercial airplanes. The task is to incorporate fuel-saving concepts into commercial aircraft design.

The potential weight savings and fuel reduction resulting from the use of advanced composites in aircraft structure, especially primary structure, are significant. However, lack of technical confidence and cost data has delayed their use in commercial aircraft.

Hardware programs conducted in a production environment were required to establish and demonstrate the structural integrity, operating-life characteristics, and manufacturing cost of advanced composite primary structures.

Boeing's approach to these problems was to obtain reliable production, technical, and cost data bases by the integration of advanced composite technology development. Realistic production costs in a commercial transport manufacturing environment were developed using these data bases. The Advanced Composite Elevator program emphasized acquiring the information needed to obtain an early production commitment by management, and was conducted in an environment consistent with production standards. This work was performed under NASA Contract NAS1-14952 and, when combined with company-supported efforts, has accelerated the use of advanced composites in aircraft structures.

Preliminary efforts involved conceiving, developing, and analyzing alternate elevator design concepts, preparing a technical plan to aid in selecting and evaluating material, identifying ancillary structural development test requirements, and defining full-scale ground and flight test requirements necessary to obtain FAA certification. Figure 1 shows the location and general arrangement of the 727 elevator.

The program was based on both precontract and contract design development activities that considered:

- Program management and plan development
- Establishment of design criteria
- Conceptual and preliminary design
- Manufacturing process development
- Material evaluation and selection
- Verification testing
- Detailed design
- FAA certification

This final report describes the work required to accomplish the contractual goals and program activities outlined in the overall program schedule summarized in Figure 2.

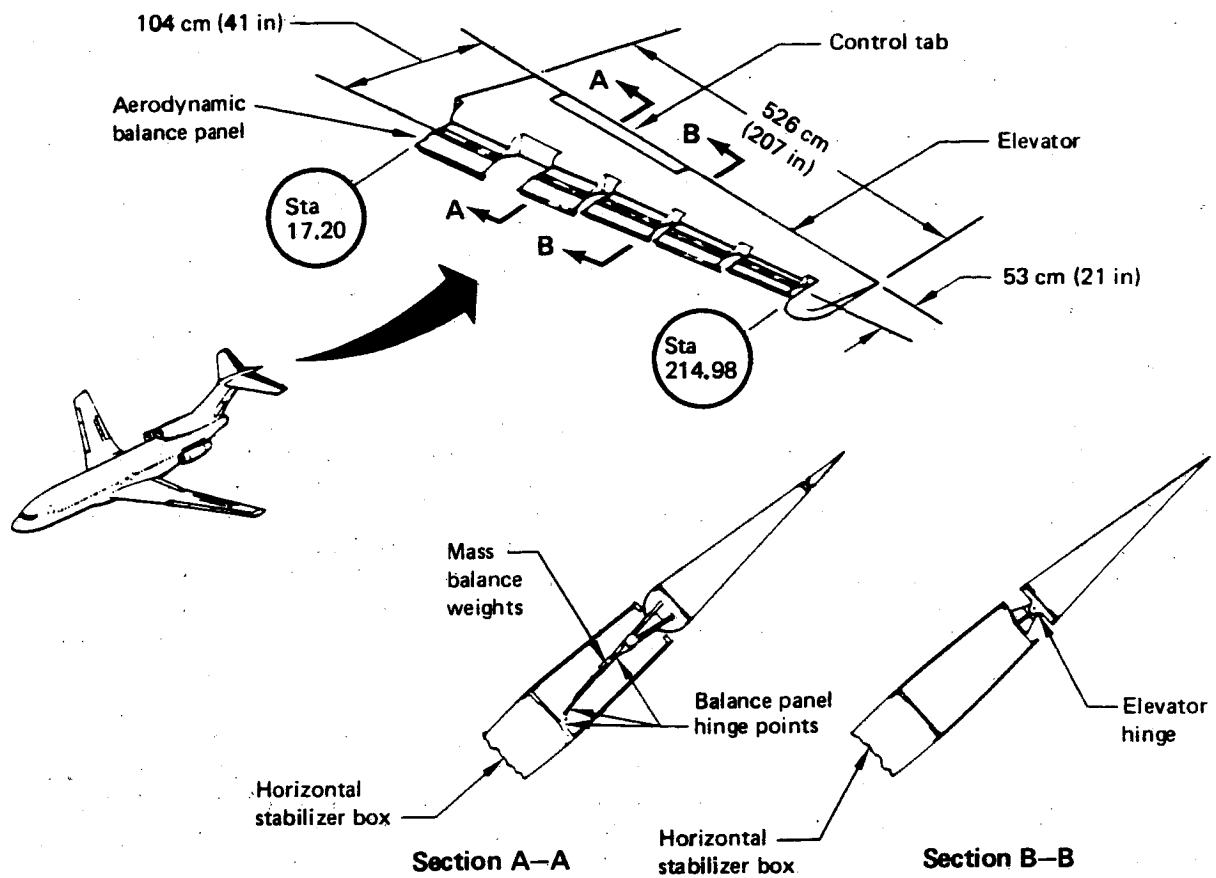


Figure 1. 727 Elevator General Arrangement

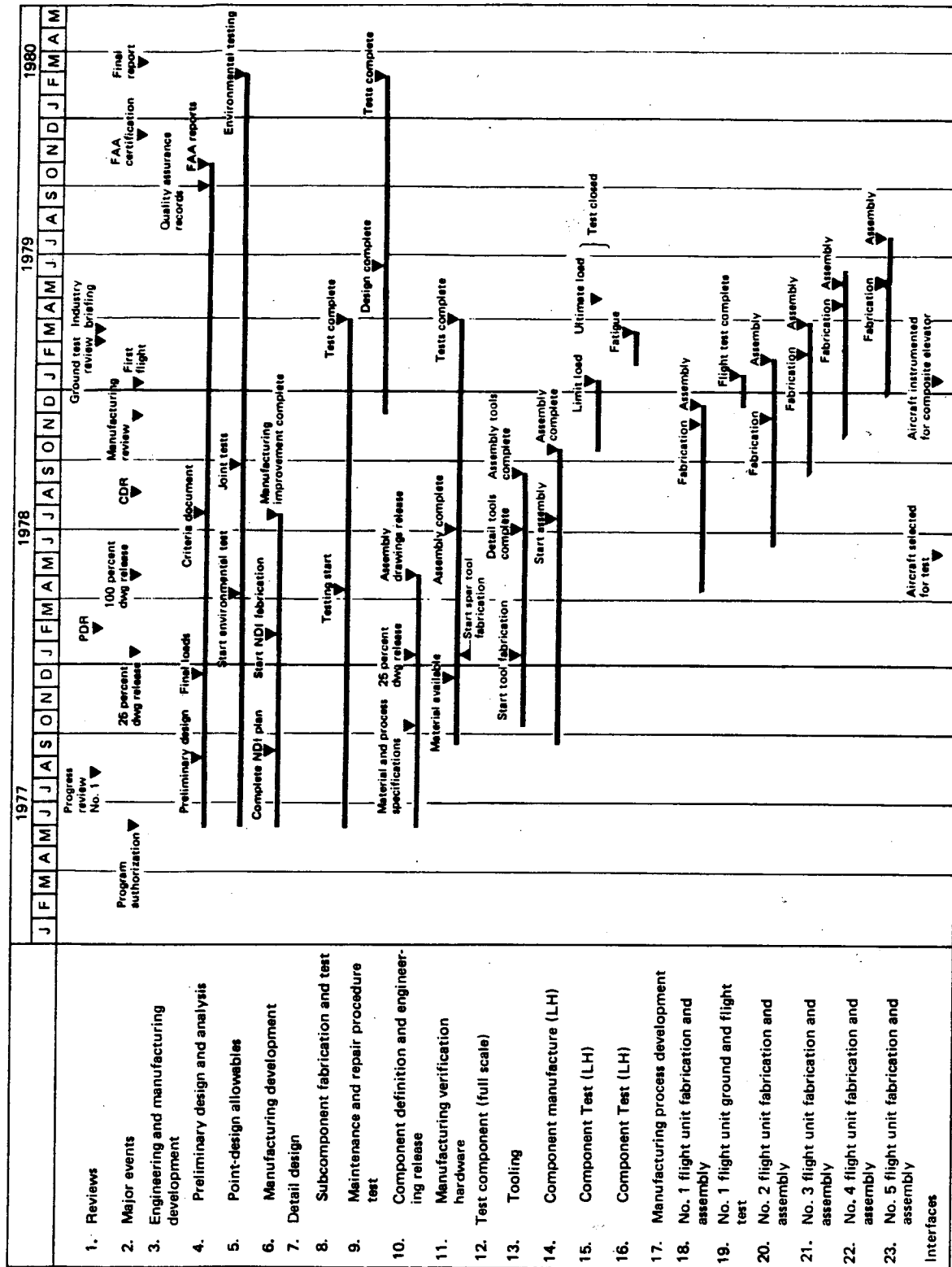


Figure 2. Advanced Composites Elevator Program Schedule

2.0 SYMBOLS AND ABBREVIATIONS

A	area
amp	ampere
ATLAS	computer program
avg	average
BAC	Boeing process specification
Bm	beam
BMS	Boeing materials standard specification
b/a	plate aspect ratio
b/t	ratio of plate width to thickness
CAR	Civil Air Regulations
C	centerline
cm	centimeter
C _N	total airplane normal force coefficient
CSK	countersink
D	diameter
dB	decibel
deg	degree (angular)
DSC	differential scanning calorimetry
DVR	correction factor
E	modulus of elasticity
EDI	electronic deflection indicator
EI	spanwise bending stiffness
E _x	modulus in x-direction
E _y	modulus in y-direction
FAA	Federal Aviation Administration
FBR	typical bearing stress
f _{brg}	applied bearing stress

F_{brg}	design value bearing stress
FEP	fluorinated ethylene propylene (Teflon)
F_{scr}	critical shear stress
g	gram
GJ	torsional stiffness
G_{xx}	inplane shear modulus
h	distance between centroid of chords
\bar{H}	hingeline
Hz	hertz
$K_{B\infty}$	B basis statistical factor
kn	knot
ksi	thousand pounds per square inch
L	length
lb	pound mass
lbf	pound force
LC	liquid chromatography, load case
m	metre
M_{CF}	material correction factor
M_D	Mach number at dive speed
MDI	master dimensioning index
MEK	methyl ethyl ketone
M_{MO}	Mach number at maximum operating speed
MS	margin of safety
MVF	material variability factor
Narmco	manufacturer of graphite-epoxy material
N	newton
NAS	National Aircraft Standard
NASA	National Aeronautics and Space Administration
NDI	nondestructive inspection

N_x	load in x-direction per unit length
N_{xcr}	critical load in x-direction per unit length
N_{xy}	shear load per unit length
N_y	load in y-direction per unit length
N_{ycr}	critical load in y-direction per unit length
OASPL	overall sound pressure level
OML	outside mold line
OSHA	Occupational Safety and Health Administration
P	load
Pa	pascal
P_A	actuator force
P_{BP}	balance panel pressure
P_c	chord load
PCM	photo contact master
P_e	elevator pressure
P_E	maximum triangular distribution elevator pressure
P_H	fastener load from hinge fitting
P_{HS}	skin load from fastener hinge fitting
Pl	plate
psi	pounds per square inch
P_t	tab pressure
P-static	precipitation static
Q	coulomb
R_{BR}	bearing stress ratio
Rd	rod
RH	relative humidity
rpm	revolutions per minute
RT	room temperature
R GR	gross area strain ratio

S	strength
S _M	mean strength of distribution
S _{MIN}	minimum strength confidence level
Sta	station
t	thickness
T	temperature
t _{face}	face thickness
TGA	thermal gravimetric analysis
T _H	torsion about the hingeline
TTU	through-transmission ultrasonic
typ	typical
V	volt
V _A	design maneuver speed
V _C	design cruise speed
V _D	design dive speed
V _F	design flap speed
VFM	variation magnification factor
V _{MO}	maximum operating speed
V _{S1}	stall speed with flaps retracted
V-n	limit load factor-velocity
W	width
W _{BP}	balance panel load per unit length
ν _{xy}	inplane Poisson's ratio
δ	vertical deflection at elevator hinge
ν	poisson's ratio
ν _{MAX}	maximum test value ratio
ε	ultimate axial strain
γ	ultimate shear strain

ϵ_c	compression strain
ϵ_{DV}	design value strain
ϵ_{GR}	gross area strain
ϵ_{IR}	infrared emissivity
$^{\circ}C$	degree Celsius
$^{\circ}F$	degree Fahrenheit
μs	microsecond
α_s	solar absorptivity
ϵ_T	thermal strain

All measurement values are expressed in International System of Units (SI), followed by U.S. customary units in parentheses. The U.S. customary units were used for principal measurements and calculations.

3.0 DESIGN

3.1 CONCEPT DEVELOPMENT

Concept development consisted of establishing design criteria and objectives, evaluating and selecting materials, and establishing an optimum baseline configuration for the advanced composite elevator. Several trade studies were conducted during the concept development phase in which durability, inspectability, producibility, repairability, and customer acceptance of various alternate design concepts were evaluated. A description of these efforts is contained in this section.

Following the concept development effort, the design of each elevator component was detailed, and drawings of the parts and assemblies were prepared. The design details of the major components are described in Section 3.2.

3.1.1 DESIGN CRITERIA AND OBJECTIVES

The advanced composite elevator was designed to meet the same criteria as those for the existing metal elevator and to comply with both Federal Aviation Regulations and Boeing design requirements.

Additional criteria used were:

- The composite elevator must be interchangeable with the existing metal elevator on all model 727 airplanes and require no change to the horizontal stabilizer.
- The aerodynamic effectiveness of the elevator will not be significantly altered; i.e., composite elevator stiffness shall closely match the metal elevator stiffness, particularly in torsion.
- The composite elevator's strength, durability, inspectability, and serviceability will be equal to, or better than, that of the existing metal elevator.
- Protection against damaging effects of lightning, static discharges, and environmental elements will be provided.
- Structural bonding shall not be used to join major assemblies.

In addition to the preceding criteria, the following contract requirements were imposed:

- The elevator weight should be reduced by a minimum of 20%.
- The recurring costs at the 200th unit should be equal to or less than those of the existing metal elevator at the 200th unit.

3.1.2 DESIGN TRADE STUDIES

3.1.2.1 Material Evaluation and Selection

Preliminary Boeing-funded development efforts were devoted to selecting and evaluating material and included the tests and manufacturing considerations discussed in this section. In addition, an evaluation of material history and current industry usage was made. The graphite fiber-epoxy resin systems investigated were as follows:

Graphite Fiber-Epoxy Resin System

Supplier

T300/5208	Narmco
T300/5235	Narmco
T300/934	Fiberite
T300/976	Fiberite
AS/3501-5A	Hercules
T300/F263	Hexcel
T300/F288	Hexcel

Each system was ordered and tested in the following forms:

- Preplied tape, 3.5-mil, two-ply
- Unidirectional tape, 5.2-mil
- Plain-weave fabric prepreg, 7.0-mil

Prepreg forms were ordered to the general requirements of Boeing Material Specification (BMS) 8-212 with specific tolerances on prepreg and cured laminate physical properties. Testing included the following:

- Resin
 - Differential scanning calorimetry (DSC)
 - Liquid chromatography (LC)
 - Thermal gravimetric analysis (TGA)
- Prepreg
 - Resin content, percent of prepreg weight
 - Volatile content, percent of prepreg weight
 - Resin gel time, minutes
 - Resin flow, percent of weight
 - Graphite areal weight
- Laminate properties
 - Fiber volume
 - Density, thickness/ply, void content
 - Weight
 - Tensile modulus
 - Elongation, tension, and compression
 - Short beam shear
 - Ultimate strength, tension, and compression
- Sandwich properties
 - Flatwise tension
 - Porosity
 - Peel
 - Weight

Manufacturing producibility was evaluated by fabricating from each candidate material a test panel representing typical layup complexity of actual structure. Drape, tack, work time, and degree of difficulty in layup were determined for each material system and form. Quality Control performed receiving inspection tests on all materials used in the evaluation. They also made a thorough comparison of suppliers' certified test data and Boeing's test results. In all instances, the suppliers' test data and Boeing's test results compared favorably within acceptable limits. A process specification (BAC 5562), which describes autoclave cure cycles, also was developed before the contract was initiated.

Material selection consisted of analysis and comparison of the above tests and included additional factors such as the following:

- Available industry data base
- Demonstrated resin durability in different environments
- Supplier production experience
- Supplier production capacity and control
- Supplier ability to provide all material forms
- Supplier cooperation for process audit

This Boeing-funded material evaluation resulted in selection of the Narmco 5208 resin system. The system was selected because it best satisfied a majority of the selection criteria.

3.1.2.2 Elevator Configuration

Major components of the metal 727 elevator are seven upper and seven lower 2024 aluminum bead-stiffened skin panels, 26 aluminum ribs, 33 aluminum nose ribs, five balance panels, five upper and five lower aluminum nose skins, aluminum front and rear spars, and a steel horn balance weight.

Four replacement preliminary composite elevator configurations (figs. 3 through 6) were considered. Concept 1 utilized a minimum number of ribs and skin panels stabilized by Nomex honeycomb core (fig. 3). This concept had been previously used in Boeing transport fiberglass control surfaces. A minimum thickness, solid laminate skin, supported by closely spaced ribs, was considered in Concept 2 (fig. 4). This design had been developed in composite control surfaces. Concepts 3 and 4 (figs. 5 and 6) used the same number of ribs as in the existing metal elevator with solid laminate skin panels stabilized by bead stiffeners and blade stiffeners. These two configurations were considered because they closely matched the existing aluminum elevator configuration.

The primary factors considered during the selection of the composite elevators configuration included weight, number of parts required for an elevator assembly, recurring assembly costs, tooling costs, and processing complexity. The results of the evaluation are summarized by concept in Table 1.

Concepts 3 or 4 would have had approximately the same part count as the existing aluminum elevator (600), of which 370 would have been graphite-epoxy. The number of parts used in Concept 2 would have been even higher than in Concepts 3 or 4. Concept 1 had the minimum number of parts (389), of which 142 were graphite-epoxy. The number of fasteners required to assemble the elevators would have been greater for the concepts with more detail parts in the assembly. The number of fasteners in Concept 1 was 1355, or 35% of the fasteners used in the existing aluminum structure. Since Concepts 2, 3, and 4 had more detail parts and fasteners than Concept 1, they would have been more expensive to fabricate than Concept 1. The bead and blade stiffeners required in Concepts 3 and 4 required significantly more processing complexity than the honeycomb-stiffened panels in Concept 1.

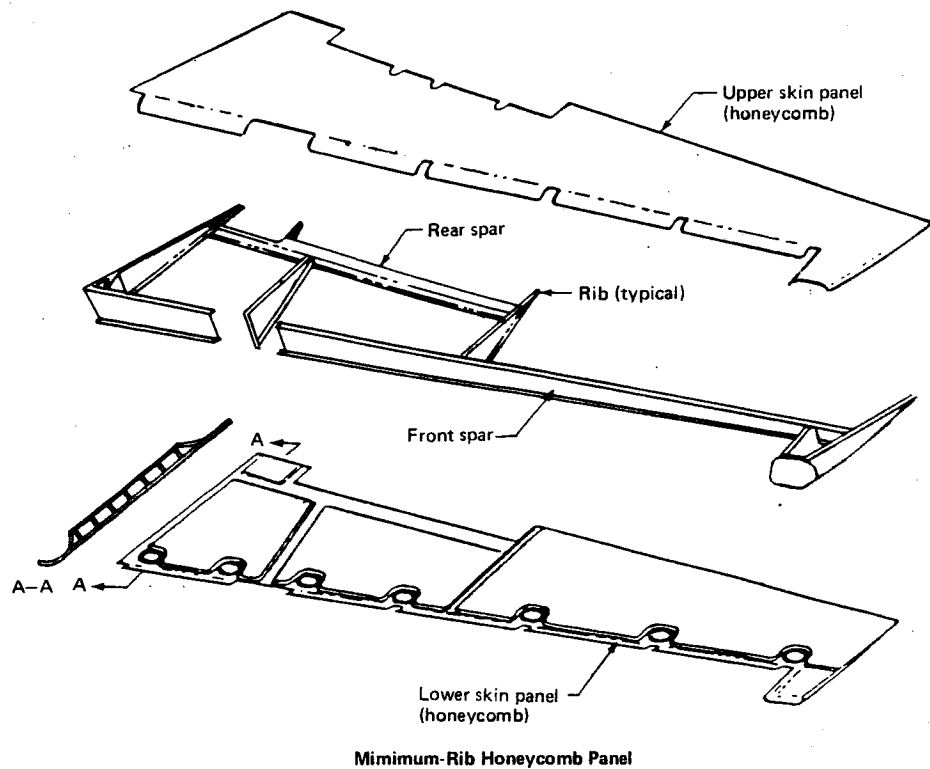


Figure 3. Preliminary Composite Elevator Configuration—Concept 1

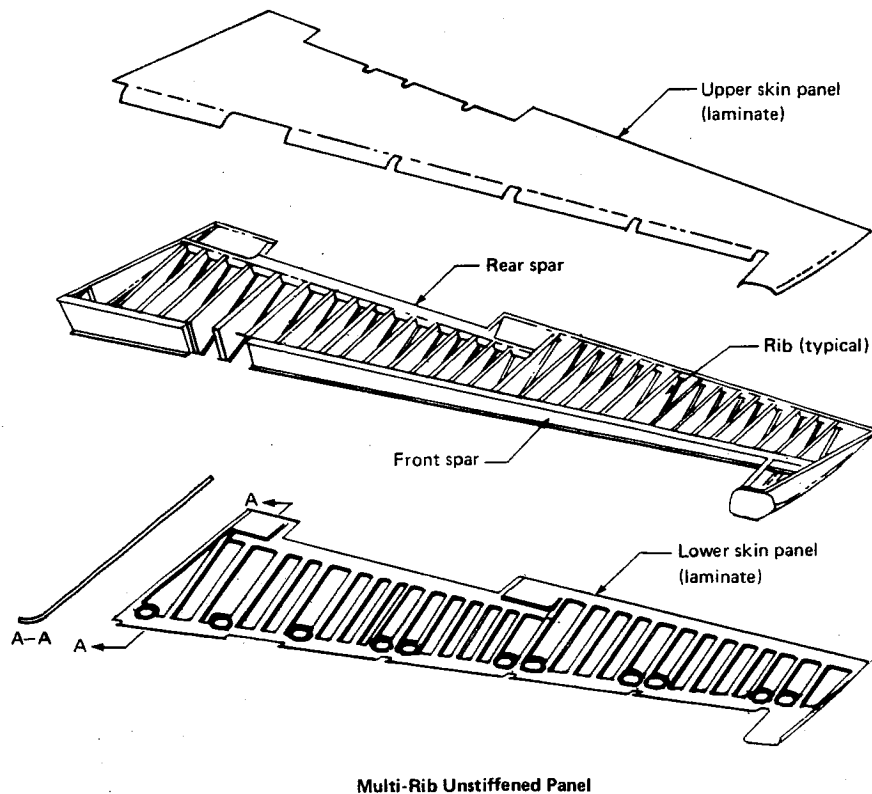


Figure 4. Preliminary Composite Elevator Configuration—Concept 2

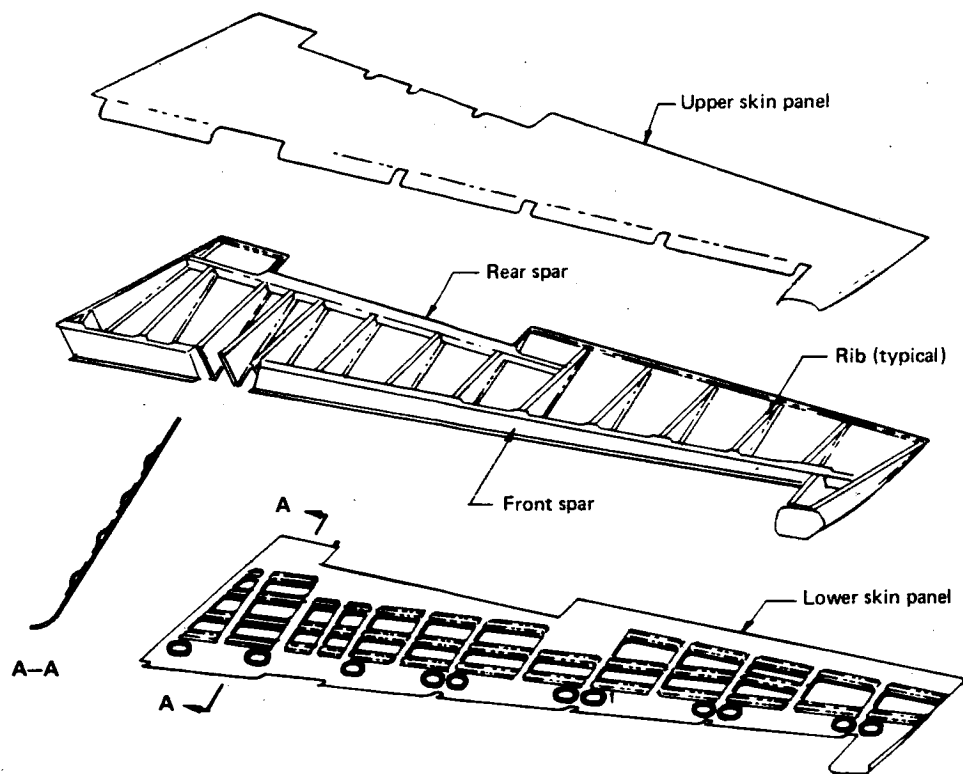


Figure 5. Preliminary Bead-Stiffened Panel Composite Elevator Configuration—Concept 3

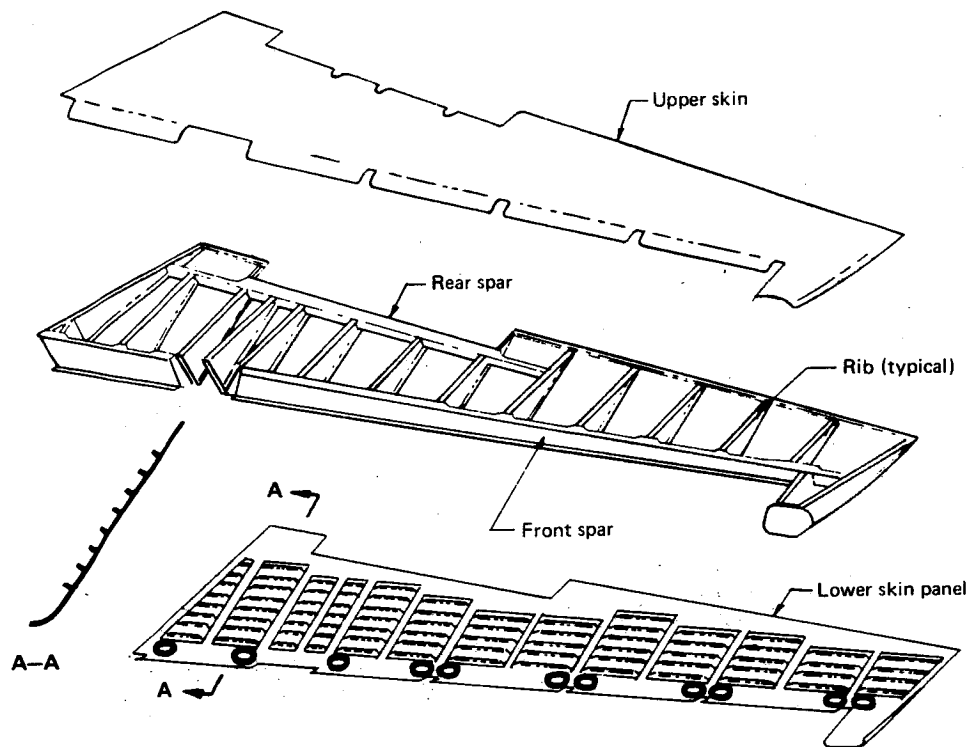


Figure 6. Preliminary Blade-Stiffened Panel Composite Elevator Configuration—Concept 4

Table 1. Concept Comparison

Concept	Rib ratio	Fastener ratio	Weight ratio	Recurring cost ratio	Remarks
1. Minimum-rib honeycomb panel design Concept 1	1.0	1.0	1.0	1.0	Simple panel tools CHOSEN CONCEPT
2. Multirib unstiffened panel design Concept 2	8.25	2.5	1.3-1.5	2.6	8 times the number of rib tools
3. Multirib bead-stiffened panel design Concept 3	3.5	1.5	1.1-1.3	1.7	3.5 times the number of rib tools More complex panel tools Difficult to cocure panels
4. Multirib blade-stiffened panel design Concept 4	3.5	1.5	1.2-1.4	1.6	3.5 times the number of rib tools More complex panel tools

The composite elevator configuration selected (Concept 1) is shown in Figure 7. This design features one-piece lightweight honeycomb upper and lower skin panels, a laminate front spar spliced at the actuator fitting, a laminate rear spar from the elevator tab inboard, and a minimum number of honeycomb ribs.

The evaluation results and the concept selected are consistent with the trends of recent Boeing commercial aircraft where fiberglass honeycomb panels are used extensively on lightly loaded control surfaces, including elevators. The selected concept is a refinement of an earlier concept that used existing hinge fittings and had ribs at each elevator hinge. A study showed that redesign of the hinge fitting (fig. 8) to introduce the overturning moment directly into the skin panels, combined with the triangular shape of the elevator box, eliminated the need to distribute torsion loads to the panels by these ribs; therefore, the hinge fitting ribs were eliminated.

3.1.2.3 Front-Spar Centerline Location

A trade study on the location of the graphite-epoxy front spar centerline was made. The first location selected for the composite elevator was 1.52 mm (0.06 in) forward of the existing aluminum design. This forward location allowed the contacting surfaces of the existing aluminum production actuator fitting to be retained, but it also meant that all 33 built-up, die-formed nose ribs and the existing aluminum thrust hinge would require modification.

During this trade study, the actuator fitting was modified to accommodate thermal expansion requirements. This influenced the trade study decision to also modify the contacting surfaces of the actuator fitting, and the graphite-epoxy front spar centerline was maintained in the same location as in the existing aluminum design. Thus, the 33 nose ribs and the thrust hinge could be retained unaltered. The new actuator fitting was machined from the existing production aluminum forging.

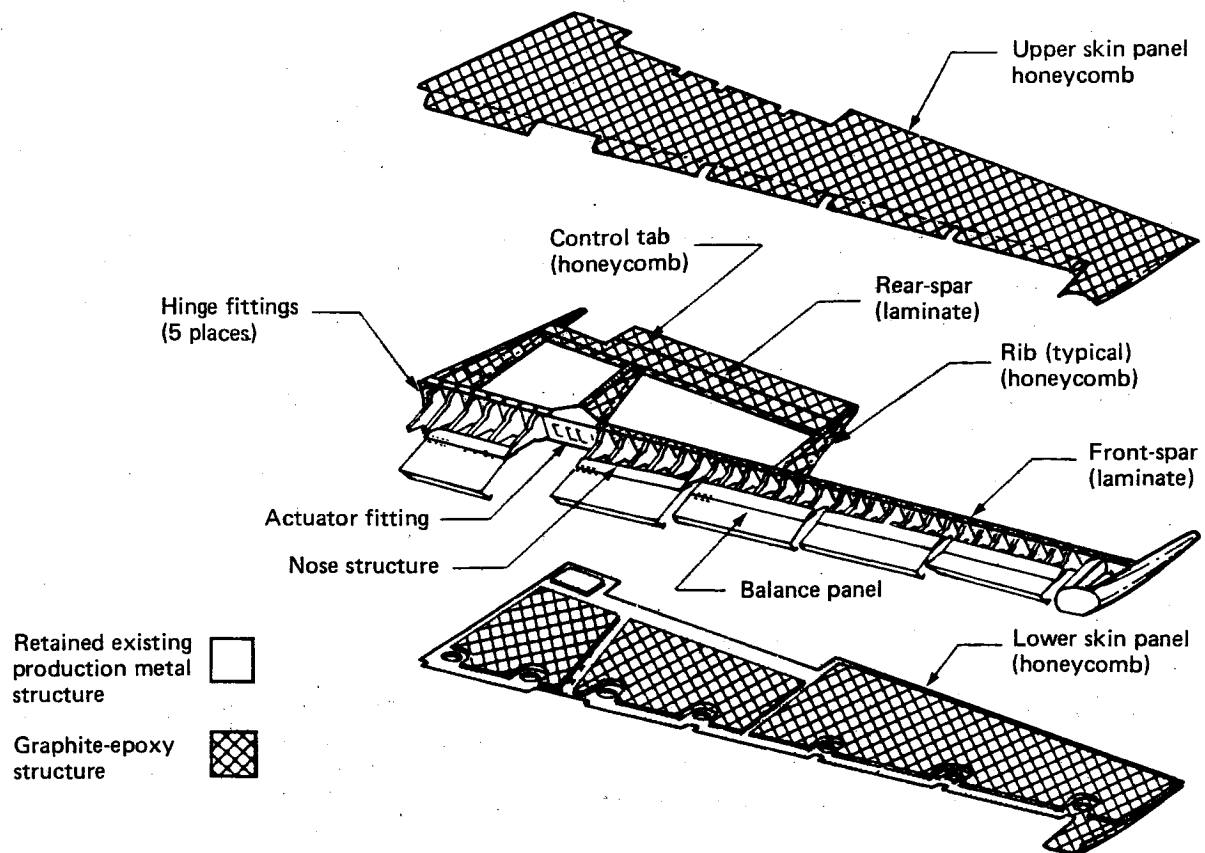


Figure 7. 727 Composite Elevator Structural Arrangement

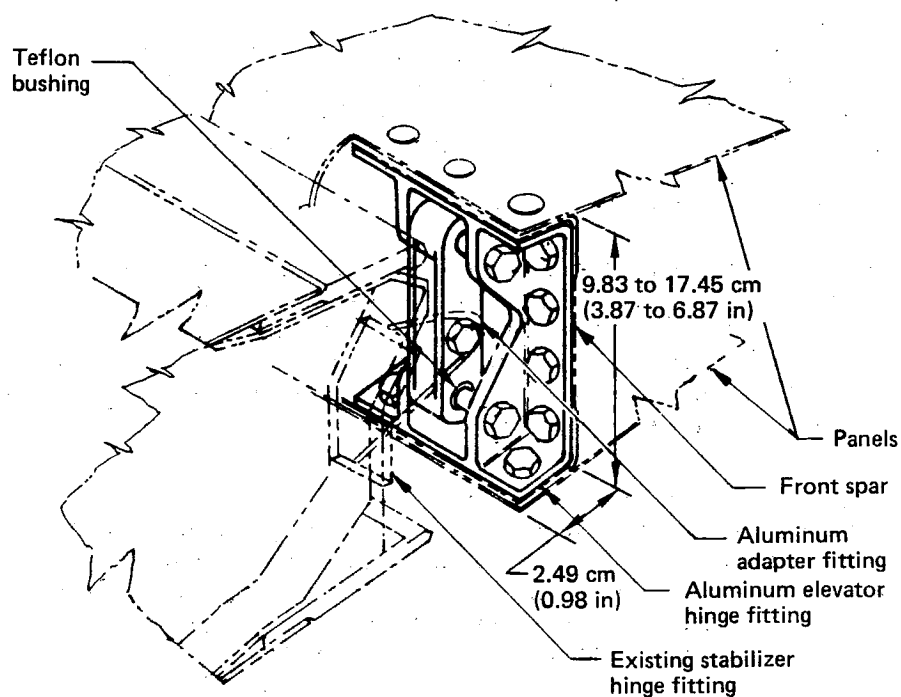


Figure 8. Sliding Block Hinge Fitting

3.1.2.4 Rear-Spar Trailing-Edge Stiffeners

A study was made of the attachment of the rear-spar trailing-edge stiffener to the rear spar. The initial design (fig. 9) of the rear-spar trailing-edge stiffener had one row of fasteners attaching it to the rear spar. An alternative to this design was to make the trailing-edge stiffener integral with the rear spar, thereby eliminating the weight and installation cost of the fasteners and additional separate parts. The complexity of the rear spar tooling and fabrication would be increased with integral parts. The selected design was integral trailing-edge stiffeners instead of separate trailing-edge stiffeners similar to those used on the existing aluminum elevator.

3.1.3 STRUCTURE COMMON TO ALUMINUM ELEVATOR

The existing production metal nose structure (consisting of nose ribs, nose skins, and aerodynamic balance panels) was retained with little or no change, as shown in Figure 7.

This structure would not have been cost effective to change—no weight savings would have been achieved because it is located forward of the elevator hinge line, and tooling for the new structure would have been necessary (i.e., for each pound of structures weight saved, a portion of that weight would have to be returned in balance weights to maintain the mass balance of the elevator). The aluminum actuator fitting also was retained with some minor machining changes, because it is a complex fitting with critical interfaces for actuator attachment and hinge connections integrated into it.

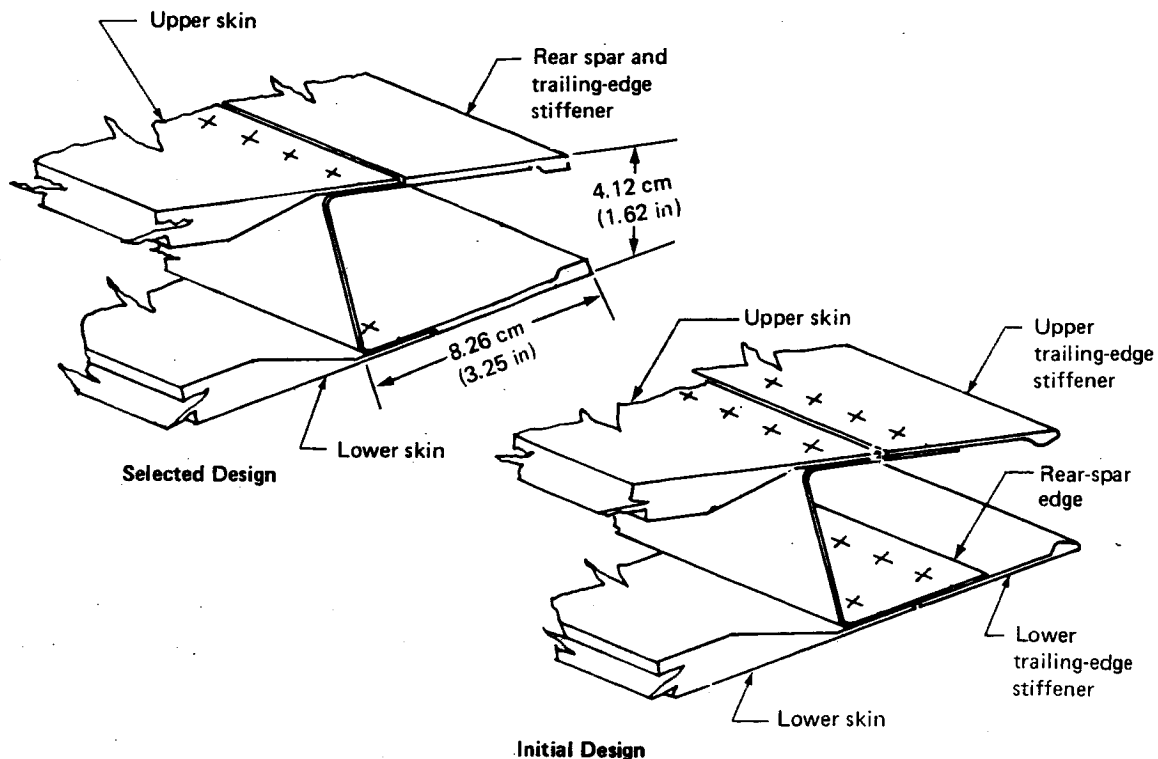


Figure 9. Rear-Spar Trailing Edge

3.2 DETAIL DESIGN—COMPONENT DEFINITION

3.2.1 UPPER AND LOWER SKIN PANELS

The skin panels are one-piece, cocured graphite-epoxy sandwich panels stabilized with Nomex nonmetallic honeycomb core.

The basic panel was designed to provide torsional stiffness equivalent to the existing aluminum panel and to carry the air pressure load without excessive deflection. A solid laminate for fastener attachment was provided along the front spar, trailing edge, rear spar, ribs, and around cutouts. Figure 10 shows the skin panel details. Before selecting the layup configuration, several candidate layups were evaluated after fabrication of sample panels. The evaluation emphasized minimizing weight, layup time, exterior surface roughness to reduce finishing time, fiber breakout on exit side of holes, and panel warpage. An evaluation summary of the other candidate panel layups follows:

- Two plies of 0.01905-cm (0.0075-in) woven fabric oriented ± 45 deg and 0/90 deg on each side of the core. The 0-deg material was inefficient because it was not required to meet stiffness or strength requirements and it added weight. The exterior surface was not smooth and would have required more finishing time.
- A layered four plies of 0.0089-cm (0.0035-in) tape in a 0, ± 45 deg, and 90-deg configuration was evaluated in two forms of preplied broadgoods; namely, two-ply (one ± 45 deg and one 0/90 deg) and single layup (0, ± 45 , and 90 deg). (Both of these material forms had production problems, as discussed in Section 5.1.1.1.)

The honeycomb core stabilizing the skin panels was 48 kg/m³ (3 lb/ft³) Nomex 1.41 cm (0.55 in) thick. This thickness gave a panel depth sufficient to prevent the air loads on the skin panel from deflecting more than the existing aluminum elevator beaded skins deflect.

The selected layup configuration consisted of 0.0089-cm (0.0035-in) thick, 30.5-cm (12-in) wide tape at 90 deg against the layup tool (exterior surface) and ± 45 -deg, 0.01905-cm (0.0075-in) thick woven fabric against the honeycomb core. The interior surface had 0.0089-cm (0.0035-in) thick, 30.5-cm (12-in) wide tape at 90 deg against the honeycomb core and ± 45 -deg, 0.01095-cm (0.0075-in) thick woven fabric on the bag side (fig. 10). This layup resulted in panels of minimum weight (no 0-deg material), reduced cost (less graphite-epoxy), and other production advantages outlined in Section 5.1.1.1. All honeycomb panels had a 0.00254-cm (0.001-in) thick sheet of Tedlar cocured on the interior surface (bag side) to provide a moisture barrier. The skin panels were cured with a layer of FM 300 adhesive weighing 0.01465×10^{-3} kg/cm² (0.03 lb/ft²) between the Nomex core and the adjacent graphite ply. This adhesive was a cocuring 176.7°C (350°F) adhesive that meets the requirements of BMS 8-245.

The exterior finish on these panels is the same as that presently used on production fiberglass panels, except that the conductive coating used on fiberglass is not required on graphite. This finish system consists of a static conditioner (pinhole filler) followed by two primer coats and polyurethane enamel.

A previous Boeing government contract (ref. 1) determined that an unprotected graphite-epoxy structure would be subject to damage if struck by lightning. Therefore, a lightning protection system was designed for the outboard end of the upper skin on the graphite-epoxy elevator, which is an area that has a high lightning strike probability. Probability of a lightning strike is extremely remote inboard of this region or on the lower skin surface.

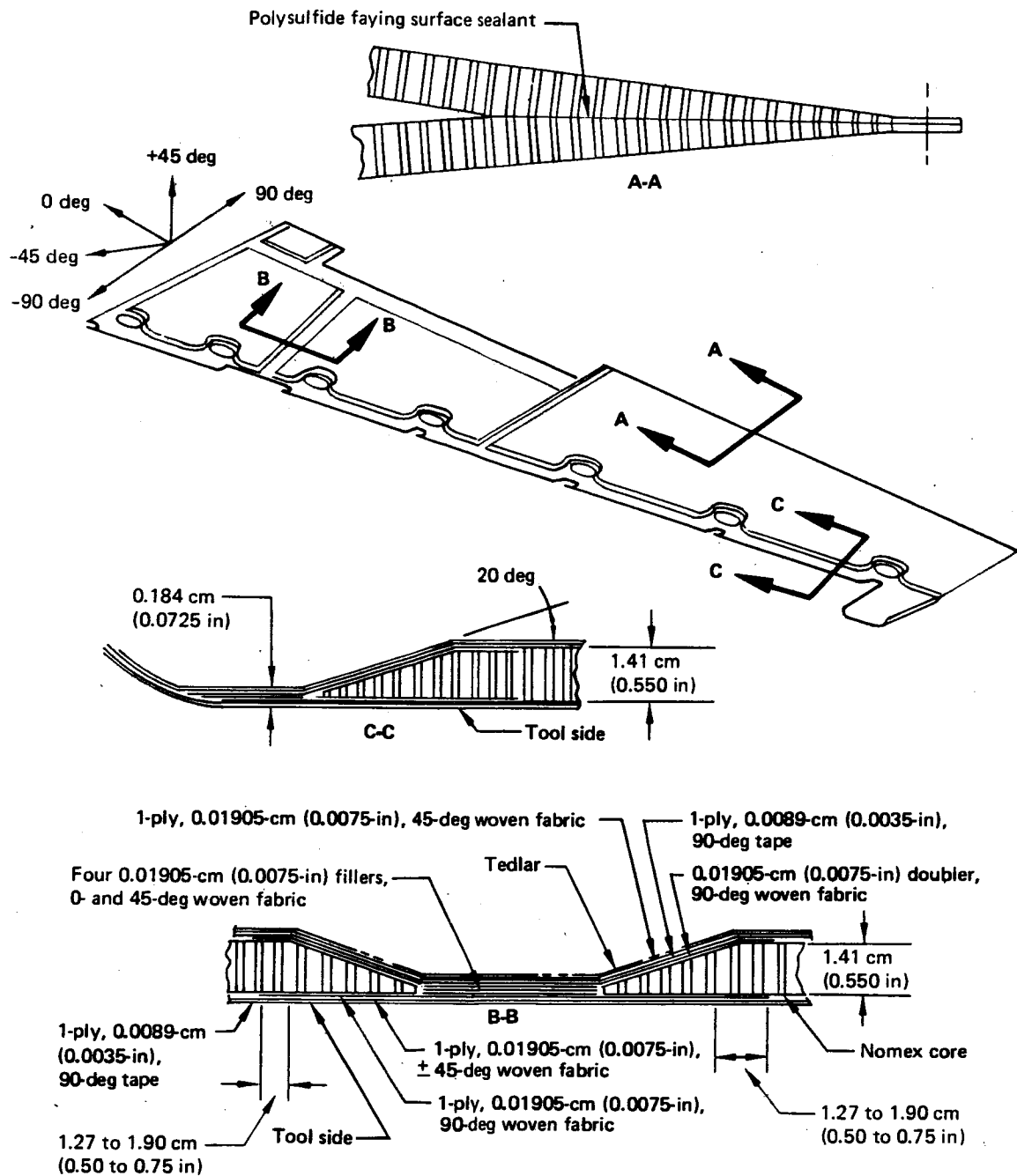


Figure 10. Elevator Skin Panel

The lightning protection system consists of an aluminum diverter strip separated from the graphite-epoxy elevator skin panel by a two-ply fiberglass dielectric layer. This system is shown in Figure 11. The aluminum diverter strips are electrically bonded to the aluminum nose skins and thus provide an electrical path in the aluminum horizontal stabilizer box. These aluminum diverter strips serve as a point of attachment for the initial lightning bolt, as well as conducting the longer term (up to 1 s) lightning current component. This lightning protection system is designed to withstand a severe lightning strike of 100,000A peak current without sustaining significant damage.

A test panel was constructed and tested to substantiate the lightning strike protection provided by this system. See Section 4.2.5 for test description.

3.2.2 RIBS

The four major ribs (inboard closure, actuator backup, station 117, and outboard closure) in the selected elevator design are honeycomb ribs. The rib configuration and layup are defined in Figure 12. Before selecting this concept, a trade study was made comparing a honeycomb rib with a sine-wave rib. Parts of each configuration were designed and fabricated. The ribs were of equal weight; however, it took longer to lay up the sine-wave configuration than the honeycomb configuration. Section 5.1.1.1 presents further details.

The rib at station 117.36 was designed to incorporate the shear-tie angle as an integral part of the rib, thus eliminating the separate shear-tie angle and one row of fasteners. Alternate designs are shown in Figure 13. One concern of the integral design lies in the mismatch that could occur between the spar and rib heights. Any mismatch in the surface contour normally would be compensated for by moving the rib toward or away from the front spar before attaching the separate shear tie. This adjustment is impossible with an integral shear tie. Contour mismatch did not prove to be a problem.

3.2.3 FRONT AND REAR SPARS

The front spar is made in two sections and spliced by the actuator fitting. Both sections are channel-shaped laminates laid up on male tools. These spars are spliced by the actuator fitting. The layup consists of 6 plies of +45-deg fabric with up to 10 plies of 0.0132-cm (0.0052-in) thick unidirectional tape interleaved with the fabric in the chord areas (fig. 14). An unstiffened laminate spar section was selected because the stiffeners required for the 33 nose rib attachments plus the hinge fittings provide all the stiffening required. The chords were designed to furnish the necessary bending stiffness, and the web was designed to carry the shear load.

High, local, spanwise loads in the lower front spar chord near the station 99 elevator-to-stabilizer hinge cutout required local reinforcement of the lower front spar chord. These loads were the result of distributed spanwise skin loads on each side of the hinge cutout being concentrated in the spar chord as the load path passes between the hinge cutout and skin panel access door at station 99. The requirement for local reinforcement was identified during final development of graphite-epoxy material design values (after the basic elevator assembly was completed). To reinforce the lower front spar chord near the station 99 hinge cutout, an external strap 3.56-cm (1.4-in) wide by 68.6-cm (27-in) long was attached to the lower surface of the elevator. This strap consisted of eight plies of 0.0132-cm (0.0052-in) thick unidirectional graphite-epoxy tape oriented spanwise interleaved with five plies of 0.01905-cm (0.0075-in) thick graphite-epoxy fabric oriented at 45 deg to the tape fiber direction. The row of elevator skin-to-front spar fasteners was used to attach the strap to the elevator. If a large elevator production run were forecast, this external reinforcement could easily be incorporated into the local spar chord flange buildup.

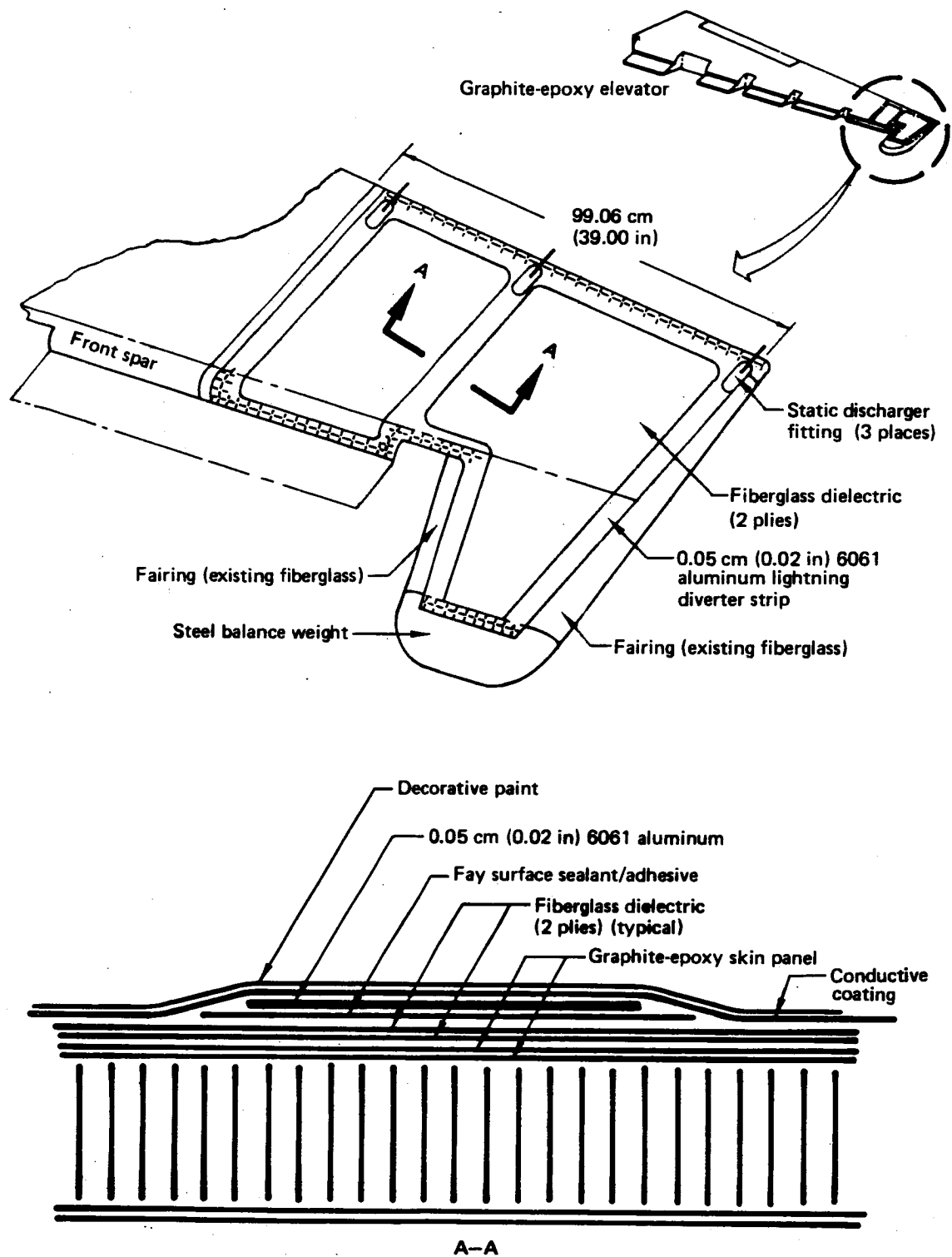


Figure 11. Lightning Protection System

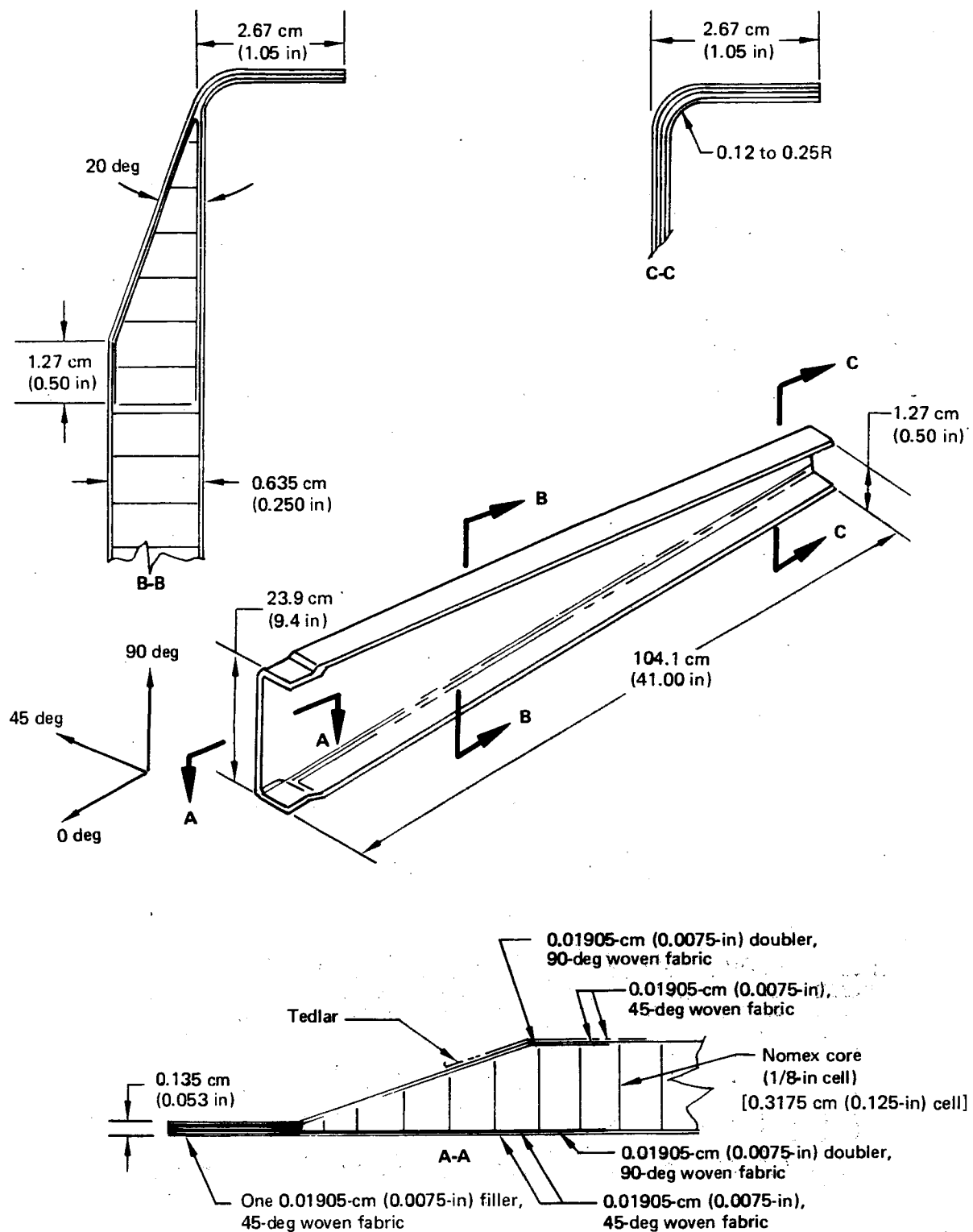


Figure 12. Graphite-Epoxy Honeycomb Rib

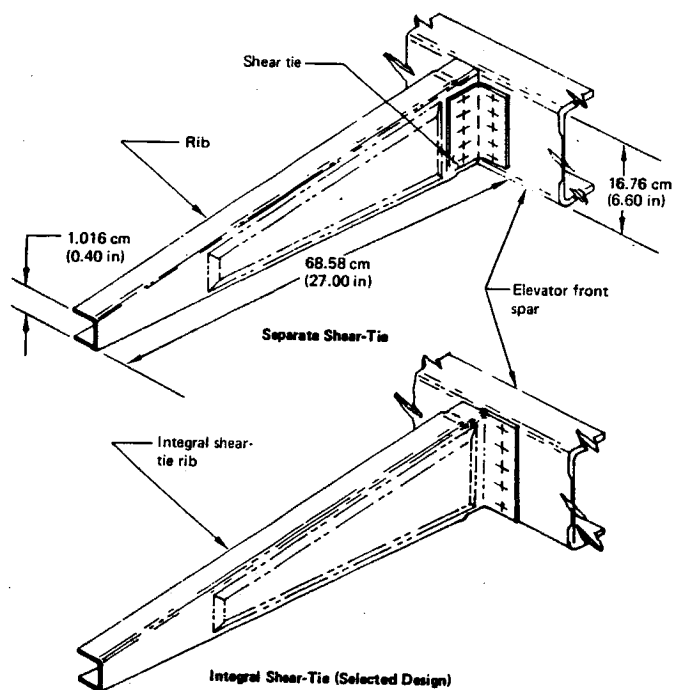


Figure 13. Rib at Station 117.36

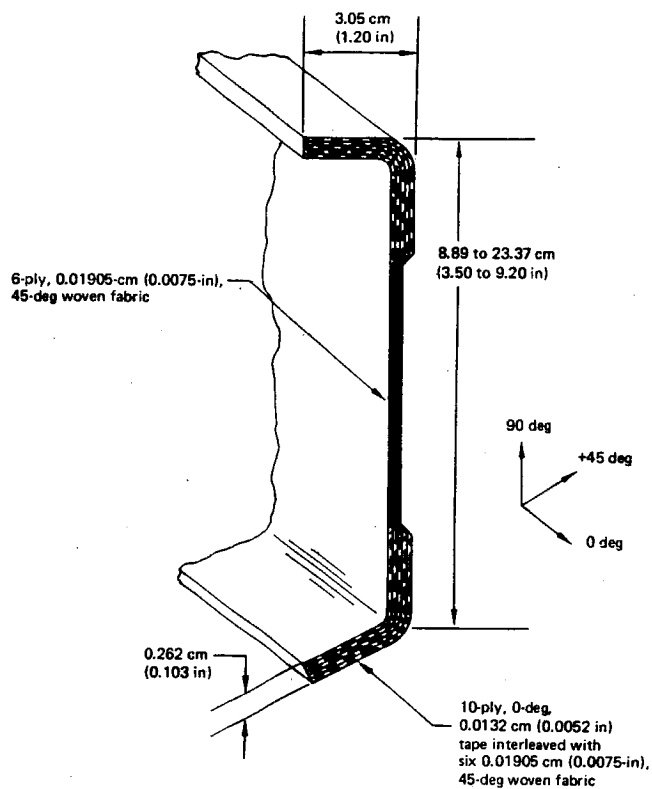


Figure 14. Front Spar

The rear spar is a channel-shaped laminate, as indicated in Figure 15. This spar ends at the outboard end of the tab and supports the five tab hinge fittings and the aft edge of the elevator panels. The layup is four plies of 0.01905-cm (0.0075-in) thick fabric, with fibers at +45 and -45 deg interleaved with two to three plies (depending on location) of 0.01905-cm (0.0075-in) thick fabric with fibers at 0 and 90 deg.

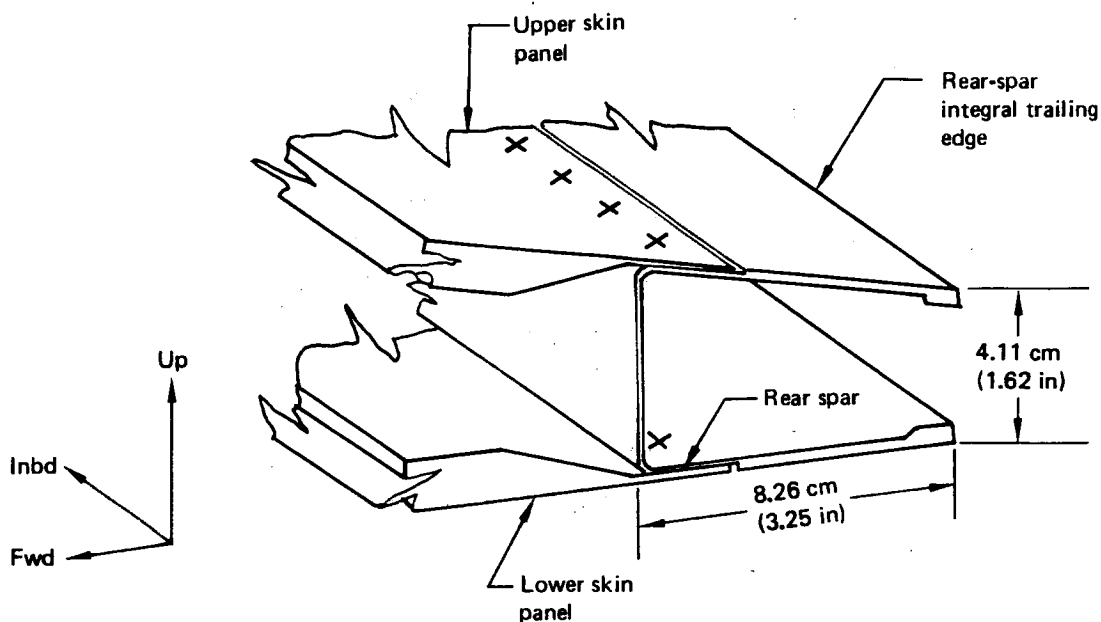


Figure 15. Rear Spar

3.2.4 ELEVATOR ASSEMBLY

The elevator components were assembled using titanium fasteners. Where access permitted, countersunk titanium bolts with modified Phillips-head recesses (Torque-set) or protruding-head titanium Hi-loks were used. These fasteners were mated with stainless-steel nuts or collars.

The lower panel surface (the first installed) was initially attached to the substructure with flush-head titanium Hi-loks. During installation of these fasteners, it was necessary to torque the stainless-steel collar to such a high level before the collar broke off that the Hi-lok head sometimes pulled into the countersunk hole excessively. Further, reacting the high torque in the hex drive of the Hi-lok pin caused the hex wrench to twist and fracture. These fasteners have been replaced by titanium bolts (Torque-set) installed with stainless-steel nuts and washers.

For the initial two assemblies, the closeout (upper) panel was attached to the substructure with titanium bolts mated with stainless steel nutplates. This material combination proved to be impractical due to the excessive torque required to seat the fastener. The tightening tool would "cam out" of the recess in the bolthead before tightening was complete. For the later eight elevator assemblies, the closeout panel was attached to the substructure using blind fasteners (Visu-loks). This fastener change significantly reduced the elevator assembly time.

The skin panels were riveted together along the trailing edge, using special harness-type double-countersunk titanium rivets that were squeeze installed. Polysulfide sealant (BMS 5-79) was used as a faying-surface sealant in this area (fig. 10).

During the assembly of the composite elevator components, gaps were noted between some mating parts before installation of the joint fasteners. These gaps mostly occurred between the aluminum nose ribs and the elevator cover panels where aluminum parts made with existing tooling had improperly contoured flanges. Some gaps occurred at the elevator trailing edge because some of the rib tools produced composite parts with too high or too low a chord height at the aft end. Normally, in a production run of composite elevators, the aluminum nose rib forming tools and the composite rib layup tools would be altered to produce parts with the correct contour, thus eliminating the gaps. For a limited run of five shipsets of elevators, the assembly gaps exceeding 0.0254 cm (0.010 in) were shimmed to minimize clamp-up stresses. Phenolic shims (MIL-P-15035, type FBM or FBG) were used to fill up gaps before installation of the joint fasteners. When shim lengths greater than 7.62 cm (3.0 in) were required, these shims were tapered to 0.051 cm (0.020 in) thick using an 80-to-1 taper ratio and then cut off leaving a minimum of 0.508-cm (0.20-in) edge margin). Shims made from liquid epoxy materials (Hysol EA 933 and EA 934) were used to fill gaps of 0.0762 cm (0.030 in) or less.

3.2.5 CONTROL TAB

The control tab is a lightweight graphite-epoxy wedge-shaped structure with minimum-thickness face sheets (one ply +45-deg graphite-epoxy fabric 0.01905-cm (0.0075-in) thick plus one ply 90-deg graphite-epoxy unidirectional tape 0.0089-cm (0.0035-in) thick) supported by full-depth 0.318-cm (0.125-in) cell, 48-kg/m³ (3.0-lb/ft³) Nomex honeycomb core, and a laminate spar (fig. 16). The five aluminum hinge fittings used on the aluminum tab were retained. One hinge was relocated spanwise to preclude interchangeability with the current aluminum tab, since elevators are a controlled mass-balanced surface.

3.2.6 BALANCE WEIGHTS

The existing elevator balance weights consist of a stainless-steel casting positioned at the elevator horn tip, balance weights located at the aft edge of the balance panels, and aluminum bronze balance panel hinges.

The lighter graphite-epoxy elevator was mass balanced by removing all balance weights from the balance panels and reducing the weight of the aluminum bronze hinges in those bays with the shorter balance arms, thus locating the balancing weight where the balance arm is longest.

3.2.7 THERMAL CONSIDERATIONS

Consistent with the current metal design, elevator side load is carried at the inboard hinge. Thermal expansion between the aluminum stabilizer and the graphite-epoxy elevators builds up to a maximum at the outboard end where the total structural relative movement between the stabilizer and elevator could be 1.32 cm (0.52 in).

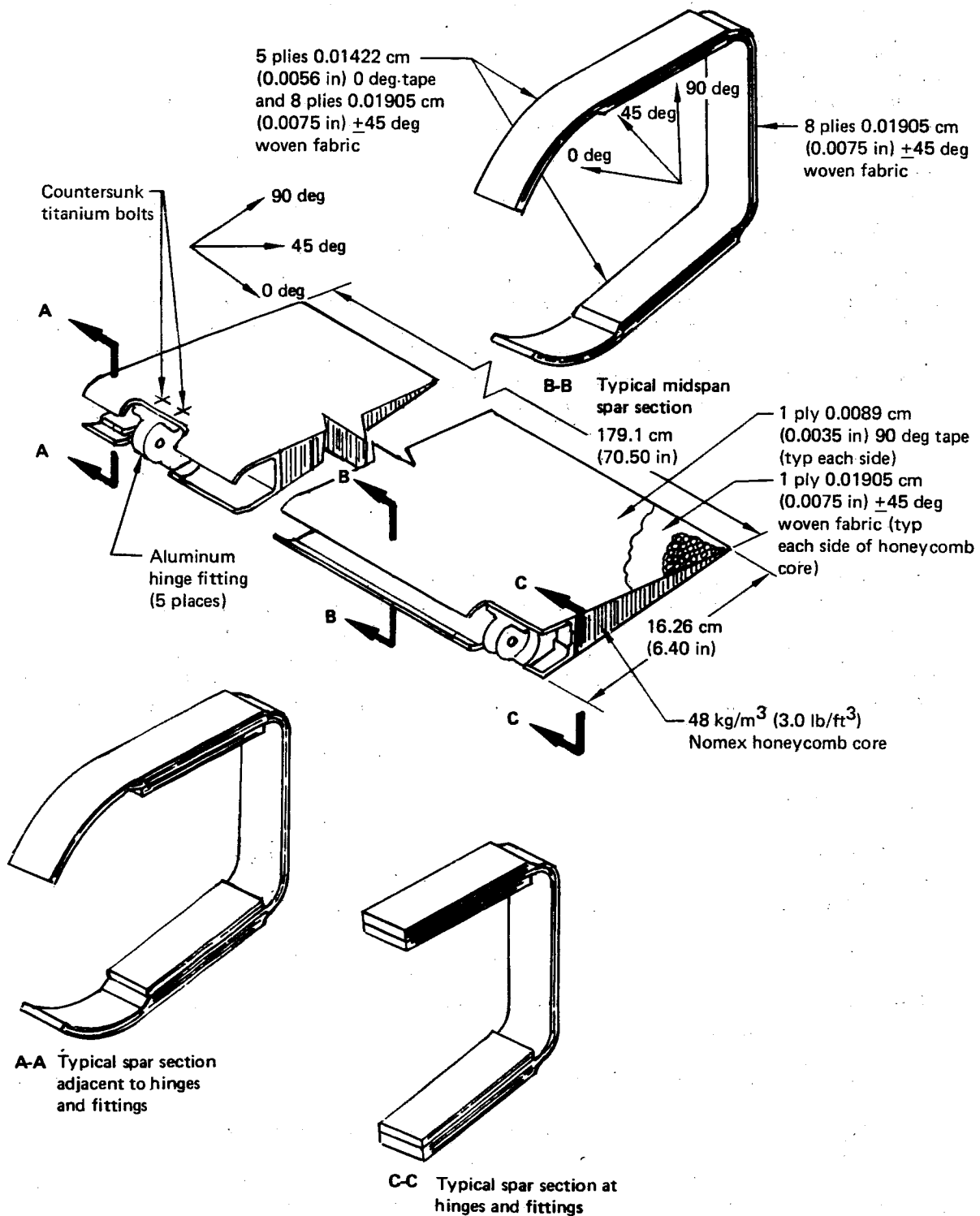


Figure 16. Control Tab

This relative motion impacted the design in three areas:

- Aerodynamic sealing of balance panels to the sides of the stabilizer hinge ribs. New, larger diameter bulb seals and new seal retainers were required to maintain this seal throughout the range of elevator operating temperatures (fig. 17).
- The piano hinge between the balance panel and the elevator. The tight fit between the balance panel hinge halves prevented any spanwise motion. A new hinge design permitted enough space between the hinge halves to allow the required spanwise motion (fig. 17). Because this loose fit between hinge halves increased pin bending, a larger diameter hinge pin was required in the new design.
- The elevator-to-stabilizer hinge connection. To provide the required spanwise motion in this area without any change to the stabilizer or stabilizer hinge fitting, two configurations were studied:
 - The first configuration involved increasing the distance between lugs to allow the required spanwise float, installing Teflon-lined bushings on each side of the stabilizer fitting, and changing the hinge pin to a higher heat-treat steel pin.
 - The second concept introduced an adapter fitting that retained the existing hinge pin by providing lugs identical to the existing elevator hinge fitting and transferring the spanwise motion to bolts that were mounted in teflon bushings above and below the hinge point. See Figure 8 for configuration details.

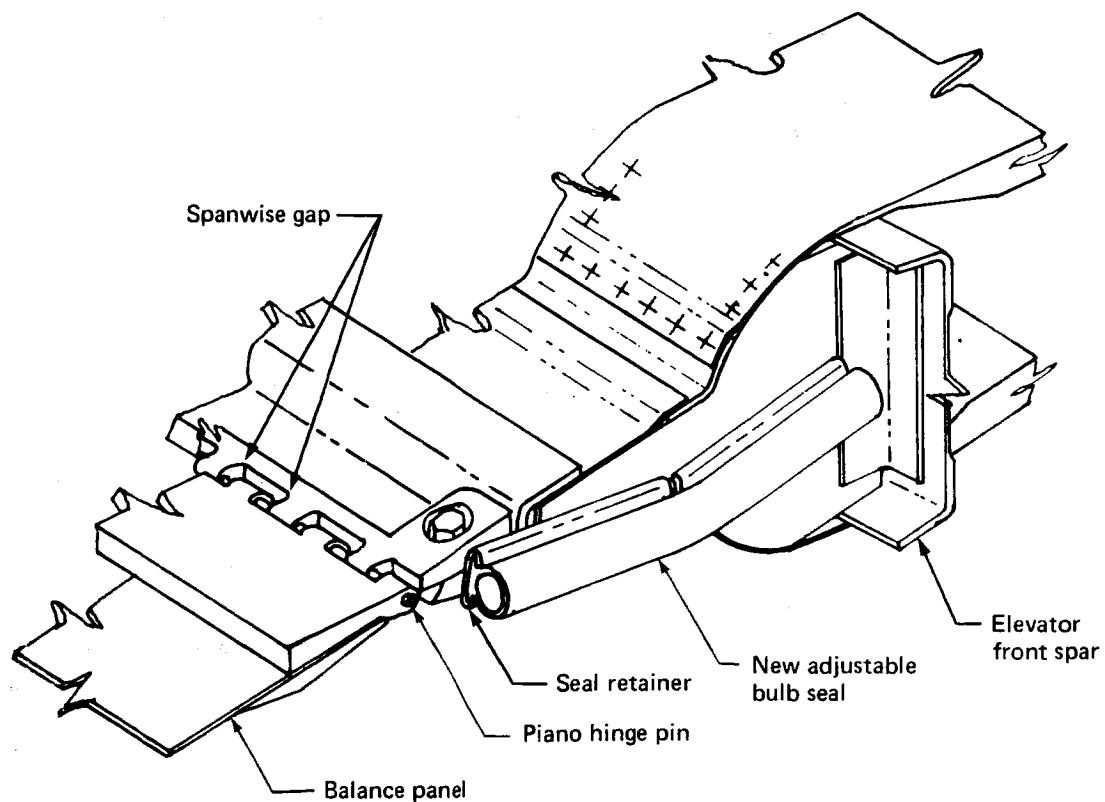


Figure 17. Adjustable Seals and Piano Hinge

Mockups were made of each of these configurations for detailed evaluation of access, producibility, and maintainability. This evaluation led to the selection of the concept that incorporates the adapter fitting (fig. 8). This concept permits considerably better access for elevator installation and/or removal and avoids the use of a special high-heat-treat hinge steel bolt at the point of interface with the stabilizer.

3.2.8 CORROSION PROTECTION SYSTEM

A baseline corrosion protection system was developed for use on the advanced composite elevator. Basically, the corrosion protection system was designed to isolate graphite-epoxy surfaces from aluminum structure to minimize the cathodic area (graphite) available for electrochemical reactions. This minimizes the potential current flow and, thus, galvanic corrosion.

The corrosion protection system provides a level of corrosion resistance for the advanced composite elevator equivalent to that of the existing aluminum elevator. This was determined by comparing the amount of corrosion products on samples that were representative of the aluminum elevator structure and the advanced composite structure after exposure to salt spray. Several corrosion protection designs (including use of fiberglass, Tedlar, paint, and polysulfide sealant to isolate the aluminum from the graphite) were investigated in a Boeing-funded study. Assemblies incorporating candidate corrosion protection systems were subjected to salt spray; conventional anodized and primed aluminum parts were used as control specimens to compare the corrosion resistance of the parts under test.

The corrosion protection system selected consisted of covering graphite-epoxy surfaces with a ply of cocured fiberglass or Tedlar in areas that are within 7.62 cm (3 in) of aluminum or interface with aluminum structure. Also, a polysulfide faying-surface seal was applied between the graphite-epoxy part and the aluminum part. Fasteners were installed with wet polysulfide sealant, and exposed graphite-epoxy edges adjacent to aluminum structure were fillet sealed. In addition to the isolation of graphite-epoxy surfaces from aluminum structure, all aluminum structure was primed and painted with an enamel paint. An example of the corrosion protection system is detailed in Figure 18.

3.2.9 STRUCTURAL REPAIR DOCUMENTATION

Structural repair requirements and techniques were developed for the advanced composite elevator and published in D6-48756, Advanced Composite Elevator for Boeing 727 Aircraft, Structural Repair Manual (Appendix A). Included are repairable damage criteria, elevator repair procedures, elevator balance limitations, and elevator balance procedures. The repair procedures were qualified by testing discussed in Section 4.2.6.

3.2.10 MAINTENANCE AND INSPECTION DOCUMENTATION

Maintenance planning recommendations were developed as a general guide for individual airlines as they establish maintenance programs for Boeing model 727-200 aircraft with advanced composite elevators installed. These recommendations were published in D6-46020, Maintenance Planning Data, 727 Aircraft Structural Inspection, Composite Elevator (Appendix B).

1 Apply static conditioner and surfacer (SRF 14.672) and one coat BMS 10-11 primer (F20.02). Then one coat BMS 10-79 type II primer plus one coat BMS 10-60 type II gloss polyurethane (7067 white) enamel (F19.41-7067).

2 1-ply Tedlar film (PVF), transparent 100 BG, 30 TR per BAC 5562 in area shown.

3 1-ply, 120 style fiberglass with Narmco 5208 resin, Cocure per BAC 5562.

4 Fillet seal using BMS 5-79 per BAC 5000.

5 Faying surface seal using BMS 5-79 per BAC 5000.

6 Alodine or anodize plus one coat BMS 10-11 type I primer (SRF 2.30).

7 Install fasteners with wet sealant using BMS 5-79 per BAC 5000.

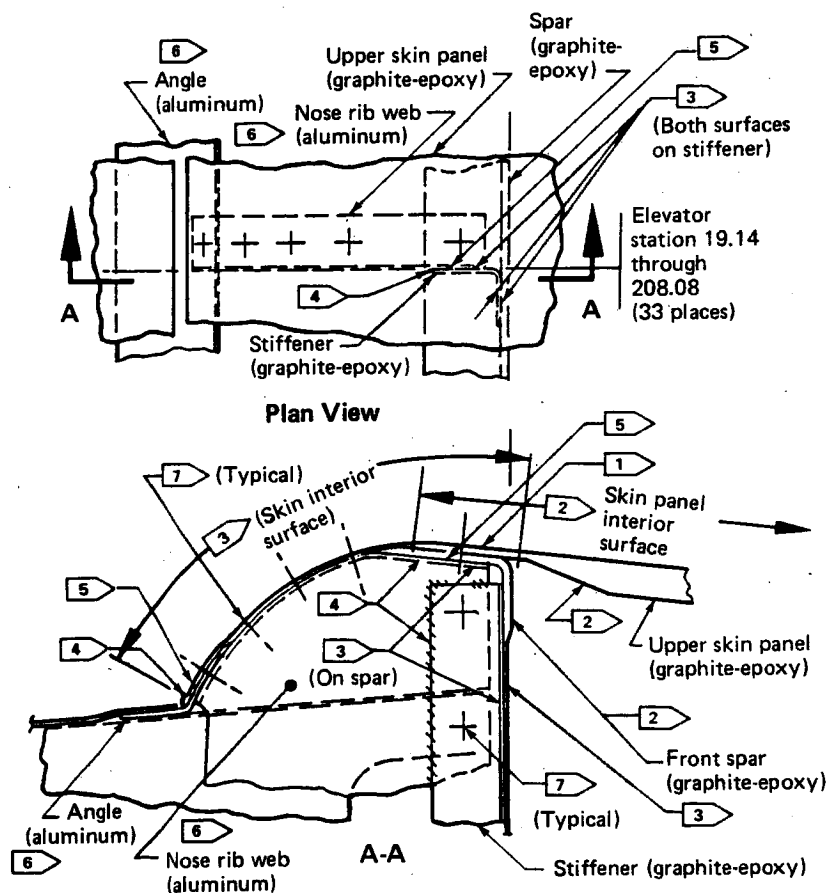


Figure 18. Corrosion Protection—Typical Graphite-Epoxy/Aluminum Interface

4.0 ANALYSIS AND TEST

Analysis and test tasks were performed during this program to substantiate the advanced composite elevator for airline flight use. Ultimate strength, flutter, and stability and control analyses were performed to provide an analytical base. Ancillary and full-scale ground structural tests, flutter, and stability and control flight tests were performed to verify the analyses.

4.1 ANALYSIS

This section presents the analysis tasks performed during the advanced composite elevator program. These analysis tasks are similar to those typically performed for similar metal structures. Moisture and temperature effects for the composite material were accounted for by using design values developed from environmentally conditioned specimens and subcomponents in the final strength analysis. This procedure is discussed in detail in Section 4.1.7.

The composite elevator was designed in accordance with applicable Civil Air Regulations (CAR 4b) (ref 2) and all applicable Boeing design documents. The Composite Aircraft Structure Advisory Circular (AC20-107) (ref 3) was used as the basic guide to show compliance with the regulations.

4.1.1 STRUCTURAL CRITERIA

Structural criteria shall be defined to provide a base for the design. In most cases, the criteria shall be based on existing metal design practices. Other criteria that are unique to composite structure shall be based on knowledge obtained from prior composite programs. Sections 4.1.1.1 through 4.1.1.5 define specific criteria.

4.1.1.1 Loads

The external loads for the advanced composite elevator shall be the maximum loads expected in service on any model of the 727 aircraft. These loads shall be adequate in scope to meet all Boeing and FAA design requirements. The airplane flight envelope (V-n diagram) remains unchanged. All components of the elevator shall be designed to withstand ultimate loads. Ultimate and limit load definitions shall be identical to those of current metal structure.

The effects of any loads due to thermal expansion differences between the elevator and horizontal stabilizer shall be accounted for in the analysis of each component.

4.1.1.2 Flutter and Vibration

A flutter analysis of the present 727 airplane with the advanced composite elevator shall be conducted. The flutter analysis is verified by ground vibration and flight tests.

The effects of elevator stiffness and mass changes on the airplane flutter characteristics shall be assessed.

4.1.1.3 Sonic

The advanced composite elevator shall be designed for the most critical local sonic environment encountered on the horizontal tail of any 727 airplane model.

4.1.1.4 Electrodynamics

Precipitation static (P-static) and lightning protection requirements shall be incorporated into the design of the graphite-epoxy composite elevator. An analysis shall be conducted to determine the extent of lightning protection required, including lightning strike damage at the contact point, possible lightning current paths through the structure, and elevator-to-stabilizer electrical bonding and ground requirements.

Figure 19 defines the potential lightning threat, as defined by SAE Committee AE4L (ref 4), that shall be accounted for in the protection system design.

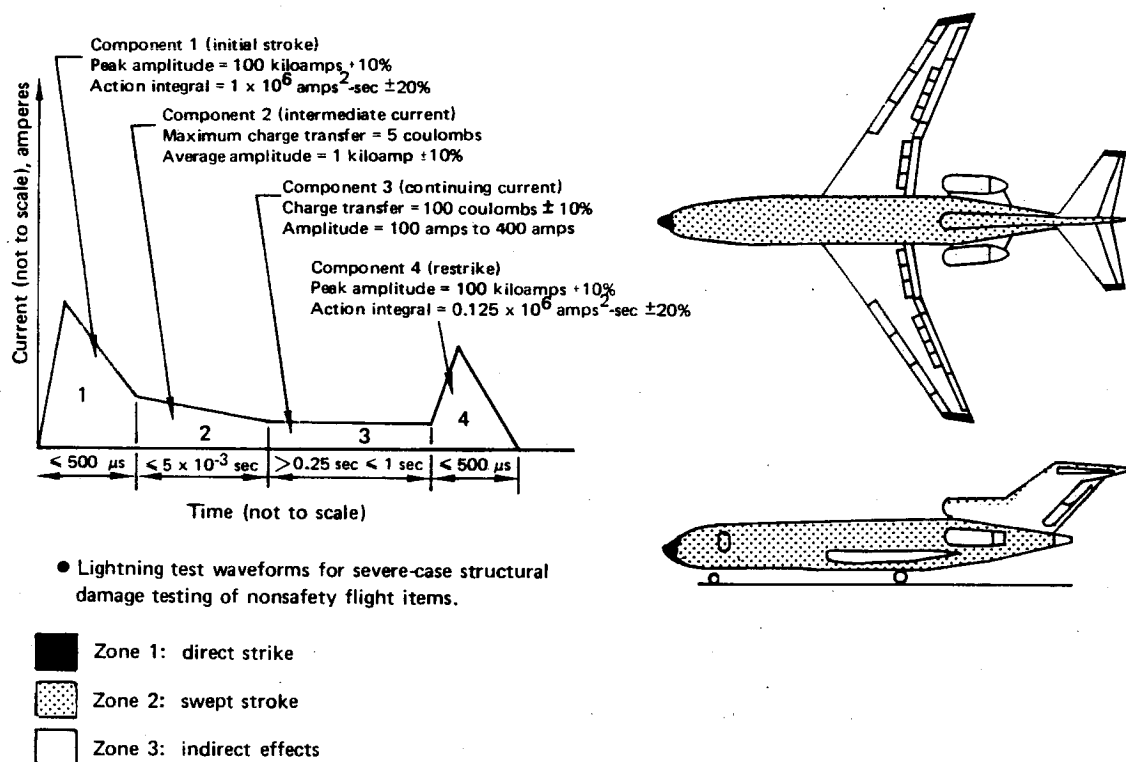


Figure 19. Lightning Strike Zones and Intensities

4.1.1.5 Environment

The advanced composite elevator shall be designed to be compatible with the current 727 airplane certified structural operational environment.

In-service moisture and temperature effects on physical and mechanical properties of structural materials shall be accounted for in the design, analysis, and testing of the advanced composite elevator. Conservative moisture and temperature envelope values for airline service exposure shall be used to establish design, analysis, and test temperature and moisture absorption levels. Moisture and temperature effects shall be accounted for when evaluating test results obtained from components exposed only to ambient temperature and humidity.

4.1.2 EXTERNAL LOADS ANALYSIS

The external loads used for the structural analysis were obtained from the most highly loaded model 727 airplane. The requirements of CAR 4b (ref 2) and Boeing design specifications were met. The load requirements included limit and ultimate loads, durability, dynamics and vibration, and flutter. The CAR 4b limit load factor-velocity (V-n) diagram is shown in Figure 20 for reference. Critical design load conditions are shown in Figure 21. The design ultimate pressures shown are the total lift pressures across the control surface. The fatigue loads were derived from the same flight-load spectrum as that used for current production airplanes.

4.1.3 STIFFNESS ANALYSIS

4.1.3.1 Stiffness Calculation

The spanwise bending stiffness (EI) and torsional stiffness (GJ) comparisons of the production aluminum elevator and the graphite-epoxy composite elevator are shown in Figures 22 and 23. Typical cross-sections of both the production aluminum elevator and the graphite-epoxy elevator, at hinge cutouts and between hinges, are shown in Figures 24 and 25.

The bending stiffness for the production aluminum elevator was calculated using the amount of compression skin effective at limit load. The entire skin area is effective on the graphite-epoxy composite elevator, since skin buckling does not occur below ultimate load.

Properties were calculated at each elevator hinge station, where the nose structure is discontinuous, and at stations midway between hinges, where the nose structure is assumed fully effective for bending stiffness. Bending stiffness values plotted are the average of the foregoing values. The nose structure is assumed fully effective for torsional stiffness except at the local hinge cutouts. Stiffnesses were determined in the same manner for the existing aluminum elevator.

4.1.3.2 Stability and Control

A static aeroelastic study was performed to establish an acceptable tolerance of elevator control effectiveness. The calculated bending and torsional stiffness for the composite elevator resulted in an elevator control effectiveness that was within the acceptable tolerance band.

Further substantiation that the graphite-epoxy elevator had acceptable stability and control aeroelastic characteristics was provided with the successful completion of the flight test program reported in Section 4.5.

4.1.3.3 Flutter

A flutter analysis was conducted for the model 727 airplane with a graphite-epoxy composite elevator. Symmetric and antisymmetric flutter analyses were performed that encompassed elevator center-of-gravity extremes with both power-on and power-off operation. In addition, power-on and power-off analyses were made for a failed elevator actuator and a failed tab control rod. The analytical results indicate that a 727 with a composite elevator does not suffer any degradation of flutter characteristics or speeds when compared to the production aluminum elevator.

Both ground vibration and in-flight flutter tests, reported in Sections 4.4 and 4.5, substantiated the results of the flutter analyses.

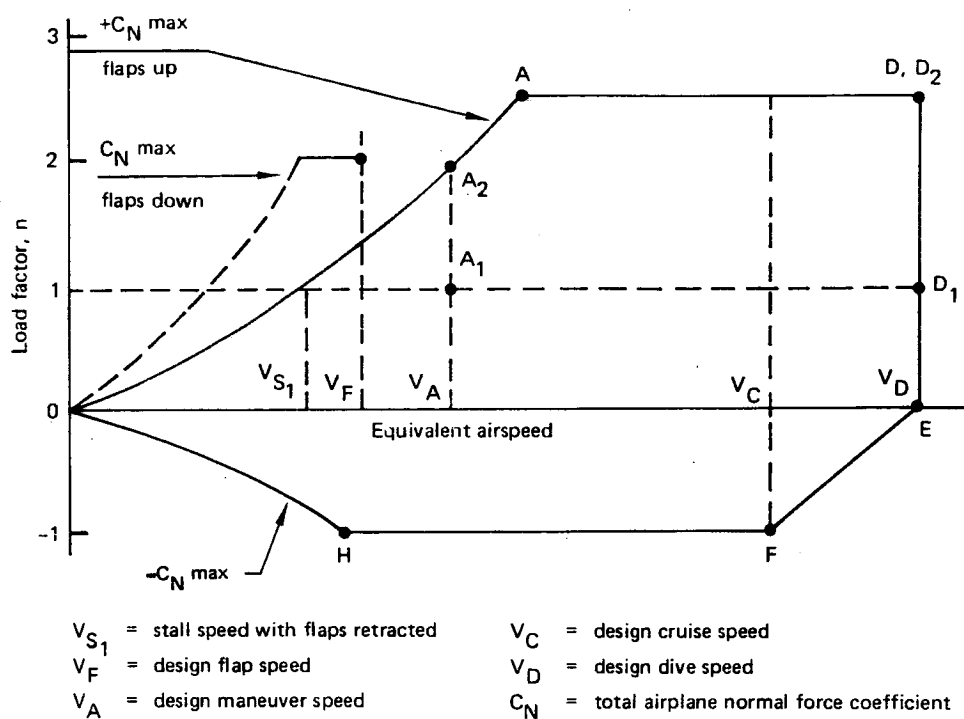
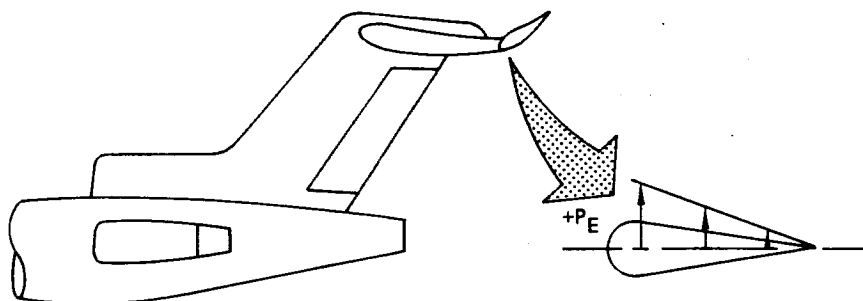


Figure 20. CAR 4b V-n Diagram



Condition	Load case	Limit load factor	Altitude, m (ft)	Speed, km/hr (kn)	Ultimate pressure P_E , kPa (lbf/in ²)
+ Maneuver at V_D	120R	2.5	4145 (13,600)	851 (460)	-23.37 (-3.39)
- Maneuver at V_D	122R	-1.0	Sea level	722 (390)	23.31 (-3.38)
Check maneuver	124	1.0	Sea level	722 (390)	-2.76 (-0.40)
Instantaneous elevator	125	1.0	Sea level	463 (250)	-22.62 (-3.28)
+ Maneuver at V_D	128	2.5	Sea level	851 (460)	-31.85 (-4.62)

Figure 21. Critical Design Conditions

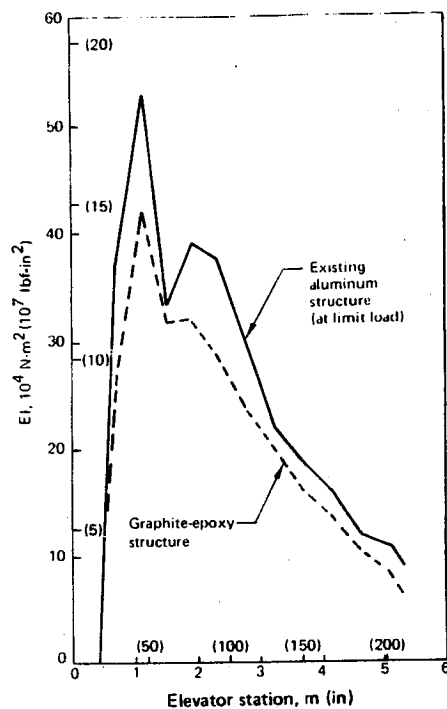


Figure 22. 727 Elevator Spanwise Bending Stiffness

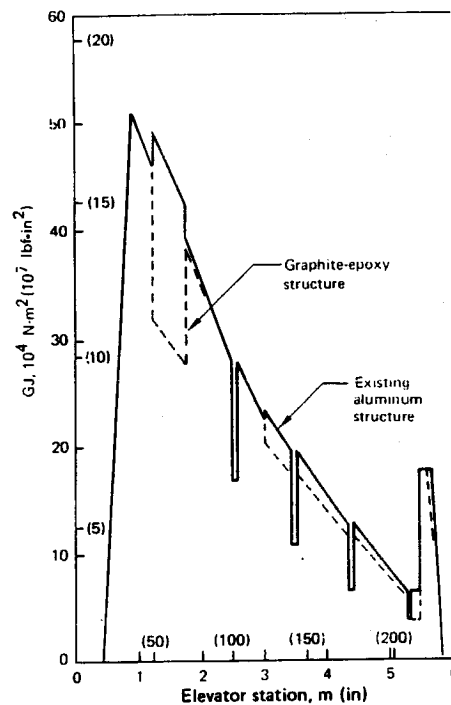


Figure 23. 727 Elevator Torsional Stiffness

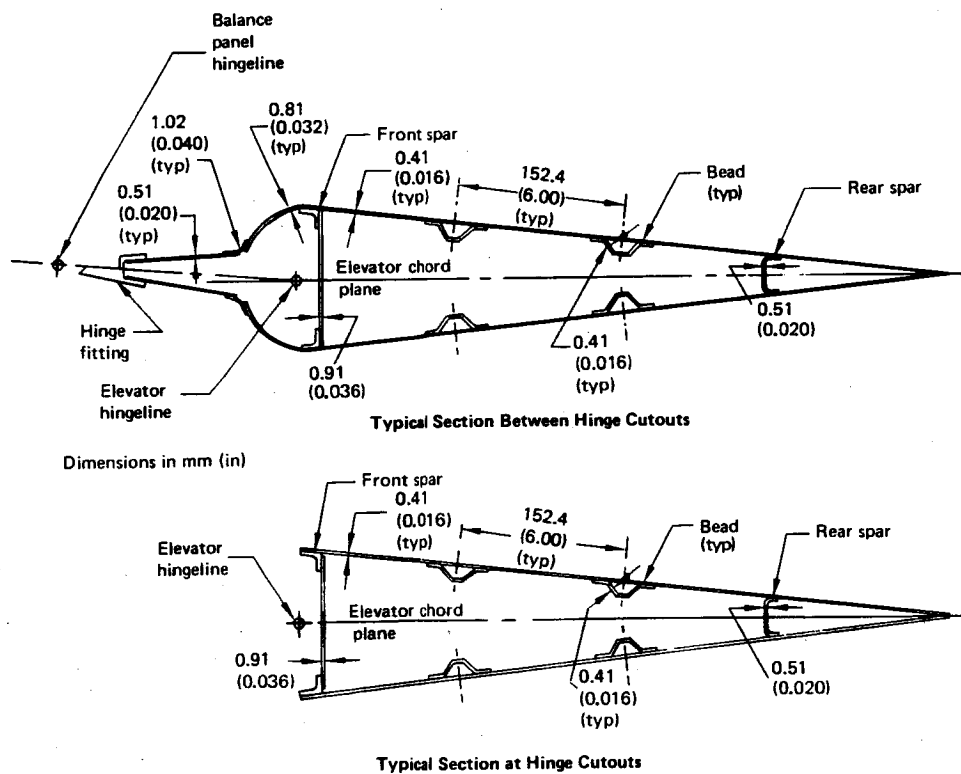


Figure 24. Production Aluminum Elevator

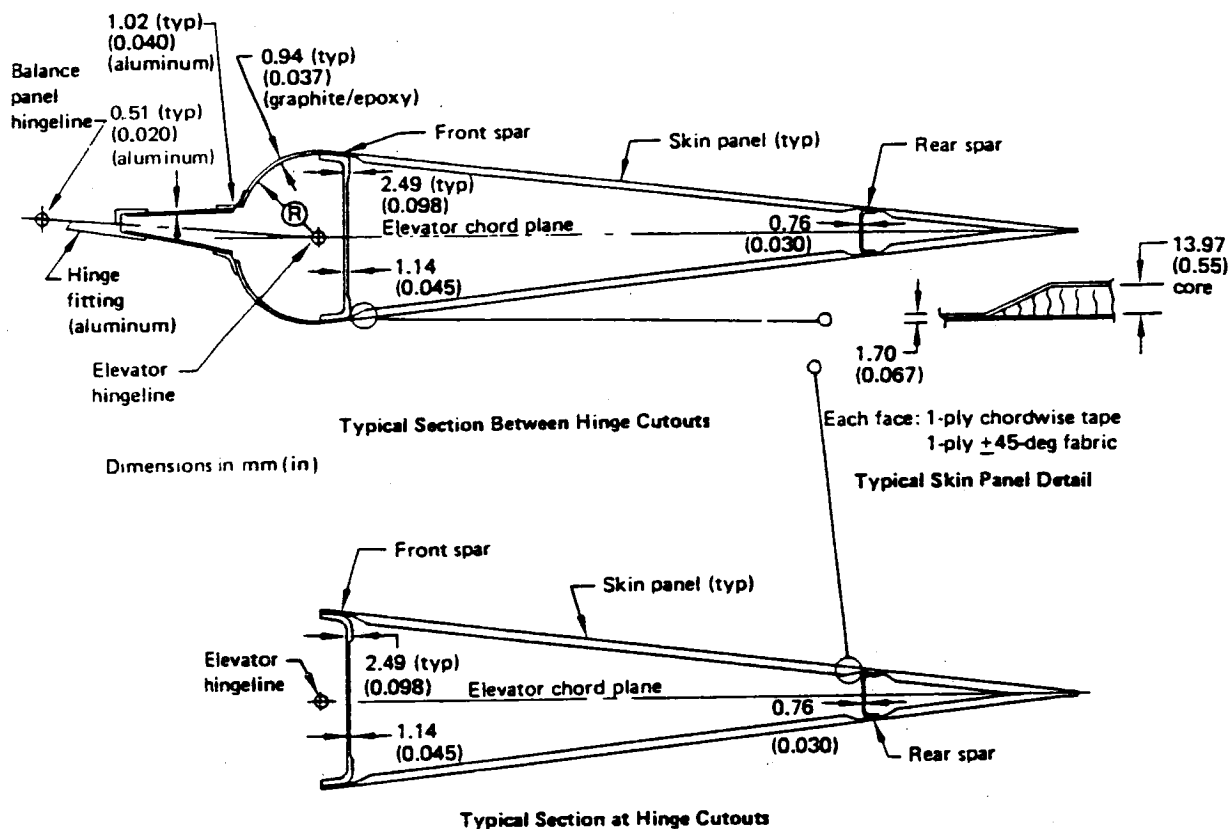


Figure 25. Graphite-Epoxy Composite Elevator

4.1.4 SONIC ANALYSIS

Maximum overall sound pressure levels (OASPL) for the lower surface of the 727 horizontal tail are shown in Figure 26. These values are based on measurements that have been adjusted to account for the highest possible OASPL attainable on any 727 airplane.

Based on the measured sonic values and the basic life requirements, the 4-hr exposure to 158-dB OASPL or the 15-hr exposure to 155-dB OASPL was equivalent to the sonic exposure experienced by the elevator during one airplane service lifetime. The sonic box test, reported in Section 4.2.3.9, was conducted at these higher noise levels to reduce test time.

4.1.5 THERMAL ANALYSIS

The temperature excursion used in the design of the graphite-epoxy elevator was established as 82 to -59°C (180 to -75°F). The maximum temperature was obtained from a thermal analysis that accounted for ambient air temperature, radiation and convection heat transfer, surface absorptivity and emissivity characteristics, and cooling effects during taxi, takeoff, and flight. The thermal model and boundary conditions established for the thermal model are shown in Figure 27. A dark paint system was conservatively assumed. The steady-state temperatures achieved in the model are shown in Figure 27 at time = 0. A transient analysis then was performed and the results are shown in Figure 27. The conditions and assumptions used for the

transient analysis were defined as 4-minute taxi run, with a constant relative wind velocity of 37.1 km/hr (20 kn), followed by constant takeoff, acceleration, and climb to 352 km/hr (190 kn) in 1.2 minutes. This point was selected as the earliest possible time that the aircraft could be subjected to significant maneuver or gust loads and would occur at 5.2 minutes after brake release (fig. 27). The ultimate load conditions were conservatively analyzed at this speed and altitude.

The thermal analysis indicated that at the end of 1.2 minutes of flight, the elevator front spar web would be at 82°C (180°F). This temperature was conservatively used for all elevator structure.

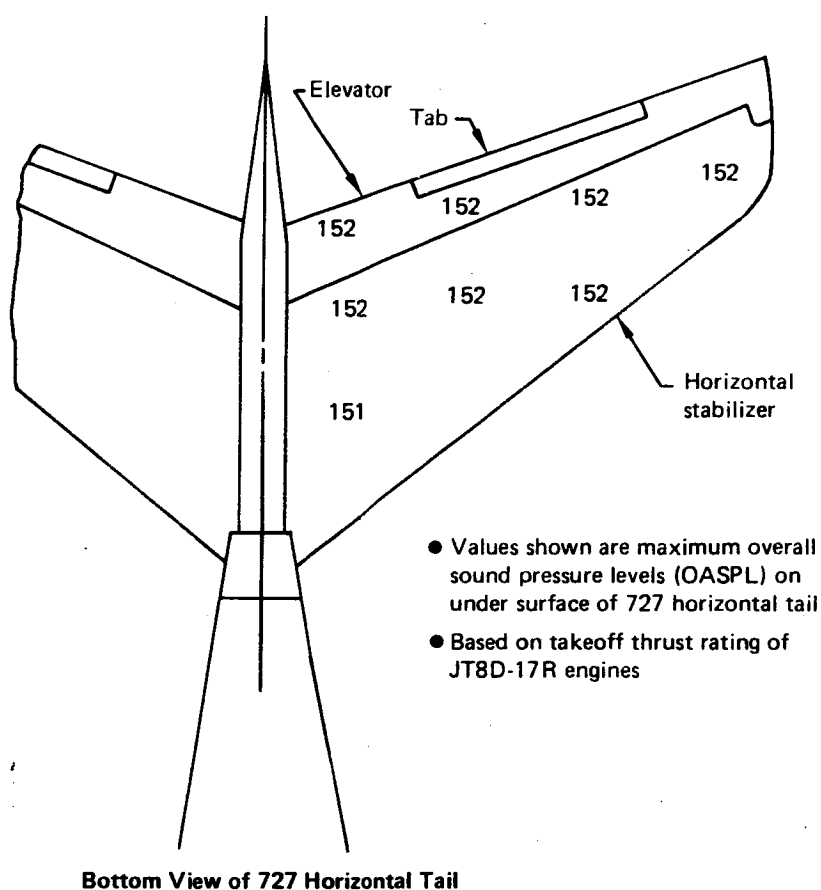


Figure 26. Maximum Overall Sound Pressure Level on 727 Horizontal Tail

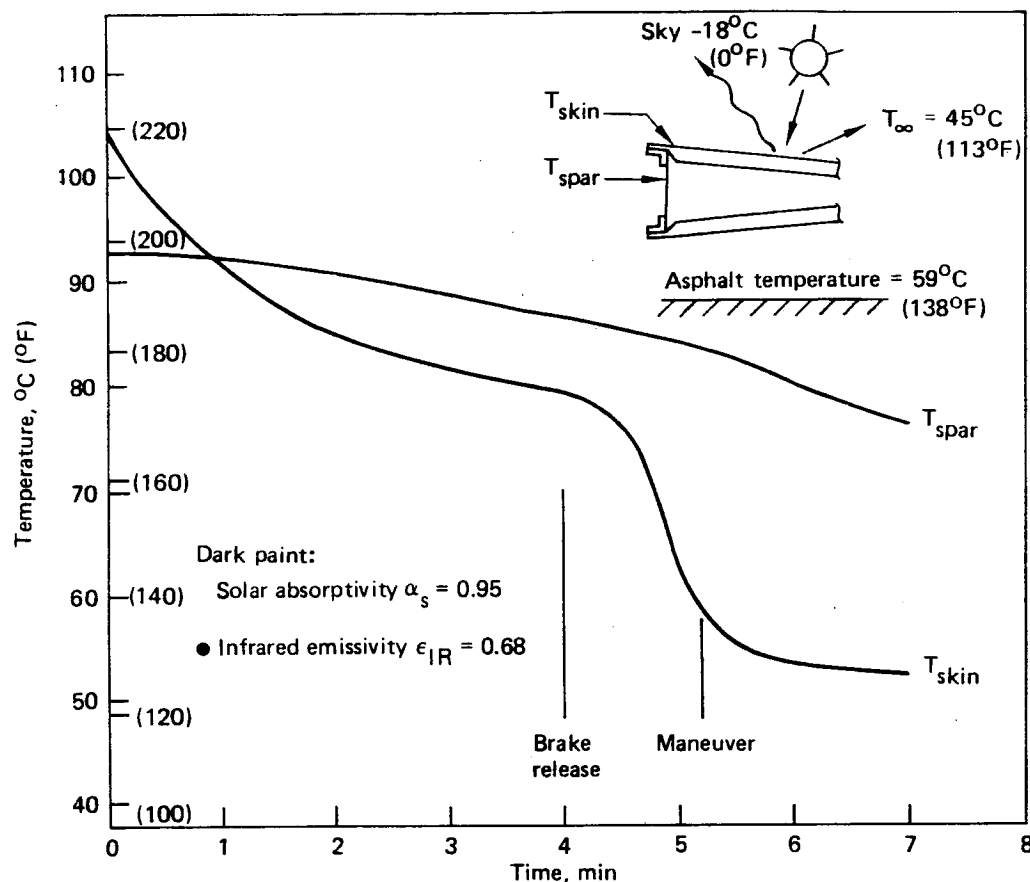


Figure 27. 727 Elevator Thermal Analysis Results

The minimum temperature of -59°C (-75°F) was based on the lowest ambient temperature experienced in flight, modified by the effect of aerodynamic heating.

4.1.6 MOISTURE ANALYSIS

The amount of moisture that can be conservatively expected to be absorbed by graphite-epoxy laminates in service was analytically determined. World environmental conditions were surveyed and existing industry data were reviewed. An analytical diffusion model was set up using average diffusivity coefficients obtained from industry. The results of this analysis indicated that a moisture content of $1.1 \pm 0.1\%$ of the total weight could be expected in the elevator structure in service.

To provide a control for moisture-conditioned test parts in the ancillary test program, a moisture rider coupon was used. The laminate moisture rider was a 12-ply fabric laminate and the honeycomb rider was a two-ply laminate of the same configuration as the elevator skins. These moisture riders were calibrated by placing them in a humidity chamber at 100% relative humidity and 60°C (140°F). Typical weight-gain curves for the 12-ply laminate and honeycomb skin laminate are shown in Figures 28 and 29, respectively. These tests were used to establish typical moisture pickup rates.

In the ancillary test program, these standardized moisture coupons were placed in the conditioning chamber along with the test specimen. When the rider coupon had attained 1.1% moisture, the test specimen was removed from the chamber and tested.

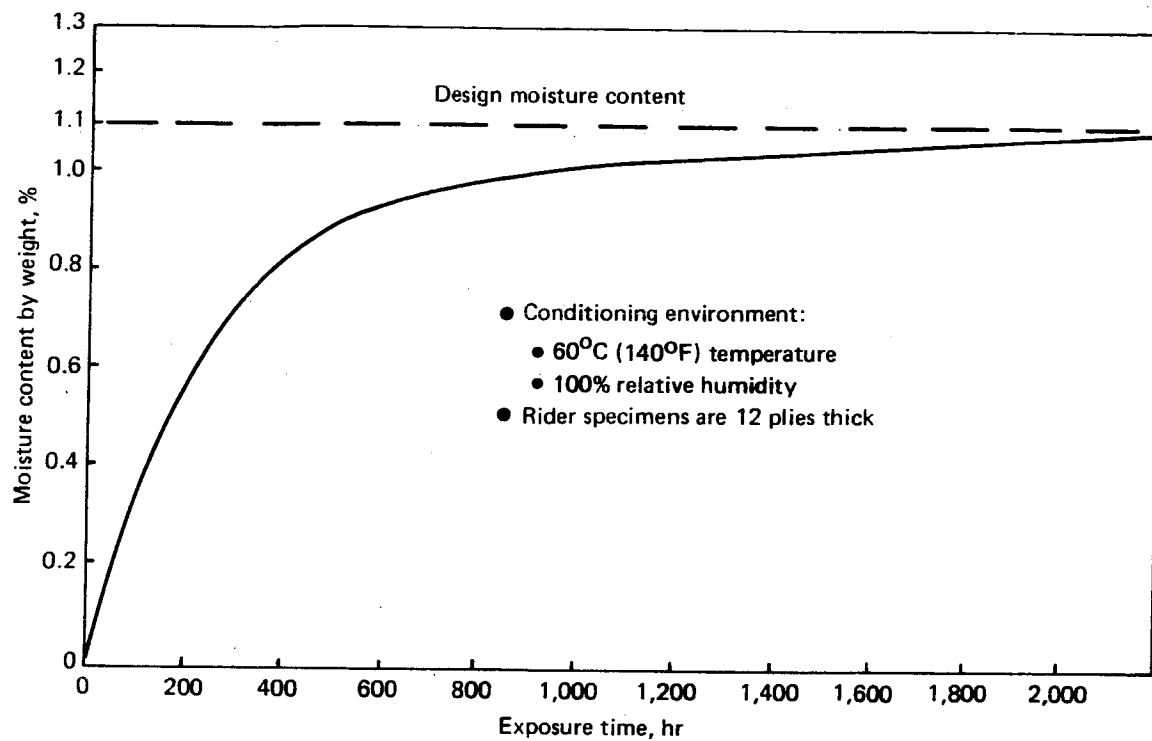


Figure 28. Exposure Time Versus Moisture Content for Laminates

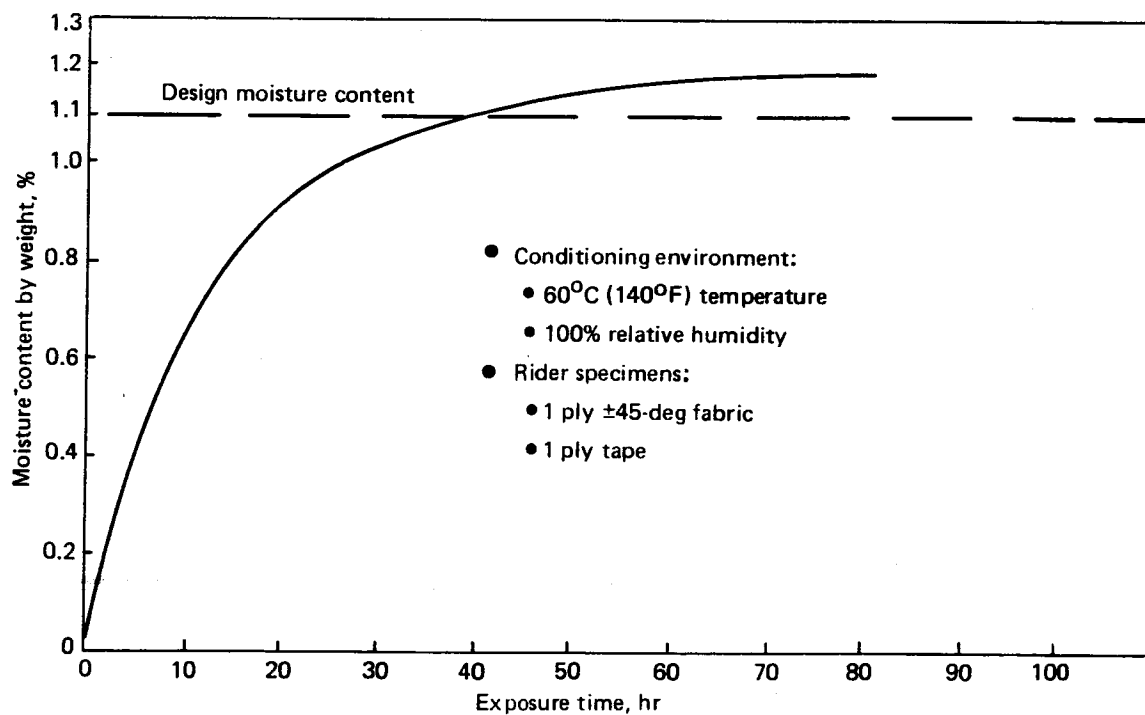


Figure 29. Exposure Time Versus Moisture Content for Sandwich Skin Panel Face

4.1.7 STRENGTH ANALYSIS

4.1.7.1 Finite-Element Model

General—An ATLAS finite-element model (ref 5) was developed for the 727 graphite-epoxy elevator and was mounted on a stabilizer model to ensure that strains induced in the elevator by the stabilizer deflected shape were accounted for within the elevator model. The stabilizer and elevator finite-element model definition is shown in Figure 30. The stabilizer was modeled with a large grid, using structural elements that produced representative bending and torsion stiffness. The elevator was modeled with a finer grid to produce a more comprehensive strain distribution.

The elevator and stabilizer were modeled in separate data sets. For each load case, the two models were merged at the attachment points (hinge points and actuator) with the elevator rotated to the appropriate angle. The tab structure was not included in the elevator model; however, the tab loads were imposed on the elevator at the five tab hinge points.

The hinge attachment points were modeled to produce the required rotational and translational freedoms. The hinge supporting structure at station 17.2 (see fig. 30) was modeled to provide a lateral restraint.

In addition to the overall elevator model, models of the tab rod cutout and hinge hand-hole areas (shown in fig. 31) were developed for detailed analysis of these areas on the lower surface.

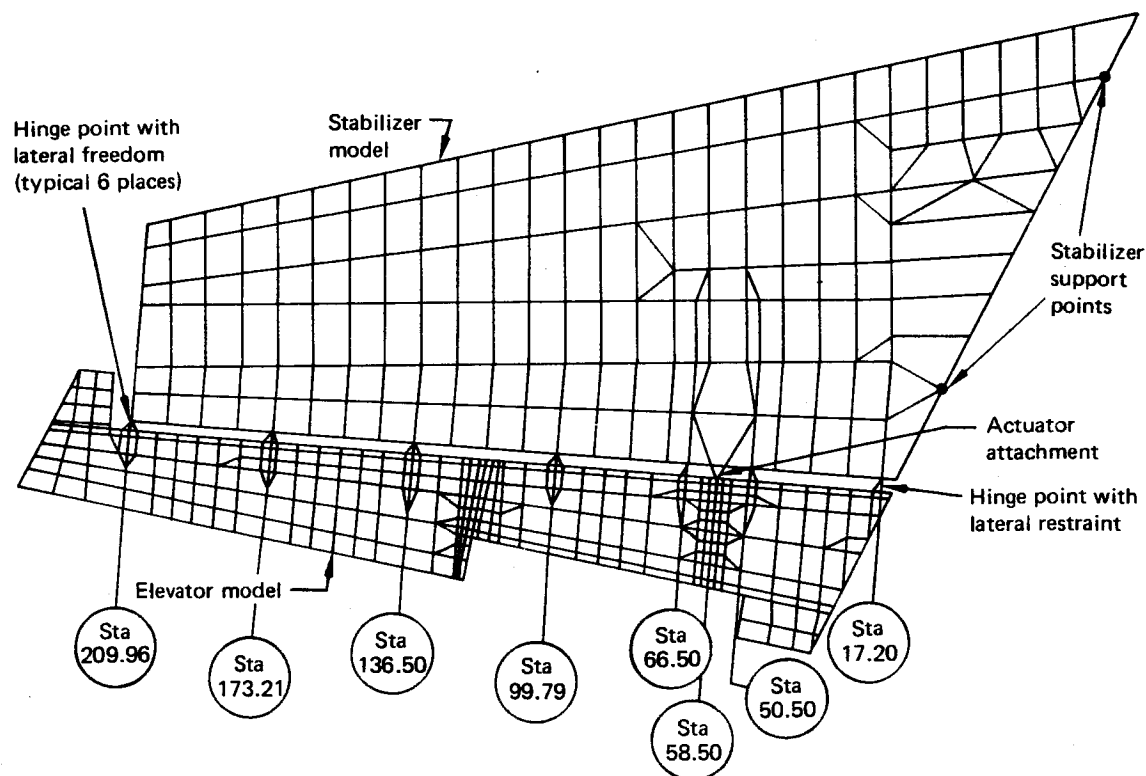


Figure 30. Elevator/Stabilizer Finite Element Model

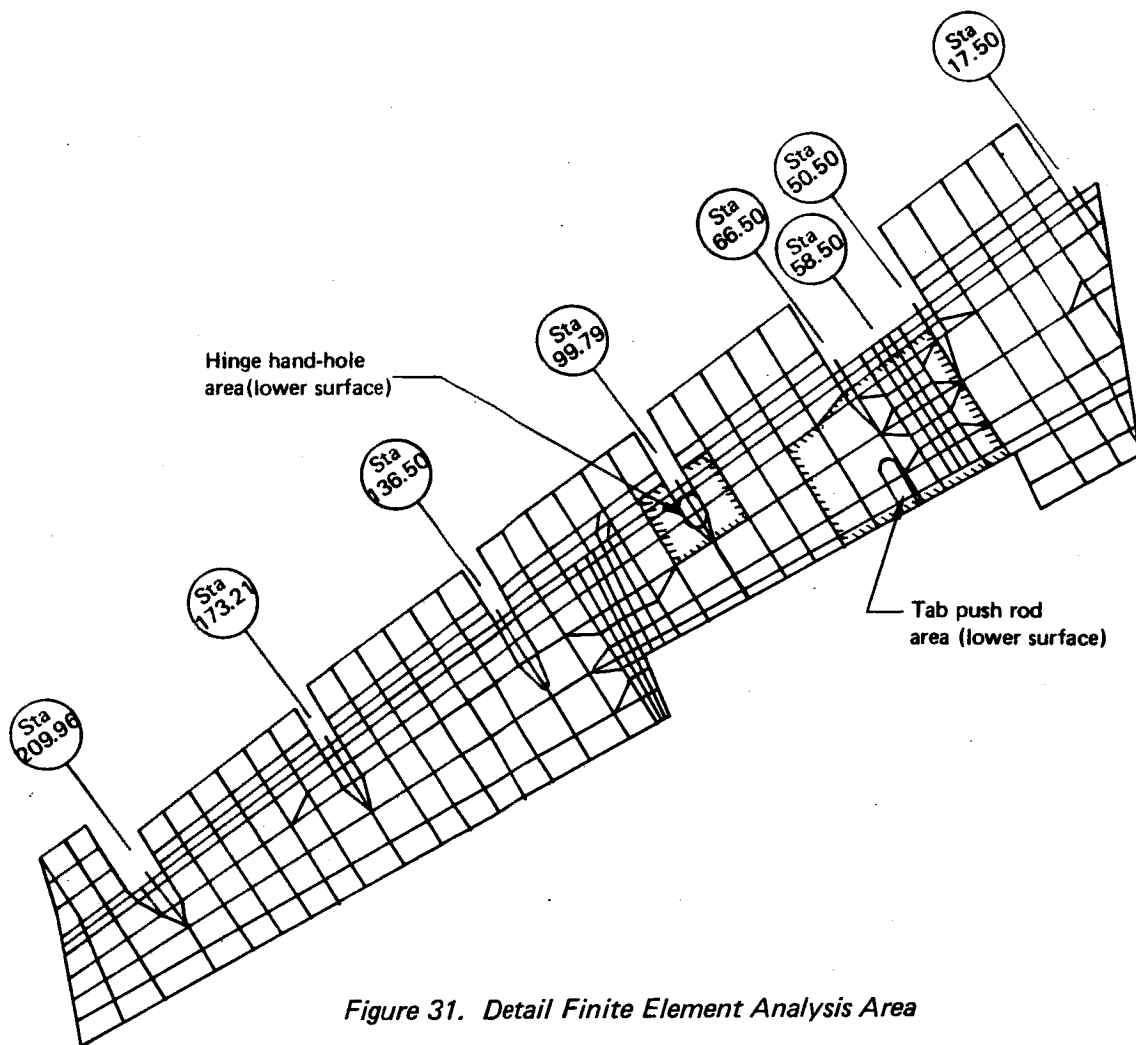
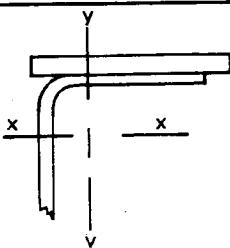
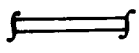

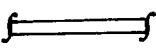


Figure 31. Detail Finite Element Analysis Area

Geometry and Material Input—Element definitions and input properties for the major elevator structural components are shown in Table 2. The material stiffness properties used in the elevator model were Boeing standard values, as shown in Table 2.

Loads—The external load cases that were used for the ultimate strength analysis are listed in Table 3. In addition to these flight load cases, two uniform temperature thermal conditions of 82 and -59°C (180 and -75°F) were analyzed. These two thermal cases represent the temperature extremes previously defined in Section 4.1.5.

Table 2. Elevator Elements and Input Properties

ATLAS element	Input properties	Structural element	Modulus 10 ⁴ MPa (10 ⁶ lbf/in ²)			Poisson's Ratio, ν
			E ₁	E ₂	G ₁₂	
Beam	 <p>Area = A Modulus = E I_{xx}, I_{yy}</p>	Front-spar upper chord	(11.4) 7.86	—	—	0.62
		Front-spar lower chord	(11.4) 7.86	—	—	0.62
		Rear-spar upper chord	(5.7) 3.93	—	—	0.41
		Rear-spar lower chord	(5.7) 3.93	—	—	0.41
Plate	 <p>t_{membrane} E₁ E₂ ν_{12} G₁₂</p>	Front-spar web	(3.0) 2.07	(3.0) 2.07	(4.25) 2.93	0.68
		Rear-spar web	(5.7) 3.93	(5.7) 3.93	(3.1) 2.14	0.41
G plate 1	 <p>t_{membrane} t_{bending} E₁ E₂ ν_{12} G₁₂</p>	Upper skin panels	(7.9) 5.45	(3.8) 2.62	(3.45) 2.38	0.66
		Lower skin panels	(7.9) 5.45	(3.8) 2.62	(3.45) 2.38	0.66
G plate 1	 <p>t_{membrane} t_{bending} E₁ E₂ ν_{12} G₁₂</p>	Upper nose skin	(9.3) 6.41	(6.3) 4.34	(2.45) 1.69	0.31
		Lower nose skin	(9.3) 6.41	(6.3) 4.34	(2.45) 1.69	0.31

1 ATLAS finite element computer code (Ref. 4-4)

Table 3. Design Ultimate Loads

Load case	Description	Altitude, m (ft)	Mach no.	Ultimate load factor 1
1. Load case 120R	Positive maneuver at V_D	4145 (13,600)	0.90	3.75
2. Load case 122R	Negative maneuver at V_D	0	0.59	0
3. Load case 124	Check maneuver maximum negative loads	0	0.59	-3.44
4. Load case 125	Instantaneous elevator balanced maneuver	0	0.39	0.12
5. Load case 128	Positive maneuver at V_D	0	0.70	3.75

1 At horizontal tail cg

Aerodynamic loads were introduced into the model as panel pressures on the upper and lower surfaces. The aerodynamic surface pressure distribution was superimposed over the ATLAS structural panel grid work and uniform panel pressures were defined by linear interpolation. The elevator pressures for each load case are shown in Table 4. These pressure profiles were considered to be constant over the span of the elevator. The pressures were applied to the ATLAS skin panel plates with two-thirds of the pressure applied to the lower surface and one-third applied to the upper surface for the load cases with down-acting airloads. The inverse distribution was applied for up-acting airloads.

Table 4. Elevator Pressures

Load case	Surface pressure
120R	<p>7.79 kPa (1.13 lbf/in²)</p> <p>Hingeline →</p> <p>15.58 kPa (2.26 lbf/in²)</p> <p>Trailing edge</p>
122R	<p>15.51 kPa (2.25 lbf/in²)</p> <p>7.79 kPa (1.13 lbf/in²)</p>
124	<p>0.92 kPa (0.13 lbf/in²)</p> <p>1.83 kPa (0.27 lbf/in²)</p>
125	<p>7.52 kPa (1.09 lbf/in²)</p> <p>15.10 kPa (2.19 lbf/in²)</p>
128	<p>10.62 kPa (1.54 lbf/in²)</p> <p>21.24 kPa (3.08 lbf/in²)</p>

The stabilizer weight was divided into eight streamwise panel sections and the weight of each panel was apportioned to the stabilizer nodes within the panel area. The elevator weight was distributed to elevator nodes along the front spar. The weight node loads were introduced into the model and factored by the appropriate ultimate load factor for each load case before being combined with the ultimate aerodynamic loads.

The accuracy of the airload interpolation and weight distribution calculations for each load case was checked by comparing the total ATLAS loads with the defined balancing tail loads. This comparison showed a maximum variation of 3%.

Strain Output—Ultimate strain levels for load case (LC) 125 for the front and rear spars, upper and lower skin panels, and actuator rib are presented in Figures 32 through 38. Typical thermal strains are presented for the front spar in Figure 39 and for one of the skin panels in Figure 40. The final design ultimate strains were obtained by algebraically combining the ultimate flight load strains with 1.5 times the thermal analysis strains.

4.1.7.2 Detail Analysis

Analyses were conducted on composite elevator structural details. Margins of safety were checked at -59, 21, and 82°C (-75, 70, and 180°F) using corresponding detail strains and design values at each temperature.

The design values used throughout the strength analysis were based on coupon or structural element test data from the ancillary test program. Average test values were reduced to the probability and confidence levels of MIL-HDBK-5B "B" basis; namely, that 90% of the population will be higher with a confidence of 95%. These reduction factors conservatively accounted for material strength variations, test specimen geometry variations, and test condition variations.

Material strength correction factors for each test condition were based on process control test results. Process control panel data were collected from the ancillary test program specimens and analyzed to establish the strength variations. A material correction factor (MCF) was used to correct each test point to the mean of the process panel population and a second factor (MVF) was used to correct the mean value to the required confidence level. These factors are illustrated in Figure 41.

A variation magnification factor (VMF) was determined that accounted for variations in test specimen geometry and test conditions. Coefficients of variation for every unique test condition and specimen geometry were calculated. A distribution analysis of these coefficients of variation was performed. From this distribution, the maximum variance with less than a 5% probability of exceedance was determined to be 9.0%. The variance magnification factor then was computed as:

$$UMF = 1 - K_{B_{\infty}} \sqrt{V_{MAX}}$$

where $K_{B_{\infty}}$ is the "B" basis factor for an infinite sample. The $\sqrt{V_{MAX}}$ is the maximum variance.

The final design values were obtained by multiplying the average test values by the three correction factors. An example of the correction factors and the calculation procedure for honeycomb flexural strength is shown in Figure 42.

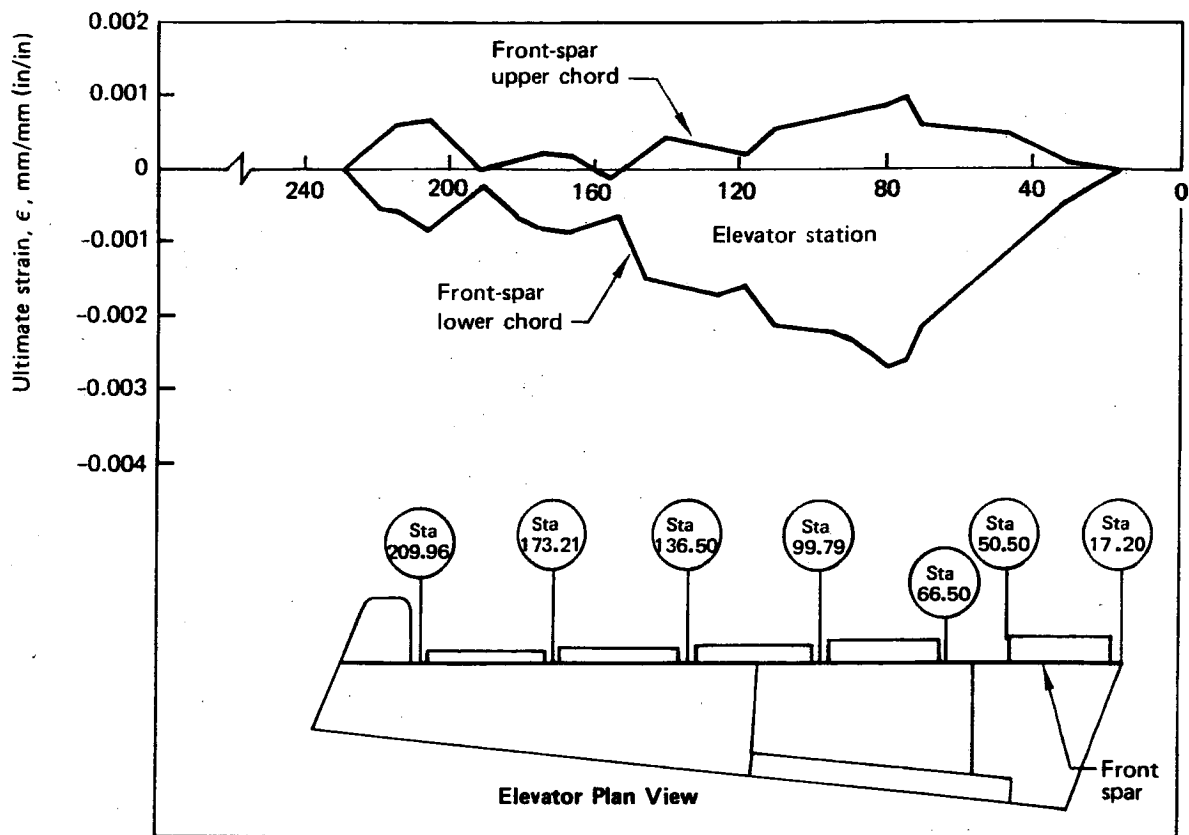


Figure 32. Front-Spar Chord Strains for Load Case 125

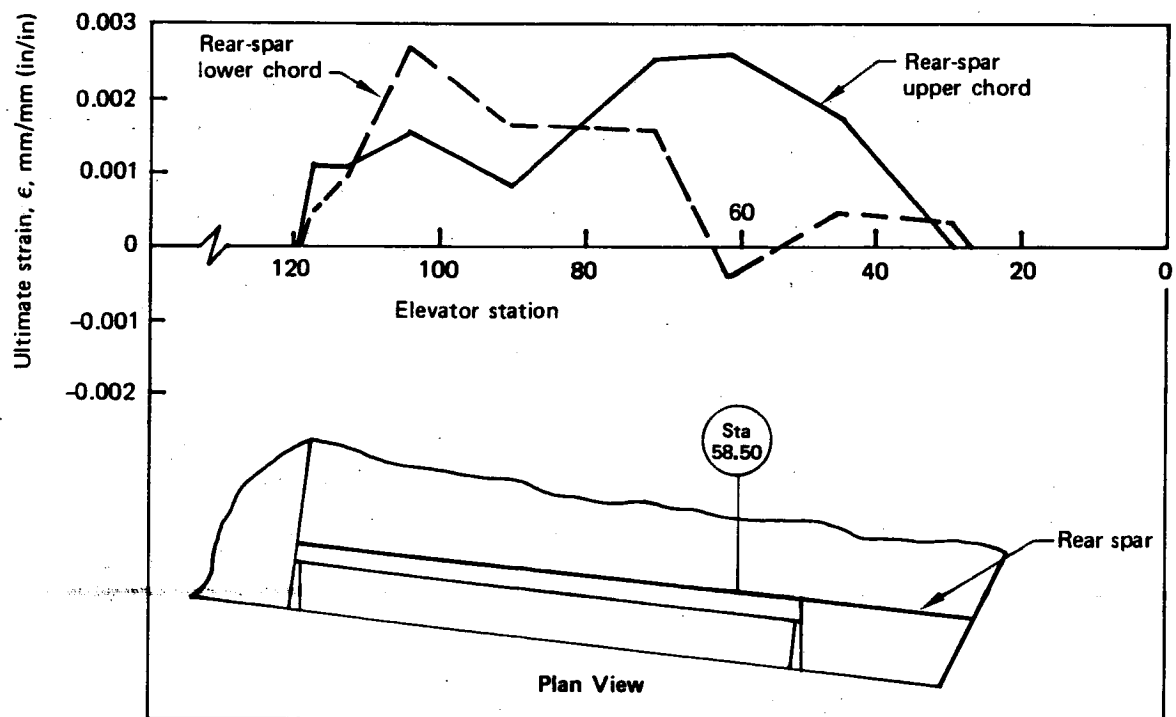


Figure 33. Rear-Spar Chord Strains for Load Case 125

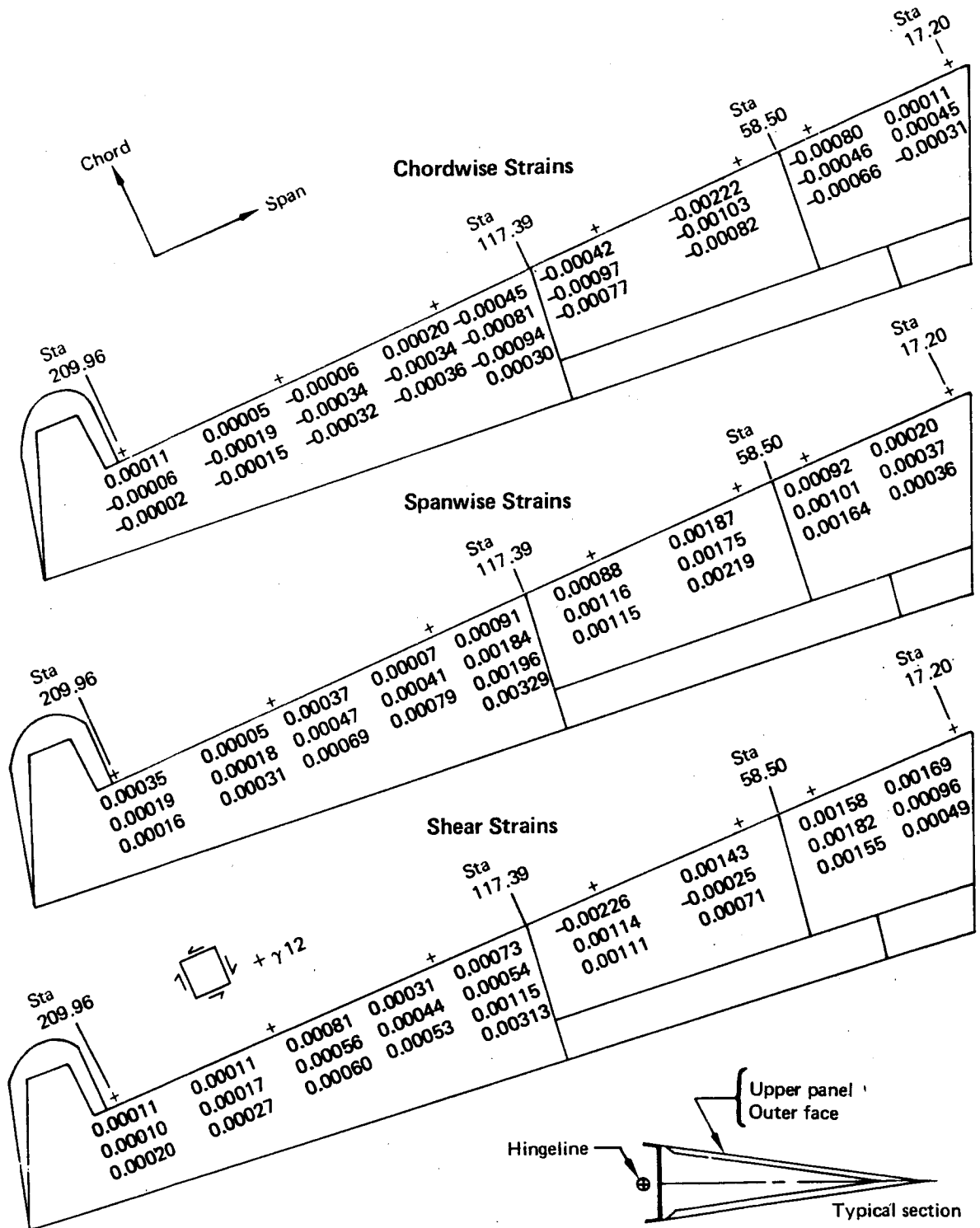


Figure 34. Ultimate Skin Panel Strains, Load Case 125

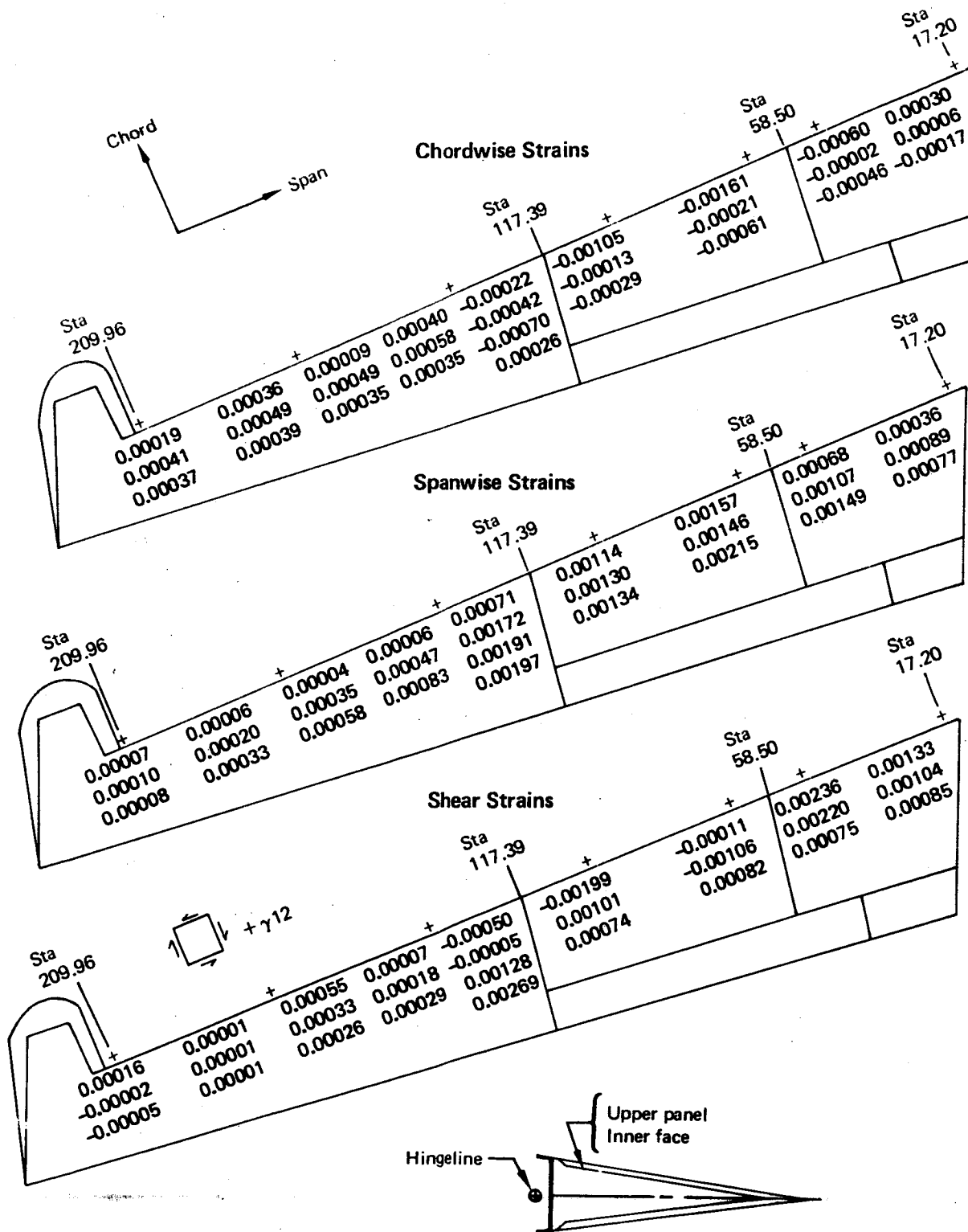


Figure 35. Ultimate Skin Panel Strains, Load Case 125

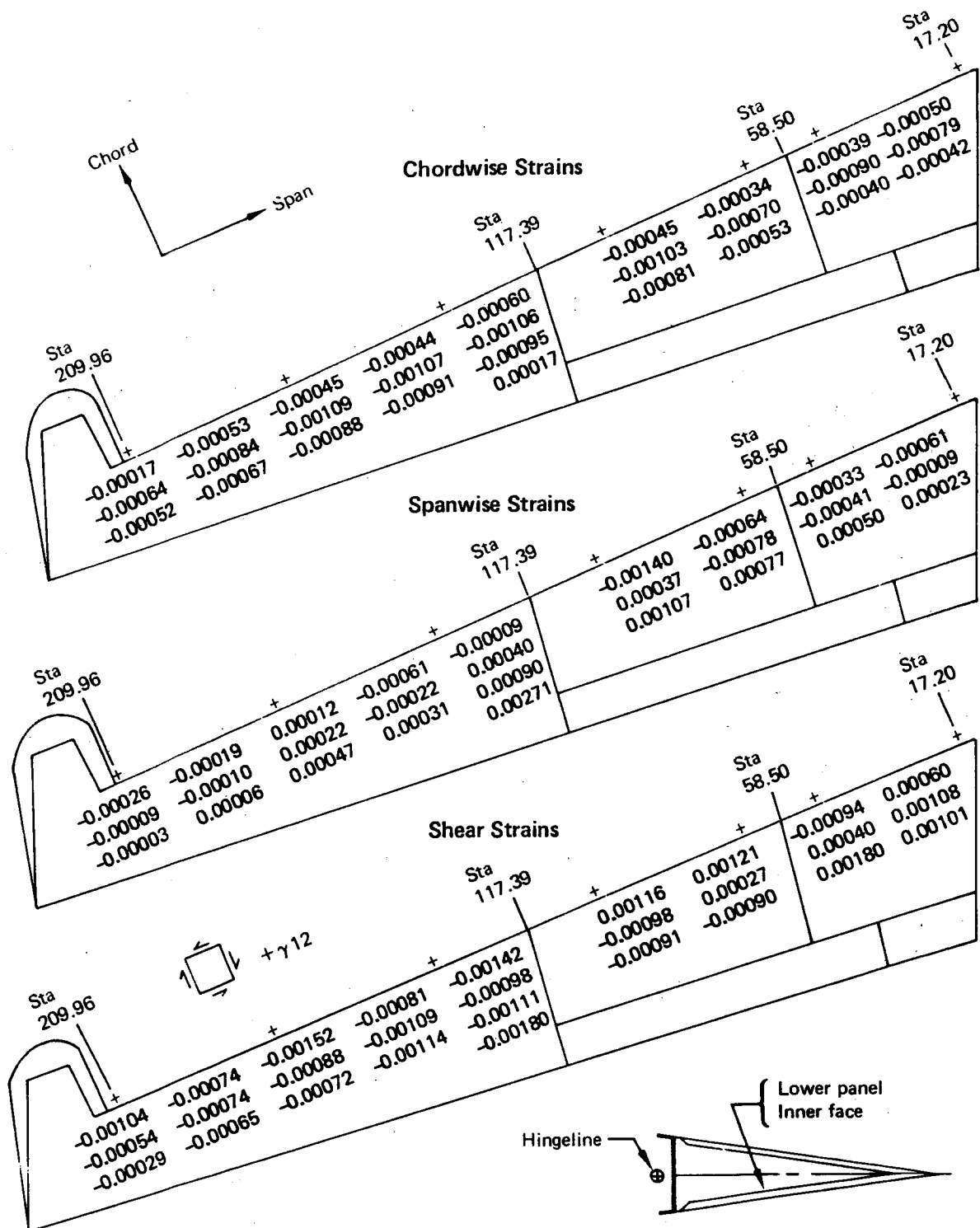


Figure 36. Ultimate Skin Panel Strains, Load Case 125

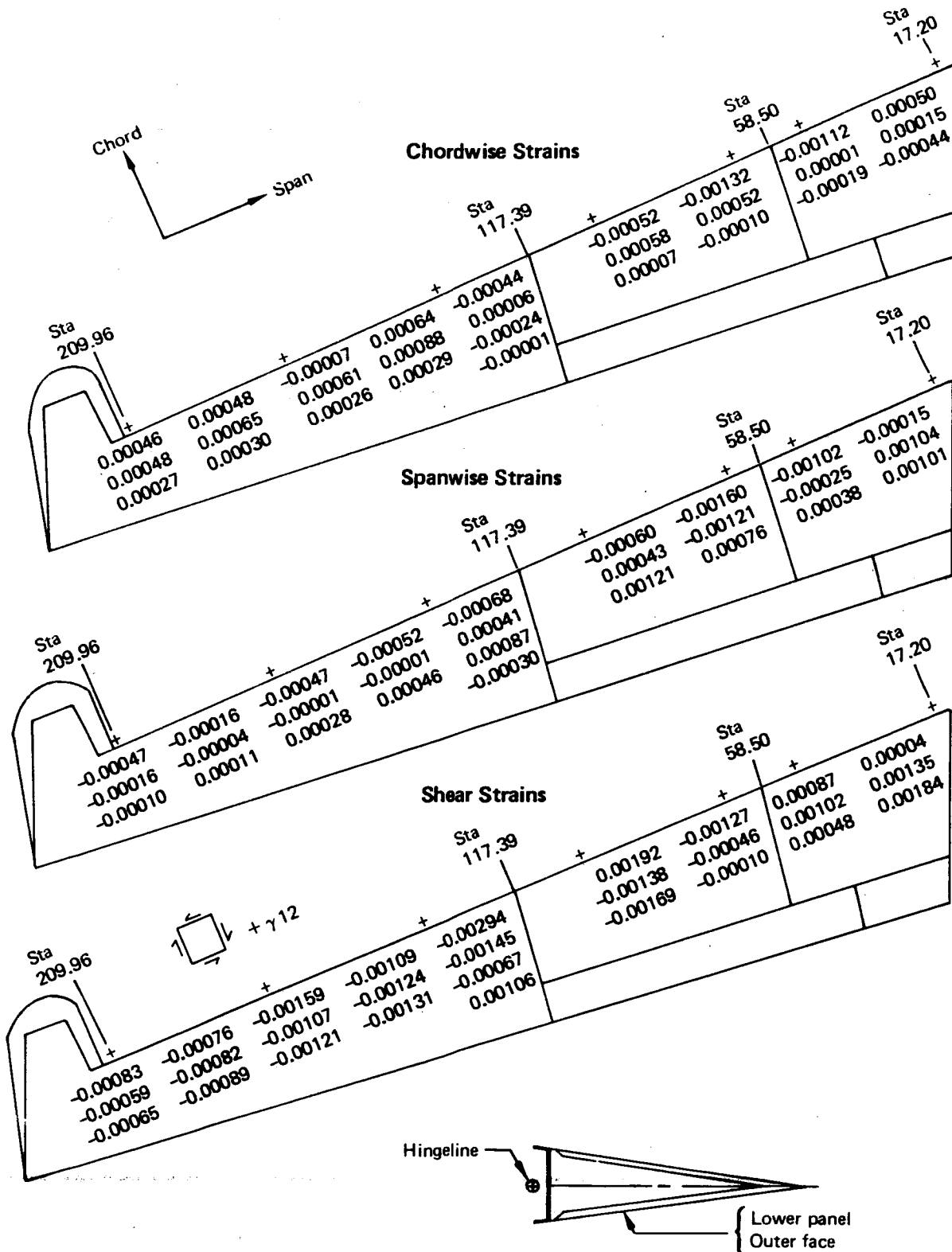


Figure 37. Ultimate Skin Panel Strains, Load Case 125

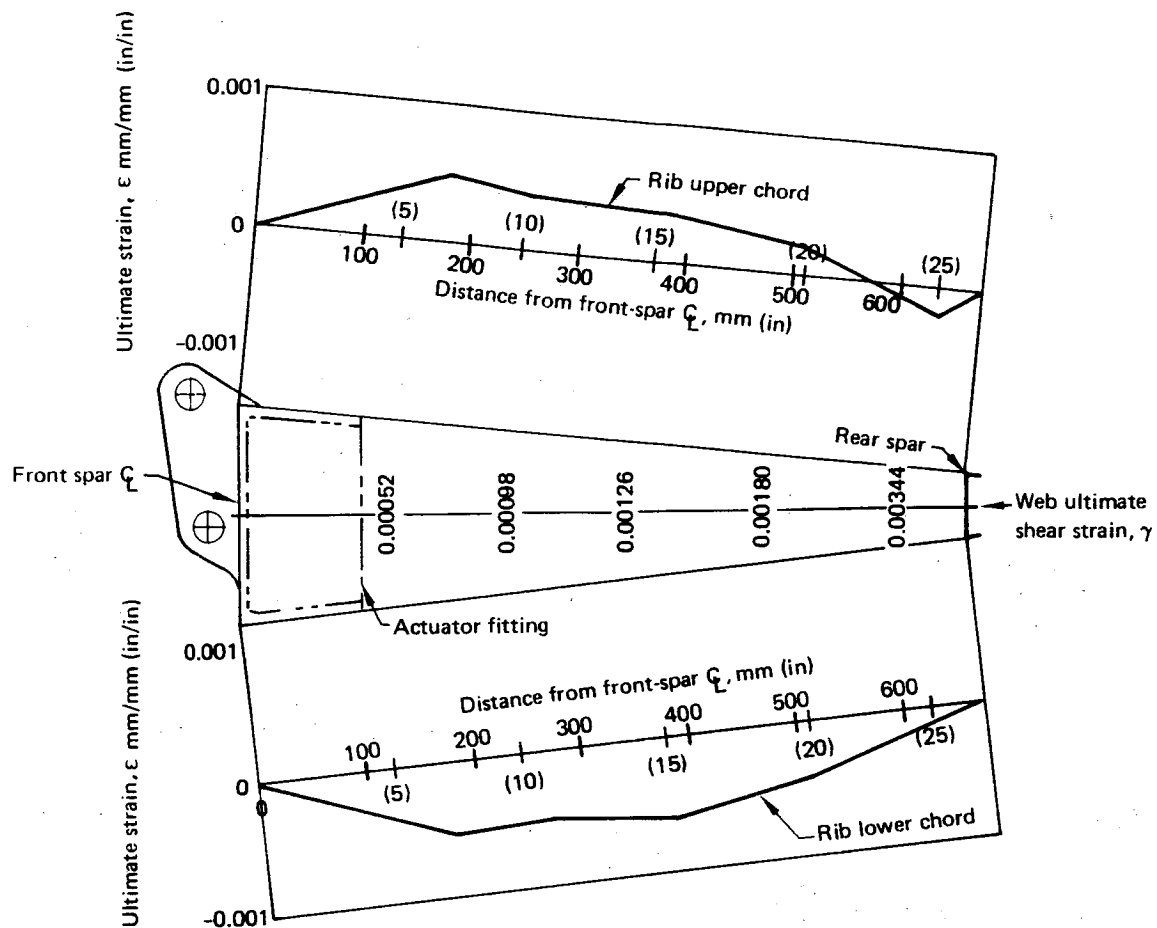


Figure 38. Actuator Rib Strains for Load Case 125.

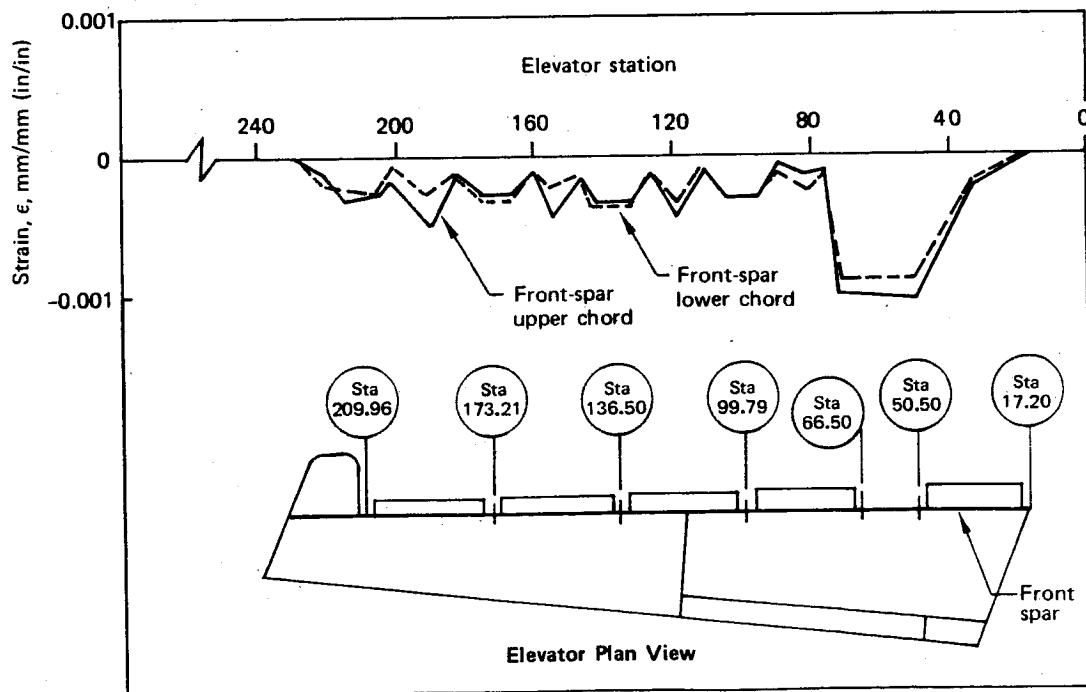


Figure 39. Front-Spar Chord Thermal Strains at -59°C (-75°F), $\Delta T = -81^{\circ}\text{C}$ (-145°F)

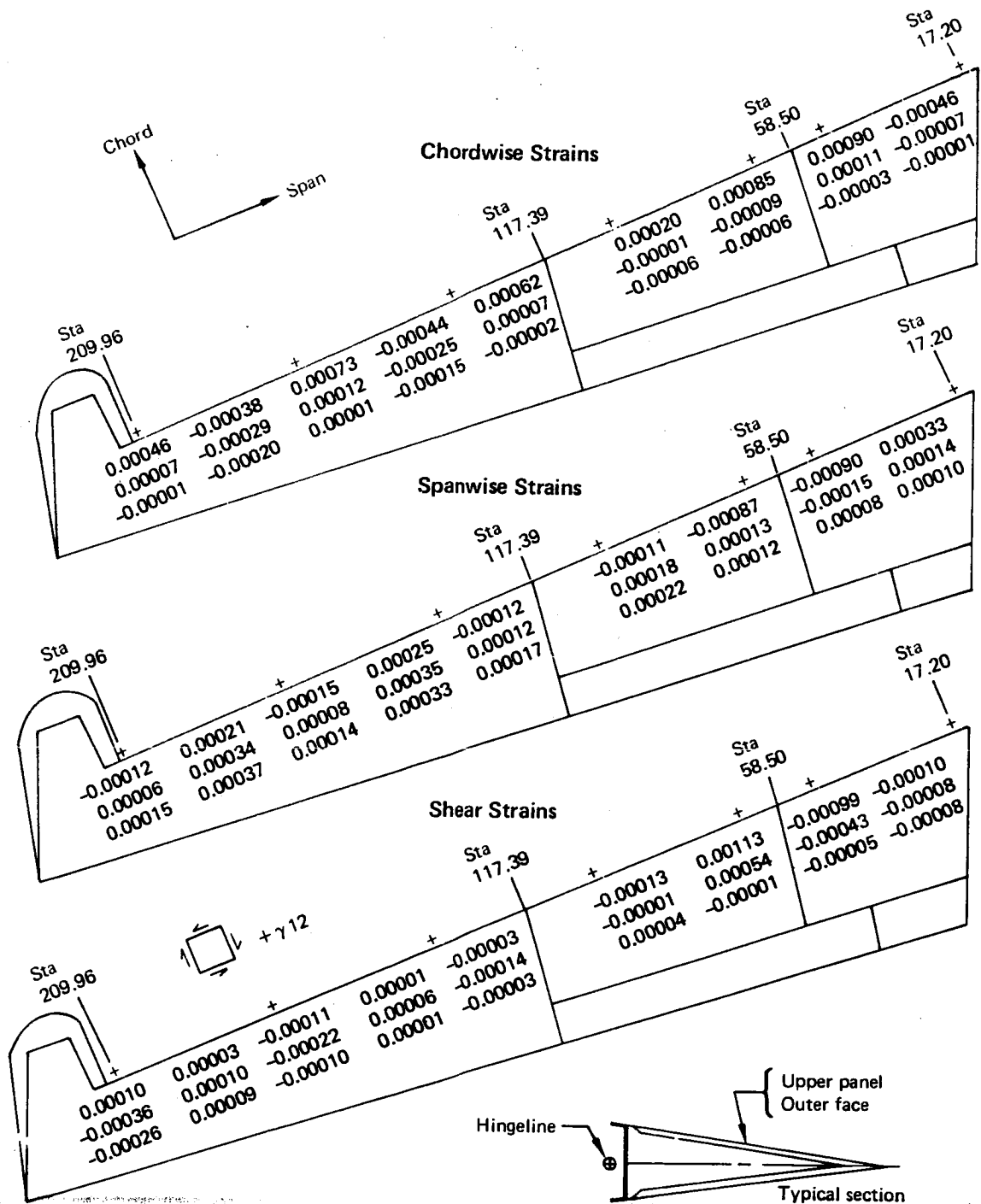
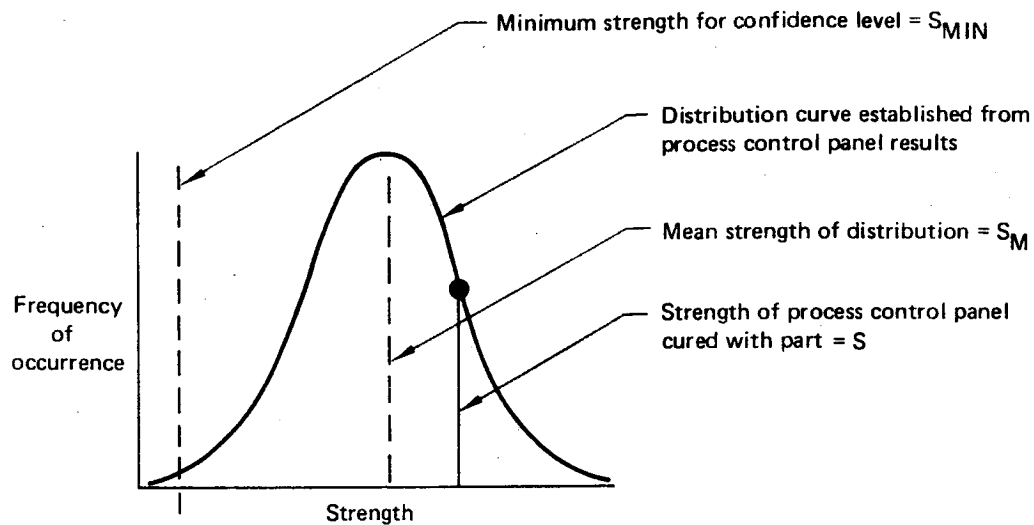


Figure 40. Skin Panel Strains, Thermal Load Case $\Delta T = -81^{\circ}\text{C} (-145^{\circ}\text{F})$
($T = -59^{\circ}\text{C} (-75^{\circ}\text{F})$)



- Material correction factor $MCF = \frac{S_M}{S}$
- Material variation factor $MVF = \frac{S_{MIN}}{S_M}$

Figure 41. Material Strength Correction Factors

Test coupon control property	MCF	MVF	VMF	DVR
Honeycomb sandwich flexural strength	0.96	0.89	0.88	0.75

- MCF—material correction factor, values vary from 0.90 to 1.1
- MVF—material variability factor
- VMF—variation magnification factor
- $DVR = (MCF) (MVF) (VMF)$
- Example calculation:
 Design value = (DVR) (average test value)
 = (0.75)(average test value)

Figure 42. Example Calculation of Design Value

Analyses of four examples of elevator structural details are contained in the following subsections. In all cases, margins of safety shown are minimums.

Front Spar Lower Chord—For LC 125, the measured strain from the full-scale test article on the front spar lower chord at station 97 exceeded the design value. The finite-element analysis results also predicted strains that would result in negative margins. Therefore, a reinforcing strap was added to reduce the strain level.

The analysis procedure to define the final margins of safety for the front spar lower chord is shown in Figure 43 and a display of the design values for this detail is shown in Figure 44.

Typical Skin Panel—The most critical upper surface skin panel is on the outer face just aft of the front spar near the outboard end of the actuator fitting. This panel region is in an area of basic honeycomb sandwich construction.

The most critical loading occurs for LC 125 at 82°C (180°F). The LC 125 strains and ultimate thermal strains in the chordwise-spanwise reference plane were combined by hand. From these strains, principal strains were calculated and compared to the appropriate design value strains to obtain margins of safety as shown in Figure 45.

The design value strains used for tension and compression were obtained from the Boeing-funded four-point beamsandwich panel tests (see figs. 65 and 66, sec. 4.2.1). A correction factor (DVR) of 0.75 (fig. 42) was used to reduce the test data to the "B" basis.

The shear strain design value was obtained from the honeycomb shear panel tests (see table 7, sec. 4.2.3.4). The test value for the wet condition was multiplied by a DVR of 0.82 to reduce the test data to the "B" basis.

Actuator Rib-to-Rear Spar Web Attachment—The critical fastener bearing stress in the actuator rib occurs at the attachment of the rib to the rear spar web. The critical condition is LC 128 at 82°C (180°F) and the analysis is shown in Figure 46.

The design value bearing stress at 82°C (180°F) was obtained from the ancillary test structural element tests (see fig. 68, sec. 4.2.3.1). A DVR of 0.74 was used to reduce the test data to the "B" basis.

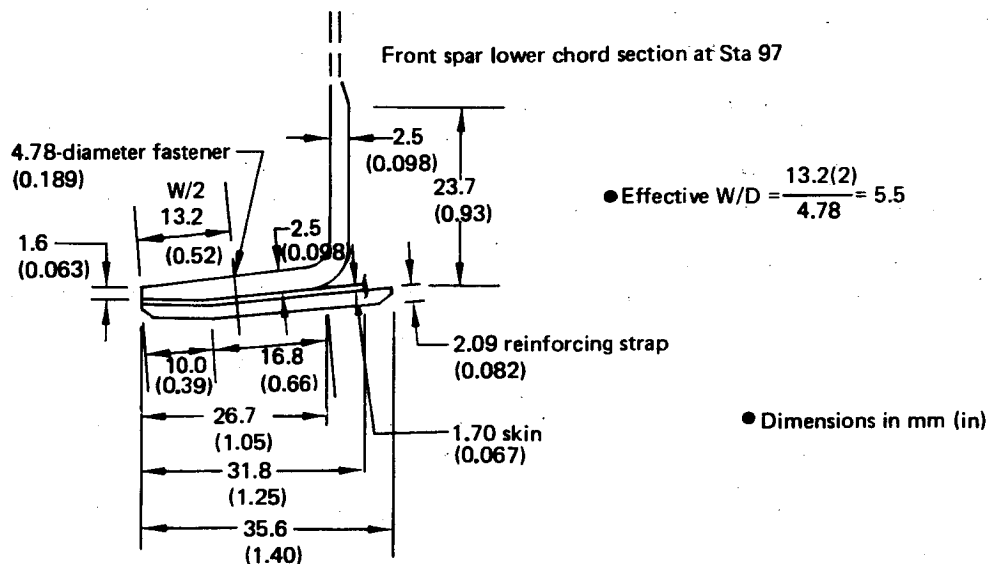
Tab Actuator Fitting Attachment—The strength analysis of the tab skin in the region of the actuator fitting is shown in Figure 47. The design value used for the skin laminate is the same as that used for the skin panel analysis (see fig. 45).

4.1.8 BUCKLING ANALYSIS

4.1.8.1 Skin Panels

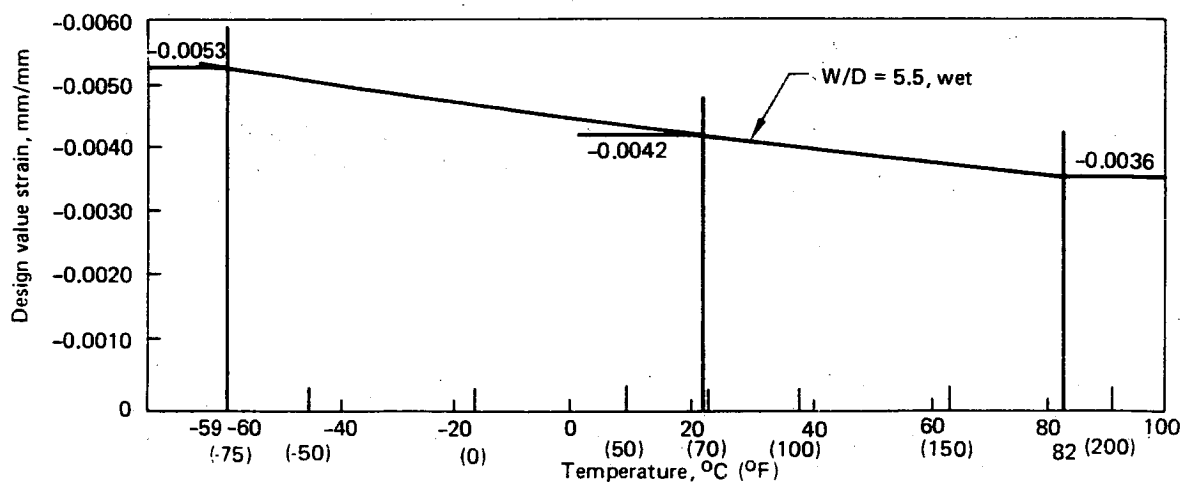
Interaction curves for orthotropic sandwich panels loaded in biaxial compression and shear were developed from the buckling analysis (ref 6) for the three main unsupported skin panels on each surface of the elevator. These curves are shown in Figures 48, 49, and 50.

The applied loads shown on each of the curves are the maximum ultimate biaxial end loads and shear load for the elevator surface panels as obtained from the ATLAS solution. A comparison between the applied loads and the analytical curves indicates that large margins exist for buckling in all three panel areas.



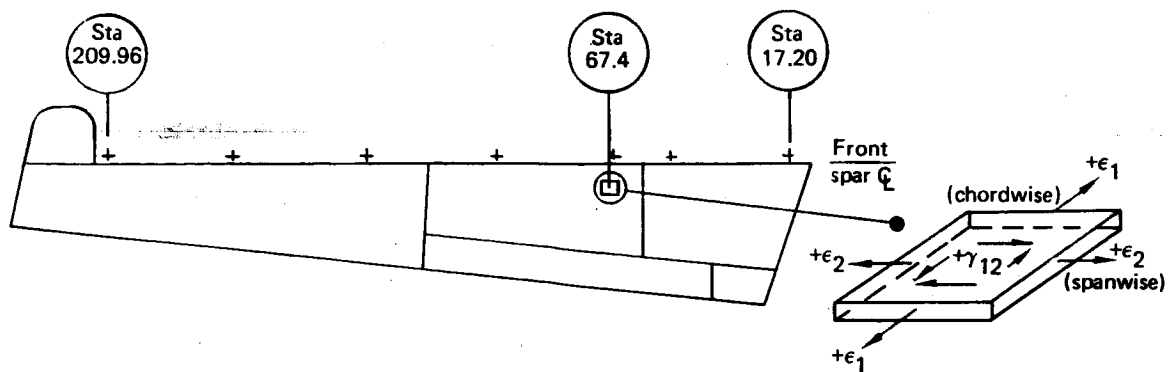
- Strain at section for ambient condition with reinforcing strap included:
 $\epsilon = -0.00321 \text{ mm/mm (in/in)}$
- Lowest margin of safety occurs at 82°C (180°F)
 Thermal strain at 82°C (180°F), $\epsilon_T = 0.000107 \text{ mm/mm (in/in)}$
- Total ultimate strain at 82°C (180°F):
 $\epsilon = -0.00321 + 1.5 (0.000107) = -0.00305 \text{ mm/mm (in/in)}$
- Design value:
 $\epsilon_{DV} = -0.0036 \text{ mm/mm (in/in)}$ for $W/D = 5.5$ at 82°C (180°F) (see fig. 44)
 $MS = \frac{-0.0036}{-0.00305} - 1 = \underline{+0.18}$

Figure 43. Strength Analysis of Front-Spar Lower Chord—Station 97 for LC 125 at 82°C (180°F)



- Data from open-hole coupon tests (see fig. 57)
- DVR of 0.77 used to reduce test data to B basis

Figure 44. Design Value Compression Strain Versus Temperature



- Critical load condition: load case 125 at 82°C (180°F)

$$\epsilon_{ult} = \epsilon_{LC\ 125} + 1.5\epsilon_{82^{\circ}C\ (180^{\circ}F)} \text{ (in the chordwise-spanwise reference plane)}$$

$$\epsilon_{1\ ult} = -0.003108 \text{ mm/mm (in/in)}$$

$$\epsilon_{2\ ult} = 0.002639 \text{ mm/mm (in/in)}$$

$$\gamma_{12\ ult} = 0.000560 \text{ mm/mm (in/in)}$$

- Principal strains:

$$\epsilon_{max} = 0.002653 \text{ mm/mm (in/in)}$$

$$\epsilon_{min} = -0.003122 \text{ mm/mm (in/in)}$$

$$\gamma_{max} = 0.005774 \text{ mm/mm (in/in)}$$

- Design values:

$$\epsilon_{tension} = 0.003260 \text{ mm/mm (in/in)}$$

$$\epsilon_{compression} = -0.003650 \text{ mm/mm (in/in)}$$

$$\gamma_{shear} = 0.006770 \text{ mm/mm (in/in)}$$

$$\bullet\ MS_{tension} = \frac{0.003260}{0.002653} - 1 = \underline{+0.23} \quad \leftarrow$$

$$\bullet\ MS_{compression} = \frac{-0.003650}{-0.003122} - 1 = \underline{+0.17} \quad \leftarrow$$

$$\bullet\ MS_{shear} = \frac{0.006770}{0.005774} - 1 = \underline{+0.17} \quad \leftarrow$$

Figure 45. Strength Analysis of Skin Panel for LC 125 at 82°C (180°F)

- Web thickness = 1.14 mm (0.045 in)

- Critical load:

Load case 128 at 82°C (180°F)

$q = 75\text{-N/mm}$ (428.3 lbf/in) ultimate 1

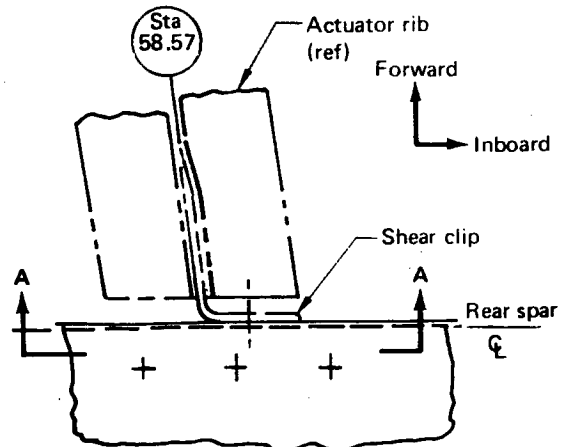
Load per fastener:

$$\frac{75 (55.9)}{2} = 2096\text{N} (471.1\text{ lbf})/\text{fastener}$$

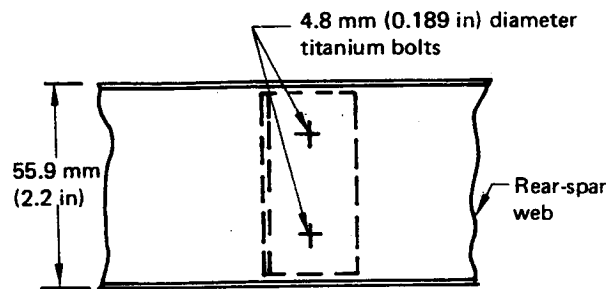
$$f_{brg} = \frac{2096}{1.143 \times 4.813} = 381\text{ MPa} (55,259\text{ lbf/in}^2)$$

$$F_{brg}\text{ design value} = 399.9\text{ MPa} (58,000\text{ lbf/in}^2)$$

$$MS = \frac{399.9}{381} - 1 = \underline{+0.05}$$



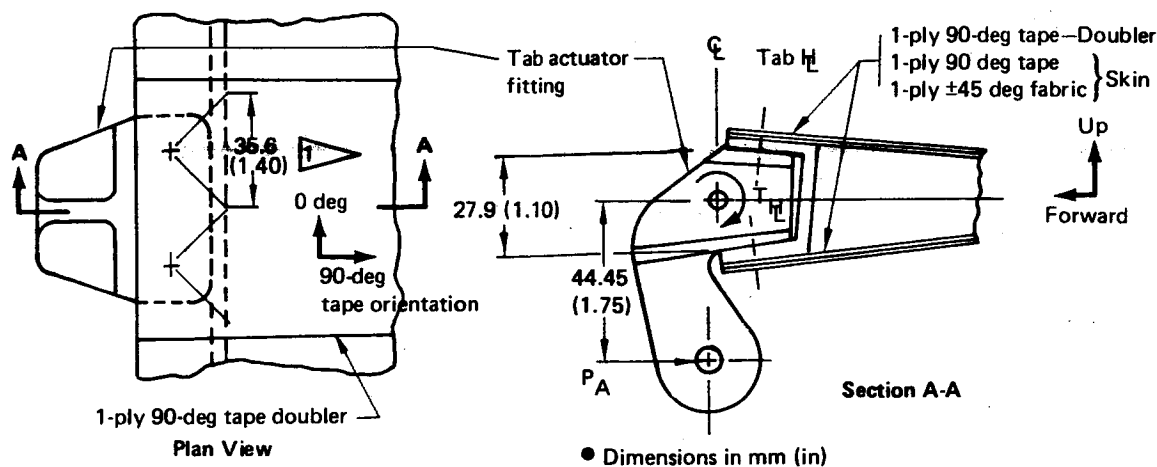
Plan View



Section A-A

1 Critical shear flow from actuator rib web

Figure 46. Strength Analysis of Actuator Rib-to-Rear Attachment for LC 128 at 82°C (180°F)



• Critical load: load case 129

$$T_H = 113 \text{ kN} \cdot \text{mm ultimate (1000 in-lbf)}$$

$$P_A = \frac{113}{44.45} = 2.54 \text{ kN ultimate (571 in-lbf)}$$

$$\text{Lower skin load, } P = \frac{2.54}{2} + \frac{113}{27.9} = 5.32 \text{ kN (1196 lbf)}$$

$$P_{\text{fastener}} = \frac{5.32}{2} = 2.66 \text{ kN/fastener (598 lbf)}$$

• Modulus in doubled area:

Material	Ply direction	t_{total}	E	$(E)(t)$
Tape (2 plies)	90 deg	0.1778 mm (0.0070 in)	$1.24 \times 10^5 \text{ MPa}$	$2.207 \times 10^4 \text{ N/mm}$
Fabric (1 ply)	±45 deg	0.1905 mm (0.0075 in)	$(18 \times 10^6 \text{ lbf/in}^2)$	$(1.26 \times 10^5 \text{ lbf/in})$
		$\Sigma = 0.3683 \text{ mm (0.0145 in)}$	$0.207 \times 10^5 \text{ MPa}$	$0.394 \times 10^4 \text{ N/mm}$
			$(3 \times 10^6 \text{ lbf/in}^2)$	$(0.225 \times 10^5 \text{ lbf/in})$
				$\Sigma = 2.601 \times 10^4 \text{ N/mm}$
				$(1.485 \times 10^5 \text{ lbf/in})$

$$E_{\text{equivalent, 90 deg}} = \frac{2.601 \times 10^4}{0.3683} = 7.06 \times 10^4 \text{ MPa (10.24} \times 10^6 \text{ lbf/in}^2)$$

$$\epsilon_{\text{compression}} = \frac{P}{AE} = \frac{2.66 \times 1000}{(35.6 \times 0.3683) \times 7.06 \times 10^4} = -0.00287 \text{ mm/mm (in/in)}$$

$$\text{Design value, } \epsilon_c = -0.00365 \text{ mm/mm (in/in)} \quad \triangleright$$

$$MS = \frac{-0.00365}{-0.00287} - 1 = +0.27 \quad \longleftarrow$$

1 Assume 45-deg load distribution cone

2 Minimum design value at 82°C (180°F)

Figure 47. Strength Analysis of Tab Skin at Actuator Fitting for LC 129 at 82°C (180°F)

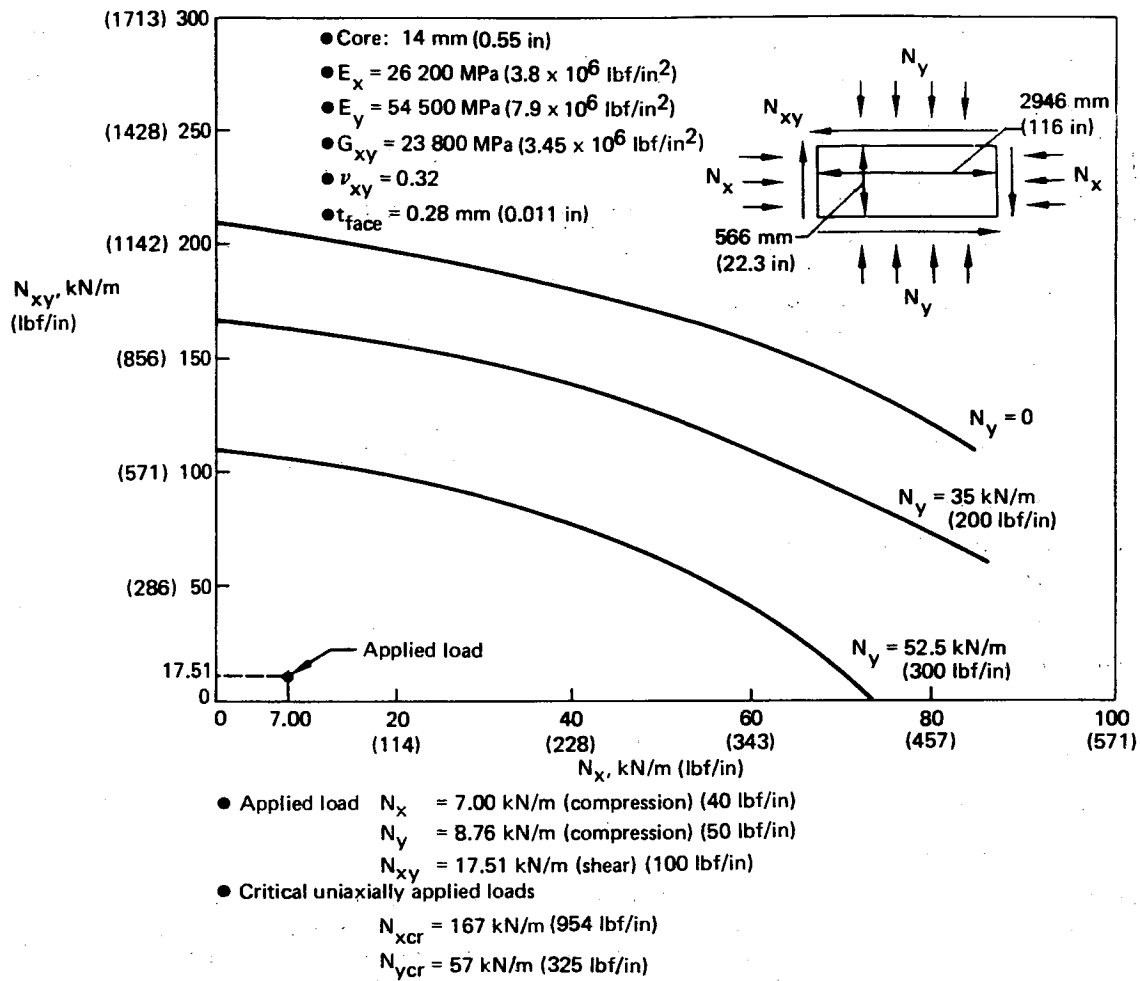
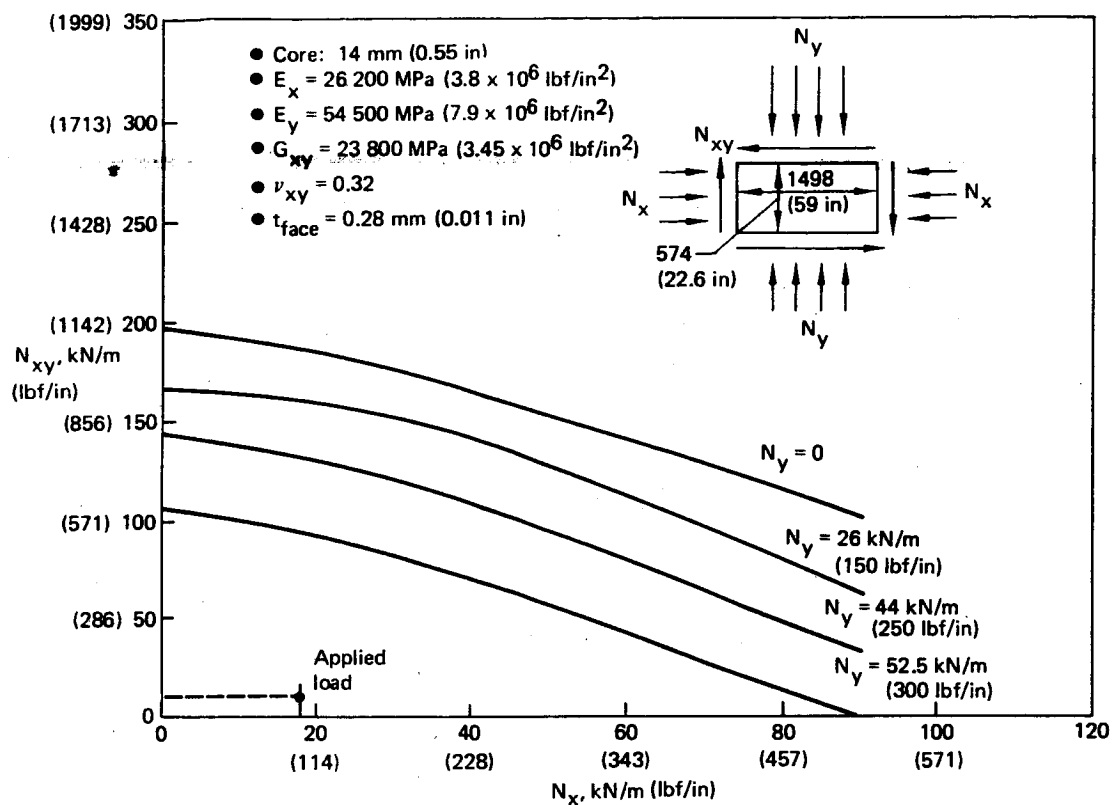


Figure 48. Interaction Curves—Outboard Skin Panel



- Applied load $N_x = 17.51\text{ kN/m}$ (compression) (100 lbf/in)
 $N_y = 3.50\text{ kN/m}$ (compression) (20 lbf/in)
 $N_{xy} = 8.76\text{ kN/m}$ (shear) (50 lbf/in)

- Critical uniaxially applied compression load

$$N_{xcr} = 164\text{ kN/m} (936\text{ lbf/in})$$

$$N_{ycr} = 70\text{ kN/m} (400\text{ lbf/in})$$

Figure 49. Interaction Curves—Skin Panel Between Actuator Rib and Transition Rib

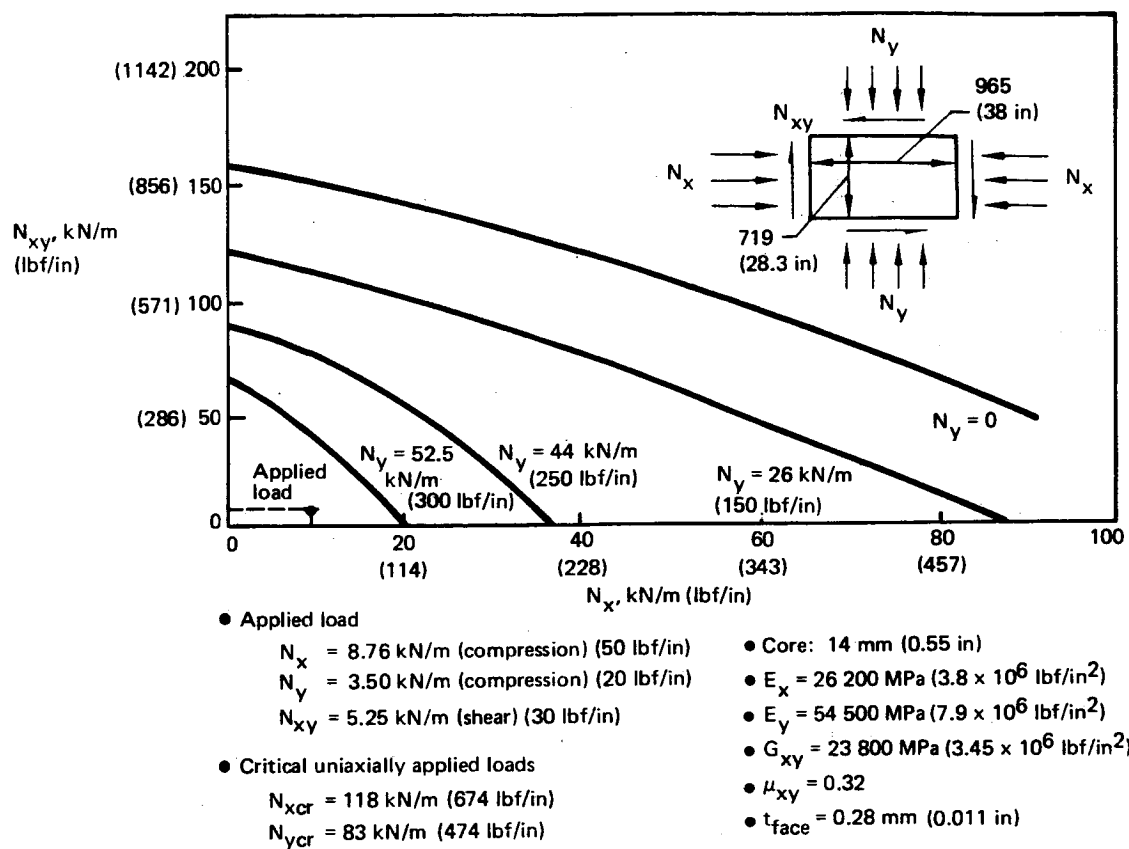


Figure 50. Interaction Curves—Inboard Skin Panel

4.1.8.2 Spar Webs

The front and rear spar webs (+45-deg fabric laminates) were designed to be shear-resistant to limit load. The spar webs were analyzed for shear buckling using the analytical procedure presented in Reference 7. A typical analytical curve is shown in Figure 51. The "a" and "b" dimensions were defined as the spar web height and stiffener spacing, respectively. Due to the low shear strains, large margins existed for all shear web panels.

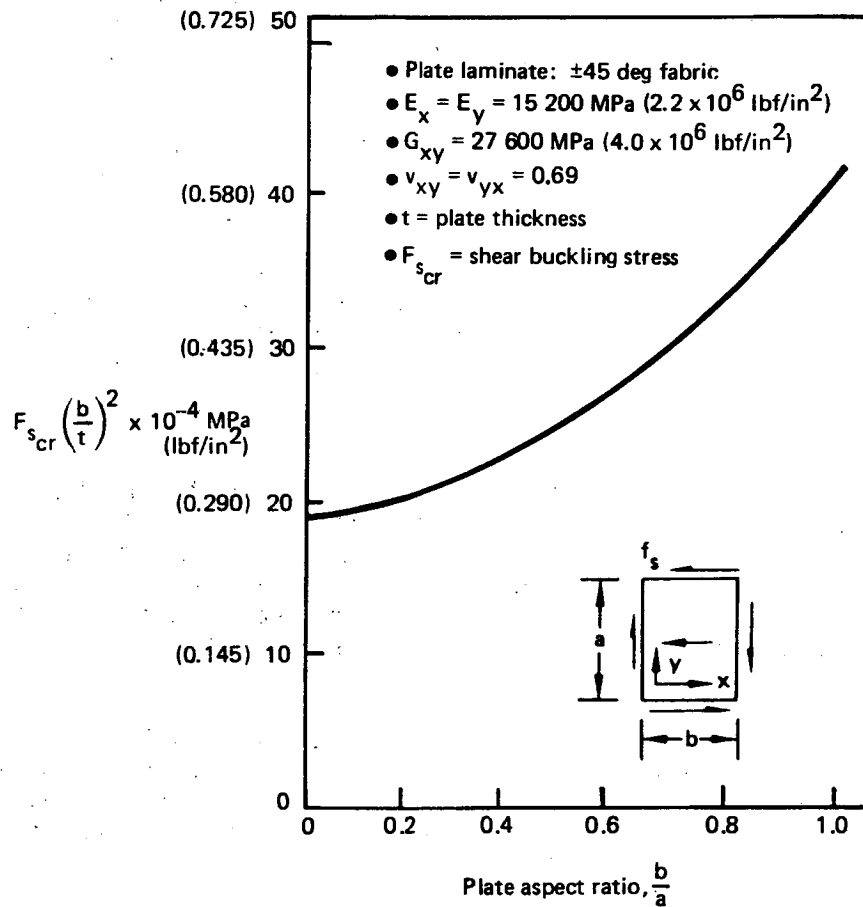


Figure 51. Shear Buckling Versus Plate Aspect Ratio—Laminate Material

4.2 ANCILLARY TESTING

An ancillary test plan, established early in the program, encompassed all testing except ground and flight tests of the full-scale component and included coupon, element, and subcomponent-sized specimens. This test plan was structured to provide the following data:

- Material design values, including environmental effects for FAA certification
- Strength and fatigue performance of specific design details
- Verification of final design details
- Real-time exposure environmental effects (moisture and temperature)
- Strength and fatigue performance of repairs

Moisture conditioning of all coupons, structural elements, and subcomponents was accomplished by placing the parts in an environmental chamber at 60°C (140°F) and 100% RH until the required moisture level was obtained as defined in Section 4.1.6.

The detailed ancillary test plans and data are presented and discussed in the following sections. All of the coupon ancillary test data are tabulated in Appendix C. Basic coupon test results that were obtained under Boeing funding to support the elevator program also are contained in the following sections and tabulated in Appendix C.

4.2.1 COUPON TESTS

The material coupon test plan, identified as NASA Test 1, is shown in Figure 52. Basic laminate strength tests funded by Boeing are defined in Figure 53. Data from these tests were used to establish design values for certification. The results from Test 1 and the basic laminate tests are discussed in the following section. In all cases, the failure strains were calculated from the failure load and the laminate modulus. The laminate modulus values are nominal Boeing values. All plotted data points are average values.

Figures 54 through 57 present the effects of temperature and moisture on failure strains of +45-deg and +45/0/90-deg fabric laminates with various ratios of width to hole diameter. The test results point out the influence that temperature and moisture have on +45-deg compression-loaded coupons due to their dependency on resin properties.

Figures 58 and 59 present the effects of temperature, moisture, and hole diameter on rail shear tests for +45-deg and +45/0/90-deg fabric laminates. The rail shear results for the +45-deg laminate indicate relative insensitivity to temperature and moisture. This result is consistent with the tension- and compression-tested coupons of the +45/0/90-deg laminate (see figs. 55 and 57), since both test configurations are fiber controlled. The results for the +45/0/90-deg laminate indicate a larger sensitivity to moisture and temperature because this laminate under shear loading is more resin dependent. This result is consistent with the tension and compression tests of the +45-deg laminate (see figs. 54 and 56).

Figure 60 presents the effects of impact and moisture on tension failure strains of +45-deg and +45/0/90-deg fabric laminates. Figure 61 shows similar data for compression failure strains.

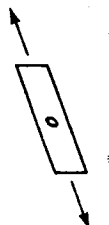
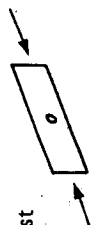
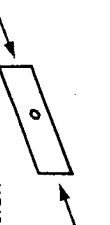
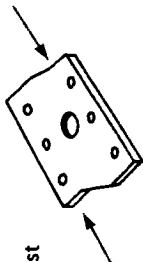
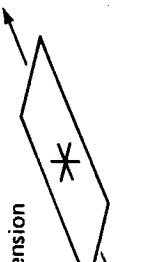
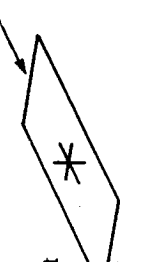
Specimen (drawing number)	Fabric layup	Size, mm (in)	Test condition	Number of specimens			Data	Purpose	Remarks
				RT	-53.9°C (-65°F)	+71°C (160°F)			
 Tension test (65C17702)	±45	381.0 (15.0) x 38.1 (1.5)	Wet Dry	3 9	3 3	3 3	Load/strain	Effect of stress con- centration	Parameters: edge margin hole size layup
	0/90/±45	381.0 (15.0) x 38.1 (1.5)	Wet Dry	3 9	3 3	3 3			
 Compression test (65C17702)	±45	381.0 (15.0) x 38.1 (1.5)	Wet Dry	3 9	3 3	3 3			
	0/90/±45	381.0 (15.0) x 38.1 (1.5)	Wet Dry	3 9	3 3	3 3			
 Defect compression test (65C17702)	±45	381.0 (15.0) x 38.1 (1.5)	Wet Dry	3 9	—	—	Residual strength	Residual strength	
	0/90/±45	381.0 (15.0) x 38.1 (1.5)	Wet Dry	3 9	—	—			
 Inplane shear test (65C17702)	±45	152.4 (6.0) x 76.2 (3.0)	Wet Dry	3 9	3 3	3 3			
	0/90/±45	152.4 (6.0) x 76.2 x (3.0)	Wet Dry	6 9	6 6	6 6			
 Impact defect-tension test (65C17702)	±45	381.0 (15.0) x 38.1 (1.5)	Wet Dry	3 12	—	—	Residual strength	Residual strength	Parameters: defect size layup
	0/90/±45	381.0 (15.0) x 38.1 (1.5)	Wet Dry	3 12	—	—			
 Impact defect- compression test (65C17702)	±45	381.0 (15.0) x 38.1 (1.5)	Wet Dry	3 12	—	—			
	0/90/±45	381.0 (15.0) x 38.1 (1.5)	Wet Dry	3 12	—	—			

Figure 52. Mechanical Properties Test Plan (NASA Test 1)


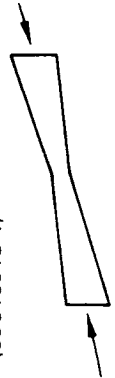
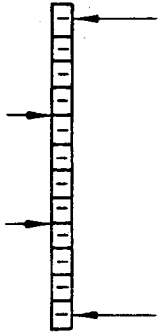
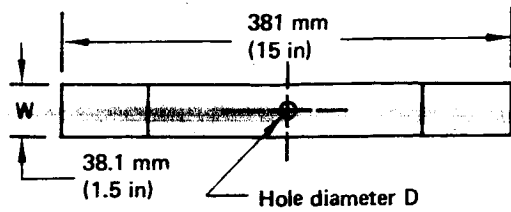
Test program	Specimen (drawing number)	Layup	Size, mm (in)	Test condition	Number of specimens				Data	Purpose
					RT	-59°C (-75°F)	86°C (180°F)	93°C (200°F)		
7313 -16	Tension test (65C19913-3) 	Fabric ±45	381.0 (15.0) x 38.1 (1.5)	Dry	5	5	4	5	Load/strain	Basic material properties
		Fabric 0/90/±45	381.0 (15.0) x 38.1 (1.5)	Dry	5	5	5	5		
	Compression test (65C19913-4) 	Fabric ±45	381.0 (15.0) x 38.1 (1.5)	Dry	5	5	5	5		
		Fabric 0/90/±45	381.0 (15.0) x 38.1 (1.5)	Dry	5	5	5	4		
7313 -36	Honeycomb sandwich beam (65C17727) 	Tape 0 Fabric ±45	406 (16.0) x 76 (3.0)	Dry	12	—	—	—		
				Wet	—	8	7	—		

Figure 53. Basic Laminate Properties Test Plan (Boeing Funded)



- 12 plies of fabric
- ± 45 -deg orientation
- Extensional modulus, $E = 2.07 \times 10^4$ MPa
(3.0×10^6 lbf/in²)
- Hole diameter
 - $D_1 = 7.95$ mm (0.313 in), $W/D = 4.8$
 - $D_2 = 2.46$ mm (0.097 in), $W/D = 15.5$
 - $D_3 = 12.7$ mm (0.500 in), $W/D = 3.0$
- Data from NASA test 1, Appendix C, Volume 2

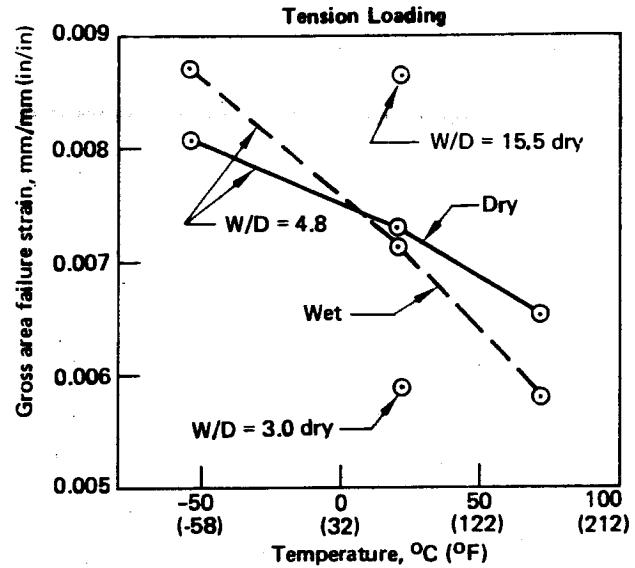
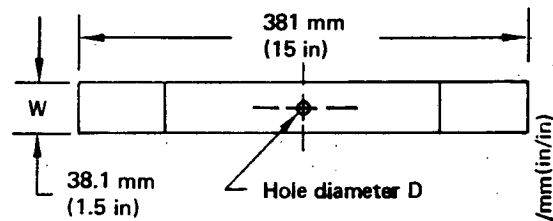


Figure 54. Effect of Moisture, Temperature, and W/D on Tension Failure Strains of ± 45 -deg Fabric Laminate Coupons



- 12 plies of fabric
- $\pm 45/0/90$ -deg orientation
- Extensional modulus, $E = 4.62 \times 10^4$ MPa
(6.7×10^6 lbf/in²)
- Hole diameter
 - $D_1 = 7.95$ mm (0.313 in), $W/D = 4.8$
 - $D_2 = 2.46$ mm (0.097 in), $W/D = 15.5$
 - $D_3 = 12.7$ mm (0.500 in), $W/D = 3.0$
- Data from NASA test 1, appendix C

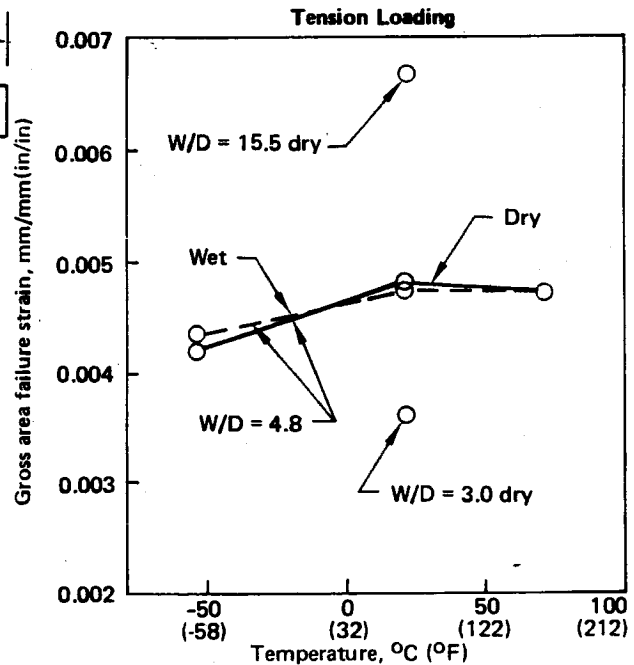


Figure 55. Effect of Moisture, Temperature, and W/D on Tension Strains of $\pm 45/0/90$ -deg Fabric Laminate Coupons

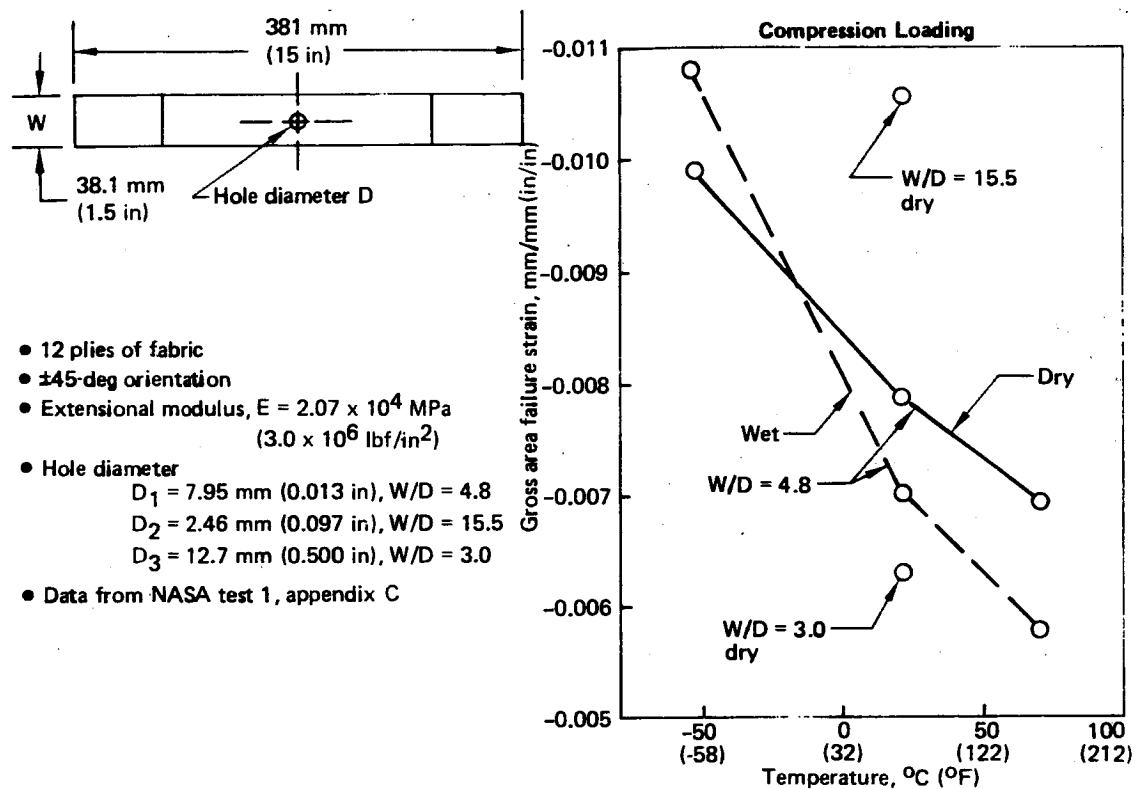


Figure 56. Effect of Moisture, Temperature, and W/D on Compression Failure Strains of ±45-deg Fabric Laminate Coupons

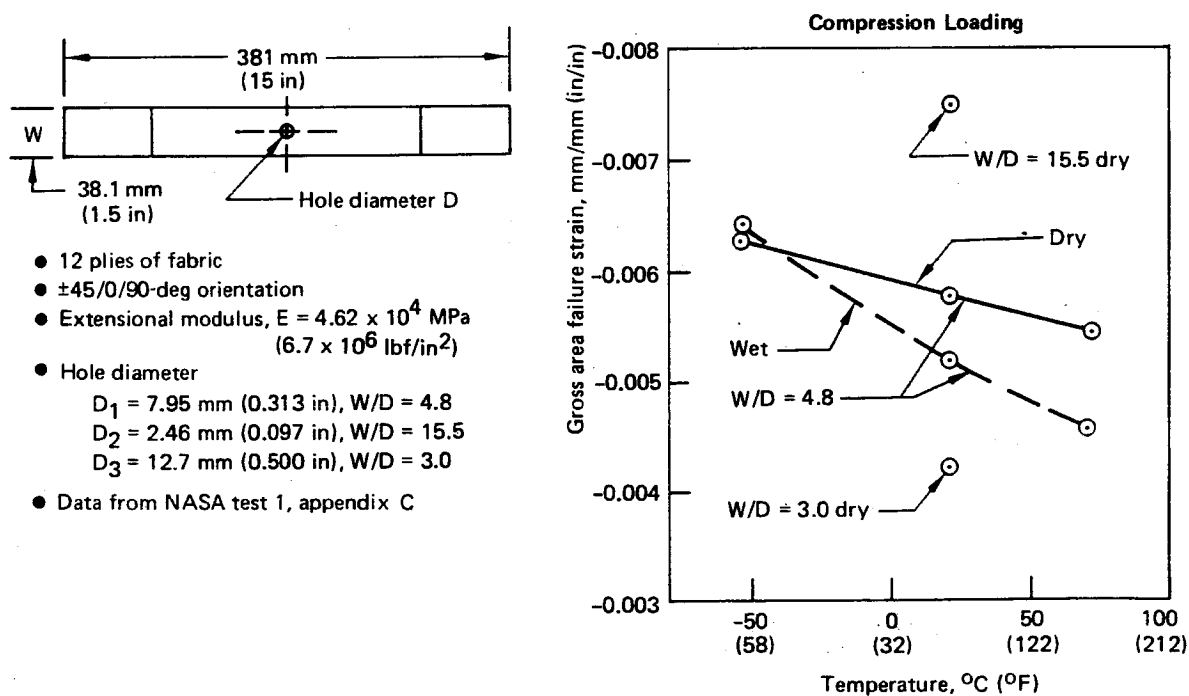
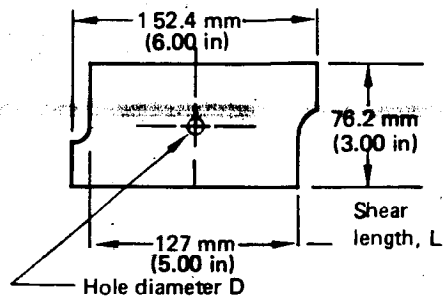


Figure 57. Effect of Moisture, Temperature, and W/D on Compression Failure Strains of ±45/0/90-deg Fabric Laminate Coupons



- 12 plies of fabric
- ± 45 -deg orientation
- Shear modulus, $G = 2.93 \times 10^4$ MPa
(4.25×10^6 lbf/in²)
- Hole diameter $D = 2.54$ mm (0.100 in),
 $L/D = 50.0$
- Data from NASA test 1, appendix C

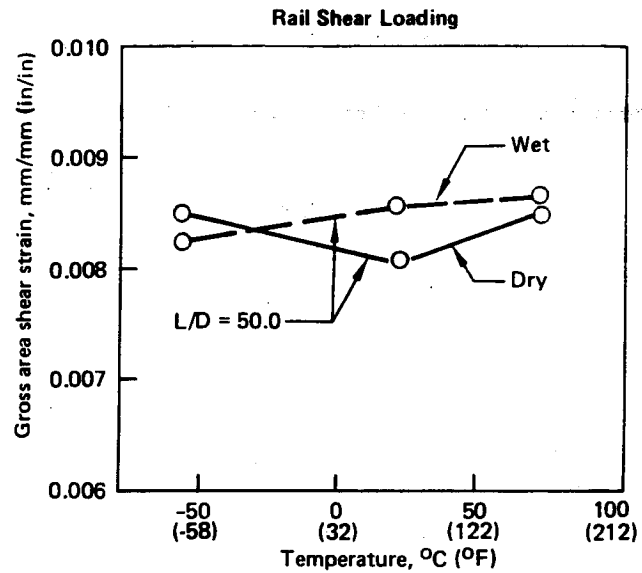
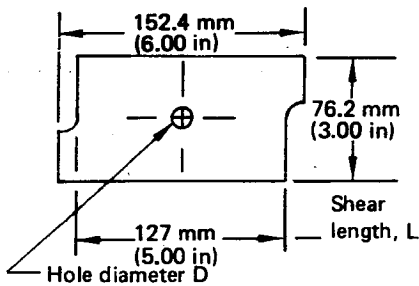


Figure 58. Effect of Moisture, Temperature, and Hole Diameter on Rail Shear Test Results for ± 45 -deg Fabric Laminate



- 12 plies of fabric
- $\pm 45/0/90$ -deg orientation
- Shear modulus, $G = 1.79 \times 10^4$ MPa
(2.6×10^6 lbf/in²)
- Hole diameter $D = 2.54$ mm (0.100 in),
 $L/D = 50.0$
- Data from NASA test 1, appendix C

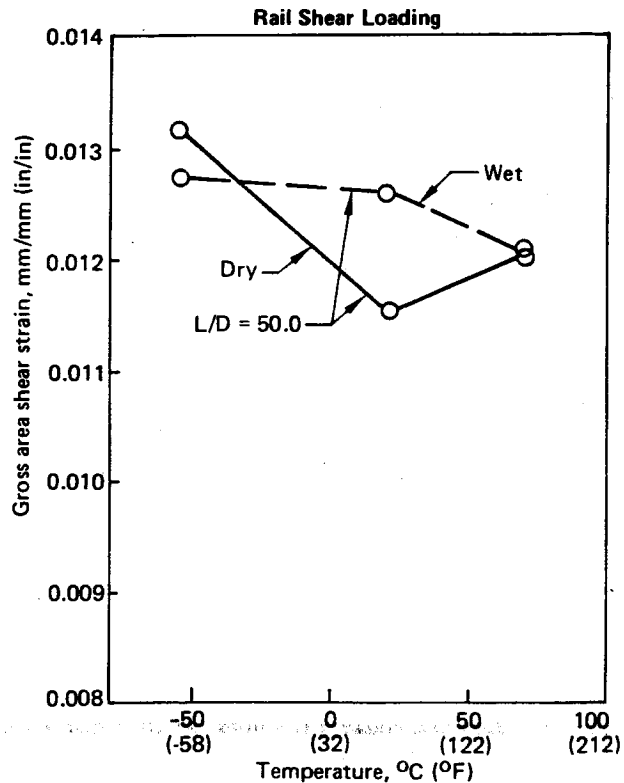


Figure 59. Effect of Moisture, Temperature, and Hole Diameter on Rail Shear Test Results for $\pm 45/0/90$ -deg Fabric Laminate

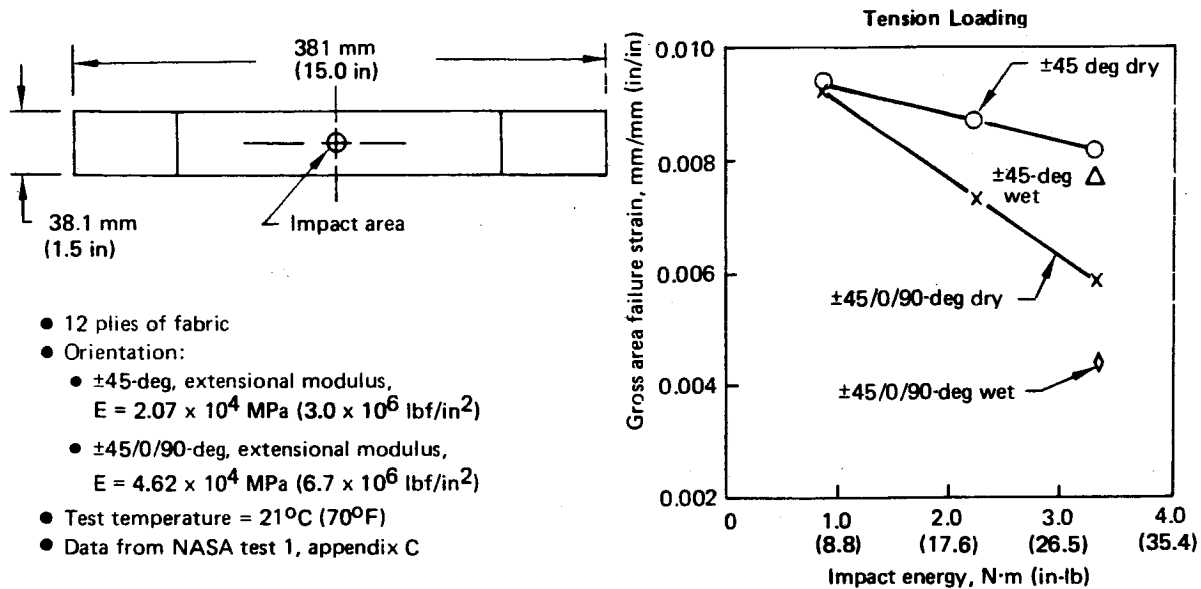


Figure 60. Effect of Moisture and Impact on Tension Failure Strains of ± 45 -deg and $\pm 45/0/90$ -deg Fabric Laminate Coupons

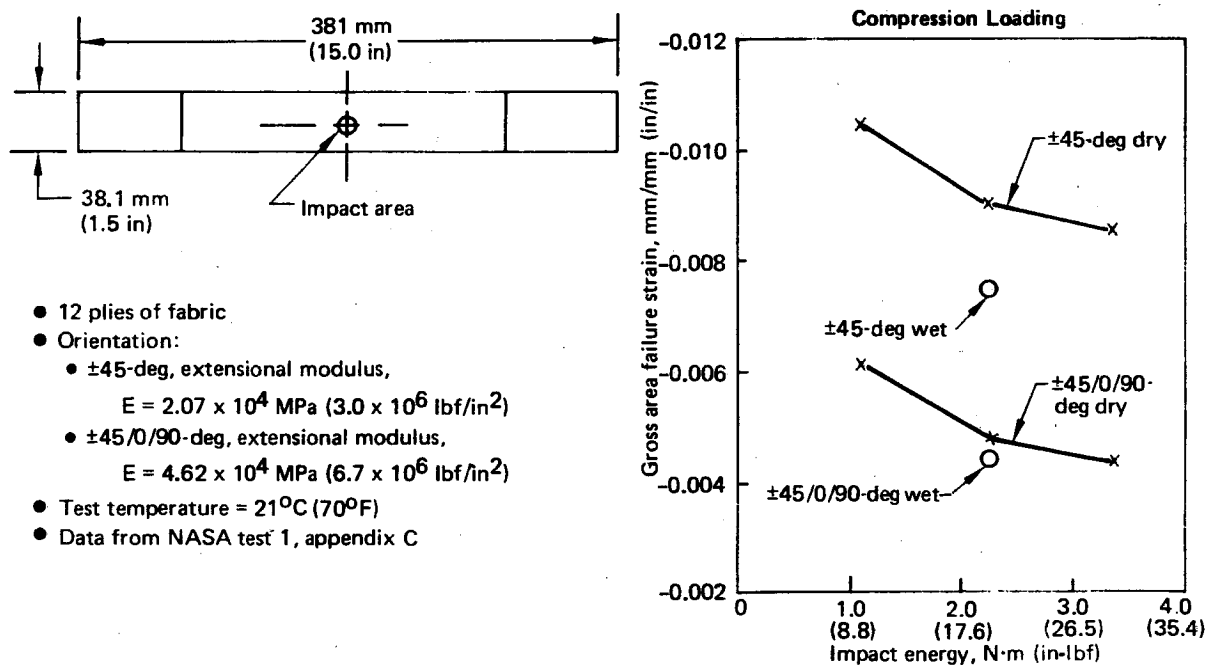


Figure 61. Effect of Moisture and Impact on Compression Failure Strains of ± 45 -deg and $\pm 45/0/90$ -deg Fabric Laminate Coupons

Figure 62 presents the effect of delaminations on ± 45 -deg and $\pm 45/0/90$ -deg fabric laminates loaded in compression. These test results, when compared to the results shown in Figure 64, indicate that delaminations of the size tested, located at the midplane of a 12-ply laminate, have minimal effect on compression failure strains.

Figure 63 and 64 present effects of temperature on tension and compression failure strains of ± 45 -deg and $\pm 45/0/90$ -deg laminates for coupons with no stress concentrations. The results for the ± 45 -deg laminate point out the significant temperature influence on coupons that are resin dominated.

Figures 65 and 66 present basic compression strengths of the elevator skin panels. These test results indicate the differences in compression strength between the tool and bag sides and between the high- and low-modulus directions of the honeycomb skin panels.

4.2.2 STRUCTURAL ELEMENT TESTS

The structural elements test plan, identified as Test 4, is shown in Figure 67. The static test results from Test 4 are summarized in the following section. Fastener bearing failure stresses were calculated using the fastener nominal diameter. All plotted points are average values.

Figure 68 shows the effects of moisture and temperature on fastener bearing stresses, Figure 69 shows the effect of fastener spacing on bearing stresses, and Figure 70 shows the effect of fastener edge margin on bearing stresses.

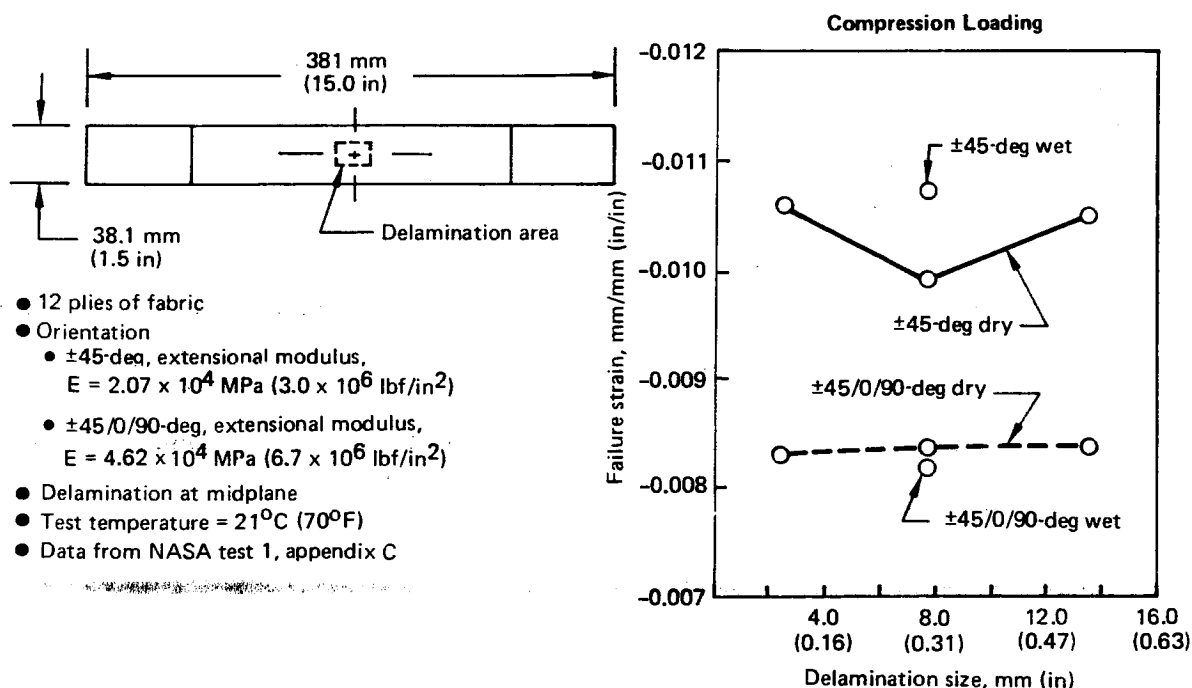
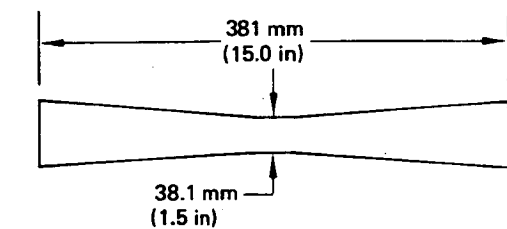


Figure 62. Effect of Moisture and Delamination Size on Compression Failure Strains of ± 45 -deg and $\pm 45/0/90$ -deg Fabric Laminate Coupons



- 12 plies of fabric
- Orientation:
 - ± 45 -deg, extensional modulus,
 $E = 2.07 \times 10^4$ MPa (3.0×10^6 lbf/in²)
 - $\pm 45/0/90$ -deg, extensional modulus,
 $E = 4.62 \times 10^4$ MPa (6.7×10^6 lbf/in²)
- Data from Boeing test 7313-16, appendix C

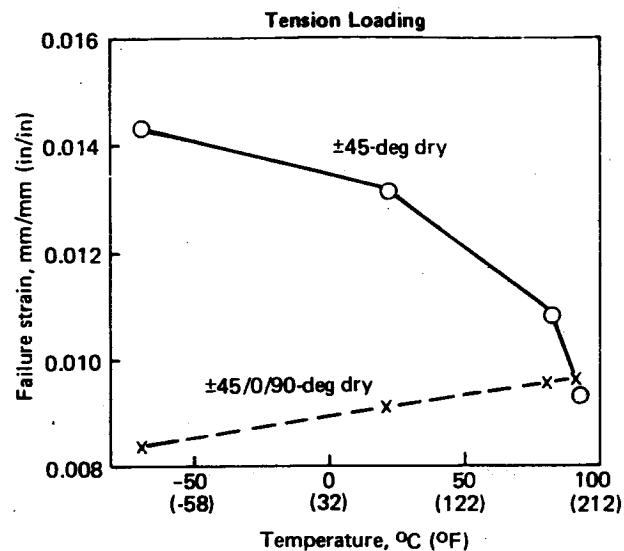
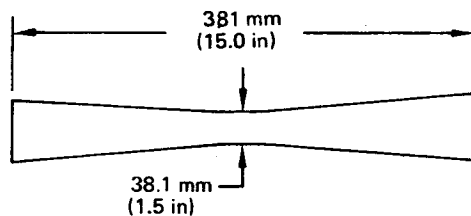


Figure 63. Effect of Temperature on Tensile Failure Strains of ± 45 -deg and $\pm 45/0/90$ -deg Fabric Laminate Coupons



- 12 plies of fabric
- Orientation:
 - ± 45 -deg extensional modulus,
 $E = 2.07 \times 10^4$ MPa (3.0×10^6 lbf/in²)
 - $\pm 45/0/90$ -deg, extensional modulus,
 $E = 4.62 \times 10^4$ MPa (6.7×10^6 lbf/in²)
- Data from Boeing test 7313-16, appendix C

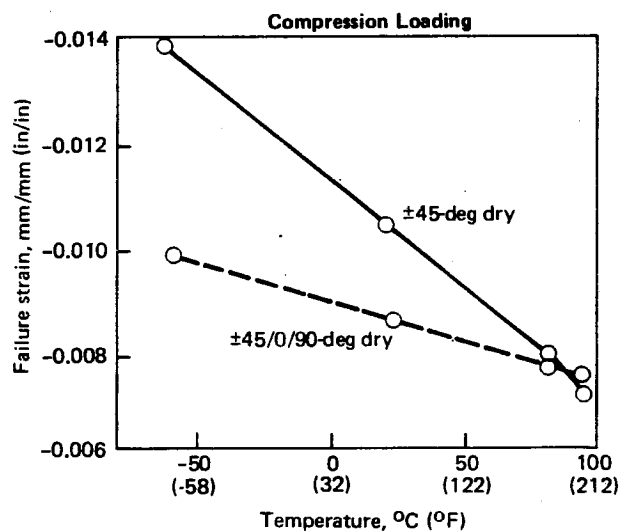
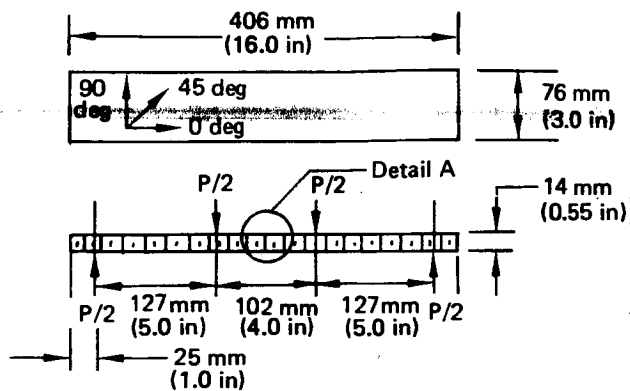
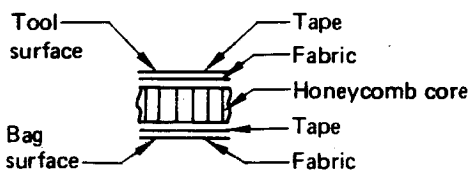


Figure 64. Effect of Temperature on Compression Failure Strains of ± 45 -deg and $\pm 45/0/90$ -deg Fabric Laminate Coupons



- Tool surface ply layup
 - Laminate 1—0-deg tape, ± 45 -deg fabric, $E = 5.38 \times 10^4$ MPa (7.8×10^6 lbf/in²)
 - Laminate 2—90-deg tape, ± 45 -deg fabric, $E = 2.62 \times 10^4$ MPa (3.8×10^6 lbf/in²)
- Tape direction same for both faces
- Tool surface in compression
- Detail A



- Data from Boeing test 7313-36, appendix C

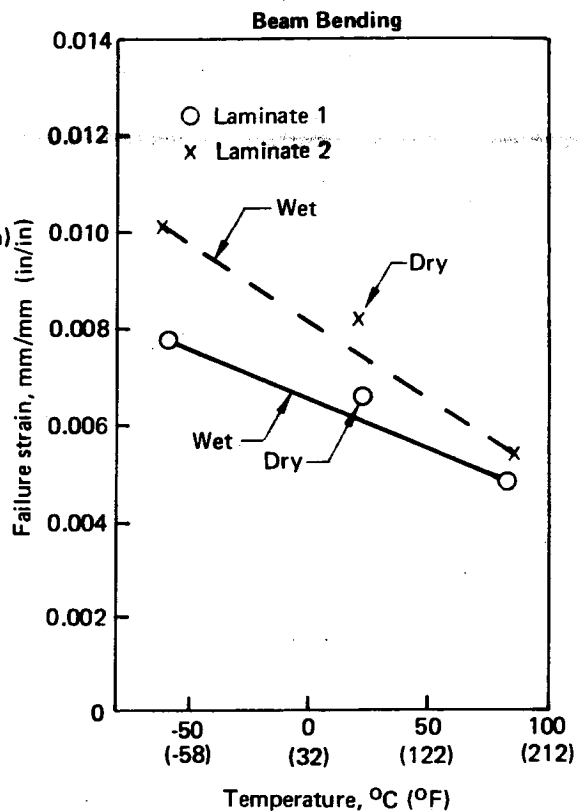


Figure 65. Effect of Temperature and Moisture on Failure Strains of Four-Point Beam-Bending Specimens—Tool Surface in Compression

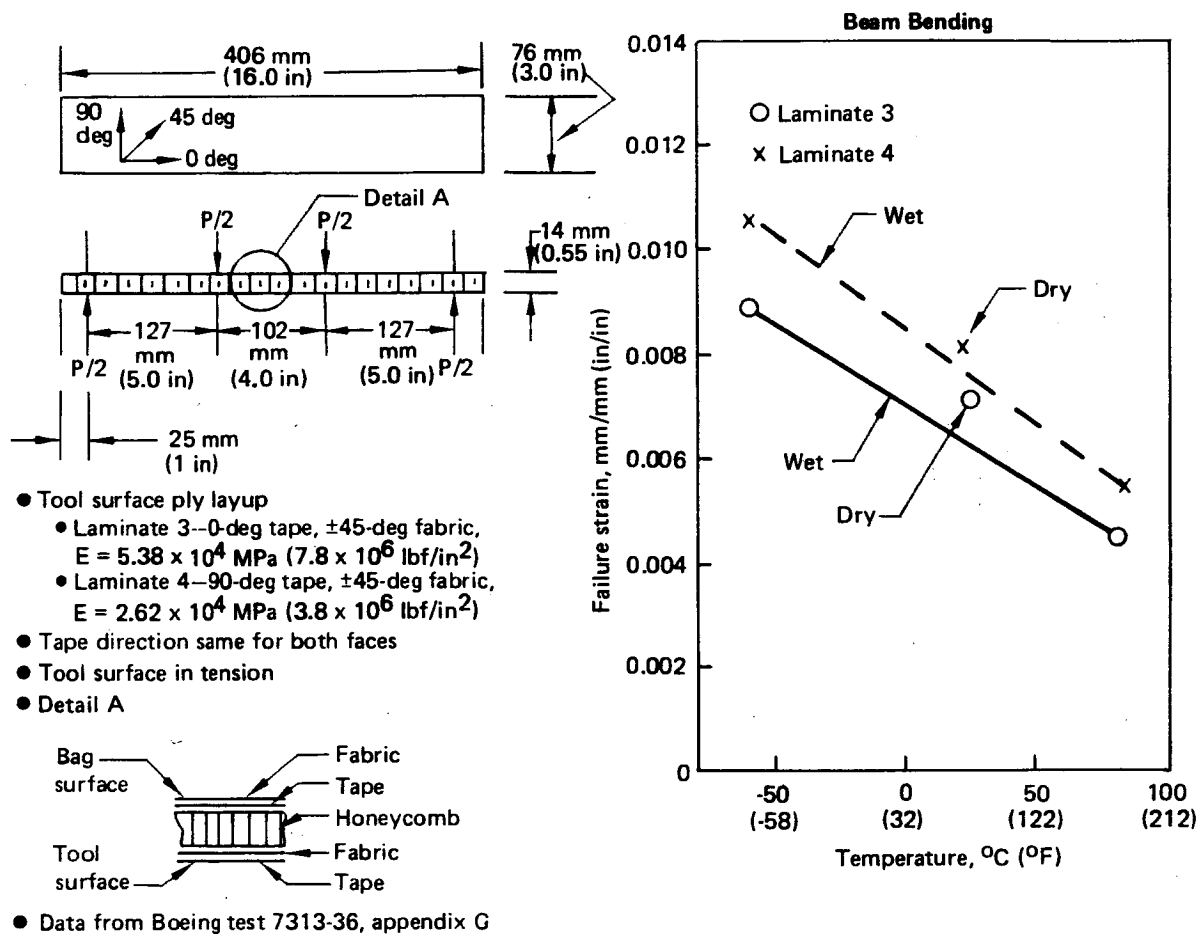


Figure 66. Effect of Temperature and Moisture on Failure Strains of Four-Point Beam-Bending Specimens—Tool Surface in Tension


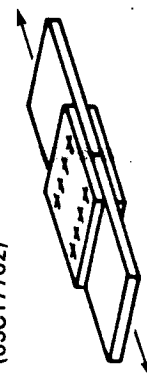
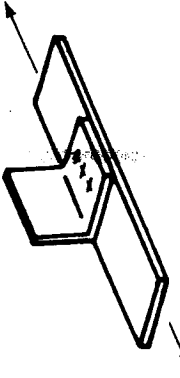
Specimen (drawing number)	Fabric layup	Size mm (in)	Condition	Number of specimens						Data	Purpose	Remarks
				Static		Fatigue R = -1.0						
				RT -53.9°C (-65°F)	+71°C (160°F)	RT -53.9°C (-65°F)	+71°C (160°F)	RT -53.9°C (-65°F)	+71°C (160°F)			
 Mechanical joint testing (65C17706)	0/90/±45	381.0 (15.0) x 38.1 (1.5)	Dry	9	—	9	3	3	Life and failure load and mode	No load transfer strength and fatigue life	Parameters: Edge margin Hole size	
			Wet	3	—	3	3	3				
 Mechanical joint testing (65C17702)	0/90/±45	Varies	Dry	33	3	33	3	3		100% load transfer joint strength	Parameters: Edge margin Fastener diameter Thickness Defects	
			Wet	15	3	15	3	3				
			Dry	6	—	6	—	—				
			Wet	6	—	6	—	—				
 Mechanical joint testing (65C17706)	0/90/±45	381.0 (15.0) x 25.4 (1.0)	Dry CSK	6	—	6	—	—	Effect of locally induced load transfer	Parameters: Thickness Defects		
			Dry non-CSK	3	—	3	—	—				
			Dry CSK	3	—	3	—	—				
			Dry non-CSK	3	—	3	—	—				

Figure 67. Structural Elements Test Plan (Test 4)

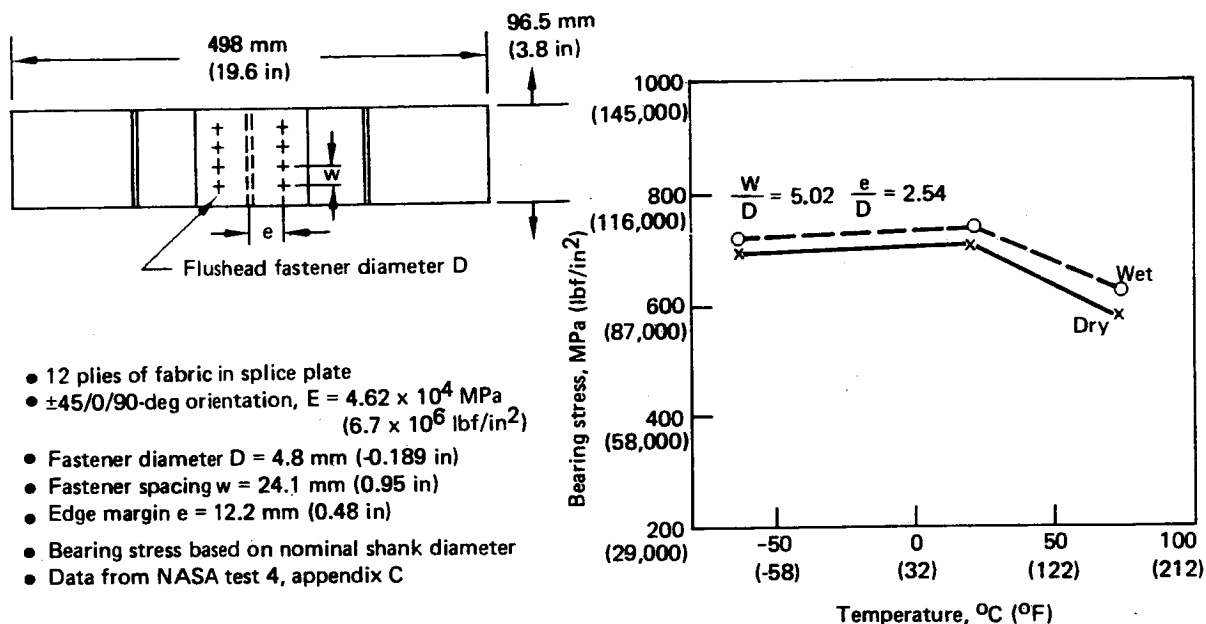


Figure 68. Effect of Moisture and Temperature on Fastener Bearing Stress

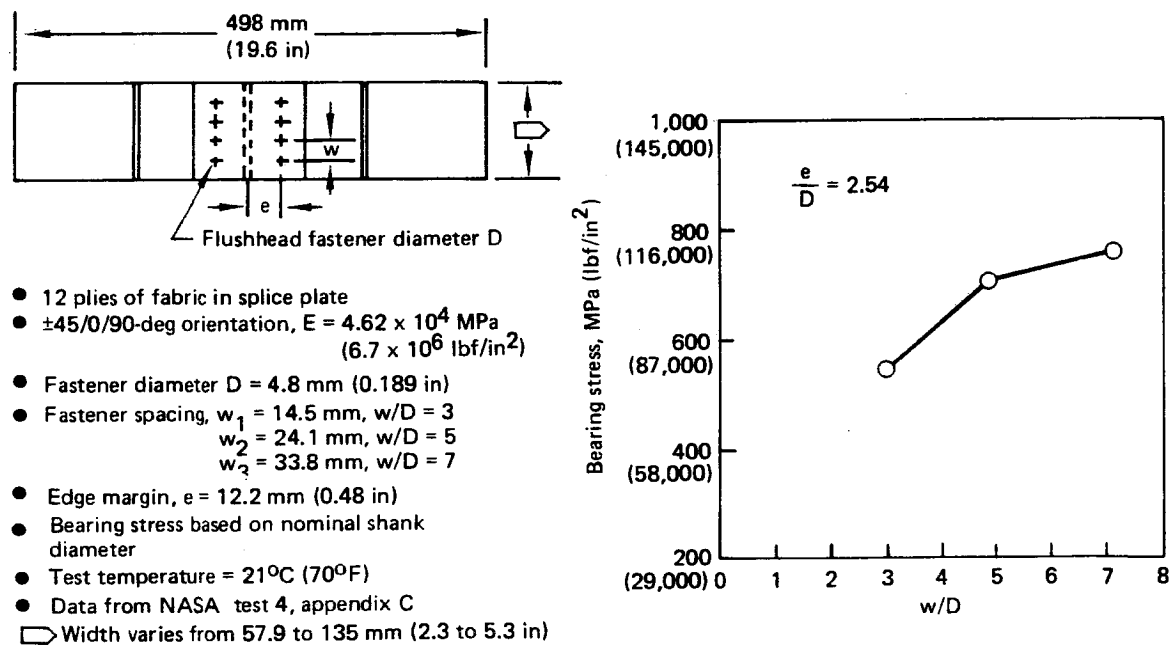
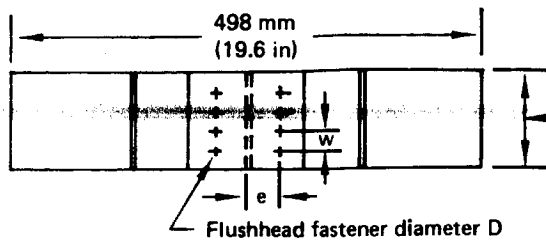


Figure 69. Effect of Fastener Spacing (W/D) on Bearing Stress



- 12 plies of fabric in splice plate
- $\pm 45/0/90$ -deg orientation, $E = 4.62 \times 10^4 \text{ MPa}$
($6.7 \times 10^6 \text{ lbf/in}^2$)
- Fastener diameter $D = 4.8 \text{ mm}$
- Fastener spacing, $w = 24.1 \text{ mm}$
- Edge margin, $e_1 = 7.4 \text{ mm}$ ($\frac{e}{D} = 1.54$)
 $e_2 = 12.2 \text{ mm}$ ($\frac{e}{D} = 2.54$)
 $e_3 = 17.0 \text{ mm}$ ($\frac{e}{D} = 3.54$)
- Bearing stress based on nominal shank diameter
- Test temperature = 21°C (70°F)
- Data from NASA test 4, appendix C

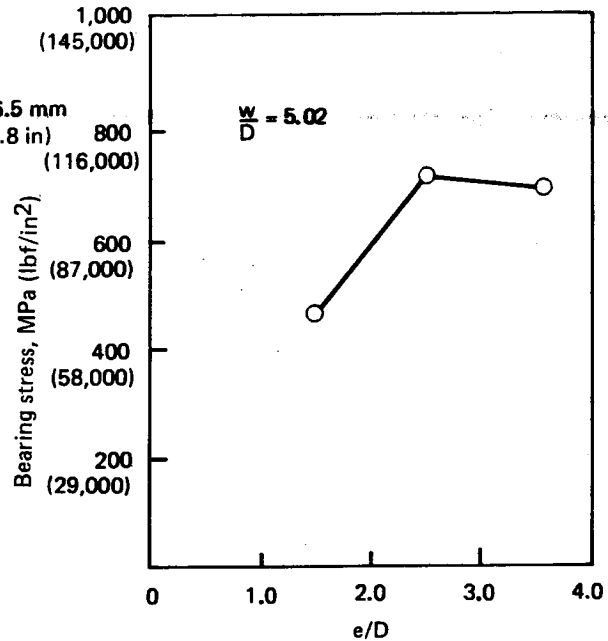
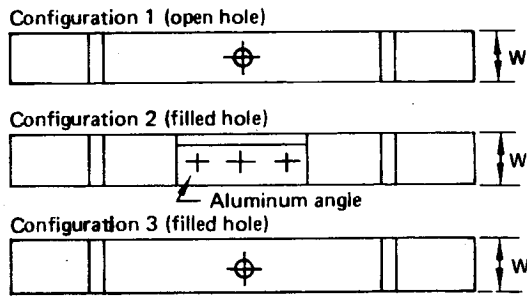


Figure 70. Effect of Edge Margin (e/D) on Bearing Stress

Figure 71 compares the results of the open-hole tests from Figure 55 with the filled-hole test data from Test 4. These results indicate that gross area failure strains are similar for the open hole, fastener-filled hole, and fastened-clip configurations for the same width-to-fastener-diameter ratio.

One hundred and eleven structural element specimens were fatigue tested as defined in the test plan (fig. 67). Test environments included ambient, -54°C (-65°F), and 71°C (160°F) and wet and dry conditions. The specimens were tested in an axial load condition at a cyclic rate of 10 Hz. All specimens were tested to 500,000 cycles with fully reversed loading ($R = -1$). The cyclic load levels varied between 20 and 40% of the static failure load. The test results are contained in Appendix C. Selected joint specimens were subsequently statically tested to failure. These test results are presented in Table 5.



- Configuration 1 data from Figure 55
- Configuration 2 from test 4, appendix C
- Configuration 3 from test 4, appendix C
- $E = 4.62 \times 10^4$ MPa (6.7×10^6 lbf/in²)
- Test temperature = 21°C (70°F)
- Dry conditions

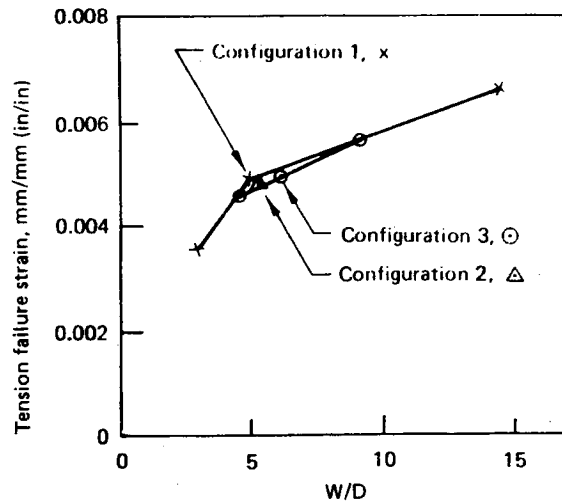


Figure 71. Effect of W/D on Tension Failure Strain Values for Open and Filled Holes

Table 5. Residual Strength Comparison of Fatigue-Conditioned Fastener Specimens

Specimen description 1	Drawing number and assembly number	Static specimen 2		Fatigue condition specimen 2 3		Comments
		Average gross stress, MPa (lbf/in ²)	Average bearing stress, MPa (lbf/in ²)	Average gross stress, MPa (lbf/in ²)	Average bearing stress, MPa (lbf/in ²)	
Four-fastener wide-mechanical joint	65C17702-53	—	708.0 (102 700)	—	565.5 (82 000)	Fatigue condition, 21.1°C dry (70°F)
	65C17702-53	—	708.0 (102 700)	—	578.5 (83 900)	Fatigue condition, -53.9°C dry (-65°F)
	65C17702-53	—	708.0 (102 700)	—	583.8 (84 700)	Fatigue condition, 71.1°C dry (160°F)
Aluminum angle hard point	65C17706-15	226.1 (32 800)	—	234.6 (34 000)	—	Fatigue condition, 21.1°C dry (70°F)
	65C17706-16	208.8 (30 300)	—	209.5 (30 400)	—	Fatigue condition, 21.1°C dry (70°F)
	65C17706-17	221.6 (32 100)	—	224.3 (32 500)	—	Fatigue condition, 21.1°C dry (70°F)
	65C17706-18	218.3 (31 700)	—	235.5 (34 200)	—	Fatigue condition, 21.1°C dry (70°F)
	65C17706-19	240.7 (34 900)	—	233.0 (33 800)	—	Fatigue condition, 21.1°C dry (70°F)
Filled hole	65C17706-21	224.7 (32 600)	—	233.8 (33 900)	—	Fatigue condition, 21.1°C dry (70°F)
	65C17706-21	224.7 (32 600)	—	238.0 (34 500)	—	Fatigue condition, -53.9°C dry (-65°F)
	65C17706-21	224.7 (32 600)	—	233.9 (33 900)	—	Fatigue condition, 71.1°C dry (160°F)
	65C17706-21	224.7 (32 600)	—	231.0 (33 500)	—	Fatigue condition, 21.1°C wet (70°F)
	65C17706-21	224.7 (32 600)	—	244.5 (35 500)	—	Fatigue condition, -53.9°C wet (-65°F)
	65C17706-21	224.7 (32 600)	—	238.6 (34 600)	—	Fatigue condition, 71.1°C wet (160°F)
	65C17706-21	224.7 (32 600)	—	—	—	—

1 Static test data in appendix C, test 4, specimen definition Figure 67

2 Static and residual test at 21.1°C (70°F) dry conditions

3 Residual strength after 500,000 cycles of fatigue loading

4.2.3 SUBCOMPONENT TESTS

The subcomponent test plan is shown in Figure 72. The test results from this phase of the program were used to verify the design and durability of specific subcomponents prior to fabrication of the first elevator unit.

4.2.3.1 Cover Panel Padup at Ribs

A section of elevator cover panel (Test 8) at a rib intersection was tested to verify the adequacy of the fastener padup region. The specimen geometry is shown in Figure 73 and a typical static test setup is shown in Figure 74. The test data are presented in Appendix C. The rib attachment angle was laterally supported during test. Five specimens of identical configuration were tension tested at ambient dry conditions. The test value strain calculations are displayed in Figure 75. The maximum spanwise strain indicated by the elevator finite-element model is 0.00283 mm/mm (in/in). Therefore, these test results indicate that the ambient dry tension capability of this detail is 2.4 times the maximum required. Three ambient-temperature wet specimens also were tested in tension and the average failure strain for these was higher than the average for the dry specimens.

Five specimens were fatigue tested at a cyclic rate of 10 Hz with fully reversed loading. The cyclic load was ± 1112 N (± 250 lbf), which approximates a ground-air-ground load level. Two specimens were tested dry and three specimens were tested wet at ambient conditions. All five specimens achieved 500,000 cycles with no detectable damage.

4.2.3.2 Spar Web Shear Test

Three sections of spar shear web (Test 9), with stiffeners attached, were tested to determine the shear strain capability of the web laminate. The specimen geometry is shown in Figure 76 and a typical test setup is shown in Figure 77. The shear web failed at an average principal shear strain of 0.005 mm/mm (in/in) at a stiffener fastener hole for all three test panels. The average shear flow in the web at time of failure was 164 N/mm (937 lbf/in), which is approximately 3-1/2 times the critical design shear flow for the front spar web. A typical moire fringe pattern, showing a well-developed diagonal tension field buckle, is shown in Figure 78.

4.2.3.3 Honeycomb Skin Panel Stability Test

Seven honeycomb panels (Test 10) were tested in compression to evaluate the buckling behavior of the panels and to determine the compression load-transfer capabilities of the panel edgeband. The panels were tested in the elevator spanwise direction and were sized to be representative of the elevator panels. The test setup and specimen geometry are shown in Figure 79. The test conditions and failure loads are shown in Table 6. All panels failed by local crippling in the edgeband region; therefore, panel buckling loads were higher than the test loads. A typical moire fringe pattern of a panel prior to failure, showing the onset of buckling, is shown in Figure 80.

The elevator finite-element model results indicate a maximum required end load of 23.5 N/mm (134 lbf/in). The wet-tested panels indicated an average failure load of 51.9 N/mm (296 lbf/in), which is 2.2 times the required value.

The impacted panel, with visible damage, failed at an end load of 45.2 N/mm (258 lbf/in), which was 1.92 times the required value. The lightning damage appeared to have minimal effect on the test panel ultimate load capability since the lightning panel failed at 92% of the average of the dry-tested panels.

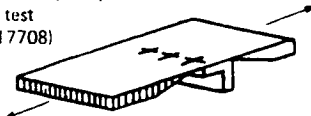
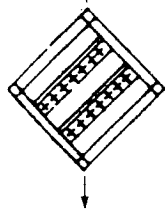
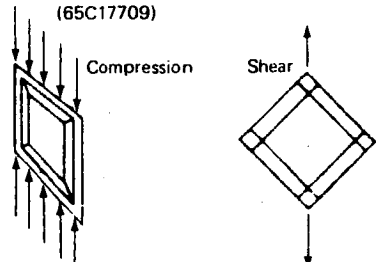
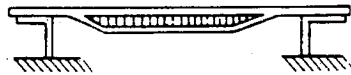
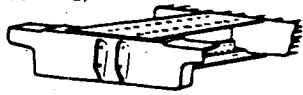

Test No.	Specimen (drawing number)	Layout	Size, mm (in)	Condition	Number of specimens		Remarks
					Static	Fatigue	
8	Cover panel padup at rib test (65C17708) 	90/±45 2-ply faces honeycomb	63.5 (2.5) x 658.0 (25.9)	RT, dry RT, wet	6 3	R = 1.0 3 3	Design verification
9	Spar shear web and stiffeners test (65C17711) 	±45	521.0 (20.5) x 521.0 (20.5)	RT, dry	4	-	Design verification
10	Honeycomb panel stability test (65C17709) 	90/±45 2-ply faces honeycomb	Com- pression 597.0 (23.5) x 610.0 (24.0) Shear 610.0 (24.0) x 610.0 (24.0)	RT, dry RT, wet RT, dry damaged RT, dry RT, wet RT, dry damaged	3 2 2 3 2 2	- - - - - -	Design verification
12	Panel edge shear and bending test (65C17710) 	90/±45 2-ply faces honeycomb	254.0 (10.0) x 50.8 (2.0)	RT, dry +load -load	3 3	R = 0 3 3	Design verification
14	Actuator rib verification test (65C17712) 	Per drawing	588.8 (23.2) x 203.2 (8.0)	RT, dry	1		Design verification
11	Front spar/actuator fitting splice test (65C17704) 	Per drawing	914.4 (36.0) x 203.0 (8.0)	RT, dry 71°C wet (160°F)	1 1	1	Design verification

Figure 72. Elevator Subcomponent Test Plan

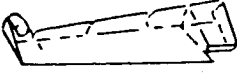
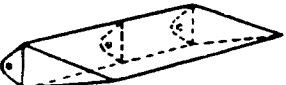
Test No.	Specimen (drawing number)	Layup	Size, mm (in)	Condition	Number of specimens		Remarks
					Static	Fatigue	
17	Elevator outboard sections (65C17707) 	Per drawing	3,000.0 (118.0) x 762.0 (30.0)	RT, dry	1	—	Design verification stiffness
15	Elevator box sonic fatigue test (65C17705) 	Per drawing	1680.0 (66.0) x 711.0 (28.0)	RT, dry	—	2	Design verification

Figure 72. Elevator Subcomponent Test Plan (Concluded)

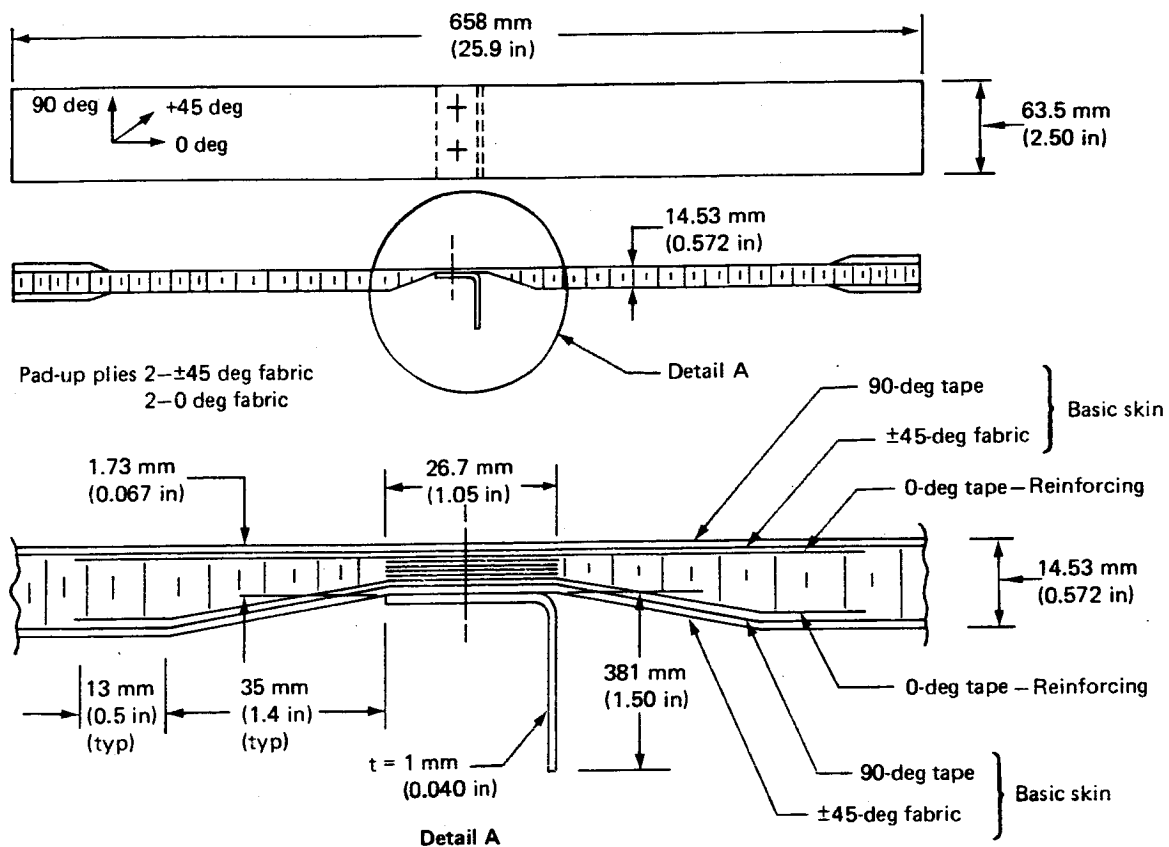


Figure 73. Cover Panel Padup Specimen Geometry (Test 8)

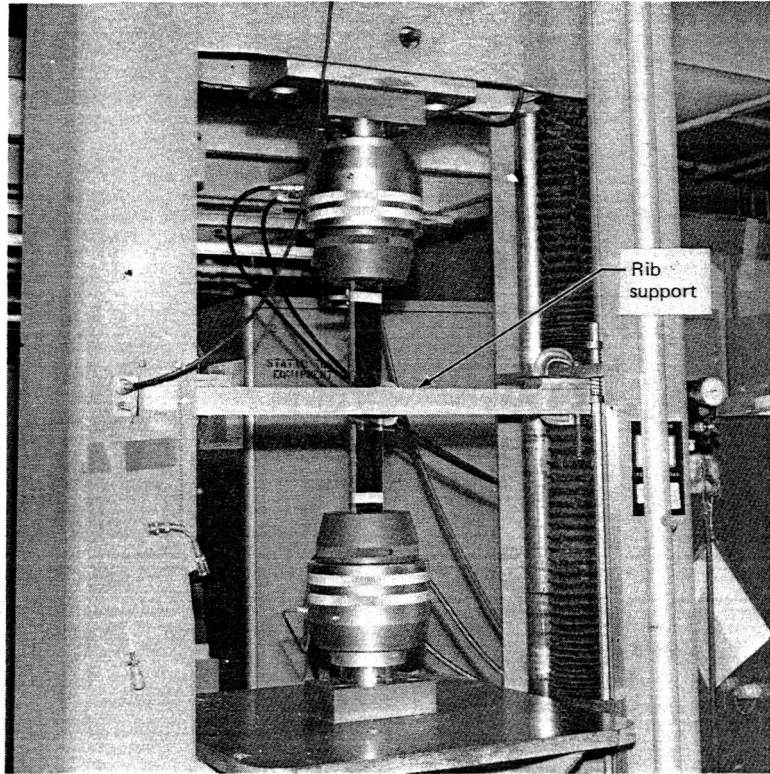
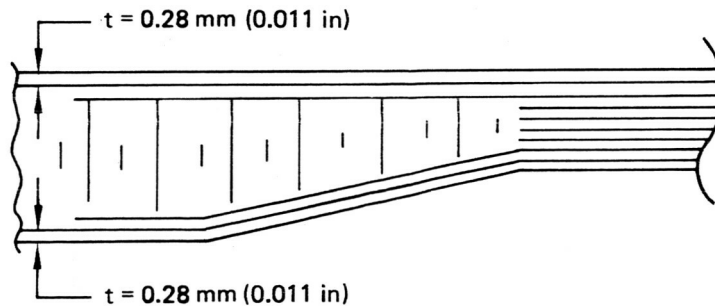


Figure 74. Cover Panel Padup at Rib Test Setup



Specimen Cross Section

- Average failure load = 6,405 kN (1440 lbf)
(NASA test 8, appendix C)
- Strain based on basic skin
 - Thickness, t = 0.28 mm (0.011 in)
 - Width, W = 63.5 mm (2.5 in)
 - Area, A = 35.56 mm² (0.055 in²)
 - E = 2.62×10^4 MPa (3.8×10^6 lbf/in²)
 - Strain, ϵ = $\frac{6.405 \times 1000 \times 10^6}{35.56 \times 2.62 \times 10^4 \times 10^6} = 0.00687$ mm/mm (in/in)

Figure 75. Cover Panel Padup Strain Calculation

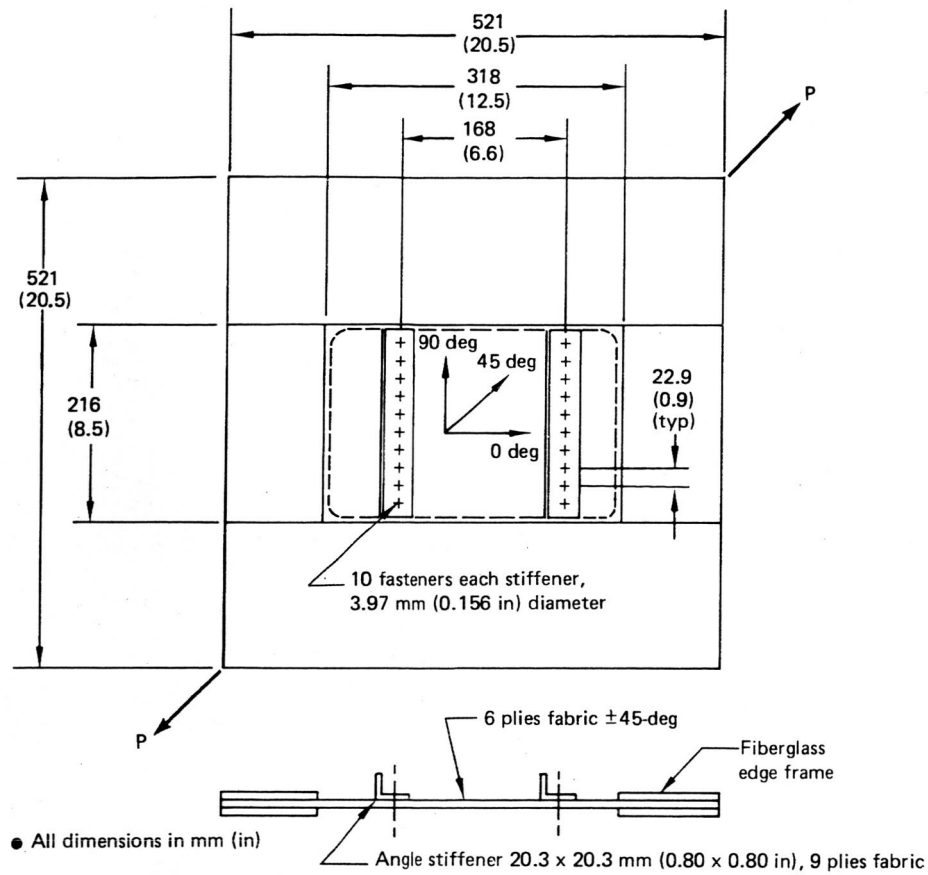


Figure 76. Spar Web Shear Test Specimen (Test 9)

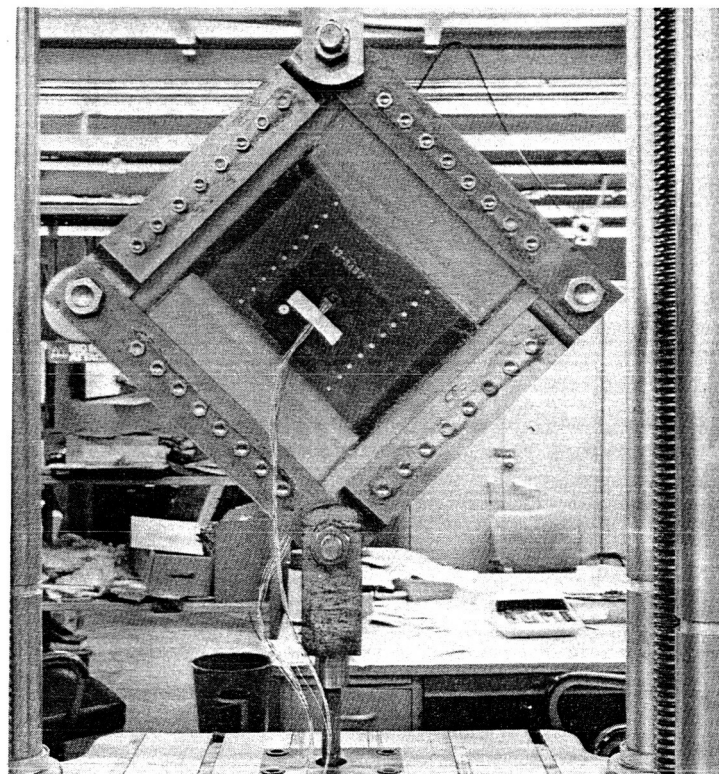


Figure 77. Spar Web Shear Test Setup

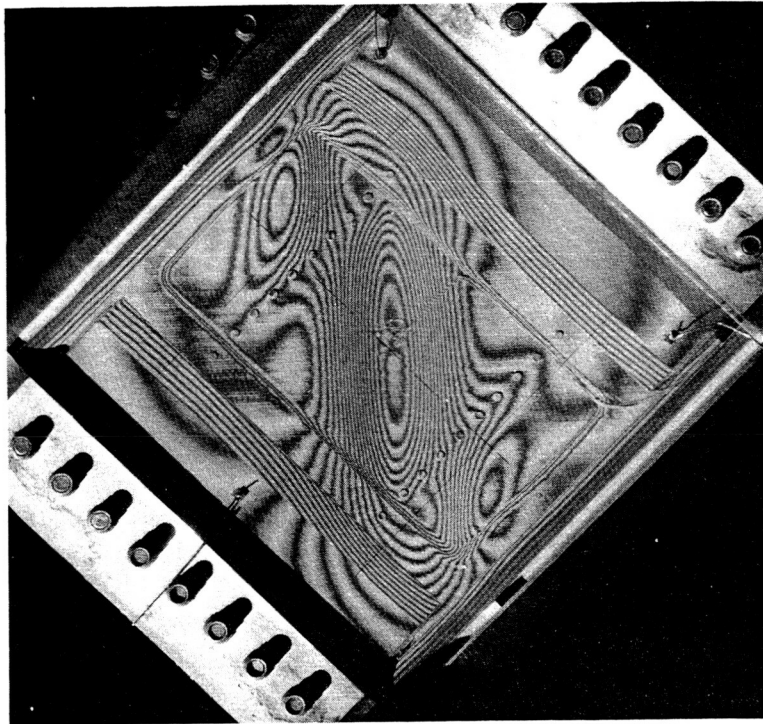


Figure 78. Typical Moire Fringe Pattern Prior to Failure for Spar Web Shear Test Panel

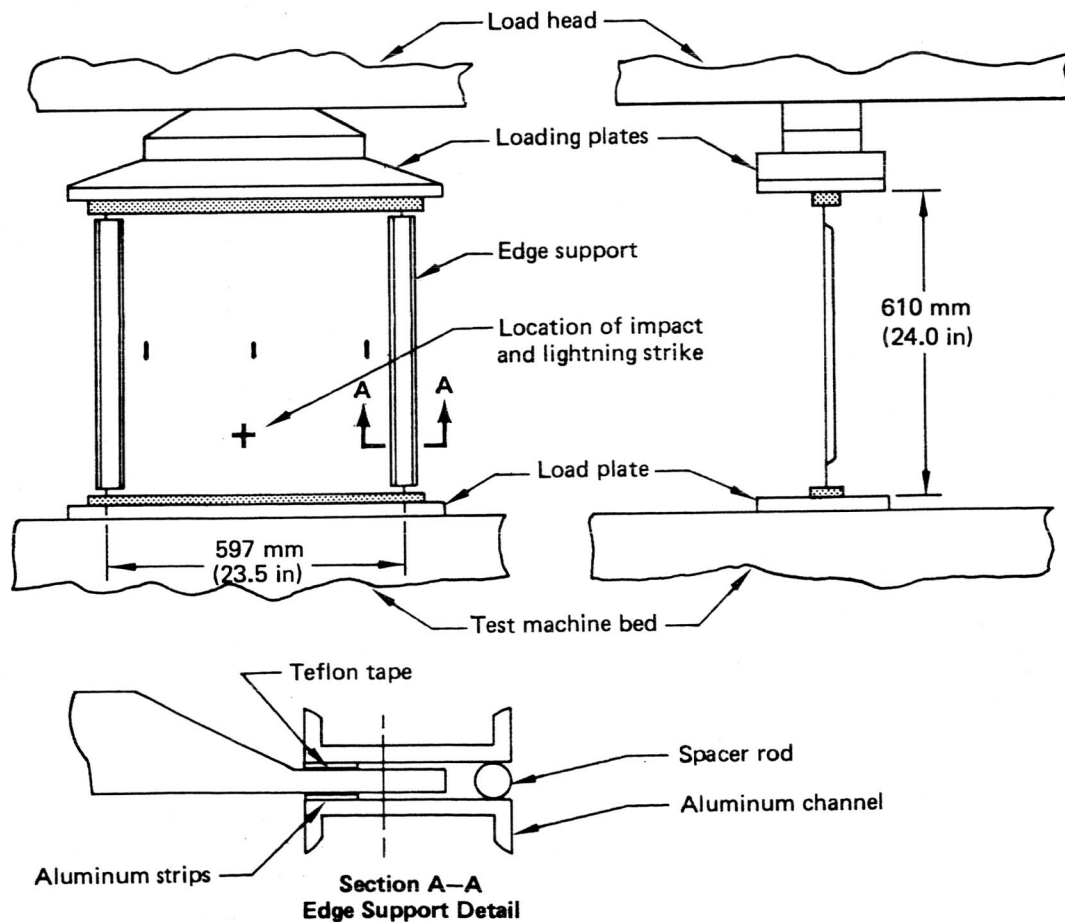


Figure 79. Honeycomb Skin Panel Compression Test Setup (Test 10)

Table 6. Honeycomb Skin Panel Compression Stability Test Results

Test condition 1	Failure load, kN (lbf)
Dry	41.37 (9300) 35.59 (8000) 34.70 (7800)
Wet	31.22 (7020) 31.14 (7000)
Dry impacted 2	26.78 (6020)
Dry lightning damage 3	34.25 (7700)

- 1 All tests at 21°C (70°F)
- 2 Impacted with 1.13 N·m (10 in-lbf) energy with 19-mm (0.75 in) spherical ended rod. Damaged fibers and some core crushing, 12.7-mm (0.50 in) diameter damaged area.
- 3 Damage from 50,000 amp current, damage area 51 by 76 mm (2.0 in by 3.0 in)

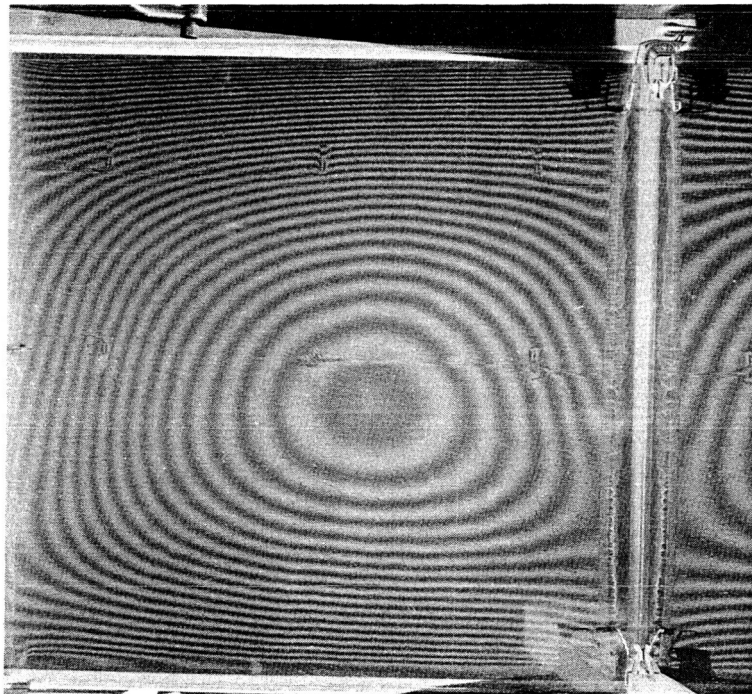


Figure 80. Moire Fringe Pattern of Honeycomb Compression Panel at a Load of 40.03 kN (9000 lbf)

4.2.3.4 Honeycomb Shear Panels

Seven honeycomb shear panels (Test 10) were tested to evaluate the shear buckling behavior of a representative elevator skin panel section. The panels were tested in a picture-frame load fixture. The test setup and specimen geometry are shown in Figure 81. The test conditions, failure loads, and principal shear strains calculated from the strain gage data are shown in Table 7. A typical moire fringe picture of a panel under load, showing initial development of a diagonal tension buckle, is depicted in Figure 82.

The first test panel failed parallel to the panel edge in the transition area between the honeycomb and the edgeband. The failure initiated in the corner radius of the panel. The next specimen was modified to eliminate the corner radius. The failure load was approximately the same as that for the first specimen, but the failure mode was changed. These failure locations and panel modifications are shown in Figure 83. Further testing was accomplished with the modified configuration.

The elevator finite-element model results indicate a maximum required principal shear strain of 0.005774 mm/mm (in/in) at 82°C (180°F) (fig. 45). The wet-tested panels at 21°C (70°F) (table 7) indicate a capability 1.4 times the required value. The lightning and impacted panels, with visible damage, indicate a capability of 1.54 and 1.45 times the required values, respectively.

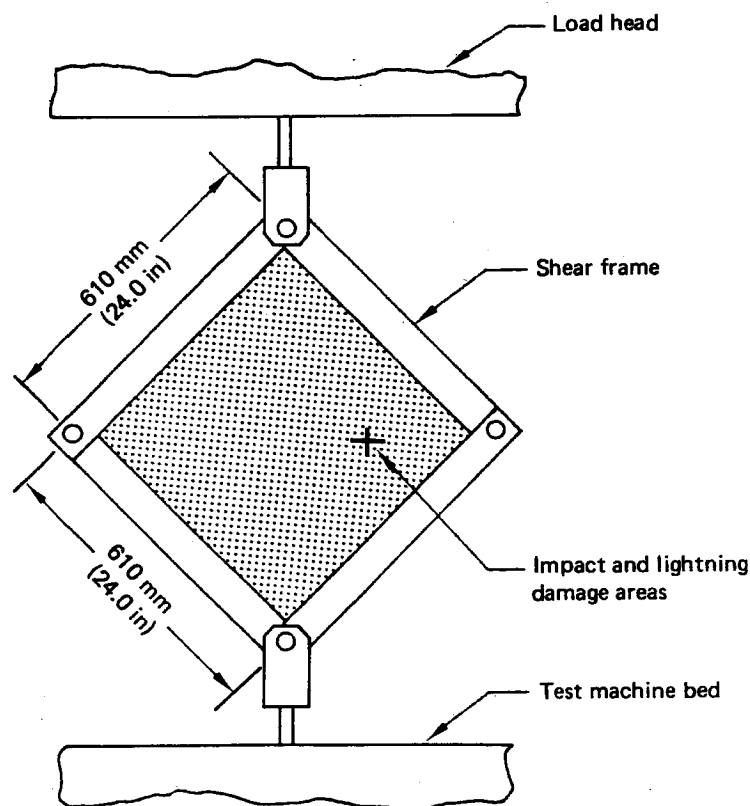








Figure 81. Honeycomb Skin Panel Shear Test Setup (Test 10)

Table 7. Honeycomb Skin Panel Shear Test Results

Test condition 	Failure load, kN (lbf)	Principal shear strain
Dry	88.30 (19,850)	0.0102
	87.01 (19,560)	0.0106
	85.63 (19,250)	0.0099
Wet	56.05 (12,600)	0.0074
	61.83 (13,900)	0.0089
Dry, impacted 	70.73 (15,900)	0.0084
Dry, lightning damage 	75.62 (17,000)	0.0089

 All tests at 21°C (70°F)

 Impacted with 1.13 N·m (10 in-lbf) energy with 19-mm (0.75 in) spherical ended rod. Damaged fibers and some core crushing, 12.7-mm (0.50 in) diameter damaged area.

 Damage from 50,000 amp current, damage area 51 by 76 mm (2.0 by 3.0 in)

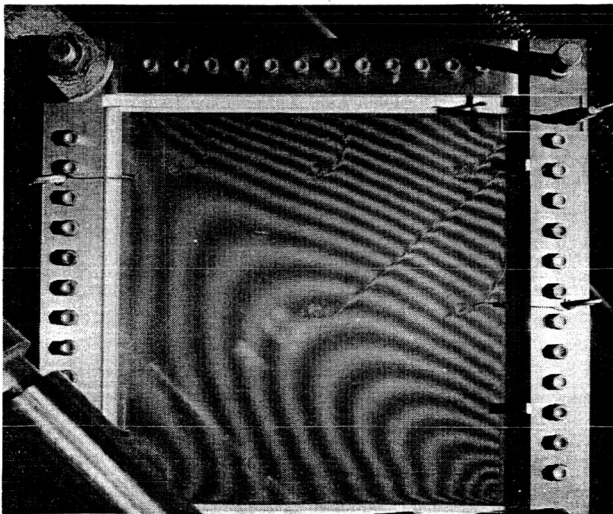


Figure 82. Moire Fringe Pattern of Honeycomb Shear Panel

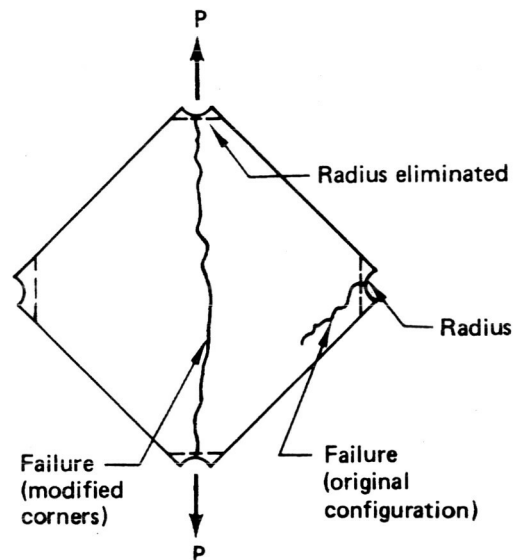


Figure 83. Honeycomb Panel Shear Test Panel Modification

4.2.3.5 Panel Edge Shear and Bending

A section of elevator cover panel (Test 12) at a spar intersection was tested to verify the adequacy of the ramp region to transfer air pressure loads to the spars. The specimen geometry and the three loading configurations that were tested are shown in Figure 84. A photograph of a typical test setup is shown in Figure 85. The failure loads are presented in Table 8 and indicate that for this particular geometry and edge constraints, the Type I loading (see fig. 84) produced the minimum load.

The maximum requirement for this detail is 4.5 N/mm (25.7 lbf/in) based on a maximum pressure shear load. The Type I specimens developed an average shear load of 9.87 N/mm (56.4 lbf/in) along the supports. Thus, these results indicate that this panel edge detail has a shear capability 2 times that required.

Three specimens were cyclically tested with a 44.5-N (10-lbf) load at $R = -1$ in the Type I load configuration. This load level represents a typical ground-air-ground pressure load. All three specimens reached 500,000 cycles with no detectable damage.

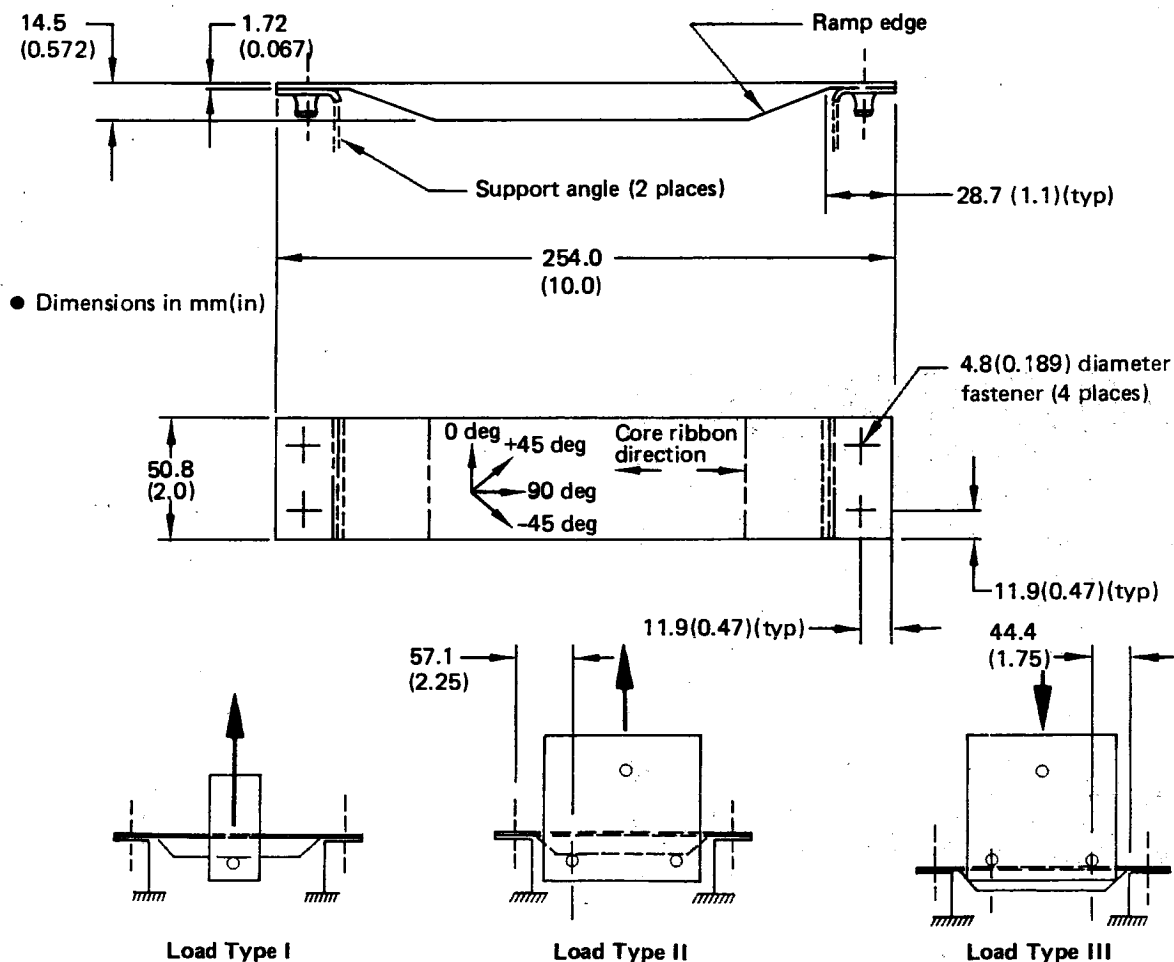


Figure 84. Panel Edge Shear and Bending Test Specimen Geometry (Test 12)

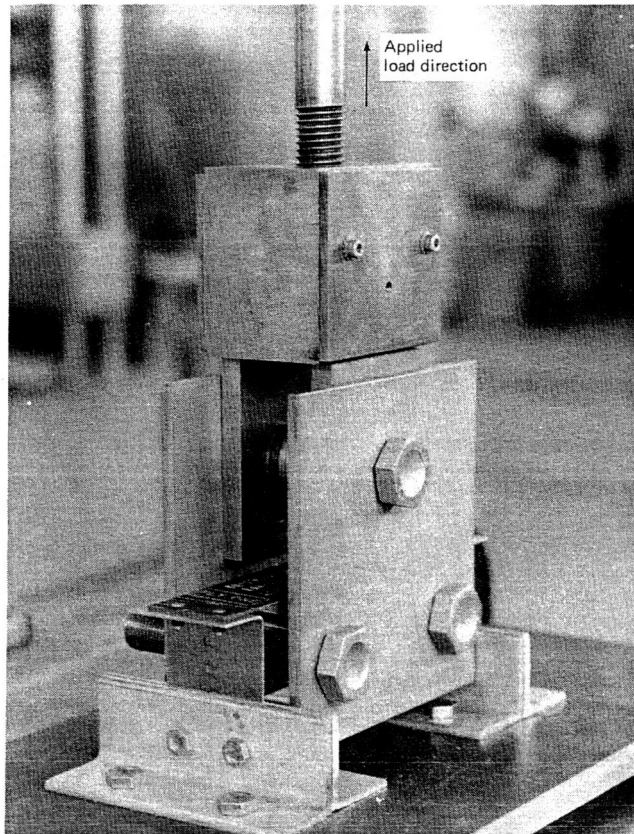



Figure 85. Panel Edge Shear and Bending Test Setup (Test 12)

Table 8. Panel Edge Shear and Bending Test Results (Test 12)

Load type 	Failure load, kN (lbf)
I	1.045 (235) 0.974 (219) 0.992 (223)
II	1.646 (370) 1.922 (432)
III	2.873 (646)

 See Figure 84.

4.2.3.6 Actuator Rib Test

A section of the elevator actuator backup rib (Test 14) was statically loaded to failure to verify the rib-to-actuator fitting joint. The test article was an assembly of the graphite-epoxy rib and an aluminum front spar actuator fitting. The specimen dimensions and a schematic of the test setup are shown in Figure 86. A photograph of the test setup is shown in Figure 87.

The required capability of the splice was based on the same strength criterion as that of the current metal design. Using this criterion, the gross area strain in the rib chords would be 0.00316 mm/mm (in/in). Figure 88 presents the calculation procedure used to determine the strain in the chords at failure. This procedure indicates that the test specimen failed at 1.33 times the design requirement. Figure 89 presents the calculation procedure used to predict the failure strain. This procedure predicts the failure strain within 11%.

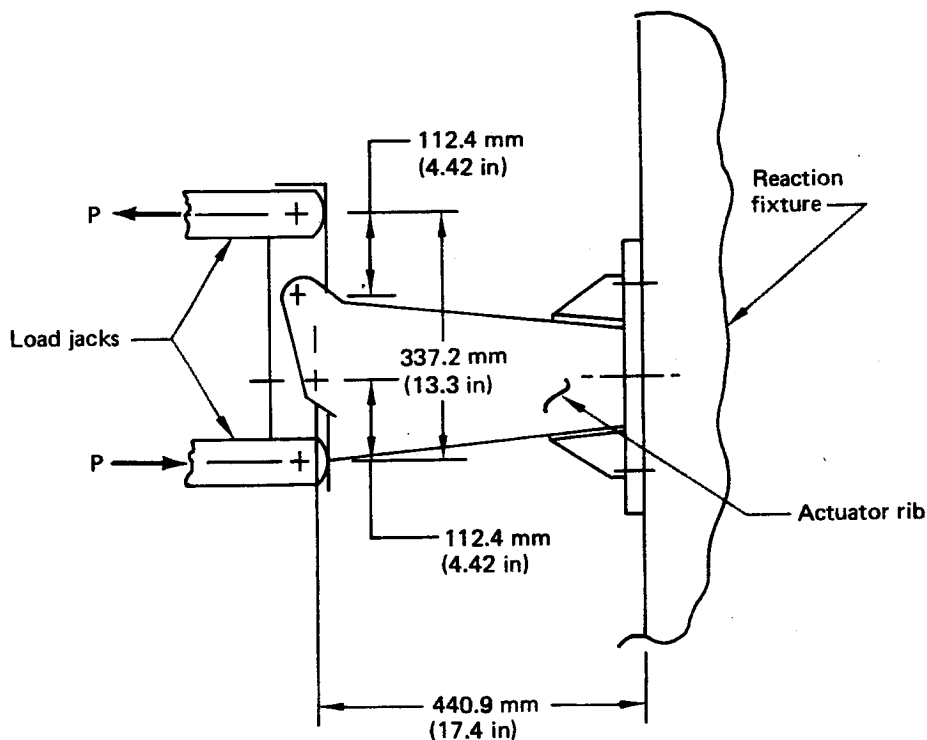


Figure 86. Actuator Rib Test Setup Schematic (Test 14)

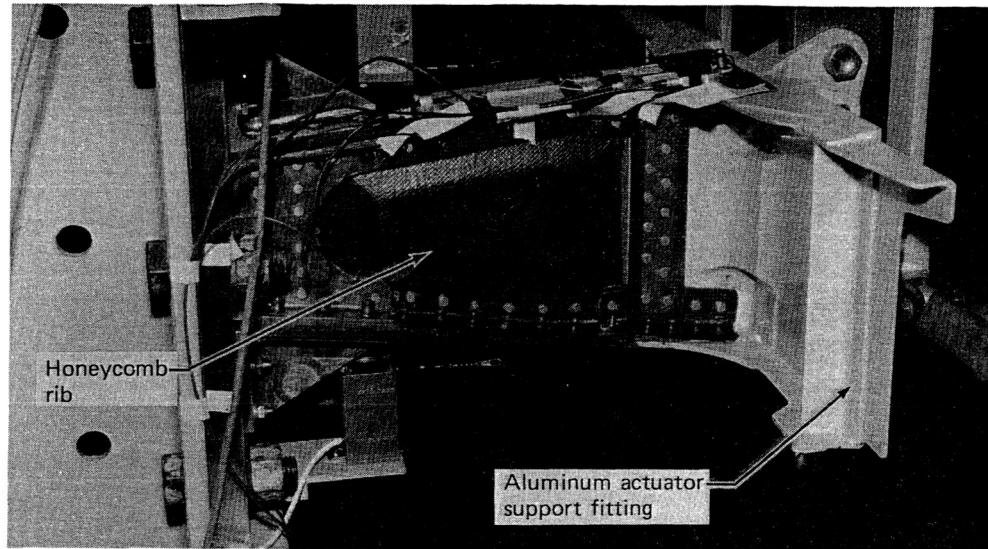


Figure 87. Actuator Support Rib Test

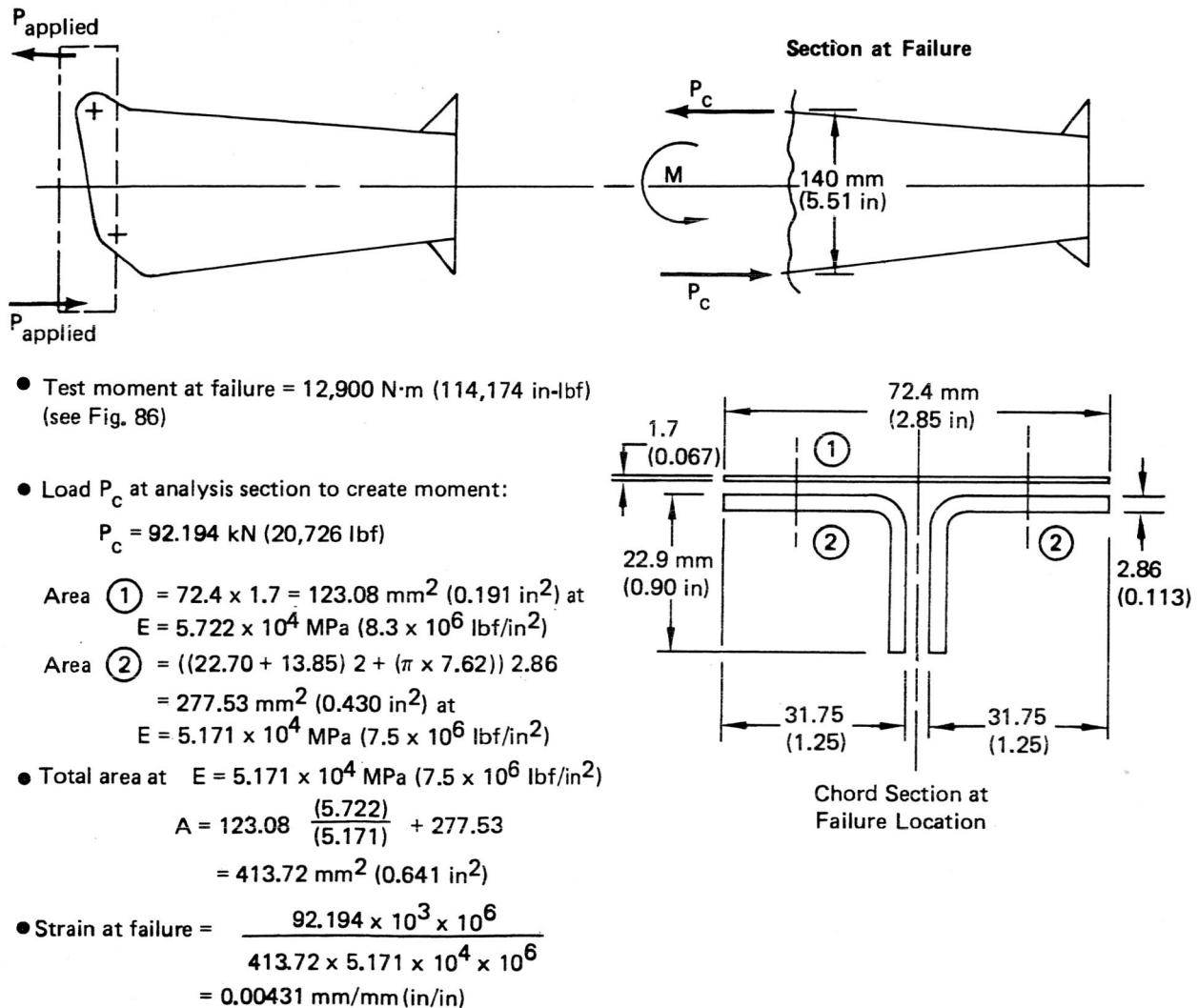


Figure 88. Actuator Rib Chord, Strain at Failure

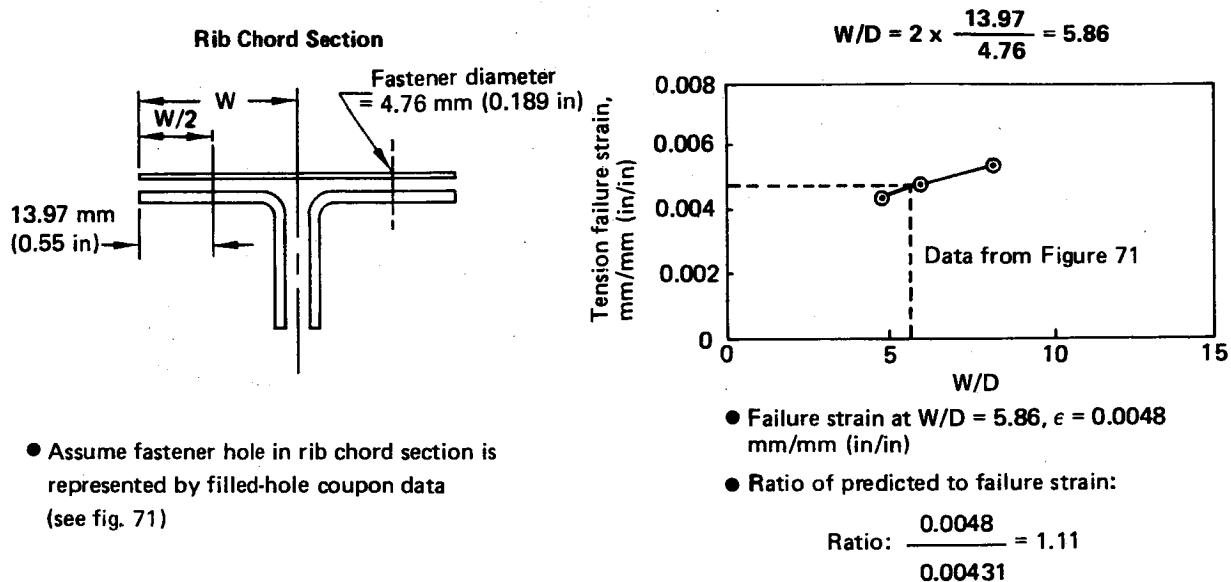


Figure 89. Actuator Rib Chord, Predicted Failure Strain

4.2.3.7 Front Spar Actuator Fitting Splice Test

Three specimens that contained the front spar actuator fitting splice region (Test 11) were subjected to static and fatigue tests. The test article consisted of a section of front spar, actuator fitting, and splice parts. The overall specimen dimensions are shown in Figure 90. The specimen was mounted as a cantilever beam with lateral restraining straps as shown in the test setup in Figure 90. Two specimens were statically tested; one specimen dry at room temperature and one specimen wet at 71°C (160°F). The third specimen was fatigue tested.

The elevated-temperature/wet static specimens were tested in an insulated plywood box that maintained the required environment during test. This test setup is shown in Figure 91. Deflections were measured along the specimen at several locations.

The room-temperature/dry static specimen failed at an applied load of 10.68 kN (2400 lbf). The failure occurred in the tension chord at a fastener hole, as shown in Figure 92.

The elevated-temperature/wet static specimen was conditioned at 60°C (140°F) in the test chamber with 100% RH for approximately 70 days. When tested at 71°C (160°F), the failure load was 11.03 kN (2480 lbf) and the failure occurred at the same location as the dry static specimen. The similarity in failure load is consistent with open-hole coupon data that indicate that for quasi-isotropic laminates, the room-temperature/dry and the 71°C (160°F)/wet tension values are similar (see fig. 55).

The maximum spanwise tension strain indicated by the elevator finite-element model in the region just outboard of the splice is 0.0019 mm/mm (in/in). For the test specimen, a strain of 0.0027 mm/mm was measured in the same region. Thus, the test results indicate that this area has a capacity 1.40 times that required.

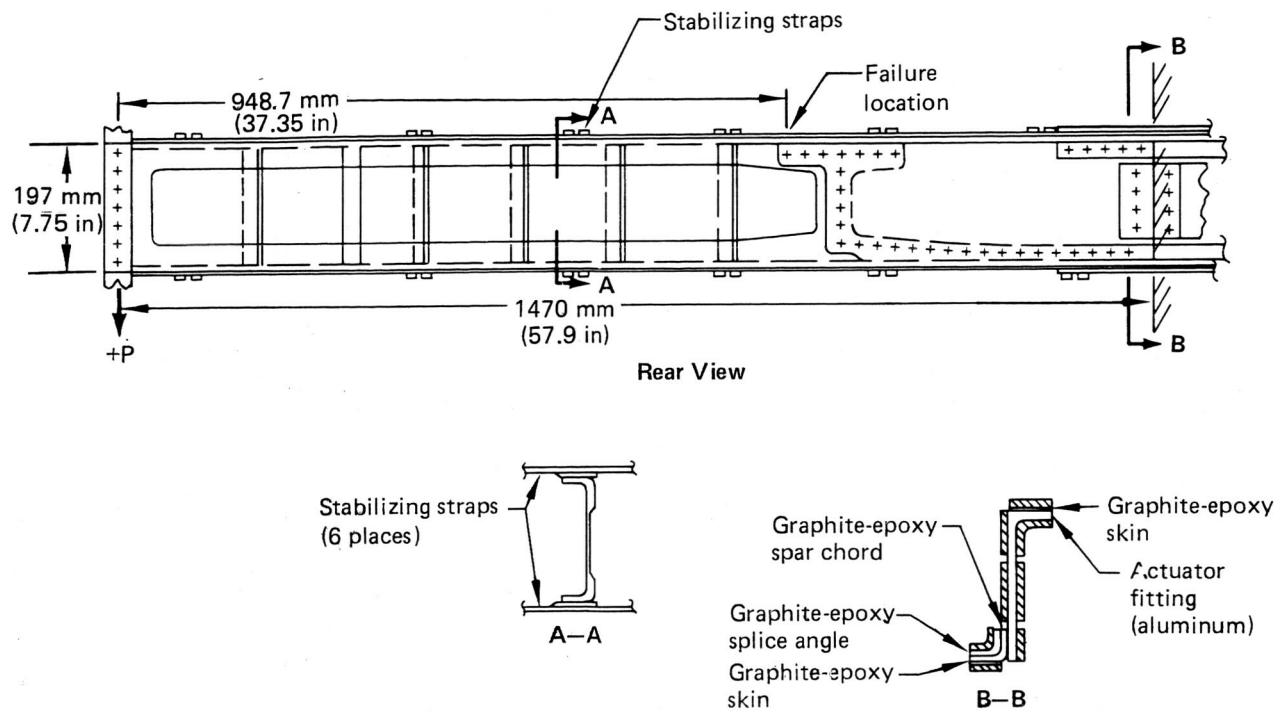


Figure 90. Front-Spar Actuator Fitting Splice Test Schematic (Test 11)

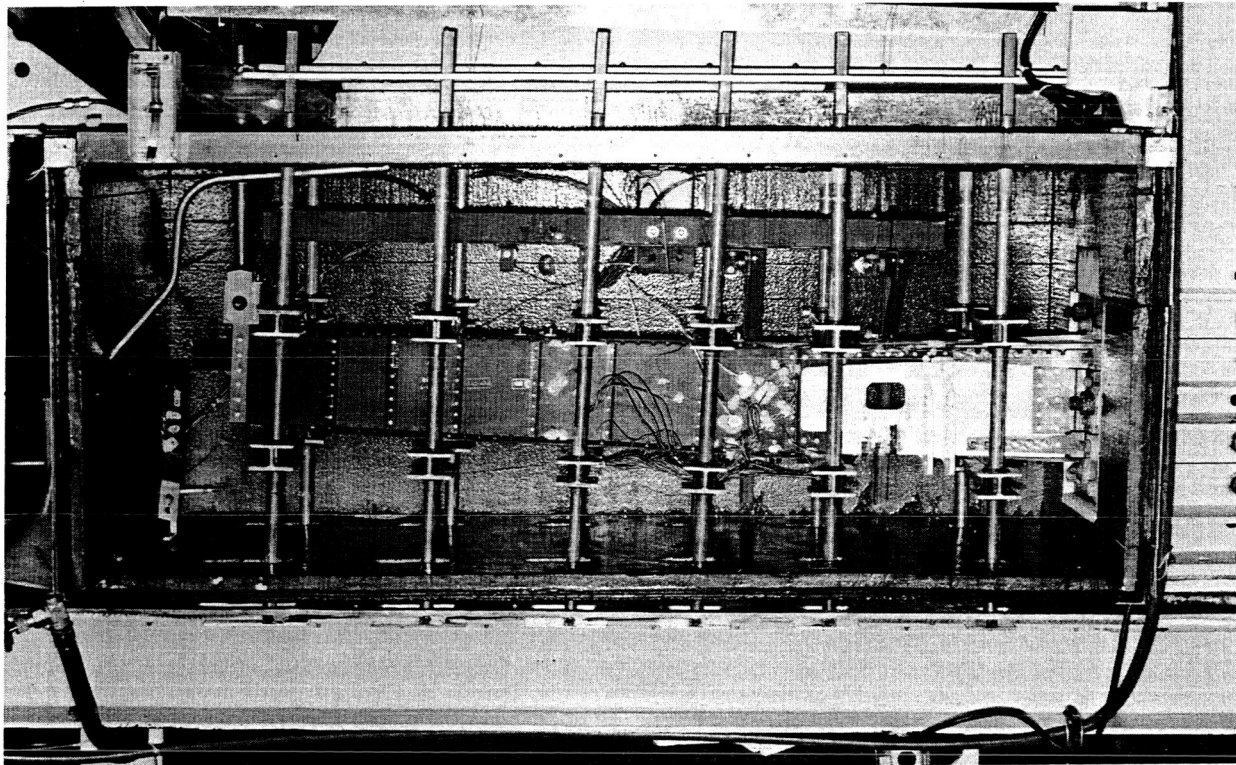


Figure 91. Front-Spar Actuator Fitting Splice Environmental Control Chamber (Test 11)

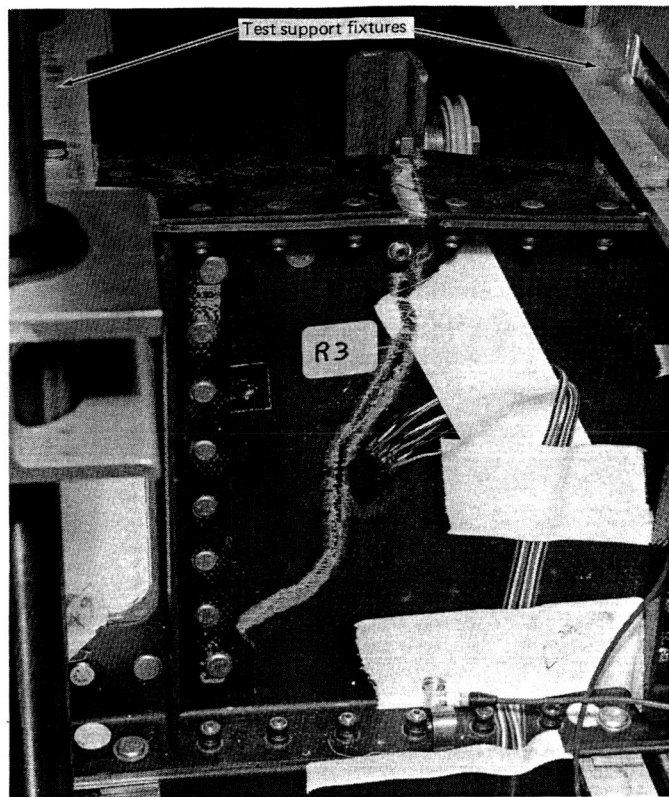


Figure 92. Front-Spar Actuator Fitting Splice Test Specimen Failure (Test 11)

The calculation procedure to predict the test failure strain is presented in Figure 93. This analysis indicates that the test and predicted values are within 9%.

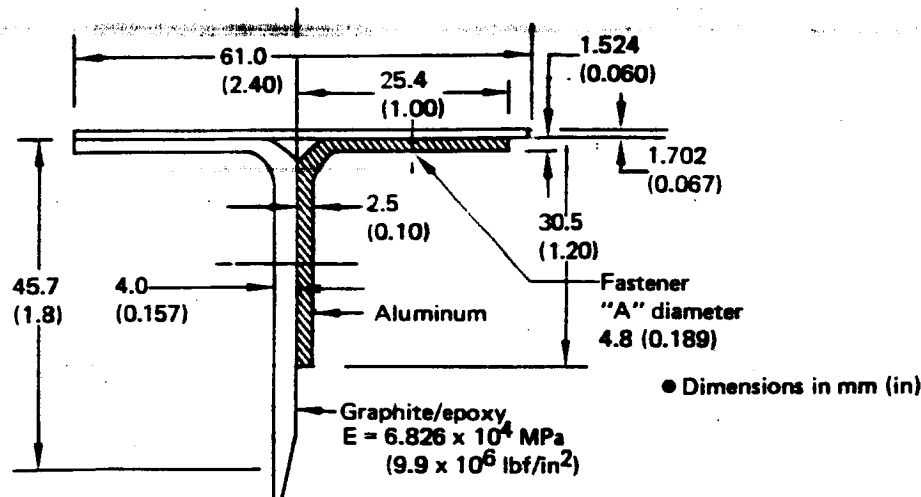
The fatigue specimen was subjected to a repeated-load test. The applied loading was 1.045 kN (235 lbf) down and 0.516 kN (116 lbf) up. Blocks of 25,000 load cycles were applied alternately in an environment of 35°C (95°F) and 100% RH, and then at laboratory ambient temperature and relative humidity.

At the conclusion of one lifetime (225,000 cycles), a design limit load was applied and deflections recorded. Cycling (elevated-temperature/wet) then was continued for a second lifetime, and deflection measurements again were recorded. Comparison of deflections taken during the room-temperature/dry static tests with those taken at the aforementioned limit load showed close agreement.

A thorough X-ray inspection of the graphite-epoxy portion of the test specimen at the conclusion of the test did not reveal any fatigue damage. An inspection of the aluminum actuator fitting also revealed no fatigue cracks.

After having undergone the equivalent of two service lifetimes (450,000 load cycles), the fatigue specimen was deliberately damaged by impact, sawcut, and delaminations at several locations. The damage locations and descriptions are shown in Figure 94. The test specimen then was subjected to a design limit load before a third equivalent service lifetime of 225,000 cycles was applied. The fatigue loads and environment were the same as for the first two lifetimes. At the completion of the third lifetime of cycling, the test specimen first was loaded to design limit load and then to design ultimate load without failure. Finally, a fourth lifetime of 225,000 cycles was applied and again, at its completion, both limit and ultimate loads were applied without structural failure.

Front Spar Actuator Fitting Splice Area, Section of Upper Chord at Failure



- At the failure section, the gross area strain is given by:

$$\epsilon_c = \frac{P_c}{A_c E_c}$$

- The area at this section is the sum of the aluminum and graphite:

Graphite area 324.5 mm² (0.503 in²)

Aluminum area = 116.1 mm² (0.180 in²)

- The total area = 441.8 mm² (0.685 in²) at

$E = 6.826 \times 10^4 \text{ MPa} (9.9 \times 10^6 \text{ lbf/in}^2)$

- On the assumption that fastener "A" loads up the aluminum adjacent to the skin to the strain ϵ_c , the load in this fastener is:

$$P_F = \epsilon_c A_A E_A$$

- On the assumption that this fastener load in the 1.702 mm (0.067 in) thick graphite skin causes a bearing failure, which initiates the final failure, the critical fastener load is:

$P_F = (\text{bearing stress}) (\text{thickness}) (\text{fastener diameter})$

Critical bearing stress = 703 MPa (102,000 lbf/in²)
(see fig. 68)

$$P_F = 703 \times 1.702 \times 4.8 = 5.759 \text{ kN} (1295 \text{ lbf})$$

- The chord strain, ϵ_c , in the aluminum is:

$$\epsilon_c = \frac{5759}{1.524 \times 25.4 \times 6.895 \times 10^4} = 0.002158 \text{ mm/mm (in/in)}$$

- Assuming that this strain exists across the total chord section, the chord strain outboard of the splice area, in the all-graphite section, would be:

$$\epsilon_{GR} = 0.002158 \frac{441.8}{(324.5)} = 0.002938 \text{ mm/mm (in/in)}$$

- The strain measured at this section in the test was 0.0027; therefore the ratio of predicted to test would be:

$$\text{Ratio} = \frac{0.002938}{0.0027} = 1.09$$

Figure 93. Front-Spar Actuator Fitting Splice Predicted Failure Load

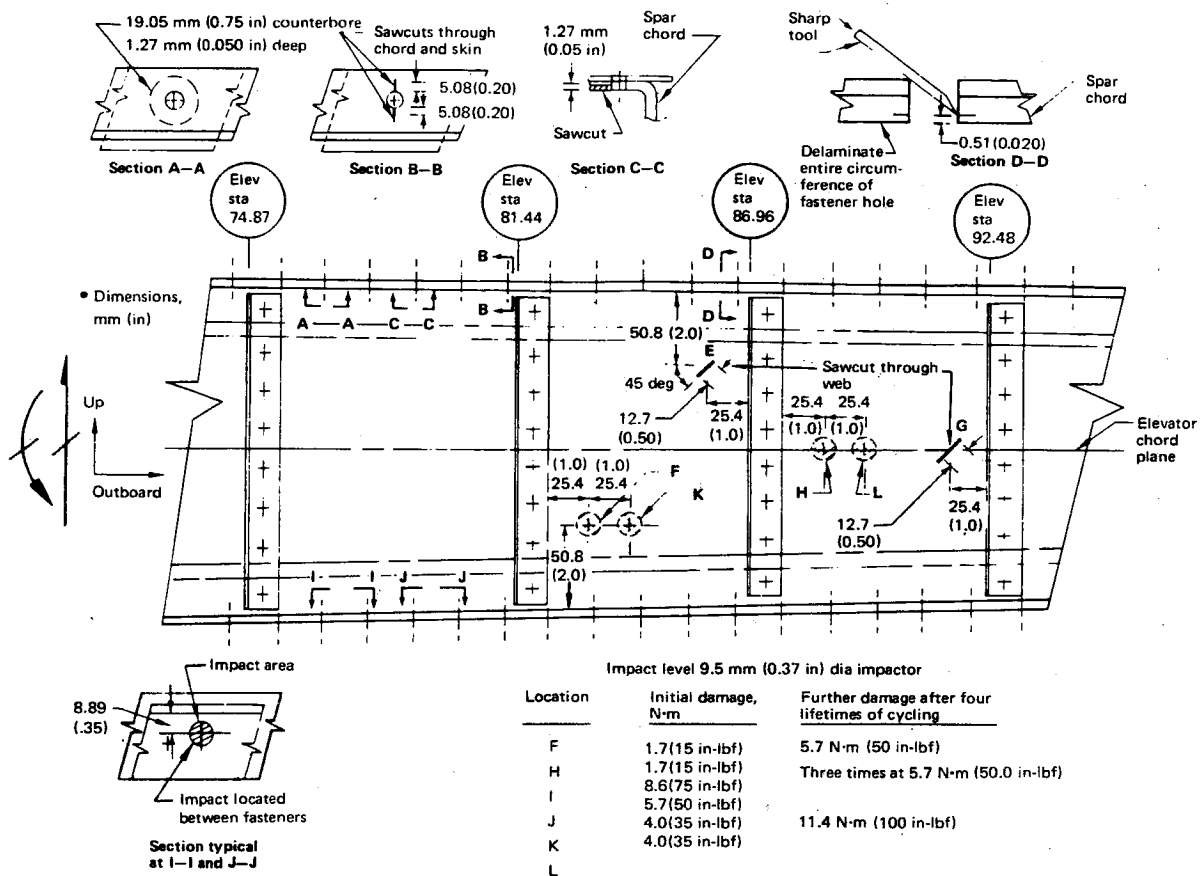


Figure 94. Front-Spar Actuator Fitting Specimen Damage Areas

Ultrasonic and X-ray inspections were conducted at 25,000-cycle intervals during the test and after application of both limit and ultimate loads at the end of each test. Evaluation of these inspections showed no damage propagation.

The damage previously inflicted was extended to create significant and easily detectable damage. One-third of the tension spar chord was cut, the compression spar chord was damaged with 11.4 N-m (100 in-lbf) of impact energy, and the spar web was damaged with 5.7 N-m (50 in-lbf) of impact energy. The tension spar chord cut is shown in Figure 95. The test specimen was loaded to design limit load in an environment of 71°C (160°F) and 100% RH without failure. Then, in an environment of ambient temperature and relative humidity, the specimen was loaded until it failed. The specimen failed at 7.59 kN (1706 lbf), failure initiating at the sawcut in the tension (upper) chord and progressing across the web, as shown in Figure 96.

Deflections were measured during both the limit load and destruction tests. A plot of the vertical deflection measured at the loaded end of the test specimen during the destruction test is shown in Figure 97. A plot of load versus deflection for both the room-temperature/dry and elevated-temperature/wet static specimens also is presented in Figure 97. This comparison indicates that all three specimens had similar stiffness.

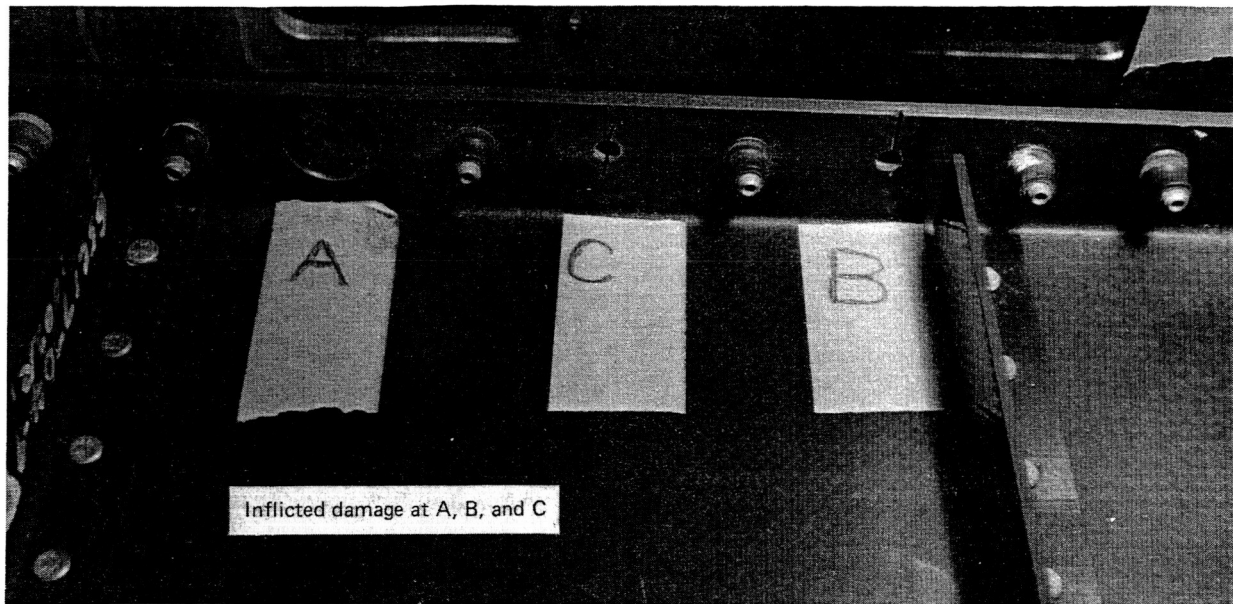


Figure 95. Front-Spar Actuator Fitting Specimen, Tension Chord Saw Cut

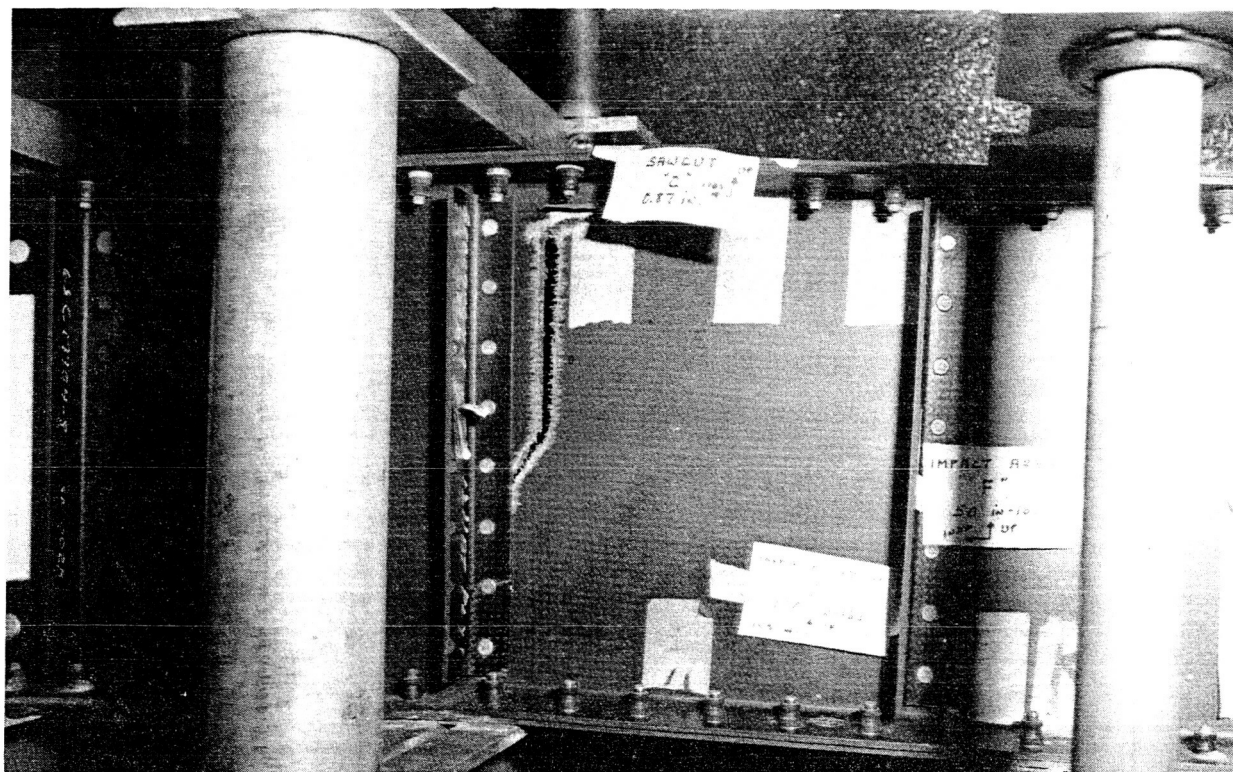


Figure 96. Front-Spar Actuator Fitting, Failed Durability Test Specimen

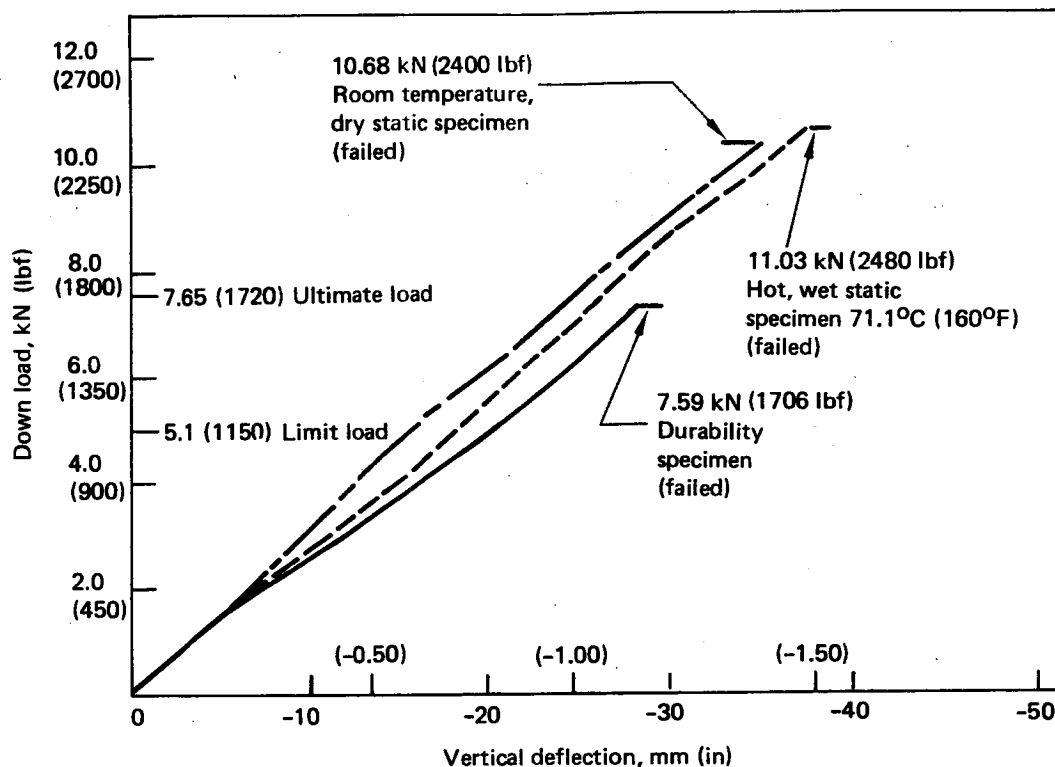


Figure 97. Front-Spar Actuator Fitting Specimen, Measured Vertical Deflections

Significant conclusions from this test program are summarized as follows:

- The apparent static strength of an undamaged test article was unaffected by the effects of absorbed moisture in a high-temperature environment (see fig. 97).
- Modulus of elasticity values were not significantly changed by environmental conditioning and fatigue cycling (see fig. 97).
- Significant detectable damage did not propagate during two service lifetimes of fatigue cycling.

4.2.3.8 Elevator Outboard Section

An outboard section (Test 17) of the 727 graphite-epoxy elevator was tested to verify the basic design and to obtain stiffness measurements. The test specimen was a full-scale outboard section complete with hinge fittings from elevator station 99.79 to stabilizer station 220.00. The section was approximately 3.0m (118 in) long and included end ribs for torsional load input and reaction. Photographs of the specimen are shown in Figures 98 and 99.

The specimen was tested on a structural test strongback and all loads were applied with hydraulic actuators. Photographs of the test setup are shown in Figures 100 and 101. Fifty strain-gage rosettes and eight deflection indicators were installed on the specimen to measure strains and deflections.

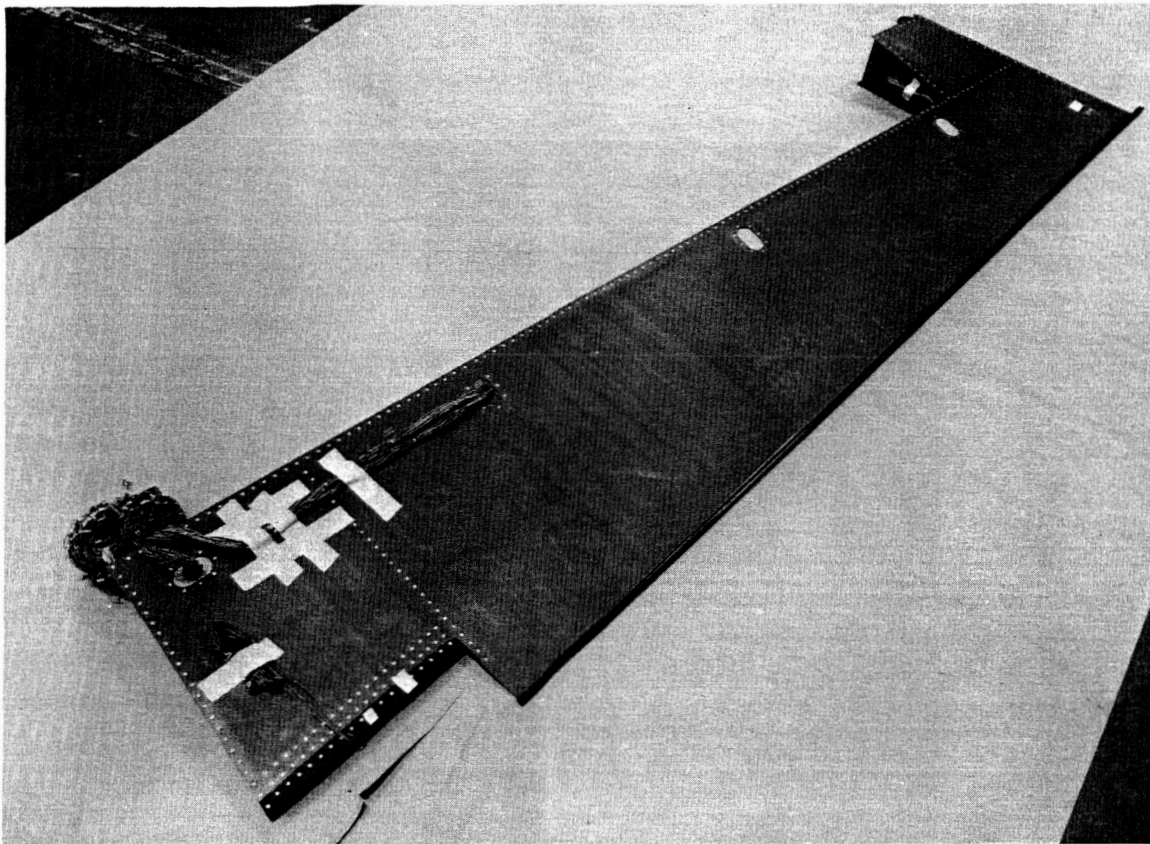


Figure 98. Elevator Test Box Lower Surface (Test 17)

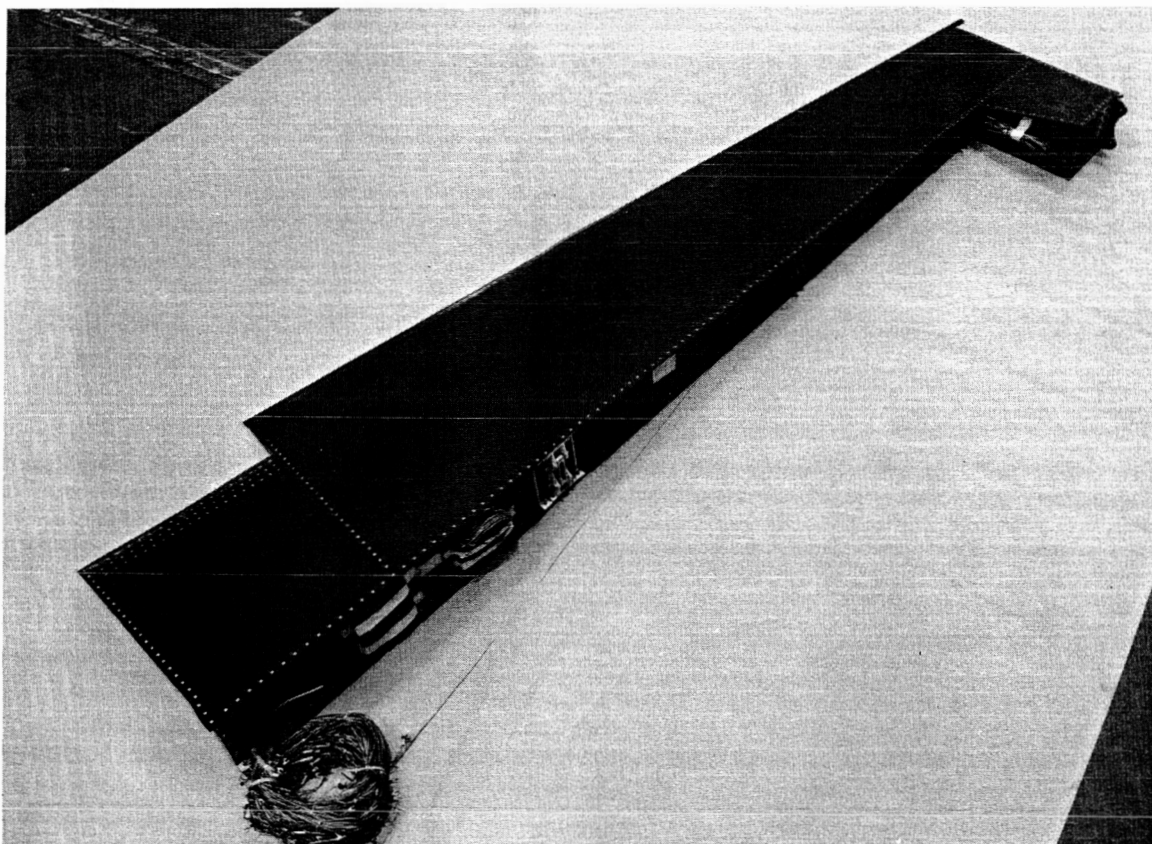


Figure 99. Elevator Test Box Upper Surface (Test 17)

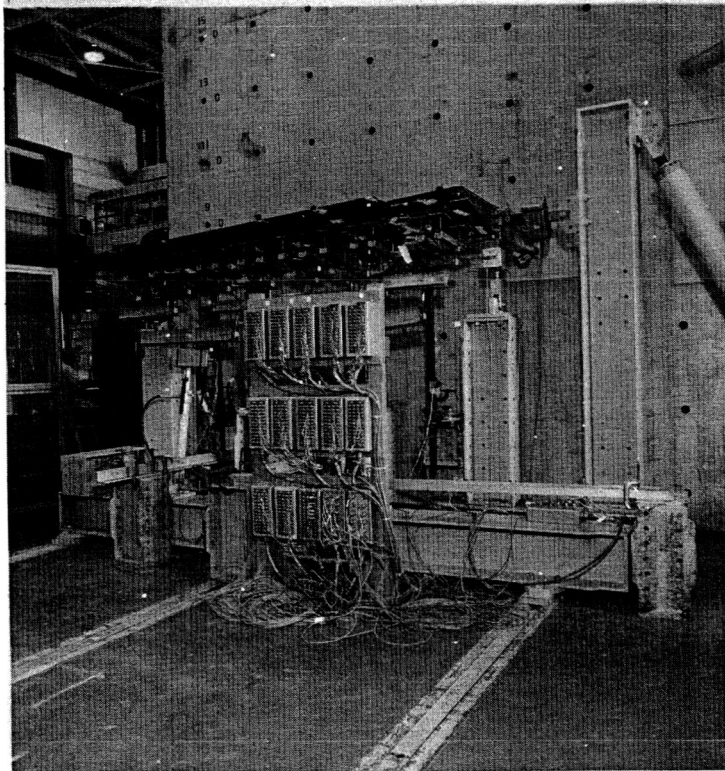


Figure 100. Elevator Outboard Box Test Setup (Test17)

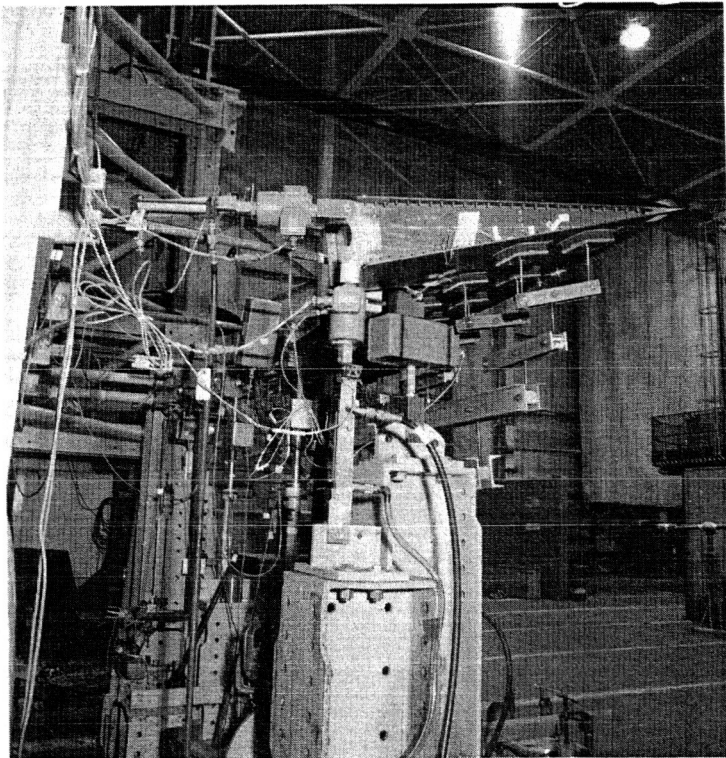


Figure 101. Elevator Outboard Box Test Setup (Test17)

An ATLAS finite-element model of the elevator outboard section was extracted from the initial complete model of the elevator and stabilizer. This finite-element model is shown in Figure 102.

A comparison in torsional windup between the test article and the finite-element model is presented in Figure 103.

The test results are summarized as follows:

- o The test box was loaded to 135% of design ultimate load with no failures. Thus, the basic design strength was verified.
- o The torsion windup of the box agreed closely with the ATLAS finite-element predictions. Thus, stiffness predictions were verified.

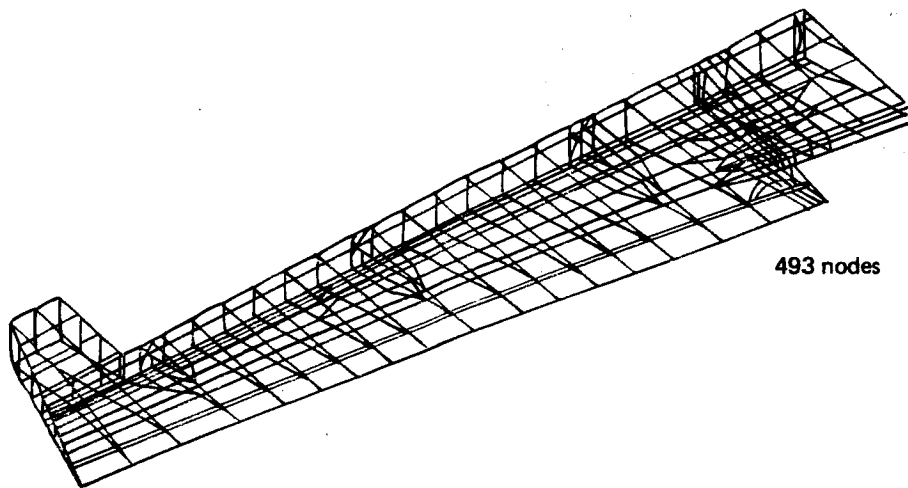


Figure 102. Elevator Outboard Box Section—Finite Element Model

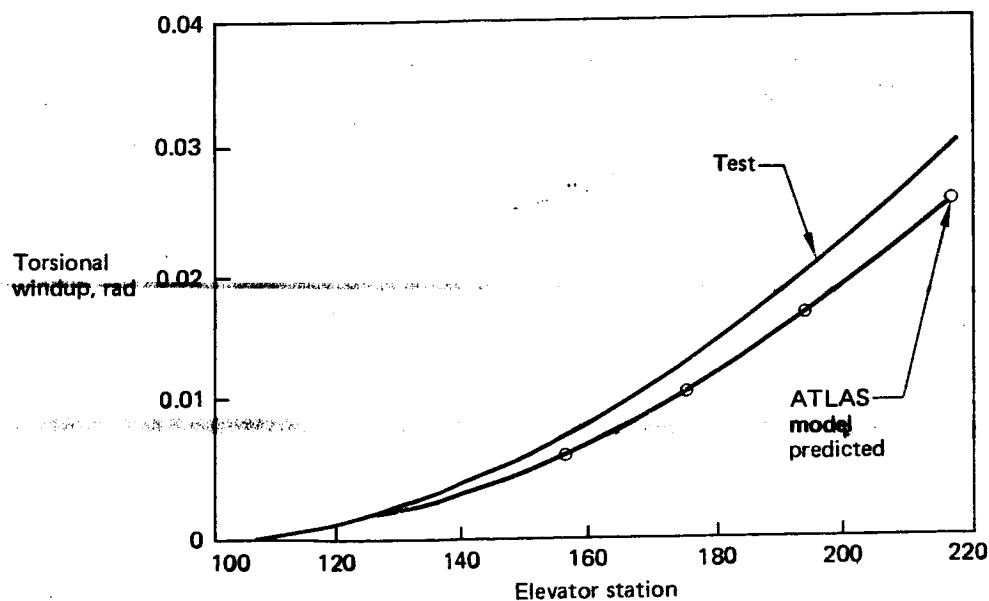


Figure 103. Elevator Outboard Box Section Test—Torsion Windup Test and Prediction Comparison

4.2.3.9 Sonic Test of Elevator Box Section

Two boxes (Test 15) were sonically tested to evaluate the effect of sonic environment on the elevator structure. The first box contained a front spar section, two closure ribs, and an upper and lower skin panel. The primary details that were evaluated in this configuration were the skin-to-spar attachment and the trailing-edge wedge detail. This elevator test section was approximately 1680 x 711 mm (66 x 28 in) and was mounted vertically in the sonic chamber as shown in Figure 104.

The box was tested for 15 hr at 155-dB OASPL and 4 hr at 158-dB OASPL. This testing represented two lifetimes of in-service damage. The box then was damaged by impacting the honeycomb panel and edgebands at 12 locations. The damaged areas were evaluated using a hand-held ultrasonic inspection instrument. The box then was tested for an additional in-service lifetime (4 hr at 158-dB OASPL). Post-test inspections revealed no apparent propagation of the damage areas.

The second box that was sonically tested contained a front spar section, two closure ribs, and a rear spar section. The primary purpose of this test was to evaluate the attachment of the skin panels to the rear spar. This test box was the same size as the first box. The box was tested for 8 hr at 158-dB OASPL and then damaged by impacting the panel and rear spar at a total of 18 locations. An additional 4 hr of testing at 158-dB OASPL did not cause any apparent propagation of the inflicted damage.

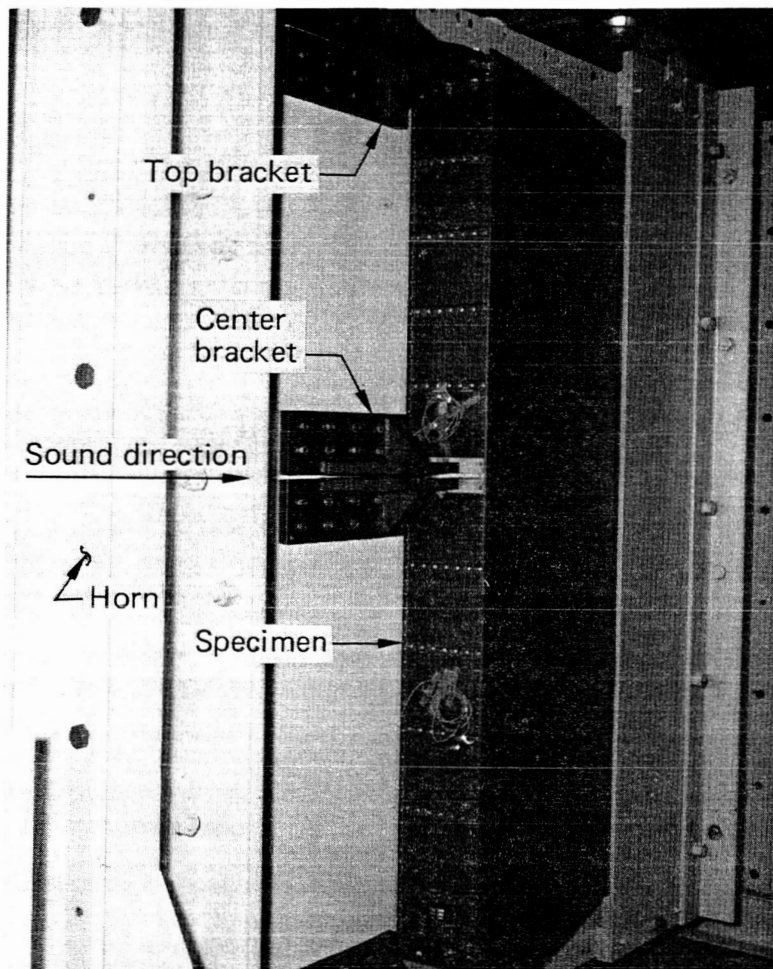
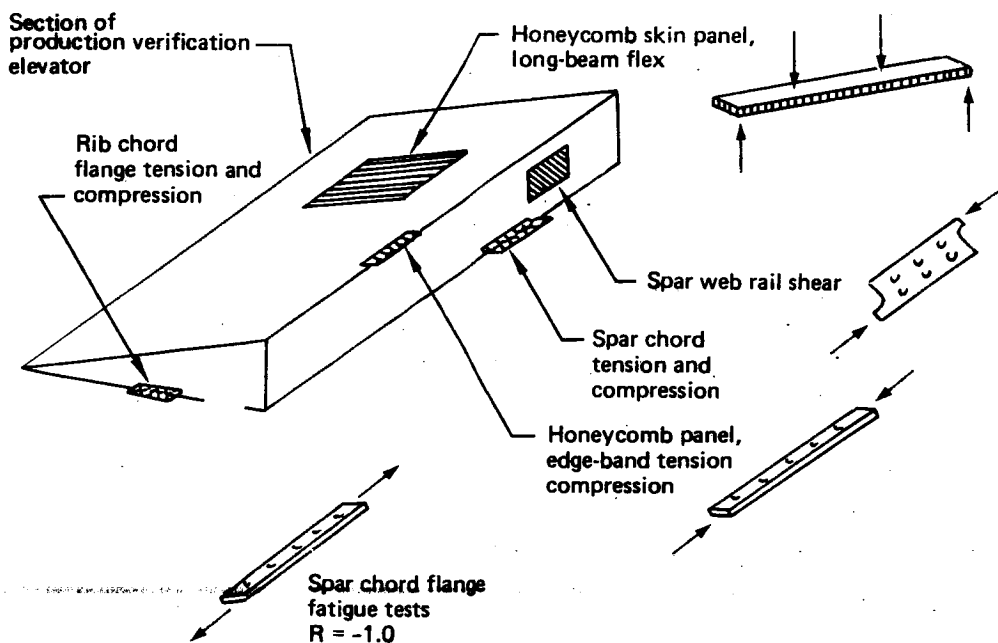


Figure 104. Elevator-Box Sonic Test Setup (Test 15)

4.2.4 PRODUCTION HARDWARE VERIFICATION TESTS

Tests of laminate and honeycomb coupons cut from an elevator production verification section were performed. The specimen configurations and the areas on the verification hardware from which the specimens were taken are shown in Figure 105. The test results are presented in Table 9 and, when compared with the ancillary test program coupon data, indicate that the production process produces an acceptable quality laminate. As noted in Table 9, six specimens were fatigue loaded to 500,000 cycles at $R = -1.0$ at a maximum load equal to 25% of the static ultimate capability. These specimens then were loaded statically to failure. When compared with similar specimens, the residual test results indicate that the applied cyclic loading at ambient conditions had no significant effect on the ultimate load capability of the tested configuration.



- Specimens taken from parts fabricated on production tools
- All tests conducted at room temperature

Figure 105. Production Verification Hardware Test Coupons

Table 9. Verification Hardware Coupon Test Results

Specimen number	Specimen location	Laminate definition	Specimen width, mm	Specimen nominal thickness, mm	Nominal area, mm ²	Failure load, N	Specimen type	Hole diameter, mm	Gross stress, MPa	Nominal modulus, GPa	Gross strain, mm/mm	
65C17719		4								5		
1	Front spar chord	1	25.43	2.565	65.23	31 450	Tension	4.724	482.2	78.60	0.0061	
2	Front spar chord	1	25.35	2.565	65.02	17 660	Compression	4.750	271.6	78.60	0.0035	3
3	Front spar chord	1	25.43	2.565	65.23	33 270	Tension	4.750	510.1	78.60	0.0065	1
4	Front spar chord	1	25.43	2.565	65.23	28 240	Tension	4.724	433.1	78.60	0.0055	
5	Rear spar chord	2	25.40	0.762	19.35	2 958	Tension	4.750	152.8	20.68	0.0074	
6	Rear spar chord	2	25.43	0.762	19.38	4 937	Compression	4.775	255.1	20.68	0.0123	3
7	Rear spar chord	2	25.37	0.762	19.33	2 615	Tension	4.750	135.1	20.68	0.0065	1
8	Rear spar chord	2	—	—	—	—	—	—	—	—	—	2
9	Rib chord	3	25.40	1.905	48.39	13 300	Compression	4.750	274.9	49.64	0.0055	
10	Rib chord	3	25.40	1.905	48.39	14 300	Tension	4.724	295.6	49.64	0.0060	
11	Rib chord	4	22.89	1.727	39.53	10 385	Tension	4.750	236.8	43.44	0.0055	
12	Rib chord	4	22.86	1.727	39.48	11 300	Compression	4.293	257.5	43.44	0.0059	
13	Skin panel	5	76.40	0.279	21.32	1 539	Beam	—	387.3	54.47	0.0071	6
14	Skin panel	5	76.45	0.279	21.33	1 503	Beam	—	378.3	54.47	0.0069	6
15	Front spar web	7	76.15	1.334	101.58	33 180	Shear	2.489	326.6	29.30	0.0111	
16	Skin edge band—front spar	6	25.43	1.702	43.28	9 185	Tension	4.750	212.2	46.89	0.0045	
17	Skin edge band—front spar	6	25.43		43.28	12 720	Tension	4.750	293.9	46.89	0.0063	
18	Skin edge band—front spar	6	25.43		43.28	10 185	Tension	4.775	235.3	46.89	0.0050	1
19	Skin edge band—front spar	6	25.40		43.23	10 275	Tension	4.775	237.7	46.89	0.0051	1
20	Skin edge band—rear spar	6	25.45		43.32	7 205	Compression	4.775	166.5	46.89	0.0036	1 3
21	Skin edge band—rear spar	6	25.45		43.32	11 610	Compression	4.801	268.2	46.89	0.0057	1
22	Skin edge band—rear spar	6	25.40		43.23	11 740	Compression	4.750	271.7	46.89	0.0058	
23	Skin edge band—rear spar	6	25.43		43.28	12 100	Compression	4.775	279.5	46.89	0.0060	
24	Skin edge band—rib	6	25.45		43.32	12 790	Tension	4.750	295.4	57.23	0.0052	
25	Skin edge band—rib	6	25.45		43.32	11 700	Tension	4.750	270.2	57.23	0.0047	
26	Skin edge band—rib	6	25.45		43.32	13 480	Compression	4.775	311.4	57.23	0.0054	
27	Skin edge band—rib	6	25.45	1.702	43.32	11 650	Compression	4.750	269.2	57.23	0.0047	
28	Front spar web	7	—	—	—	—	—	—	—	—	—	2
29	Front spar web	7	76.07	1.334	101.48	38 250	Shear	2.515	377.2	29.30	0.0129	
30	Skin panel	5	76.45	0.279	21.33	1 370	Beam	—	344.8	54.47	0.0063	6
31	Skin panel	5	76.48	0.279	21.34	1 383	Beam	—	348.1	54.47	0.0064	6
32	Skin panel	5	76.45	0.279	21.33	1 454	Beam	—	366.0	54.47	0.0067	6
33	Skin panel	5	76.48	0.279	21.34	1 517	Beam	—	381.7	54.47	0.0070	6



Residual strength after fatigue test



Specimen lost during fabrication



Invalid test, specimen did not fail in test section



Structural laminate definition—all plies are fabric except as noted

1— 10 plies 0 deg tape

6— 2 plies 90-deg tape

6 plies ±45 deg

4 plies ±45 deg

2— 4 plies ±45 deg

4 plies 0/90 deg

3— 4 plies ±45 deg

7— 6 plies ±45 deg

6 plies 0/90 deg

4— 4 plies ±45 deg

5 plies 0/90 deg

5— 1 ply ±45 deg Each

1 ply 90-deg tape face



Modules in test direction



Honeycomb panel: 13.97-mm thick core—
0.279-mm thick face sheet

Table 9. Verification Hardware Coupon Test Results (Continued)

Specimen number 65C17/19	Specimen location	Laminate definition 4	Specimen width, in	Specimen nominal thickness, in	Nominal area, in ²	Failure load, lb	Specimen type	Hole diameter, in	Gross stress, lbf/in ²	Nominal modulus, lbf/in ² × 10 ⁶ 5	Gross strain, in/in	
1	Front spar chord	1	1.001	0.101	0.1011	7070	Tension	0.186	69,931	11.4	0.0061	
2	Front spar chord	1	0.999	0.101	0.1008	3970	Compression	0.187	39,385	11.4	0.0035	3
3	Front spar chord	1	1.001	0.101	0.1011	7480	Tension	0.187	73,986	11	0.0065	1
4	Front spar chord	1	1.001	0.101	0.1011	6350	Tension	0.186	62,809	11.4	0.0055	
5	Rear spar chord	2	1.000	0.030	0.0300	665	Tension	0.187	22,167	3.0	0.0074	
6	Rear spar chord	2	1.001	0.030	0.0300	1110	Compression	0.188	37,000	3.0	0.0123	3
7	Rear spar chord	2	0.999	0.075	0.0300	588	Tension	0.187	19,600	3.0	0.0065	1
8	Rear spar chord	2	-	-	-	-	-	-	-	-	-	2
9	Rib chord	3	1.000	0.075	0.0750	2990	Compression	0.187	39,867	7.2	0.0055	
10	Rib chord	3	1.000	0.075	0.0750	3215	Tension	0.186	42,867	7.2	0.0060	
11	Rib chord	4	0.901	0.068	0.0613	2335	Tension	0.187	34,338	6.3	0.0055	
12	Rib chord	4	0.900	0.068	0.0612	2540	Compression	0.169	37,353	6.3	0.0059	
13	Skin panel	5	3.008	0.011	0.0330	346	Beam	-	56,169	7.9	0.0071	6
14	Skin panel	5	3.010	0.011	0.0330	338	Beam	-	54,870	7.9	0.0069	6
15	Front spar web	7	2.998	0.02525	0.1575	7460	Shear	0.098	47,365	4.3	0.0111	
16	Skin edge band—front spar	6	1.001	0.067	0.0671	2065	Tension	0.187	30,775	6.8	0.0045	
17	Skin edge band—front spar	6	1.001		0.0671	2860	Tension	0.187	42,623	6.3	0.0063	
18	Skin edge band—front spar	6	1.001		0.0671	2290	Tension	0.188	34,128	6.3	0.0050	1
19	Skin edge band—front spar	6	1.000		0.0670	2310	Tension	0.188	34,478	6.3	0.0051	1
20	Skin edge band—rear spar	6	1.002		0.0671	1620	Compression	0.188	24,143	6.3	0.0036	1 3
21	Skin edge band—rear spar	6	1.002		0.0671	2610	Compression	0.189	38,897	6.3	0.0057	1
22	Skin edge band—rear spar	6	1.000		0.0670	2640	Compression	0.187	39,403	6.3	0.0058	
23	Skin edge band—rear spar	6	1.001		0.0671	2720	Compression	0.188	40,536	6.8	0.0060	
24	Skin edge band—rib	6	1.002		0.0671	2875	Tension	0.187	42,846	8.3	0.0052	
25	Skin edge band—rib	6	1.002		0.0671	2630	Tension	0.187	39,195	8.3	0.0047	
26	Skin edge band—rib	6	1.002		0.0671	3030	Compression	0.188	45,156	8.3	0.0054	
27	Skin edge band—rib	6	1.002	0.067	0.0671	2620	Compression	0.187	39,046	8.3	0.0047	
28	Front spar web	7	-	-	-	-	-	-	-	-	-	2
29	Front spar web	7	2.995	0.0525	0.1572	8600	Shear	0.099	54,707	4.3	0.0129	
30	Skin panel	5	3.010	0.011	0.0330	308	Beam	-	50,000	7.9	0.0063	6
31	Skin panel	5	3.011	0.011	0.0330	311	Beam	-	50,487	7.9	0.0064	6
32	Skin panel	5	3.010	0.011	0.0330	327	Beam	-	53,084	7.9	0.0067	6
33	Skin panel	5	3.011	0.011	0.0330	341	Beam	-	55,357	7.9	0.0070	6

- 1 Residual strength after fatigue test
 2 Specimen lost during fabrication
 3 Invalid test, specimen did not fail in test section
 4 Structural laminate definition—all plies are fabric except as

- notes
 1— 10 plies 0 deg tape 6— 2 plies 90-deg tape
 6 plies ±45 deg 4 plies ±45 deg
 2— 4 plies ±45 deg 4 plies 0/90 deg
 3— 4 plies ±45 deg 7— 6 plies ±45 deg
 6 plies 0/90 deg
 4— 4 plies ±45 deg
 5 plies 0/90 deg
 5— 1 ply ±45 deg Each
 1 ply 90-deg tape face

- 5 Modulus in test direction
 6 Honeycomb panel: 0.55-in thick core—
 0.011-in thick face sheet

4.2.5 LIGHTNING PROTECTION PANEL TESTS

Lightning protection system validation tests were performed on the elevator outboard upper surface. The lightning protection system was previously shown in Figure 11. Figure 106 shows the elevator lightning protection system test article. The test article incorporated the production configuration of the graphite-epoxy elevator skin panel and its attachment to the aluminum elevator nose skin panel. A production configuration aluminum bus bar grid and discharger bases were included. Production fasteners and material finish systems were used at all interfaces. Balance panel bay number 5 (elevator station 173.21 to 209.96) aluminum area, consisting of the elevator nose skin and balance panel, was simulated with a stiffened 457 x 914-mm (18 x 36-in) aluminum sheet as shown in Figure 106.

The test setup consisted of lightning test generators electrically connected to the test article by means of remote switches that allowed sequencing of the Zone 1B discharge, as schematically shown in Figure 107. The titanium strap length controlled the resistance of the test circuit. Circuit parameters were calculated and displayed by the computerized oscilloscope. Figure 108 shows the lightning test waveform and test values used for the test.

The test article, after the Zone 1B test was accomplished, is shown in Figure 109. There was no visible damage and subsequent NDI evaluation of the test article indicated no damage.

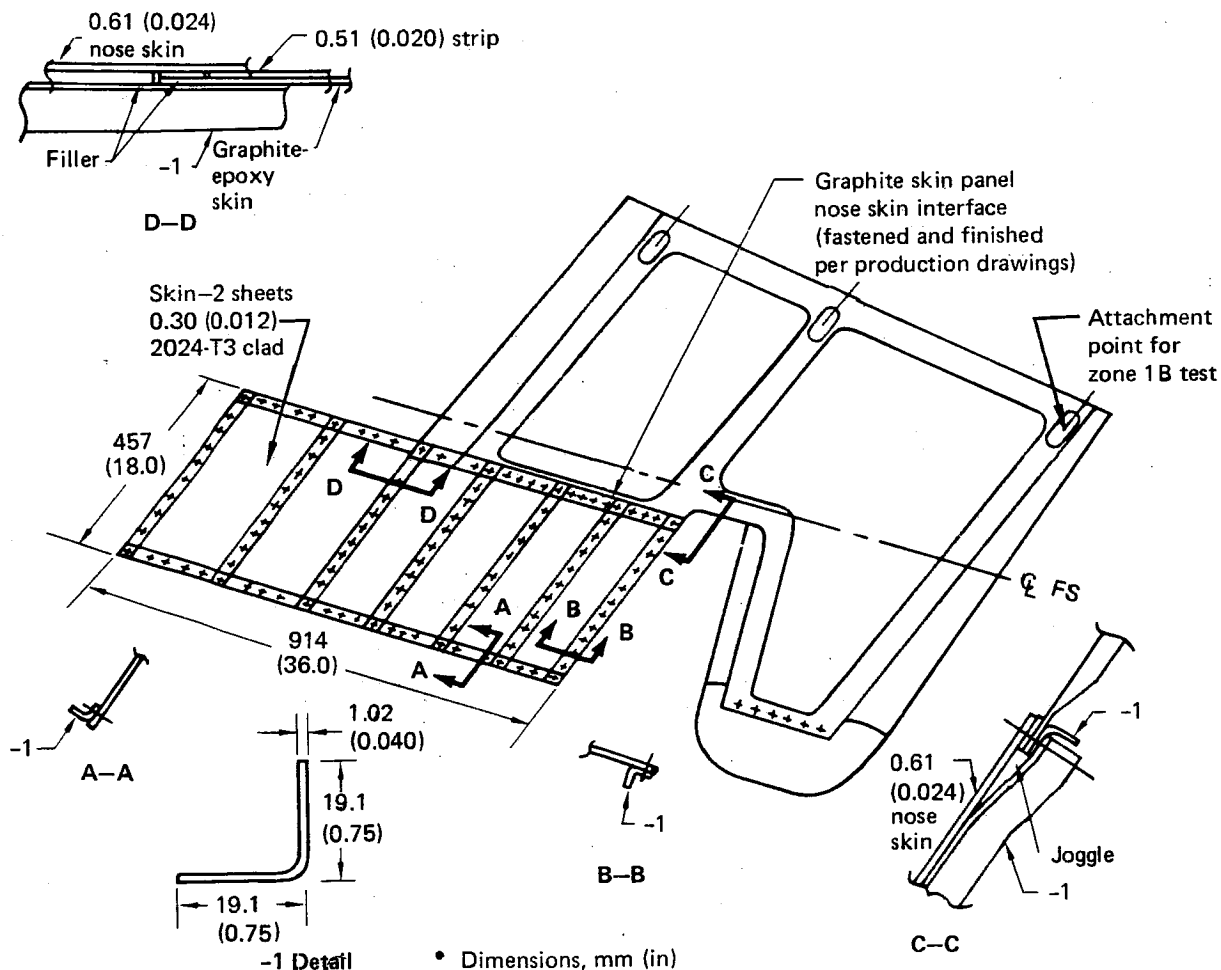


Figure 106. Graphite-Epoxy Elevator Lightning Test Article

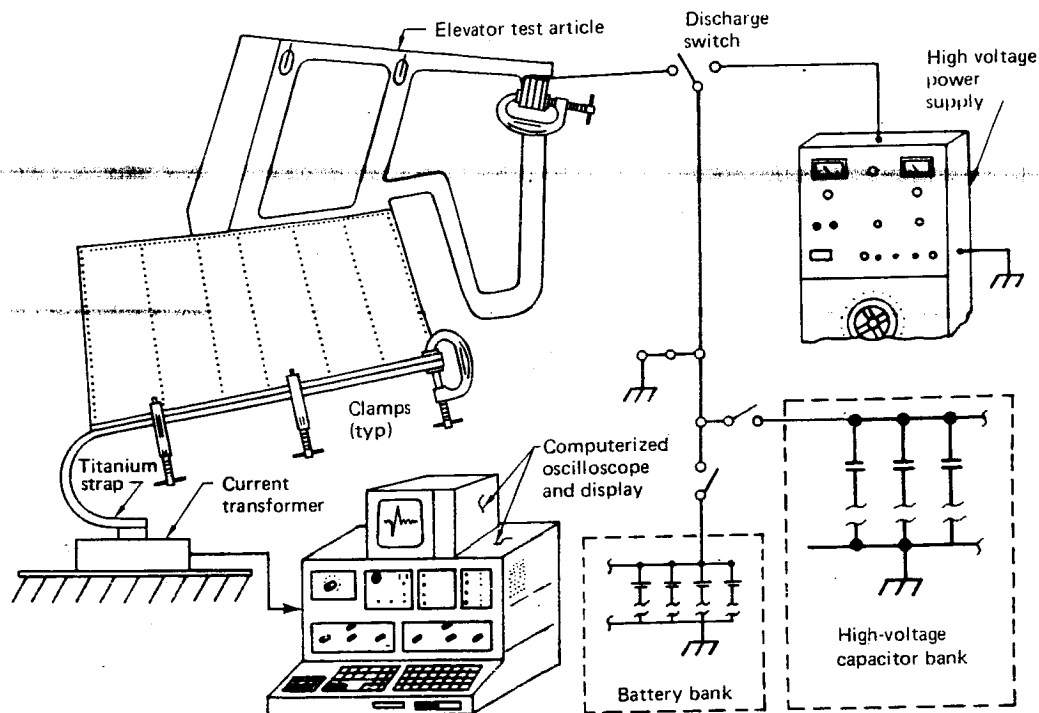
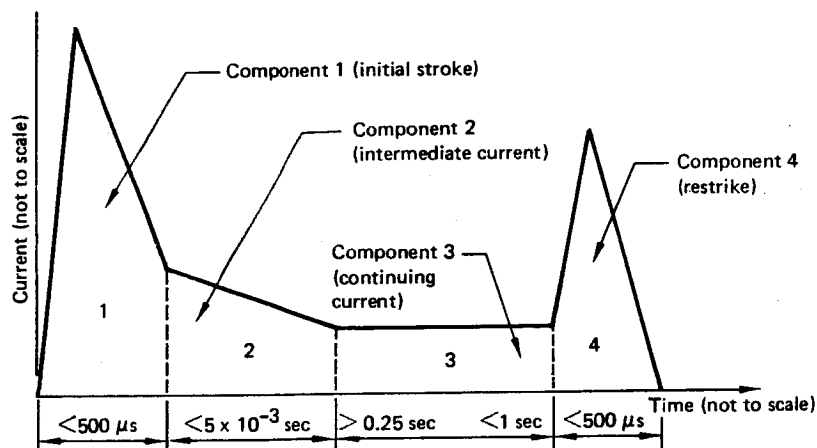


Figure 107. Lightning Laboratory Test Setup



Test waveform	Parameter	Boeing test value
Component 1	Peak current	211,000 amps
	Action integral	$3.95 \times 10^6 \text{ amps}^2\text{-sec}$
Component 2	Average current	2,030 amps
	Charge transfer	11.2 coulombs
Component 3	Average current	621 amps
	Charge transfer	230 coulombs
Component 4	Peak current	129,000 amps
	Action integral	$0.97 \times 10^6 \text{ amps}^2\text{-sec}$

Figure 108. Zone 1B Lightning Test Waveform and Test Values Used for Testing

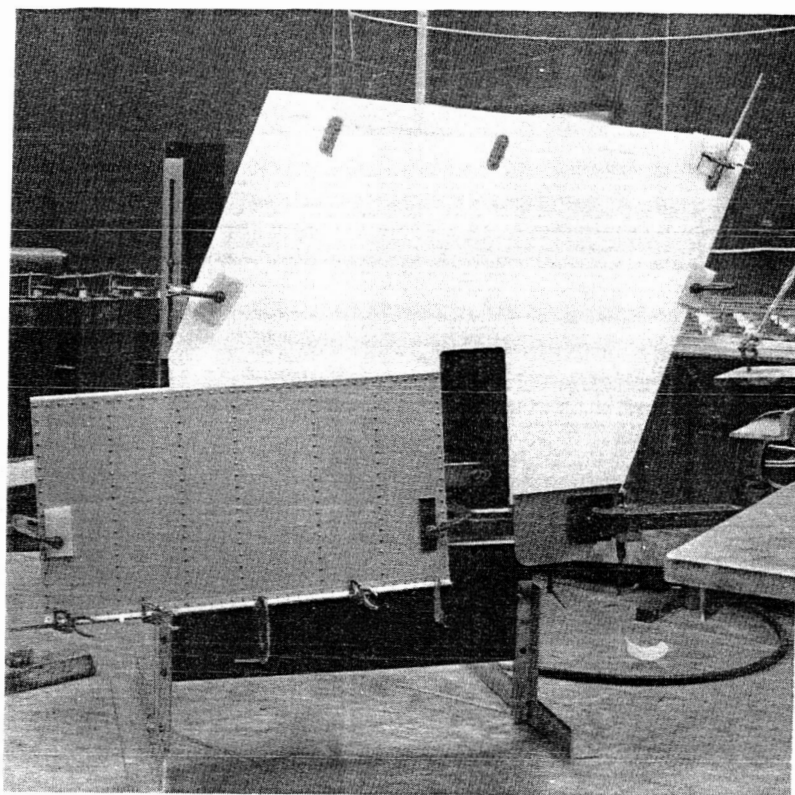


Figure 109. 727 Composite Elevator Test Article After Zone 1B Lightning Test

4.2.6 REPAIR TESTS

The objective of this test was to evaluate the strength of a typical honeycomb skin panel repair. Typical skin panels were damaged on one side, the damaged skin and core was removed, and the area was repaired using the procedures described in Appendix B.

The specimens were tested using a four-point beam bending specimen as shown in Figure 110. Undamaged specimens were tested to establish a baseline value. The wet specimens were moisture conditioned prior to being repaired to simulate parts being repaired after some flight-service time.

The repaired specimens were tested with the repair patch in compression, thus allowing the stability of the repaired area to be a contributing factor to the failure mode. Several specimens were impacted, tested, and compared to the baseline specimens. Results of these tests are summarized in Figure 110 and show that the repaired specimens were comparable to the baseline specimens at ambient test conditions. The results also showed that the repaired specimens had strength capabilities similar to the basic honeycomb panels (fig. 65) at hot and cold test temperatures. Both dry and wet impacted specimens showed lower strength capabilities than the baseline and repaired specimens.

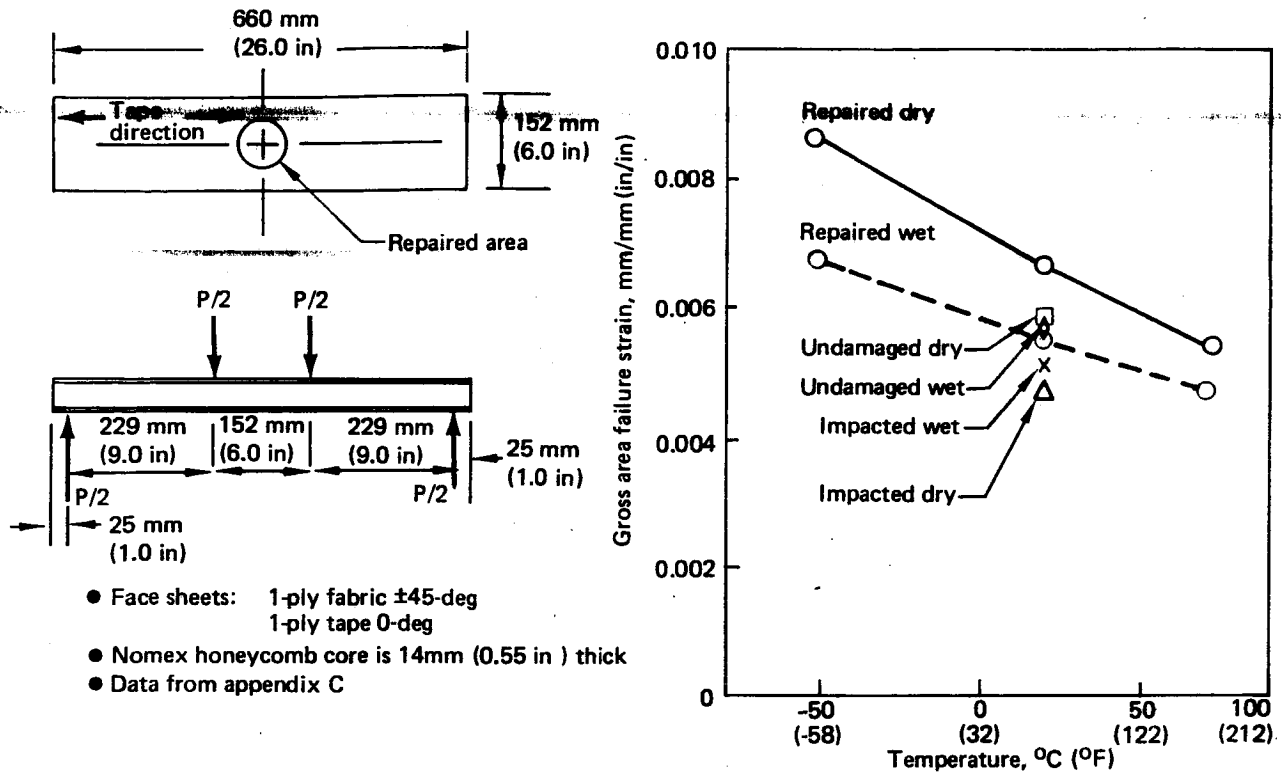


Figure 110. Honeycomb Repair Test Results

4.2.7 REAL-TIME EXPOSURE ENVIRONMENTAL TESTS

A test program to determine the effects of various real-time environmental exposures on several specimen configurations is defined in Figure 111. As noted in the test plan, specimens will be selected and tested after 12, 24, and 36 months of exposure.

The laboratory specimens were exposed to ambient conditions in the test laboratory. These specimens served as a baseline for comparison with the other three exposure conditions at comparable time intervals.

The outdoor exposure specimens were mounted on racks on the roof of the test laboratory building in Seattle, Washington; Figure 112 shows a typical installation. The specimens were positioned in a southern exposure under a sustained load of approximately 25% of their ultimate failure load. All specimens had aircraft-quality painted surfaces.

The environmental chamber specimens were subjected to cyclic pressure, temperature, and humidity; a typical exposure cycle is shown in Figure 113. The specimens were loaded in tension to approximately 25% of their ultimate failure load in sustained-load fixtures as shown in Figure 114.

The humidity chamber environment was a constant 60°C (140°F) and 100% RH. The specimens in this chamber were strained during exposure in the same load fixtures as shown in Figure 114.

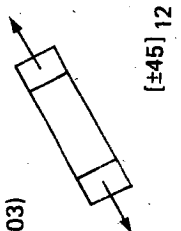

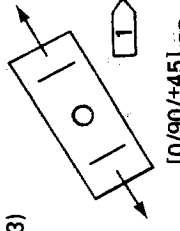


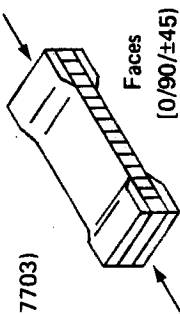




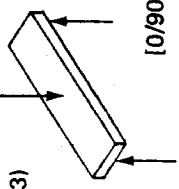


Specimen configuration (7-mil fabric) (drawing number)	Size, mm (in)	Exposure conditions	Exposure time (months and hours)				Type of test after exposure (test at room temperature)	Exposure conditions	
			Exposure time (months and hours)						
			0	12	24	36			
			0	8760	17520	26280			
(65C17703) 	304.8 (12.00) x 25.4 (1.00)	I II  IV V	6	6	6	6	Static tension	I Laboratory shelf exposure II Outdoor rack exposure strained during exposure IV Environmental chamber temperature, humidity, and pressure cycling, strained during exposure V Humidity chamber exposure, strained during exposure	
			6	6	6	6			
			6	6	6	6			
			6	6	6	6			
(65C17703) 	304.8 (12.00) x 50.8 (2.00)	I II  IV	6	6	6	6	Fatigue test to failure R = -1.0	 Three of each series of six specimens will be initially fatigue cycled to equivalent flight cycles corresponding to scheduled calendar time of exposure	
			6	6	6	6			
			6	6	6	6			
			6	6	6	6			
(65C17703) 	304.8 (12.00) x 25.4 (1.00)	I II  IV V IV  V 	5	5	5	5	Static compression	 One side painted (all other honeycomb specimens unpainted)	
			5	5	5	5			
			5	5	5	5			
			5	5	5	5			
(65C17703) 	15.2 (0.60) x 6.35 (0.25)	I II  IV V	6	6	6	6	Static interlaminar shear test	 Both sides painted (no ultraviolet exposure of unpainted specimens)	
			6	6	6	6			
			6	6	6	6			
			6	6	6	6			

Figure 111. Environmental Test Plan

At present, test data have been obtained for the ± 45 -deg tension coupons and the honeycomb compression coupons after 12 months of exposure. The 12-month exposure data are compared to the time-zero data in Figures 115 and 116. These results indicate a slight increase in strength for both specimen configurations.

This program is scheduled to continue as planned and complete program results will be published in a separate document.

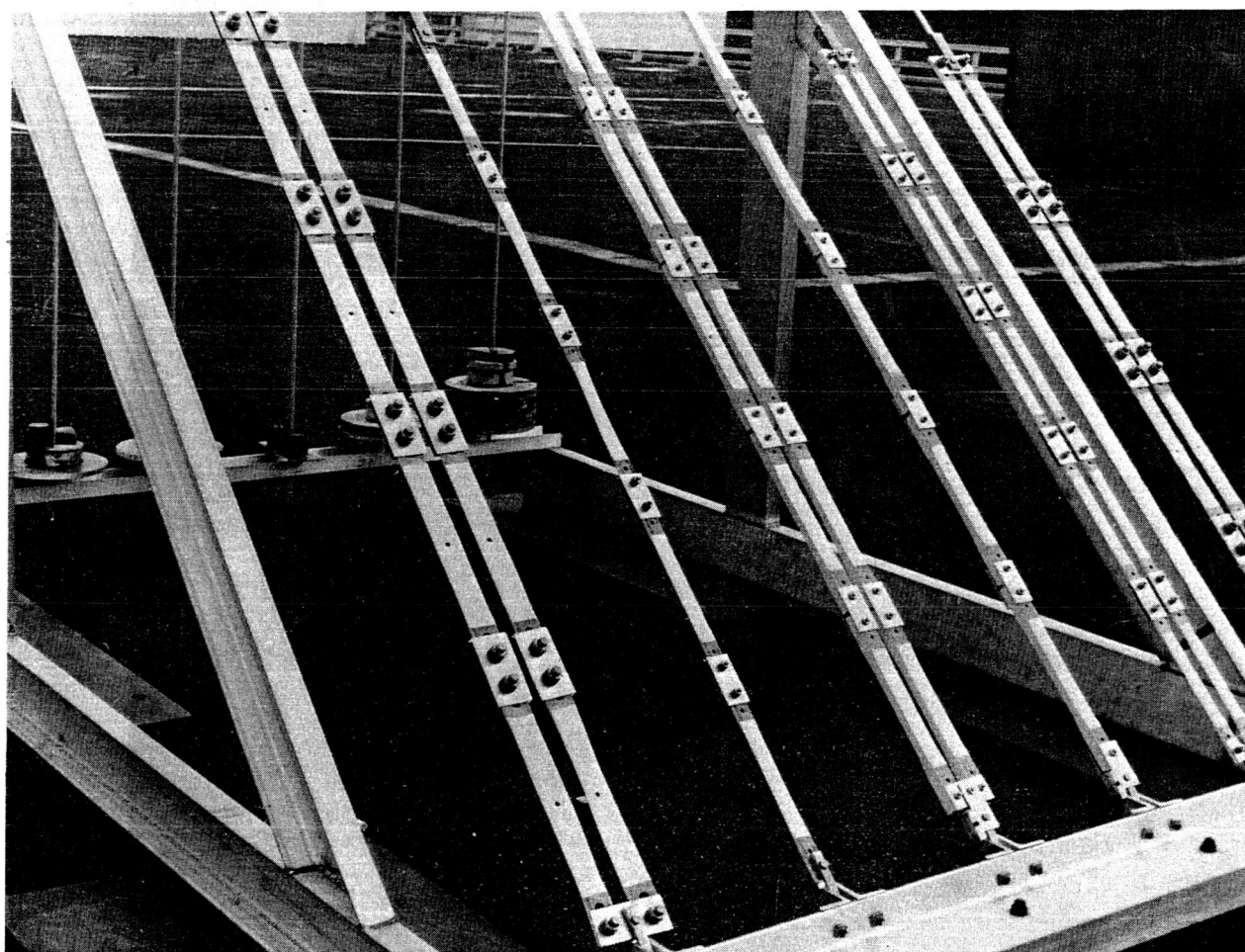


Figure 112. Outdoor Rooftop Specimen Rack

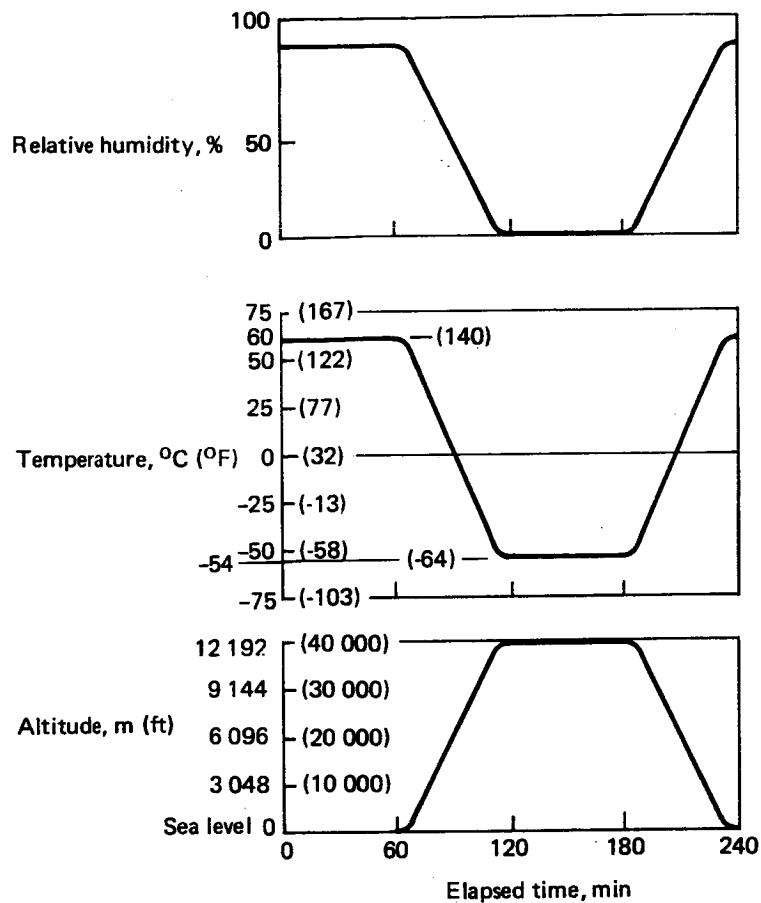


Figure 113. Environmental Chamber Cycle

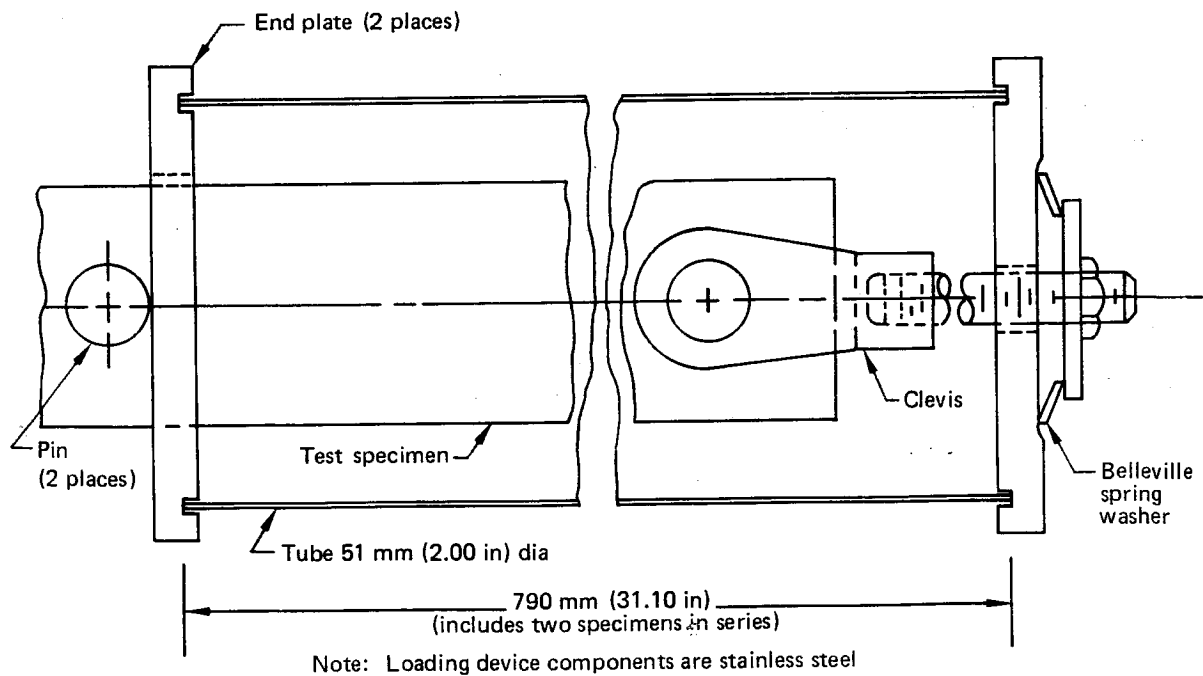
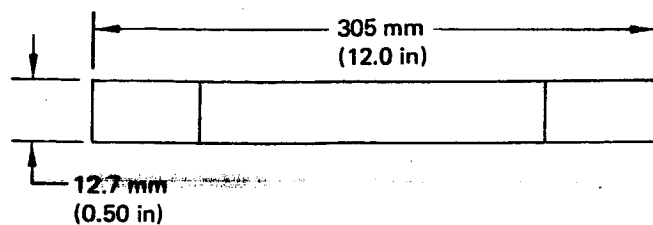


Figure 114. Environmental Test Specimen Loading Device



- 12 plies of fabric
- Orientation: ± 45 deg
- Extensional modulus, $E = 2.07 \times 10^4$ MPa (3.0×10^6 lbf/in²)
- Data from NASA Test 3, Appendix C

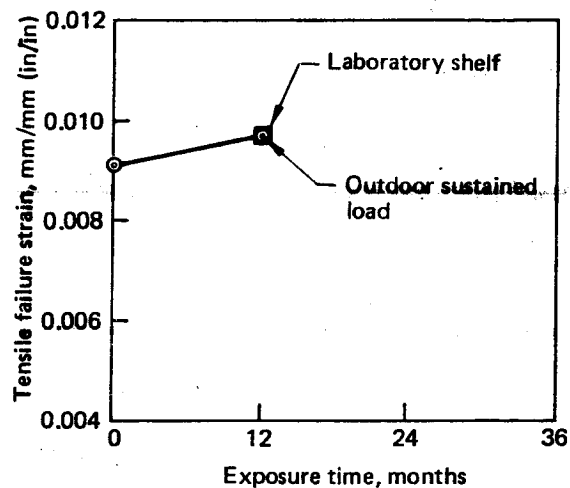
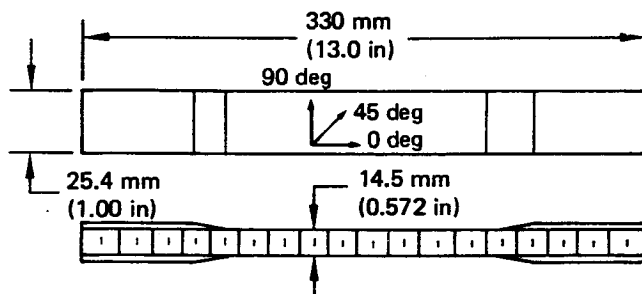


Figure 115. Tension Coupon Environmental Exposure Test Results



- Face sheets: 1-ply tape, 1-ply fabric
- Orientation:
 - Tape: 90 deg
 - Fabric: ± 45 deg
- Extensional modulus, 2.62×10^4 MPa (3.8×10^6 lbf/in²)
- Data from NASA Test 3, Appendix C

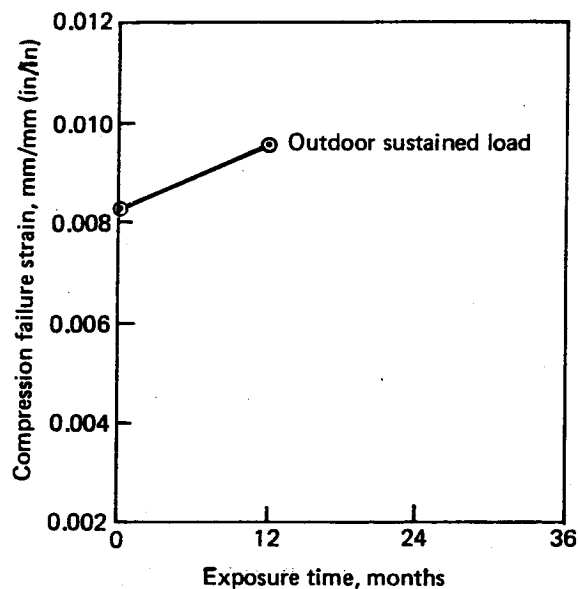


Figure 116. Honeycomb Compression Coupon Environmental Exposure Test Results

4.3 FULL-SCALE GROUND TEST

4.3.1 DESCRIPTION OF TEST SETUP

The test elevator was supported in a vertical position (trailing edge up) by steel pedestals at each hinge fitting, as shown in Figure 117. The pedestals were calibrated with strain gages so that fore-and-aft loads in the stabilizer chord plane and loads normal to the stabilizer chord plane could be determined at each hinge. The elevator hinge moment was reacted by a simulated actuator rod and reaction link that were calibrated with strain gages to read load directly.

Pedestal bases at the inboard end hinge and the four outboard hinges were moved in a plane normal to the stabilizer chord plane by hydraulic jacks to duplicate the bending induced by the stabilizer. The pedestal bases of the two hinges on the actuator support fitting and the support for the actuator rod reaction link were held immobile and were used as a datum reference for deflection of the other five hinge points. These fixed and movable hinge points are defined in Figure 118.

Elevator airloads were applied to the lower and upper surfaces through pads bonded to the skin panels, as shown in Figure 119. The portion of the balance panel loads reacted by the elevator, and the elevator nose airloads (forward of the elevator hinge line), were applied as uniform running loads along each of the five balance panel aft hinge lines. Figure 117 shows the test elevator in the test rig while testing was in progress.

The pad locations and load distributions were optimized to match (1) vertical shear along the elevator, (2) hinge moment along the elevator, (3) skin panel out-of-plane moment along the front spar, and (4) maximum normal skin panel deflections.

One hundred and fifteen rosette strain gages and 16 axial strain gages were installed to measure strains at critical areas and verify internal load distributions.

Structural deflections were measured at 26 locations by electronic deflection indicators (EDI) and dial indicators. Feedback from the EDIs at each elevator hinge location was used by a computer to control the hinge pedestal hydraulic jack movement to position each hinge to the predetermined stabilizer-induced deflection.

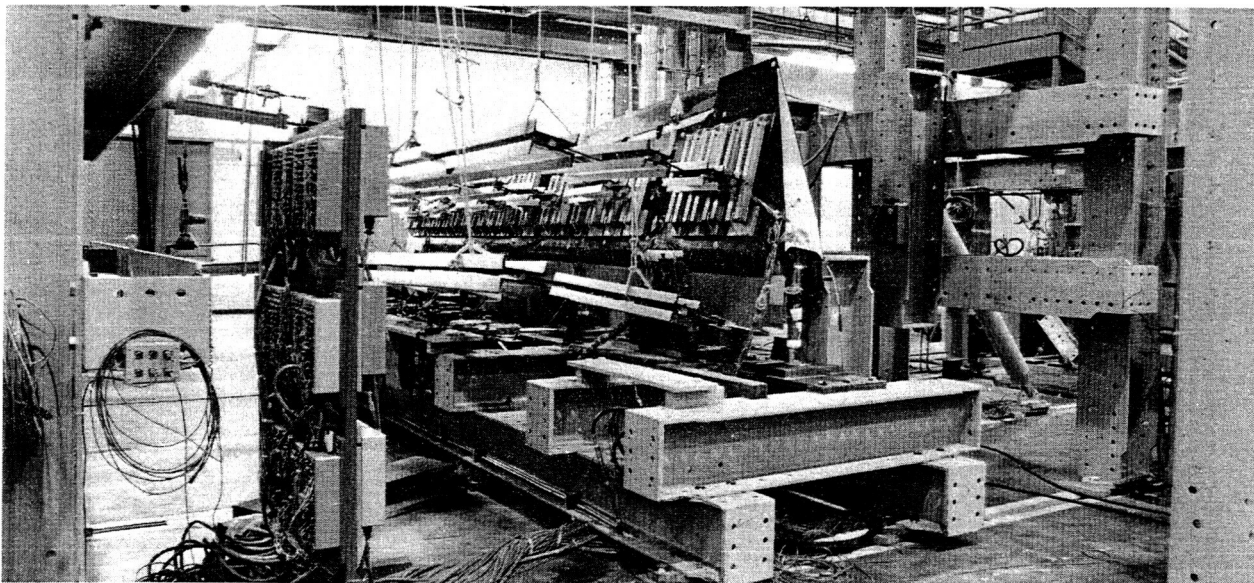


Figure 117. Elevator Ground Test Setup

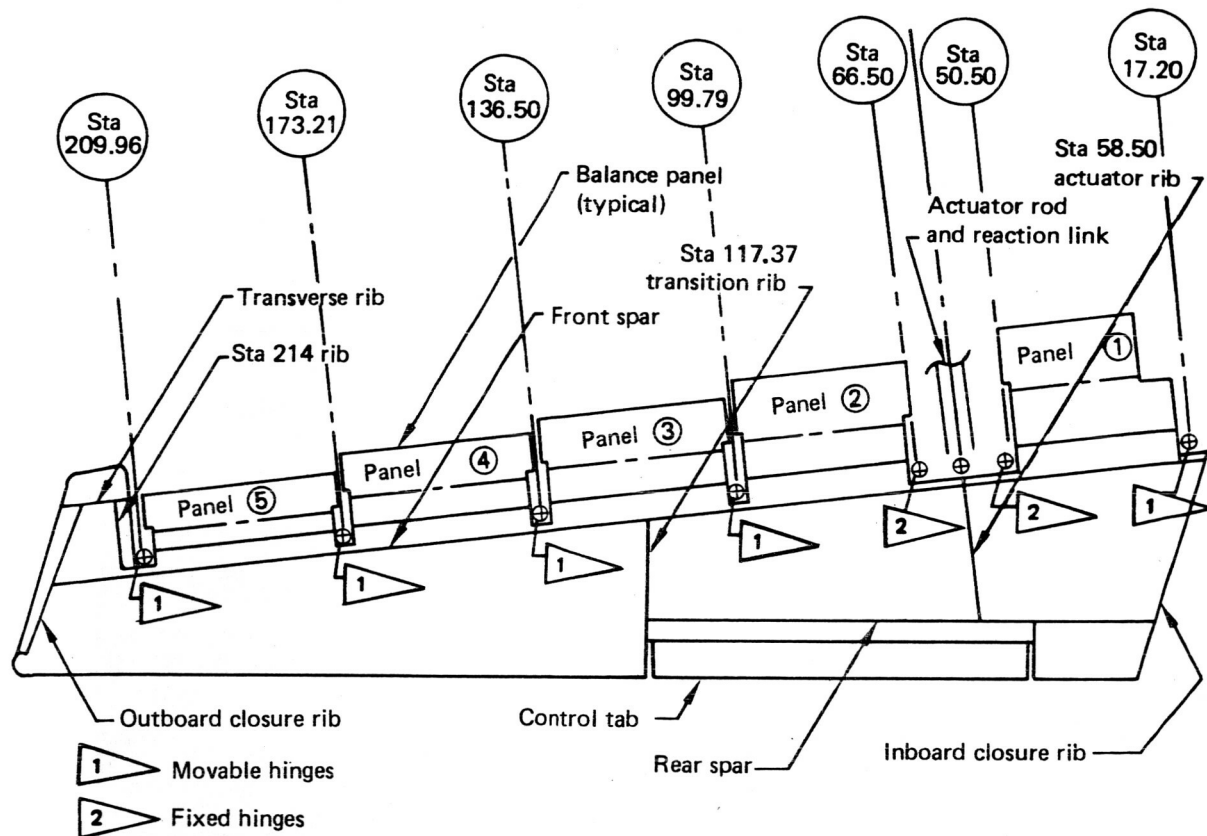


Figure 118. 727 Composite Test Elevator Hinge Locations

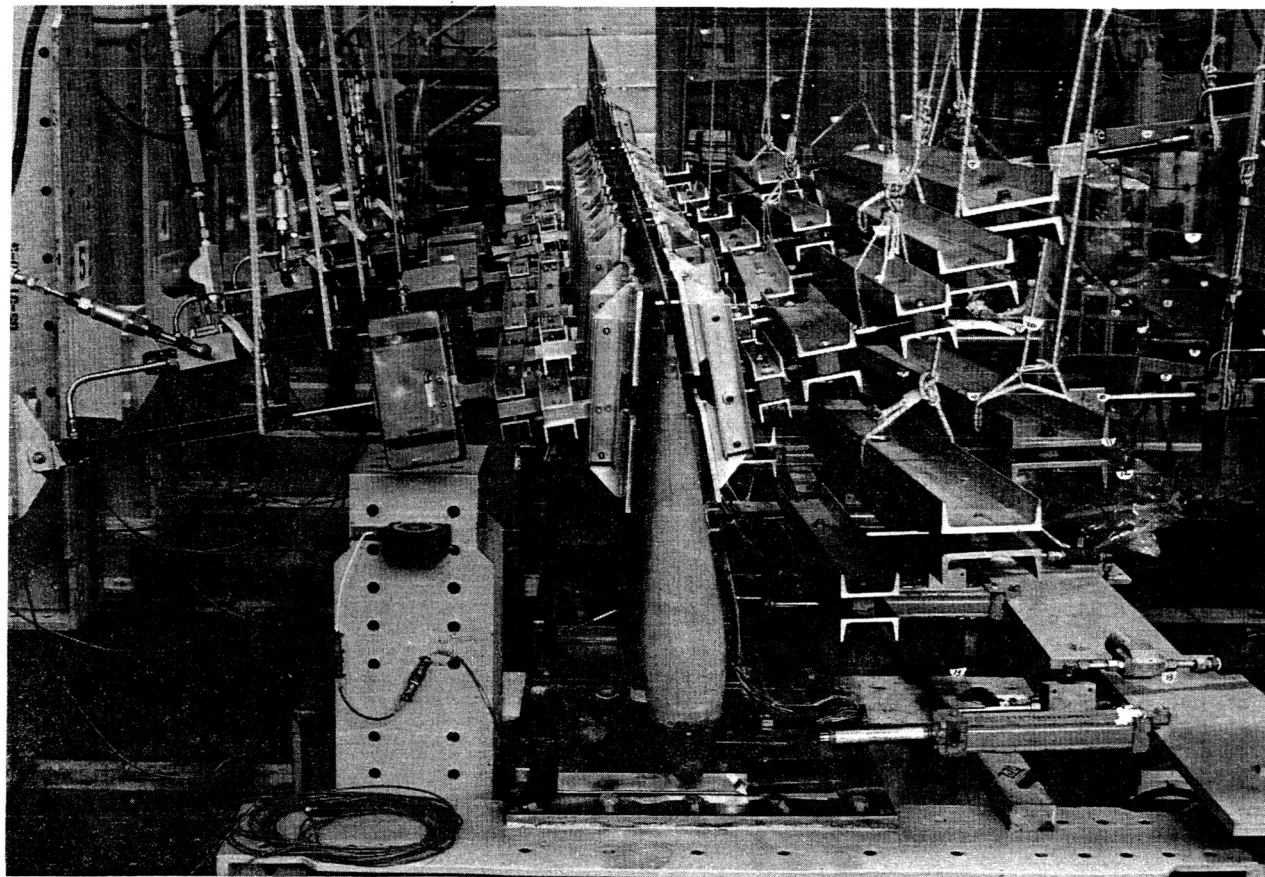


Figure 119. Elevator Ground-Test Setup Showing Bonded Pads

Thirteen hydraulic jacks were used to apply the tension and compression pad loads, the balance panel loads, and the movable elevator hinge pedestal loads. A load cell was installed in series with each hydraulic jack to measure its applied load.

4.3.2 STATIC LOADS

The composite elevator was subjected to two static load conditions (see fig. 21) defined as follows:

1. LC 128—positive maneuver at 851 km/hr (460 kn) at sea level
2. LC 125—instantaneous elevator at 463 km/hr (250 kn) at sea level

The applied loads and induced deflections for both static load cases are tabulated in Table 10. The airloads, induced deflections, and panel pressure loads are shown schematically in Figure 120. The pressure, P_e , is constant over the entire span and the balance panel running load, W_{BP} , is uniform for each balance panel. The skin panel pressure loads were applied two-thirds to the negative pressure surface and one-third to the positive pressure surface.

Table 10. Static Test Loads and Deflections

Load type		Design ultimate load cases	
		125 instantaneous elevator	128 positive maneuver at V_D
Balance panel pressure, P_{BP} , kPa (lbf/in ²)	Panel 1 2 3 4 5	-19.79 (-2.87) -22.06 (-3.20) -24.20 (-3.51) -23.58 (-3.42) -21.17 (-3.07)	-26.41 (-3.83) -30.82 (-4.47) -32.27 (-4.68) -32.27 (-4.88) -28.41 (-4.12)
Balance panel load at hingeline, W_{BP} , kN/m (lbf/in)	Panel 1 2 3 4 5	-3.20 (-18.3) -3.19 (-18.24) -3.07 (-17.55) -2.57 (-14.71) -1.93 (-11.05)	-4.27 (-24.42) -4.46 (-25.48) -4.10 (-23.40) -3.52 (-20.12) -2.60 (-14.83)
Elevator pressure, P_e , kPa (lbf/in ²)	—	-22.62 (-3.28)	-31.85 (-4.62)
Tab pressure, P_t , kPa (lbf/in ²)	—	3.38 (0.49)	5.03 (0.73)
Vertical deflection at elevator hinges δ , mm (in)	Deflection δ 1 2 3 4 5 6 7	0 -28.19 (-1.11) -38.35 (-1.51) -77.47 (-3.05) -134.84 (-5.31) -200.15 (-7.88) -269.24 (-10.6)	0 -24.64 (-0.97) -38.61 (-1.52) -74.42 (-2.93) -124.97 (-4.92) -181.61 (-7.15) -243.33 (-9.58)

1 See Figure 118 for balance panel location.

2 See Figure 120.

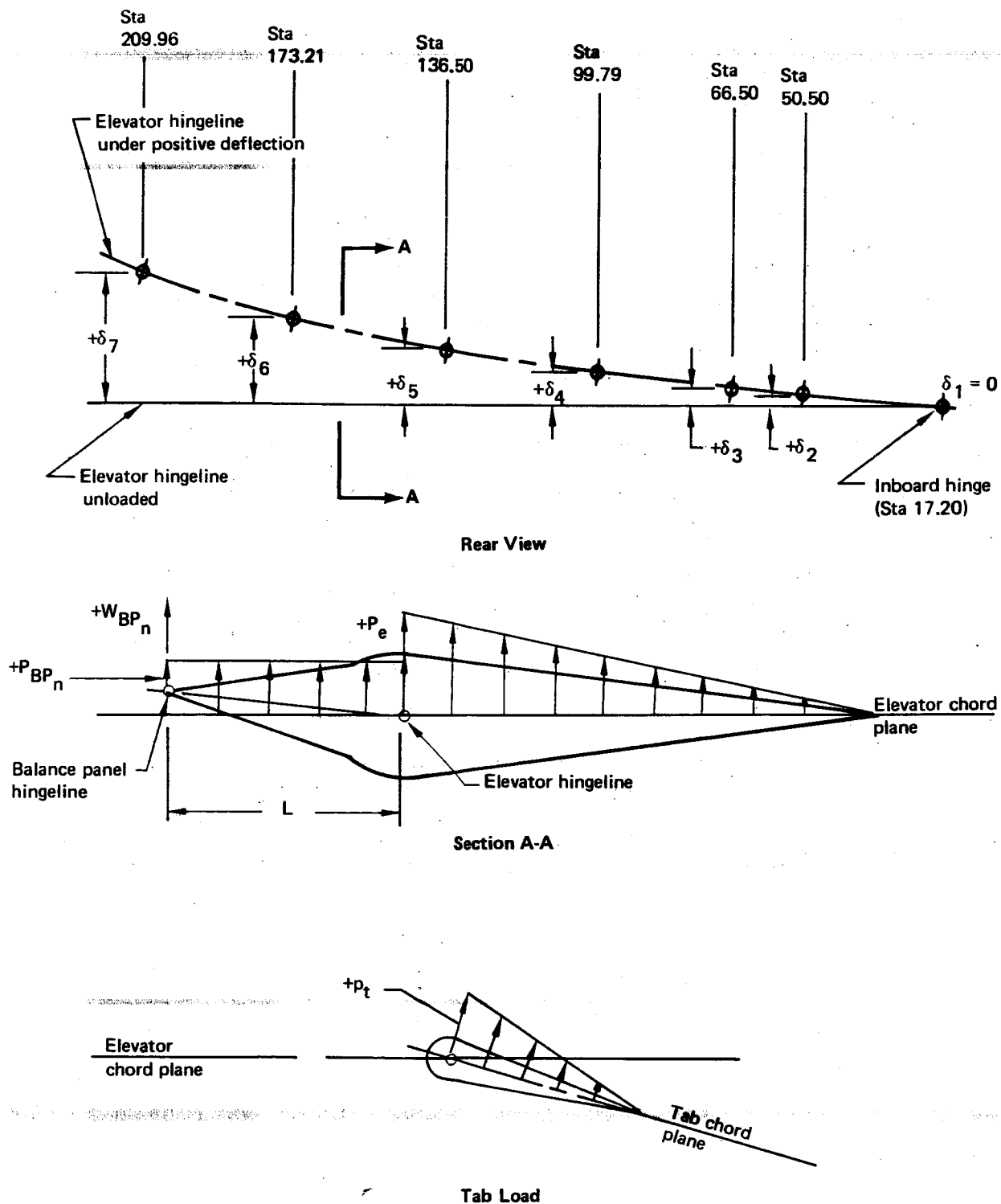


Figure 120. Induced Deflections, Air Loads, and Panel Pressure Loads

4.3.3 TEST RESULTS

4.3.3.1 Limit Load Test

The elevator was successfully tested to 67% of design ultimate LC 128 with no damage to the specimen. Strain, deflection, and load readings were recorded. Examination of measured strains, deflections, and hinge and actuator loads showed agreement with the finite-element ATLAS model values.

4.3.3.2 Durability Testing

After the limit load test, the elevator was subjected to 280,000 load cycles, which is equivalent to two service lifetimes. The cyclic loading consisted of initially deflecting the elevator down (airplane reference) to a position determined by the horizontal stabilizer during a typical flight and locking it in that position. Then the cyclic airloads and inertia loads were applied alternately as down loads to the elevator lower surface and the balance panel aft hinge, and then as up loads to the elevator upper surface and the balance panel aft hinge.

Strain and deflection surveys were conducted for both up and down airloading before cycling began and again after 100 cycles had been applied. Similar surveys were conducted before resuming cycling for a second lifetime of testing. The respective measured strain and deflection values were in close agreement at each survey.

Visual inspections were conducted of all accessible structure at scheduled intervals during the testing. Ultrasonic inspections were made of critical areas at less frequent intervals, and an X-ray inspection was performed before resumption of the second lifetime of cycling. Table 11 shows the inspection plan that was followed during the test. Figures 121 and 122 show the areas that were inspected.

Table 11. Full-Scale Ground-Test Inspection Schedule

Number of load cycles	Type of inspection			Number of load cycles	Type of inspection		
	Visual	Ultrasonic	X-ray		Visual	Ultrasonic	X-ray
5 000	X			160 000	X	X	
10 000	X			180 000	X	X	
15 000	X	X	X	200 000	X		X
20 000	X			220 000	X	X	
25 000	X			230 000	X		
30 000	X		X	240 000	X		
40 000	X	X		250 000	X	X	X
50 000	X			260 000	X		
75 000	X	X		270 000	X	X	
100 000	X			280 000	X	X	X
120 000	X	X					
140 000	X	X	X				

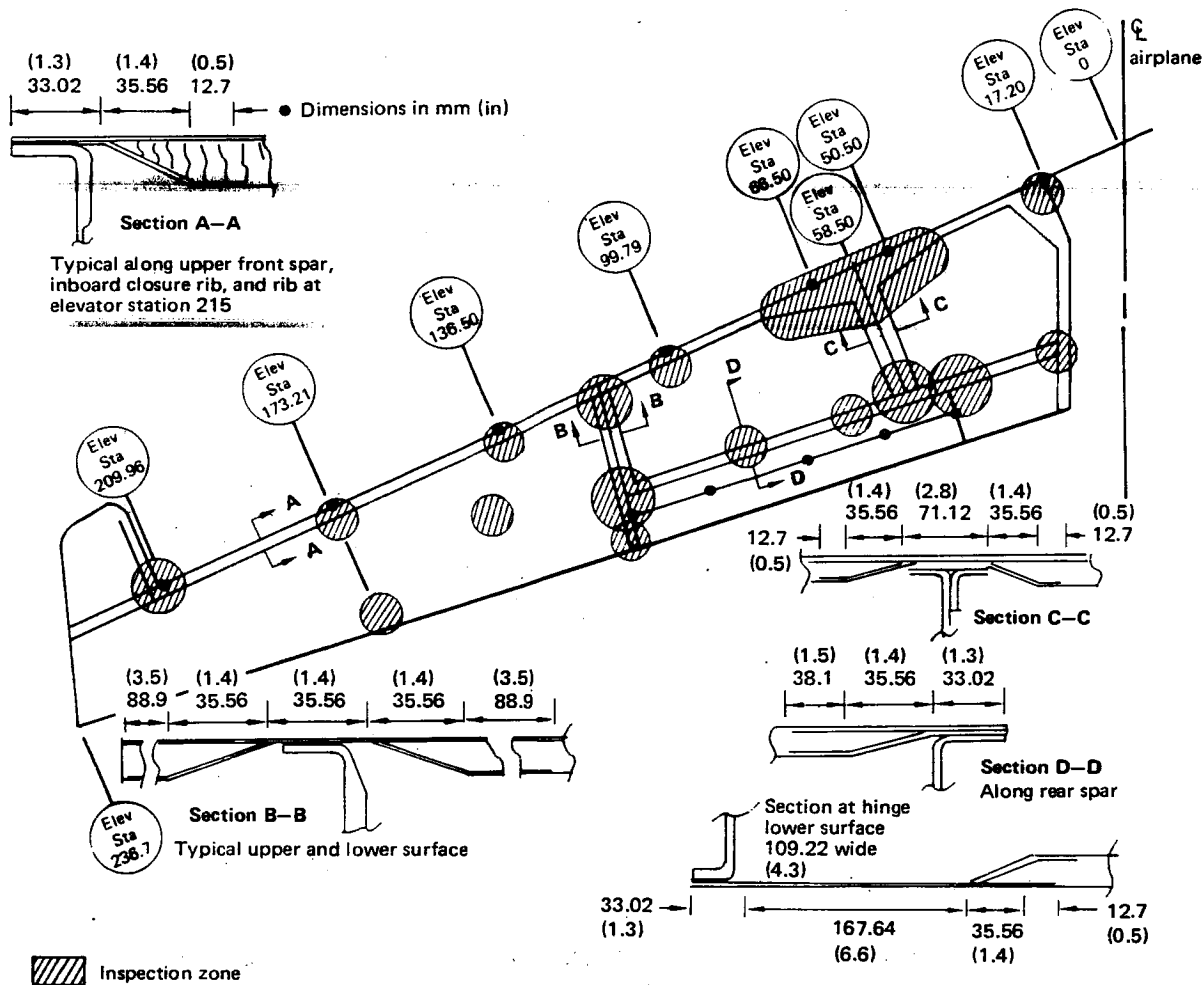


Figure 121. Full-Scale Ground-Test Locations For Ultrasonic Inspection—Upper and Lower Skin Panels

The second equivalent service lifetime of 140,000 load cycles then was applied, which concluded the cyclic testing with a total of 280,000 cycles.

Strain and deflection surveys were conducted and comparisons with values from earlier surveys showed close agreement.

The inspection schedule shown in Table 11 was followed during the second lifetime of testing. No indication of structural damage was found during any inspection.

4.3.3.3 Ultimate Load Test

The elevator was loaded to 100% of LC 128 (positive maneuver at dive speed ultimate condition). The strain-gage data showed good agreement with the linearly extrapolated limit load data.

The elevator then was subjected to LC 125 (instantaneous elevator). During this test, the elevator suffered a local skin buckle at the elevator station 99.79 hinge cutout at 60% of the design ultimate load. The local skin buckle area is shown in Figure 123. The applied hinge deflections at elevator stations 99.79 and 17.20 were inadvertently higher than those specified for 60% design ultimate load, and this incorrect loading contributed to the local skin buckling.

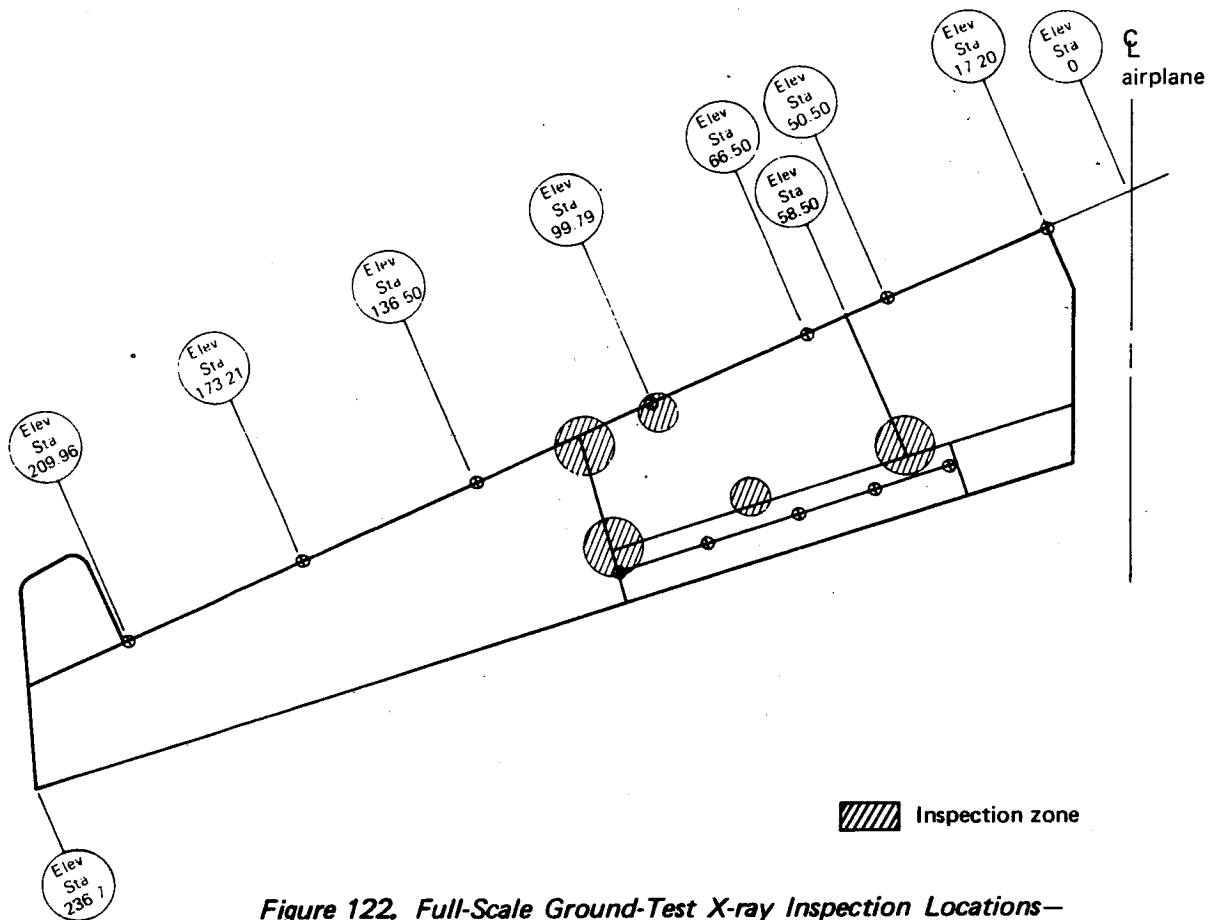


Figure 122. Full-Scale Ground-Test X-ray Inspection Locations—Upper and Lower Skin Panels

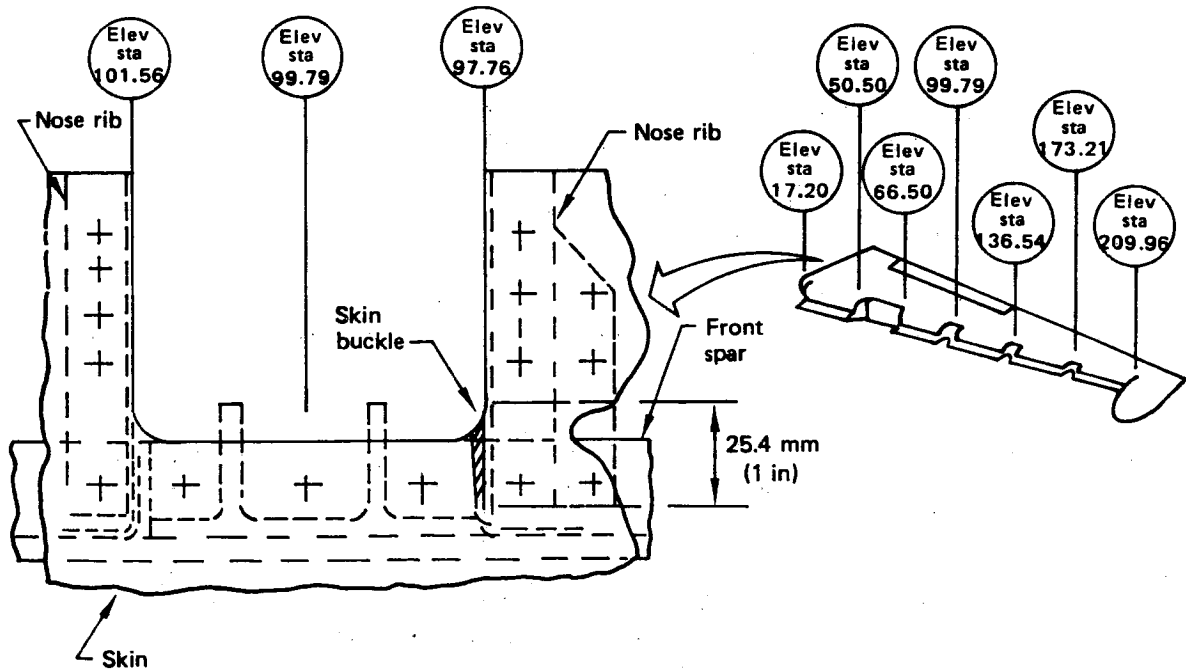


Figure 123. Skin Buckle Location

A structural modification involving a reduction of skin overhang at the cutout corner radius and the addition of a fastener common to the skin and nose rib was made at elevator stations 68.34, 97.76, and 101.56. These details are presented in Figure 124.

The ultimate load test for LC 125 was rerun successfully to 100% and subsequent inspections indicated that no further structural damage occurred.

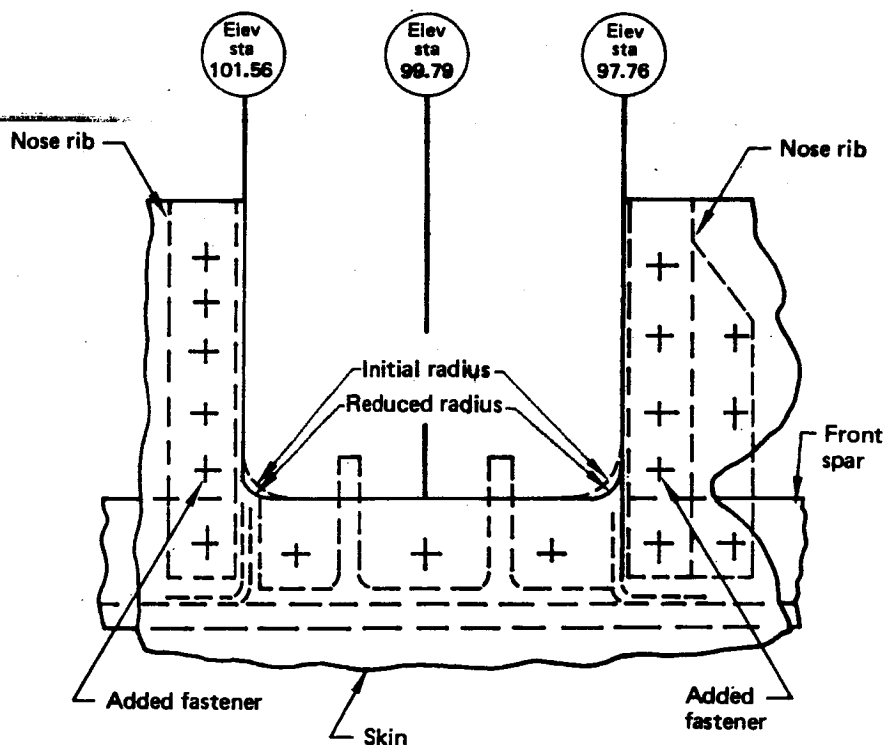


Figure 124. Elevator Nose Skin Structural Modification

Figures 125 and 126 show strain comparisons between the test elevator and the predicted finite-element model values for LC 128.

Figure 127 shows the hinge and actuator ultimate loads, predicted versus test, for LC 128.

Figure 128 shows the elevator torsional rotation comparison between test and predicted values for LC 128.

4.3.3.4 Damage Tolerance Tests

The elevator was set up for a Boeing-required fail-safe test by removing the station 209.96 hinge pin (see fig. 118). The test objective was to achieve the fail-safe load level with the hinge failed. The LC 128 loading configuration was used for the test. At 60% of LC 128 design ultimate load, the elevator upper surface skin, (tension surface) spar chord, and web failed at station 172. The failure is shown in Figures 129 and 130. The load at failure was equivalent to 96% of the fail-safe load condition. A failure analysis was performed, which included a review of the finite-element model predicted strains, strain gage data, and coupon test data.

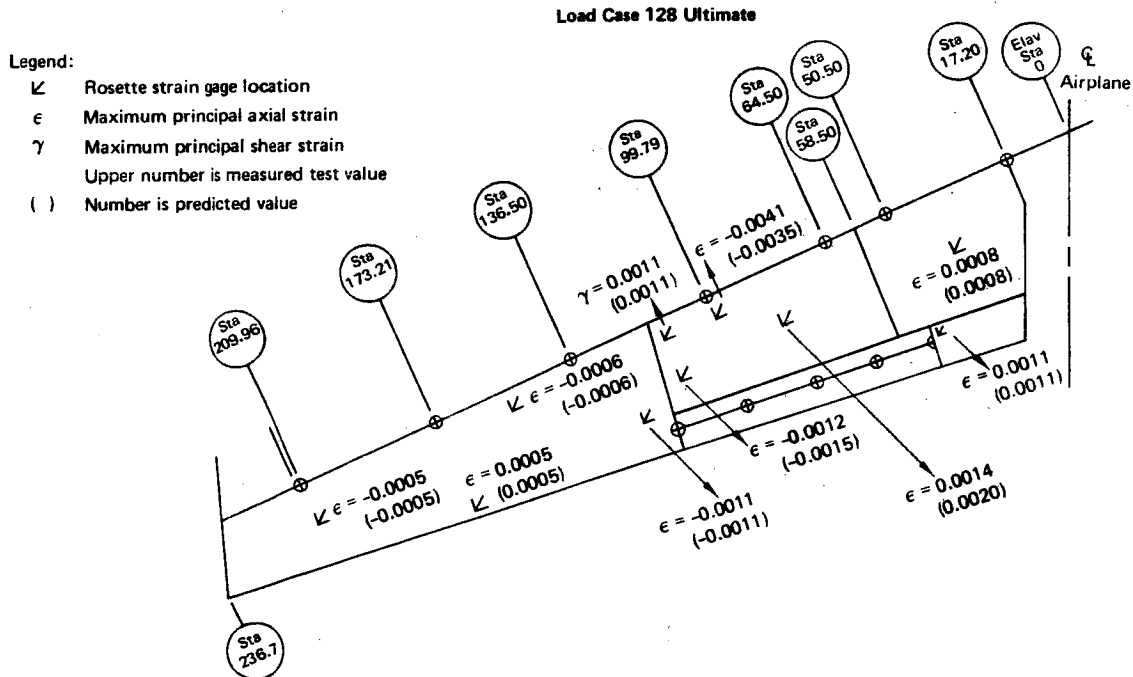


Figure 125. Lower Skin Panel Outer Face Strain Comparisons—Predicted Versus Test

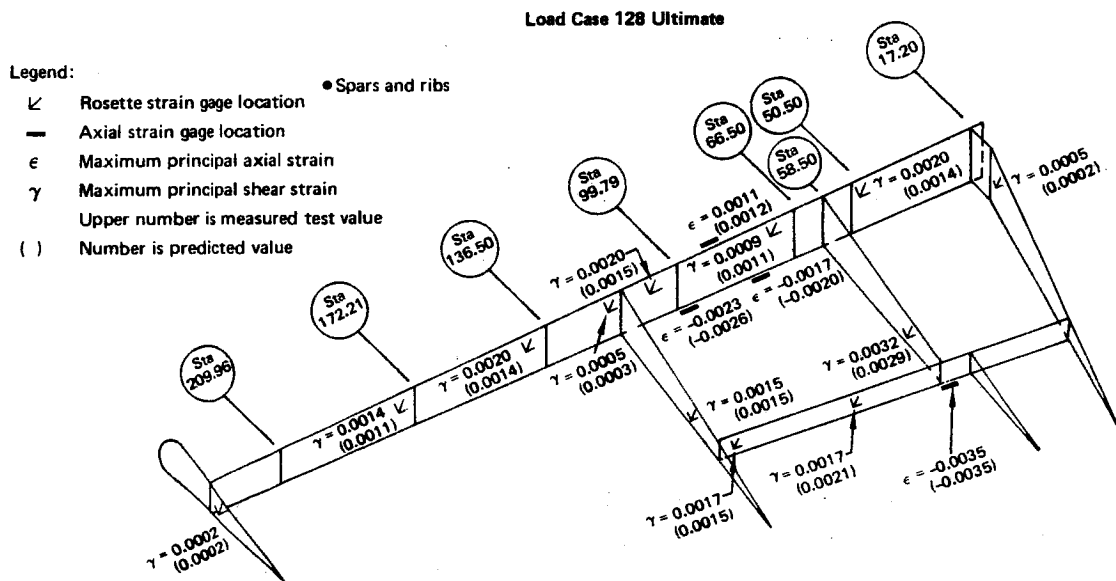


Figure 126. Spar and Rib Strain Comparisons—Predicted Versus Test

Legend:

- Upper number is measured test value, kN (lbf)
- () Number is prediction from ATLAS finite element analysis, kN [lbf]

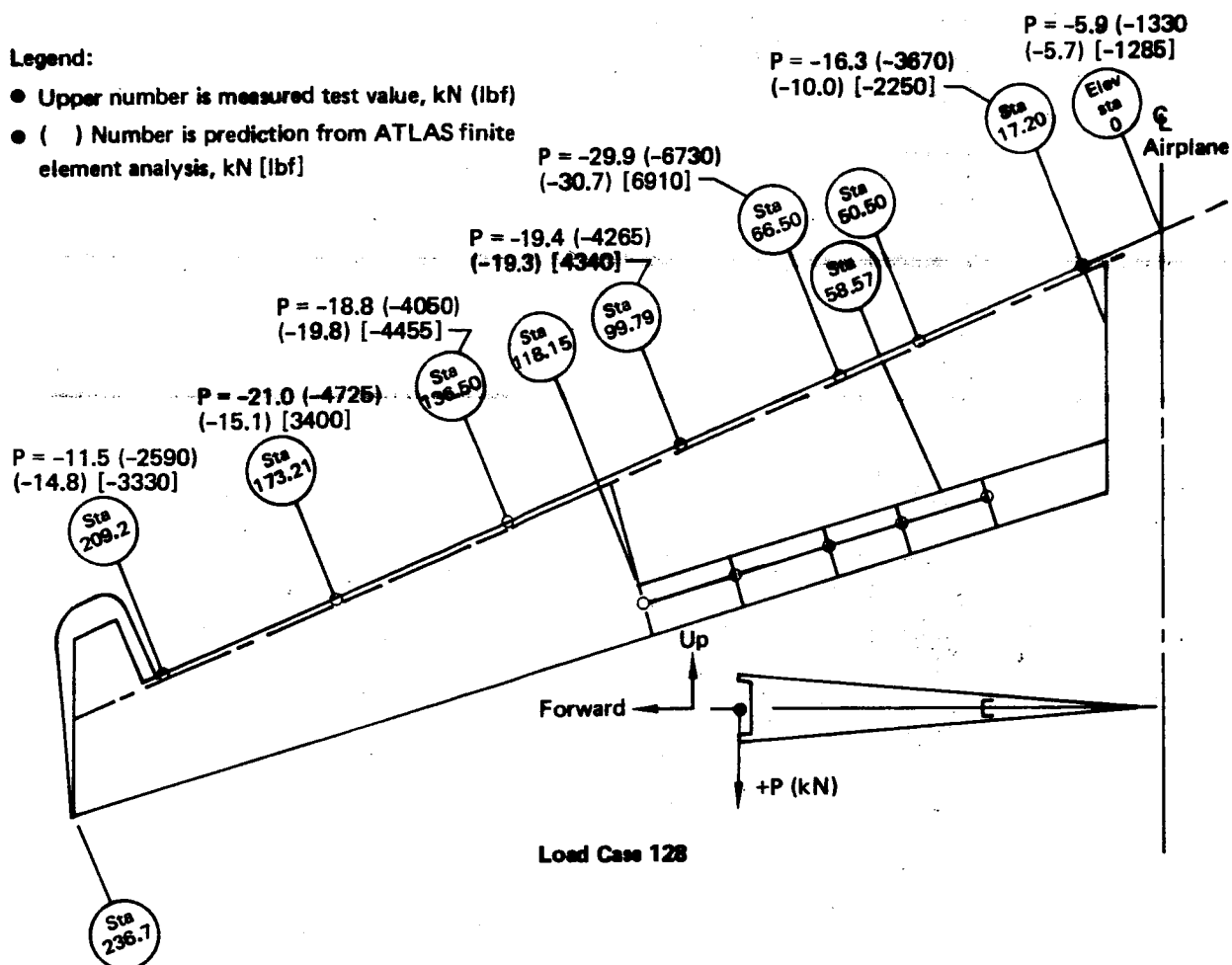


Figure 127. Hinge-Load Ultimate Loads—Predicted Versus Test

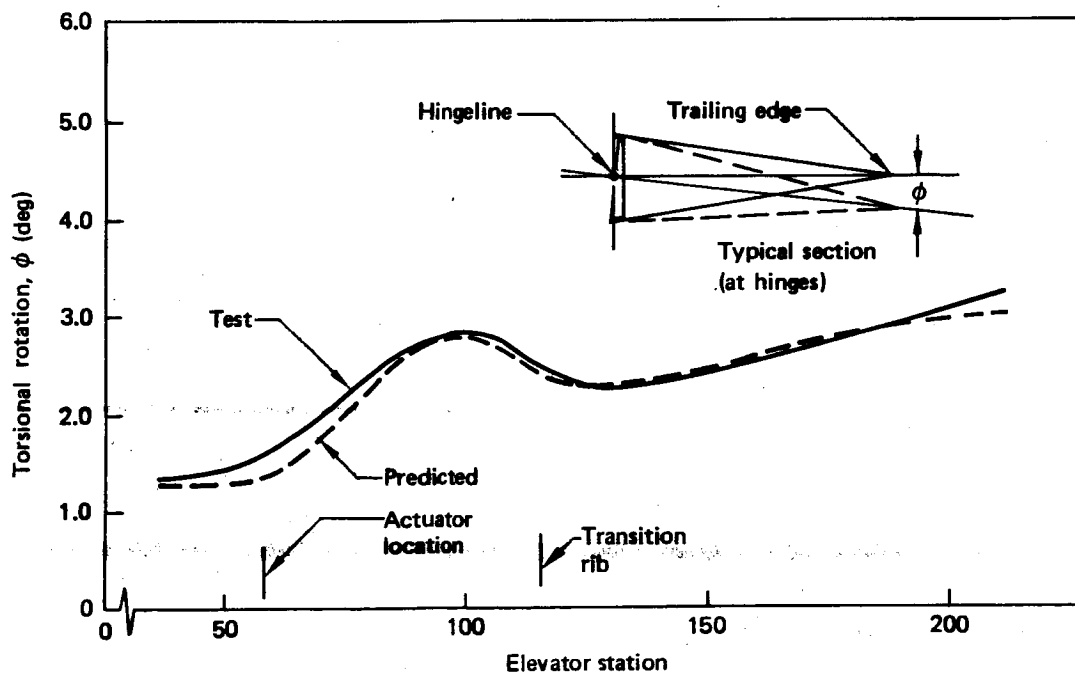


Figure 128. Elevator Rotation Comparison for Load Case 128

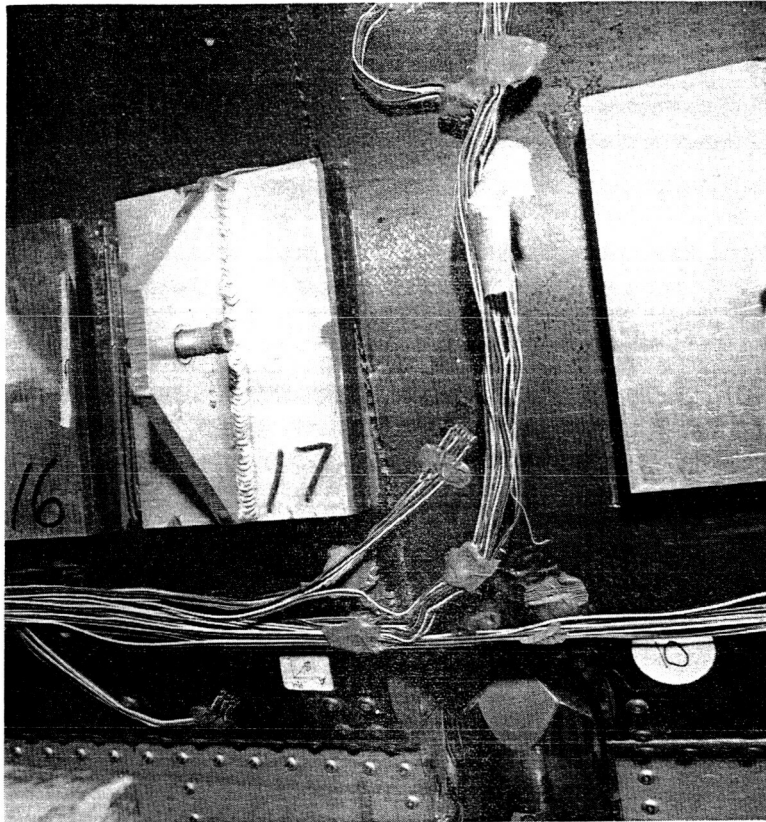


Figure 129. Full-Scale Test Elevator Upper Surface Failure at Station 172—Fail-Safe Test

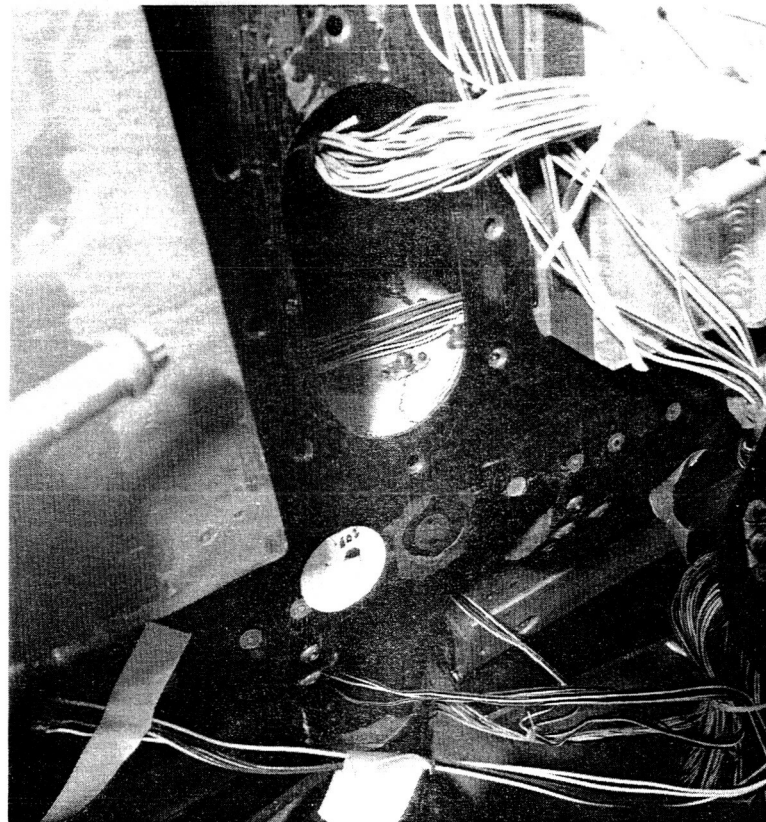


Figure 130. Full-Scale Test Elevator Front-Spar Failure at Station 172—Fail-Safe Test

The failure in the tension skin passed through the spar/skin fastener at station 172, as shown in Figure 131. The loads that existed at the analysis location were the bypass strain due to overall elevator bending and a fastener bearing stress due to the hinge loads. The fastener bearing stress acts normal to the bypass strain. Figure 132 presents the calculations that were used to obtain the bypass strain and bearing stress.

Test data from the ancillary test program were reviewed and room-temperature/dry test values of bearing stress and bypass strain that would apply in the failure area were obtained. The maximum fastener bearing stress was established as 709 MPa (102 800 lbf/in²) (fig. 68) and the maximum bypass strain was established as 0.0046 mm/mm (in/in) (fig. 71). These values are plotted on an interaction curve of fastener bearing stress versus bypass strain in Figure 133. The values of bearing stress and bypass strain that existed on the elevator at failure, from Figure 132, are plotted in Figure 133. The test point, displayed in Figure 133, defines an interaction curve for combining fastener bearing stress normal to a tension bypass strain. The 100% level of the fail-safe load condition is plotted in Figure 133 as a reference.

The test failure and subsequent analysis provided a good correlation between coupon and full-scale test results.

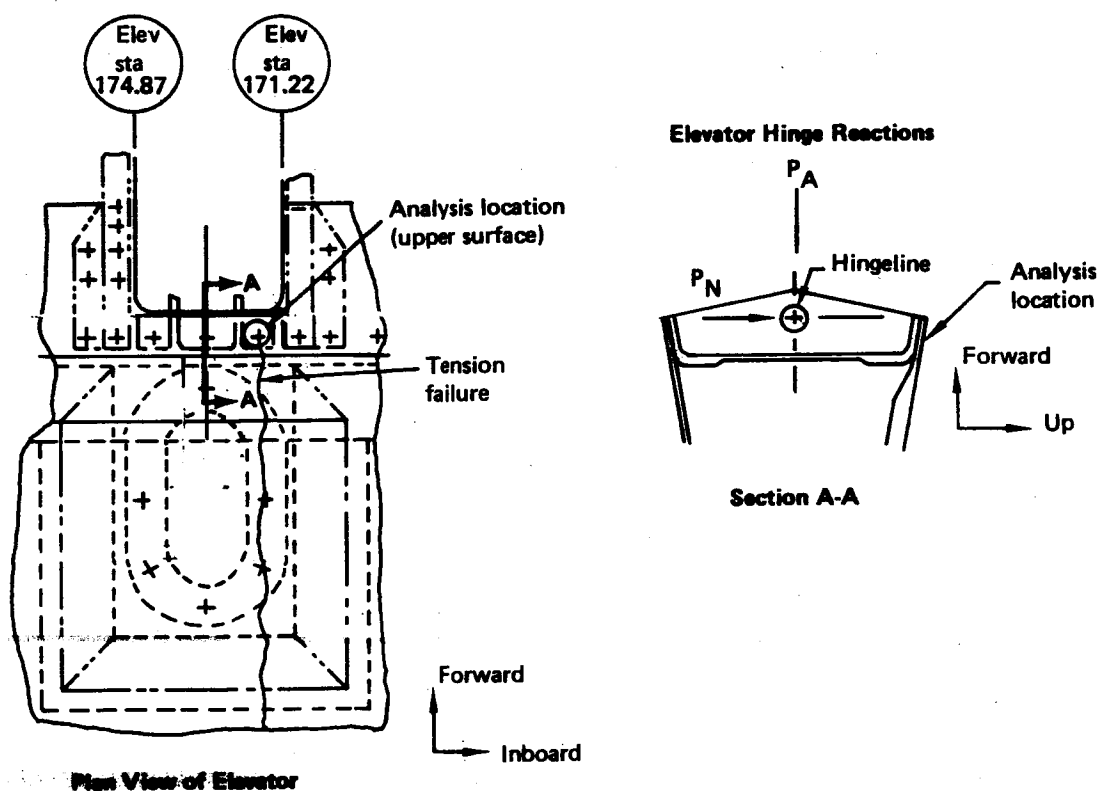


Figure 131. Fail-Safe Loading Failure Analysis Location

- Load from hinge fitting, $P_F = 5.0 \text{ kN (1124 lbf)}$

- Load taken by skin, determined from thickness ratio:

$$P_{FS} = 5.0 \left(\frac{1.7}{1.7 + 2.49} \right) = 2.03 \text{ kN (456 lbf)}$$

- Bearing stress based on thickness and effective fastener diameter:

$$F_{BR} = \frac{2.03}{(1.7)(4.8)} = 249 \text{ MPa (36 100 lbf/in}^2\text{)}$$

- Gross area bypass strain determined from strain gage and ATLAS data:

$$\epsilon_{GR} = 0.0042 \text{ mm/mm (in/in)}$$

- Dimensions, mm (in)

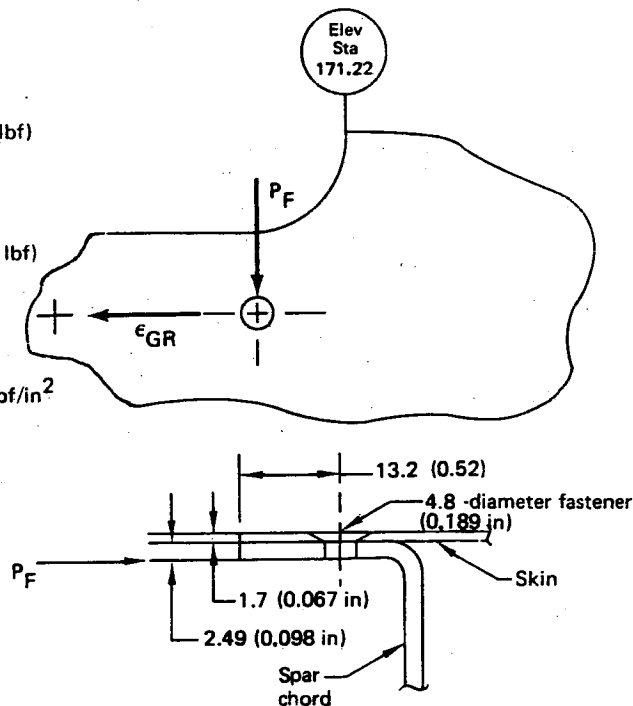
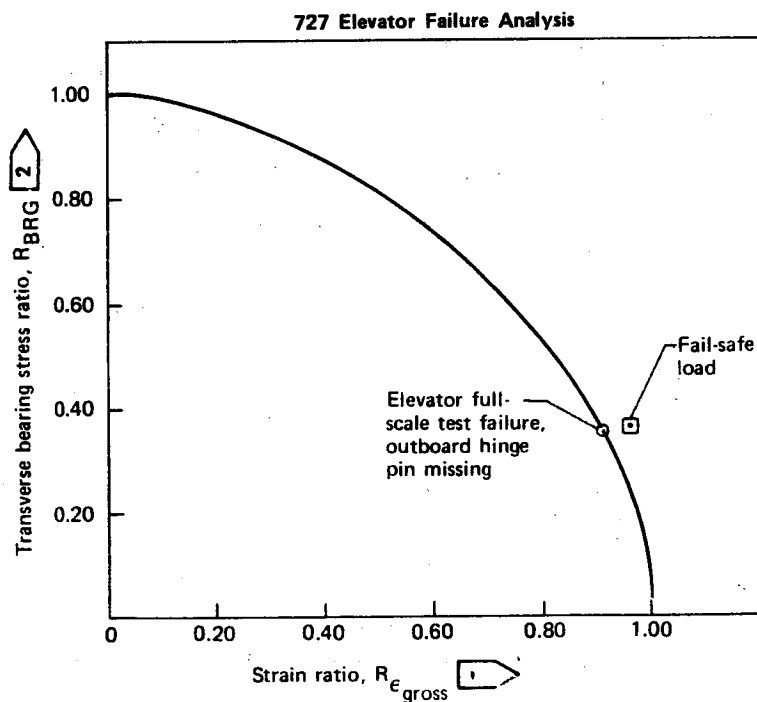


Figure 132. Fail-Safe Loading Failure Analysis



① $R_{\epsilon_{gross}}$ of 1.00 based on $\epsilon_{gross} = 0.0046 \text{ mm/mm, (in/in)}$, from room temperature, dry test specimens (fig 71)

② R_{BRG} of 1.00 based on $f_{BRG} = 709 \text{ MPa (102 800 lbf/in}^2\text{)}$ from room temperature, dry test specimens (fig 63)

Figure 133. Interaction Curve Bearing Versus Tension Bypass Strain

4.4 GROUND VIBRATION TEST

Ground vibration testing was performed on the model 727 flight test aircraft with the composite elevator installed. The primary purpose of these tests was to compare the measured natural frequencies of the composite elevators with the values used in the flutter analysis.

The test airplane was positioned on a level surface in an operating-empty weight configuration. The airplane was supported on the main and nose gears with reduced tire pressure. Portable vibration shakers were used to excite the elevator with the horizontal stabilizer in the neutral position. A typical test setup is shown in Figure 134. Tests were conducted with hydraulic power on and off, and with the right- and left-hand elevator excitation in and out of phase.

Accelerometers, located on both right- and left-hand stabilizers, elevators, tabs, and control columns, were used to measure control system natural frequencies, mode shapes, and damping characteristics. The measured natural frequencies of the advanced composite elevators were in close agreement with those used in the flutter analysis, as shown in Table 12.

4.5 FLIGHT TESTS

Boeing-funded flight tests were conducted to demonstrate flutter clearance and stability and control performance.

Flight flutter tests were conducted at the speeds and altitudes shown in Figure 135. Measured displacement and rotation of the fin, rudder, stabilizer, and elevator, due to sharp control inputs from the elevator and rudder, were used to evaluate the natural frequency and damping characteristics of the empennage with graphite-epoxy elevators.

Stability and control flight tests consisted of two phases. Phase I flight tests were conducted on a production aluminum elevator to establish baseline data. For Phase II, the aluminum elevator was replaced by the composite elevator and Phase I flight tests were repeated. The effect of the composite elevator on the stability and control characteristics and autopilot operation of the model 727 was evaluated by comparing the two sets of test data. These test results indicated no detectable difference in aircraft response between the composite and production aluminum elevators. The flight-test airplane was flown by an FAA pilot as part of the stability and control and autopilot certification flight testing.

4.6 FAA CERTIFICATION

The flight flutter and stability and control test results were submitted to the FAA. Both sets of test results indicated that all FAA requirements had been achieved.

A formal strength analysis of the graphite-epoxy elevator was submitted to and accepted by the FAA. Certification of the graphite-epoxy elevator was granted on December 7, 1979.



Figure 134. Typical Ground Vibration Test Setup

Table 12. Comparison of Ground Vibration Test and Analysis Natural Frequencies

Vibration mode		Frequency, Hz	
		Analysis	Test
First stabilizer bending	Symmetrical	6.64	6.72
	Asymmetrical	6.96	7.12
Second stabilizer bending	Symmetrical	18.3	18.2
	Asymmetrical	23.4	23.5
Torsion	Symmetrical	27.1	26.6
	Asymmetrical	28.4	28.8
Elevator rotation		13.4	13.4
Elevator torsion		28.7	27.7
Column—tab		28.3	28.4
Tab rotation		34.3	40.0

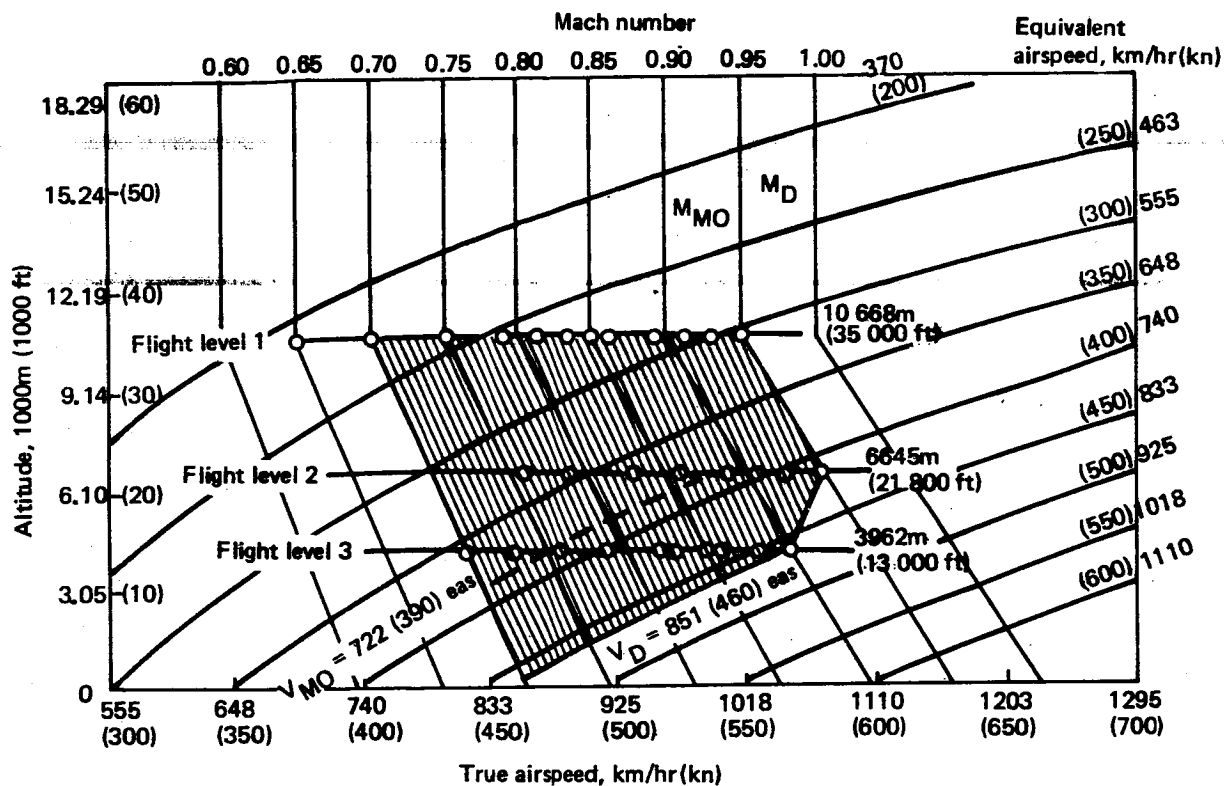


Figure 135. Flight Flutter Altitude and Speed Test Conditions

4.7 WEIGHTS

4.7.1 TECHNICAL APPROACH

Early in the program, the method used for test component weight evaluation was the same as that currently used for fiberglass components; volume times density. Inconsistencies were experienced using this method when predicted weights were compared to actual values. The reasons for these discrepancies were determined to be primarily material-related. Fluctuations in resin content/fiber volume and subsequent cured ply thickness variations were found.

Weight predictions of component parts on a ply-by-ply basis, using (area of ply) times (number of plies) times (nominal resin-impregnated material areal weight) was established early in the advanced composite elevator program. This method provides the following advantages:

- Material area can be extracted from the calculations for each style of fabric and/or grade of tape
- Thicknesses of laminate areas do not require the summation of nominal cured ply thicknesses
- Revisions to ply layups, such as ply additions, deletions, or substitutions, can be readily made

This methodology for weight predictions has provided predicted weights that have shown close correlation to the actual weights of the respective component parts.

4.7.2 ANALYSIS

The elevator system is a statically balanced primary control surface. Because of its direct bearing on aircraft flight safety, the prevention of flutter of the control surfaces is of primary concern. Flutter is a form of dynamic instability in which the amplitude of the self-induced vibration may increase until the surface suffers structural damage or actual destruction. One method of flutter prevention is to have a proper mass distribution of the control surface about the hinge line of that surface.

The static balance system is comprised of the balance panels, the aluminum bronze balance panel hinges, and the corrosion-resistant steel horn weight. This structure, together with the remaining elevator structure forward of the elevator-hinge centerline, balances the tab assembly and elevator structure aft of the elevator-hinge centerline. A balance adjust weight system is included in the elevator design to "fine tune" the balance to within the limits specified by the Flutter and Vibration group.

In the design of the elevator system, the use of graphite-epoxy for structure aft of the elevator-hinge centerline allows a reduction in weight of the balance system structure forward of the elevator-hinge centerline, from that used in the baseline metal elevator system. An additional balance system weight reduction results from the Flutter and Vibration groups re-analysis of the specific lateral weight distribution to which the metal elevator system is subjected. This enables the required balancing mass to be located at the most advantageous moment arms.

The total weight reduction of the revised balance system structure is 40.3 kg (88.6 lb), representing a 28.7% savings from the comparable metal baseline structure.

The weight reduction of the redesigned structure aft of the elevator hinge centerline is 27.7 kg (61.0 lb). This represents a 23.6% savings from the comparable metal baseline structure.

An analysis of the areas of application of graphite-epoxy material, for component parts in the elevator surface and tab assembly, shows a 26.5% weight reduction from the baseline aluminum components.

4.7.3 WEIGHT/TIME HISTORY

Figure 136 shows the trend of the elevator system weight through the program.

The predicted weight at the beginning of the program was developed from preliminary design information and layout drawings. As more detailed definitions became available, the predicted weights were refined to reflect updating of the earlier information, and the addition of corrosion and lightning protection systems.

A weight reduction early in 1978 reflects the introduction of FM 300 adhesive, and the reduction in quantity of trailing-edge faying-surface sealant (BMS 5-79). With 100% drawing release, an increase in weight occurred when the analysis of these drawings, replaced the previous layout drawing predictions. As actual weights of detailed parts became available these were substituted for the production drawing weights and a small weight decrease occurred. The total weight then remains unchanged except for the addition of straps to the lower skin panels.

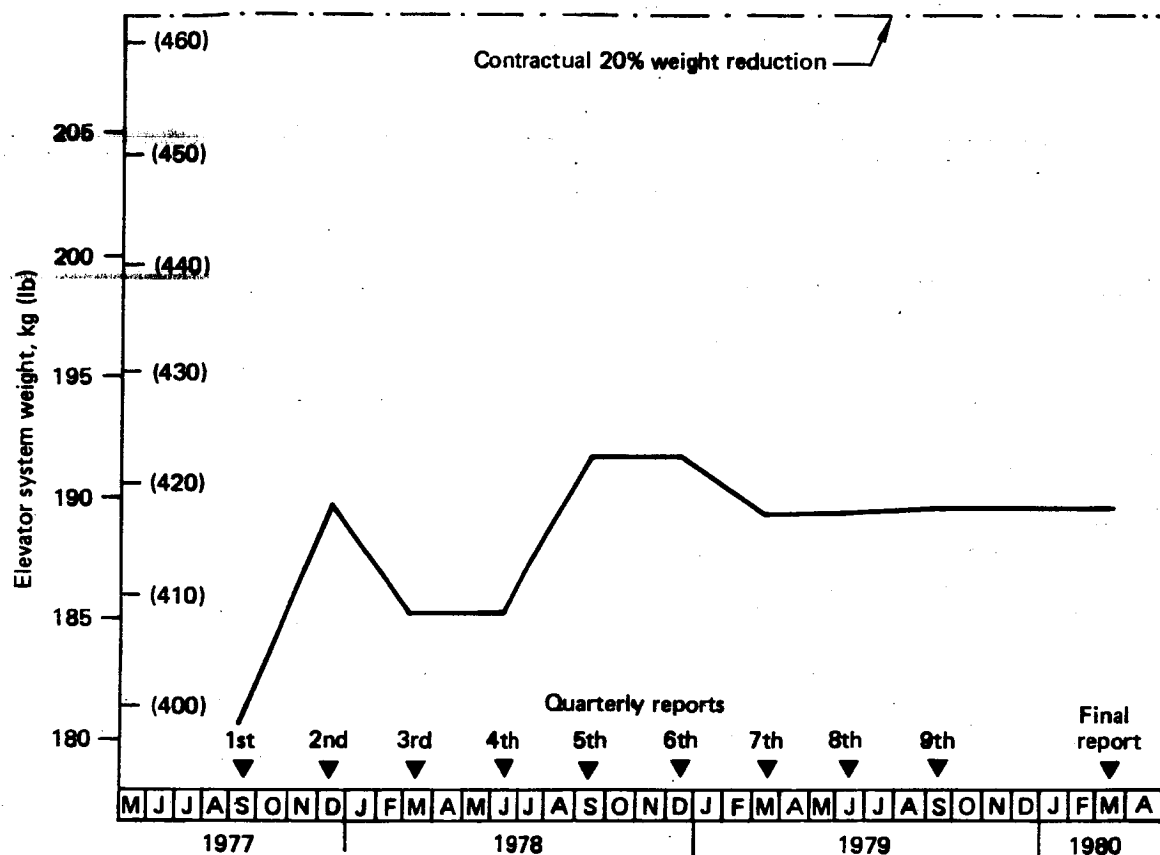


Figure 136. Advanced-Composite Elevator System Predicted Weight/Time History

4.7.4 CONCLUSIONS

The five graphite-epoxy elevator systems have shown weight reductions, from the comparable metal elevator system, of 26.4 to 27.3%. Table 13 gives the component weights for the metal baseline elevator and the predicted component weights for the graphite-epoxy elevator.

Figure 137 shows the actual weight and cg location for five shipsets of elevator systems, together with the predicted values. The plot shows a decreasing weight trend throughout the program attributable to design improvements. The reduction in shipsets No. 4 and No. 5 is partly attributed to the deletion of surfacer from the skin panel outer surfaces.

Table 13. Weight Comparison [kg (lb)/airplane]

Item	Baseline aluminum elevator, kg (lb)/airplane		Predicted advanced composites elevator kg (lb)/airplane		Weight difference, kg (lb)/airplane	Percent weight difference
Front and rear spars	35.2	(77.7)	28.4	(62.7)	-6.8 (-15.0)	-19
Ribs—inspar	12.0	(26.6)	4.4	(9.6)	-7.6 (-17.0)	-64
Skin panels	52.8	(116.3)	45.4	(100.2)	-7.4 (-16.1)	-14
Control tab	11.1	(24.4)	6.8	(15.0)	-4.3 (-9.4)	-39
Horn rib fairings	6.0	(13.2)	3.8	(8.4)	-2.6 (-4.8)	-36
Corrosion protection	0	(0)	0.6	(1.3)	+0.6 (+1.3)	—
	0	(0)	0	(0)	0	—
Replace structure	117.1	(258.2)	89.4	(197.2)	-27.7 (-61.0)	-24
Balance panel weights	32.0	(70.6)	0	(0)	-32.0 (-70.6)	-100
Balance panel hinges	54.6	(120.3)	38.3	(84.4)	-16.3 (-35.9)	-30
Horn balance weight	18.8	(41.5)	23.6	(52.1)	+ 4.8 (+10.6)	+26
Elevator adjust weight	0	(0)	1.8	(4.0)	+ 1.8 (+4.0)	—
Nose ribs and skins	18.9	(41.6)	20.1	(44.4)	+ 1.2 (+2.8)	+7
Balance panel structure	16.0	(35.2)	16.2	(35.7)	+ 0.2 (+0.5)	+1
Revised structure	140.3	(309.2)	100.0	(220.6)	-40.3 (-88.6)	-29
Total elevator system, kg (lb) airplane	257.4	(567.4)	189.4	(417.8)	-68.0 (-149.6)	-26.4

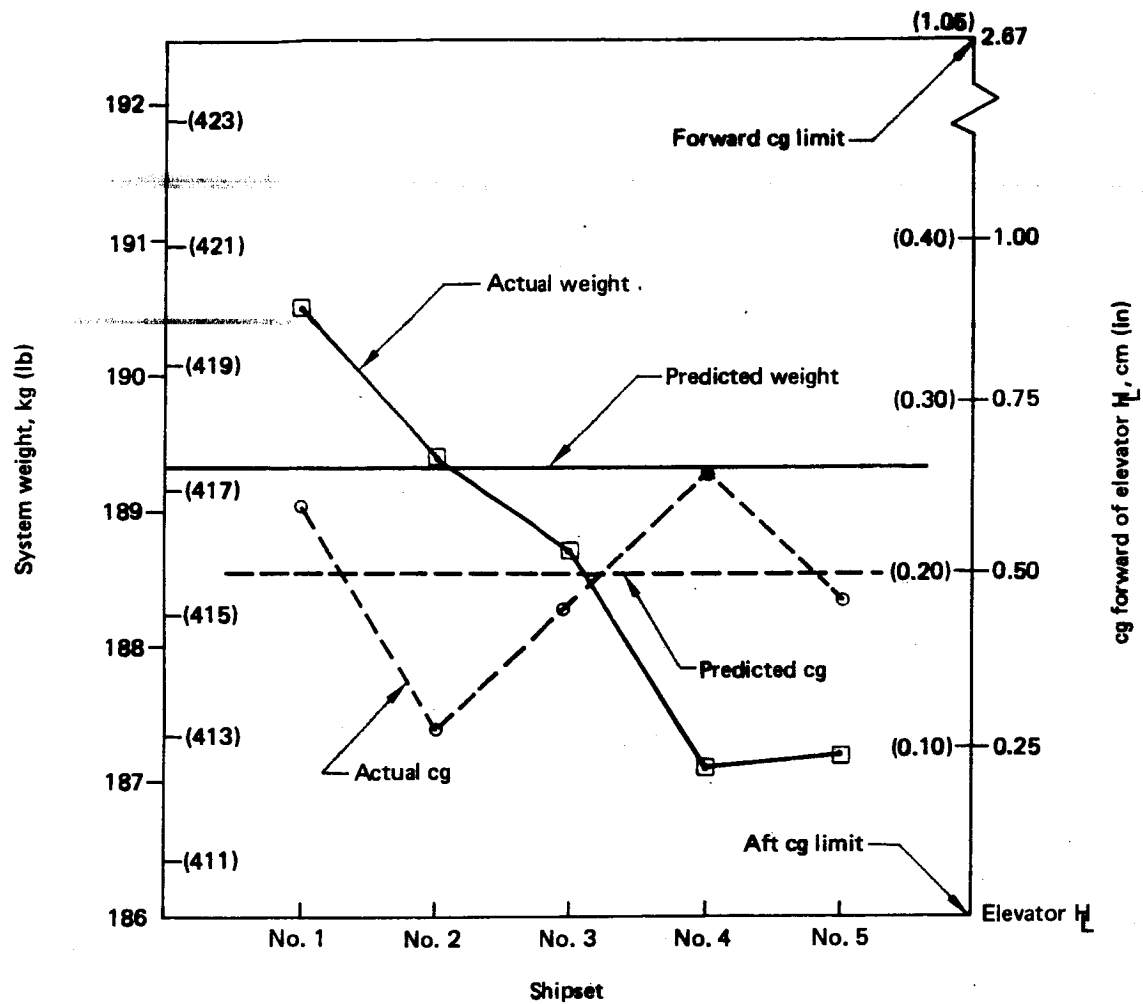


Figure 137. Elevator System Actual Weight and Balance Data (Elevator Surface, Control Tab, and Balance Panels)

5.0 OPERATIONS

This section presents the results of manufacturing efforts in the development of tooling and fabrication procedures, ancillary test part production, and quality assurance standards and nondestructive inspection techniques.

5.1 MANUFACTURING DEVELOPMENT

Section 5.1 contains the history and results of manufacturing efforts to establish and evaluate the fabricability of engineering designs and to determine the effectiveness of the developed manufacturing tooling and processes.

5.1.1 PRODUCIBILITY STUDIES

The following paragraphs describe the work done to determine producibility of the elevator components and the cost-effectiveness of varying design elements and production procedures.

5.1.1.1 Trade Studies

Precontract feasibility and cost studies determined the need for manufacturing development of the minimum rib/honeycomb-sandwich elevator configuration. The subsequent detail studies and their results are discussed below.

Rib Design—This study showed that the honeycomb sandwich rib could be produced in less than one-half the labor hours required to fabricate the corrugated laminate rib. Also, tool side bridged areas in the female portion of the sinewave required repair and rework in production. The honeycomb sandwich and corrugated designs are shown in Figure 138.

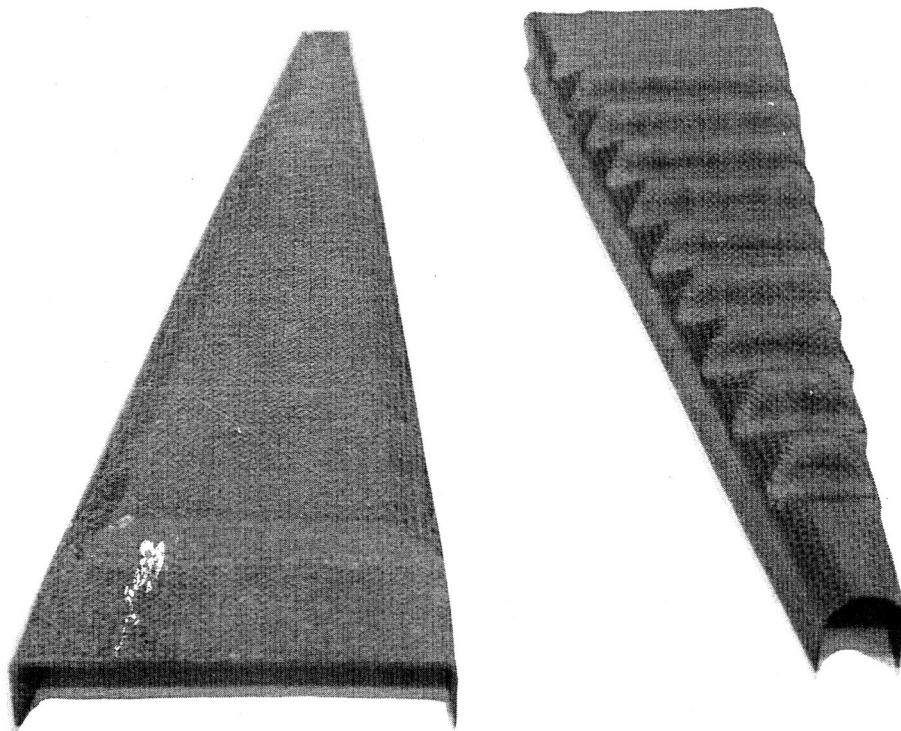


Figure 138. Honeycomb Sandwich and Corrugated Laminate Ribs

Elevator Section Feasibility Hardware—A full-scale, 125-cm (49-in) long elevator section was fabricated, demonstrating the producibility and establishing acceptability of the tooling approach and resulting tolerances. Also, cost-effectiveness calculations were performed for the no-bleed resin system with woven, or two-ply, preplied, unidirectional broadgoods versus the higher resin content surface bleed system with 30.5-cm (12-in) wide unidirectional tape. The results indicated that use of the no-bleed system would provide a 15% cost savings over the surface-bleed type.

Skin Panel Material Form—A woven fabric, when compared to tape, was shown to be the most cost-effective material form for two reasons: less layup labor was required and there were fewer rejections due to fiber breakout when drilling through the panels than on unidirectional or preplied tapes. Photographs of the layup processes are shown in Figures 139 and 140. Table 14 compares relative cost for the different material forms.

Surface Finish Study—Surface finishing time, using static conditioner, epoxy primer, and topcoat on different material forms, was greatest for woven fabric. However, overall fabrication with woven fabric remained the most cost-effective (table 14).

Skin Panel Configuration—A sandwich feasibility panel, using tape on the outside surfaces with fabric doublers and fillers on edgebands, met most manufacturing objectives; i.e., reduced layup time, elimination of lateral core crush in chamfered areas, surface finish equivalent to all-tape construction, and acceptable fiber breakout on drilling and countersinking. The feasibility skin panel shown in Figure 141 was selected as the basic cover panel configuration.

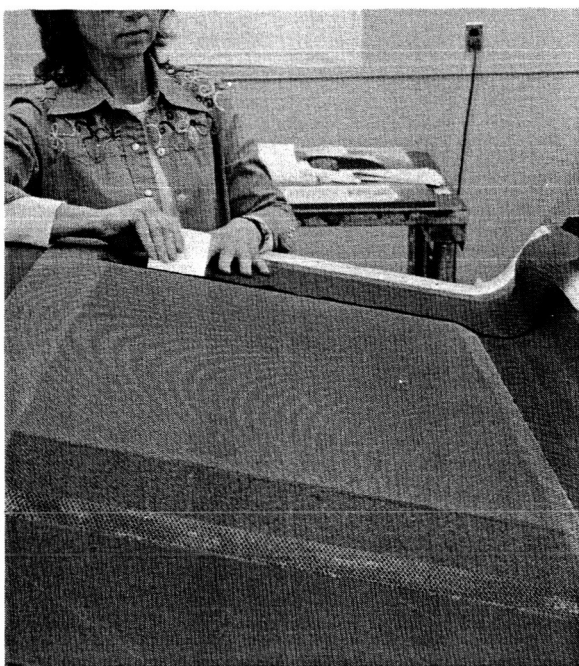


Figure 139. Layup of Fabric Skin Panel



Figure 140. Layup of Preplied Tape Skin Panel

Table 14. Material Form and Finishing Cost Study

Material form	Relative Cost	
	Without finishing	With finishing
Woven fabric	1.00	1.00
2-ply preplied tape	1.25	1.21
4-ply preplied tape	1.10	1.05
30.5-cm (12-in) wide unidirectional tape	1.39	1.35

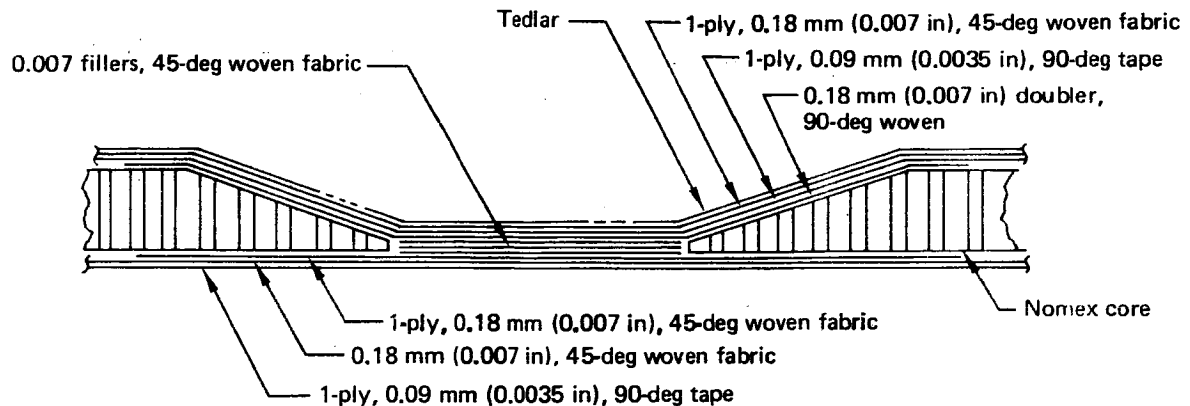


Figure 141. Graphite-Epoxy Feasibility for Skin Panel

Rib Configuration—A producibility trade study made during rib layup showed that substitution of one ply of unidirectional tape for fabric on the tool side of the rib improved surface finish, but resulted in unacceptable fiber breakout on drilling. A solution was to add a single ply band of fiberglass on the hole breakout side.

5.1.1.2 Trailing-Edge Tolerance Panel

Tooling and processing methods were developed in this study to maintain 0.15-cm (0.06 in) bondline tolerance between cover panels at the elevator trailing edge (fig. 142). These methods were used in the fabrication and assembly of the test and verification hardware and the five and a half production shipsets. A brief description of the methods follows.

Improved Core Location—The core runout, as opposed to the chamfered edge, was used as the reference point for locating the core on the tool (fig. 143).

Improved Bonding Surfaces—Use of a caul plate during cure to fair out bond surfaces at the trailing edge minimized interference fit between the cover panels during assembly (fig. 142).

Adhesive Application and Assembly—The amount of adhesive applied was controlled by use of a serrated sweeper having proper pitch and spacing, as illustrated in Figure 144. The holding fixture (fig. 145) was designed and constructed to hold the skins in alignment and provide controlled sealant flow during cure.

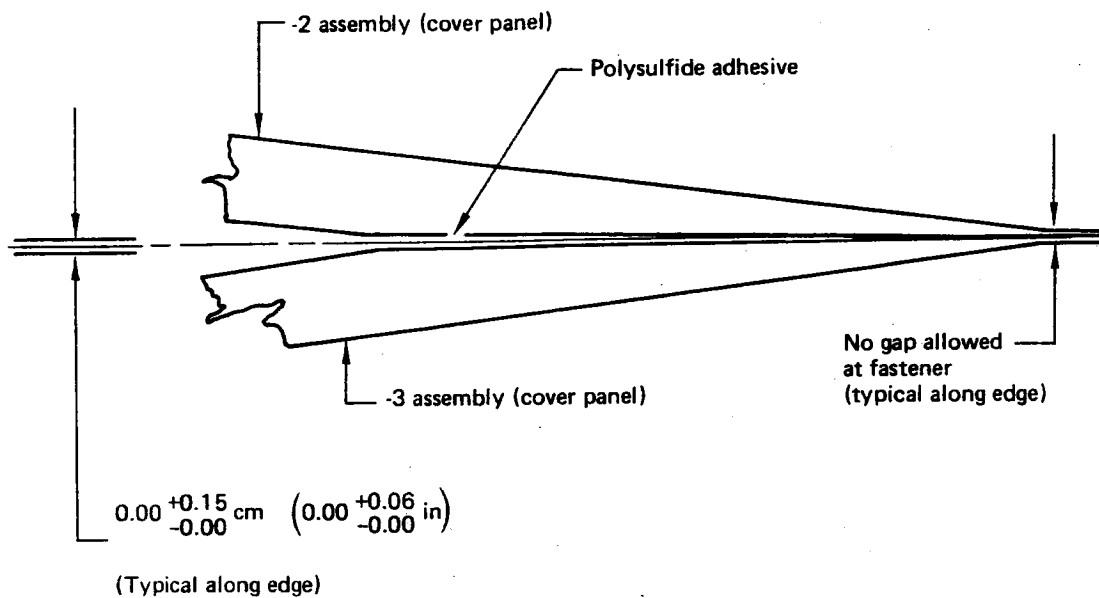


Figure 142. Trailing-Edge Tolerance

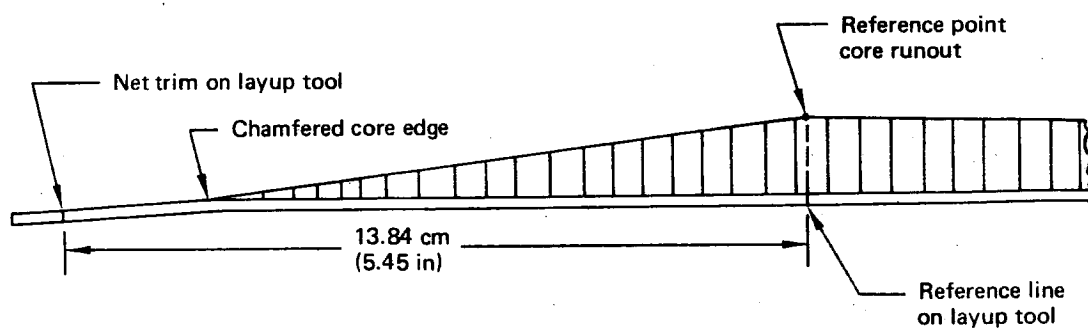


Figure 143. Core Locating Method

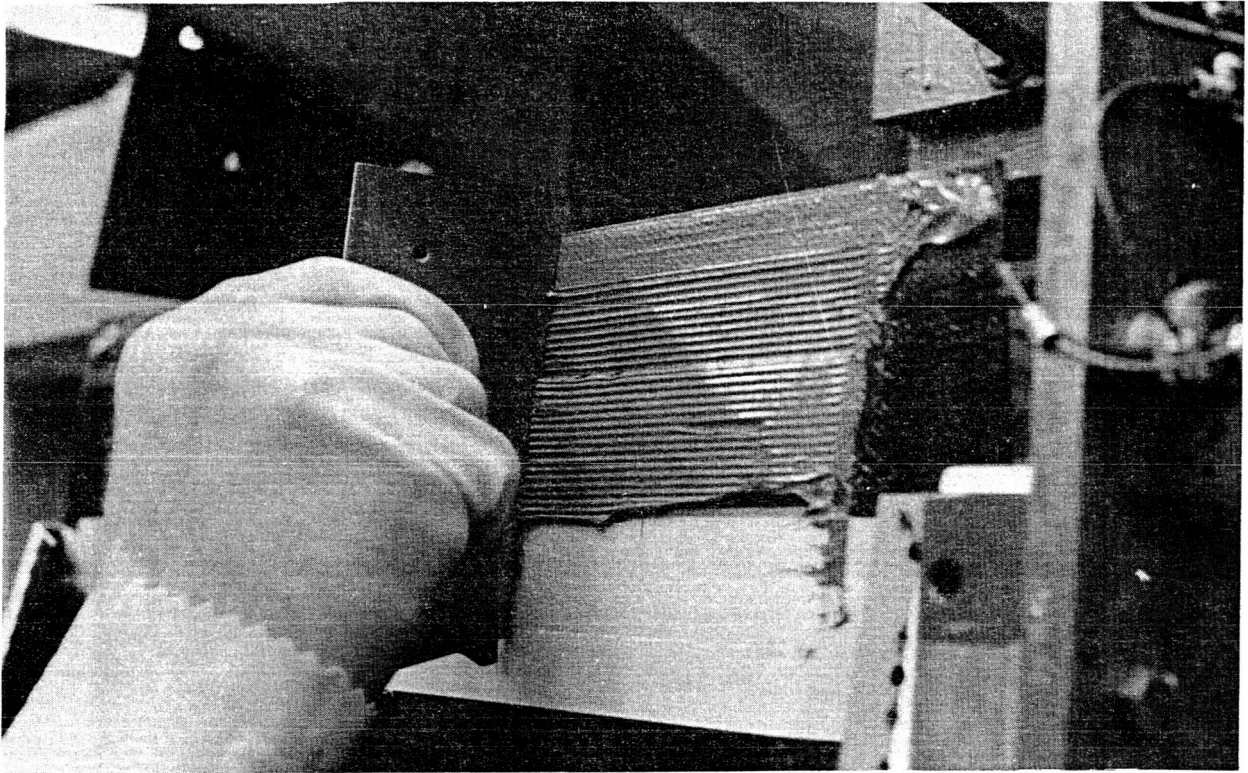


Figure 144. Application of Trailing-Edge Sealant and Adhesive

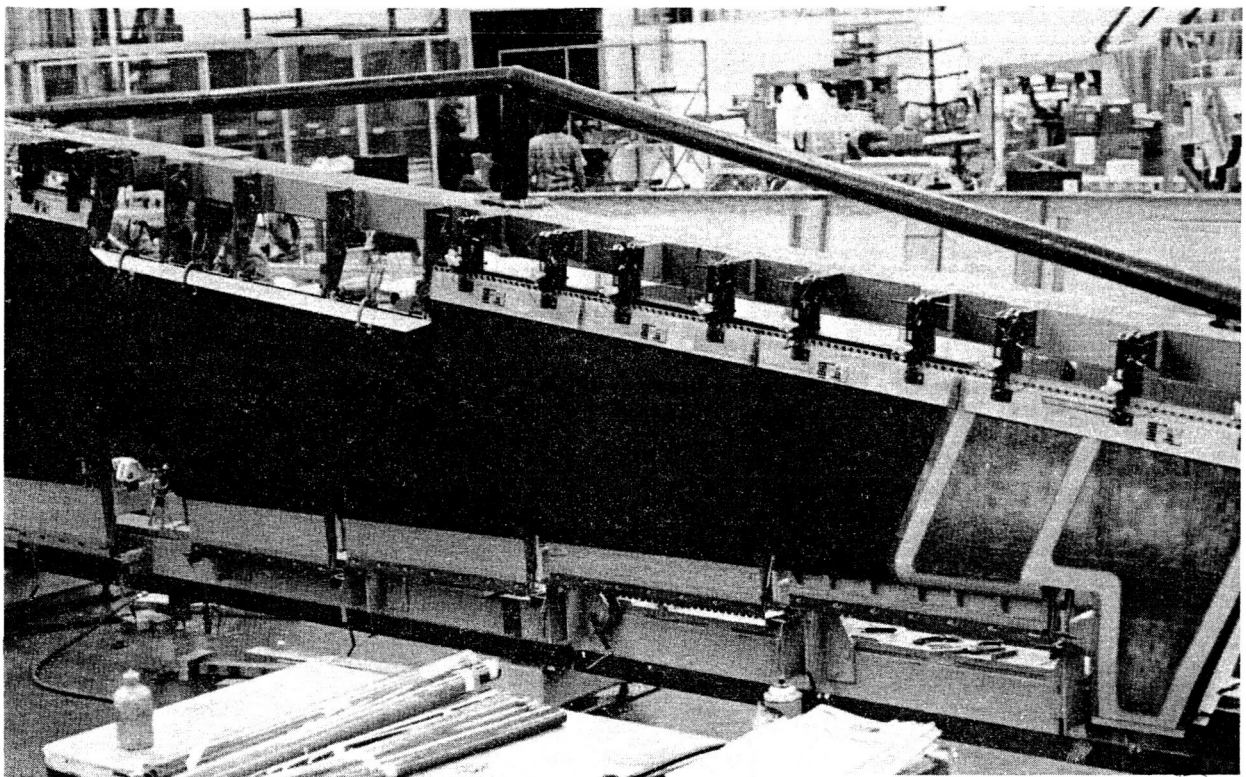


Figure 145. Elevator Major Jig Position Showing Upper Skin Panel in Position During Sealant Cure

5.1.1.3 Lightning Strike Protection

To provide the required lightning strike protection of the elevator outboard tip, a 0.05-cm (0.02-in) thick aluminum strip was bonded to the upper cover panel (fig. 146 and 147). A full-size lightning strike protection panel was fabricated for test and to verify the manufacturing technique for bonding the aluminum strips on the outer surface. The selected bonding process consisted of:

1. Cleaning the aluminum detail, phosphoric-acid anodizing, and coating with corrosion-inhibiting primer
2. Lightly abrading the outboard edge of the upper cover panel and then solvent wiping
3. Applying a thin coat of flexible polysulfide adhesive to the mating surfaces
4. Curing under vacuum pressure to obtain a thin, uniform bondline thickness

Layup of graphite-epoxy skins and Nomex core is shown in Figures 148 through 152. The aluminum strip bonded on the outside mold line (OML) of the test panel, using polysulfide adhesive and under vacuum pressure, is shown in Figure 152. After bonding, a protective finish system was applied that consisted of:

- Static conditioner to the fiberglass insulation
- Conductive coating
- Handling primer
- Epoxy primer
- Enamel

The finished panel, with static dischargers attached, is shown in Figure 153.

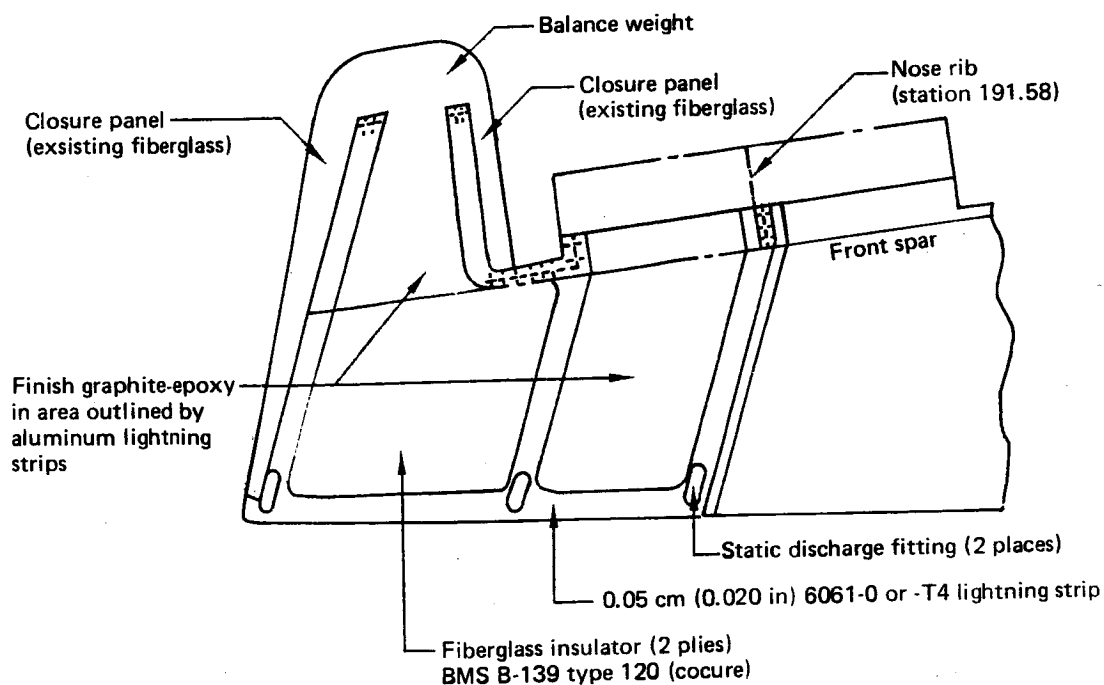


Figure 146. Lightning Strike Panel

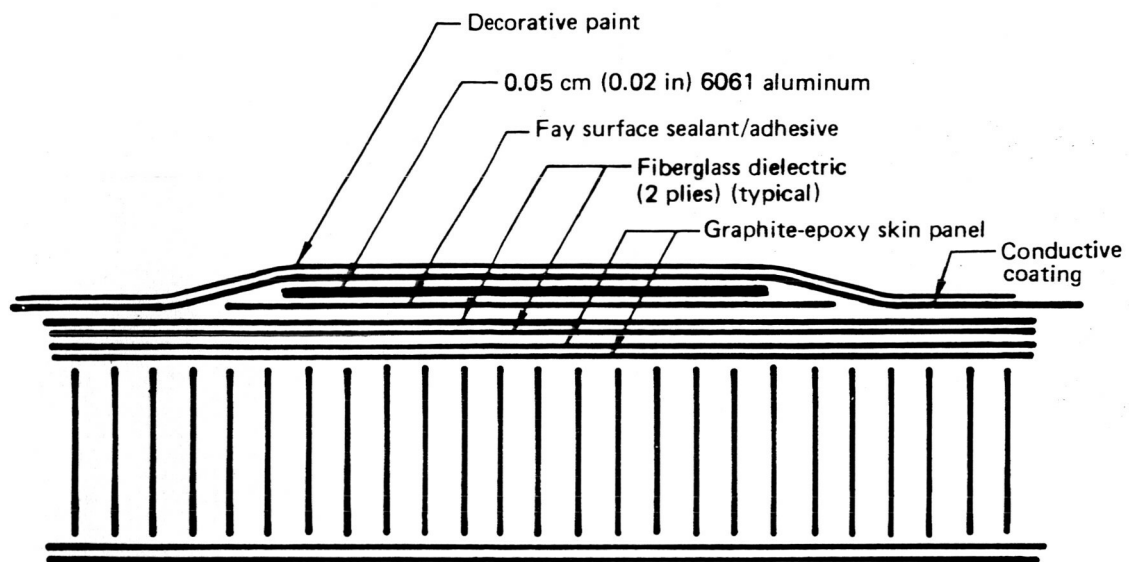


Figure 147. Layup of Lightning Protection System

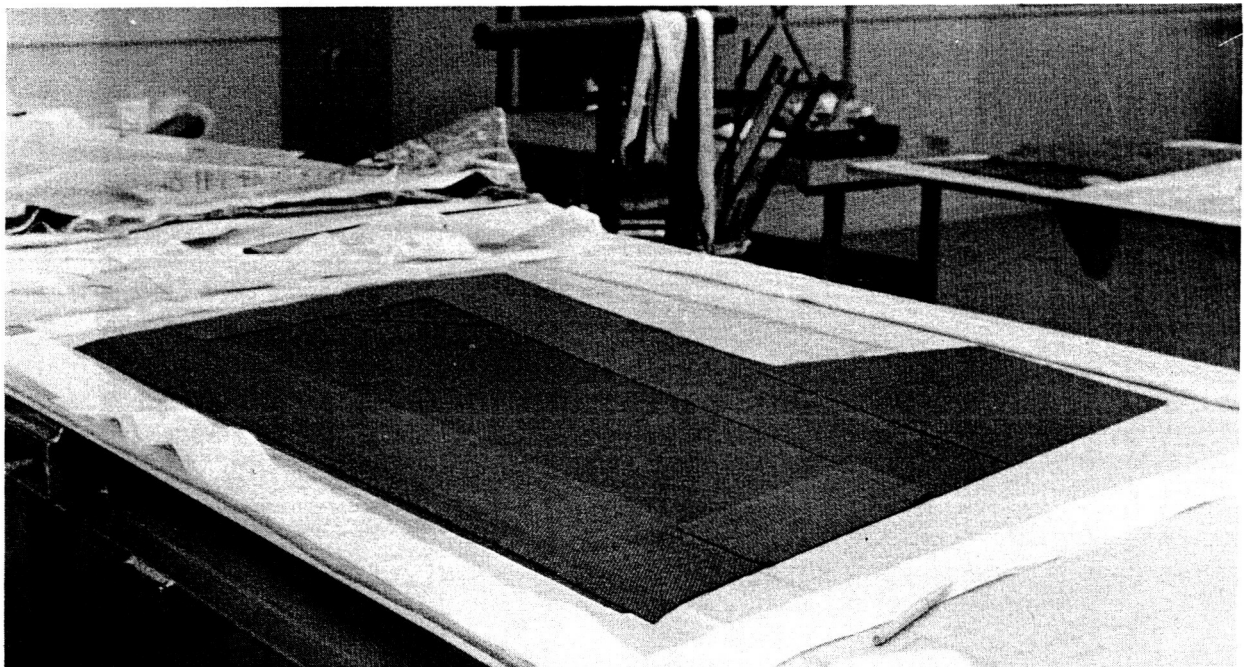


Figure 148. Lightning Strike Panel Showing Layup of Doublers and Outer Skin

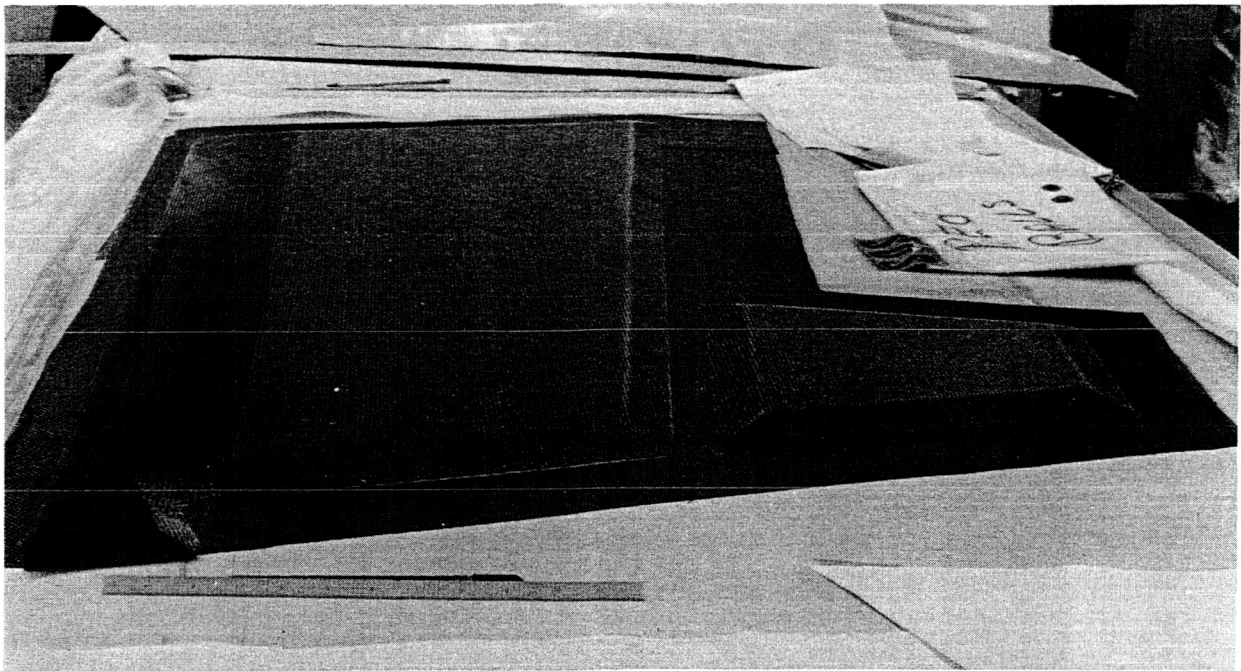


Figure 149. Lightning Strike Panel Showing Core in Place on Outer Skin

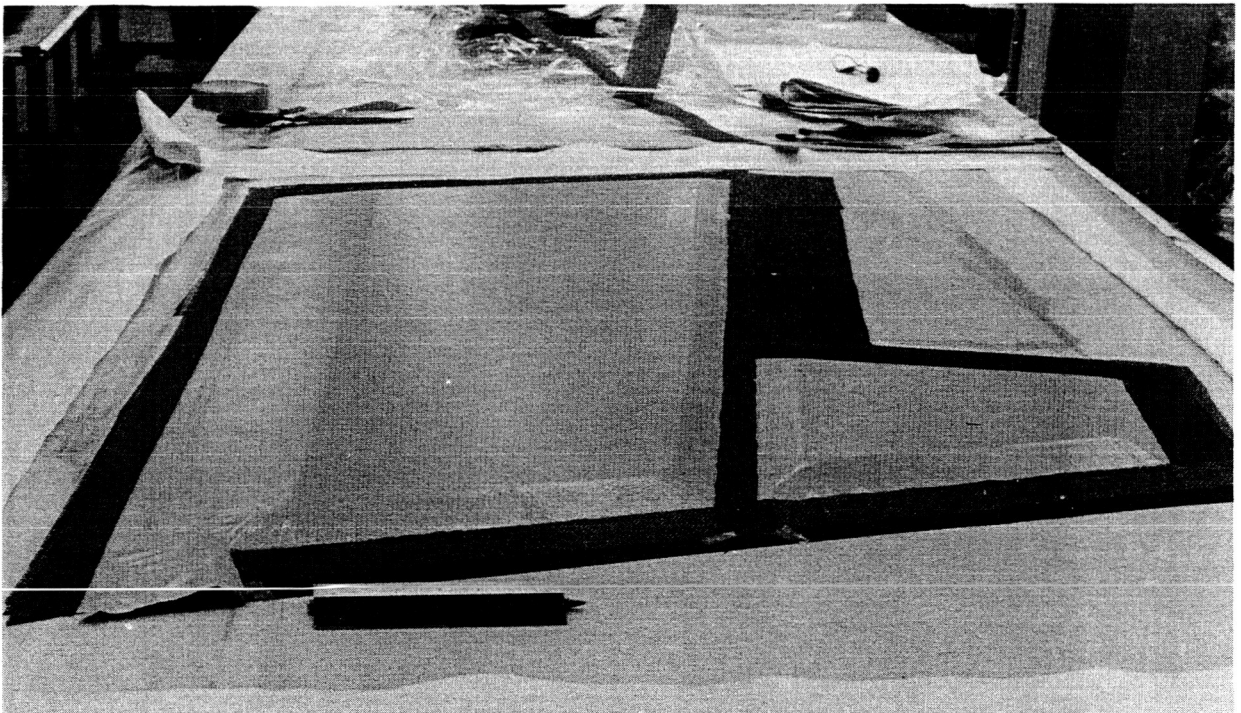


Figure 150. Lightning Strike Panel Showing FM 300 Adhesive on Core

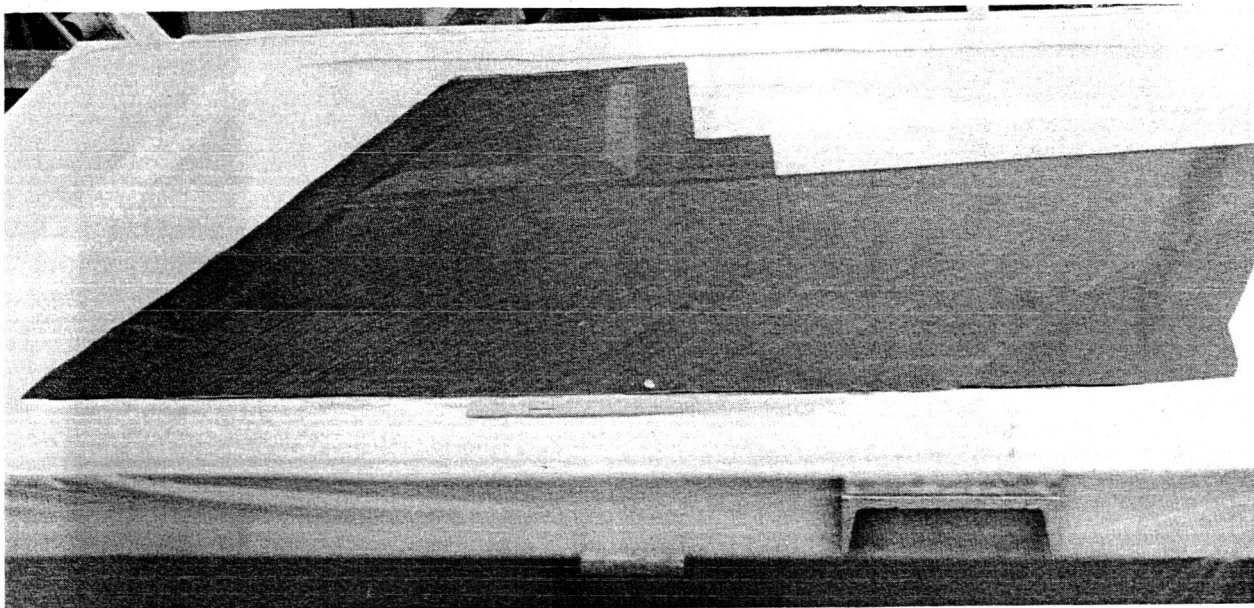


Figure 151. Lightning Strike Panel Showing Completed Layup Ready For Bagging

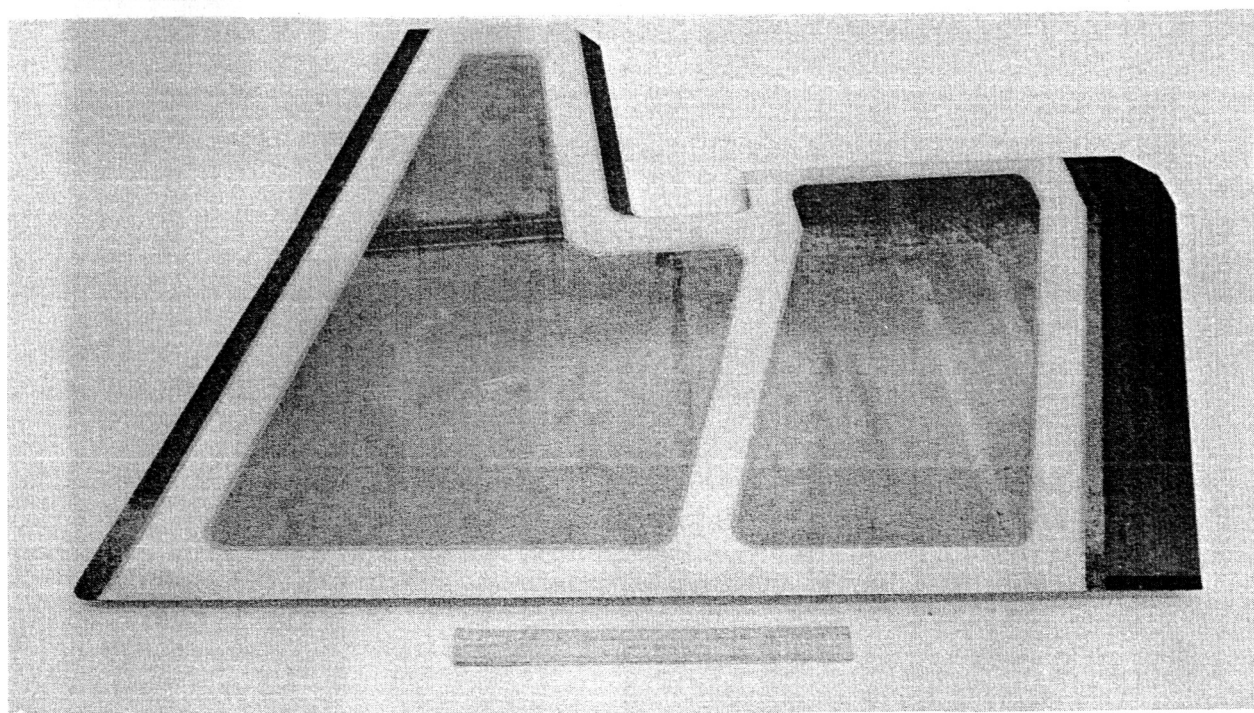


Figure 152. Lightning Strike Panel with Bonded Aluminum Strip

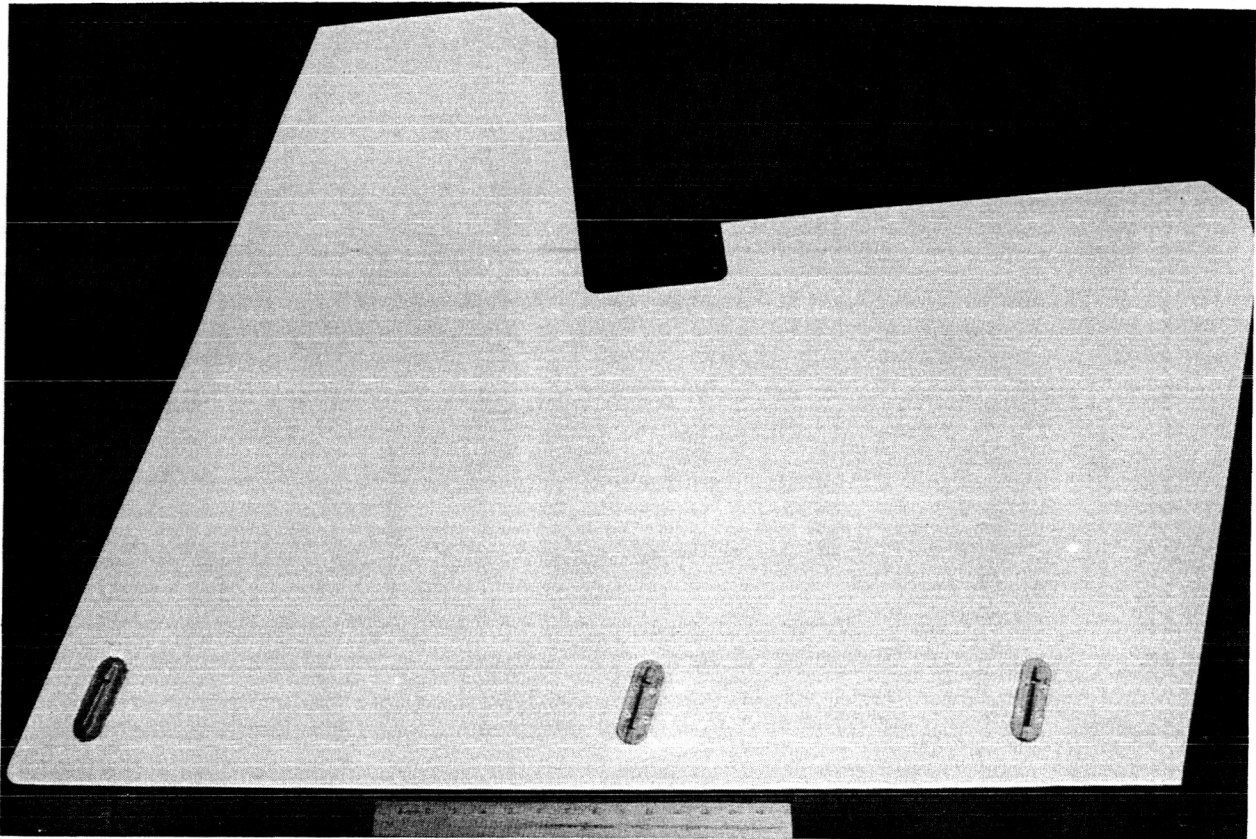


Figure 153. Lightning Strike Panel—Finished Part Ready for Test

5.1.1.4 Elevator Rear Spar

The improved design of the rear spar (fig. 9), incorporating the trailing-edge stiffeners as an integral part of the spar and eliminating one row of riveting, required the tool design and process development illustrated in Figures 154 through 159.

The first test part verified the one-piece tooling concept and design; the closed angle was easily sprung from the tooling. There was, however, some bridging in the radius areas at the upper edge of the precured filler (fig. 154). To remedy this condition, tape plies were added to the filler radii of a second test part and exterior pressure plates were added to provide a smooth transition across the spar surface in the area opposite the radii. Additionally, warpage of 0.91 cm (0.36 in) in the spanwise direction was corrected by changing the unidirectional tape layup of the precured filler to a quasi-isotropic layup of fabric. Warpage of 0.13 cm (0.05 in) on the second test spar could be eliminated with slight hand pressure and was, therefore, acceptable.

5.1.2 ANCILLARY TEST HARDWARE FABRICATION

Production of test hardware required to obtain engineering data is discussed in the following subsections. Results of studies undertaken to resolve fabrication problems are included.

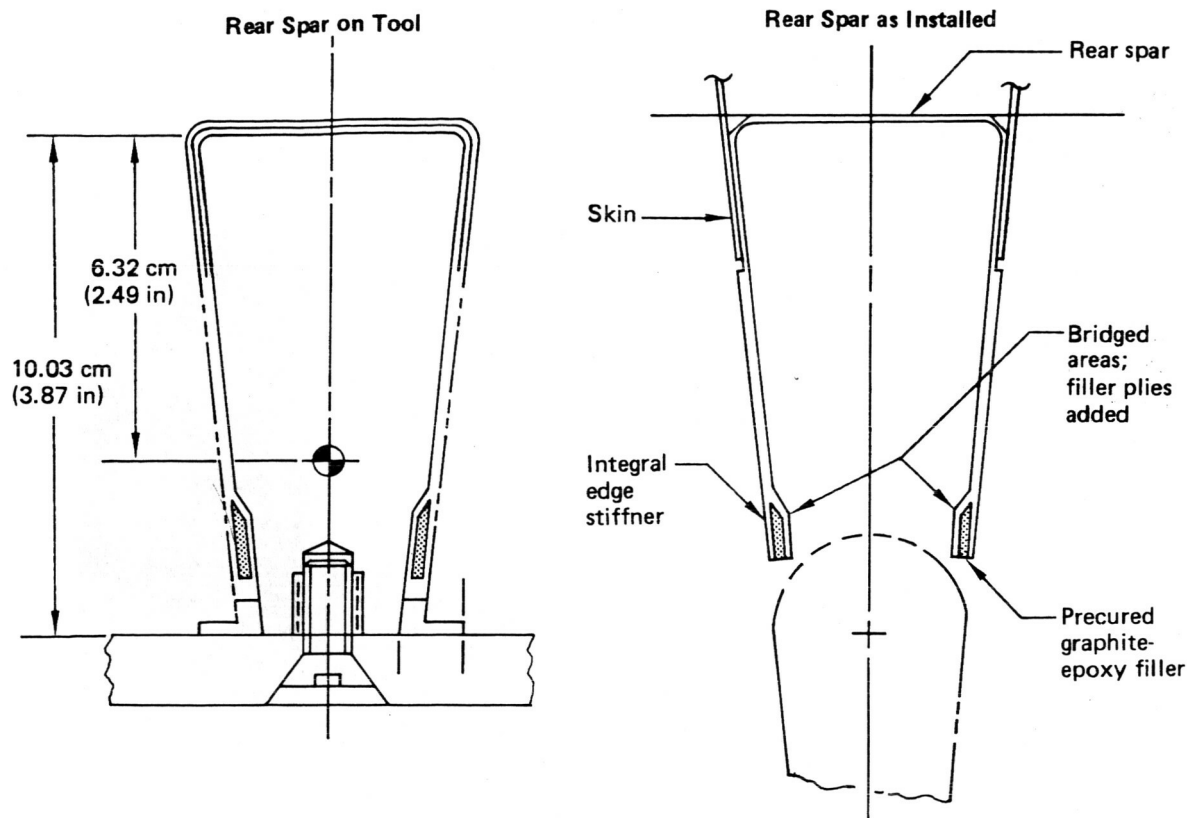


Figure 154. Rear-Spar Feasibility Hardware

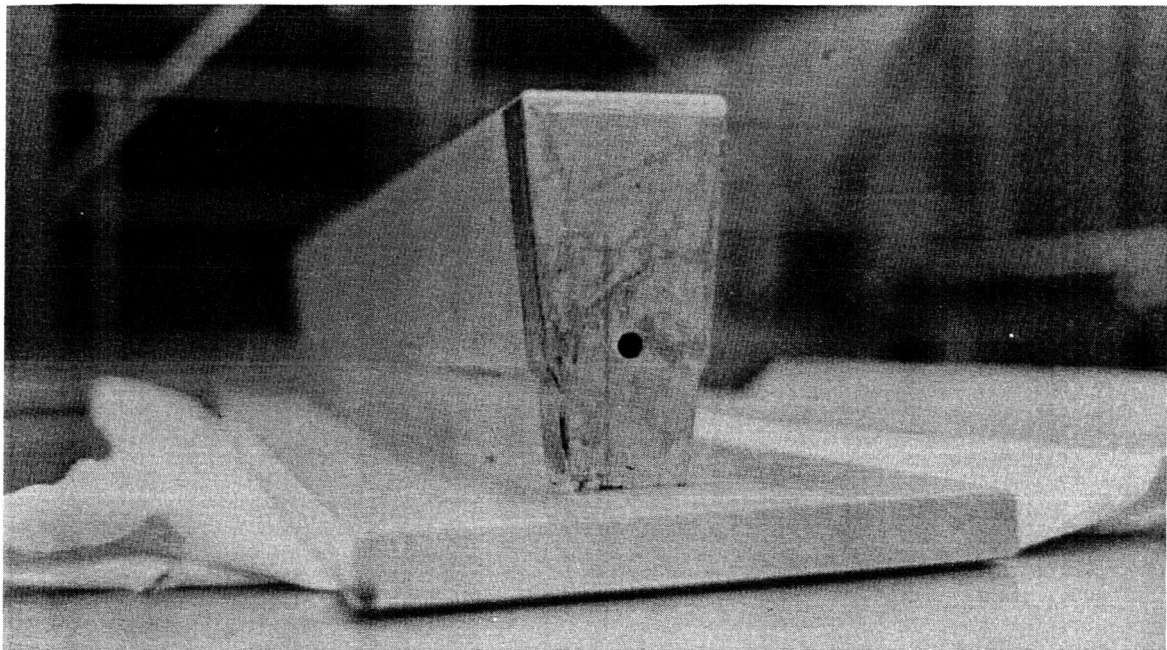


Figure 155. Rear-Spar Layup Material

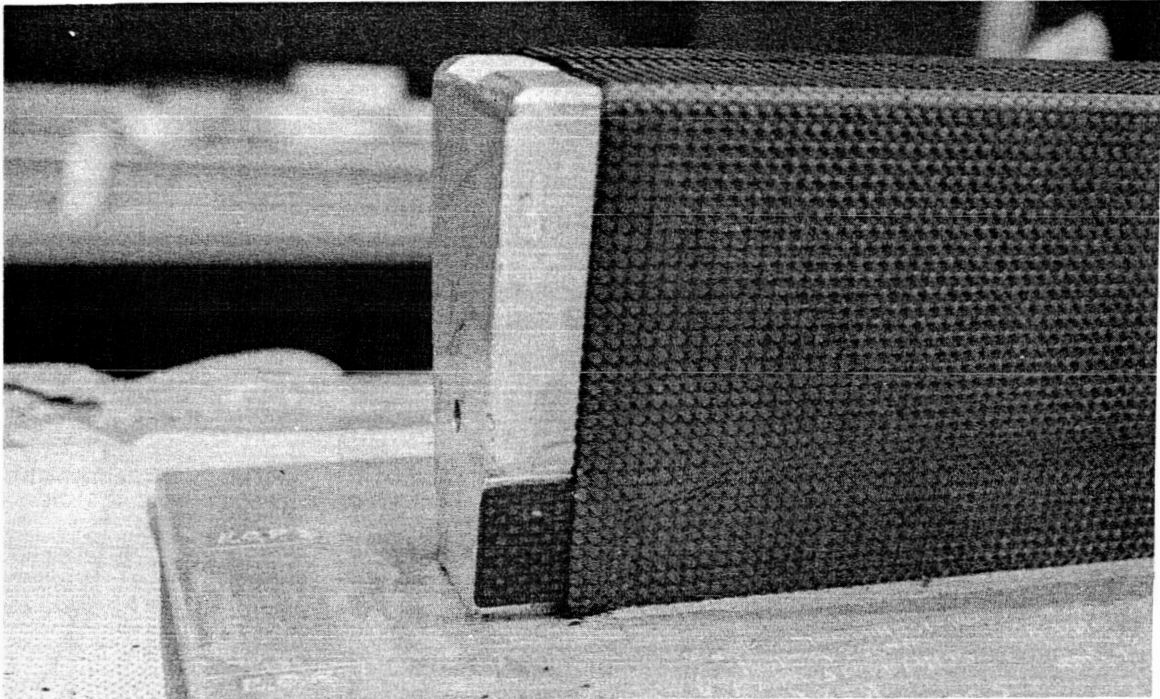


Figure 156. Rear-Spar Test Part Showing Initial Ply Layup Before Precured Filler



Figure 157. Rear-Spar Test Part Showing Application of Adhesive for Precured Filler

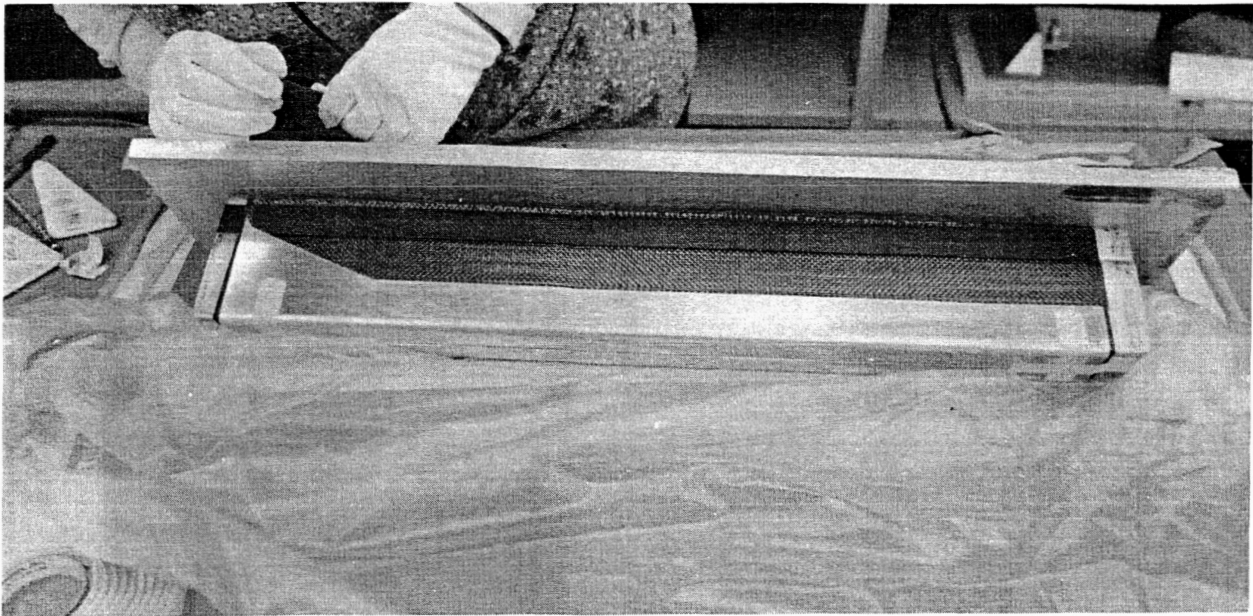


Figure 158. Rear-Spar Test Part Showing Location of Precured Filler

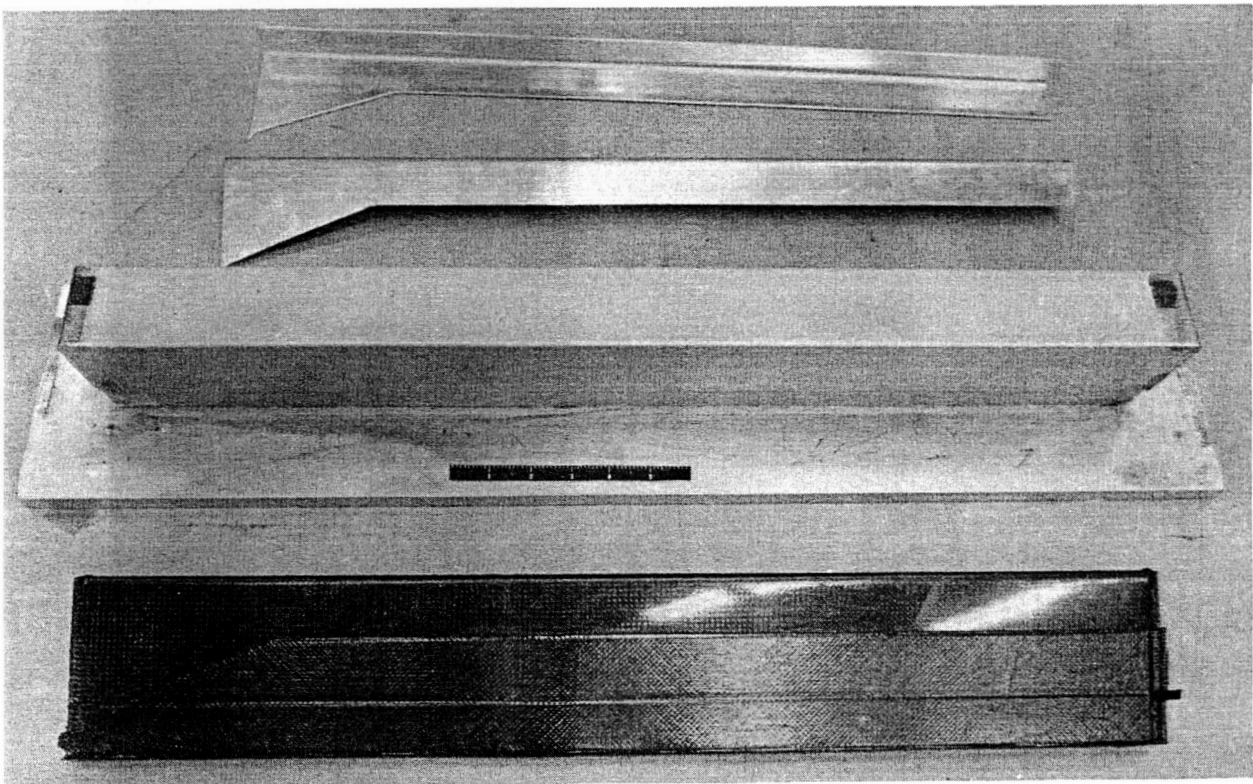


Figure 159. Rear-Spar Test Part Showing Finished Part With Tooling

5.1.2.1 Allowables and Environmental Effects

Hardware fabricated for this portion of the ancillary test program included laminate and honeycomb panels to provide coupons for tensile, compression, and shear strength determinations as required by the test program. During this phase of the contract, problems were identified that included out-of-tolerance dimensions, improper identifications, and errors in ply orientation. To correct these problems, a task force that included representatives from Manufacturing, Tool and Production Planning, Manufacturing R&D, Quality Control R&D, and Factory Quality Control was organized. The team developed the following:

- A procedure for "kitting" graphite-epoxy prepregs to minimize errors in ply orientation and drawing interpretation. Upon release of the Engineering Drawing, a prepreg kit is developed and incorporated into the Manufacturing Plan. Each detail is pictured in an isometric drawing showing skin, doubler, and filler ply locations. Refinements and revisions of the kit are made during the first-part fabrication.
- A procedure to reduce waviness in the specimens where mismatch occurred at the transition where the honeycomb core was prepotted for gripping test specimens. This required the substitution of BMS 5-28 Type 13 potting compound for BMS 5-28 Type 7 and cocuring with the graphite-epoxy face sheets.
- A procedure for bonding fiberglass grip tabs on laminate specimens, which brought associated waviness within drawing tolerances. This incorporated perforated Teflon (FEP) on each side, and fiberglass plies at the perimeter with a flat caul plate in an envelope bag and cured at 241 kPa (35 lb/in²).
- A quality control procedure for measuring waviness, using a profilometer on an inspection surface table.

5.1.2.2 Concept Verification

This portion of the ancillary test program included process and assembly verification of the following test structures and development of the requisite tooling and processes:

- Panel-to-rib pad, Test 8 (fig. 160)
- Spar/aluminum splice, Test 11 (fig. 161)
- Honeycomb panel stability, Test 10 (fig. 162)
- Panel edge shear, Test 12
- Rib design, Test 14; shown on layup tool in Figure 163
- Sonic test box, Tests 15 and 18 (figs. 164 through 166)
- 10-ft outboard test box, Test 17 (figs. 167 through 169)

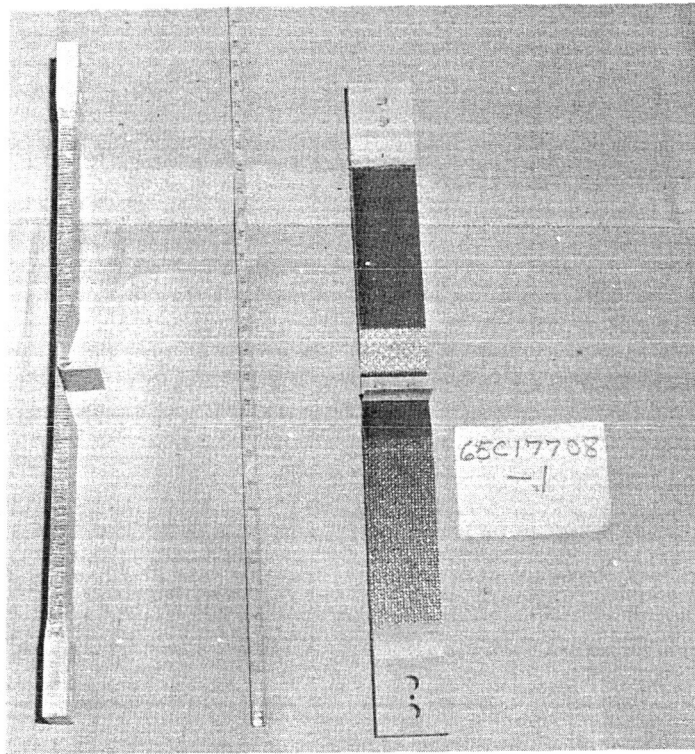


Figure 160. Panel-to-Rib Pad (Test 8) Showing Typical Test Specimen

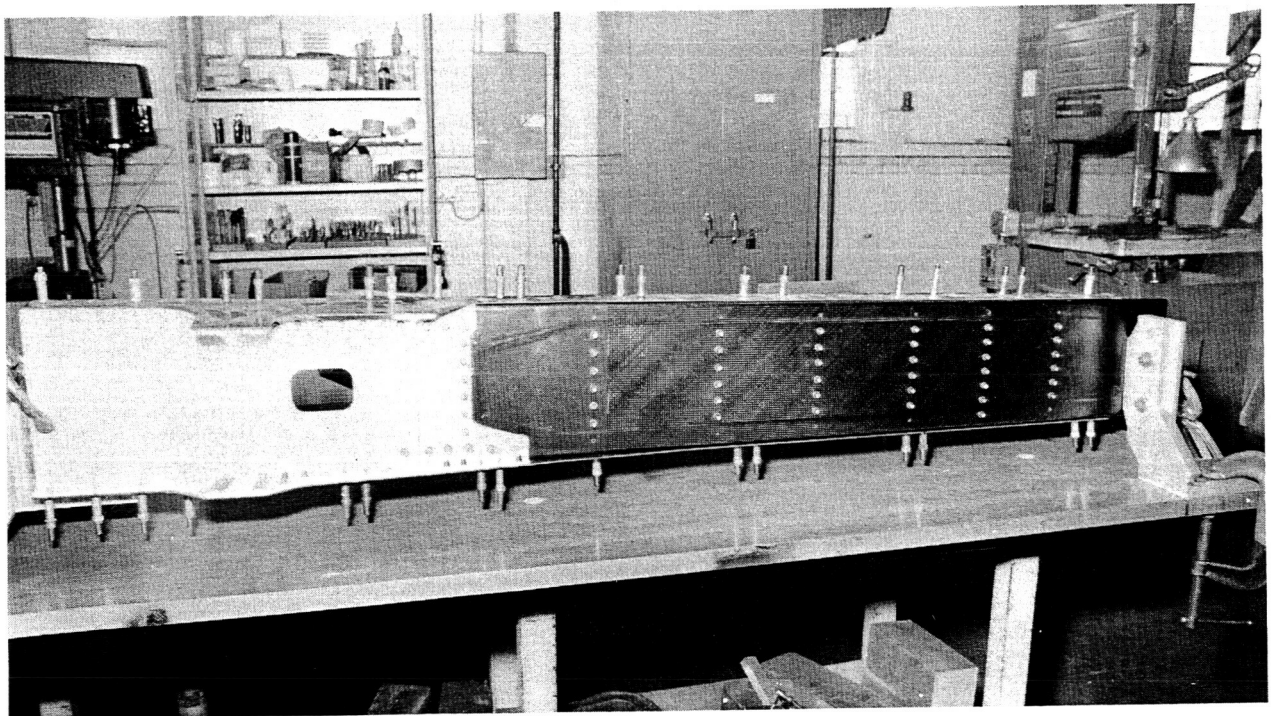


Figure 161. Spar/Aluminum Splice (Test 11) Showing Test Part Being Assembled

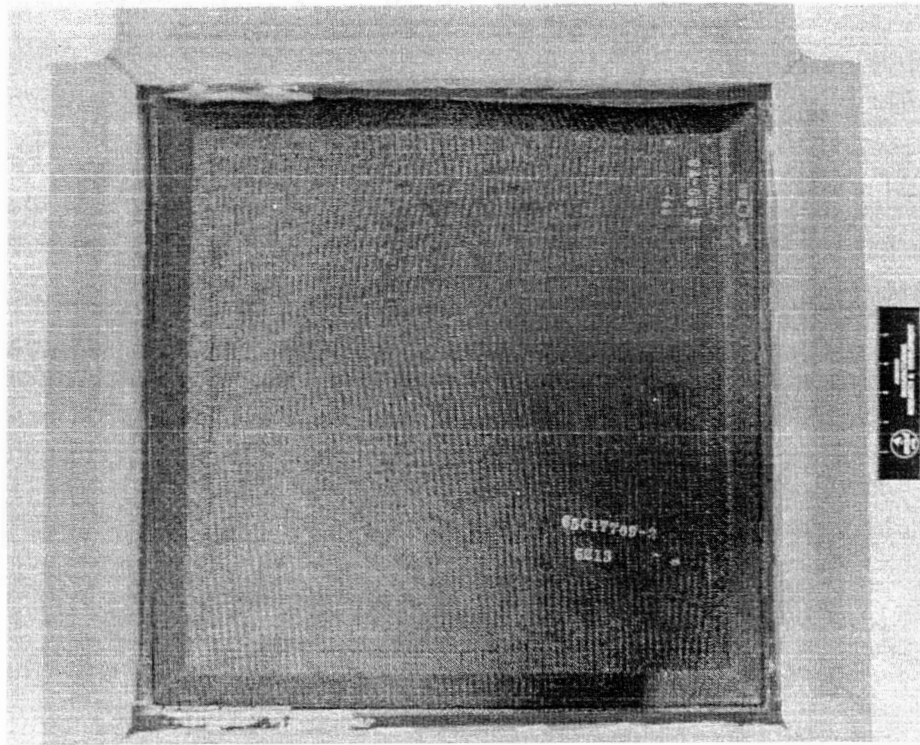


Figure 162. Honeycomb Panel (Test 10) Showing Honeycomb Panel with Grips



Figure 163. Rib Verification (Test 14) Showing Rib Ready for Cure

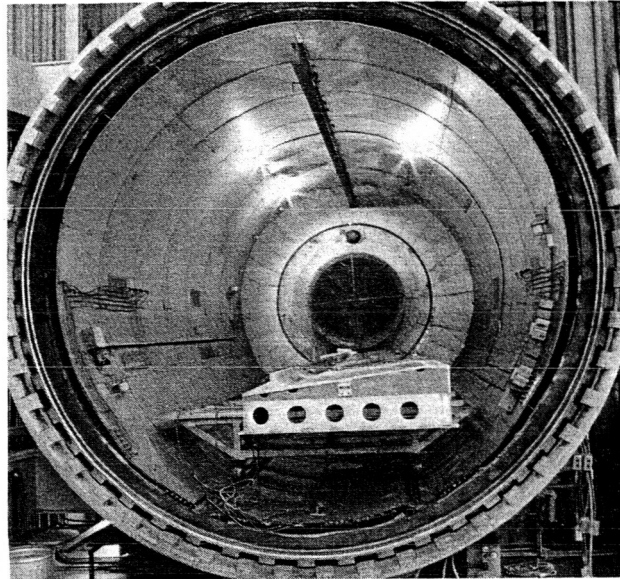


Figure 164. Second Sonic Box (Test 18) Showing Skin Panel in Autoclave

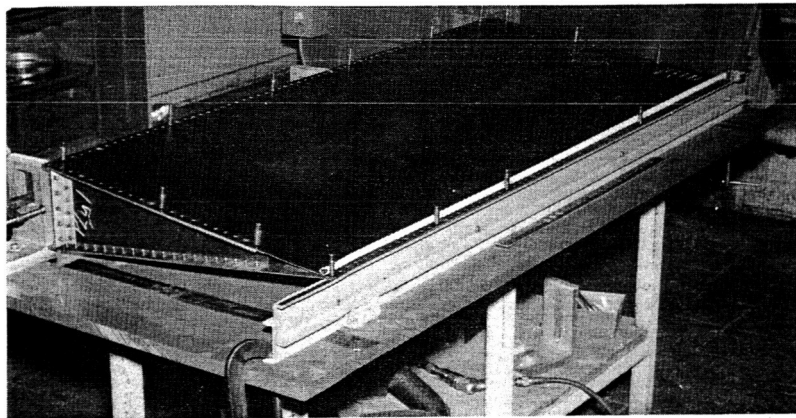


Figure 165. Sonic Test Box (Test 15) Showing Test Box Being Assembled

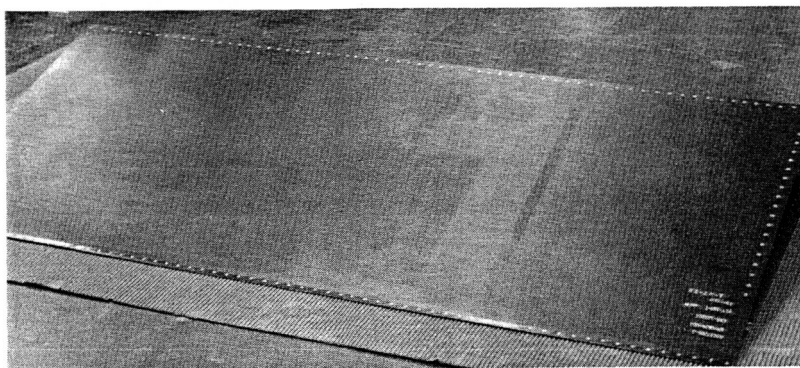


Figure 166. Sonic Test Box (Test 15) Showing Assembled Test Box

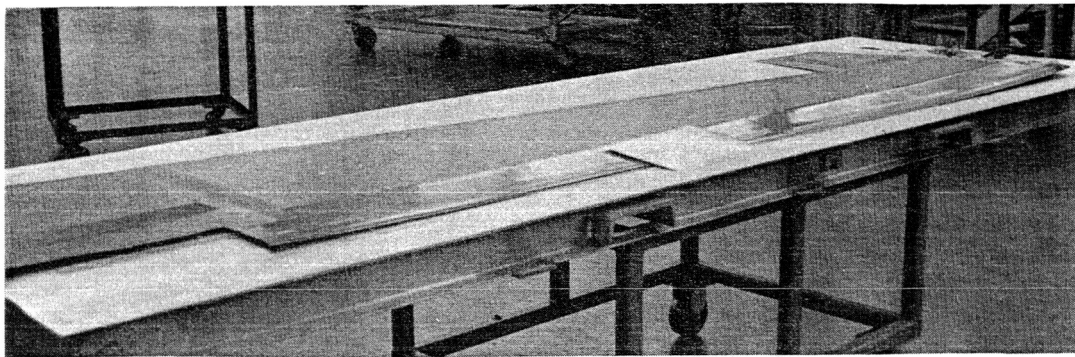


Figure 167. 10-ft Test Box (Test 17) Showing Complete Cover Panel

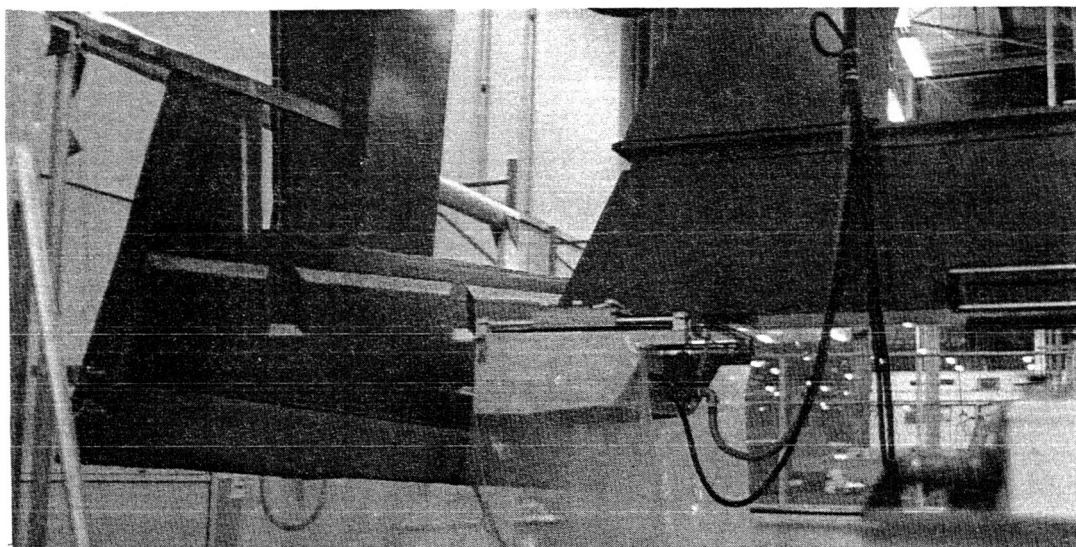


Figure 168. 10-ft Test Box (Test 17) Showing Cover Panel Being Inspected by Through-Transmission Ultrasonic

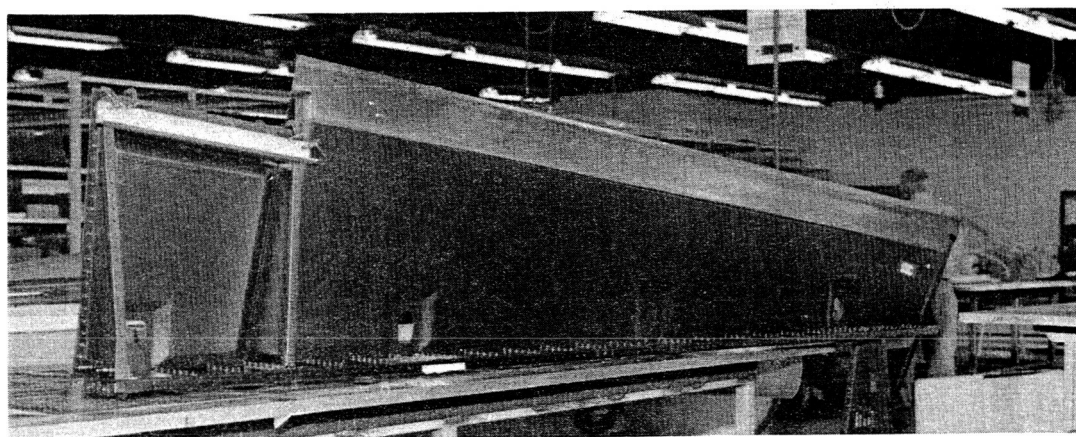


Figure 169. Assembly of Test 17 Outboard Test Box, Showing Assembled Lower Skin, Ribs, and Rear Spar

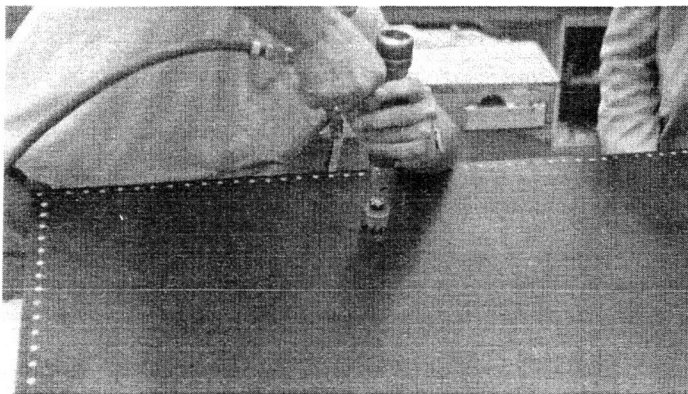
5.1.2.3 Damage Repair

To repair accidental impact damage to the honeycomb skin panel of the sonic test box, the following procedure (illustrated in fig. 170 through 175) was developed and used:

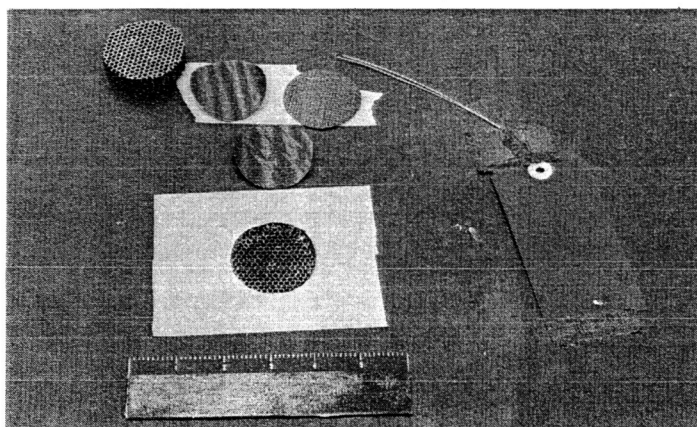
1. Locate damage area.
2. Drill 0.64-cm (0.25-in) pilot hole in center of damaged area. Maximum depth 0.64 cm (0.25 in). Use drill stop.
3. Cut a 5.08-cm (2.0-in) diameter hole through the graphite-epoxy skin, using a carbide-tipped hole saw with a pilot. Use drill stop to prevent pilot from extending deeper than 0.64 cm (0.25 in).
4. Carefully remove cut-out graphite-epoxy.
5. Sand exposed core to a depth of 0.64 cm (0.25 in) with a disc sander. Vacuum residue.
6. Install one layer of 120°C (250°F) curing epoxy adhesive, BMS 5-101, to exposed core surface.
7. Install one layer of cured graphite-epoxy fabric (one ply) after sanding surfaces and methyl ethyl ketone (MEK) wiping.
8. Install one layer of BMS 5-101.
9. Cut a Nomex core plug 0.952 cm (0.375 in) thick with a 5.08 cm (2.0 in) diameter.
10. Wrap a layer of foam adhesive around the core plug edge.
11. Insert the core plug into the hole area being repaired.
12. Bag and cure under vacuum (use heating blanket).
13. After cure, sand core plug flush to graphite-epoxy skin surface with a disc sander.
14. Prepare cured patch (one ply 45-deg fabric plus one ply 90-deg tape) and cut 10.16-cm (4-in) square with 1.27-cm (0.5-in) radius on corners. Sand bond surfaces of patch and graphite-epoxy skin and MEK wipe.
15. Apply BMS 5-101 to bond surface of patch.
16. Install patch, centered on repair area, in same ply orientation as graphite-epoxy skin. Mask around patch periphery to control adhesive flash.
17. Bag and cure under vacuum (use heating blanket).
18. Remove masking.



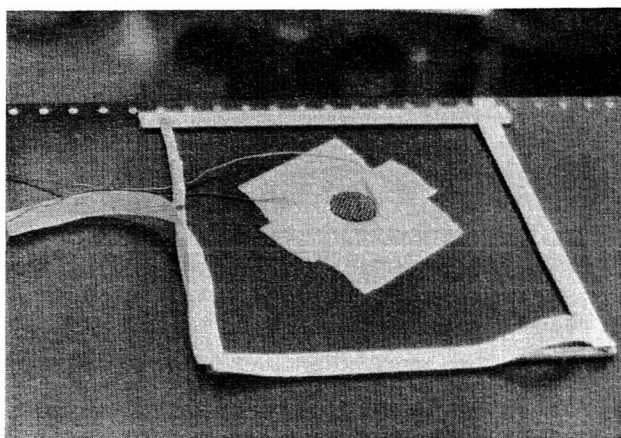
*Figure 170. Sonic Test Box (Test 15)
Equipment Used in Repairing
Damage to Test Box*



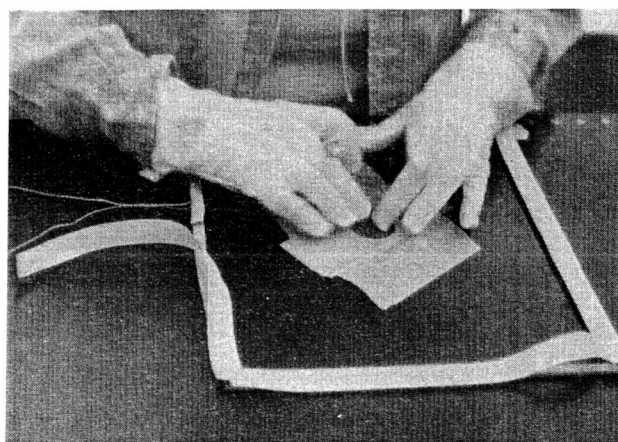
*Figure 171. Sonic Test Box (Test 15) Showing
Start of Repair*



*Figure 172. Sonic Test Box (Test 15) Showing Adhesive,
Precured Graphite-Epoxy, and Core for Repair*



*Figure 173. Sonic Test Box (Test 15)
Showing Core in Place*



*Figure 174. Sonic Test Box (Test 15)
Showing Precured Graphite-Epoxy
Skins Being Positioned*

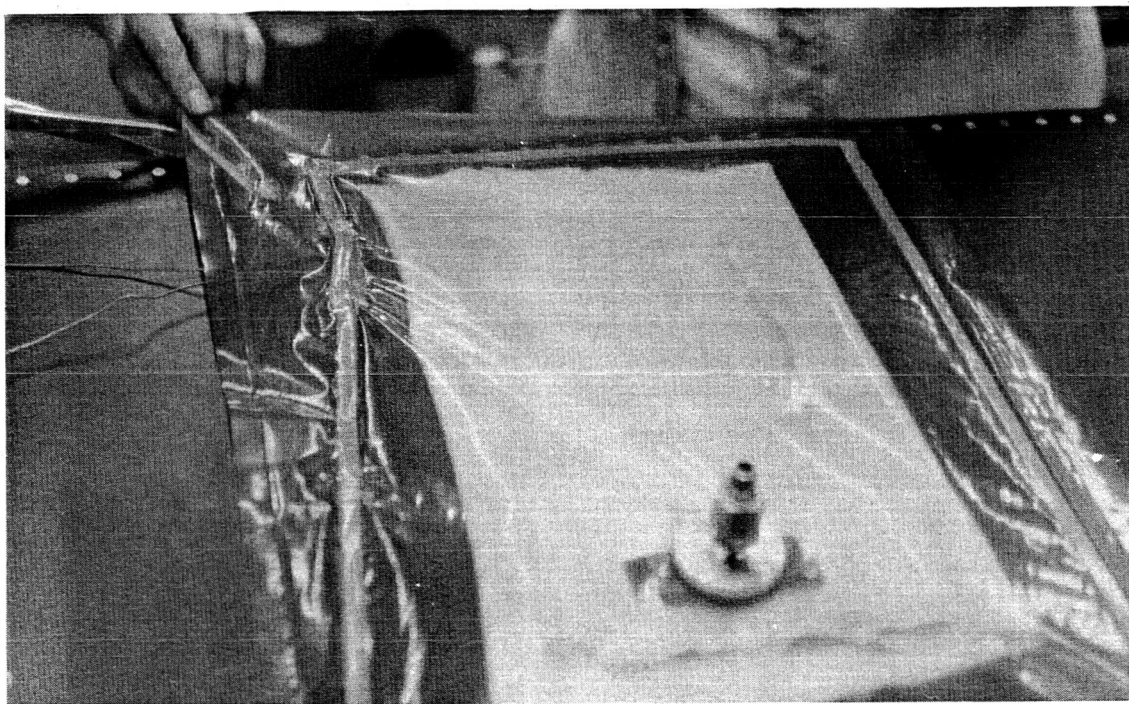


Figure 175. Sonic Test Box (Test 15) Showing Repair Ready for Cure

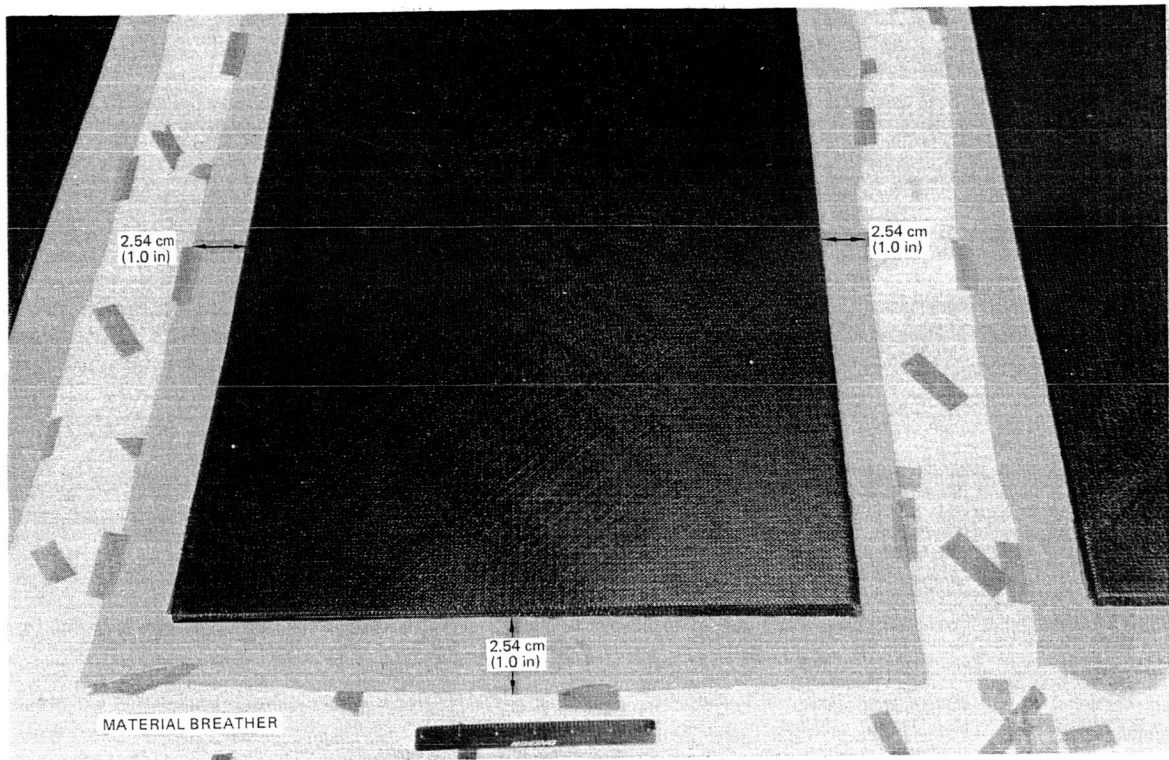
5.1.2.4 Material Processing

Several elevator test parts, fabricated using the Narmco 5208 resin system, were rejected for high fiber volume fraction. Investigation showed that this occurred during the cure cycle. When pressure was applied at 120°C (250°F), the low-viscosity resin flowed into the edge breather area, resulting in high fiber-to-resin volume ratios in the finished part.

To resolve this typical problem, bagging techniques were changed to limit contact between the part and the edge breather material and the cure cycle was modified to apply pressure at the start of the cycle. These changes minimized bleed-out and ended rejection for high fiber volume fraction (fig. 176).

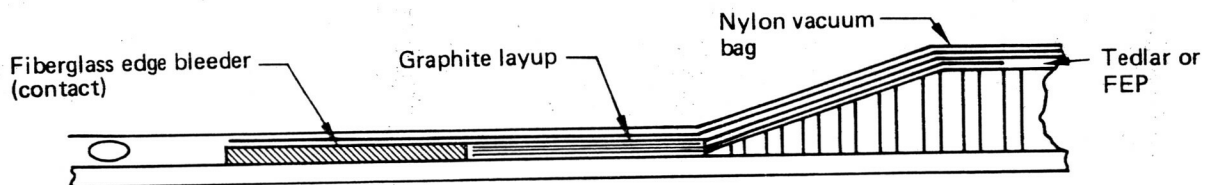
5.1.2.5 Hole Preparation Improvements

Studies were undertaken to improve hole quality, as defined by dimensional control and fiber breakout, and to determine inspection requirements for both ancillary test components and production hardware. The first study compared holes drilled in graphite-epoxy fabric and tape panels on a conventional drill press with holes drilled using a Boeing-modified, hand-held, high-speed drill (figs. 177 and 178). In both cases, a special fluted carbide drill was used. Hole diameters were measured and appearances were evaluated before radiographic inspection, then rated on a relative scale based on measured diameter variation and the extent of fiber breakout. The study showed that hole tolerances went out of range 0.0 ± 0.008 cm (0.003 in) in panels 0.152 cm (0.060 in) or thinner, when drilled using the high-speed, hand-held drill. Additionally, unacceptable fiber breakout occurred on tape face drill exit surfaces.

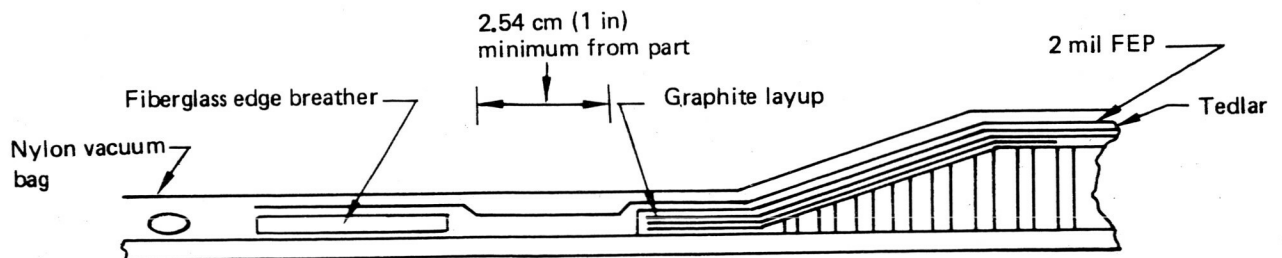


The photograph shows the breather material placed 2.54 cm (1.0 in) away from the panel to reduce or eliminate resin bleedout.

- Parts were cured using the step cure cycle with a bleeder system as shown below.

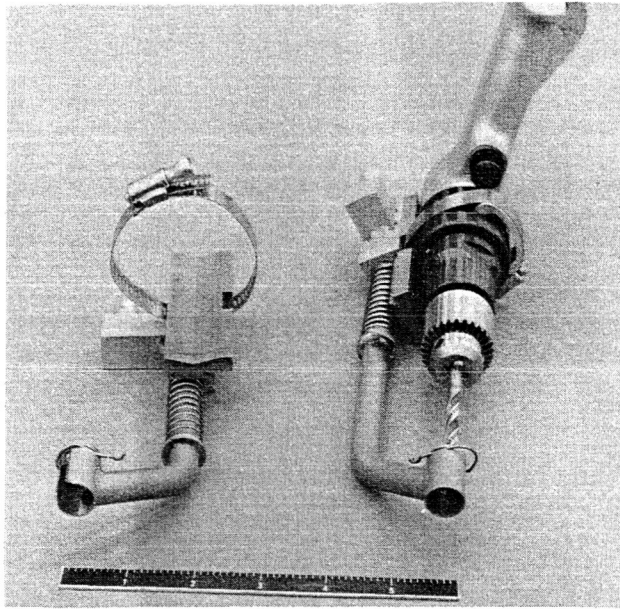


- The cure was changed to pressure applied at the start of the cure cycle and breather (not bleeder) applied as shown below.



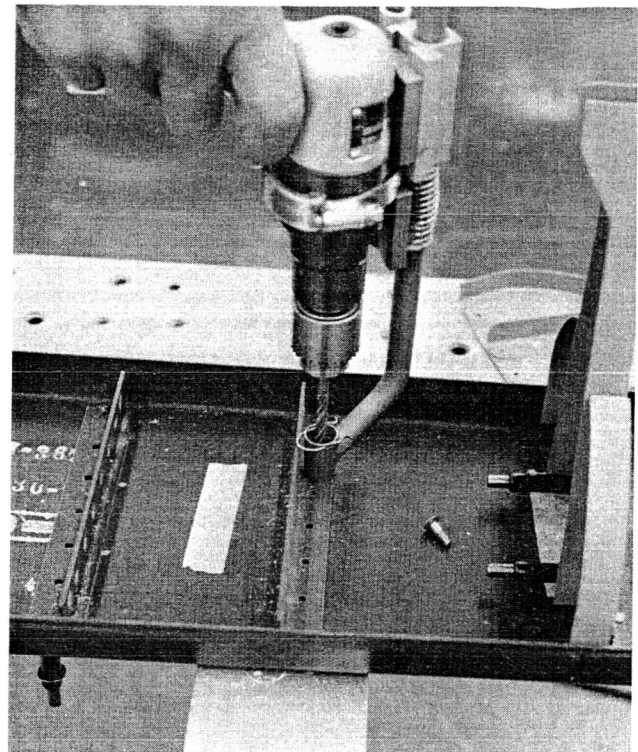
- The bagging eliminated excessive resin bleed.

Figure 176. Improved Flow Characteristics of Narmco 5208 Resin



Note:
Vacuum unit can be used with tooling
designed to provide a positive guide.

*Figure 177. Hand Drill (Right), Showing
Standard Vacuum Unit and Modified
Vacuum Unit (Left)*



*Figure 178. Drilling Attach Angles on Front
Spar, Showing Interference Between Angle
and Vacuum Collar*

The second study was conducted using the 36 panels, four holes per panel, of the Boeing-funded countersunk bearing fastener tests. Each panel was inspected radiographically after hole drilling and again after countersinking. The radiographic procedure included application of a radiographically opaque penetrant and X-ray exposure at low kilovoltage. The hole quality was evaluated on the same basis as in the first study. After structural tests of the fastened panels, the relative fiber breakout ratings were compared with the failure loads obtained. No correlation existed between fiber breakout rating and failure load.

From these results, it was concluded that extensive radiographic inspection was not required to ensure hole quality. The cost savings in inspection operations effected through these studies is calculated to be 83 labor hours per elevator shipset; this is based on 1/2 minute per hole for penetrant application and radiographic inspection at a rate of 30 minutes per 20 holes.

5.1.2.6 Fastener Studies

Because of limited accessibility when using standard tools during installation of titanium Hi-lok bolts with corrosion-resistant steel collars in the rear spar, lower skin, and actuator rib areas, Torque-set bolts with slotted heads and standard nuts were substituted, resulting in an estimated 8-hr reduction in installation time for the rear spar.

The time-consuming installation of nut plates used in the upper skin closeout was reduced by substituting Visu-lok blind fasteners in conjunction with a stainless-steel Visu-lok washer bonded to the back side of the graphite-epoxy. This solution provided a fabrication time saving in spite of the washer bonding requirement. The bigfoot blind fastener was not qualified for nor used on the elevator.

A hollow-end, flared titanium rivet with requisite tooling and installation techniques was developed to reduce assembly costs of the elevator trailing edge and to prevent damage to the graphite-epoxy from rivet expansion during installation.

5.1.2.7 Machining of Cured Graphite-Epoxy

An assessment of machining operations (other than hole preparation) resulted in the following observations and actions:

- Machining/trimming processes (milling, routing, shaping, bandsawing, circular sawing, and surface grinding) can consistently achieve edge-quality standards within the limits of the graphite-epoxy process specification, 0.076-cm (0.030-in) maximum delamination, providing the external plies are not unidirectional graphite-epoxy tape.
- Where external plies are unidirectional graphite-epoxy tape, all conventional machining/trimming processes result in splintering of the external plies from the basic resin matrix. The extent of this splintering normally can be contained within 0.25 cm (0.10 in) of the machined edge. Consequently, splintering allowance is required up to 0.25 cm (0.10 in) from the machined edge in all external unidirectional plies. The Boeing process specification has been revised to reflect the 0.25-cm (0.10-in) splintering allowance.
- Although respirable particles of dust generated during machining of advanced composite materials are not classified as carcinogenic, they are considered to be inert nuisance dusts. OSHA recommends a maximum operator exposure of 10 mg of inert dust per m^3 of air space. Appropriate dust-collection systems are being used in the designated graphite-epoxy machining areas (figs. 179 and 180). A particle count verified collection system performance with escaping particles measuring less than 5% of the allowed maximum of 10 mg/m^3 (0.0004 lb/in^3) of air.

5.2 MANUFACTURING VERIFICATION HARDWARE

A full-scale, 203-cm (80-in) long section of the elevator was fabricated to test production detail tools and ensure that no major assembly problems would be encountered during production of the five and a half shipsets. Significant steps in this process are shown in Figures 181 through 188. Three significant facts developed from the fabrication of the verification hardware:

1. The fabrication should have been used to train production assembly personnel rather than being done by research mechanics.
2. Fabrication of a short length of a structure does not always identify all of the problems associated with the manufacture of a complete full-scale structure. The 203-cm (80-in) front spar section and short rear spar of the verification elevator section showed only slight, 0.13 cm, acceptable cross-section warpage after fabrication. The first full-length production spars, however, developed excessive warpage of 0.91 cm, resulting in rejection (see sec. 6.3). From this experience, it was concluded that verification hardware should be made full-scale.

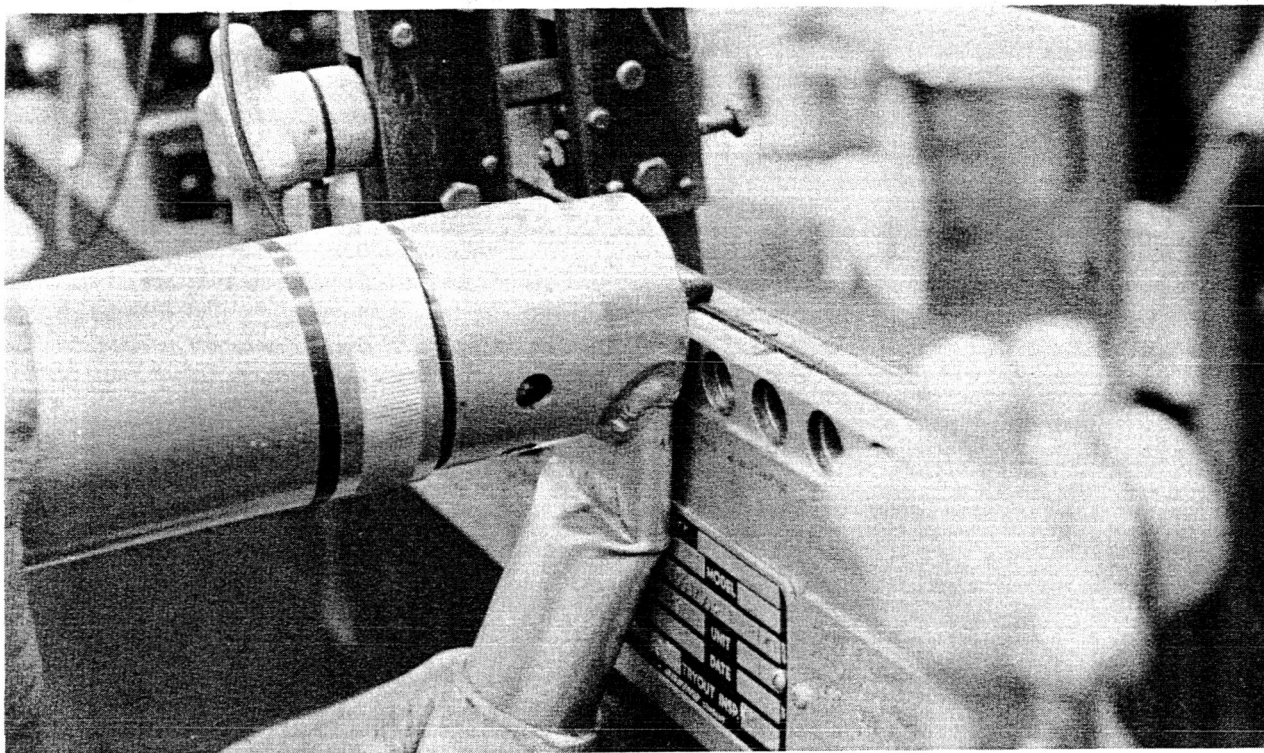


Figure 179. Vacuum Dust Collector Mounted on Standard Router

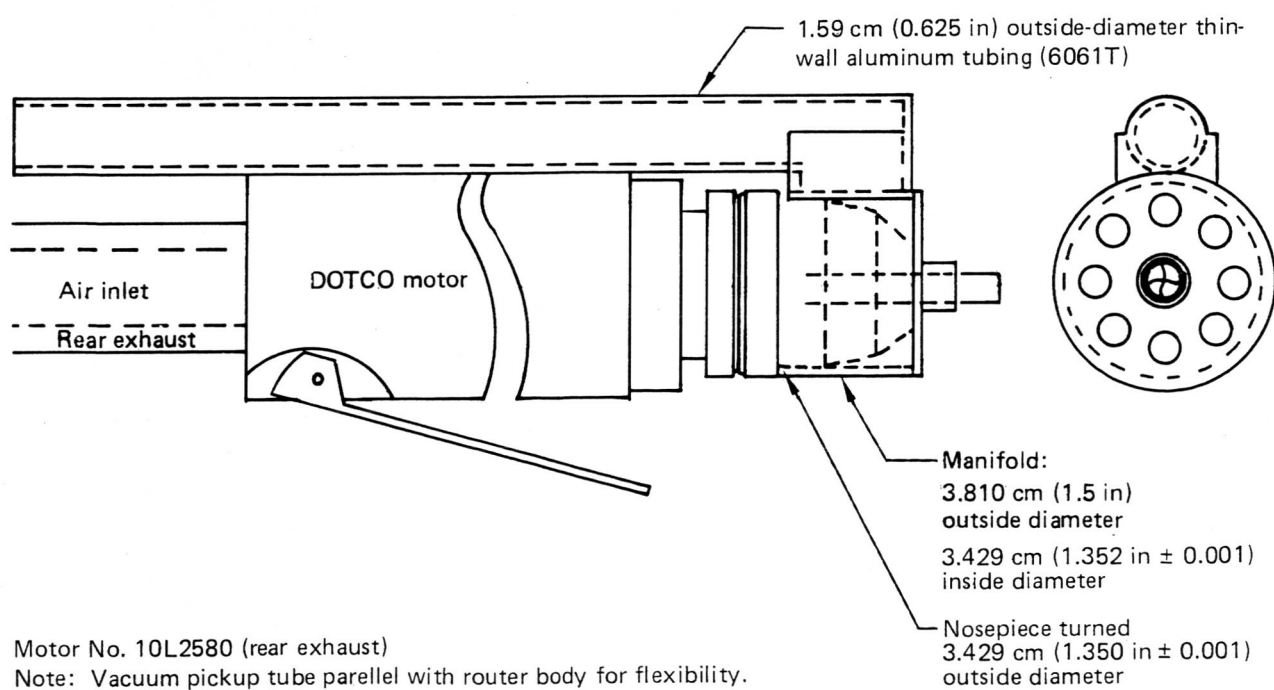


Figure 180. DOTCO Router Motor

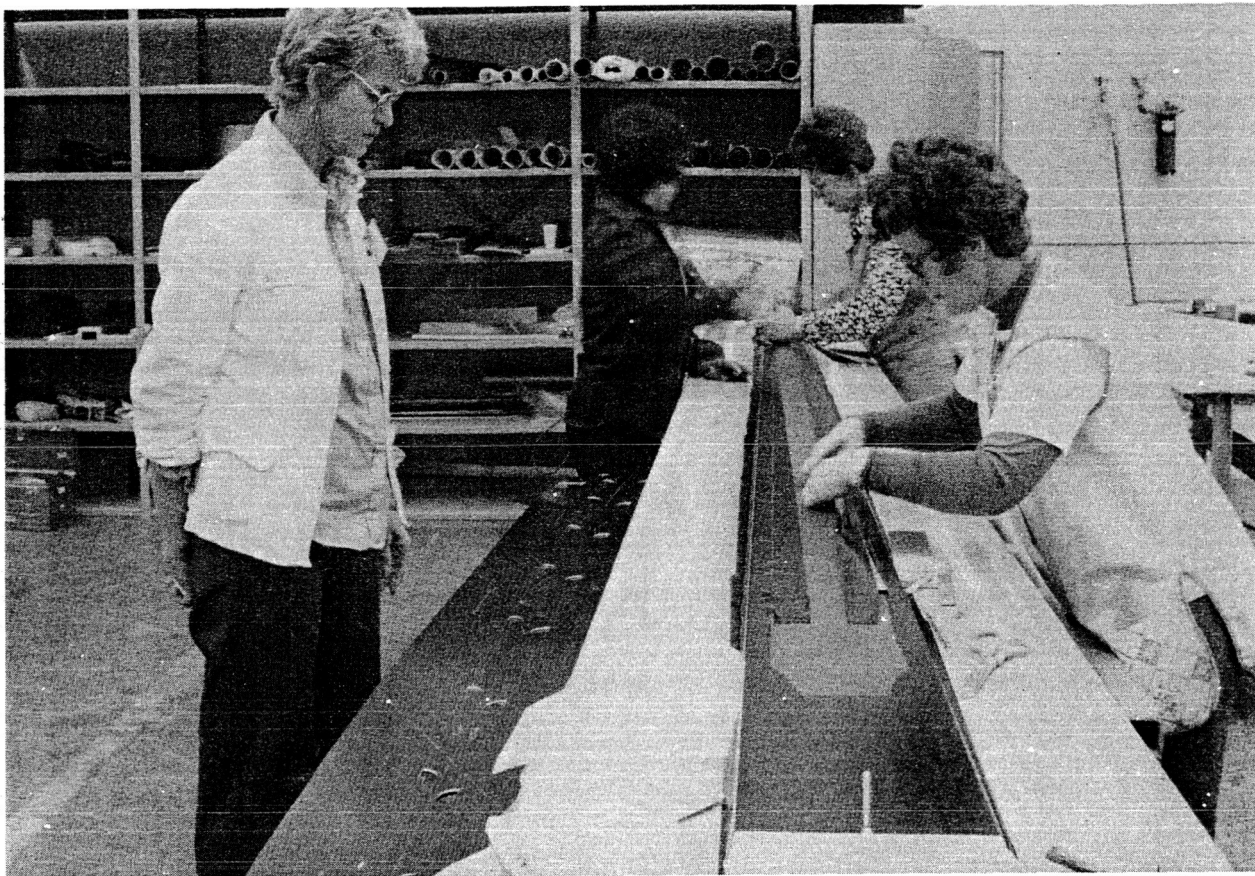


Figure 181. Manufacturing Verification Hardware (Test No. 16) Showing Front Spar Being Laid Up

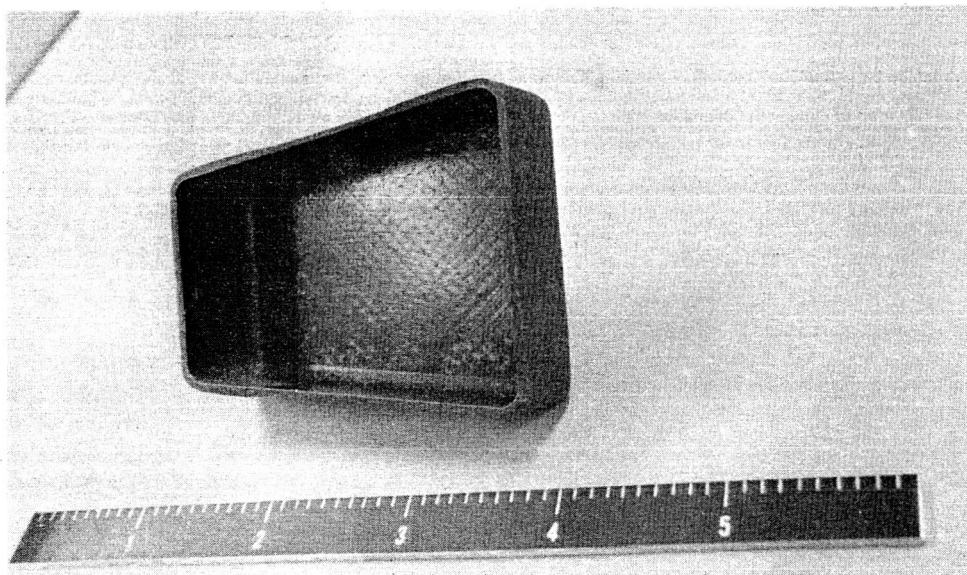


Figure 182. Manufacturing Verification Hardware (Test No. 16) Showing Completed Rear-Spar Header

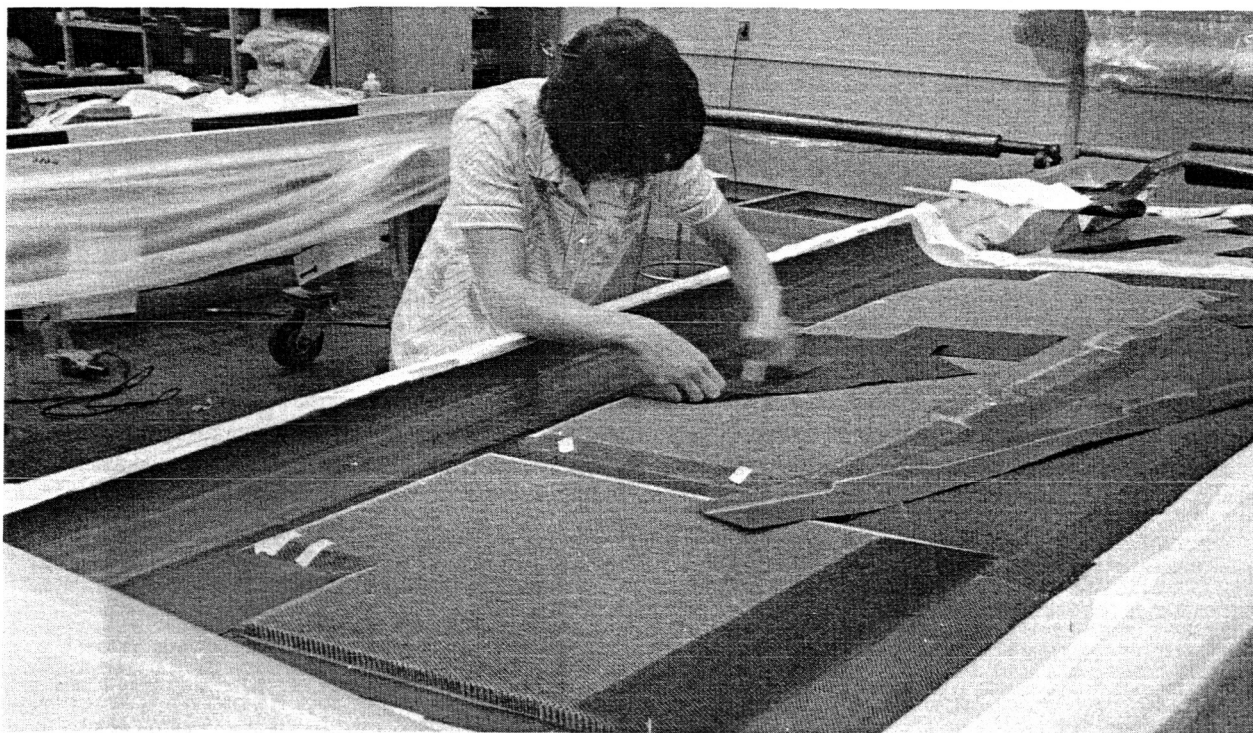


Figure 183. Manufacturing Verification Hardware (Test No. 16 Skin Panel) Showing Doubler Being Laid Up

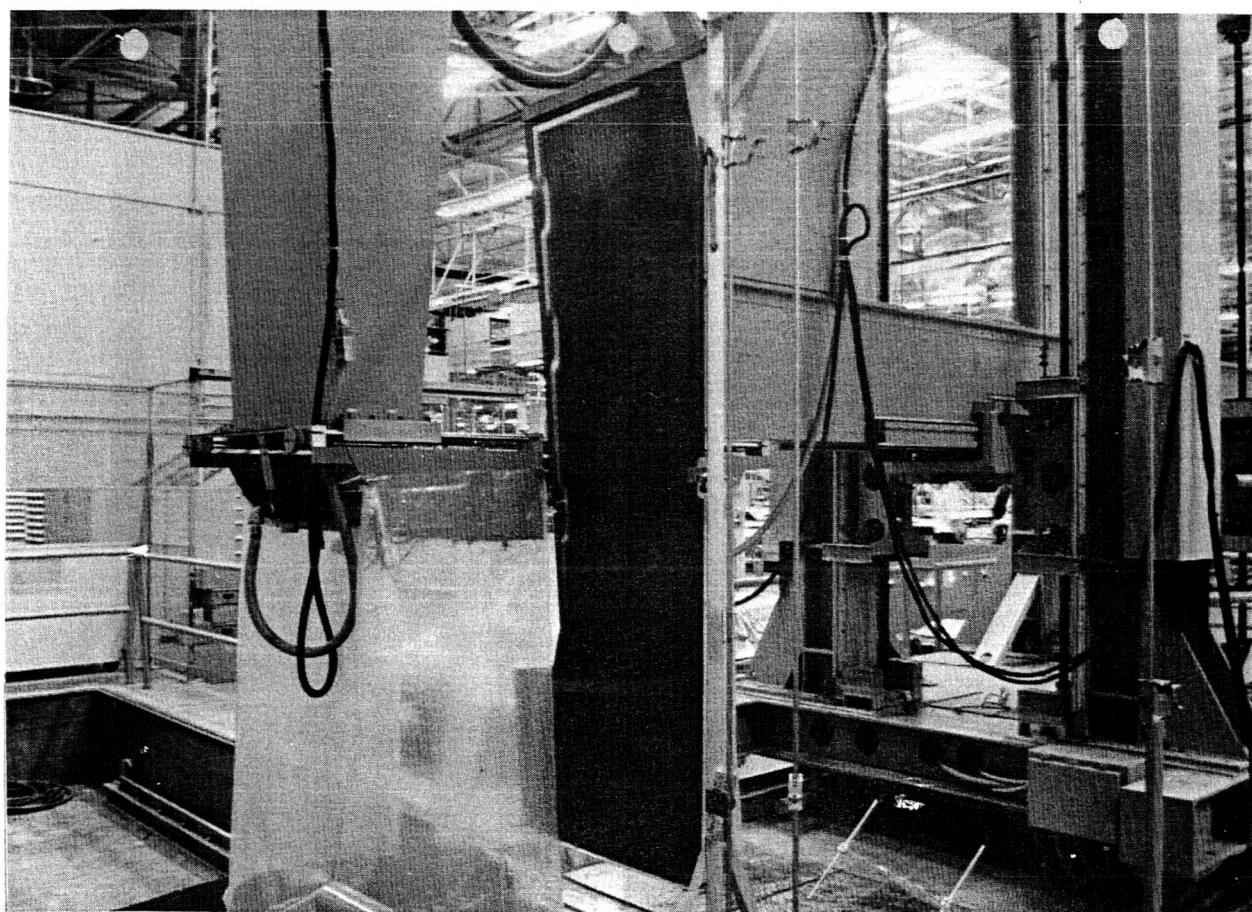


Figure 184. Manufacturing Verification Hardware (Test No. 16) Showing Skin Panel in TTU Inspection

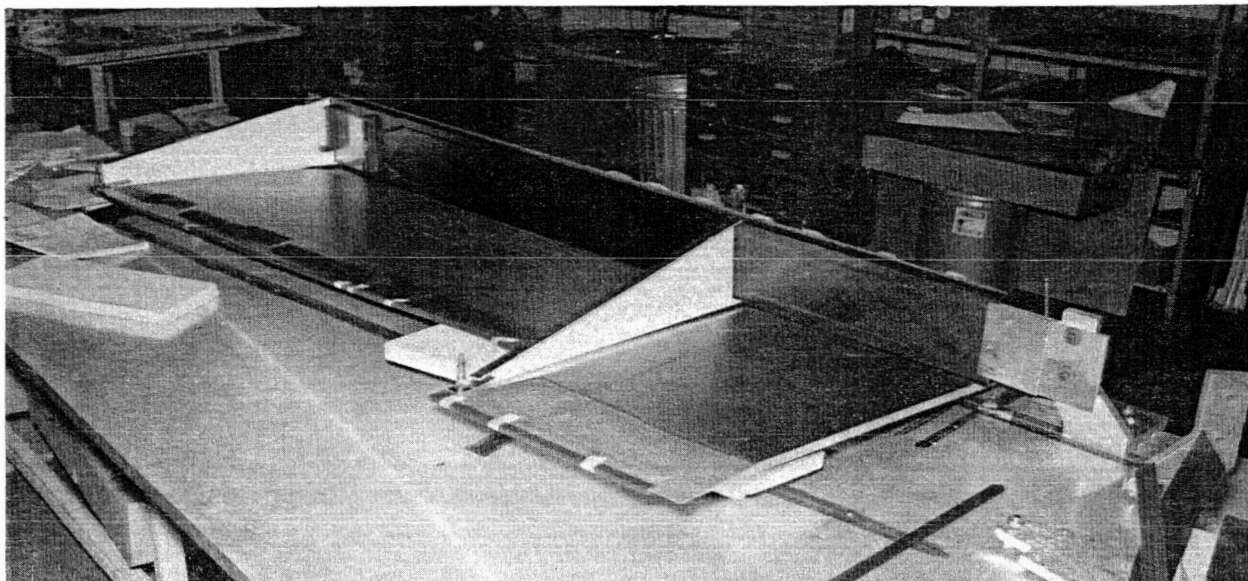


Figure 185. Manufacturing Verification Hardware (Test No. 16) Showing Front Spar, Two Ribs, and Lower Skin Being Assembled

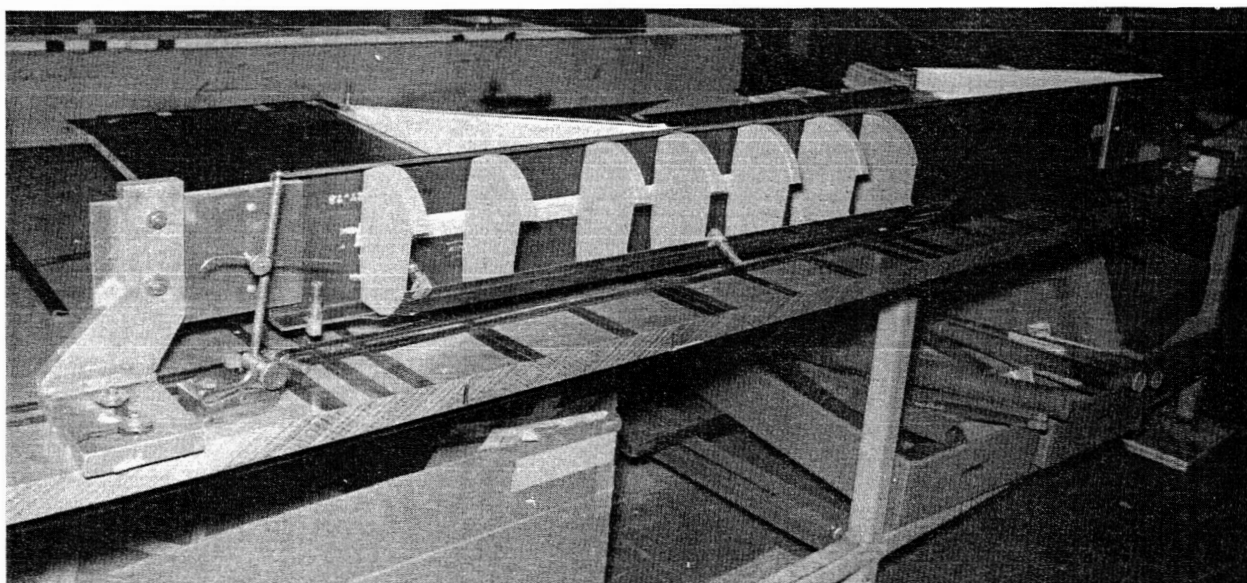


Figure 186. Manufacturing Verification Hardware (Test No. 16) Showing Aluminum Nose Ribs Being Attached to Front Spar

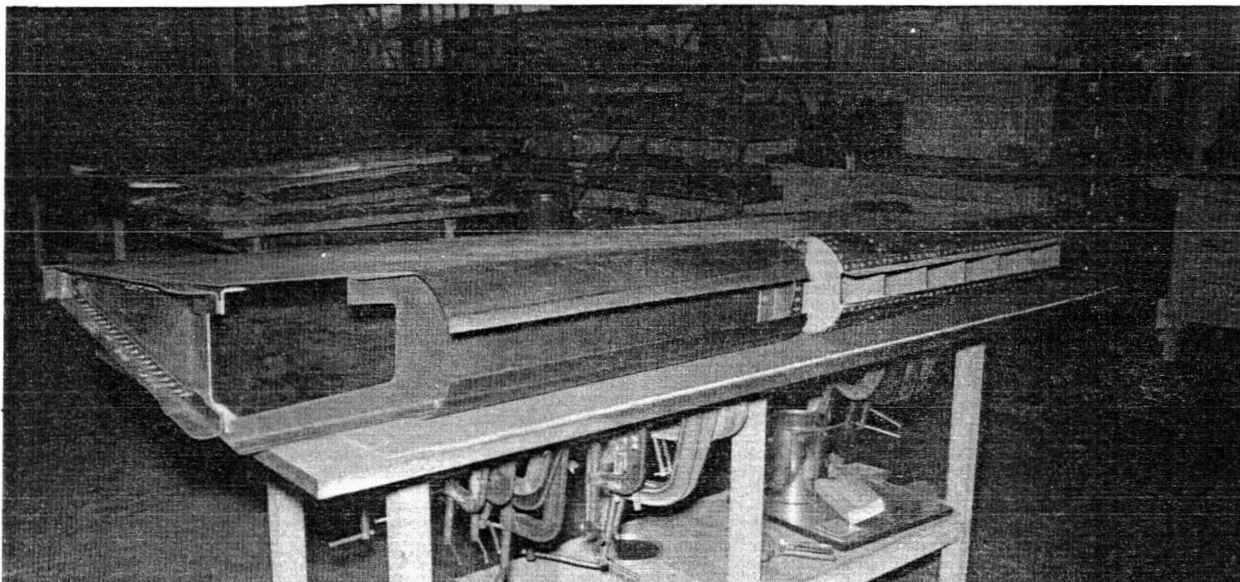


Figure 187. Manufacturing Verification Hardware (Test No. 16) Showing View of Completed Assembly

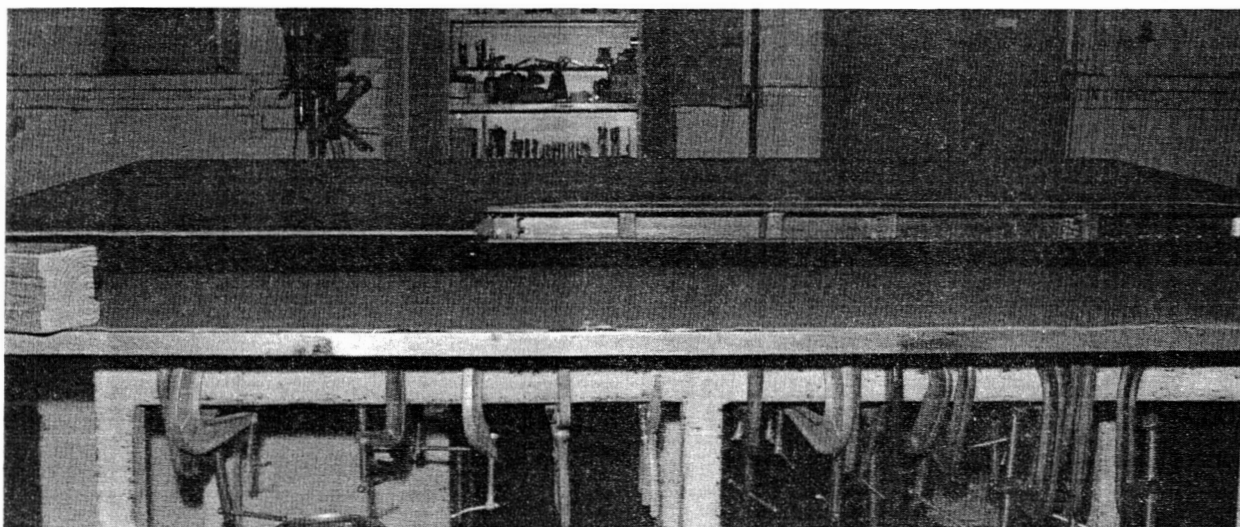


Figure 188. Manufacturing Verification Hardware (Test No. 16) Showing Rear View of Completed Assembly

3. Assembly fitup discrepancies between rib spars and skins in the concept verification hardware were caused by dimensional inaccuracy in the male rib tool that had been designed by scaling the photo contact master (PCM) drawing. Ribs for the subject verification hardware were fabricated on production male tools made using master dimensioning index (MDI) data. No dimensional discrepancies were found in these ribs.

5.3 QUALITY ASSURANCE STANDARDS AND NONDESTRUCTIVE TEST DEVELOPMENT

The quality assurance system for the NASA advanced composite 727 elevator consisted of material control, process control, complete part inspection, NDI standards development, NDI technique evaluations, assembly inspection, record retention, and analysis of production records. Other activities included design review for inspectability, inspection of damage-repaired areas, and evaluation of test assemblies during static and fatigue testing.

5.3.1 MATERIAL CONTROL

Quality Control procedures verify that composite prepreg materials, honeycomb core, and adhesives are stored and handled per specification requirements. In addition, Quality Control verifies that materials incorporated into a part meet material and procurement specification requirements. A complete record of materials used, test records, material rejections, etc. is maintained with each Manufacturing Plan.

5.3.2 PROCESS CONTROL

Inspection during processing of graphite-epoxy parts is a critical part of the fabrication operation. The inspection sequence is recorded on the Manufacturing Plan, with inspections performed to the requirements of Boeing process specification BAC 5562. Layup sequence and ply orientation are inspected on a ply-by-ply basis. The cure cycle is monitored for temperature, pressure, and time with process control test panels, representative of part structures, cured with each autoclave load.

Each process control record is verified to ensure that information is complete; e.g., manufacturer, batch number, lot number, roll number, autoclave load number, test panel acceptance, and discrepancy corrections are all incorporated.

5.3.3 COMPLETED PART INSPECTION

Completed parts receive final inspection per BAC 5562 and all other drawing requirements. Final inspection includes:

- Trimmed dimensions
- Warpage
- Voids and delamination
- Resin starvation
- Resin bleedout and surface ridges
- Material inclusions
- Crushed core
- Fabric wrinkles or distortion
- Surface defects and finish quality

5.3.4 ASSEMBLY INSPECTION

Assembly inspection is performed to ensure that the 727 elevator is assembled per drawing, process, and material requirements. During the assembly of five and a half shipsets, the following items were monitored to ensure the overall quality of workmanship:

- Verification of individual parts and subassemblies for serialization and Quality Control acceptance
- Proper fitup and location of parts and subassemblies prior to drilling and fastener installation
- Hole drilling and countersinking
 - Dimensional inspection
 - Visual inspection for breakout
 - Visual inspection for, and measurement of, delamination. Use of X-ray inspection with radiographically opaque dye where indicated.
- Evidence of sealant barrier between graphite and metal surfaces to prevent electrochemical corrosion
- Fastener installation to ensure correct fastener, fastener length, washer, and torque requirements
- In-process inspection during repair and nondestructive inspection of completed repair
- Inspection of trailing-edge seal
 - In-process inspection for uniform application plus squeeze-out of sealant when pressure clamps are tightened
 - X-ray inspection for sealant voids

5.3.5 REPAIR EVALUATION

Graphite composite repairs are monitored to evaluate their bonding characteristics and structural integrity. Three types of inspection are used to ensure a high-quality repair:

1. In-process inspection includes surface preparation, cleanliness, material verification, and quality control acceptance of cure cycle for temperature, pressure, time, and heating rate during actual repair.
2. Visual inspection for obvious defects; e.g., bubbles, blisters, or other not-bonded areas.
3. Nondestructive inspection includes Through Transmission Ultrasonic (TTU), Soudicator, and/or Fokker Bond Tester for bonding, X-ray for voids and porosity.

Figure 189 shows an acceptable repair to a 727 graphite composite elevator skin panel. Figure 190 shows the Fokker Bond Tester being used to inspect bonding characteristics of a repair on the lower skin panel surface of a 727 graphite composite elevator. Figure 191 shows X-rays of two repairs to skin panels on a 727 graphite composite elevator.

5.3.6 QUALITY ASSURANCE RECORDS

Procedures that meet record maintenance and traceability requirements for the NASA Advanced Composites Program were established with a controlled area (Records Retention) located at the Fabrication Division, Auburn, Washington. Records retained and logged include Composite and Adhesive Material Identification and Test, Manufacturing Engineering Planning with rejection tags and disposition, and Quality Control Process and Nondestructive Inspection Data and Recordings. All records are maintained for the life of the NASA programs and are available for selected program personnel and NASA evaluation.

Production records for the program have been collated, analyzed, and the results tabulated. A total of 1828 details and assemblies, fabricated during February 1978 through April 1979, yield 937 discrepant conditions with some parts having more than one condition reported. These data are summarized in Table 15 and Figure 192.

Further analysis of the data showed that process failures comprised 25% of all rework and 58% of all scrap. Human errors, including operators and planning, contributed 75% of the rework and 42% of the scrap. This is comparable to metal structures early in the program.

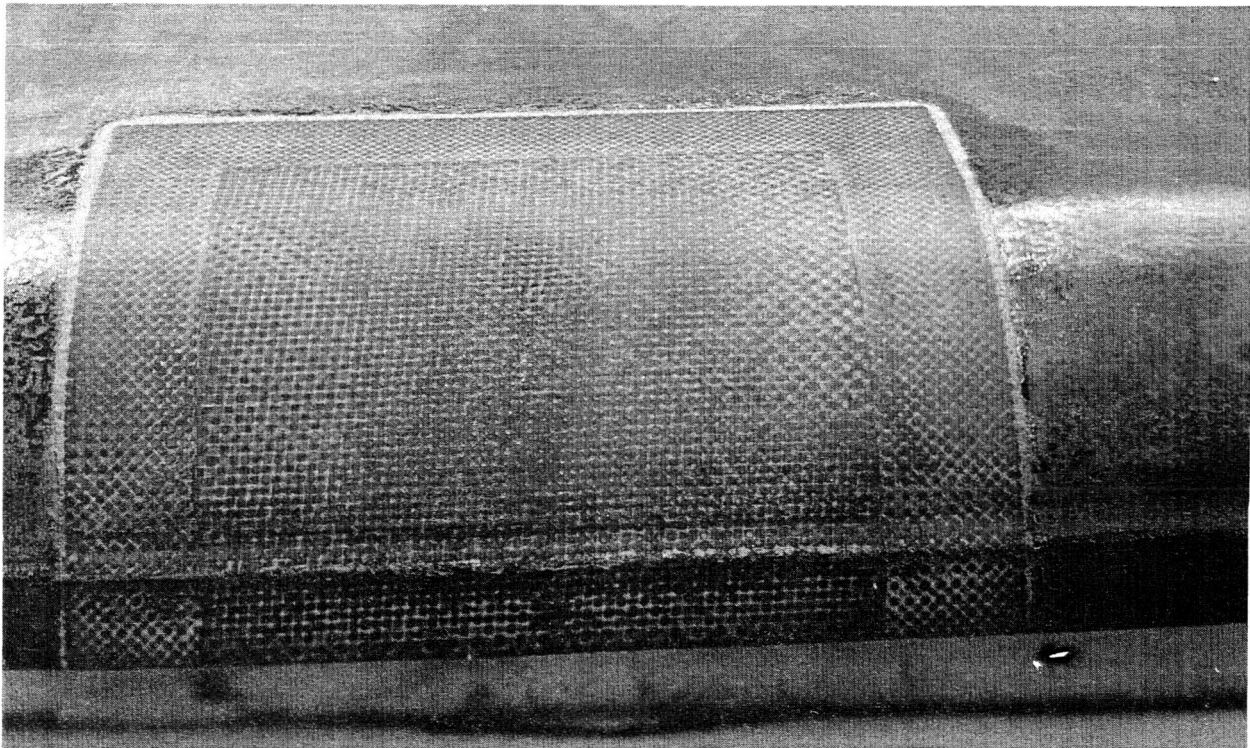


Figure 189. Visually Acceptable Repair to Skin Panel

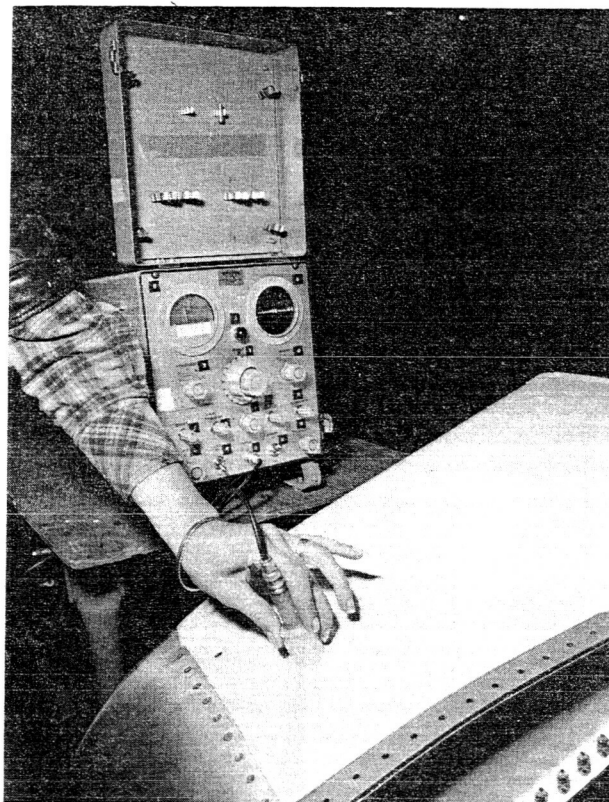


Figure 190. Fokker Bond Tester Inspection of Repair to Skin Panel

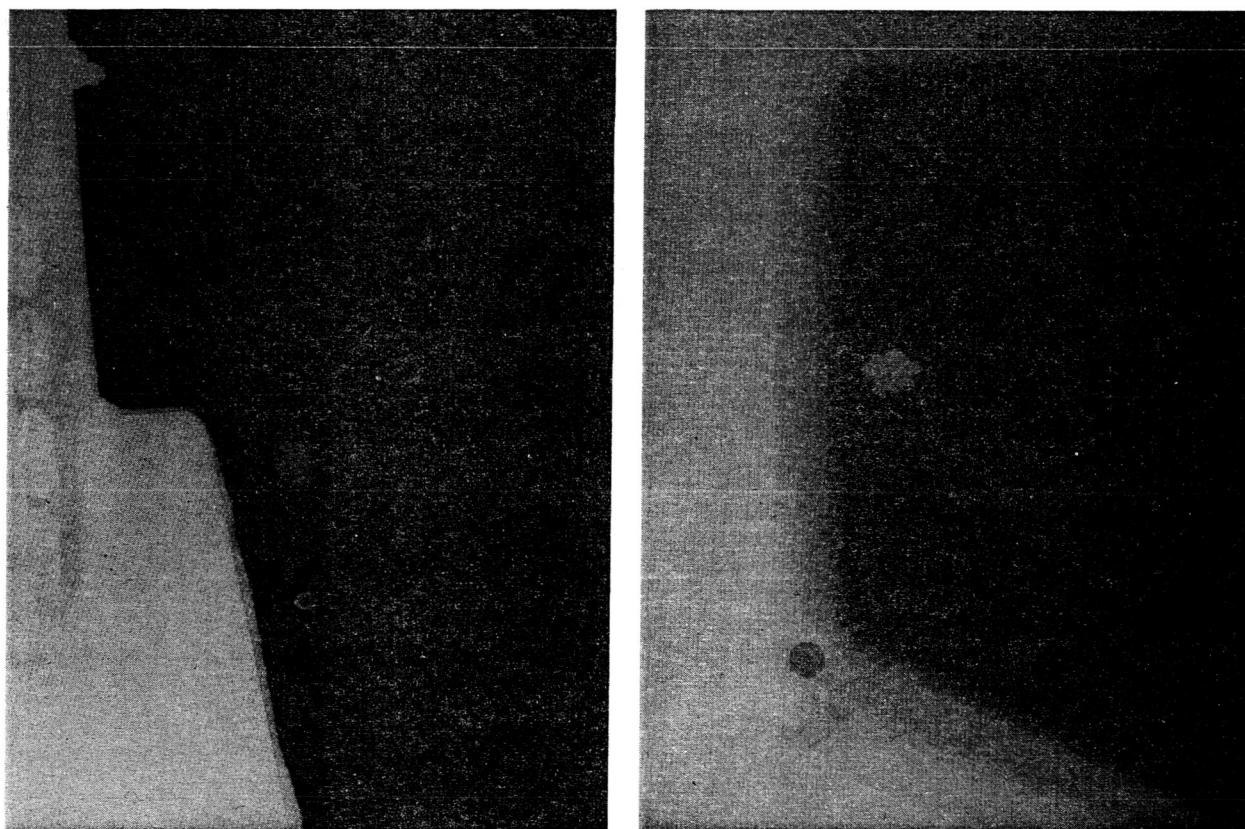


Figure 191. Examples of X-ray Examination of Repairs to Skin Panels

Table 15. 727 Elevator Quality History

Month/year	Parts assemblies per month	Discrepant parts/month (%)	Scrap parts/month (%)	Month/year	Parts assemblies per month	Discrepant parts/month (%)	Scrap parts/month (%)
2/78	108	33	10	10/78	119	60	15
3/78	74	13	3	11/78	102	98	2
4/78	110	7	12	12/78	157	24	2
5/78	128	4	16	1/79	123	26	7
6/78	148	6	17	2/79	137	25	7
7/78	117	14	8	3/79	90	40	0
8/78	173	35	13	4/79	78	15	0
9/78	164	28	10	Totals	1,828	25	8

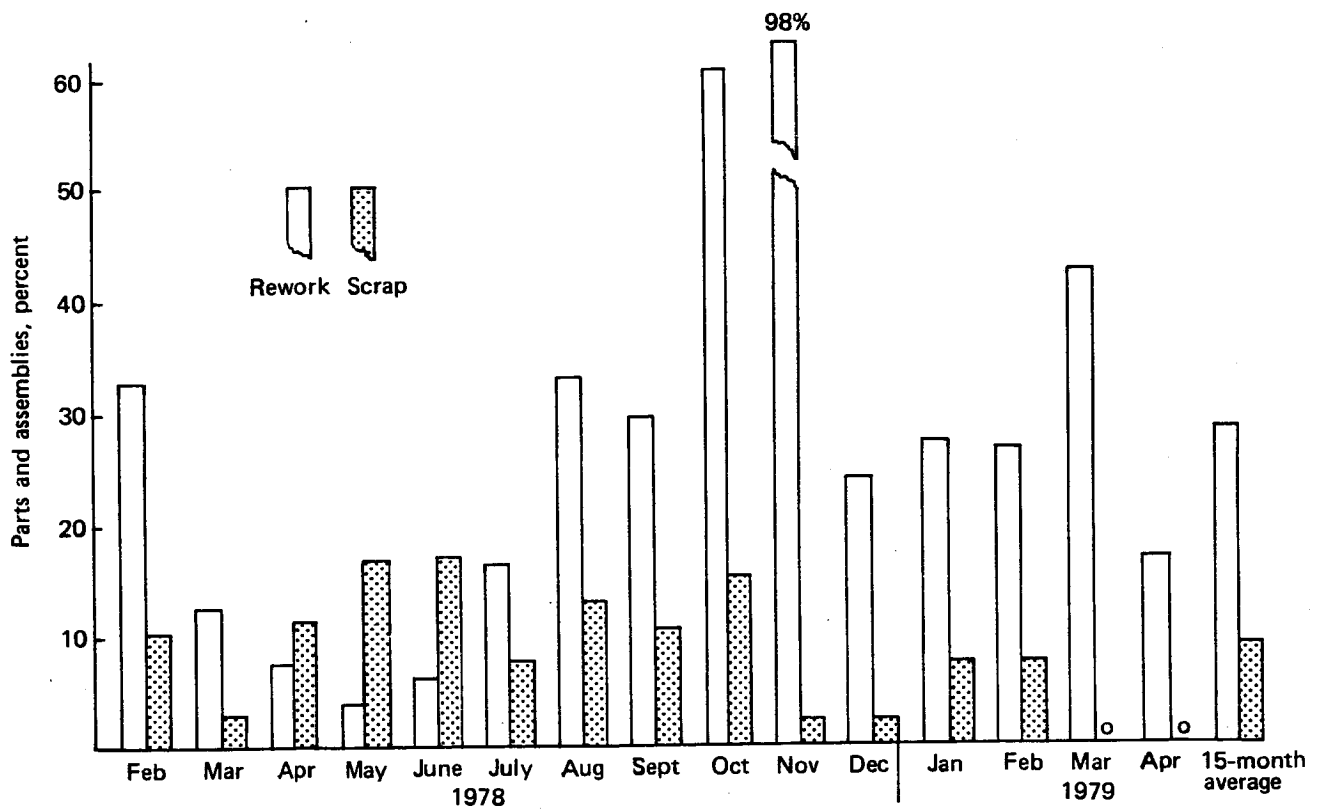


Figure 192. Rework and Scrap History

5.3.7 NONDESTRUCTIVE INSPECTION STANDARDS

The following NDI standards, fabricated to represent production designs, were built with defects consisting of two shims of 2-mil Teflon. In the layup of the preliminary standards, the defects replaced cutout fabric or tape; in the production standard layup, they were introduced between the fabric or the tape layers. Preliminary standards consisted of:

Laminate Standard—This standard was built with 0.64 x 0.64 cm (0.25 x 0.25 in) defects. It was required to qualify NDI techniques per Boeing Advanced Composites Process Specification. See Figures 193 and 194.

Honeycomb Standard—This standard, built with 0.64 x 0.64 cm (0.25 x 0.25 in) defects, was required to qualify NDI techniques. See Figures 193 and 195.

Laminate Step Standard—This standard consists of eight laminate steps with 0.64 x 0.64 cm (0.25 x 0.25 in) and 1.27 x 1.27 cm (0.5 x 0.5 in) defects in each step. The thicknesses of steps are 2P, 4P, 6P, 8P, 10P, 12P, 14P, and 15P. See Figures 196 and 197.

Skin Panel Standard—This standard has 0.64 x 0.64 cm (0.25 x 0.25 in), 1.27 x 1.27 cm (0.5 x 0.5 in), and 2.54 x 2.54 cm (1 x 1 in) defects. The standard was designed to duplicate upper and lower skin panels. See Figures 198 through 200.

Taper Edge Standard—This standard was designed to investigate defects in the taper area of the skin panels. The defect sizes were in the taper area of the skin panels. The defect sizes were 1.27 x 1.27 cm (0.5 x 0.5 in) and 2.54 x 2.54 cm (1 x 1 in). See Figure 201.

Front Spar Chord Standard—This standard has 1.27 x 1.27 cm (0.5 x 0.5 in) defects in various thickness levels. See Figures 202 and 203.

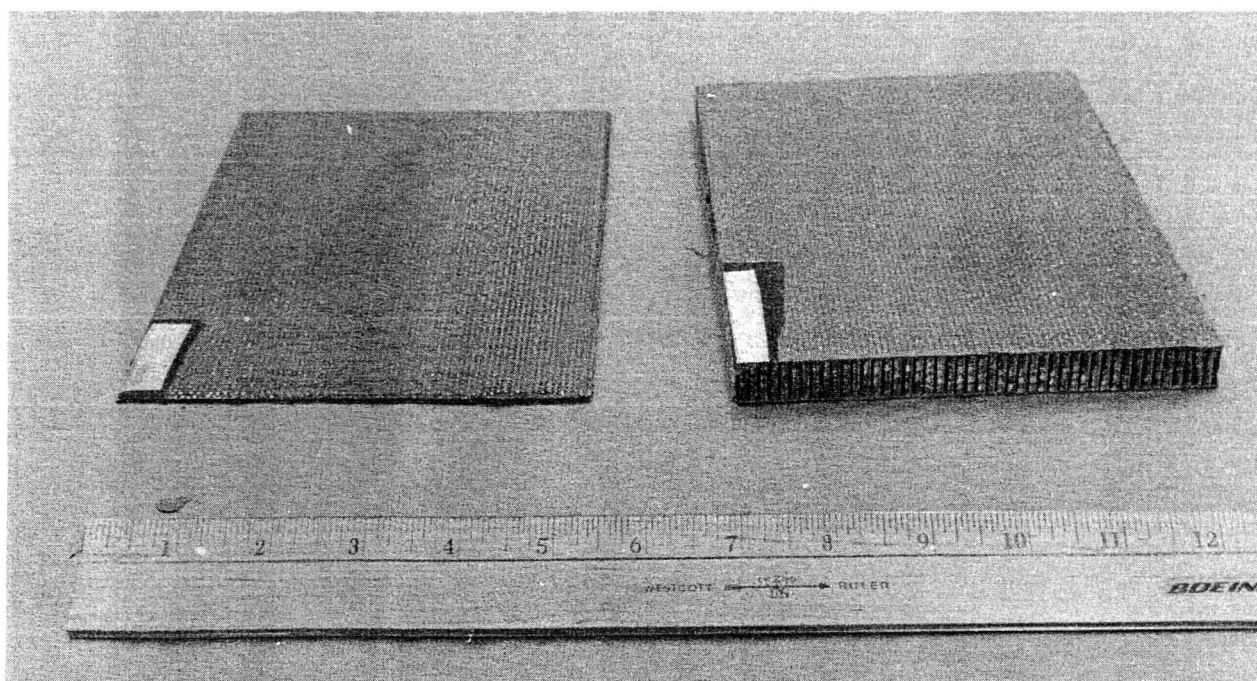
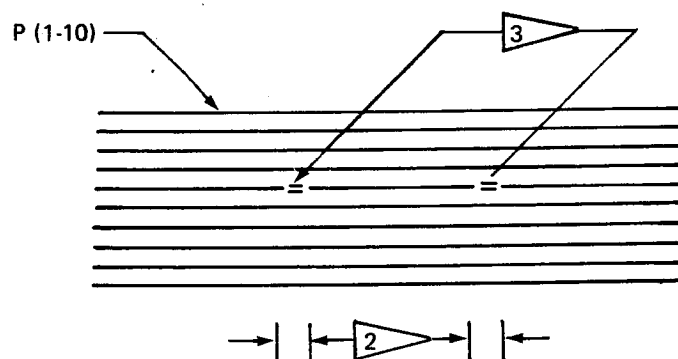
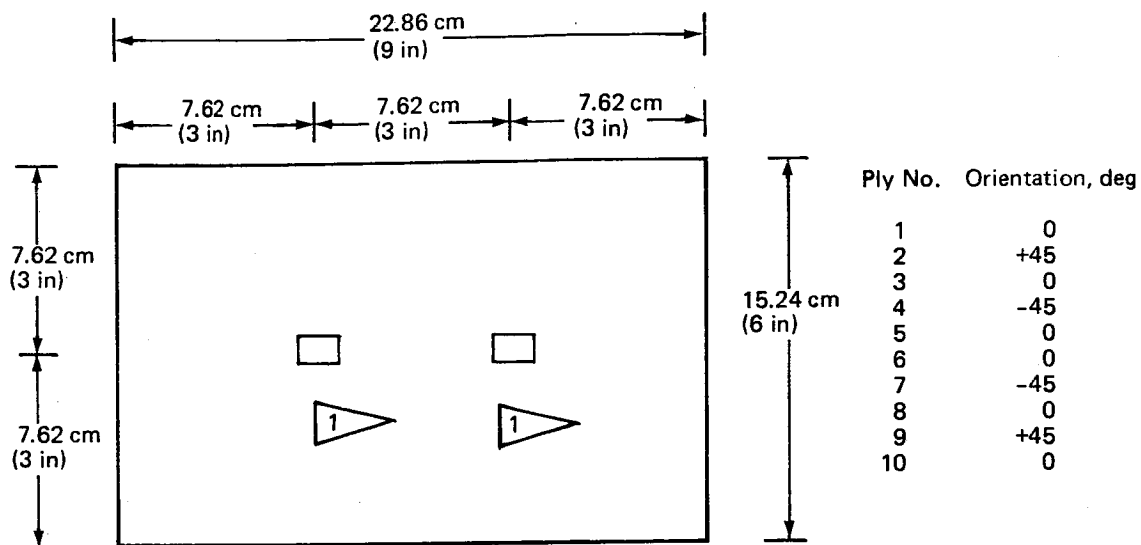

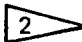
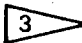


Figure 193. NDI Standards—Laminate and Honeycomb Panel



10 plies
BMS 8-212
Type II
Class 2
Style 3K-70-P

-  0.64 x 0.64 cm (0.25 x 0.25 in) disbond
-  0.64 x 0.64 cm (0.25 x 0.25 in) fabric cutout
-  Two 0.64 x 0.64 cm (0.25 x 0.25 in) Teflon shims—2 mil thickness

Fabricate per BAC 5562

Figure 194. NDI Reference Standard—Graphite-Epoxy Laminate

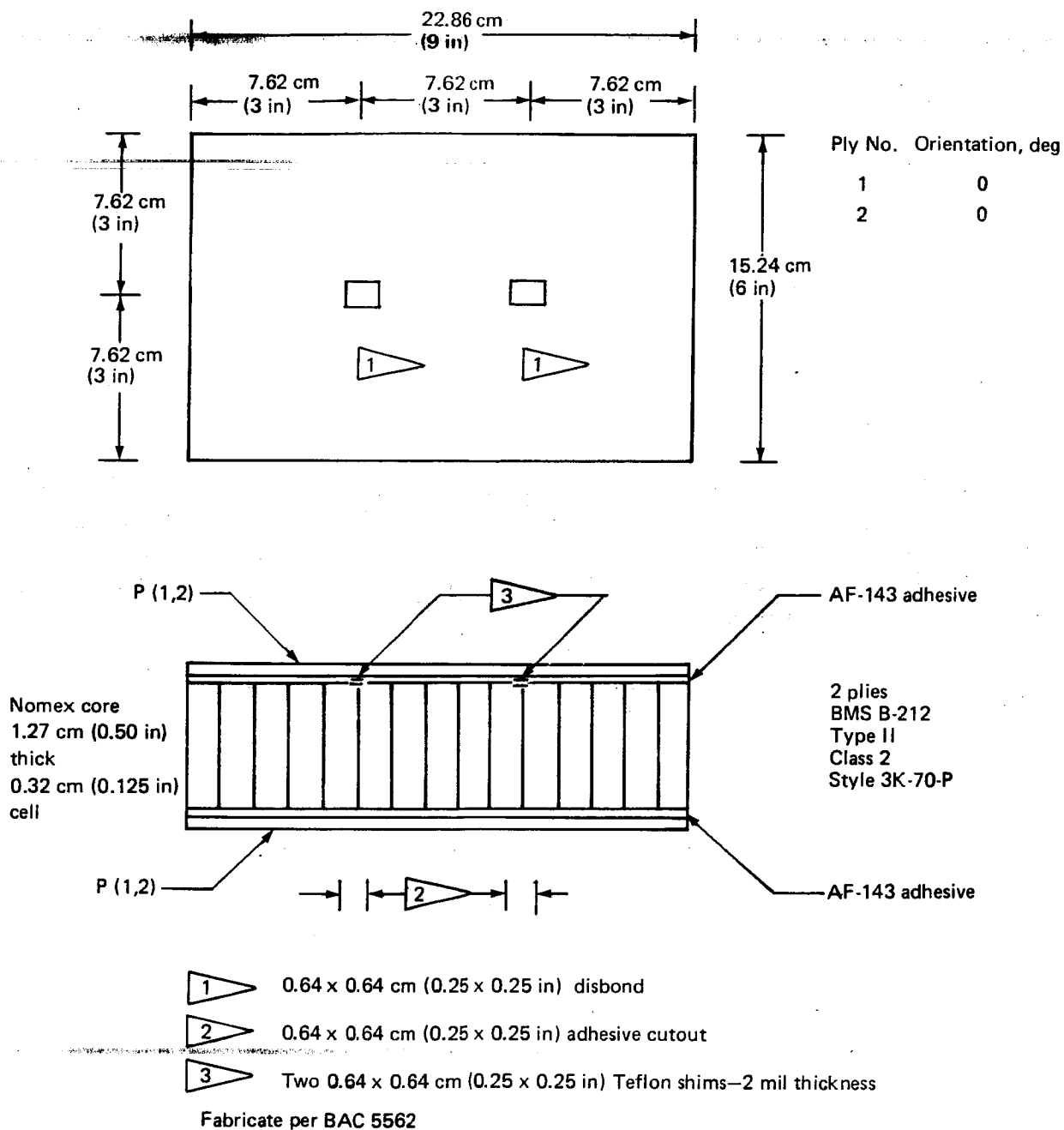


Figure 195. NDI Reference Standard—Graphite-Epoxy Honeycomb

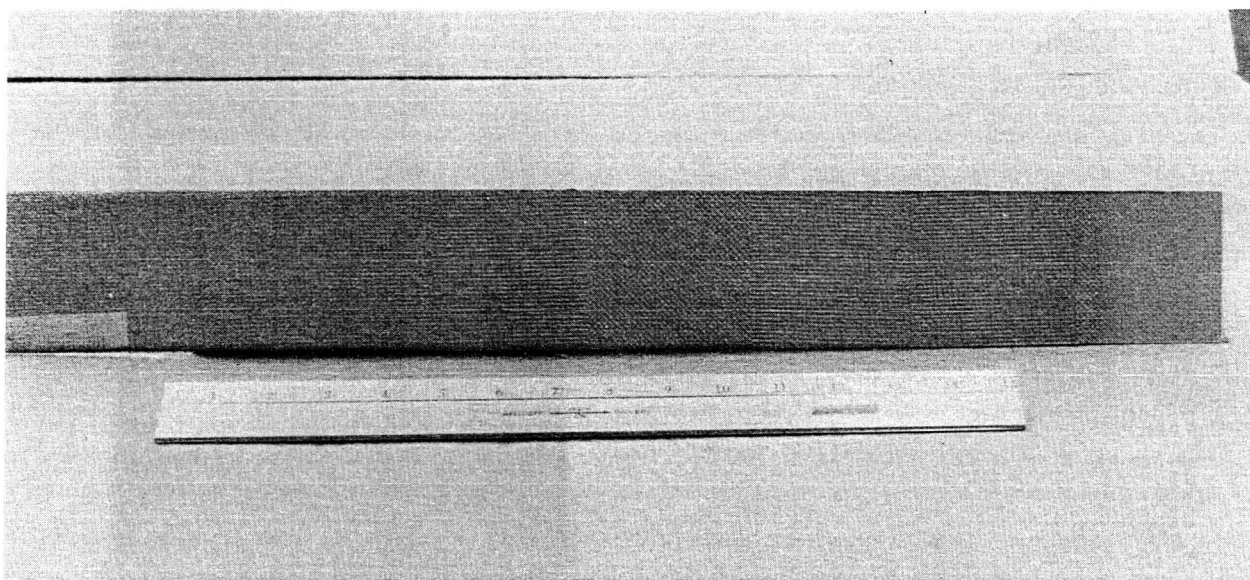
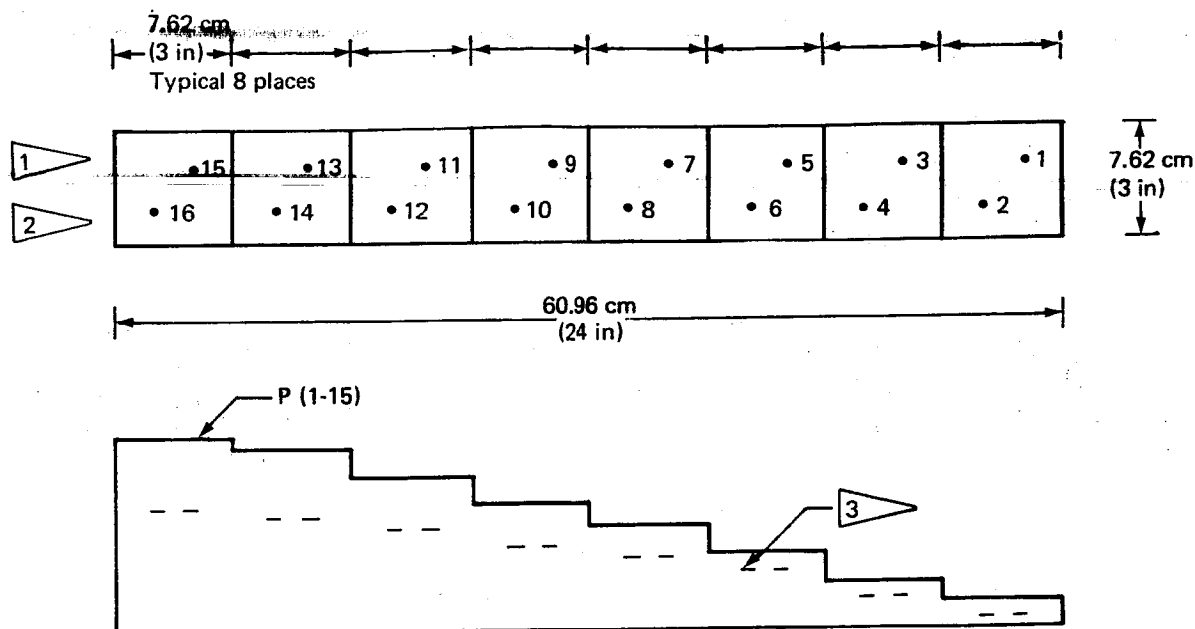


Figure 196. NDI Standard—Step Laminate



Defect No. 1 and 2 between P1 and P2
 Defect No. 3 and 4 between P3 and P4
 Defect No. 5 and 6 between P4 and P5
 Defect No. 7 and 8 between P5 and P6
 Defect No. 9 and 10 between P6 and P7
 Defect No. 11 and 12 between P7 and P8
 Defect No. 13 and 14 between P8 and P9
 Defect No. 15 and 16 between P9 and P10

BMS 8-212
 Type II
 Class 2
 Style 3K-70-P

- 1 0.64 by 0.64 cm (0.25 by 0.25 in) defect
 2 1.27 by 1.27 cm (0.5 by 0.5 in) defect
 3 Two 0.005 cm (0.002 in) Teflon shims of specified defect size

Ply No.	Orientation, deg	Ply No.	Orientation, deg
1	0	8	+45
2	+45	9	0
3	90	10	90
4	0	11	-45
5	-45	12	0
6	90	13	90
7	0	14	+45
		15	0

Figure 197. Laminate Step Standard

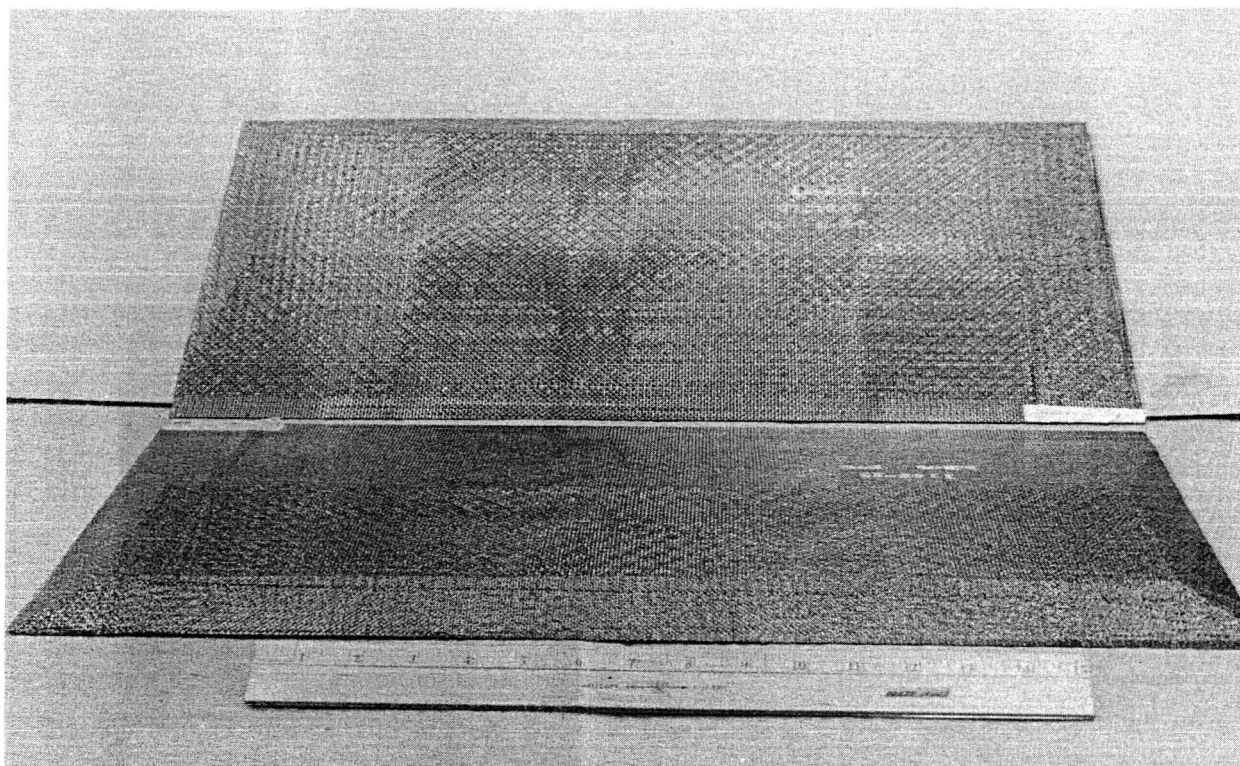


Figure 198. NDI Standard—Two Honeycomb Skin Panels

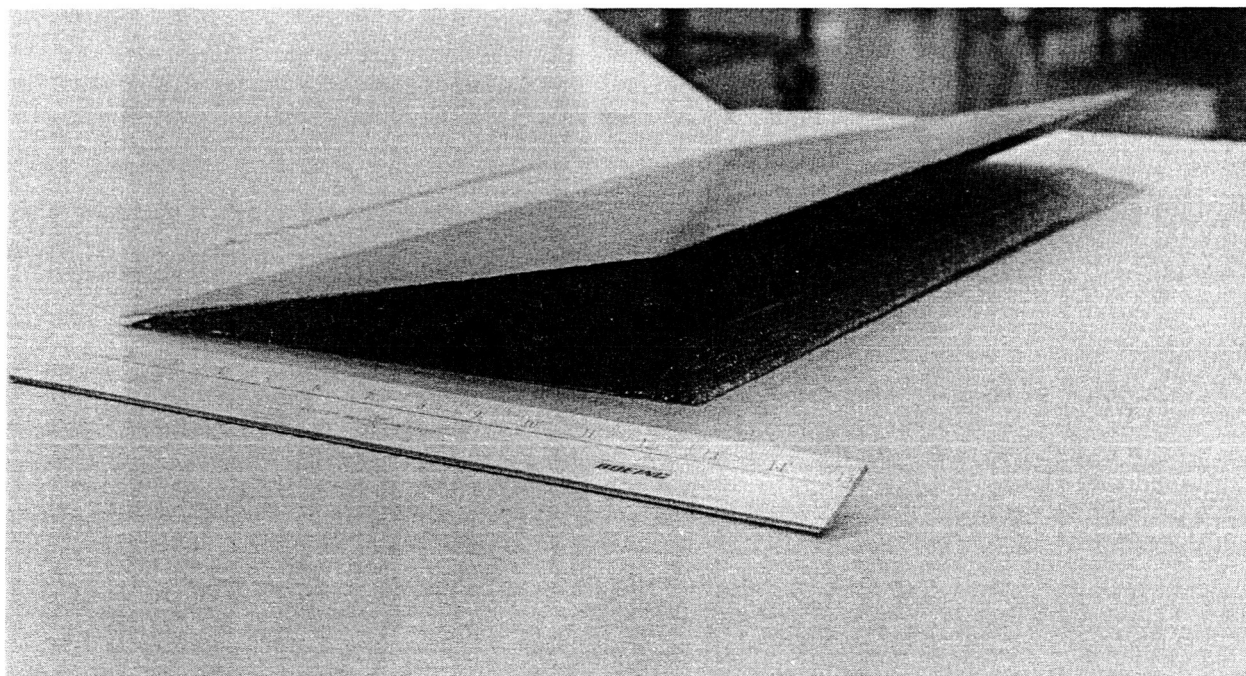


Figure 199. NDI Standard—Honeycomb Skin Panels Simulating Trailing-Edge Assembly

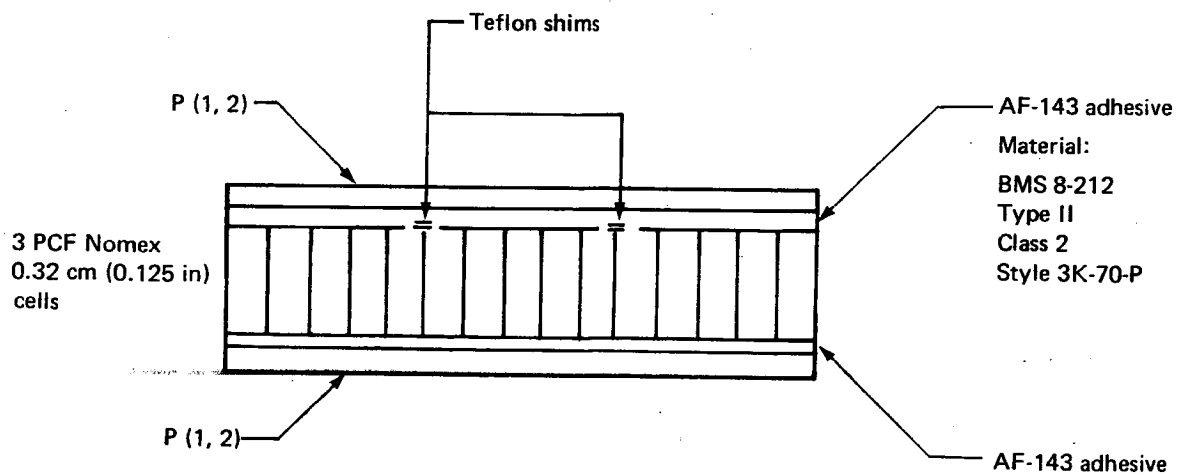
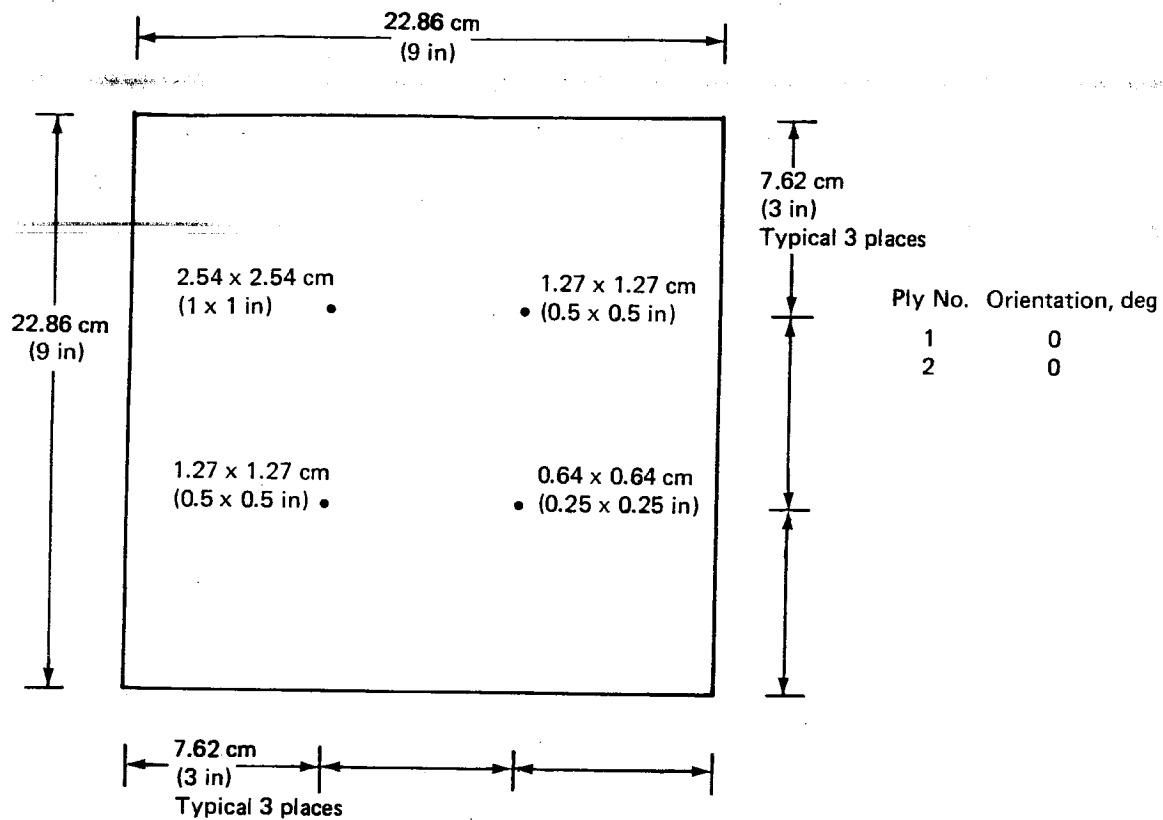


Figure 200. Skin Panel Standard

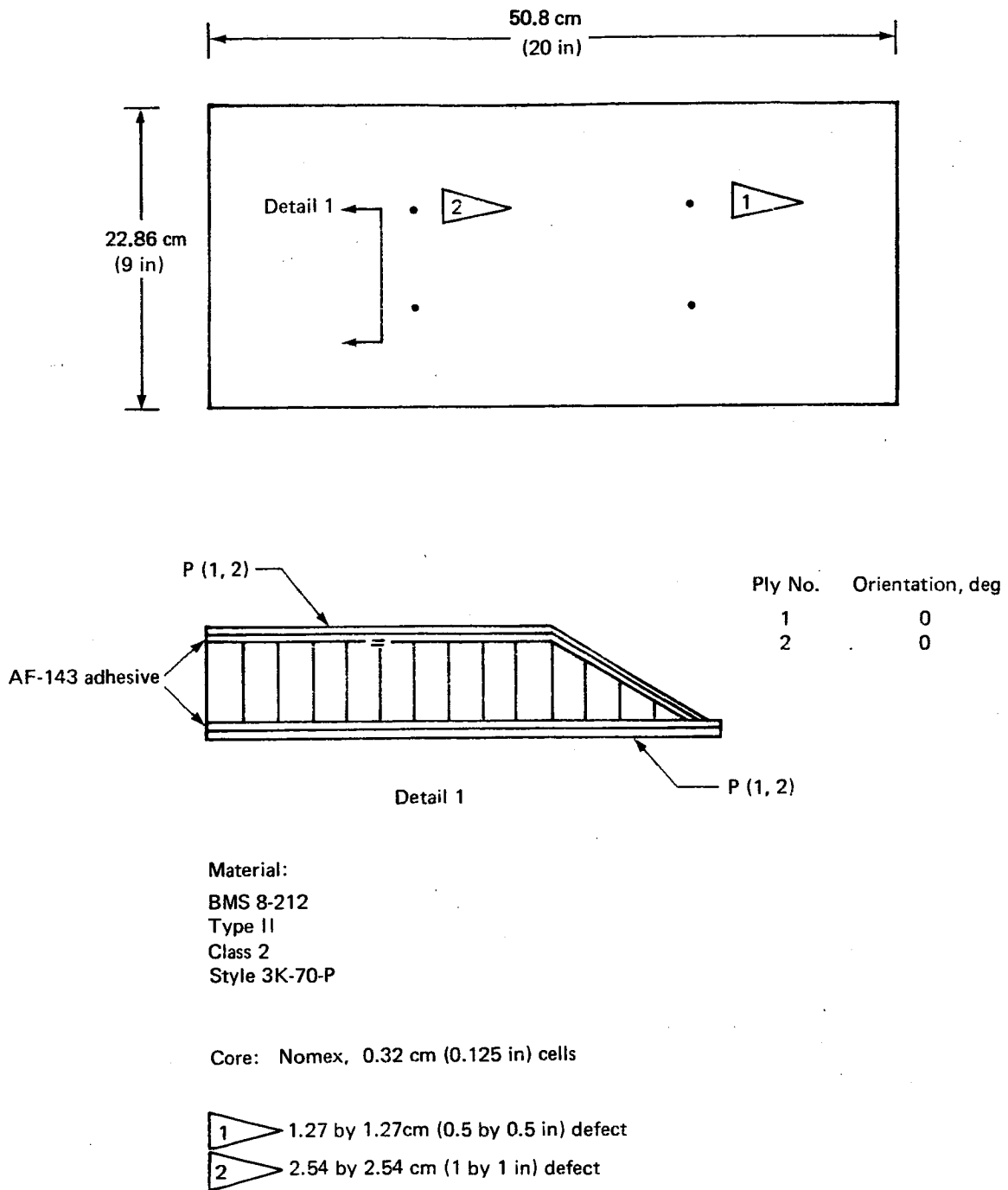
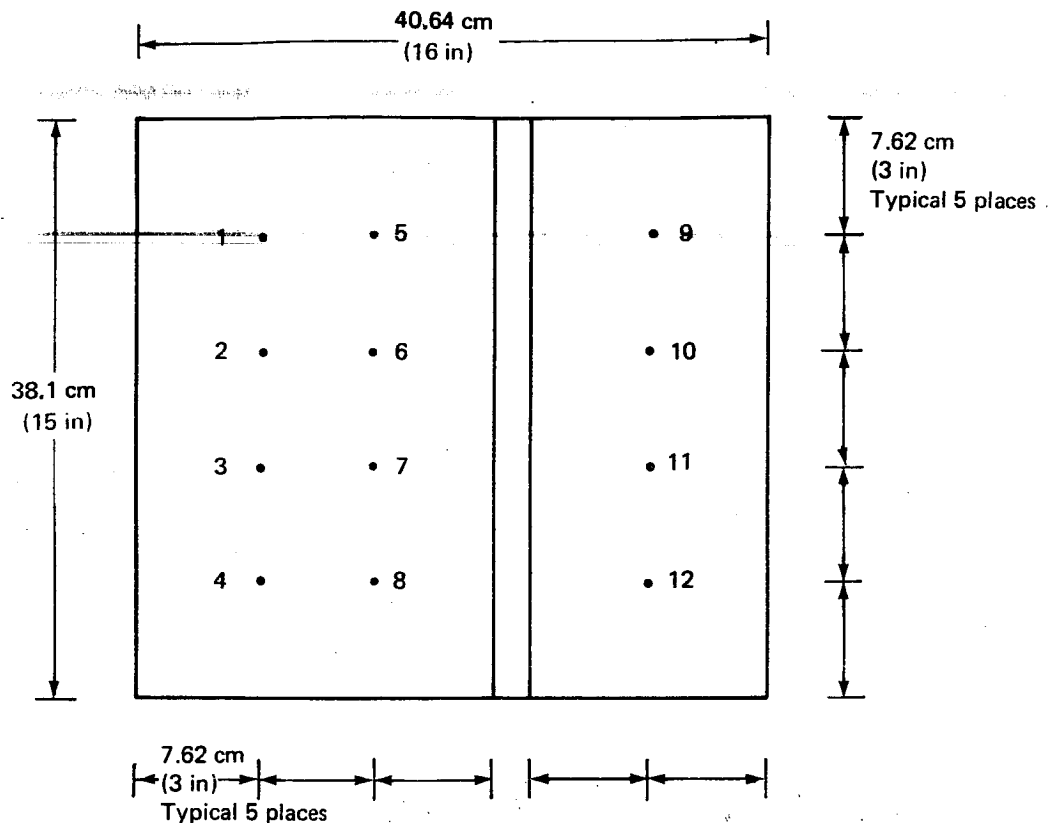


Figure 201. Taper Edge Standard



6 plies (fabric)
Material:
BMS 8-212
Type II
Class 2
Style 3K-70-P

All defects 1.27-by 1.27 cm (0.5 by 0.5 in) 2-mil Teflon shims

Defect No. 1 between P17 and P16
Defect No. 2 between P16 and P15
Defect No. 3 between P15 and P14
Defect No. 4 between P14 and P13
Defect No. 5 between P13 and P12
Defect No. 6 between P12 and P11

Defect No. 7 between P11 and P10
Defect No. 8 between P10 and P9
Defect No. 9 between P17 and P14
Defect No. 10 between P14 and P11
Defect No. 11 between P11 and P7
Defect No. 12 between P7 and P4

11 plies (tape)
Material:
BMS 8-212
Type II
Class 1
Grade 145

Figure 202. Front-Spar Chord Standard

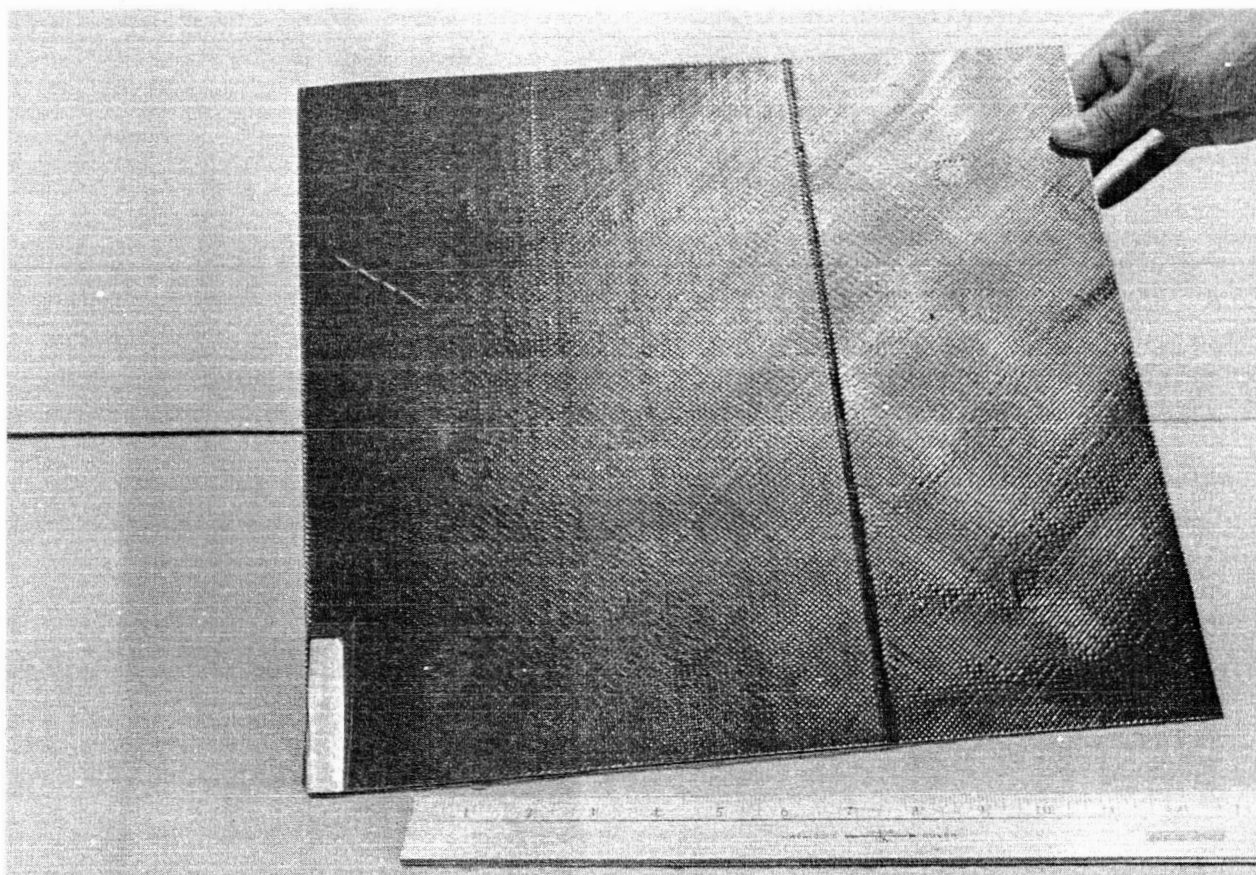


Figure 203. Preliminary NDI Standard—Front-Spar Chord

Production NDI standards, designed to duplicate production parts but with built-in defects, were fabricated in accordance with a Boeing specification.

- Upper and lower skin panel sections were fabricated per drawing 65C-17707-902 and 65C-17707-903 from station 136.50 to 173.21. The built-in defects, ranging from 0.64 x 0.64 cm (0.25 x 0.25 in) to 2.54 x 2.54 cm (1 x 1 in), were introduced throughout the panels, as shown in Figure 204.
- The two additional skin panels were fabricated and then sealed at the tapered end to make a trailing-edge assembly. The incorporated defect size ranged from 1.27 x 1.27 cm (0.5 x 0.5 in) to 5.08 x 5.08 cm (2 x 2 in). The details are shown in Figure 205.
- The rear spar standard, Figure 206, was built per drawing 65C-17707-9006E, from station 117.0 to 99.79. The defects ranged from 0.64 x 0.64 cm (0.25 x 0.25 in) to 2.54 x 2.54 cm (1 x 1 in).
- The front spar standard, Figure 207, was built per drawing 65C-17707-9006E, from station 149.34 to 129.19, with defects ranging from 0.64 x 0.64 cm (0.25 x 0.25 in) to 2.54 x 2.54 cm (1 x 1 in).
- The rib standard, Figure 208, was built per drawing 65C-17707-4E, full size. The defects ranged from 0.64 x 0.64 cm (0.25 x 0.25 in) to 2.54 x 2.54 cm (1 x 1 in).

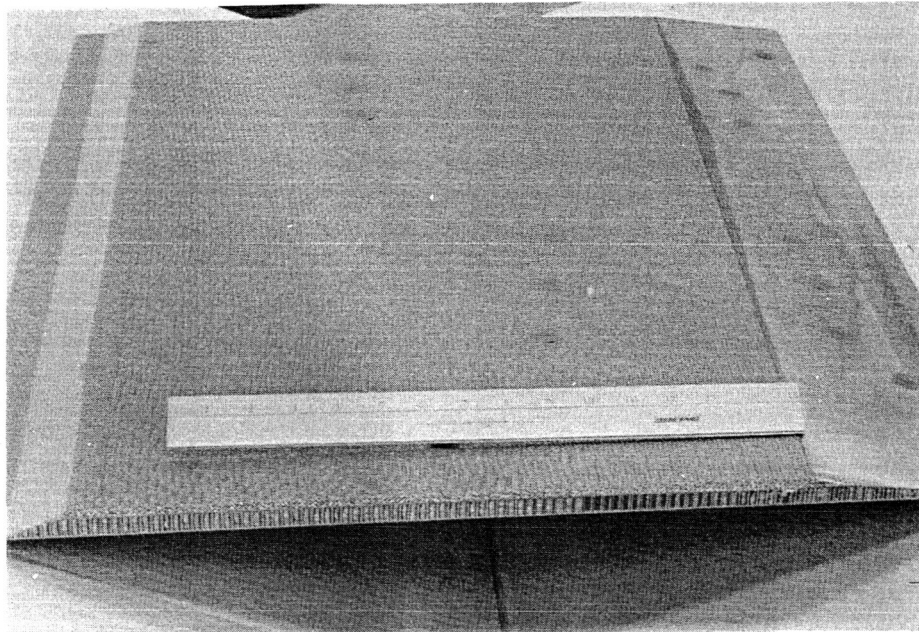


Figure 204. 727 Advanced Composite Elevator Skin-Panel Standard

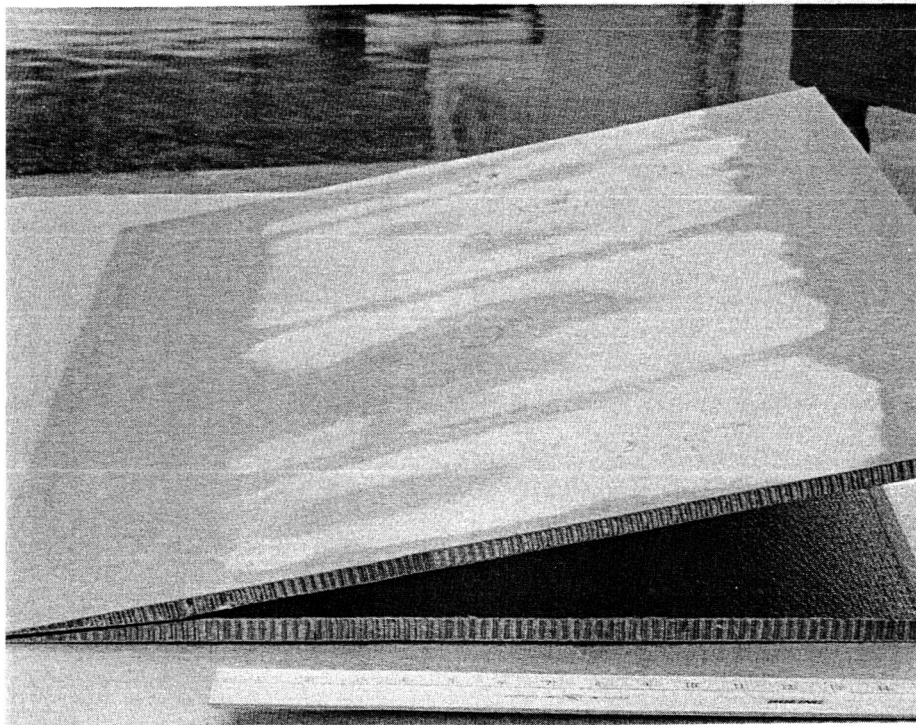


Figure 205. 727 Advanced Composite Elevator Trailing-Edge Assembly Standard

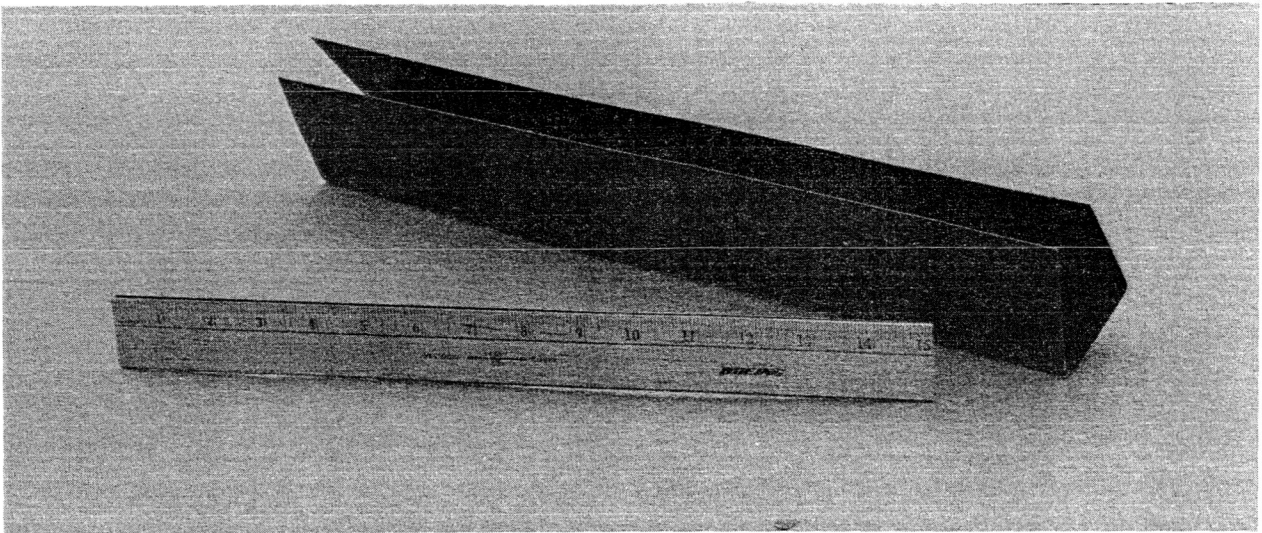


Figure 206. 727 Advanced Composite Elevator Rear-Spar Standard

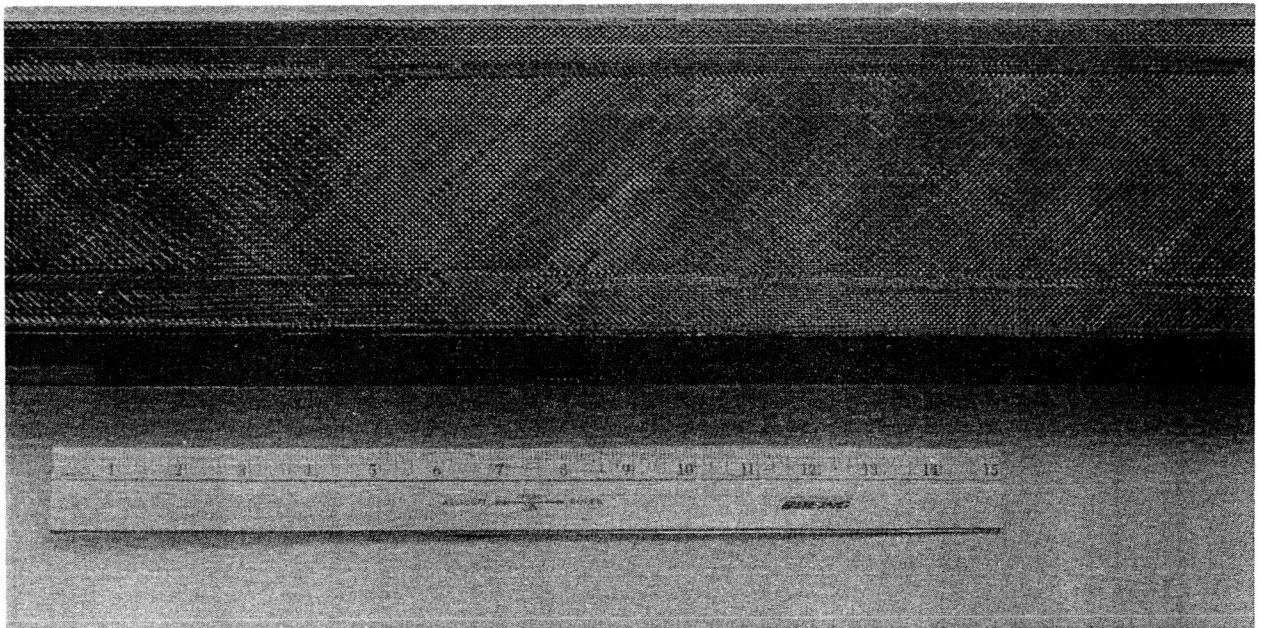


Figure 207. 727 Advanced Composite Elevator Front-Spar Standard

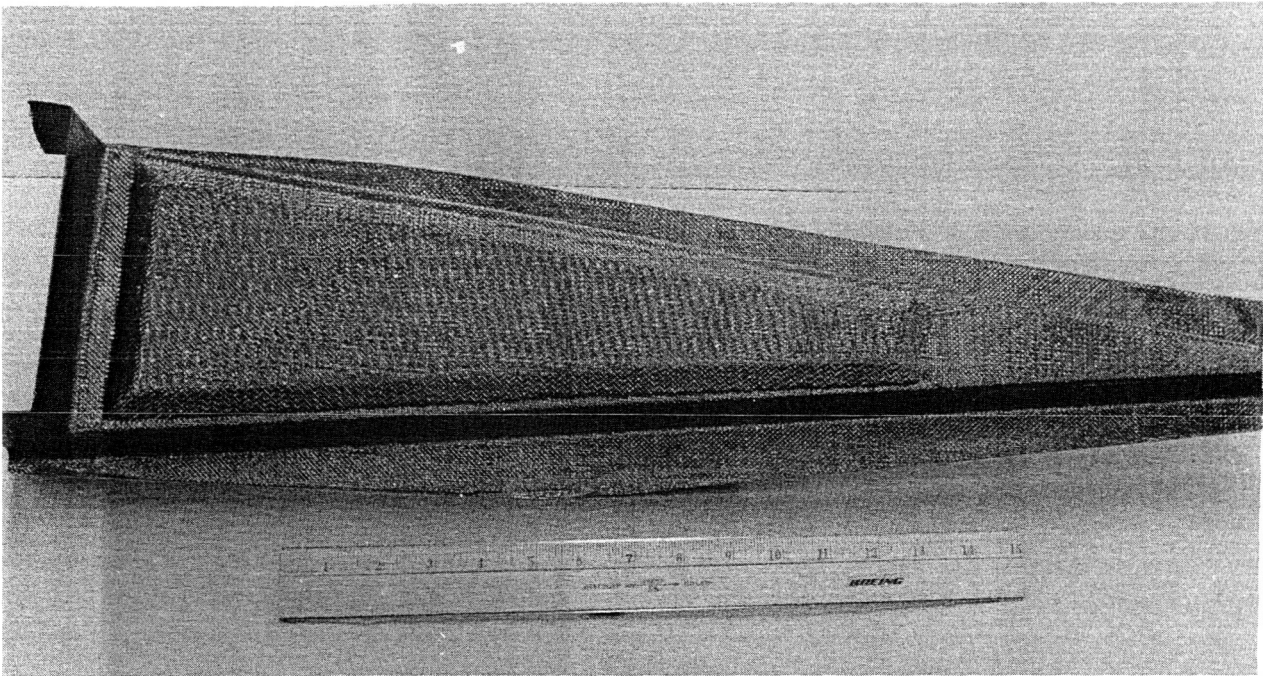


Figure 208. 727 Advanced Composite Elevator Rib Standard

5.3.8 NONDESTRUCTIVE INSPECTION TECHNIQUES

The following NDI techniques were evaluated during this investigation:

- Through-Transmission Ultrasonic (TTU) with automated scanning and computerized C-scan recording and/or a visual display (figs. 209 and 210)
- Portable and semi-portable TTU, manual scanning with light meter and audible defect indication (figs. 211 and 212)
- Sondicator, Models -1 or S-2B; manual ultrasonic inspection (fig. 213)
- Fokker Bond Tester (fig. 214)
- Radiographic inspection, low-kilovoltage (15--40 kV)

All preliminary and production standards were evaluated using one or more of the above techniques. It was found that TTU was the most sensitive test method and the computerized C-scan capability provided a permanent record (fig. 206). Voids and delaminations are shown in darker areas of the scan. Semiportable and portable equipment and techniques were used without C-scan capability, but having a light meter and audible defect indicators (figs. 207 and 208). TTU C-scan inspection was capable of reliable defect detection to 0.64 x 0.64 cm (0.25 x 0.25 in). Using portable and semiportable TTU with manual scanning, the detection capability was limited to defects 1.27 x 1.27 cm (0.5 x 0.5 in). The latter techniques were used in rib sections, flange, and spar areas (fig. 209).

The Sondicator and Fokker Bond Tester also were used for defect detection in those areas where manual scanning was required. Both were effective down to a detection limit of 1.27 x 1.27 cm (0.5 x 0.5 in). In the sealed area of the trailing edge, radiographic inspection was determined to be the only suitable technique for detecting minute voids in the sealant. In-service and maintenance inspection can be performed using the Sondicator, Bond Tester, and/or X-ray (when practical). Under these conditions (outside the laboratory or production environment), the realistic defect detection capability is expected to be 2.54 x 2.54 cm (1.0 x 1.0 in) or larger.

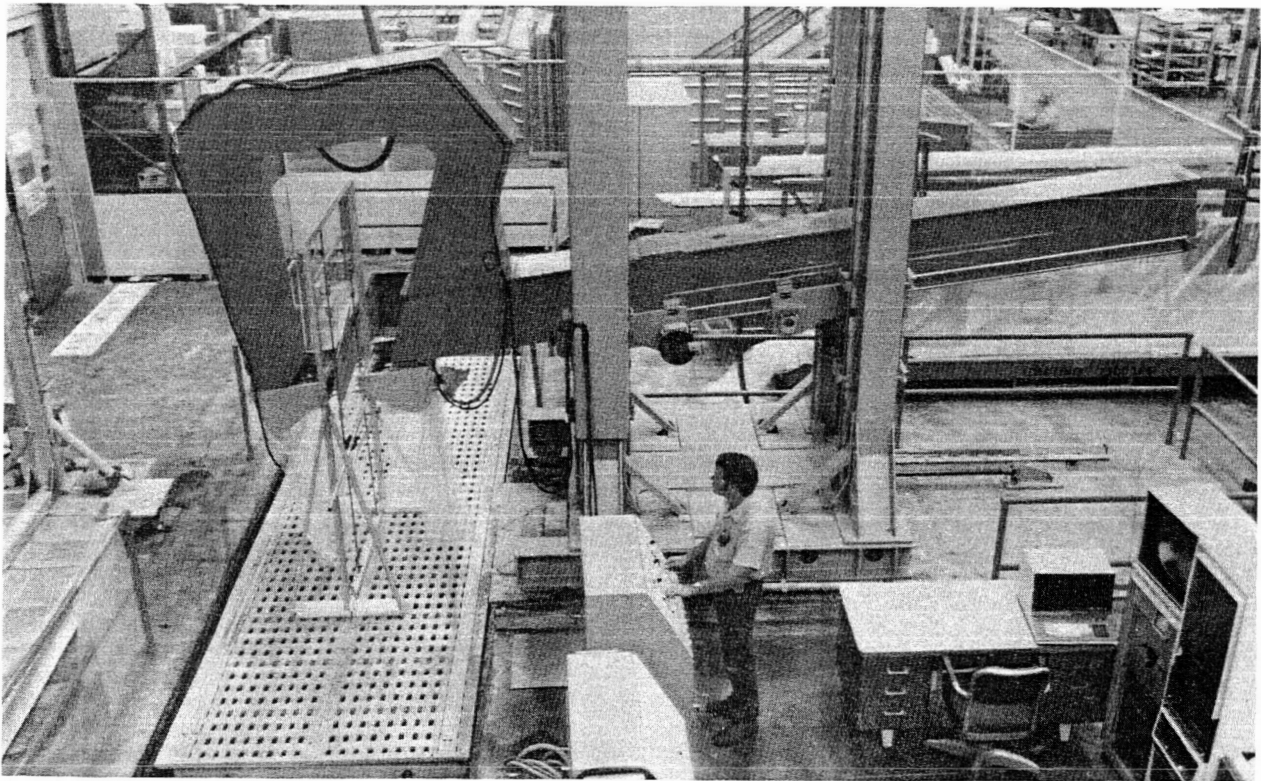


Figure 209. Automated TTU Scanner

GRAPHITE TEST PANEL
 PART NUMBER = 11423A
 DATE = 3/9/78
 SCANNER INDEX = 60 THOUSANDTHS
 X SCALE = 1 Y SCALE = 1
 PLOTTING SEQUENCE = 1,0,0,0,0,0.

SERIAL NUMBER = 000
 CALIBRATION PROCEDURE = L4
 SCAN PATTERN = A
 SCAN DIRECTION = LEFT
 NUMBER OF OPERATIONAL CHANNELS = 1

SIGNAL IDENTIFICATION LEVELS
 LEVEL MAX VOLTS*100

0	1000
1	700
2	335
3	285
4	255
5	225
6	190
7	155
8	115
9	75
10	50
11	30
12	15

PLOTTED SYMBOLS

1000	.GT. BLANK	.GE.	700
700	.GT.	.GE.	335
335	.GT. 1	.GE.	285
285	.GT. 2	.GE.	255
255	.GT. 3	.GE.	225
225	.GT. 4	.GE.	190
190	.GT. 5	.GE.	155
155	.GT. 6	.GE.	115
115	.GT. 7	.GE.	75
75	.GT. 8	.GE.	50
50	.GT. 9	.GE.	30
30	.GT. 10	.GE.	15
15	.GT. 11	.GE.	0

TOTAL NUMBER OF BLOCKS = 210

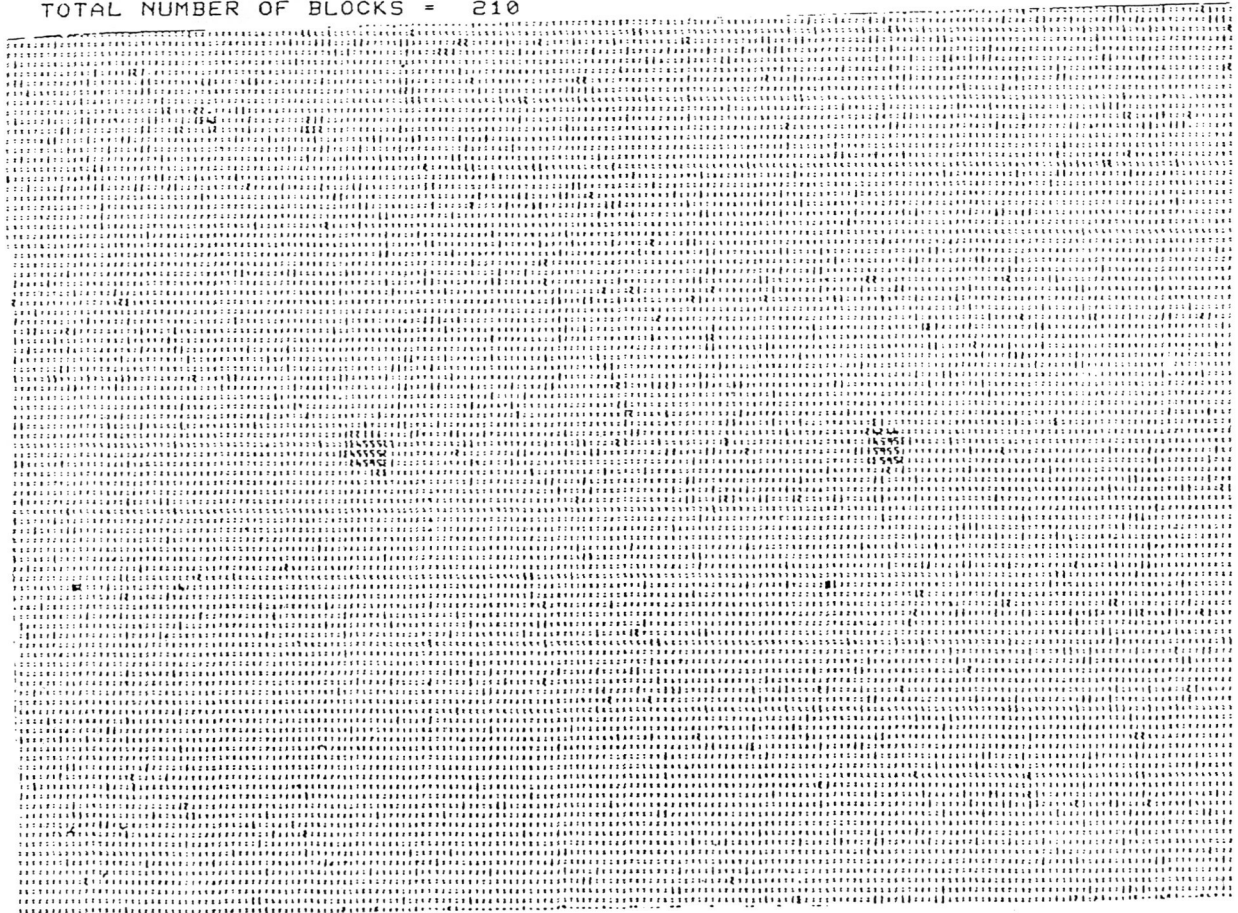


Figure 210 Graphite-Epoxy Test Panel Standard, Computerized C-Scan Recording

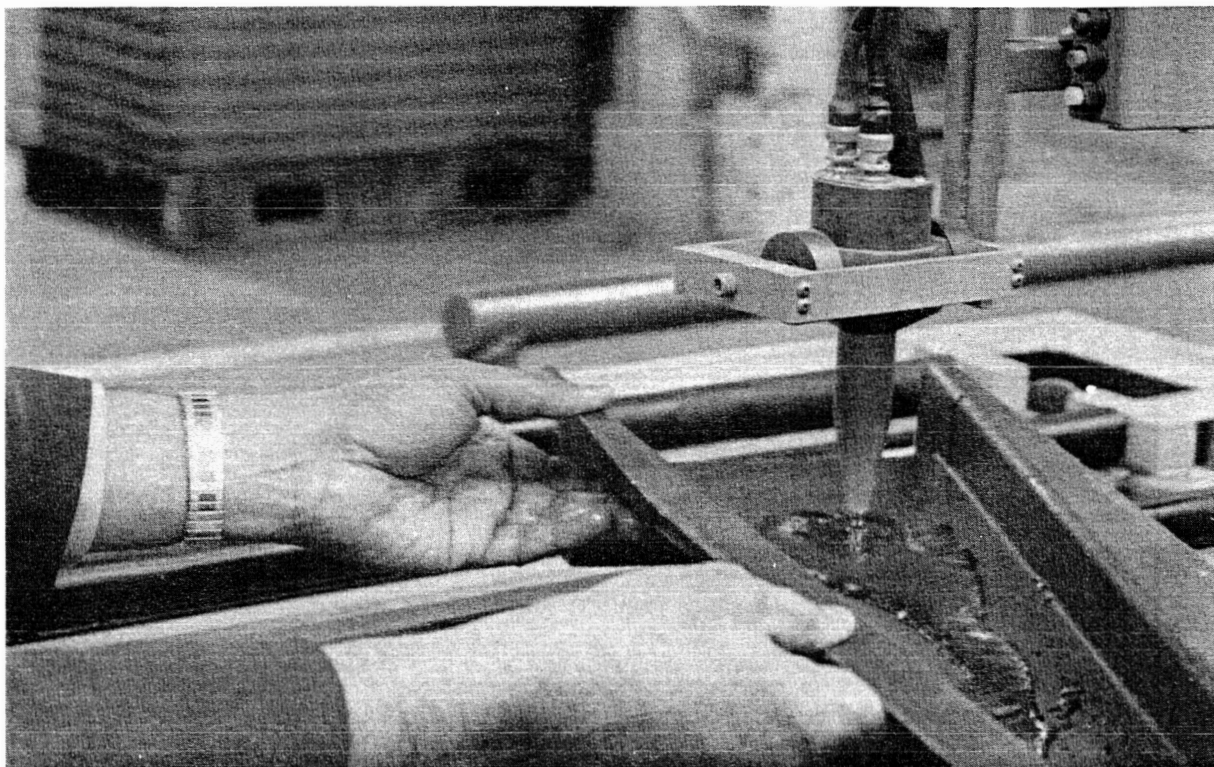


Figure 211. Semiportable TTU Scanner without C-Scan Capability



Figure 212. Portable TTU Scanner, Showing Inspection of Flange Area by Hand-Held TTU Unit

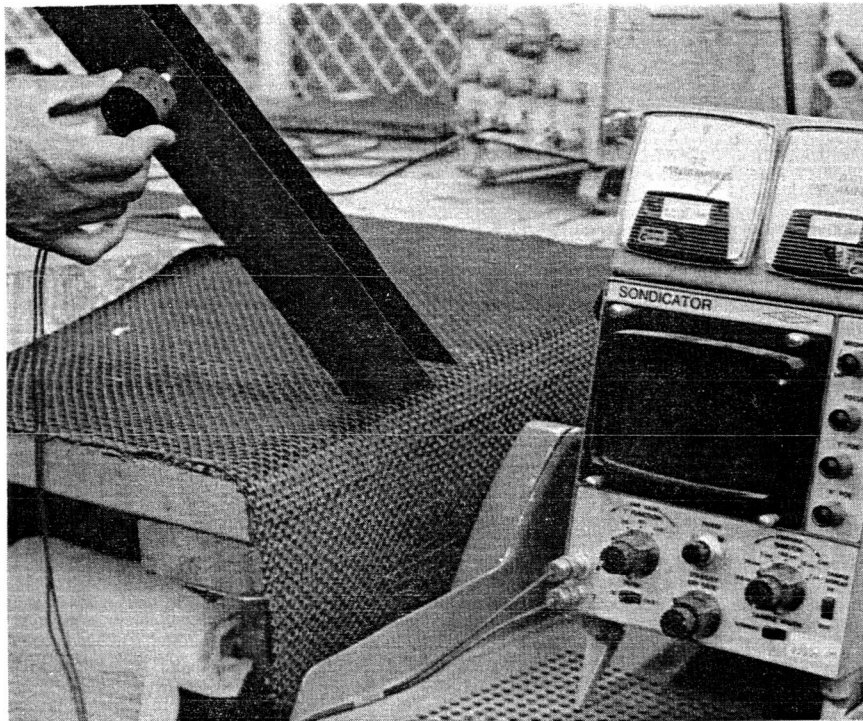


Figure 213. Sondicator Inspection of Configuration Not Suitable for TTU Scan

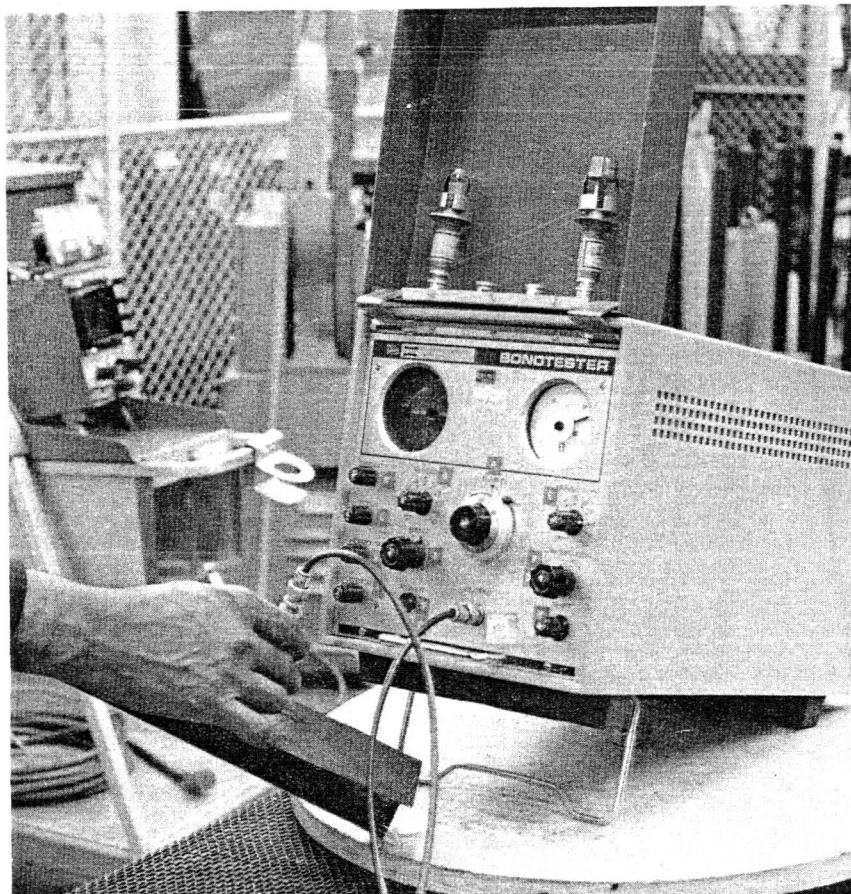


Figure 214. Fokker Bond Testing of Configuration Not Suitable TTU Scan

6.0 PRODUCTION

The production phase of the NASA model 727 elevator program began in April 1978 with fabrication of composite components and was completed in July 1979 when the last of the five and a half shipsets had been assembled. Composite elevators, composite control tabs, and metal balance panels were included in the program (fig. 215). Five full shipsets were manufactured to a flight configuration ready for installation on any given 727 trijet and one half shipset was manufactured for Engineering test. The first full shipset produced was installed on a Boeing-owned airplane for flight testing. The five shipsets were installed on commercial airplanes.

From the proposal stage on, Boeing's approach to the program was to use past fiberglass-epoxy fabrication and assembly experience as a basis for program planning and to accomplish manufacturing efforts in a production environment. This approach established comparative cost, schedule, and technological data essential to follow-on production commitment decisions.

Production facilities at Boeing's Fabrication Division in Auburn, Washington were used to produce advanced composite components and certain new metal components. Assembly of the elevators, tabs, and balance panels was accomplished at the production assembly facilities of the 707/727/737 Division in Renton, Washington. Some modification of the facilities was required to accommodate the unique processing requirements of the composite materials.

The systems and procedures used for ongoing commercial airplane manufacture also were employed, so that a go-ahead production decision could be readily implemented. Computer systems that play a vital role in Boeing's everyday activities were programmed to handle advanced composites program engineering releases, planning releases, parts ordering and control activities, and scheduling of program events. Personnel assignments were made from the pool of production and tooling workers already engaged in normal fiberglass and metal manufacturing operations.

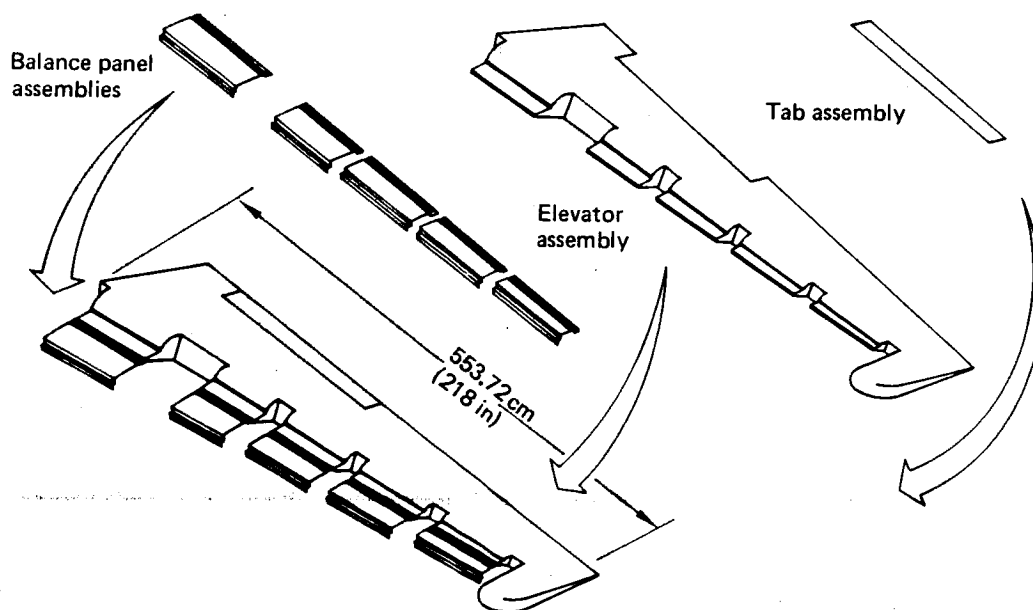


Figure 215. Elevator/Tab/Balance Panel Assembly

Detail and assembly tools were designed and fabricated to support a full-scope production program, rather than a limited run. Also, because previous development programs were designed to verify tooling approaches and fabrication processes that would be used in the production mode, the production tools were used wherever feasible to produce developmental hardware.

This section of the report addresses the methods and concepts used in the detail and assembly tooling and fabrication sequences of the program as a result of developmental efforts and the production environment approach.

6.1 DETAIL TOOLING

As previously noted, detail tools for the fabrication of composite components were designed and constructed to production standards and used for fabrication of verification hardware. Because the test box built for verification encompassed only 304.8 cm (10 ft) of the 548.64-cm (18-ft) elevator, a number of tools were tried for the first time at the startup of production operations. Also, only those portions of the large skin panel and spar tools that were contained within the test box had prior tryout. As a result, some tool development was necessary during production of the full-size article, but there were no major deviations from original concepts based on prior fiberglass tooling experience.

Both male- and female-configured layup tools were used for the program. Male tooling was preferred and most commonly used because tool fabrication and layup and bagging operations were less costly. Female tools were used wherever necessary to avoid having honeycomb core against the tool surface. Difficulties experienced with laying up composite materials to female-type tools are covered in Section 6.3.

Layup mandrels were designed and fabricated for multiple use wherever possible; i.e., the tool was capable of producing both left- and right-hand components.

Aluminum, steel, and fiberglass materials were used for the tools. Material selection was based on part size and complexity. Although lower thermal expansion made steel the desired material, its weight and low heatup rate were factors that led to the selection of aluminum for large parts such as skin panels and spars. Shrink factors were developed for both metals to account for tool thermal expansion during 176.5°C (350°F) cure cycles. Laminated fiberglass had limited usage.

Other tools used to fabricate composite details were core-locating templates, core-trim templates, setup templates, shaper fixtures, and hand router fixtures. The core-locating template was primarily used to locate honeycomb core(s), but in some instances also was used to locate graphite plies, doublers, and fillers. The core-trim template was used to fabricate core details. The setup template, shaper fixture, and hand router fixture were used to trim the parts to drawing or manufacturing configuration. Trim tool selection was dependent upon the part configuration and type of cut to be made. These tools were used in conjunction with either abrasive carbide, abrasive diamond, or carbide cutters.

The following sections describe the tooling packages developed for various composite components of the elevator.

6.1.1 FRONT SPAR

Layup Mandrel--A tool used to lay up inboard and outboard sections of spar (figs. 216 and 217).

Core-Locating Template--An aluminum tool used to locate graphite full and filler plies.

Setup Template--An aluminum tool used to show net trim of part and chamfer angle of flanges.

Shaper Fixture--An aluminum tool used to trim part to net size.

6.1.2 REAR SPAR

Layup Mandrel--This tool is shown in Figures 218 and 219.

Core-Locating Template--An aluminum tool used to locate graphite full and filler plies.

Hand Router Fixture--A fiberglass tool used to trim part to net size.

6.1.3 INBOARD CLOSURE RIB

Layup Mandrel--A female-configured tool due to core location (figs. 220 and 221).

Core-Locating Template--A fiberglass tool used to locate core detail and graphite doubler and filler plies.

Shaper Fixture--A fiberglass tool used to trim part to net size.

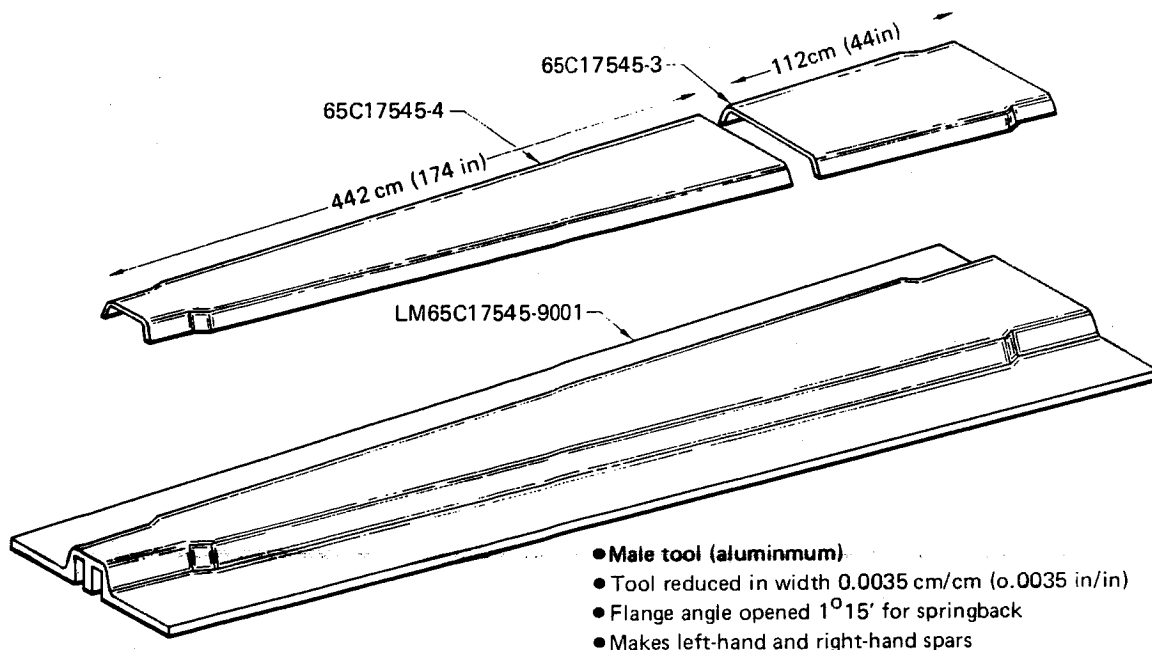


Figure 216. Front Spar and Layup Mandrel

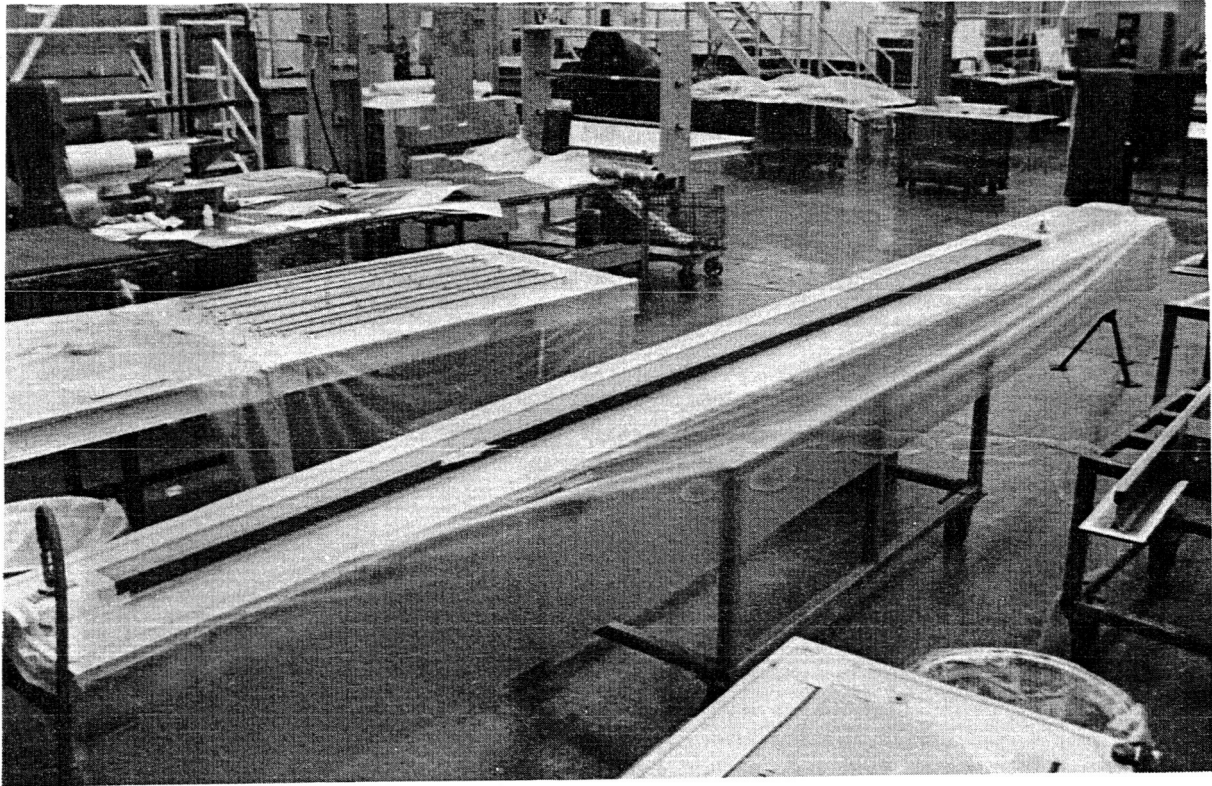


Figure 217. Front-Spar Assembly Tool with Outboard Spar Detail

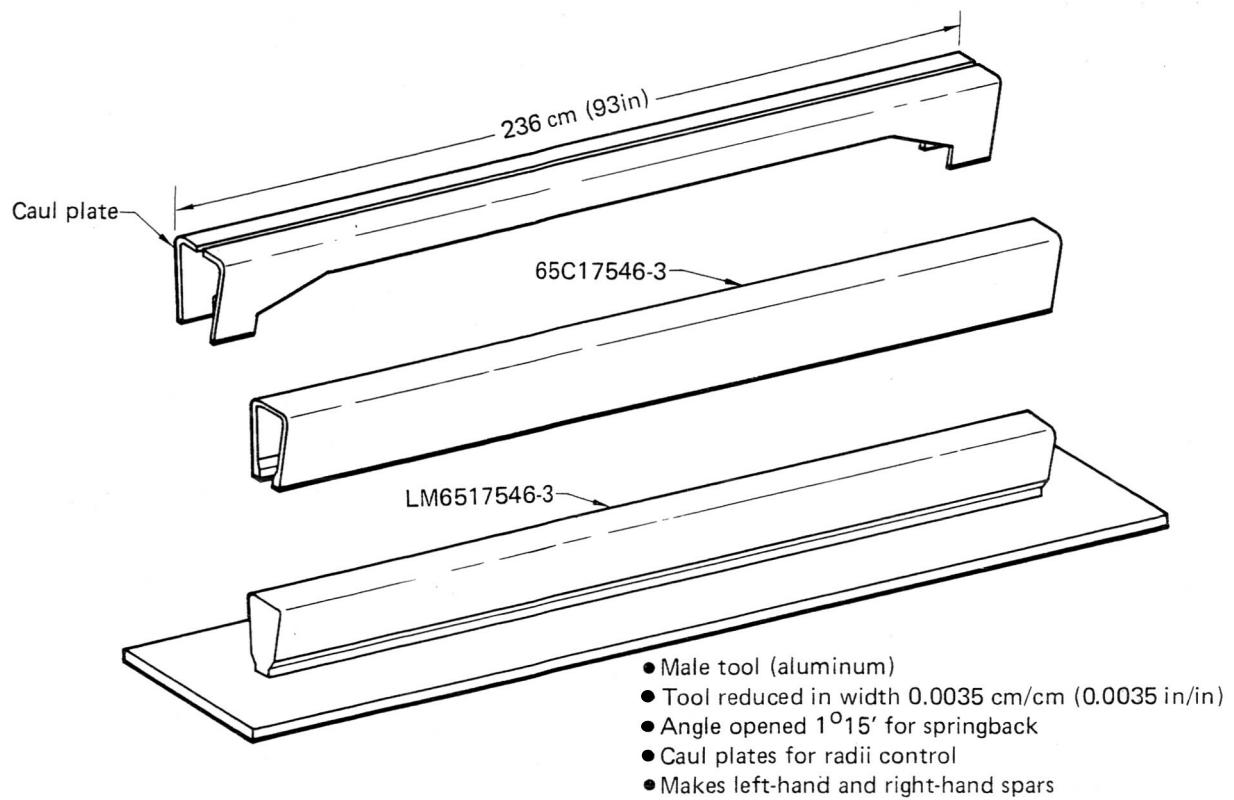


Figure 218. Rear Spar and Layup Mandrel

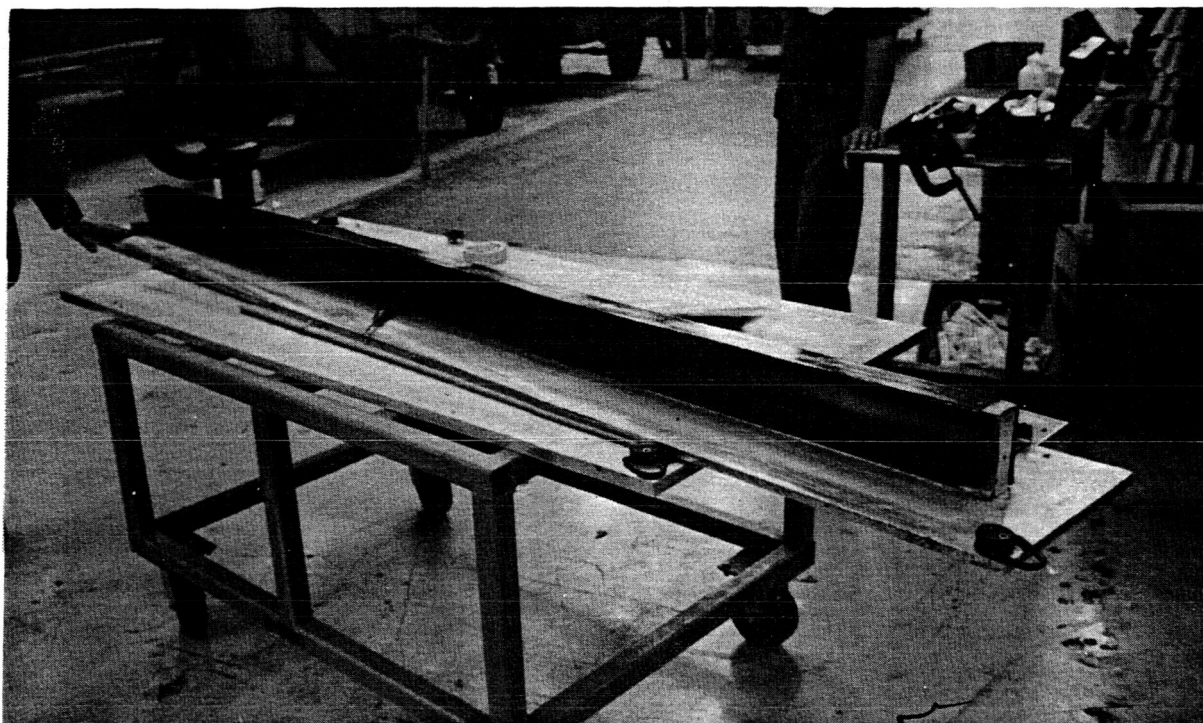


Figure 219. Rear-Spar Detail on Layup Mandrel

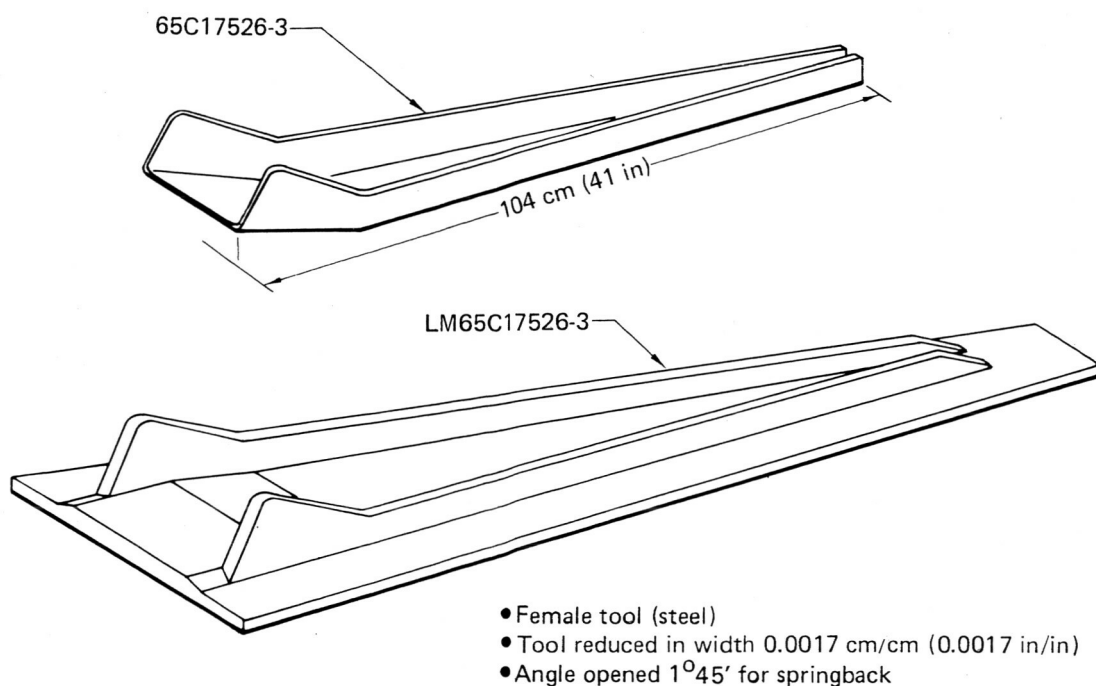


Figure 220. Inboard Closure Rib and Layup Mandrel

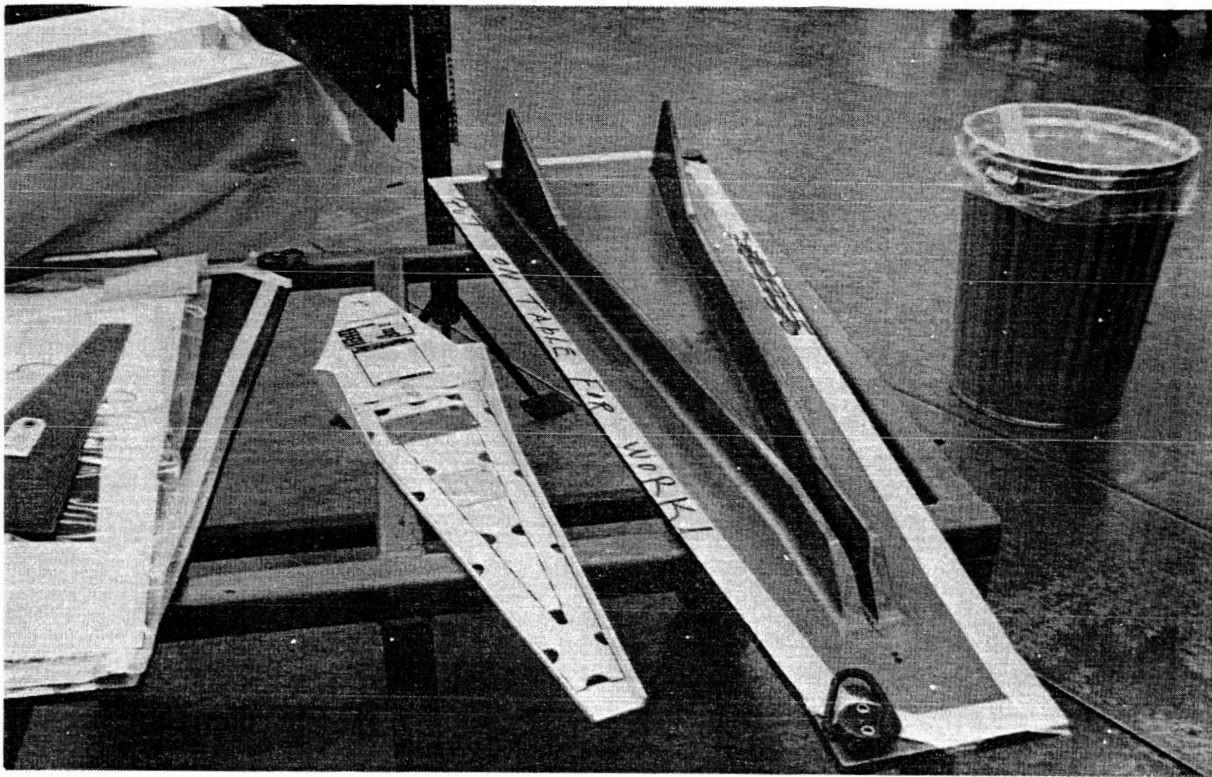


Figure 221. Inboard Closure Rib Layup Tools

6.1.4 OUTBOARD CLOSURE RIB

Layup Mandrel—This tool is shown in Figure 222.

Core-Locating Template—A Mylar tool used to locate core and graphite doubler and filler plies.

Shaper Fixture—A fiberglass tool used to trim part to net size.

6.1.5 RIB—STATION 117.37

Layup Mandrel—These tools are shown in Figures 223 and 224.

Core-Locating Template—A Mylar tool used to locate core detail and graphite doubler and filler plies.

Shaper Fixture—A fiberglass tool used to trim part to net size.

6.1.6 REAR-SPAR HEADER

Layup Mandrel—A tool that uses silicone rubber pressure caps and makes eights parts (fig. 225).

Shaper Fixture—A fiberglass trim tool used to trim detail to net size.

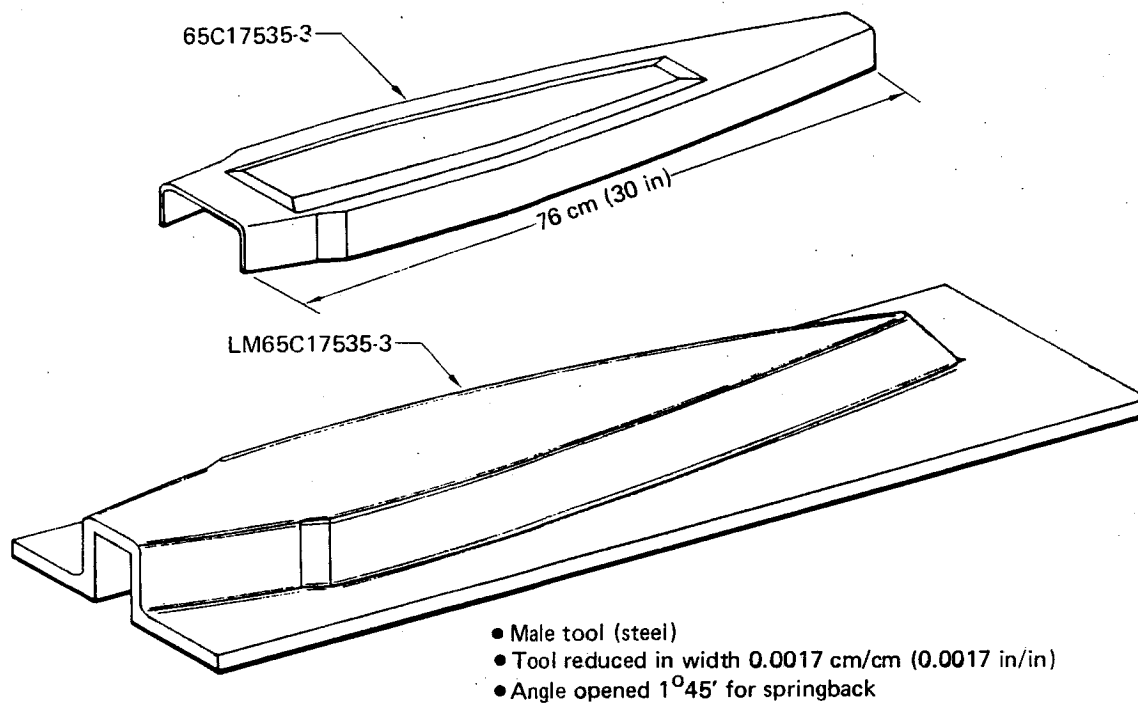


Figure 222. Outboard Closure Rib and Layup Mandrel

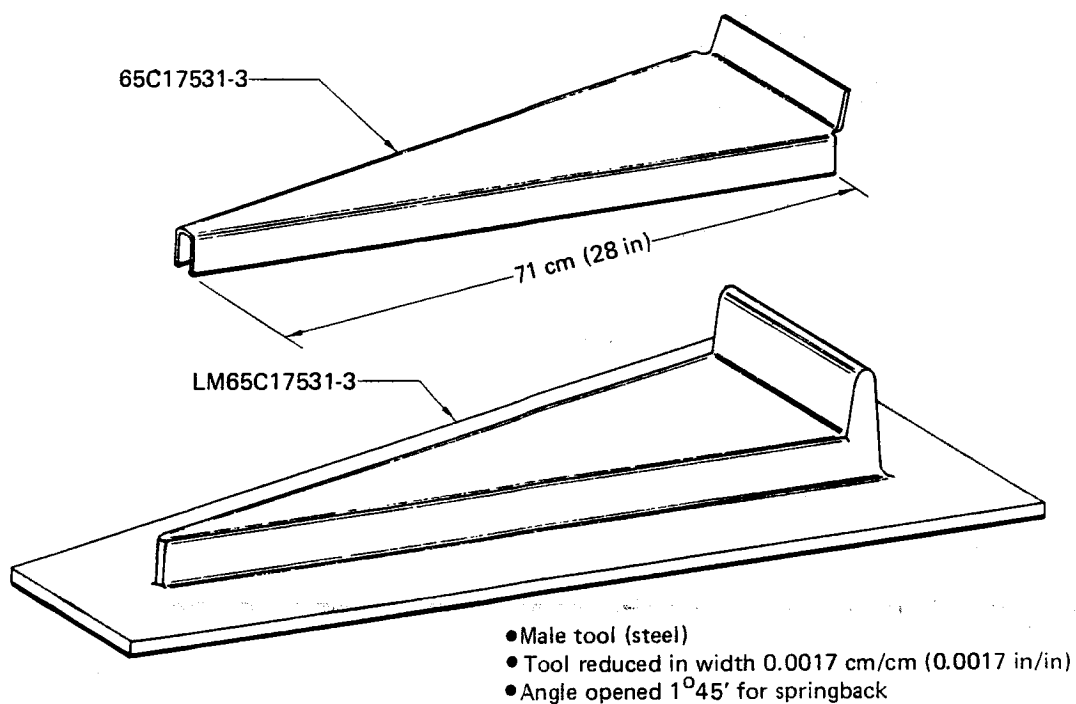


Figure 223. Rib—Station 117.37 and Layup Mandrel

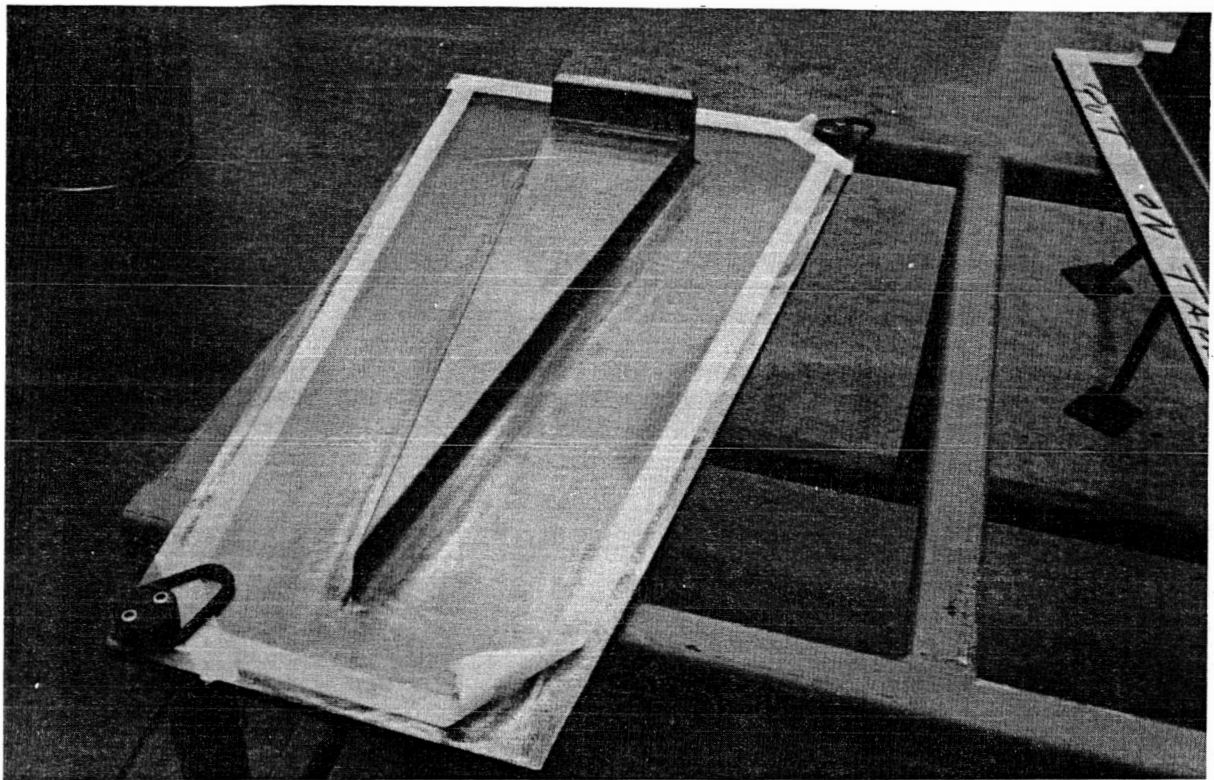


Figure 224. Station 117.37 Rib Layup Tool

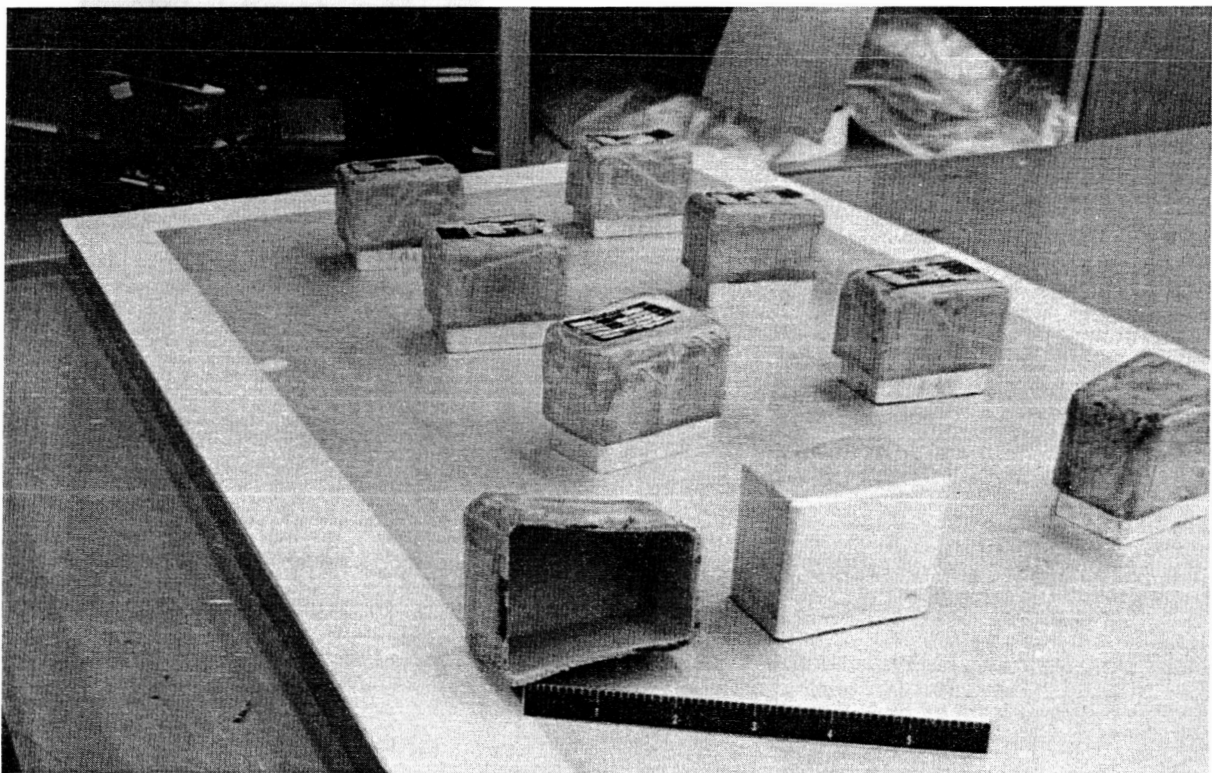


Figure 225. Rear-Spar Header Layup Mandrels

6.1.7 ACTUATOR FAIRING

Layup Mandrel—This tool is shown in Figure 226.

Core-Locating Template—A fiberglass tool used to locate graphite filler plies.

Shaper Fixture—A fiberglass tool used to trim part to net size.

6.1.8 SKIN PANELS

Layup Mandrels—These tools are shown in Figures 227 through 229.

Core-Locating Template—A Mylar tool used to locate core details and graphite doubler and filler plies. Two core-locating templates are used to locate core details along the trailing edge. An aluminum caul plate is used along the trailing edge to control bonding plane.

Hand Router Fixture—A fiberglass tool used to trim detail with excess trimmed after assembly is completed.

6.1.9 CONTROL TAB

Bonding Assembly Jig—A tool used for three stages of bonding of spar, core, doublers, and skins (fig. 230).

Bonding Mill Fixture—A tool used to hold first-stage bond assembly to mill taper.

Setup Template—A tool used to locate precured doublers along the spar for bonding.

Hand Router Fixture—A tool used to trim assembly to net size, including forward edge of spar.

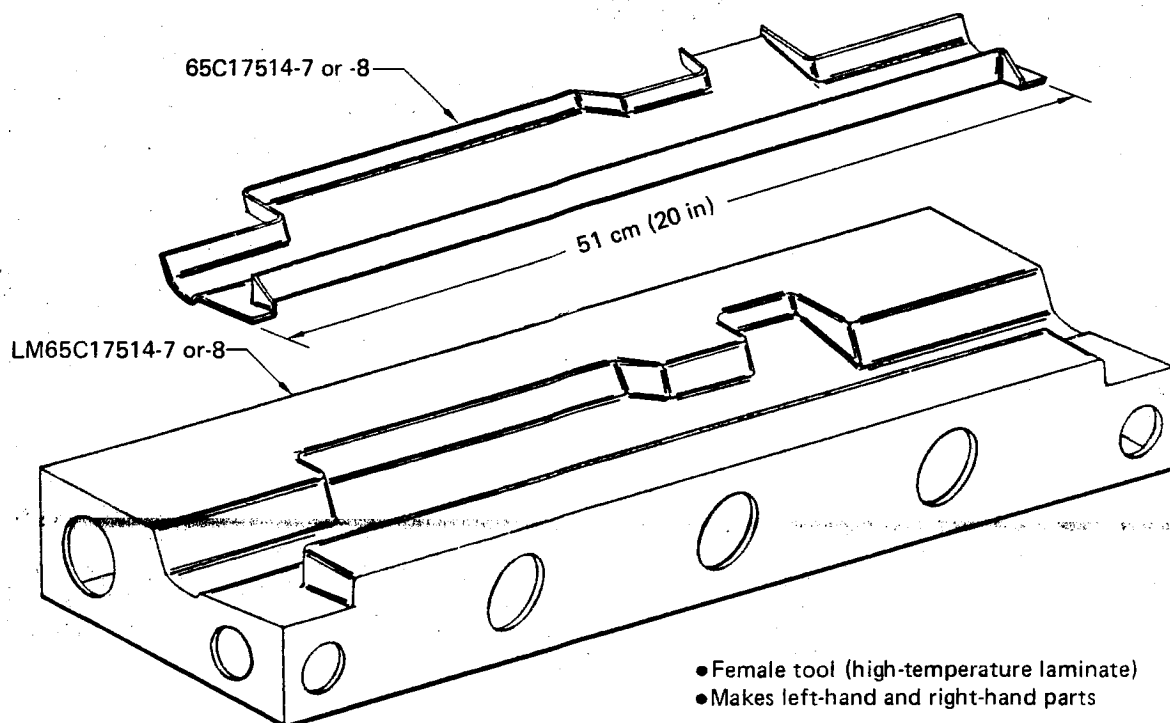


Figure 226. Actuator Fairing and Layup Mandrel

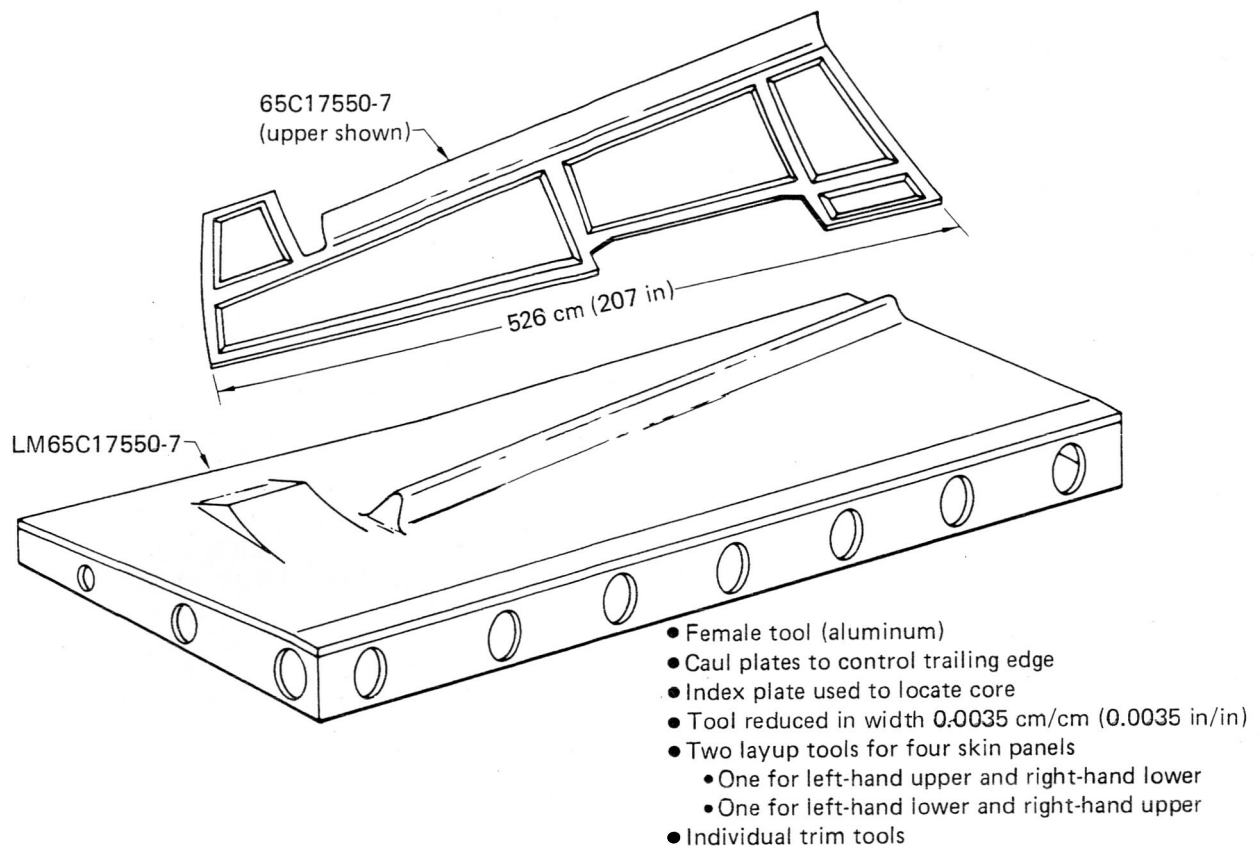


Figure 227. Skin Panel and Layup Mandrel

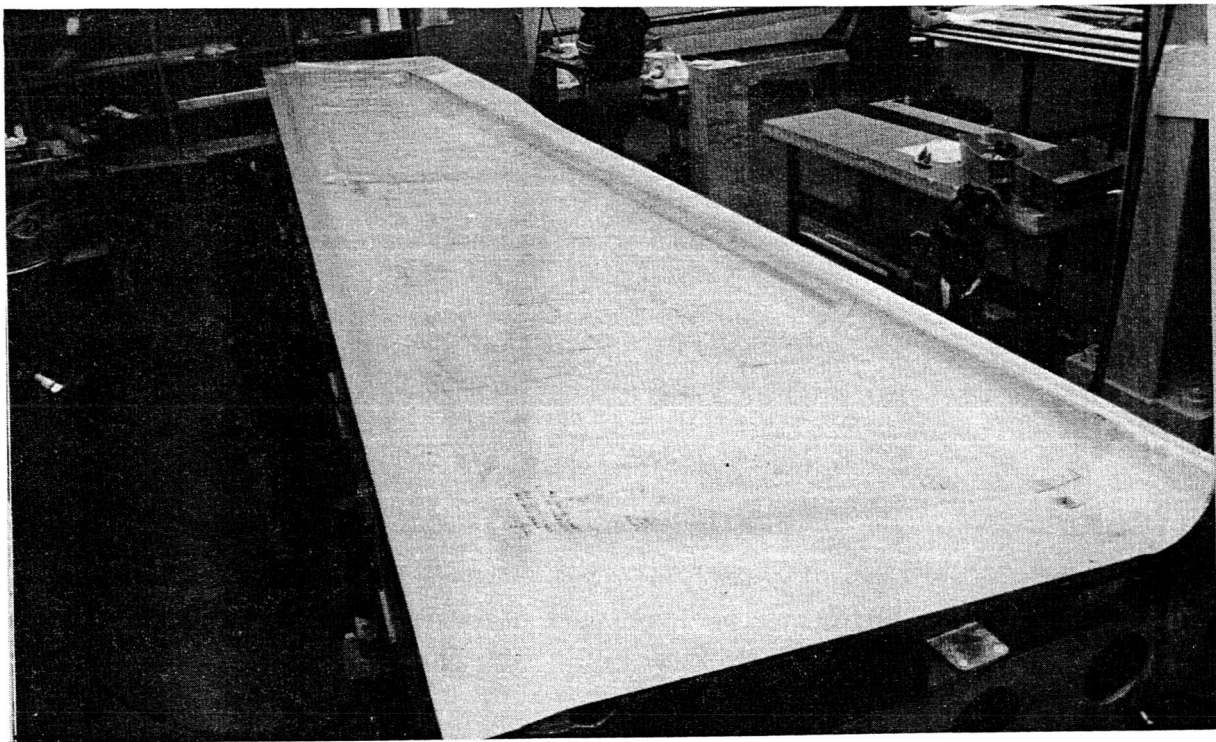


Figure 228. Skin Panel Layup Tool

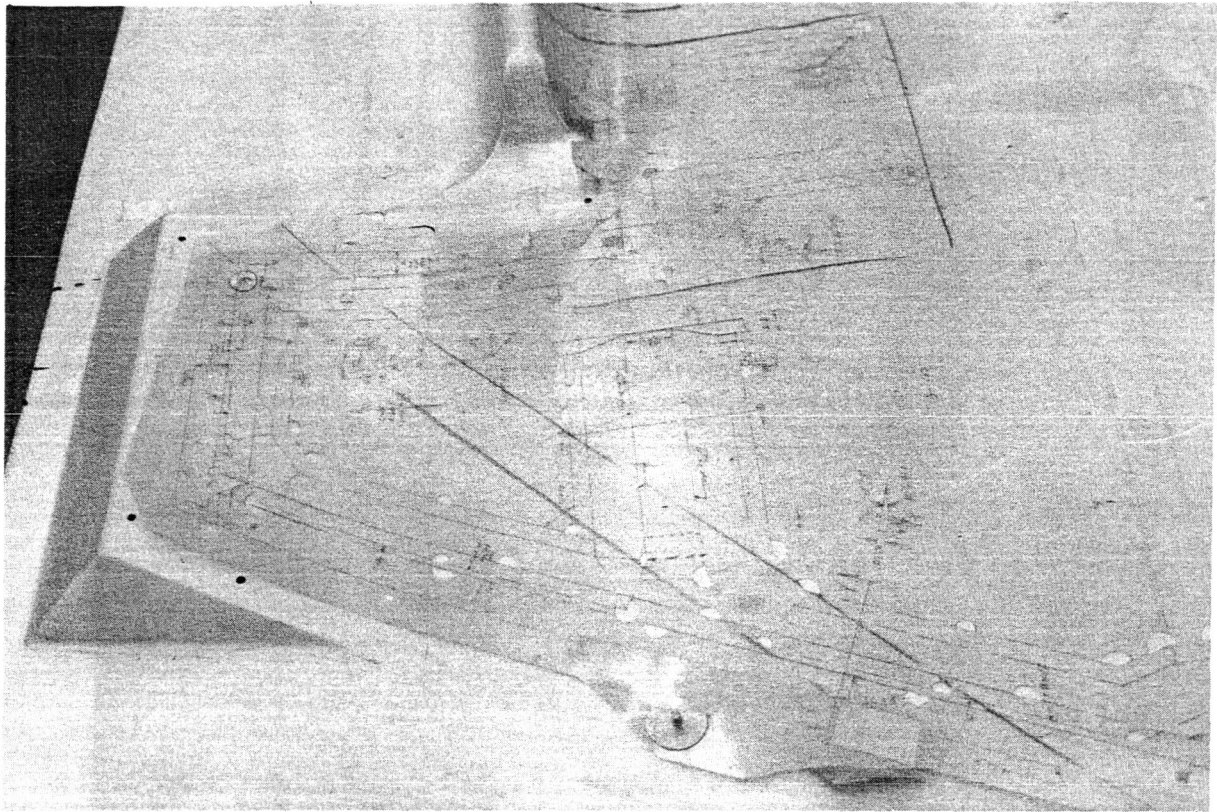


Figure 229. Skin Panel Layup Tool Showing Outboard End and Forward Layup Areas

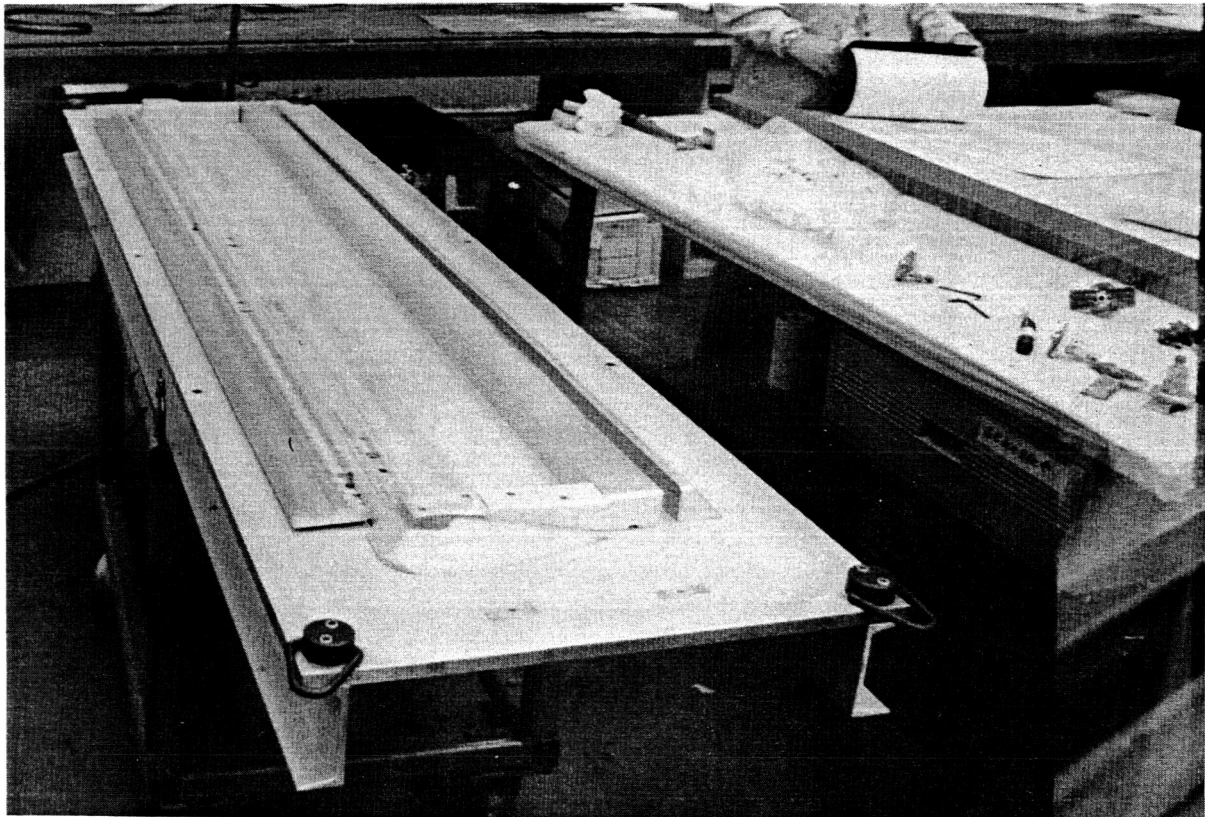


Figure 230. Control Tab Bonding Tool

6.1.10 CONTROL TAB SPAR

Layup Mandrel—This tool is shown in Figures 231 and 232.

Core-Locating Template—A Mylar tool used to locate graphite full and filler plies.

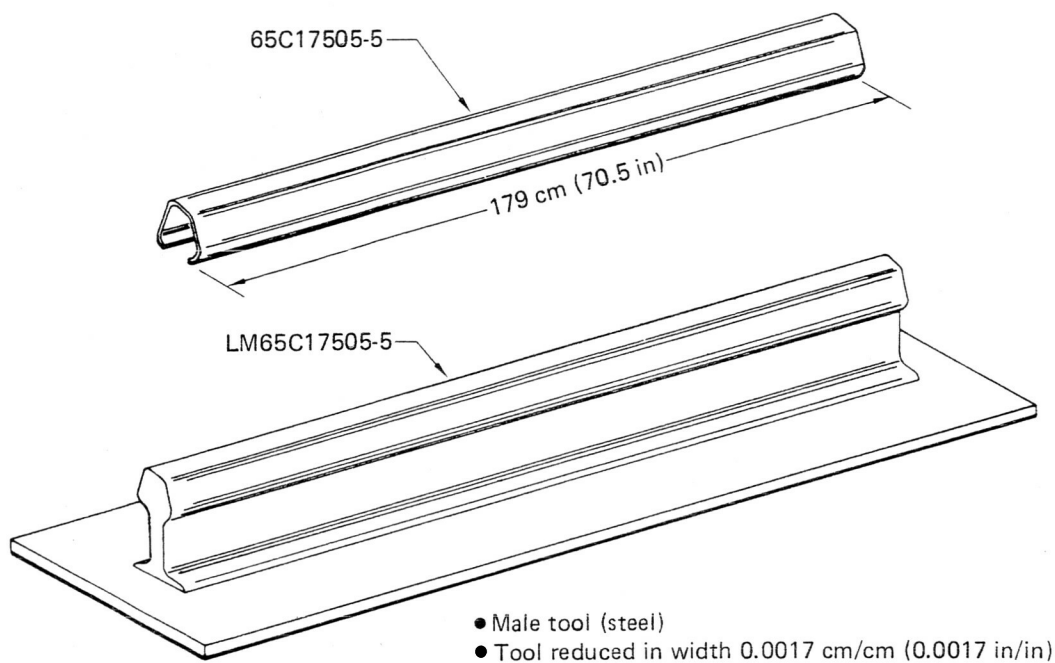


Figure 231. Control Tab Spar

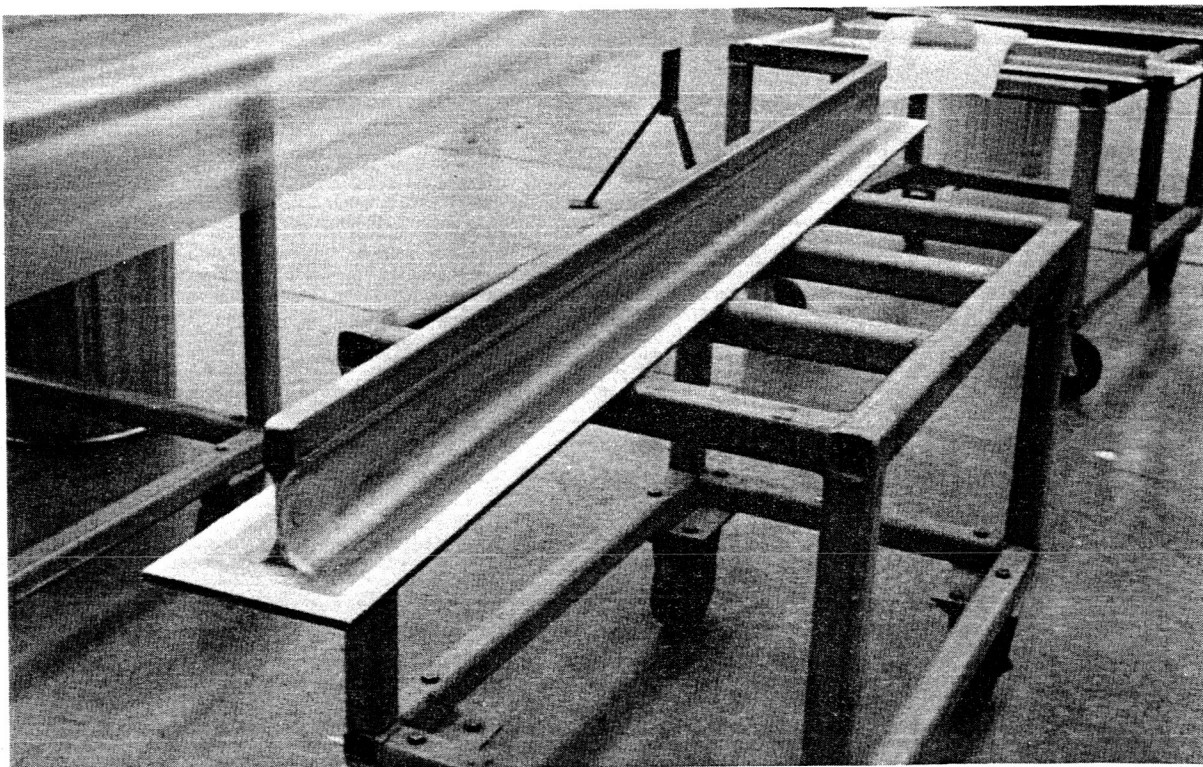


Figure 232. Control Tab Rear-Spar Layup Tool

6.2 ASSEMBLY TOOLING

New tools were designed and fabricated for elevator assembly operations. These tools are similar to existing metal elevator tools, but are fewer in number because the major assembly work is accomplished in one stage versus three stages for the metal elevator. The 727 metal elevator structure is shown in Figure 233. The reduced number of internal structural members and one-piece cover panels for composite units allowed one-stage operation. These features and other engineering design variances disallowed using existing tool designs and constructing dual-purpose tools for elevator production. Tooling consisted of left- and right-hand units for rear spar, front spar/leading edge, and major assembly operations. Figures 234, 235, and 236 display this tooling. Existing master tooling was used as a control medium to ensure interchangeability at the stabilizer/elevator hinge centerline. A new master gage was constructed for control of the tab/elevator hinge line.

Existing control tab and balance panel tools were revised such that either metal- or composite-configured assemblies could be produced.

Conventional tooling methods were used to design and construct all tools, but unique features were included to accommodate the special equipment developed for drilling and trimming composite parts. This equipment included such items as high-speed (18,000 rpm) tapered drills, diamond-coated router bits, and dust collection systems. For the latter, vacuum nozzles adapted to drill motors and router units were used in conjunction with portable vacuum canisters, as shown in Figures 178, 180, 181, and 237.

Index holes sized to the drill motor vacuum nozzle diameter were used in assembly tool drill plates to provide positive dust management during drilling operations, as well as proper hole location and drill alignment (fig. 238). Restricted access prevented use of this system in some areas of the spars and major assemblies. In these areas, a hand-held vacuum hose was used.

As a result of tool tryout conducted during assembly of the left-hand test elevator and shipset No. 1, modifications were made to improve tool use, but for the most part, the conventional tool approach worked quite effectively.

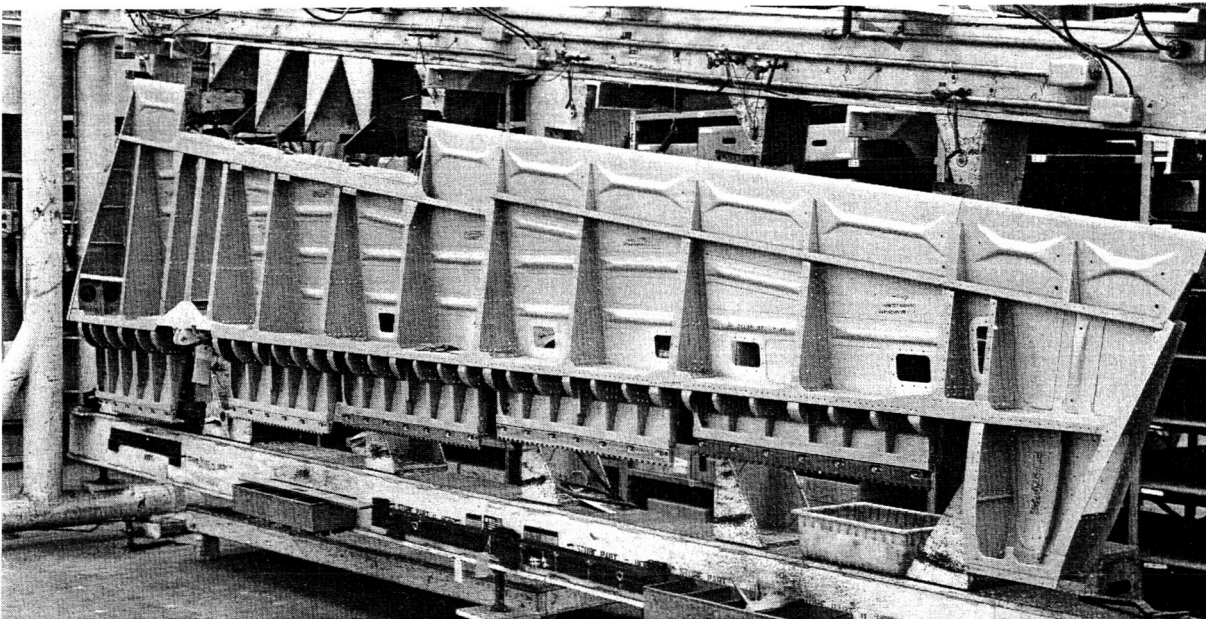


Figure 233. Model 727 Metal Elevator Structure

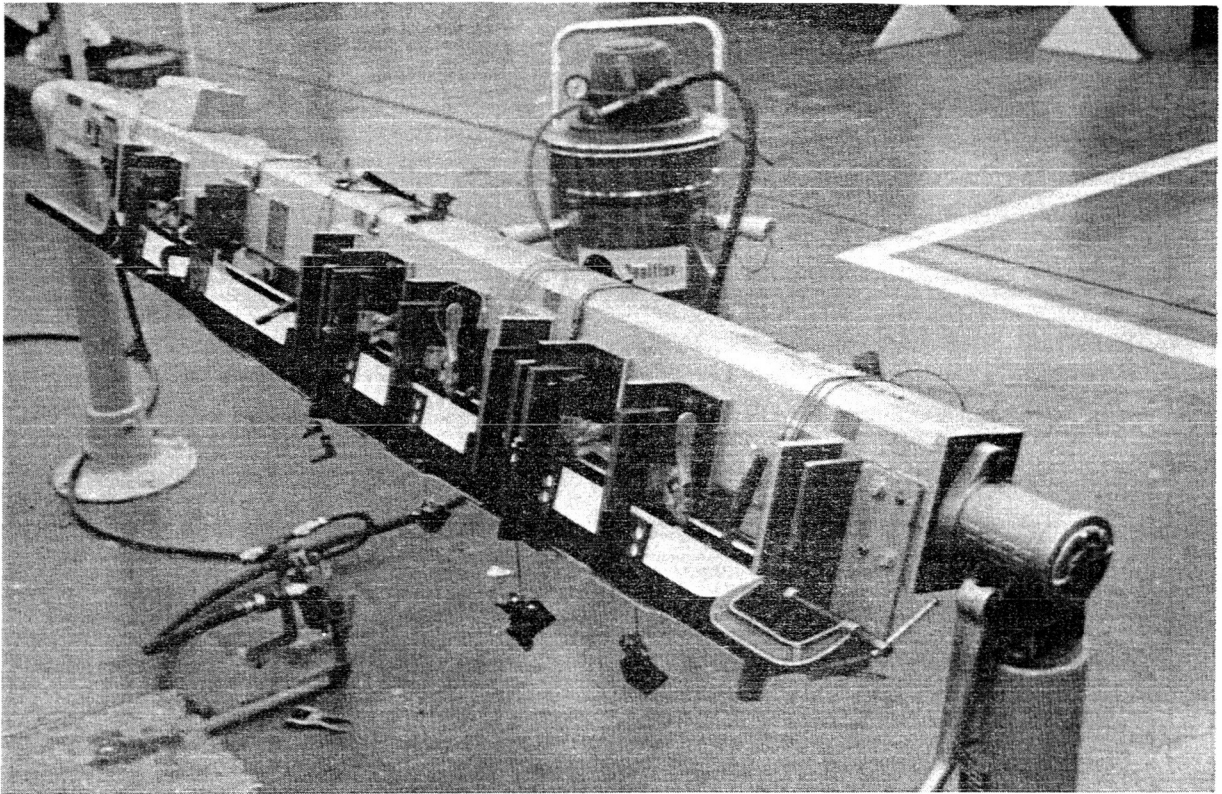


Figure 234. Rear-Spar Assembly Tool

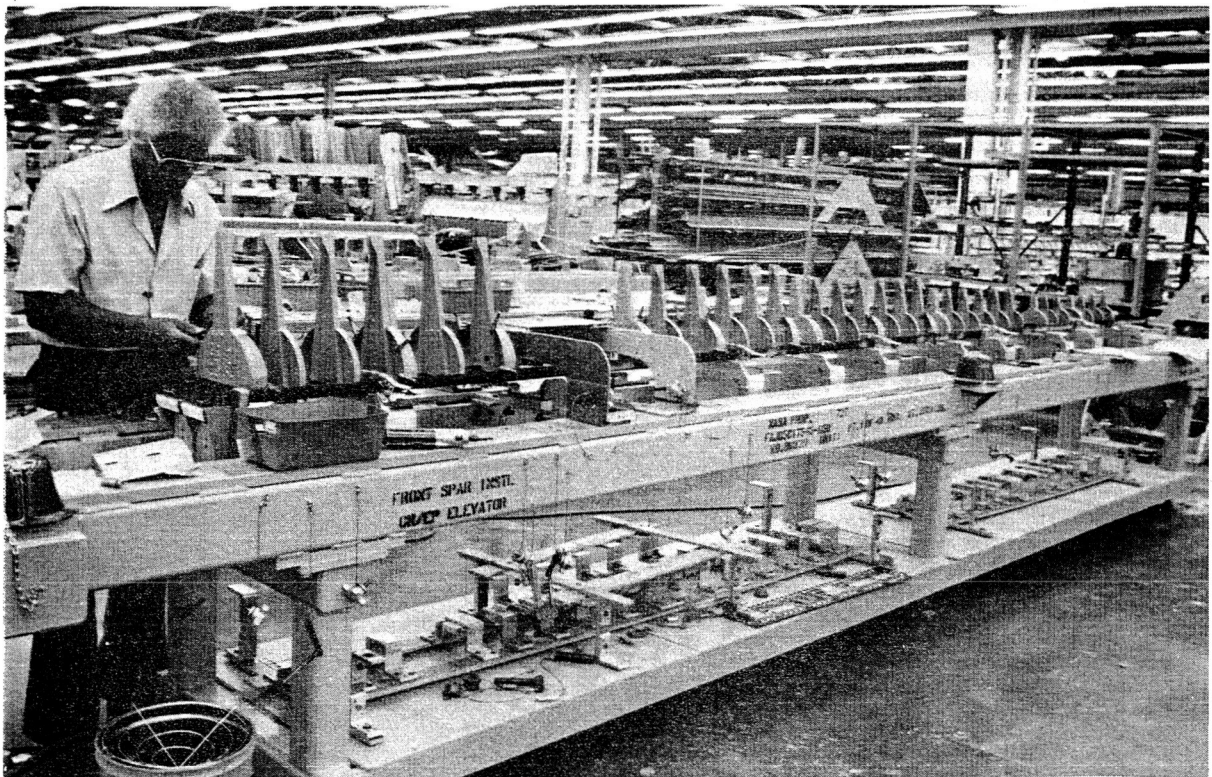


Figure 235. Front-Spar/Leading-Edge Assembly Tool

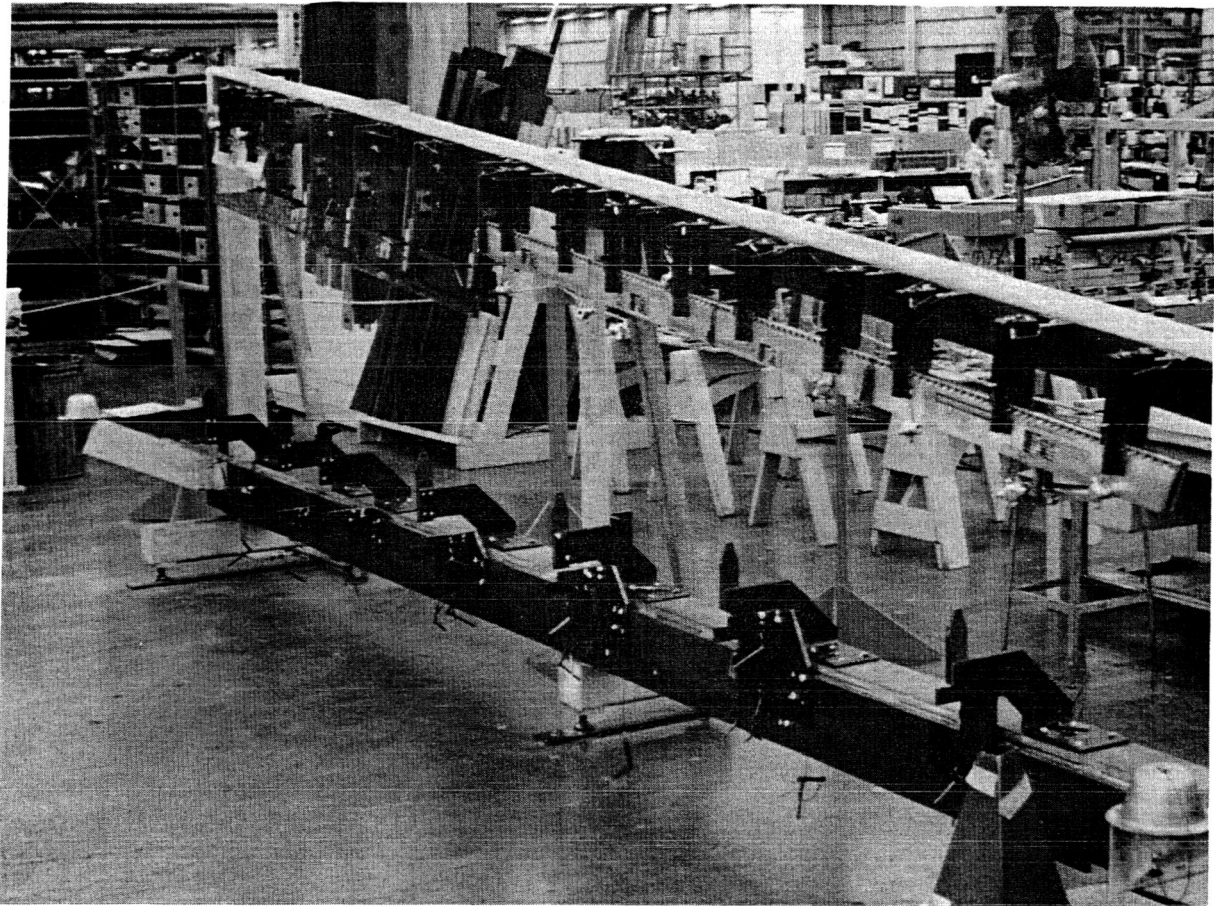


Figure 236. Elevator Major Jig

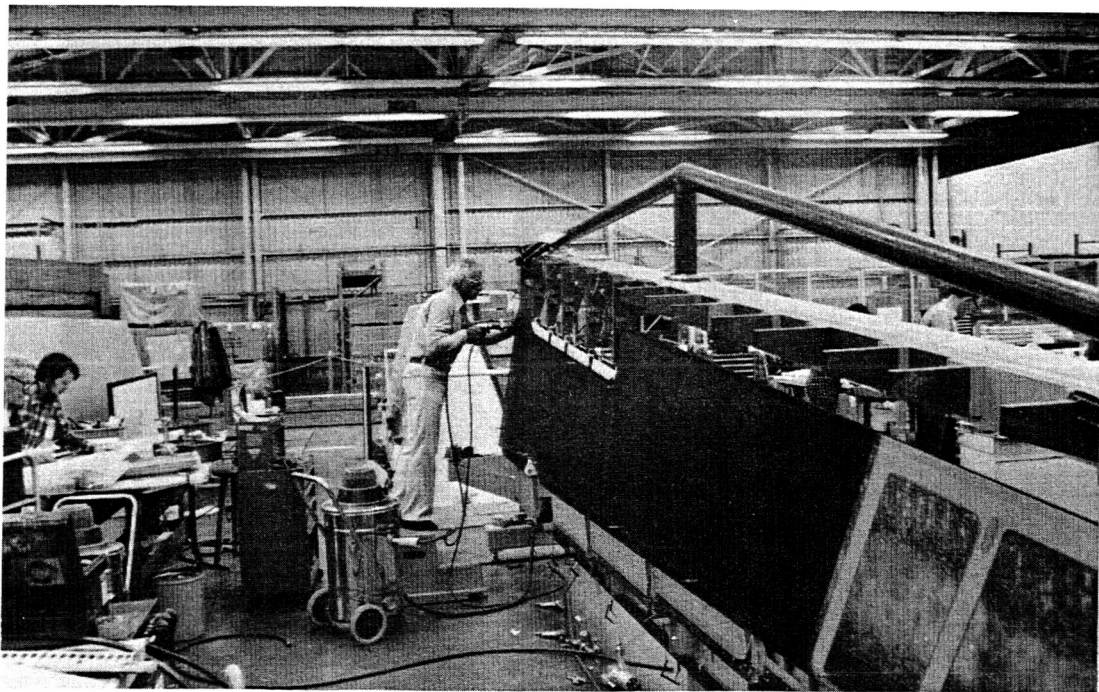


Figure 237. Elevator Assembly Showing Vacuum System Used for Dust Collection

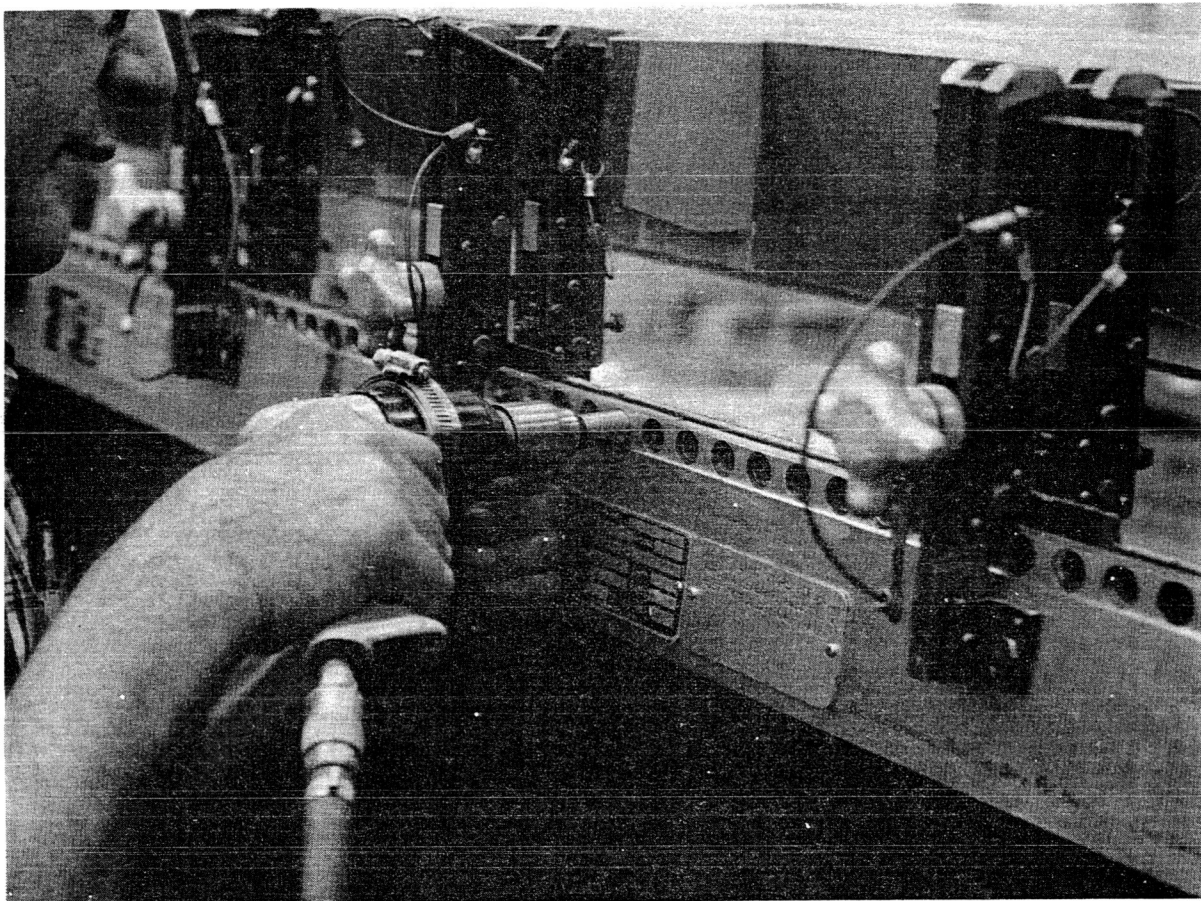


Figure 238. Drilling Operation Using Index Holes Sized to Vacuum Nozzle

6.3 COMPONENT MANUFACTURE

A no-bleed resin system with a 176.5°C (350°F) cure cycle was used to fabricate all composite components. Figure 239 illustrates the typical operational flow for these components. Both laminates and honeycomb structures followed the kitting, layup, cure, inspection, and trim cycles shown.

Layup of the graphite fabric and tape materials was accomplished manually with templates used to assist in proper location, orientation, and final sizing of the plies. Templates also were used to locate honeycomb cores.

The transition from developmental and verification hardware fabrication to the production phase of the program was accomplished as planned without major deviation from the operational guidelines and specifications developed through these prior programs. However, some problems were experienced during fabrication of full-size components that were not evident in the smaller test components. Also, some development was required to correct problems with parts that were not included in the test program.

Warpage, a condition that seems to be inherent to structures made from graphite materials, was a problem with full-size spars and skin panels, as well as the control tab.

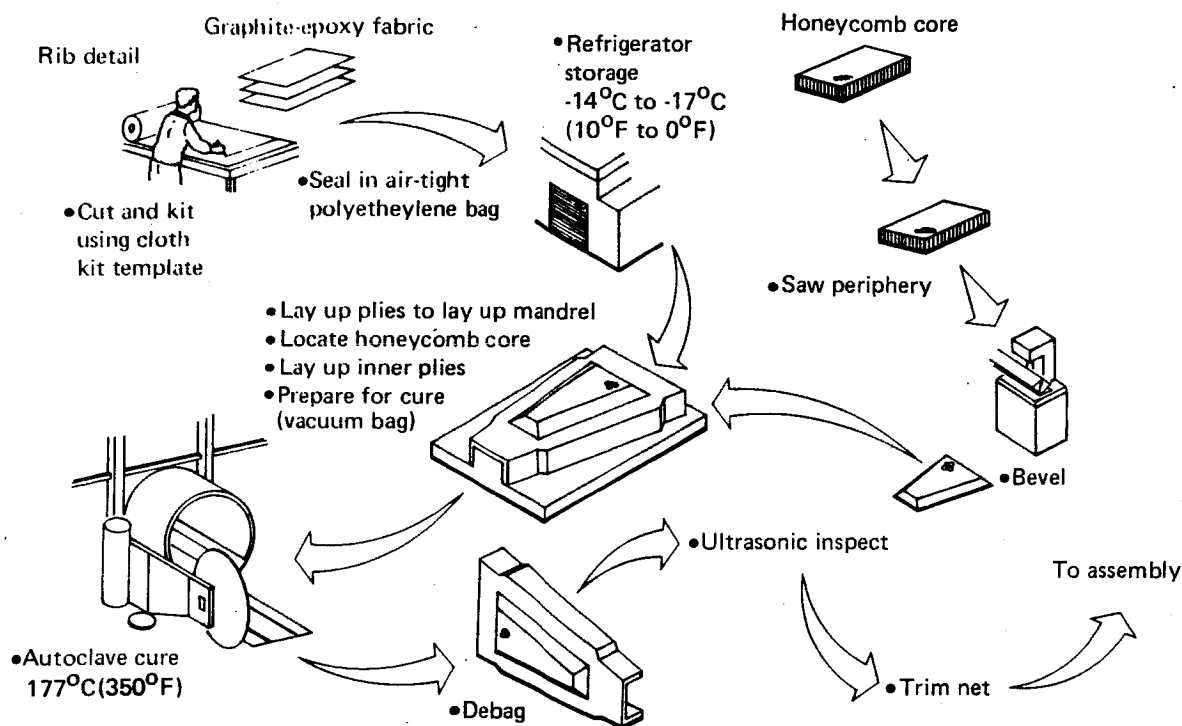


Figure 239. Typical Advanced Composite Fabrication Process

The outboard portion of the front spar exhibited a cross-section warp on all five and a half shipsets of parts. Because assembly tool clamping and installation of spar stiffeners and nose rib attach angles straightened the spars, changes to the layup were not introduced during the contracted program (refer to sec. 6.4). Investigations continued in an effort to isolate specific causes of the warp. As a result, Manufacturing recommendations for changing ply sequence and orientation and using worked fabric were submitted for Engineering design consideration.

The rear spar exhibited a spanwise warp relative to the spar centerline. Revisions were introduced that changed the layup to all fabric with revised ply orientation, and warpage was reduced to acceptable levels. Again, as with the front spar, assembly tooling provided final straightening. One other concern with these parts was the variance in final flange angularity that affected the opening at the trailing edge (refer to sec. 6.4). A tool development program was considered, but because assembly operations were not adversely affected, this was not pursued.

Full-size production skin panels have a span of 526 cm (207 in), which caused concern about proper core locations and maintenance of edgeband tolerance during the cure cycle. Since graphite-epoxy cured on the large aluminum tools grows to the point of ~~resin-gel as a function of aluminum expansion~~, it was determined that a growth factor must be incorporated into the layup of core details. This growth factor is shown in Figure 240. To compute the growth factor for the panels, a 61-cm (24-in) wide simulated panel was laid up on the production tool. Four 127-cm (50-in) long core sections were located across the span of the panel, and their location was measured from a reference point on one end. Following the cure cycle, measurements were

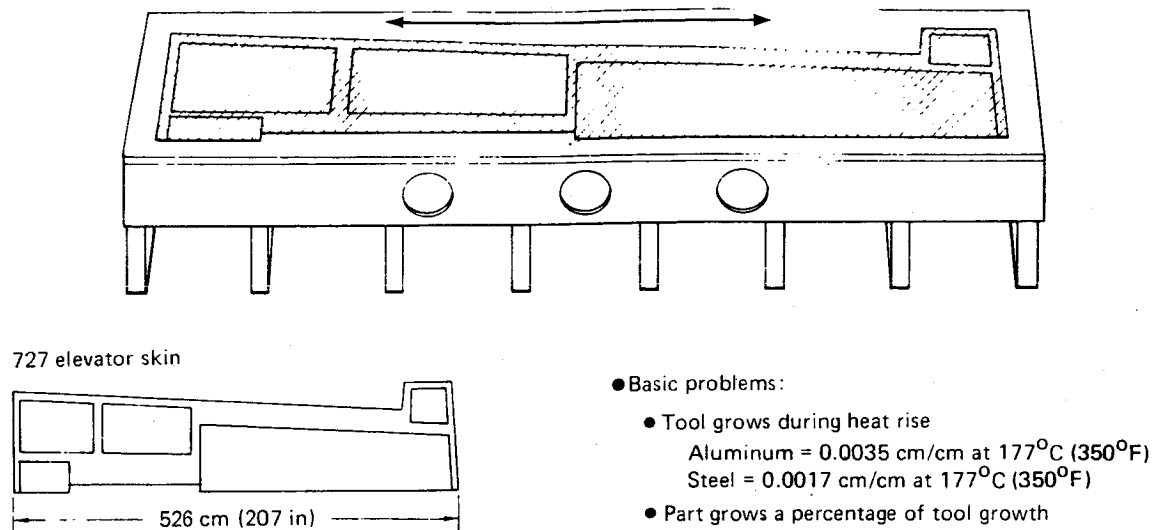


Figure 240. Growth Factors

rechecked. Results showed an overall length increase of 1.02 cm (0.4 in) or 0.0019 cm/cm (0.0019 in/in) for the core and graphite-epoxy (fig. 241). From these data, core-location templates were reworked to incorporate the growth factor, as displayed in Figure 242. As a result, production units exhibited proper core location after cure. Figures 243 through 252 show the sequence of skin panel fabrication.

The skin panels also warped away from the tool surface after cure (refer to sec. 6.4). Inspection of the condition, against specification warp allowances, showed the panels to be acceptable. However, further checks were conducted during the assembly stages to determine if the panels would assume proper fair and mating to substructure. This proved to be the case. Therefore, a program of design and tool analysis to eliminate the warp was not required.

Trailing-edge warpage of the control tab bonded assembly was a difficult problem. The first assembly made for a left-hand test unit was at the limit of warp acceptability, but subsequent units exceeded this limit.

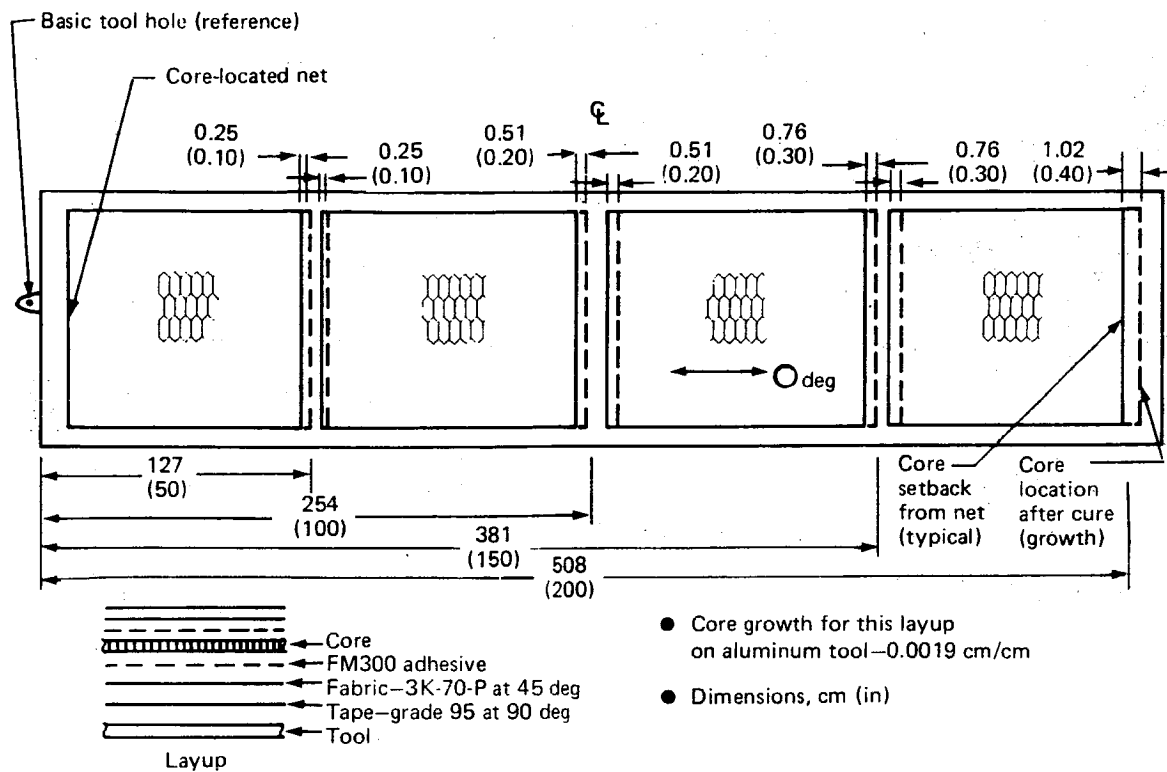


Figure 241. Core Growth Test Panel

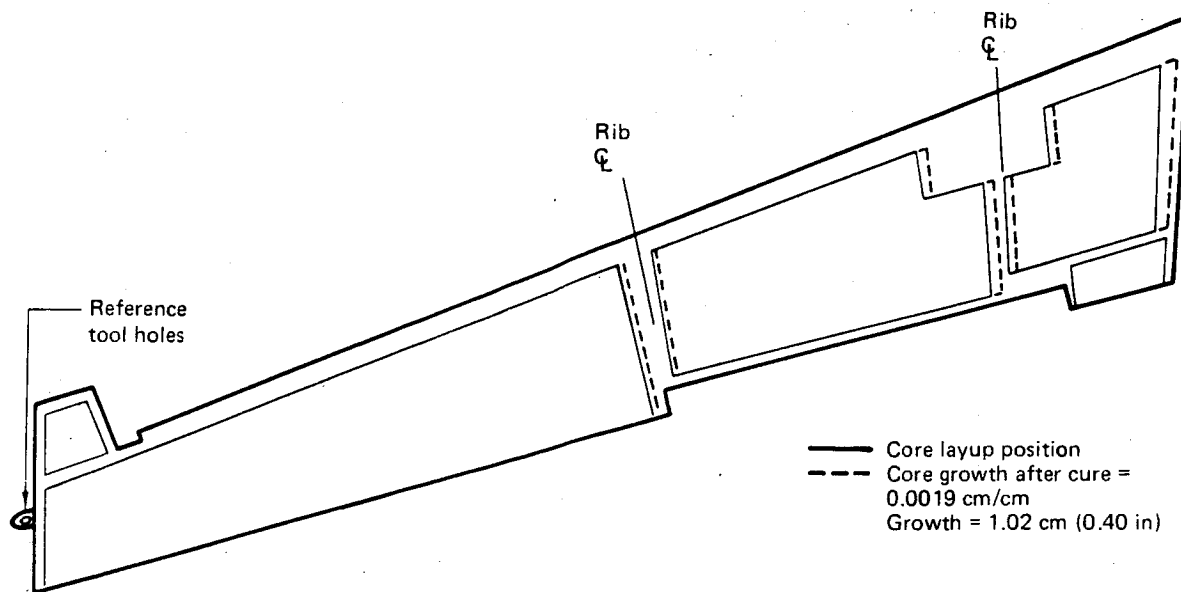


Figure 242. Core Setback on Elevator Skin Panels Prior to Cure

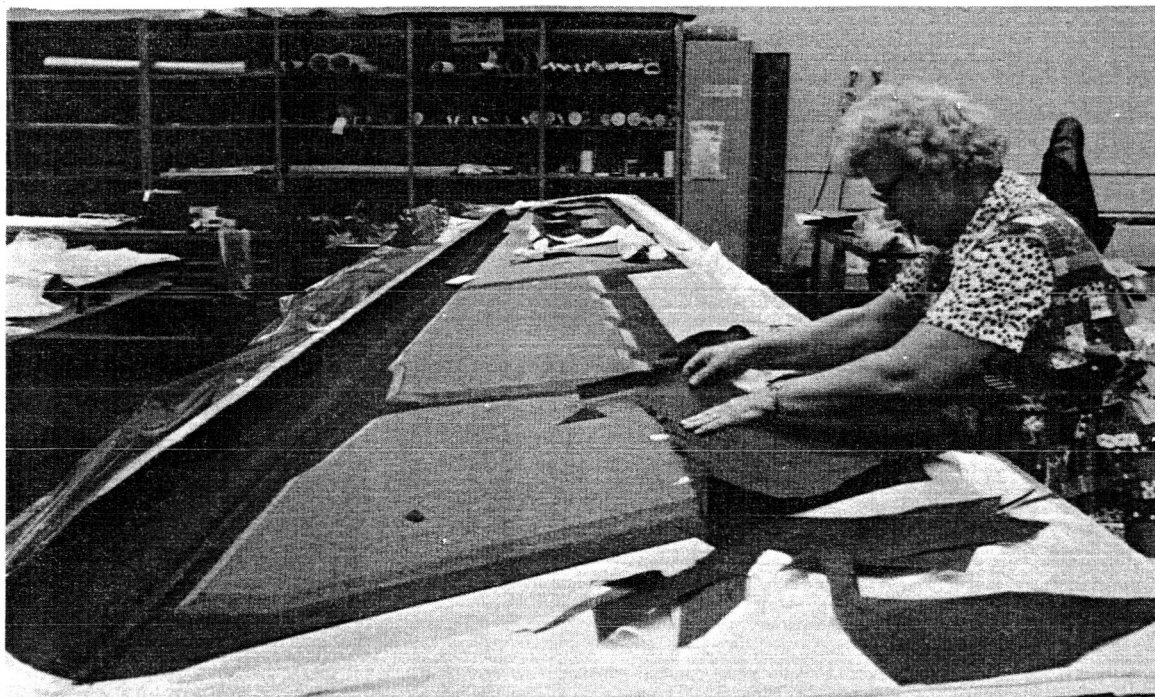


Figure 243. Layup of Skin Panel

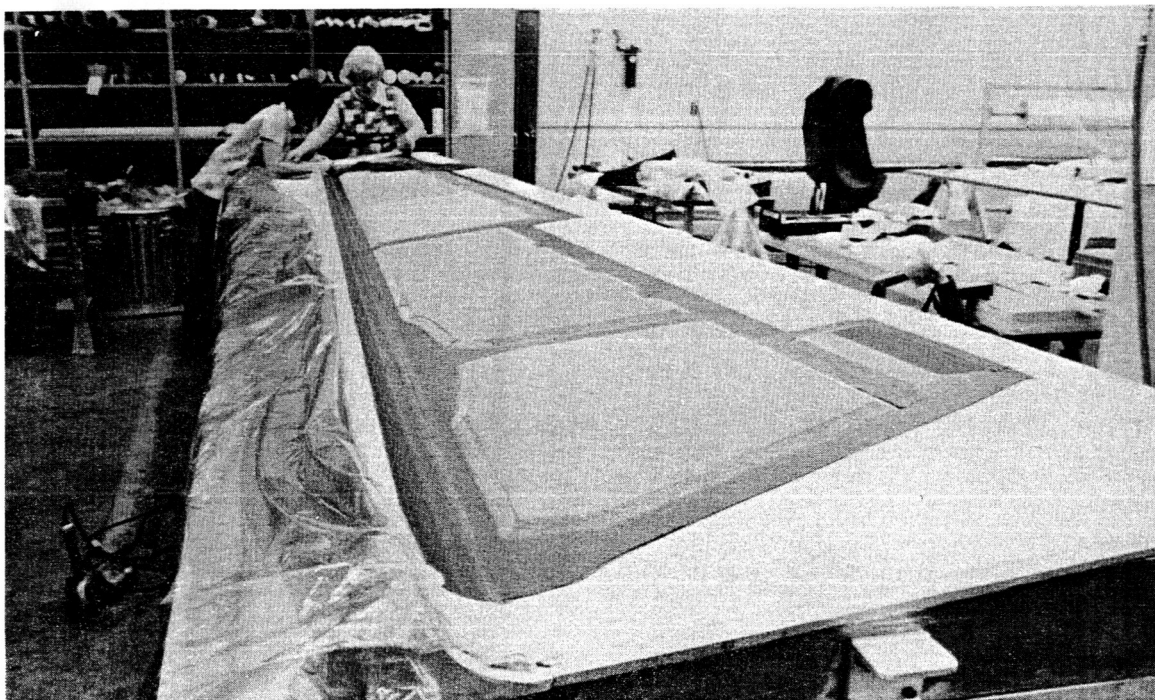


Figure 244. Skin Panel with Outer Layup and Honeycomb Core in Place

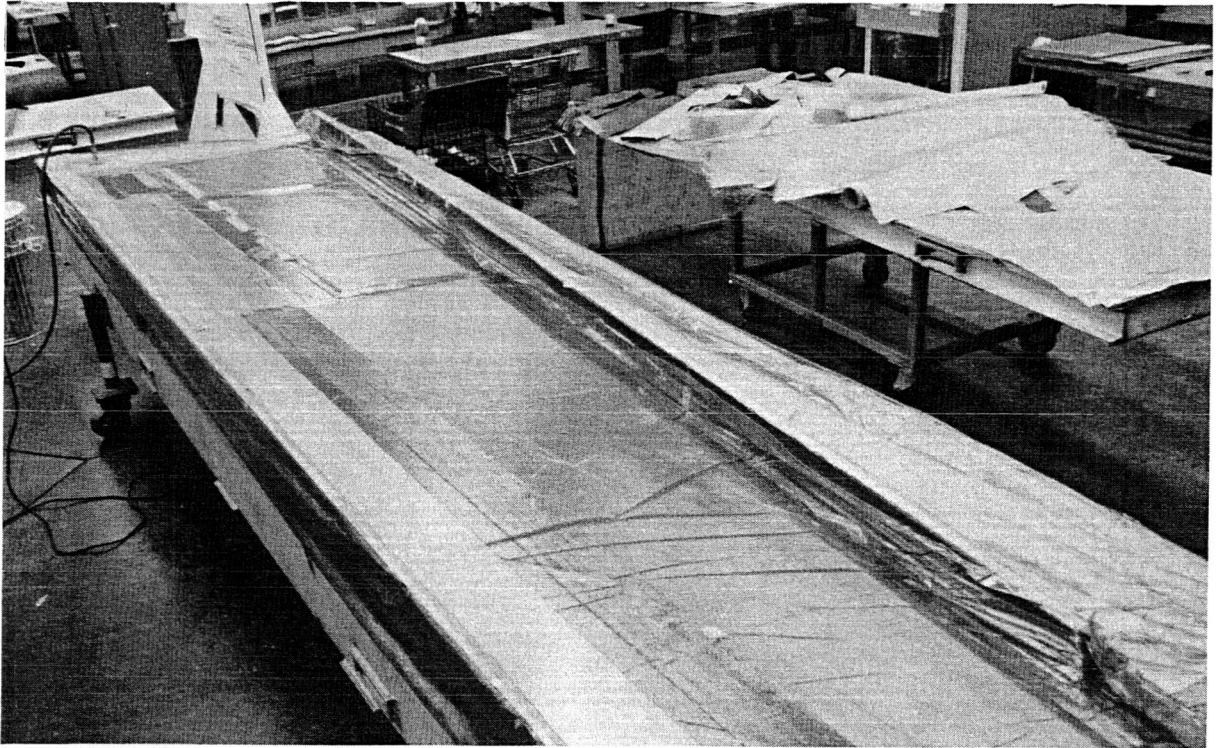


Figure 245. Skin Panel Compaction with Vacuum

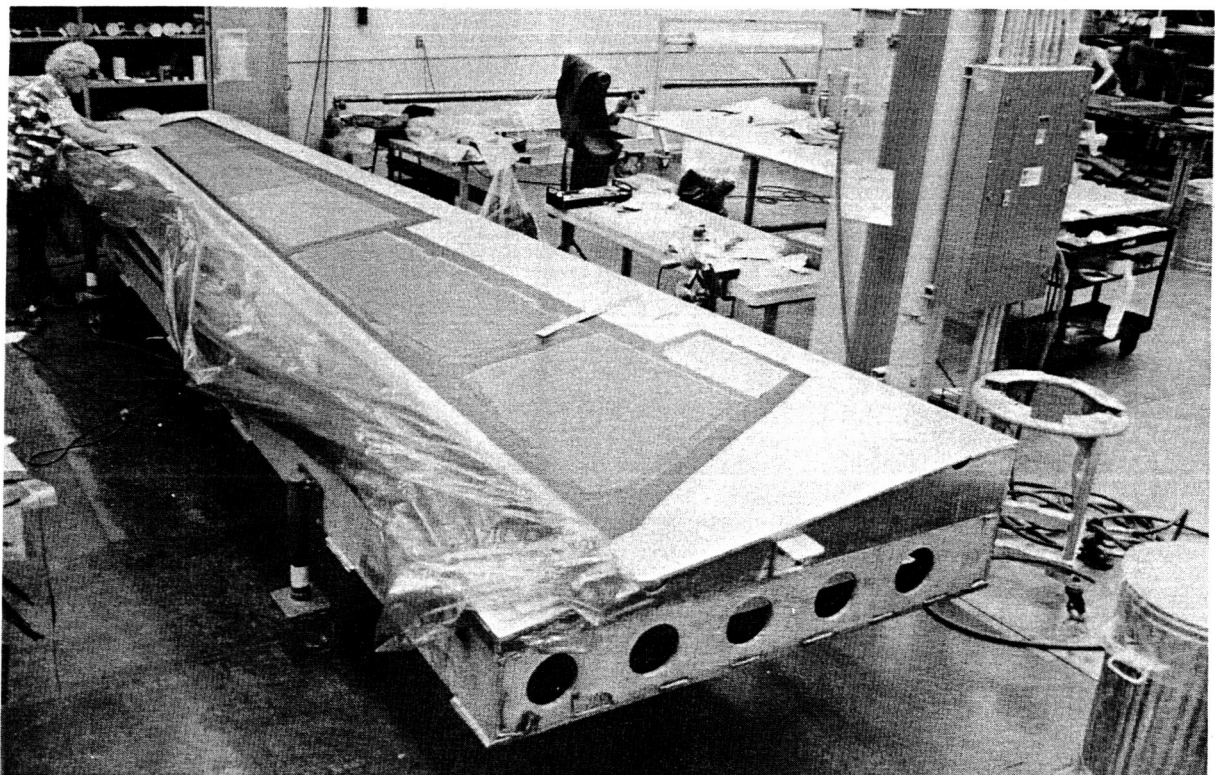


Figure 246. Application of FM 300 Adhesive to Core of Skin Panel

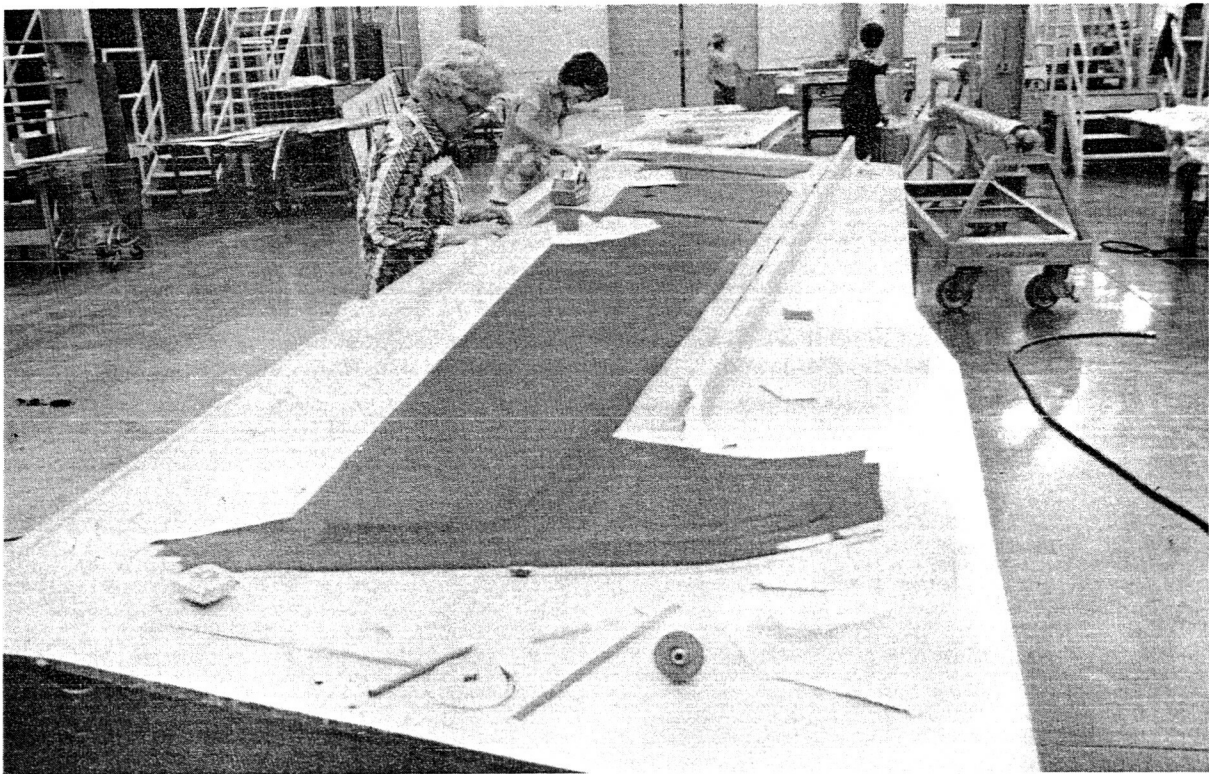


Figure 247. Application of Fiberglass Layer to Trailing Edge of Skin Panel



Figure 248. Upper Skin Panel Ready for Autoclave Cure



Figure 249. Upper Skin Panel After Autoclave Cure

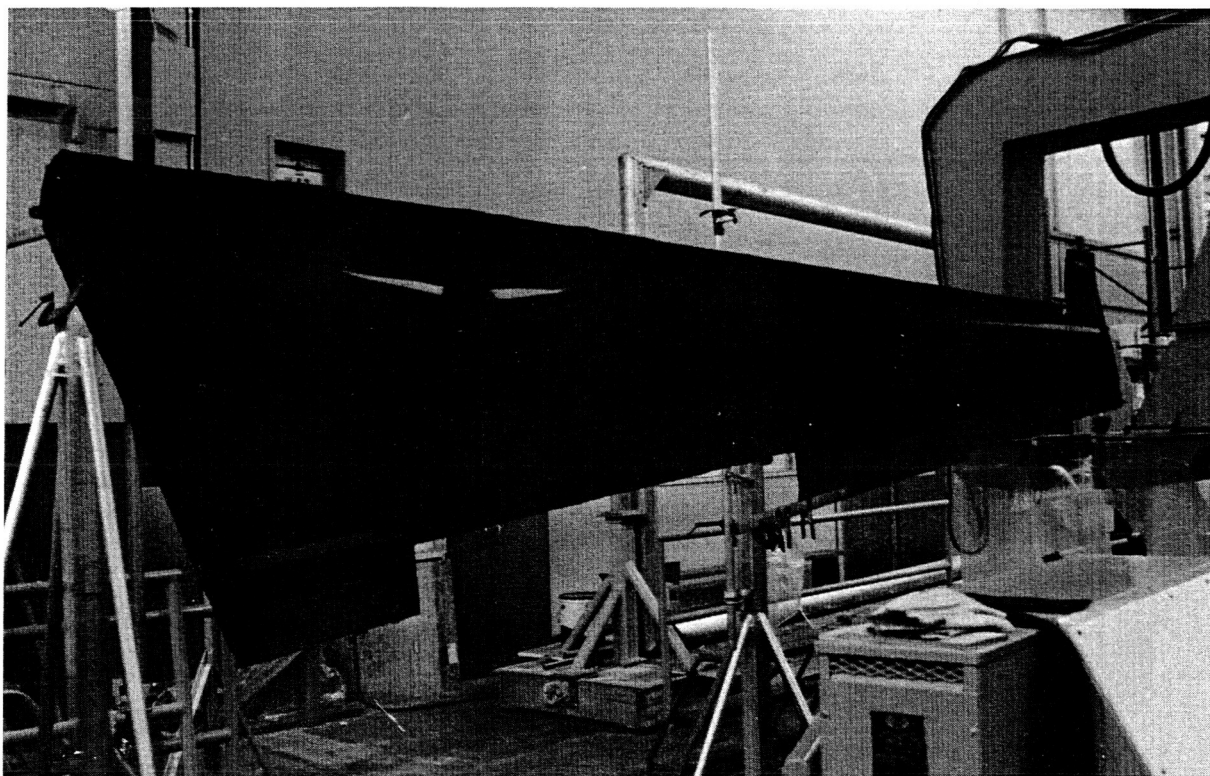


Figure 250. Upper Skin Panel in TTU Inspection

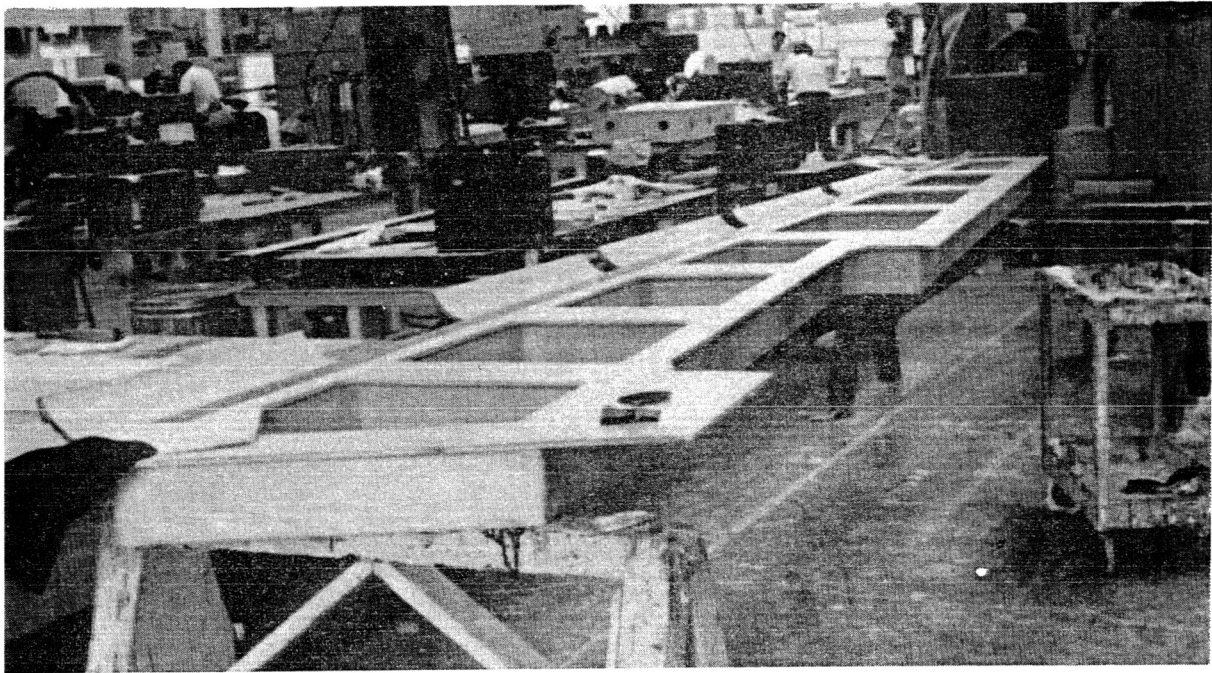


Figure 251. Trim Tool for Upper Skin Panel

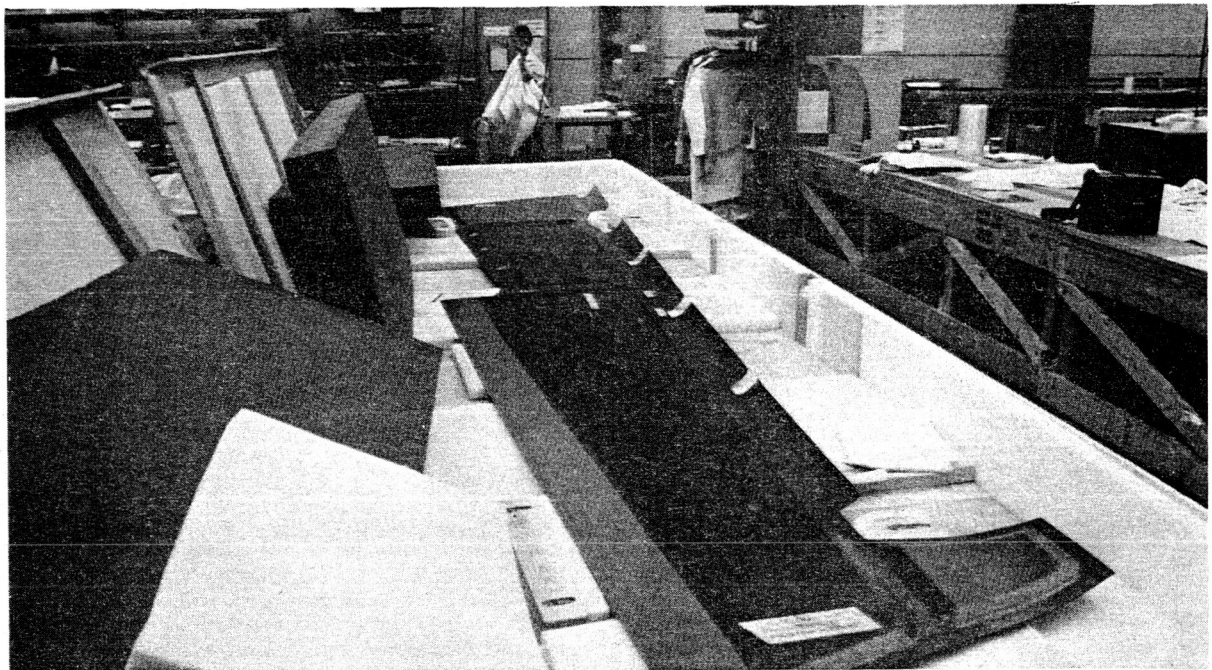


Figure 252. Upper Skin Panel Ready for Transport to Assembly Shop

The tab is fabricated in three stages of bonding. In the first stage, a block of core is bonded to the precured graphite-epoxy spar. The tool-side skin and trailing-edge fillers then are laid up and bonded to the core and spar. The final stage, after the core and fillers are milled to proper taper, consists of laying up and bonding the opposite, or bag-side, skin. This stage is shown in Figure 253.

A detailed analysis of each of the bonding operations and the engineering design indicated two areas of potential reasons for the warpage. One was an unbalanced layup between the tool-side skin and the cocured trailing-edge filler plies. A change in filler layup from nine plies $+45$ -deg fabric to nine plies alternating $0/45$ -deg fabric was instituted to correct this condition. The other suspect area was cocuring of the bag-side skin. Changing this skin to a precured component for final-stage bonding, coupled with the filler layup change, reduced tab warpage to within acceptable limits (see fig. 254).

Female layup mandrels presented problems with bridging of materials in the outside radius of flanges, which created resin ridges and voids. Typical of parts exhibiting this condition were the inboard closure rib (fig. 255), the station 117.37 rib spar attach flange (fig. 256), the joggled area along the skin panel leading edge, and radius areas on the actuator fairing. Changes to radius size, where allowable, and staged compaction corrected some of the problem, but not completely. Because analysis of representative areas indicated that structural properties of the parts were not affected, sanding of ridges and filling of voids with adhesive were authorized and applied to finish the parts.

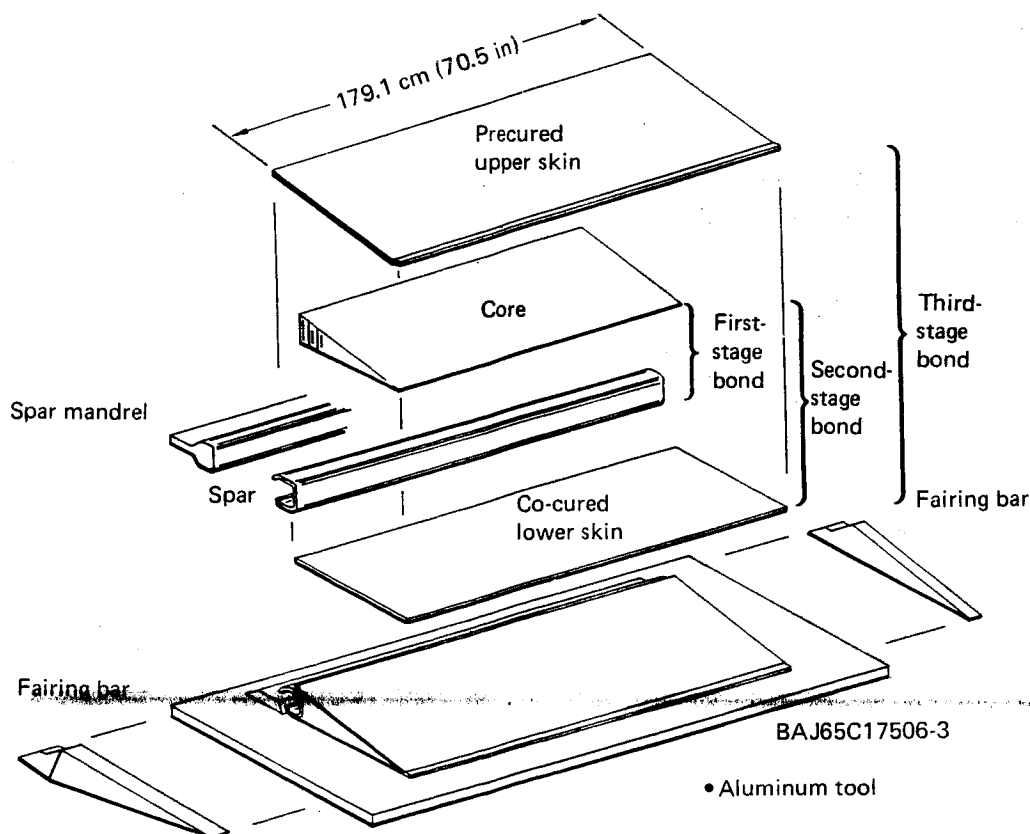


Figure 253. Control Tab Bonding Sequence

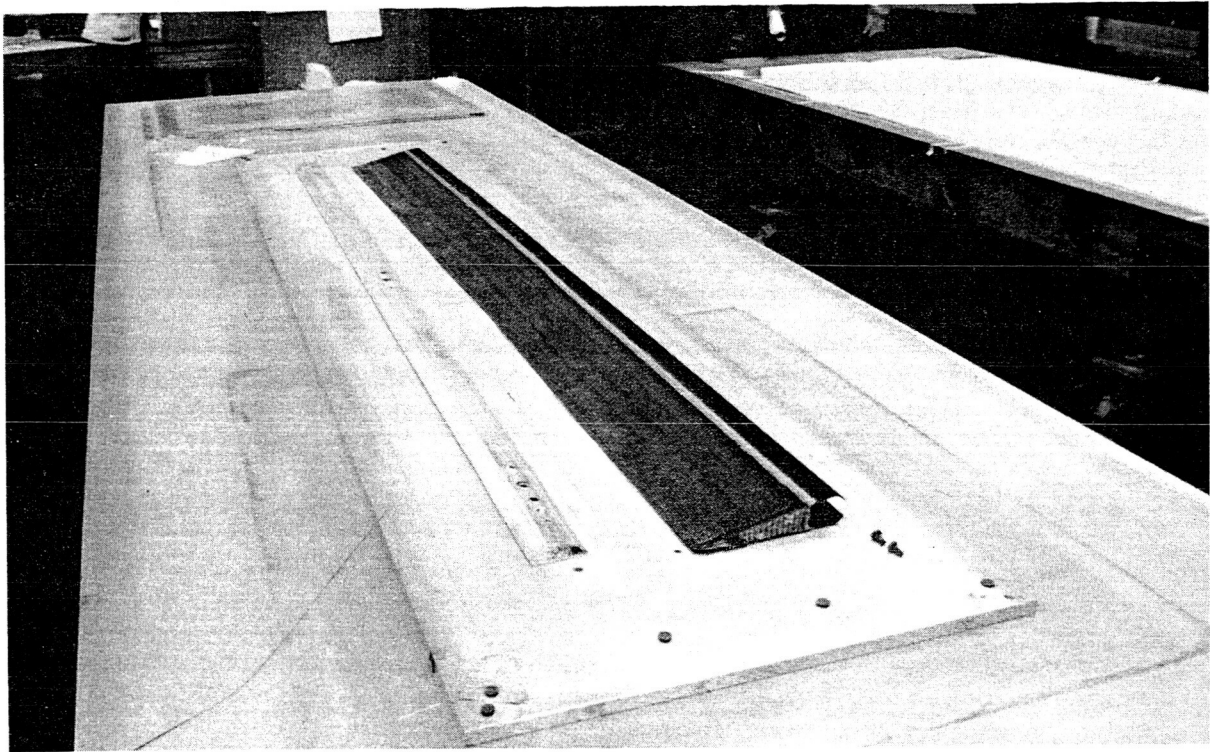


Figure 254. Control Tab Second Stage Bond Showing Spar, Core, Toolside Skin, and Trailing-Edge Fillers

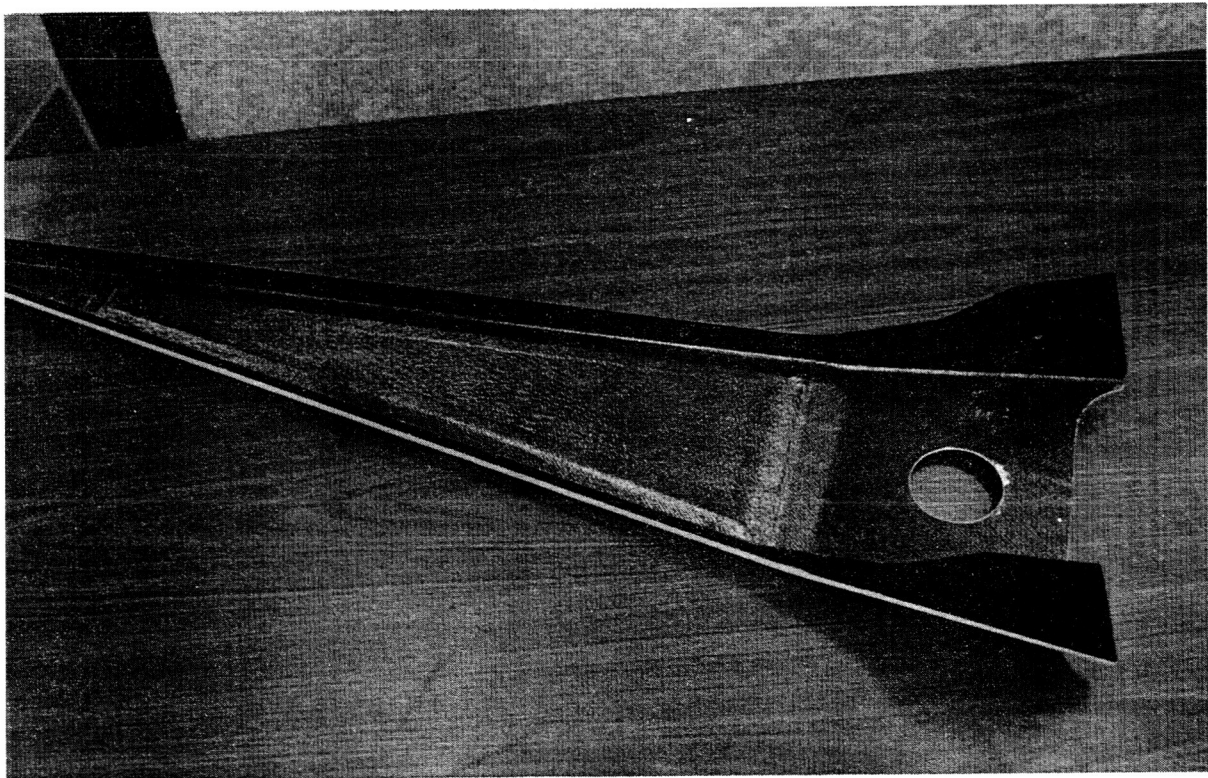


Figure 255. Inboard Closure Rib

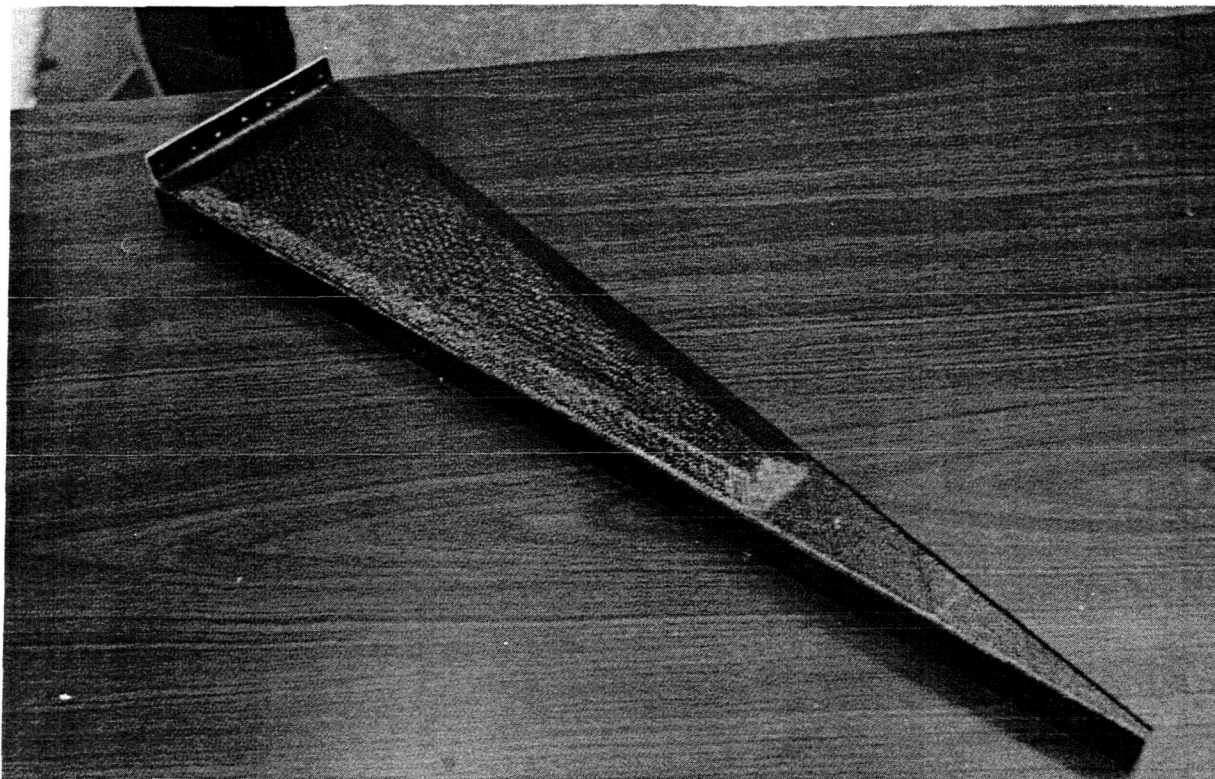


Figure 256. Station 117.37 Rib

In retrospect, the five-and-a-half-shipset production program did verify the program approaches established early in the proposal phases, but at the same time demonstrated that fabricating parts from composite materials was more complex than originally anticipated. However, the experience gained from the program was essential to the refinement of production systems procedures and data that will be the basis for future production commitment decisions.

6.4 ASSEMBLY OPERATIONS

Assembly of the composite elevators was accomplished per manufacturing plans developed during the proposal stages of the program. No significant deviations from those plans were required to attain the objective of producing hardware in accordance with engineering designs and maintaining interchangeability at the hinge centerlines. The sequence of assembly is depicted in Figure 257, and Figures 258 through 266 display the assembly stages. Significant elements of the work performed are discussed in this section, along with associated problems.

6.4.1 PART FITUP

Fitup of components was not the problem originally anticipated, although there were areas, such as the skin-panel-to-nose interface, where shimming was required. Warpage of the spars and skin panels during cure cycles was a problem during detail fabrication that caused concern relative to fitup on assembly. However, assembly operations were not appreciably affected.

The front-spar parts exhibited a cross-section warp (fig. 267) that normally could be removed by the clamping action of the assembly tool and installation of nose rib attach angles (fig. 268). There were only two instances where shimming was required to allow proper fastener installation.

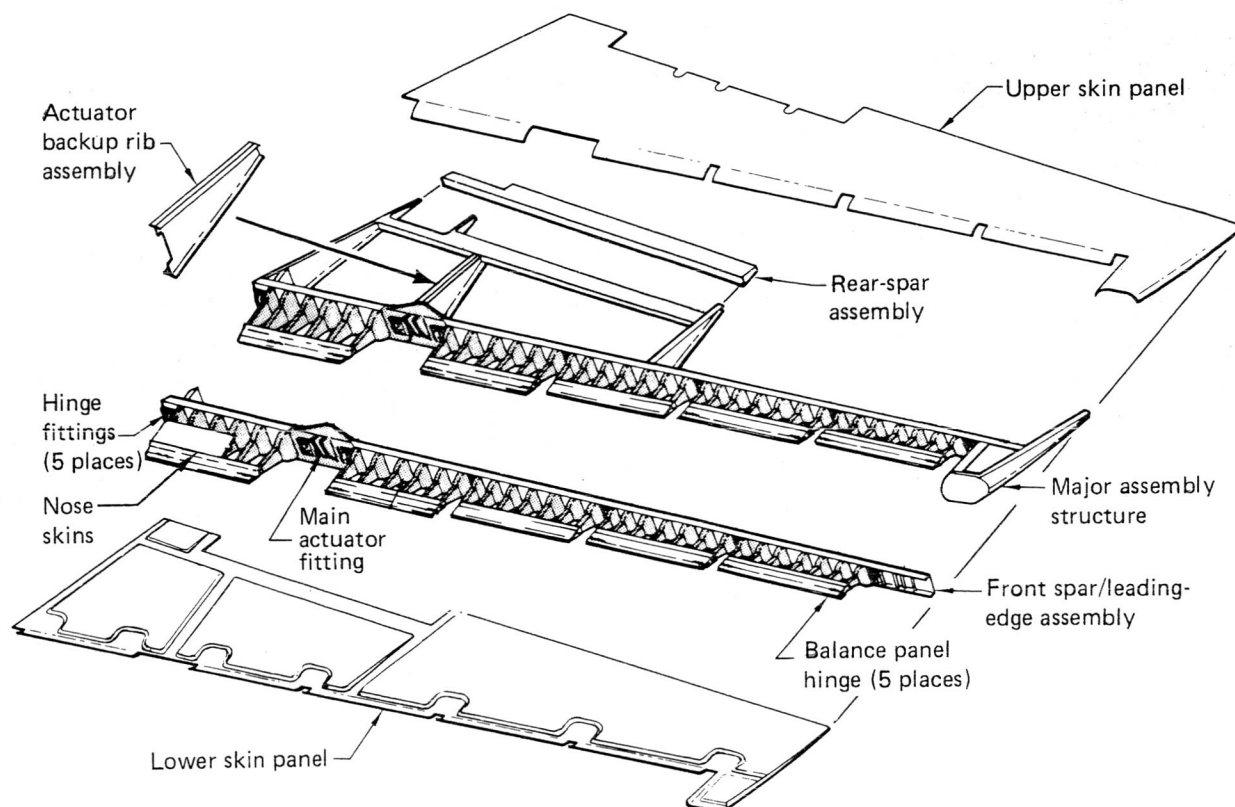


Figure 257. Elevator Assembly Breakdown

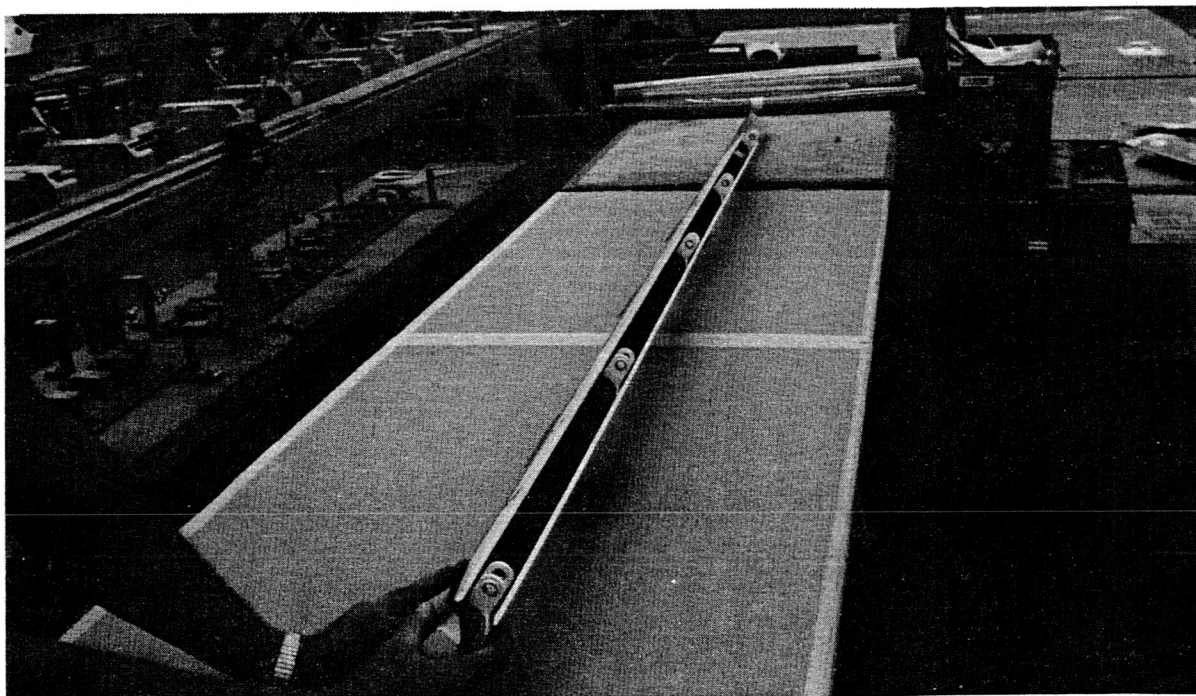


Figure 258. Rear-Spar Assembly

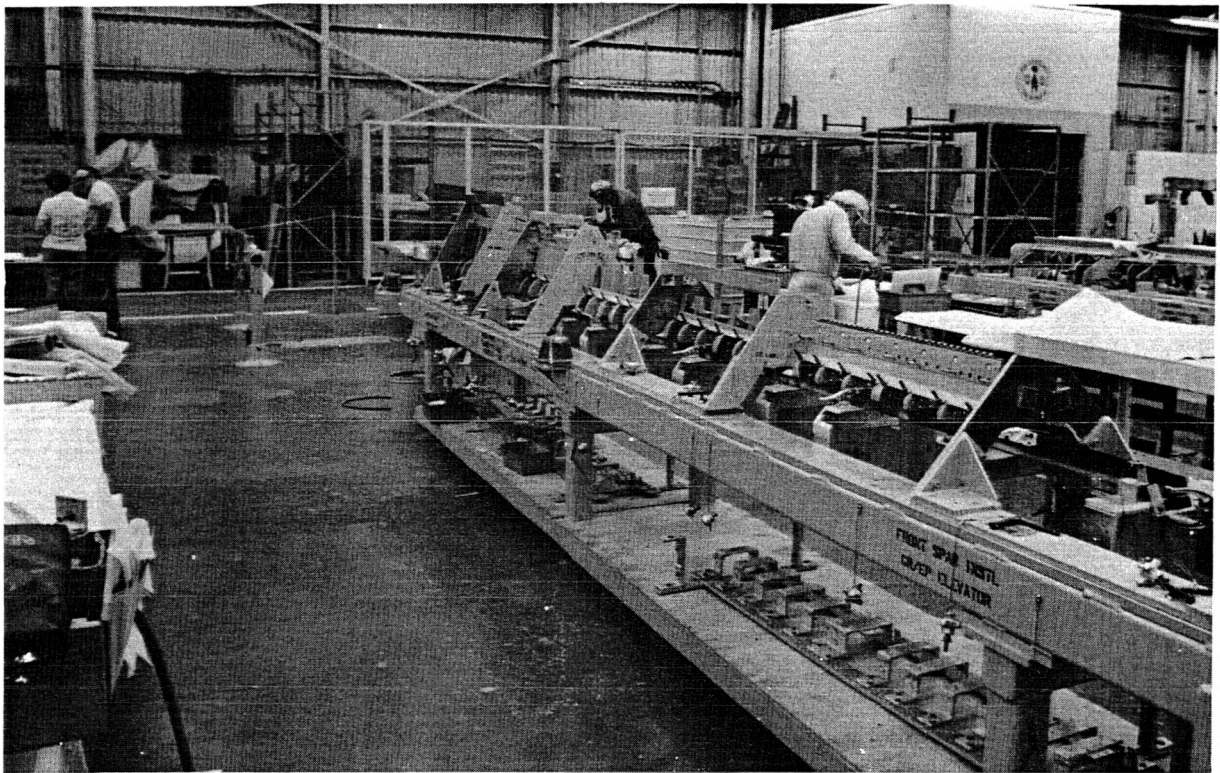


Figure 259. Front Spar/Leading-Edge Assembly Buildup

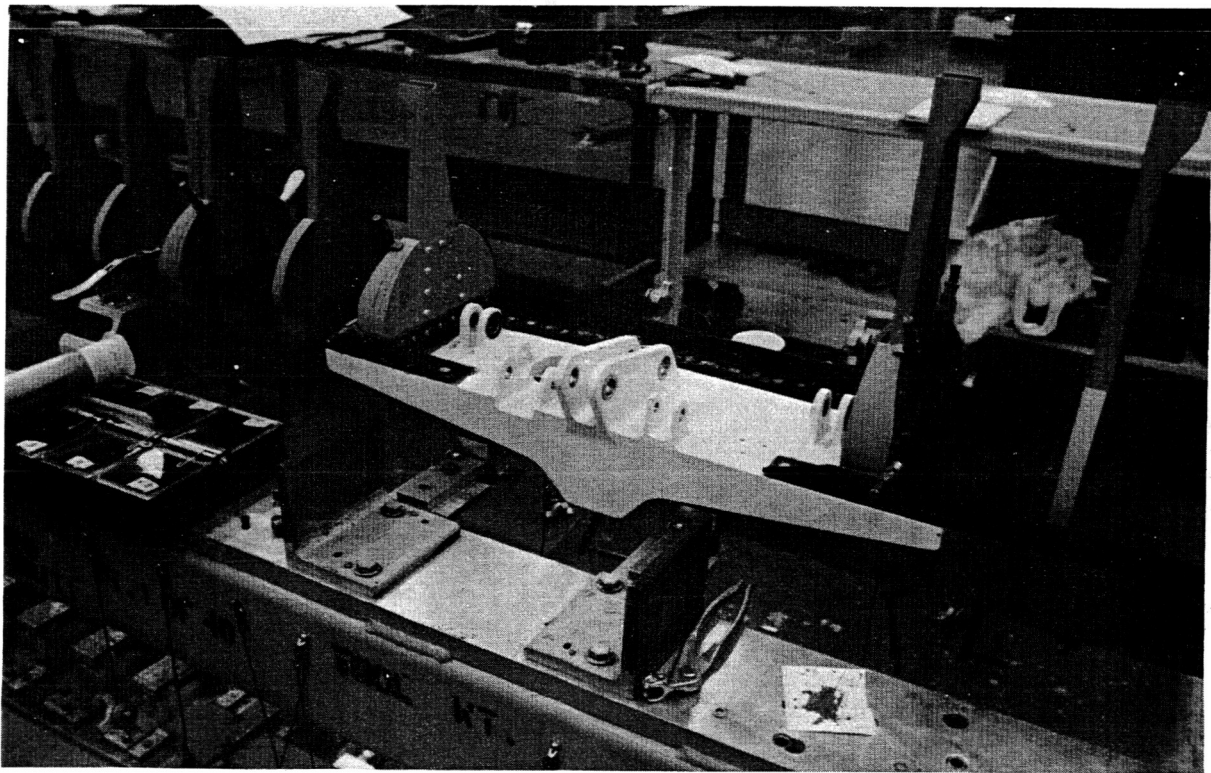


Figure 260. Closeup View of Actuator Fitting in Front Spar

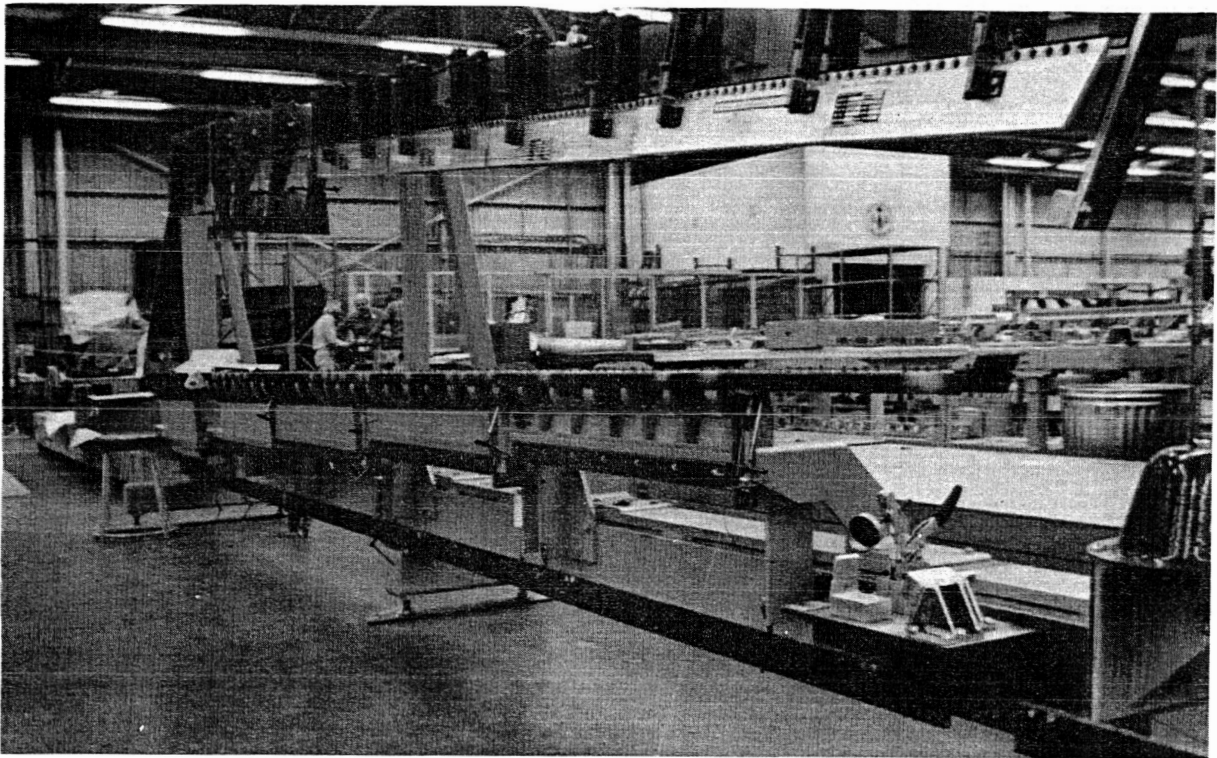


Figure 261. Front-Spar/Leading-Edge Assembly Located in Major Jig

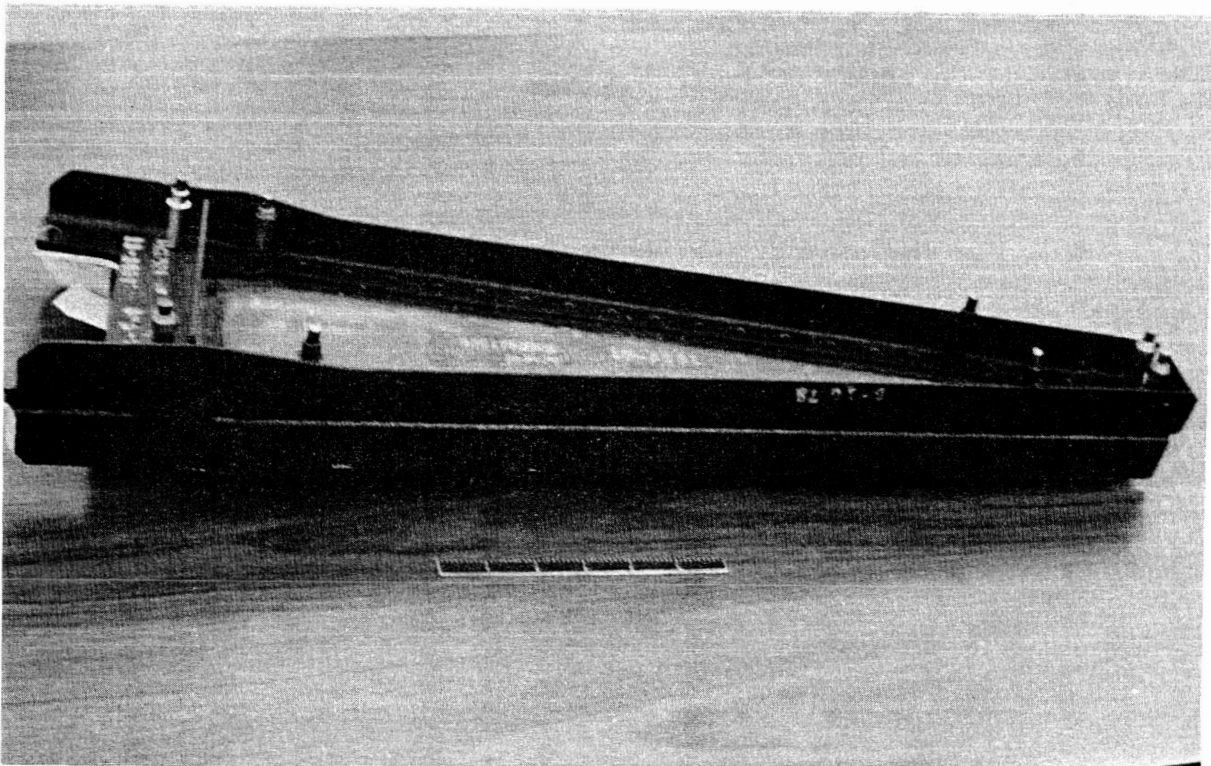


Figure 262. Actuator Backup Rib Assembly

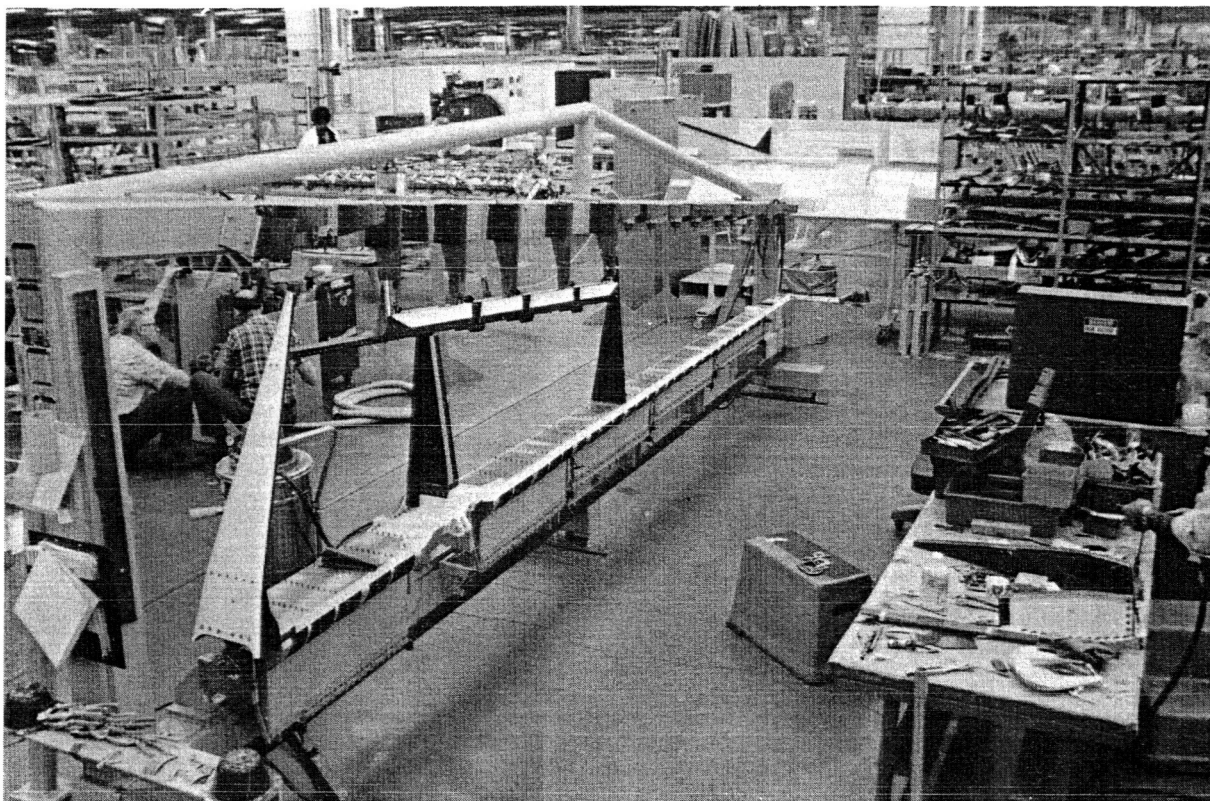


Figure 263. Elevator Major Assembly Tool

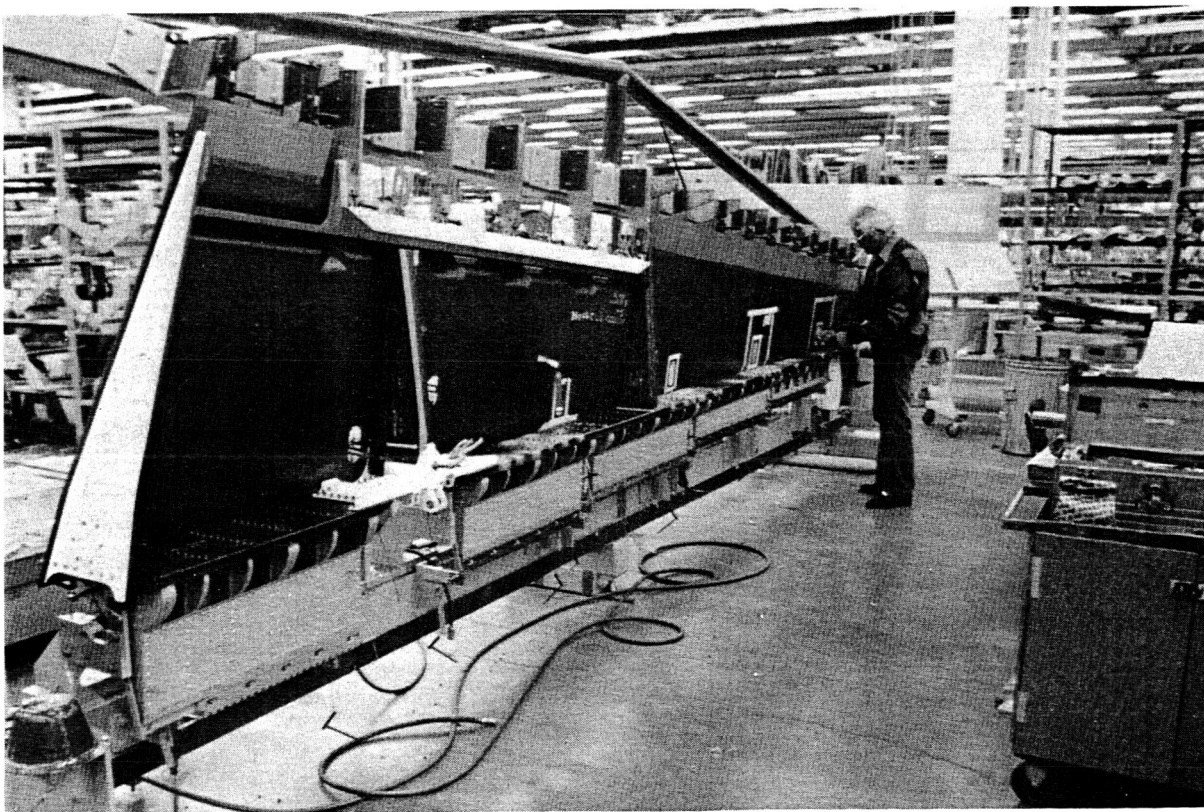


Figure 264. Lower Skin Panel in Place with Internal Structure of Elevator—Major Jig Position

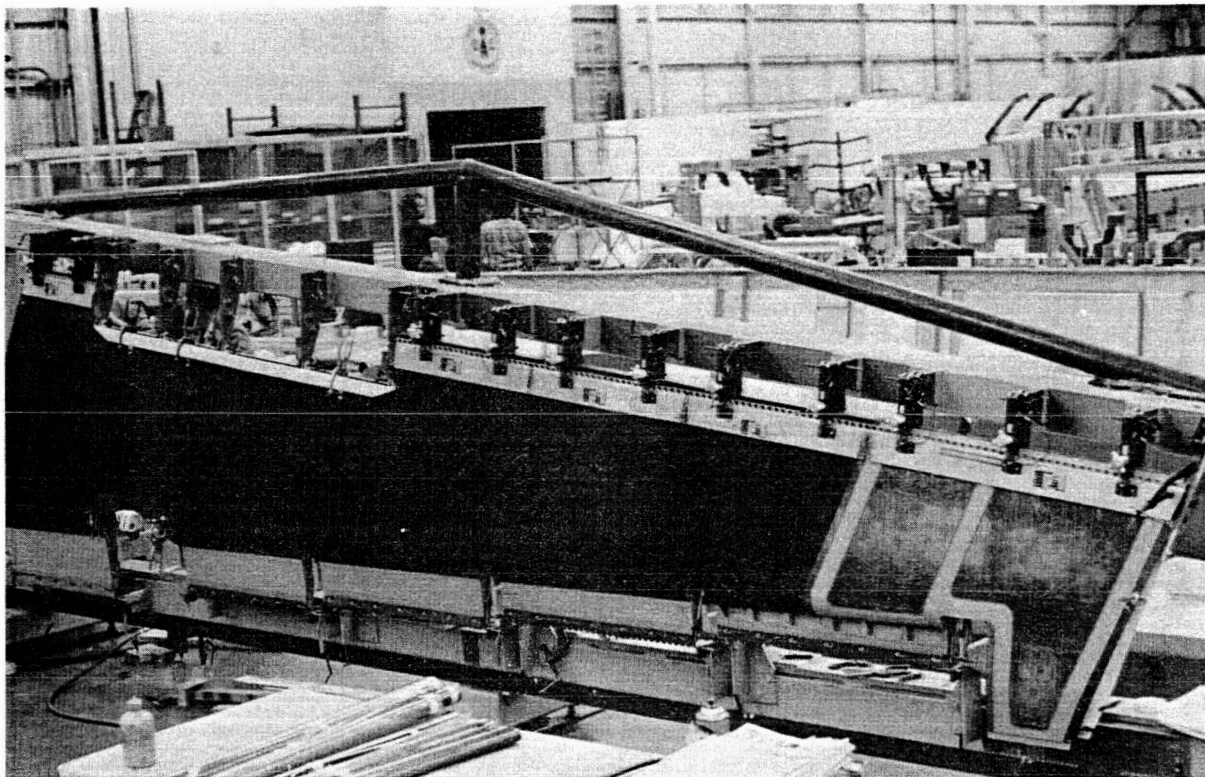


Figure 265. Upper Skin Panel in Position in Major Jig

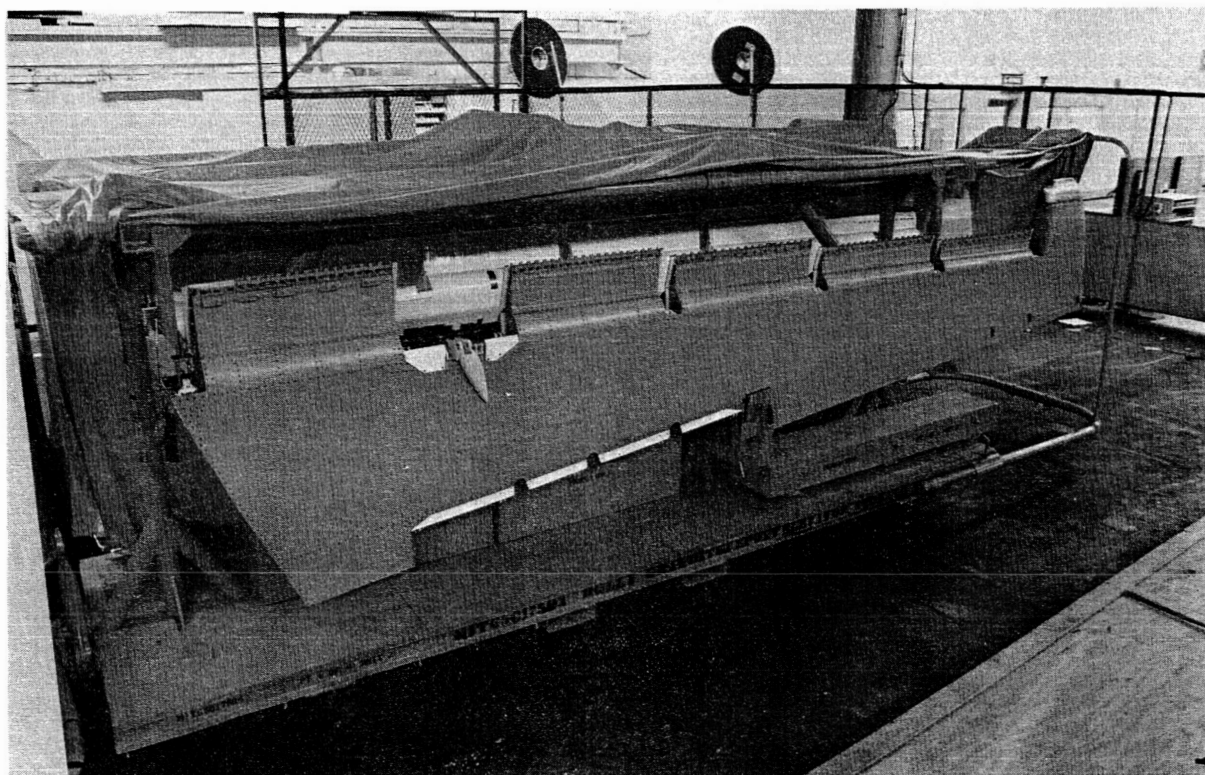


Figure 266. Completed Elevator Assembly

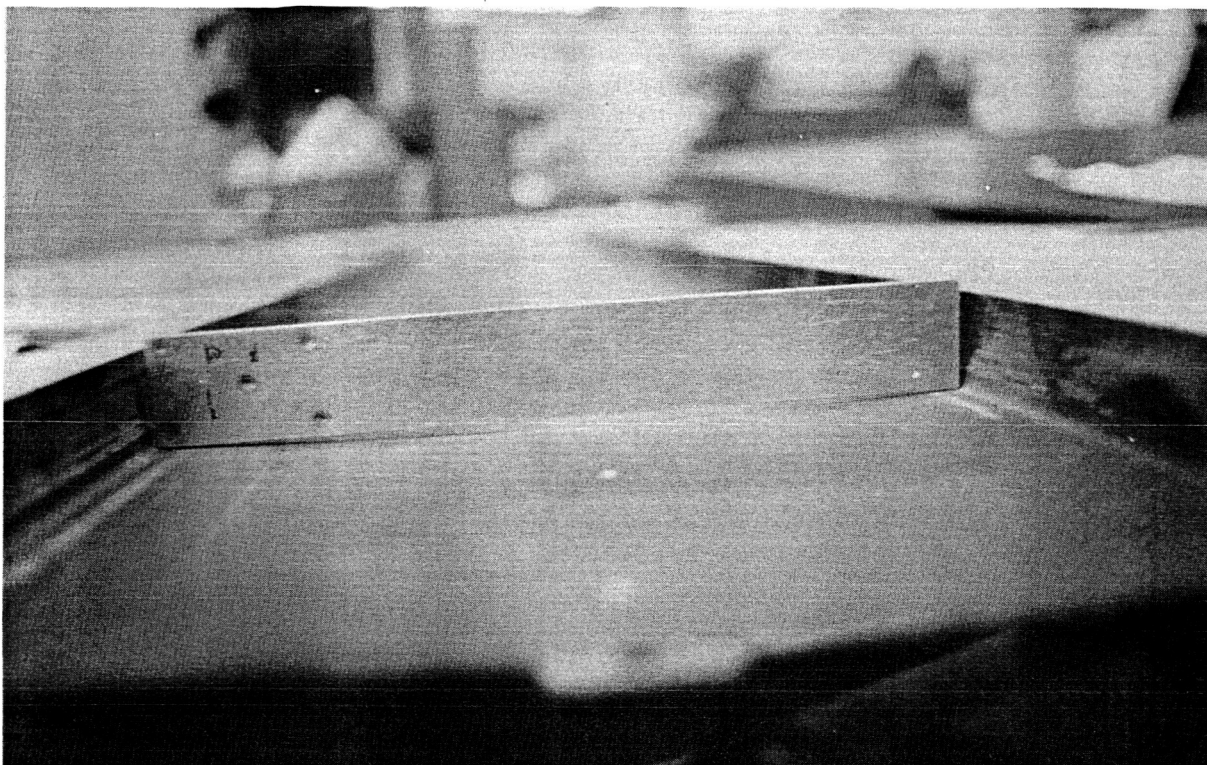


Figure 267. Front Spar Showing Warp Removed on Assembly

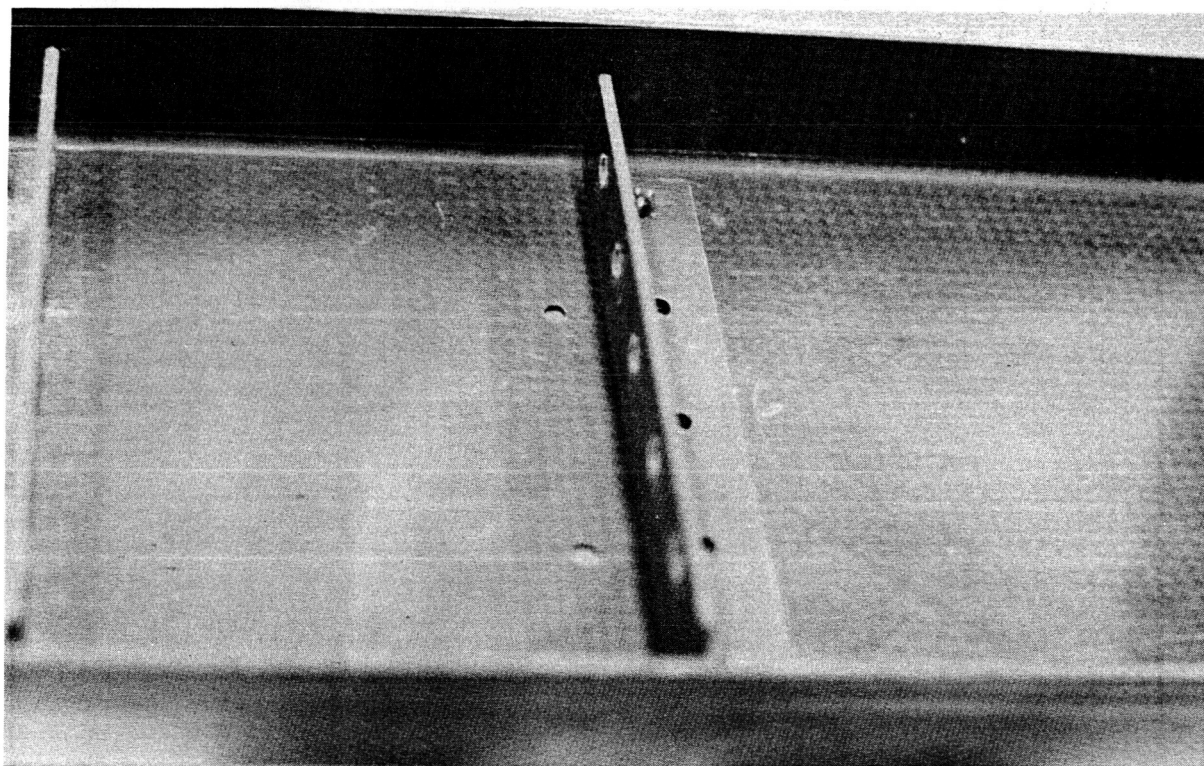


Figure 268. Front-Spar Rib Attach Angle

The rear-spar channel, shown in Figure 269, exhibited a lengthwise warp relative to the spar centerline and, here again, the clamping action of assembly tools could hold the channel in position without excessive preload. Also, the channel legs had a tendency to close in toward the trailing edge when curing, as depicted in Figure 270. In most instances, the channel could be opened sufficiently by hand or by tool pressure to allow installation of rear-spar headers and tab hinge fittings even though the amount of closedown varied from shipset to shipset.

Warpage across the width of the skin panels (figs. 271 and 272) was a prevalent condition, but positioning to the inspar structure could be accomplished without excessive pressure on preloading. The main trouble area was along the leading edge where the stiffness and warp of the panels, coupled with tolerance variance in the metal nose ribs, often created shimming requirements for part separation. Shimming was necessary to avoid preloading and to reduce part separation at the fastener to an allowable standard.

6.4.2 HOLE PREPARATION

Drilling and countersinking techniques were developed during fabrication of verification hardware and were carried over into the production cycle through training sessions. Quality of this work was directly related to this preassembly training as well as the experience gained during several units of production work. Hole preparation methods and problems are discussed in the following paragraphs.

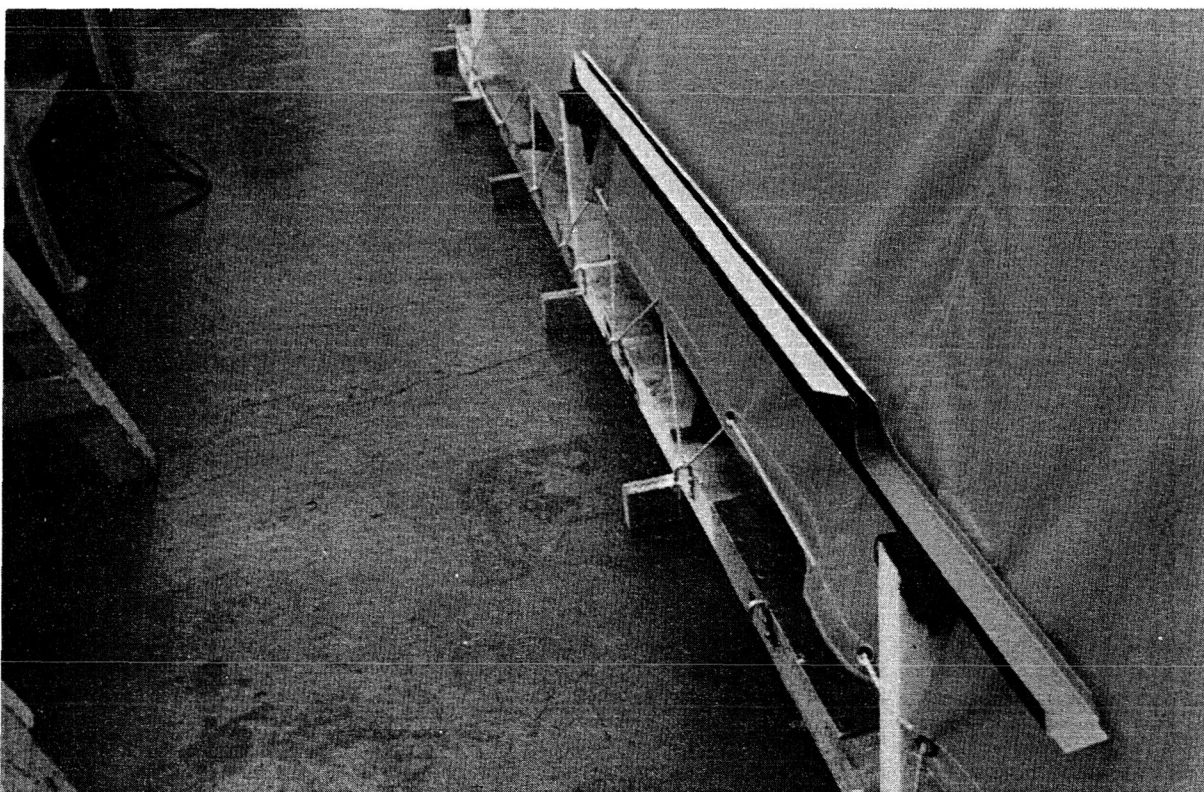


Figure 269. Rear-Spar Channel

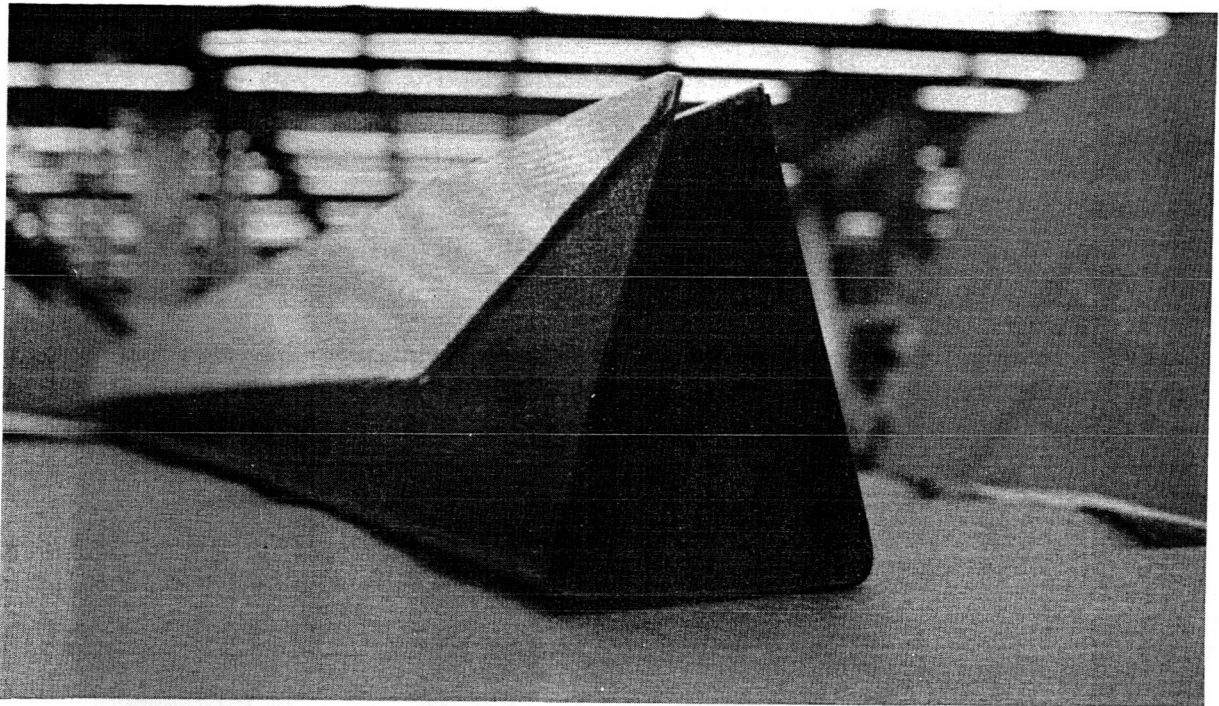


Figure 270. Rear-Spar Channel Showing Trailing-Edge Gap

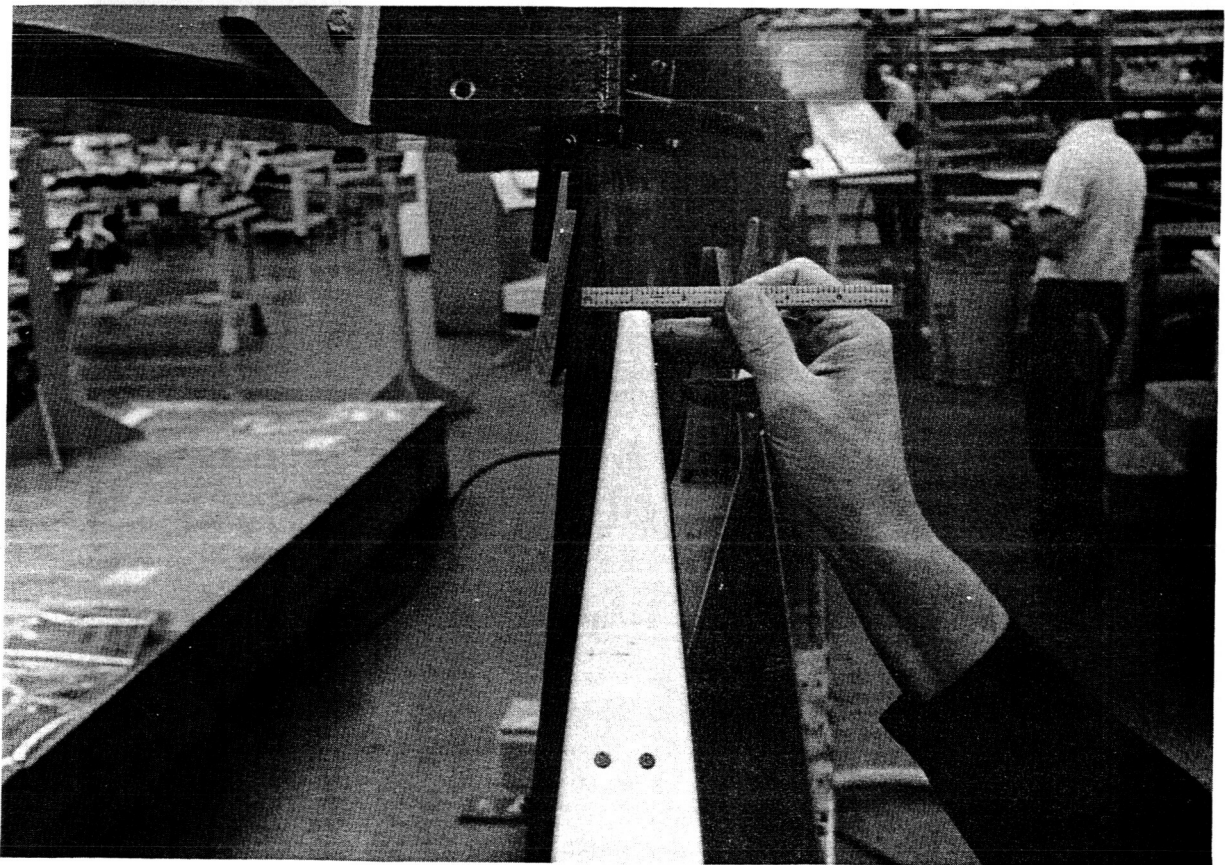


Figure 271. Lower Skin Panel Showing Warp at Inboard End

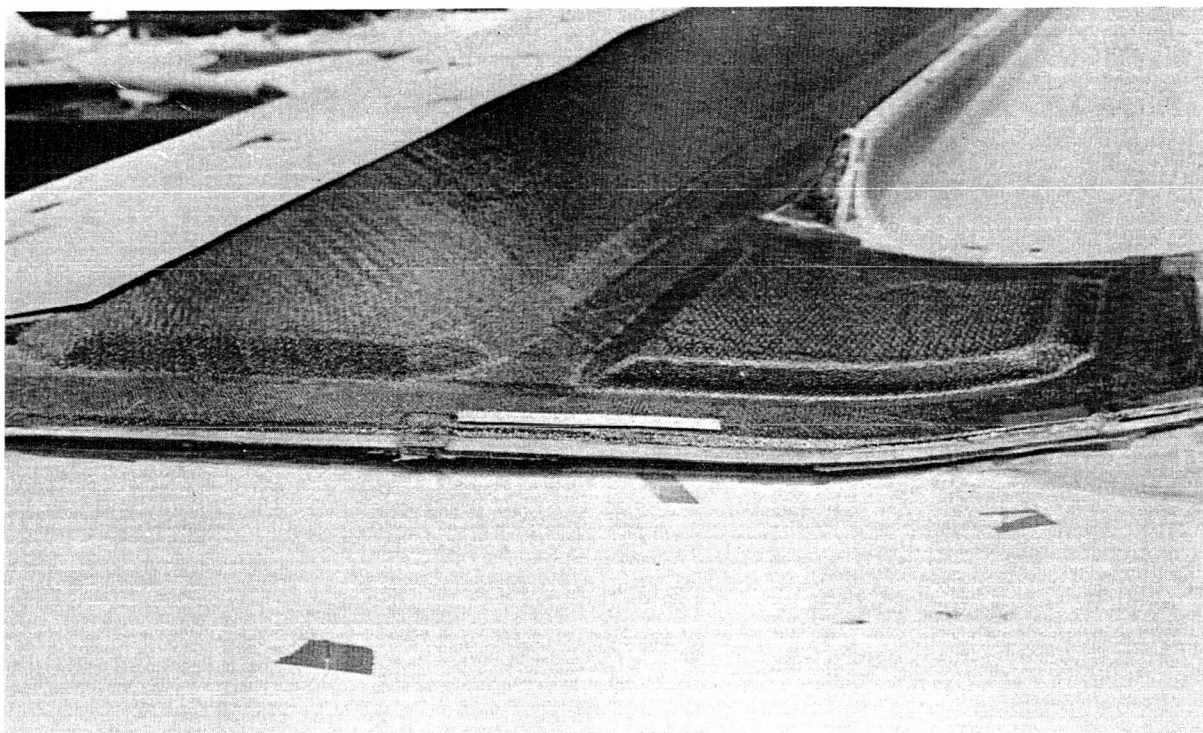


Figure 272. Upper Skin Panel Showing Warp at Outboard End

6.4.2.1 Composite Stackup

Drilling through composite materials was accomplished with 18,000-rpm air motors and special high-speed tapered drills that were made with carbide materials. Hole preparation by this method was trouble free, except where conditions required that the drill exit through the outer surface of the skin panels. The outer layers of the panels are tape material rather than fabric, and breakout of the graphite fibers occurs as the drill exits. Breakout that was experienced generally cleaned up during countersink operations so that it was within drawing allowances except on one particularly troublesome area along the trailing edge where a strip of fiberglass fabric was added to the exterior ply of the panels to eliminate the problem.

Wherever possible, provisions were included on the assembly tools for positioning and positive guidance during drilling operations since the taper drill cut through quite rapidly and the flutes can cut sidewise like a router if misguided. There were a number of places, particularly in the front-spar area, where hole positioning was provided from pilot holes in a part in lieu of tool provisions. In these instances, extra caution had to be exercised by the mechanics to avoid oversizing of the finished hole.

6.4.2.2 Composite/Aluminum Stackup

A one-step operation with carbide-tipped twist drills operating at 2,000 rpm was used to prepare the holes. Where the metal was entered first, no problems were experienced. However, in the leading edges where the graphite skin panel was entered first, a problem with fiber breakout caused by metal chips backing up the drill flutes was experienced. To correct this problem, a two-step operation was employed. First, the hole was drilled undersize with a carbide-tipped twist drill and then brought to full size with the special taper drill.

6.4.2.3 Countersinking

Tool life, depth control, surface quality, and fiber breakout were startup problems that required the most attention. From the different approaches used on early units, it was determined that three fluted cutters with carbide inserts provided the desired quality and tool life. The addition of a nylon pad to the nose of the microstop countersink tool effectively controlled the depth and size of the countersink and provided pressure close around the cutting area such that breakout was eliminated. The modified countersink tool is shown in Figure 273. Operator training and techniques contributed to proper countersinks.

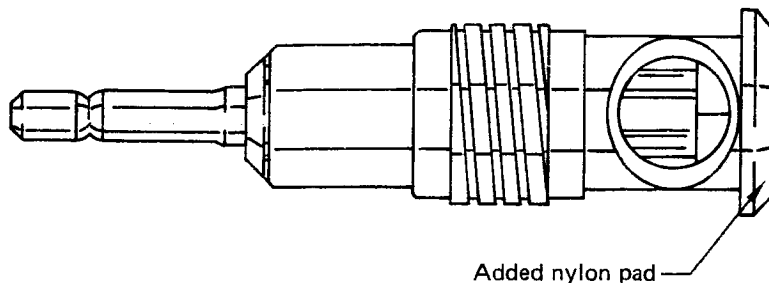


Figure 273. Modified Countersink Tool

6.4.3 FASTENING SYSTEMS—HI-LOK BOLT

Titanium Hi-lok bolts with corrosion-resistant steel collars and washers were the predominant fasteners used for mechanical joining of assembly components. However, installation problems prompted changing to alternative fasteners in the rear spar and lower skin panel areas. Problem items were:

1. Accessibility of standard tools to the collar and Allen pin recess (fig. 274)
2. High torque range for collar breakoff
3. Size of Allen pin recess

The first item resulted in excessive installation time, and items two and three caused the Allen pin in the drive tool to round off or twist and in some cases the pin sheared off. In an effort to correct these problems, Hi-lok bolts were replaced by Hi-torque bolts that had slotted heads (fig. 275), and Hi-lok collars were replaced with self-locking nuts. This change allowed driving the bolts from the outside and eliminated the Allen pin problem. It was found, however, that the Hi-torque bolt head was difficult to grip and presented problems in obtaining proper clamp-up torque (fig. 275). To offset this condition, a new bolt (the Torque-set) was qualified and used in place of the Hi-torque bolt. This bolt has an offset Phillips-head configuration that provides a positive grip without a high degree of pressure being applied to keep the drive tool seated. Figures 276 and 277 show this new bolt.

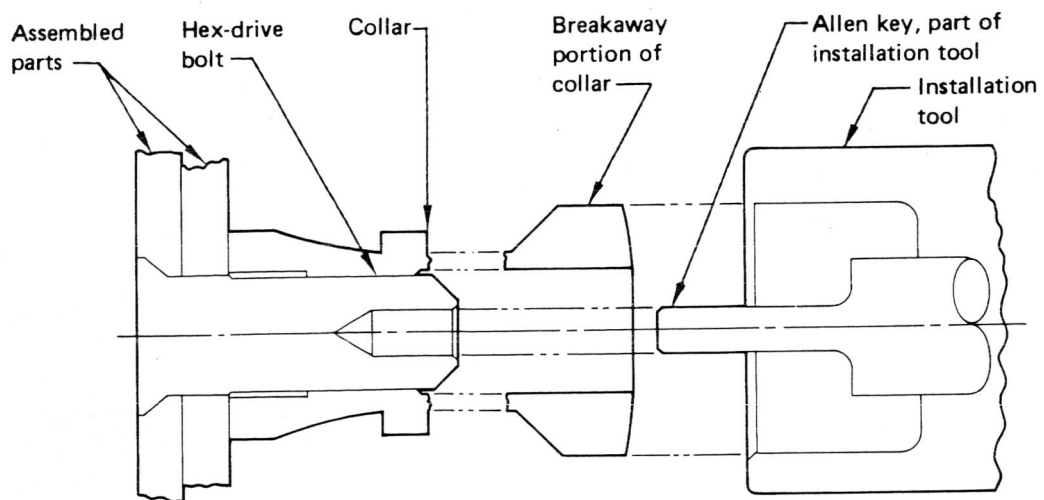


Figure 274. Hi-Lok Fastener Hex-Drive Bolt and Collar Installation

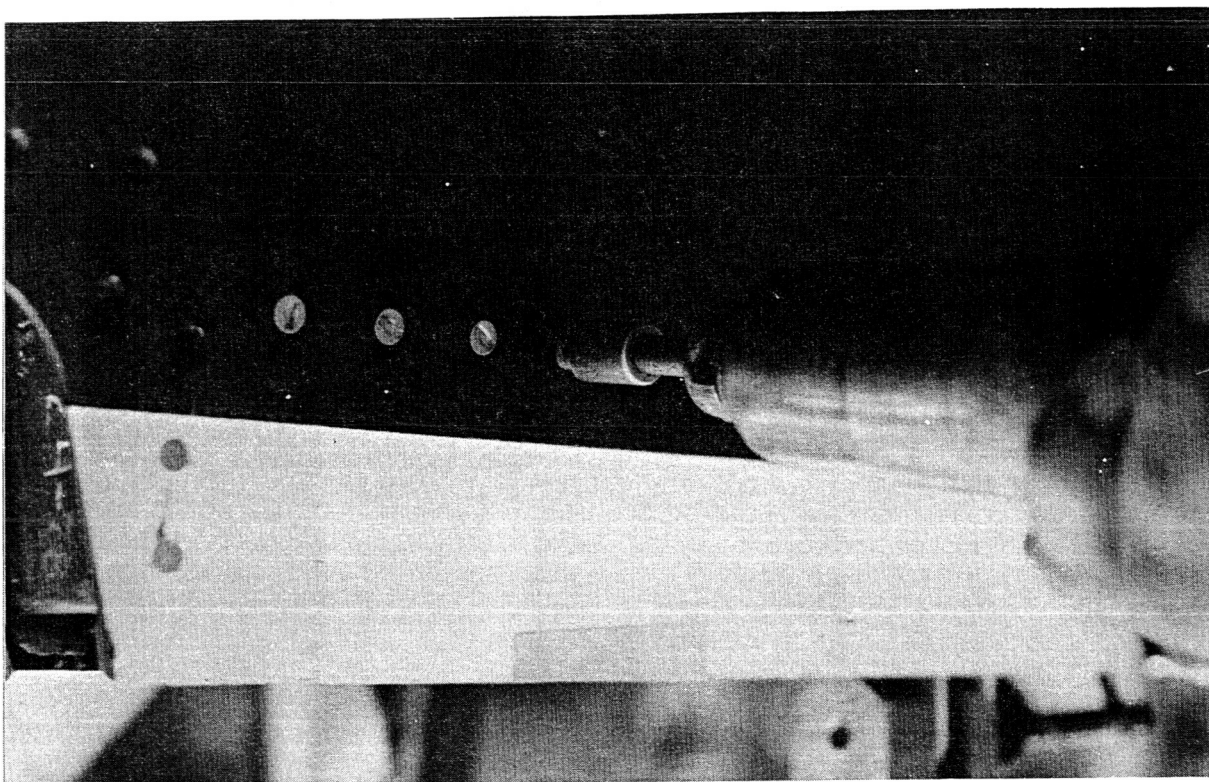


Figure 275. High-Torque Bolt Installation

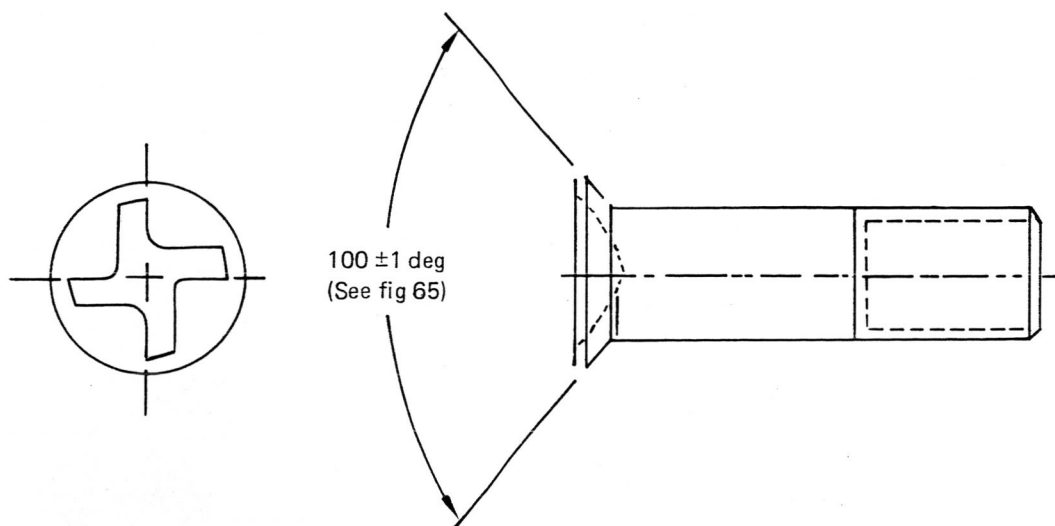


Figure 276. Torque-Set Bolt, 100-deg Flush-Reduced Head

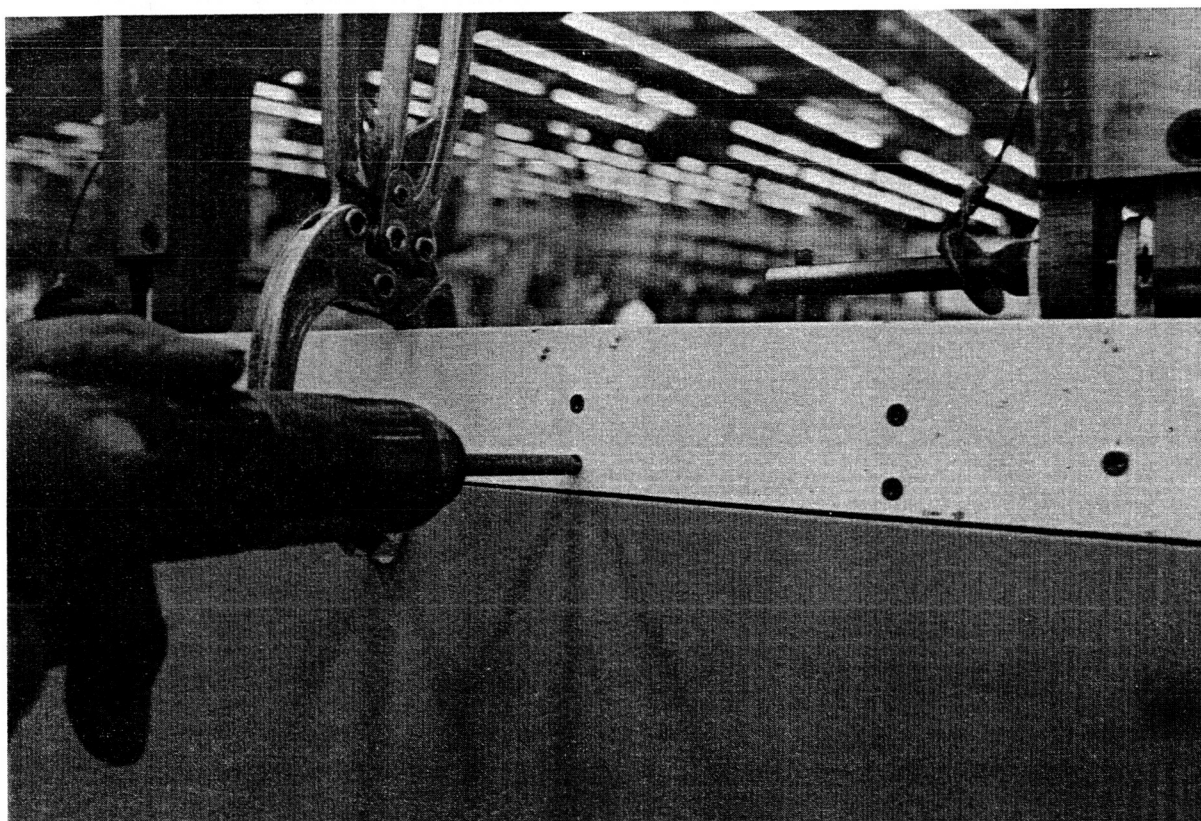


Figure 277. Torque-Set Bolt Installation

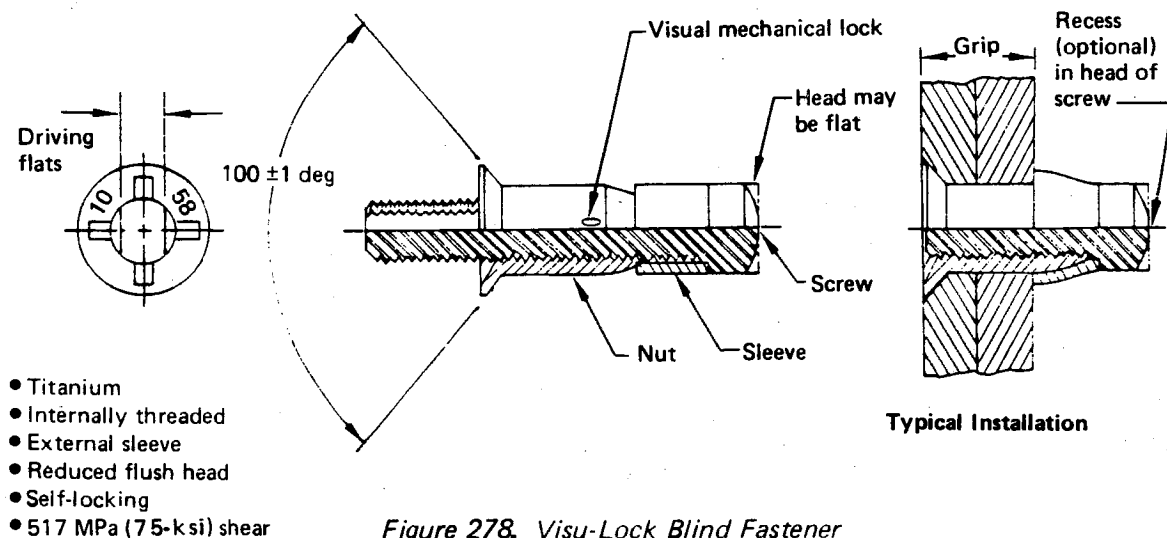
6.4.4 FASTENING SYSTEMS--NUTPLATES

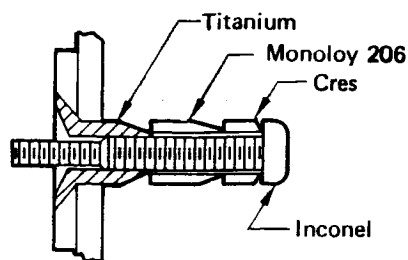
The nutplate/Hi-torque bolt fastening was the primary system used to install the upper skin panels, which is the closeout side of the assembly. Blind rivets, along with the nutplate/bolt fastener, were used in the nose rib area and hollow-ended rivets in the trailing edge. The nutplate installation was time-consuming, and the Hi-torque bolts presented the same grip problem as noted in Section 6.4.3. To correct these problems, blind fasteners were qualified and substituted at the majority of these fastener locations. The Visu-lok blind fastener (fig. 278) was used in conjunction with a stainless-steel washer bonded to the inner surface of the composite stackup. Even with the time involved to bond the washers in place, overall installation time for the upper panels was reduced considerably. Use of the "Bigfoot" blind fastener (fig. 279), which was qualified after completion of the fifth shipset of elevators, will eliminate the washer requirement.

There were no significant problems with installation of the NAS blind fasteners in the nose rib area, but the hollow-ended rivets used along the trailing edge required development of special rivet dies. Figure 280 shows the installation of these rivets.

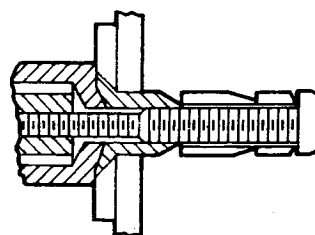
6.4.5 CONTROL TAB ASSEMBLY

Mechanical assembly efforts for the control tabs consisted of installing hinge fittings and mass balance weights. There were no significant problems with fastener installation, and modifications to the metal control tab assembly tool to produce composite tabs work as planned.

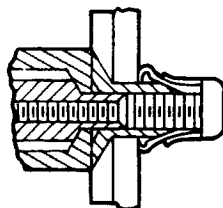




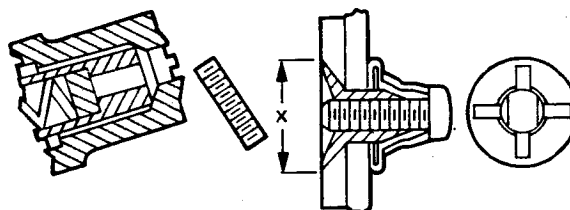
Bigfoot fastener is inserted in hole drilled through members to be joined.



Standard NAS 1675 installation tooling with modified wrench adapter and nose adapter is applied to Bigfoot fastener with nose adapter engaging the nut and the wrench adapter engaging the slabbed portion of the screw shank.



Power is applied and screw is wrenched while nut is held. The bearing sleeve, compressed between the nut and the column sleeve, expands and is drawn over the tapered shank of the nut. The column sleeve is drawn over the bearing sleeve, forming a large head that grips the mating surfaces of the material being joined.



Positive sheet clamp-up is simultaneously effected. Slabbed portion of screw shank is snapped off as soon as Bigfoot is fully driven.

- Diameters = 4.76 mm (3/16 in) to 7.94 mm (5/16 in) plus 0.79 mm (1/32 in) oversize
- Grip lengths = increments of 1.27 mm (0.050 in)
- Flush/protruding head

Figure 279. Installation Procedure of Monogram/Aerospace "Bigfoot" Fastening System

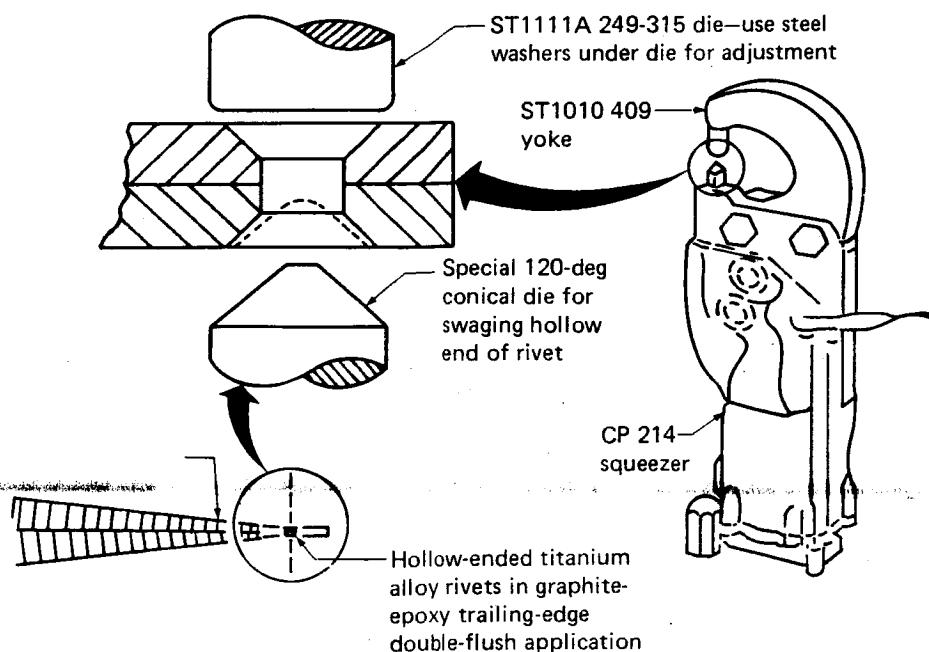


Figure 280. Elevator Trailing-Edge Rivet Installation

7.0 COST ANALYSIS

This section presents the analysis of production cost data for the five-and-one-half-shipset production run. Except for the ground test labor hours that are shown in Table 16 as information of special interest, this section addresses only those costs directly incurred in producing five-and-one-half shipsets of 727 composite elevators using the methods and techniques developed during the preproduction phases of the program. Manufacturing process, assembly and tool development considerations, and their production applications are discussed in detail in Sections 5.0 and 6.0 of this report.

Total production program costs shown in Figure 281 reflect the fabrication and manufacturing processes used in a semiproduction environment for the five-and-one-half-shipset program. Tooling and component manufacturing percentages are relative to overall costs in dollars; engineering costs are not included.

Work was performed in production shops by employees whose experience and skill levels were representative of a cross section of the shop work force. Component fabrication was performed with hand cutting and layup of broadgoods, ply-by-ply inspection, and hand trimming. Tooling was designed for extended production; however, the tool rework and improvement effort was restricted to the five-and-one-half-shipset contract.

These activities were representative of the production processes that would, insofar as practical, be used to produce a large number of elevators. It is likely, however, that through the adoption of improved manufacturing processes, the per-unit cost of elevators produced in a regular production environment would be significantly lower. Projections of production cost trends are discussed in Section 7.3.

Table 16. Ground Test Labor Hours—727 Composite Elevator

Fixture	
Design	3,097
Fabrication	<u>2,821</u>
TOTAL	5,918
Testing	
Static	3,372
Fatigue	3,055
Fail-safe (damage tolerance)	<u>1,164</u>
TOTAL	7,591

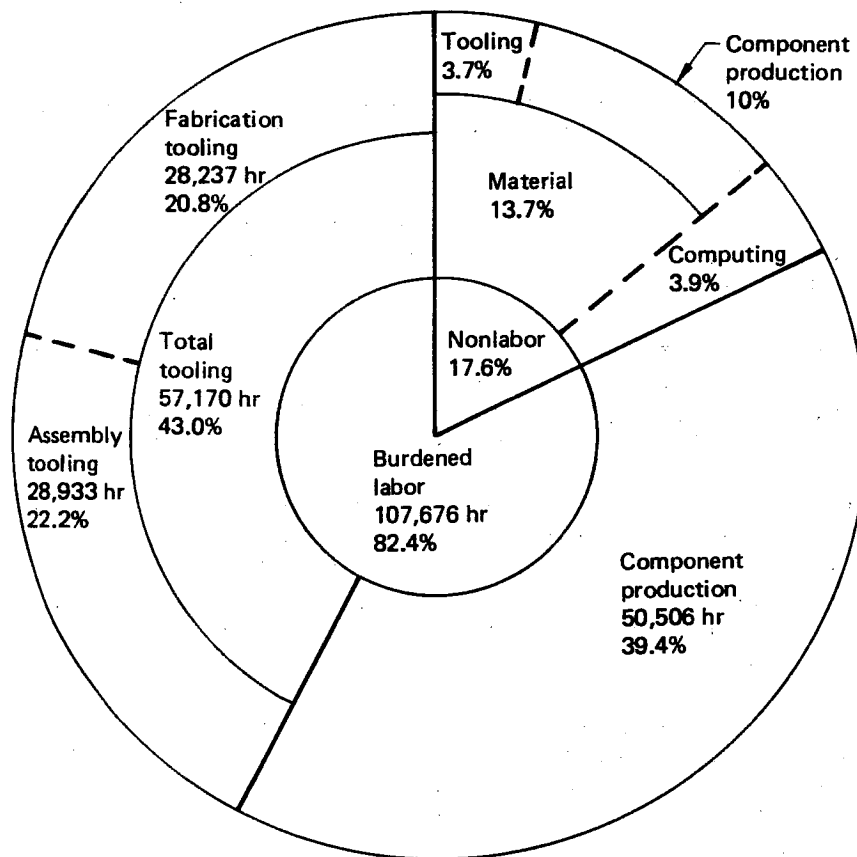


Figure 281. Total Recurring and Nonrecurring Production Costs by Major Element—5½ Shipsets

7.1 LABOR COSTS

Assembly labor hours were recorded manually for each shipset and compiled by the Industrial Engineering organization. All other labor hour data were taken from sources accessing The Boeing Company's central labor cost accumulation and distribution system. Total recurring labor costs by shipset are detailed in Table 17. Separate costs are recorded for the larger process assembly items (i.e., cover panels, ribs, spars, and tab assemblies) since they are produced from single unit orders. Costs of lot-time items are prorated equally among the shipsets and are included in the unit costs.

Many nongraphite parts used in the composite elevator are common to both the metal and the composite elevator. Some of these had to be modified from the configuration provided by the part vendor or metal elevator subcontractor to make them usable in the composite elevator assembly. The rework costs of these parts have been segregated and are identified in Table 17 and Figures 282 and 283. The hours required to fabricate the parts are not included.

Figure 282 and Table 18 show the total recurring and nonrecurring component production labor expenditures excluding tooling. The data provide a breakdown of the labor expenditures into the categories of component fabrication, Manufacturing Research and Development (MR&D), and assembly. The MR&D effort was liaison support to the fabrication and assembly work. Figure 282 shows that 61.8% of the total labor was for component fabrication including planning. This compares to only 28.0% for assembly including planning and 10.2% for liaison support.

Table 17. Recurring Labor Hours, 5½ Shipsets—727 Composite Elevator

Description	Ship-set no.	Ground test unit L-H	Lefthand					Righthand				
			1	2	3	4	5	1	2	3	4	5
Front spar—inboard		18.9	54.8	②144.3	65.7	③48.5	35.6	38.1	24.9	20.3	21.7	—
Front spar—outboard		115.9	46.2	44.3	105.5	50.1	④153.4	42.1	40.6	60.6	⑤138.9	32.0
Rear spar		93.0	93.2	42.0	43.4	111.4	46.2	45.8	26.3	32.2	39.2	41.2
Ribs		401.8	254.2	232.5	233.0	229.5	218.4	254.2	232.5	233.0	229.5	218.4
Upper skin panel ①⑥		527.1	116.6	144.6	182.3	123.9	178.3	222.8	276.6	202.4	161.3	192.6
Lower skin panel		129.7	171.8	130.2	121.4	150.6	115.8	165.7	175.1	161.4	⑦166.0	239.7
Trim tab		168.5	227.2	⑧236.1	⑨225.7	199.1	211.0	174.2	⑩251.9	204.5	177.3	187.2
Graphite components		1454.9	964.0	974.0	977.0	913.1	958.7	942.9	1027.9	914.4	933.9	911.1
Nongraphite components		377.0	340.8	344.0	347.5	323.9	340.8	334.0	364.4	323.9	330.6	323.9
Blanket time		287.1	272.9	275.7	278.3	259.4	272.9	267.5	291.9	259.4	264.8	259.4
Manufacturing Engineering—Planning		—	74.0	50.0	40.0	35.0	30.0	74.0	50.0	40.0	35.0	30.0
Quality assurance		1079.0	514.8	519.9	525.0	489.3	514.8	504.6	550.5	480.3	499.5	489.3
Fabrication recurring		3198.0	2166.5	2163.6	2167.8	2020.7	2117.2	2123.0	2284.7	2018.0	2063.8	2013.7
Elevator assembly		1298.0	704.0	651.0	609.0	548.0	488.0	704.0	651.0	609.0	548.0	488.0
Distributive		690.0	196.0	181.0	170.0	153.0	137.0	196.0	181.0	170.0	153.0	137.0
Manufacturing Engineering—Planning		—	66.0	61.0	57.0	52.0	45.0	66.0	61.0	57.0	52.0	45.0
Quality Assurance		373.0	315.0	202.0	190.0	170.0	92.0	315.0	202.0	190.0	170.0	64.0
Manufacturing R&D—QA		2617.0	746.0	245.0	275.0	167.0	117.0	746.0	245.0	275.0	167.0	117.0
Assembly recurring		4978.0	2027.0	1340.0	1301.0	1090.0	879.0	2027.0	1340.0	1300.0	1090.0	851.0
Engineering Liaison/Sustaining		777.0	1161.0	519.0	232.0	72.0	81.0	1161.0	519.0	232.0	72.0	80.0
Total recurring		8953.0	5354.5	4022.6	3700.8	3182.7	3077.2	5311.0	4143.7	3551.0	3225.8	2944.7

Component labor hours are raw data taken from the automated cost collection system and are not subject to adjustment at this level of detail. Disproportionately high figures in these data are explained by footnote where the reasons are known and results identifiable. Assembly hours were collected manually by shipset and are divided equally between left-hand and right-hand units.

Labor Hours Lost Due to Scrapped Parts

①	12/5/8	One wedge scrapped—resin starved—for total of five shipsets	28.6 hr
②	6/14/8	Scrap—bleed out Ply buildup mislocated	38.6 60.9
③	3/20/9	Scrap—warping	25.5
④	4/25/9	Scrap—damaged in shipping	40.4
⑤	4/10/9	Scrap—spar warpage	34.2
⑥	10/11/8	Assumed that one part mischarged to ground test unit, rather than five-shipset total	145.5
⑦	4/25/9	Scrap—incorrect dimensions	98.1
⑧	10/6/8	Scrap—dimensions	87.0
⑨	12/5/8	Scrap—delamination	5.5
⑩	10/23/8	Scrap—resin bleedout	32.5
⑪	11/29/8	Scrap—transition slope—redesign of tool Rework—indentation, resin ridges, cure cycle	78.9

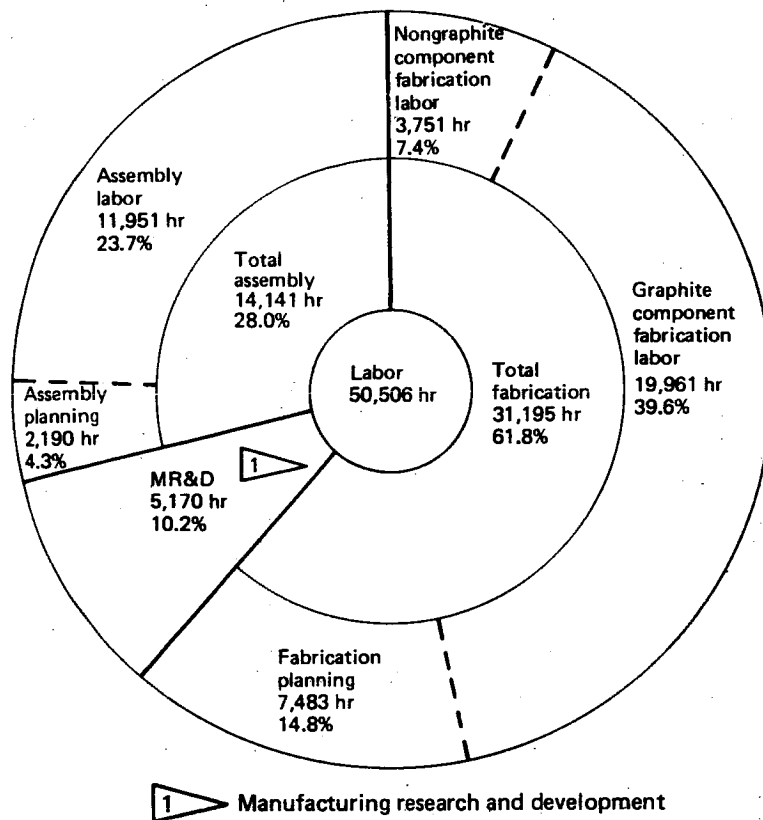


Figure 282. Total Recurring and Nonrecurring Component Production Labor Hours—5½ Shipsets

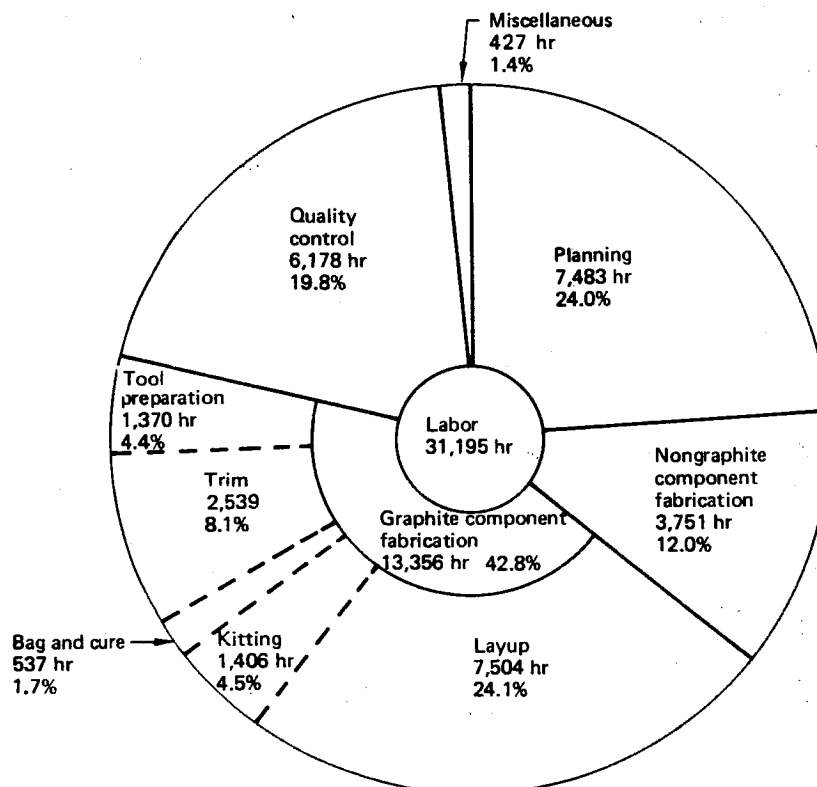


Figure 283. Total Recurring and Nonrecurring Fabrication Hours—5½ Shipsets

**Table 18. Component Production Labor Expenditures—Total
Recurring and Nonrecurring (Excludes Tooling)**


	Labor hours		
	Ground test unit	Five shipsets	Totals
Recurring			
• Fabrication (excluding planning)	—	20,001	20,001
• Fabrication planning	—	458	458
• Subtotal fabrication	—	20,459	20,459
• Assembly (excluding planning)	—	9,582	9,582
• Assembly (planning)	—	563	563
• Subtotal assembly	—	10,145	10,145
• Manufacturing research and development (MR&D)	—	1,276	1,276
• Subtotal MR&D	—	1,276	1,276
• Total recurring	—	31,880	31,880
Nonrecurring			
• Fabrication (excluding planning)	3,711	—	3,711
• Fabrication (planning)	4,344	2,681	7,025
• Subtotal fabrication	8,055	2,681	10,736
• Assembly (excluding planning)	2,369	—	2,369
• Assembly (planning)	1,060	567	1,627
• Subtotal	3,429		3,996
• Manufacturing research and development (MR&D)	2,617	1,277	3,894
• Subtotal MR&D	2,617	1,277	3,894
• Total nonrecurring	14,101	4,525	18,626
Total recurring and nonrecurring	14,101	36,405	50,506

Figure 283 provides a further breakdown of the recurring component fabrication labor hours. The primary cost element is layup, which accounts for 24.1% of the total fabrication labor. Graphite component fabrication (including layup, kitting, bag and cure, and trim) accounted for 38.4% of the total labor expenditures. Nongraphite fabrication (part modification) accounted for 12.0% of the expenditures.

Table 19 shows total production tooling hours. Fabrication tooling labor hours were 49.4%, while assembly tooling labor hours were 50.6%. Recurring tooling labor hours were only 3.6%, while nonrecurring tooling hours, which included all left-hand test article tooling, were 96.4%.

Figure 284 provides a breakdown of the total recurring and nonrecurring labor expenditures for component assembly. The primary cost element is assembly labor, which comprises 67.9% of the total. The balance consists of planning (16.0%) and quality control (16.1%).

Table 19. Production Tooling—727 Elevator

	Labor hours		
	Design	Fabrication	Total
Recurring			
Fabrication tools	70	586	656
Assembly tools	64	1326	1390
SUBTOTAL	134	1912	2046
Nonrecurring 			
Fabrication tools	2431	25150	27581
Assembly tools	225	27318	27543
SUBTOTAL	2656	52468	55124
GRAND TOTAL	2790	54380	57170

 All left-hand test article tooling is nonrecurring

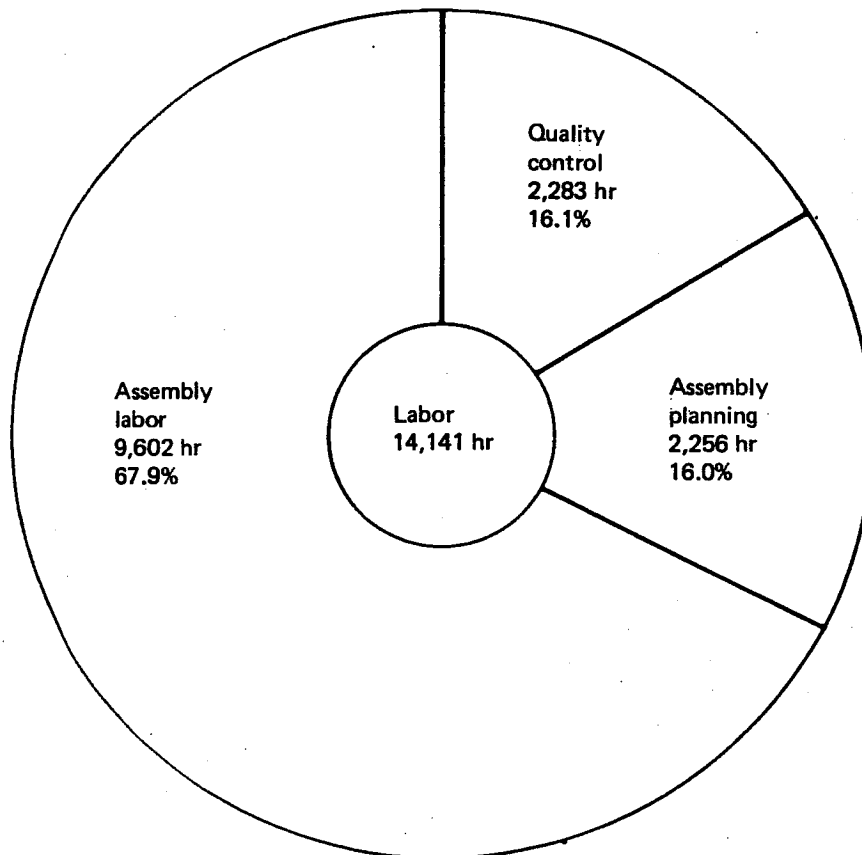
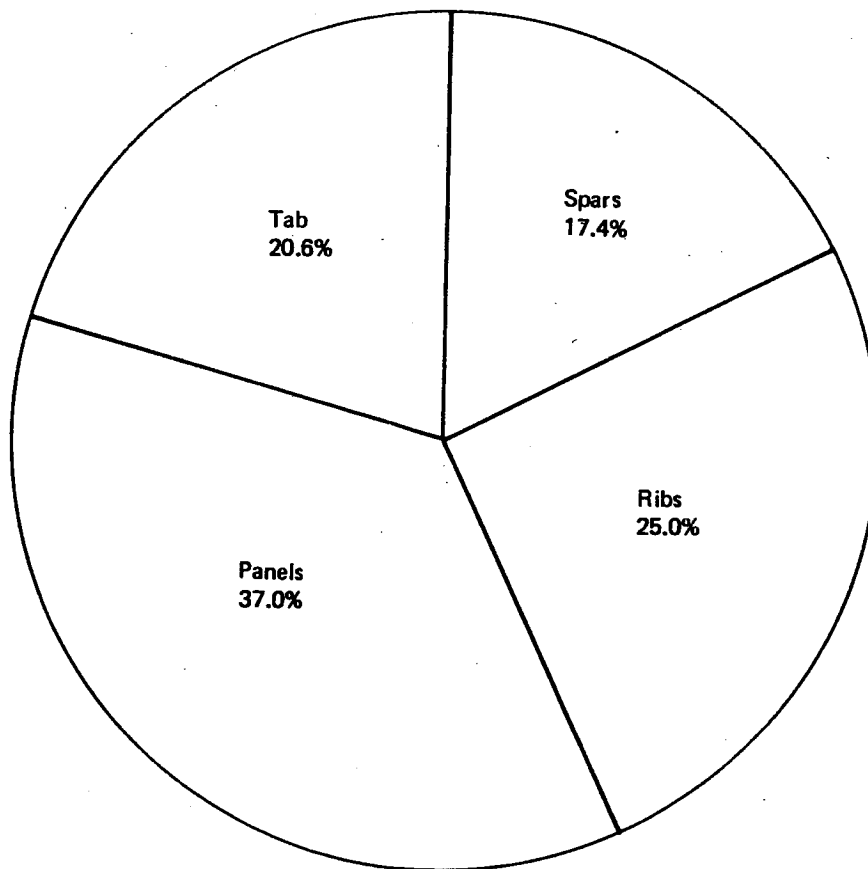


Figure 284. Total Recurring and Nonrecurring Assembly Labor Hours —5% Shipsets

Figure 285 shows a percentage breakdown of the recurring fabrication labor hours for the major graphite components. Figure 286 shows the percentage breakdown of the recurring direct labor hours for the 727 composite elevator component fabrication and assembly. The MR&D effort, which is included in Figure 286, was expended in support of fabrication and assembly work and was not expended in the developmental hardware programs. Planning that occurred before 1979 was considered nonrecurring and was not included. Kitting, layup, bag and cure, and trim were based on hours generated by the applicable shops associated with those functions.



Component labor hours are raw data taken from the automated cost collection system and are not subject to adjustment at this level.

Figure 285. 727 Composite Elevator—Graphite Components Percentage of Component Labor ▷ Recurring Costs—5½ Shipsets

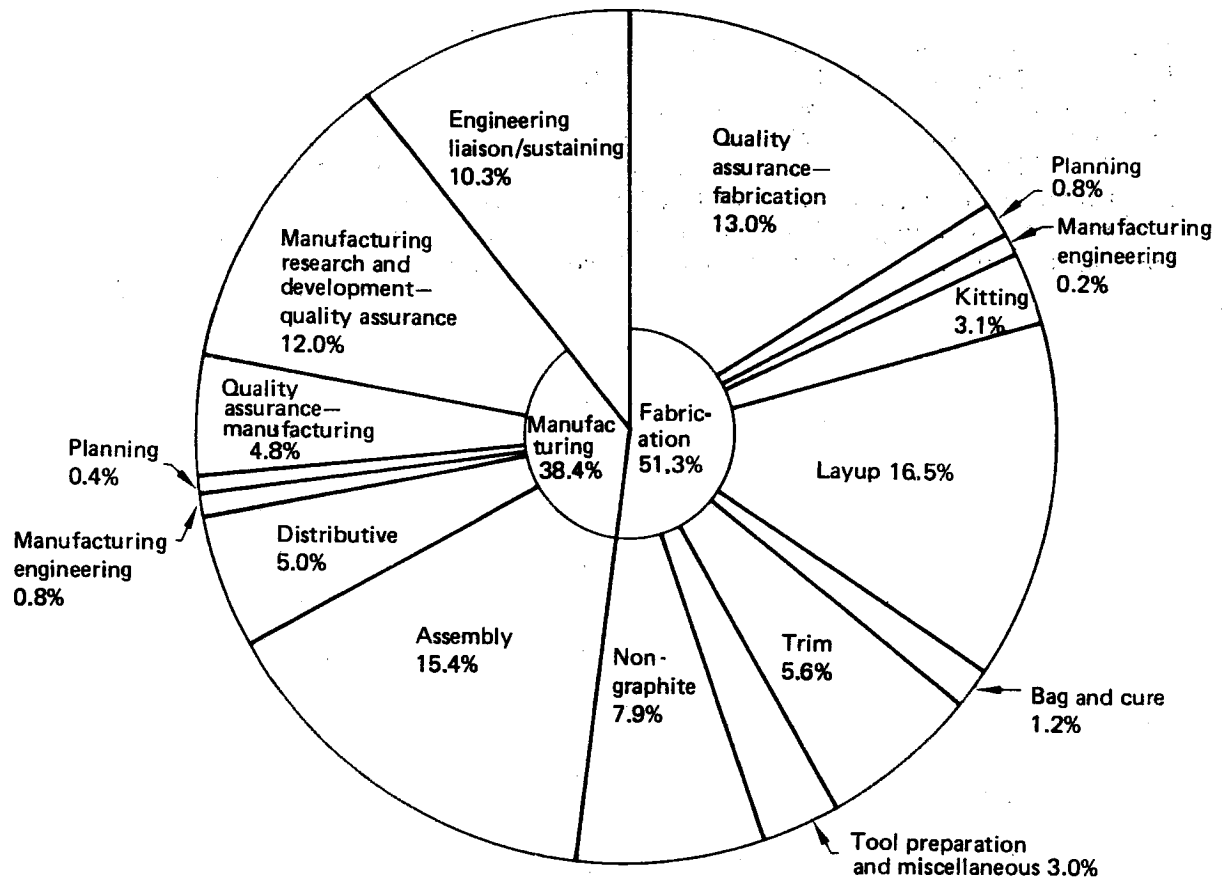


Figure 286. Fabrication and Assembly Recurring Costs Percentage of Labor Hours—5½ Shipsets

7.2 USAGE FACTORS

Usage factors experienced for graphite-epoxy materials were 0.78 kg (1.8 lb) of tape and 1.22 kg (2.8 lb) of fabric for each pound of graphite-epoxy flyaway weight in the finished elevator. This included indirect usage for receiving tests, kitting trim loss, process test panels, process and miscellaneous rejections, and layup trim loss. It is estimated that these factors could be reduced to 1.5 and 2.0, respectively over a 200 shipset program, with more uniform quality materials, revised handling methods, and improved manufacturing processes. With the advent of automated material cutting/part nesting and new layup and processing technology, these factors would be further reduced.

Based on costs incurred in producing the five-and-one-half shipsets of composite elevators, the average cost of 200 shipsets is estimated to be 40% higher than the average cost of the first 200 shipsets of the current all-metal configuration. However, this cost penalty would be substantially reduced and possibly be eliminated through the adoption of improved manufacturing processes, including use of the aforementioned automated tape layup and cutting machines, more efficient utilization of material, and a reduction in material prices in real terms through increased production volume.

The effect of improved technology on the trend of competitive cost averages for initial 200-shipset quantities of model 727 composite elevators at current and at future time periods is depicted in Figures 287 and 288. These figures show that the present 40% cost penalty could be reduced to 13% by 1985 and possibly eliminated or turned into an advantage by 1990 based on the current elevator design and the assumptions listed in Table 20. Further optimization of the design would be expected to produce additional cost benefits.

The cost projection comparison of 200 shipsets of metal versus composite elevators shown in Figures 287 and 288 are based on the following ground rules:

- Estimated production costs are scoping level.
- No additional engineering or developmental sustaining effort is required.
- Nonrecurring costs such as production release and duplicate tooling are excluded.
- Recurring costs include only material, outside production, and outside operations labor to be expended directly on the deliverable end item.

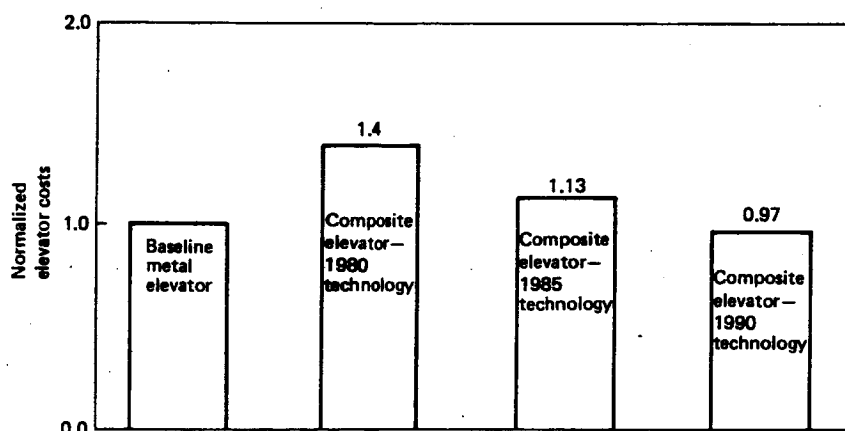


Figure 287. Relative Elevator Cost Comparison (For Initial 200 Shipsets)

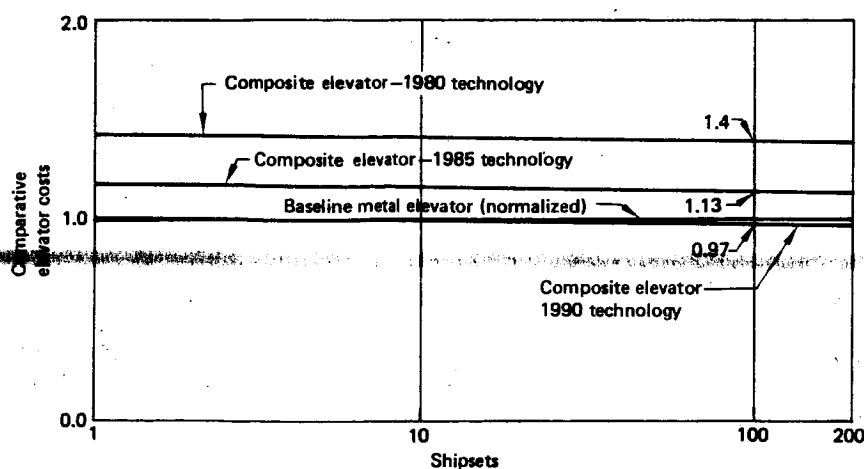


Figure 288. Relative Elevator Cost Trends (For Initial 200 Shipsets)

Table 20. Metal Elevator Versus Composite Elevator Cost Comparison Assumptions

	1980 technology	1985 technology	1990 technology
Metal elevator	<ul style="list-style-type: none"> Current production 	<ul style="list-style-type: none"> Aluminum material escalation of 152% in 5 years based on producers' price index Labor rate escalation of 147% in 5 years 	<ul style="list-style-type: none"> Aluminum material escalation of 224% in 5 years based on producers' price index Labor escalation of 216% in 5 years
Composite elevator	<ul style="list-style-type: none"> Hand layup and cutting High material usage High material cost 	<ul style="list-style-type: none"> Automatic tape layup and cutting Material waste cut by 72% Material price per lb cut 20% due to increased industry usage Labor rate escalation of 147% in 5 years 	<ul style="list-style-type: none"> Advanced manufacturing technology Material waste cut by 72% Material price per lb cut 20% due to increased industry usage Labor rate escalation of 216% in 5 years

- Production delivery rate for a 200-airplane production program is 12 shipsets per month.
- Supplier quoted cost per pound of composite material will decrease by 20% as industry usage doubles.

Other ground rules are the average of high and low cost projection factors as follows:

For the high cost projection, it is assumed that:

- 707/727/737 Division assembly hours--80% learning curve
- Fabrication Division process assembly hours--85% learning curve
- Composite material dollars include a 2.0 usage factor

For the low cost projection, it is assumed that:

- 707/727/737 Division assembly hours--75% learning curve
- Fabrication Division process assembly hours--75% learning curve
- Composite material dollars include a 1.5 usage factor

The following assumptions apply to both the high and the low cost projections:

- Fabrication Division sheet metal and machine hours--90% learning curve
- Production material--95% improvement curve

The difference between the normalized baseline metal elevator costs and the projected composite elevator costs shown in Figures 287 and 288 is based on the assumptions presented in Table 20.

7.3 CONCLUSIONS

It is projected that advanced composite material waste will be reduced with the implementation of advanced manufacturing technology and more uniform quality material. It also is projected that cost per pound of advanced composite material will decrease 20% as industry usage of the material increases. Based on these projections, the production experience gained during this program, and assumptions of other cost-reducing factors as detailed in Section 7.2, the cost of advanced composite elevators will become comparable to the cost of similar metal components.

When the increasing value of weight reduction is considered together with the adoption of innovative manufacturing methods and engineering designs, the economic justification for advanced composite aircraft structure is assured.

8.0 CONCLUDING REMARKS

Key program results are highlighted below:

- Weight saving of 27% over current metal assembly achieved.
- Components were produced on schedule.
- Parts and assemblies were readily produced on production-type tooling.
- Quality assurance methods were demonstrated.
- Repair methods were demonstrated in factory production and airline service.
- Strength and stiffness analytical methods were substantiated.
- Cost data base information was accumulated in a semiproduction environment.
- FAA certification was achieved.
- Five shipsets were committed to routine airline revenue service.

The program was successful and timely and provided the necessary Company confidence to commit usage of graphite composite structure in similar applications on a new generation of aircraft.

It is now time to pursue the next major step in a similar type of NASA/industry program directed toward usage of graphite composites in larger (wing/body) type structures.

9.0 REFERENCES

1. AFFDL-TR-77-127; Schneider, S. D., Hendricks, C. L., Olsen, G. O.; Vulnerability/Survivability of Composite Structure-Lightning Strike; The Boeing Company, Feb. 1978.
2. Civil Air Regulations, Part 4b, Airplane Airworthiness, Transport Category; Federal Aviation Agency; Sept. 1962.
3. AC 20-107; Advisory Circular, Composite Aircraft Structure; Federal Aviation Administration, July 1978.
4. Lightning Test Waveforms and Techniques for Aerospace Vehicles and Hardware; Report of SAE Committee AE4L; June 20, 1978.
5. NASA CR 159043; ATLAS Finite Element Computer Code; 1979.
6. Davenport, O. B. and Bert, C. W.; Buckling of Orthotropic, Curved, Sandwich Panels in Shear and Axial Compression; Journal of Aircraft, vol. 10, no. 10; Oct. 1973.
7. NASA TN D-7996; Housner, J. M. and Stein, M.; Numerical Analysis and Parametric Studies of the Buckling of Composite Orthotropic Compression and Shear Panels; Oct. 1975.
8. D6-46023; Boeing Document; Static Balance Requirements; Dec. 20, 1979.

APPENDIX A

D6-46020

MAINTENANCE PLANNING DATA—

AIRCRAFT STRUCTURAL INSPECTION, COMPOSITE ELEVATOR

BOEING COMMERCIAL AIRPLANE COMPANY
A DIVISION OF THE BOEING COMPANY
SEATTLE, WASHINGTON

DOCUMENT NO. D6-46020

TITLE: MAINTENANCE PLANNING DATA -

AIRCRAFT STRUCTURAL INSPECTION COMPOSITE ELEVATOR

MODEL 727

ISSUE NO. _____ TO: _____ (DATE) _____

PREPARED BY	<u>George Truslove</u> G. Truslove	<u>10-16-79</u>
SUPERVISED BY	<u>Howard Syder</u> H. Syder	<u>10-16-79</u>
APPROVED BY	<u>A. E. McCarty</u> A. E. McCarty	<u>10-14-79</u>
APPROVED BY	<u>S. T. Harvey</u> S. T. Harvey	<u>10-19-79</u>
		(DATE)

LIST OF ACTIVE PAGES

SECTION	PAGE NUMBER	REV SYM	ADDED		DELETED		PAGE NUMBER	REV SYM	ADDED		DELETED	
									PAGE NUMBER	REV SYM	PAGE NUMBER	REV SYM
0-1	1	A					1					
							2					
	1	A					3					
							4	A				
							5	A				
0-2												
0-3	1											
0-4	1						1					
	2						2					
1-0	1											
	2											
	3											
	4											
	5											
	6											
	7											
	8											
	9											
	10											
	11											
	12											
2-0	1											
	2											
	3											
	4	A										
	5											
3-0	1											
	2											
	3	A										

REVISIONS			
Rev Sym	DESCRIPTION	Date	Approved By:
A	<p>Section 2, page 4; section 3, page 3</p> <p>1. Deleted frequency recommendation</p> <p>Section 4, page 4</p> <p>1. Deleted frequency recommendation</p> <p>2. Added to internal and external inspection recommendations</p> <p>Section 4, page 5</p> <p>1. Deleted frequency recommendation</p>	<p>12/17/79</p> <p>12/17/79</p>	<p><i>[Signature]</i></p> <p><i>[Signature]</i></p>

TABLE OF CONTENTS

List of Active Pages	Section
Revision Page	0-1
Table of Contents	0-2
Introduction	0-3
General Information	0-4
Preflight, Transit, and "A" Check	1-0
"B" Check	2-0
"C" Check	3-0
Appendix Examples—X-Ray Inspection	4-0

INTRODUCTION

This document provides general guidance in establishing individual airline maintenance programs for current production 727-200 airplanes, using a composite (graphite/epoxy) elevator and control tab, and deals with only these composite (or composite-related) installed parts. (See Document D6-8766 for the remainder of the airplane maintenance procedure.) Work items in this document are recommendations, and should not be considered all-inclusive or mandatory. Each airline has the final responsibility of deciding what work to do, and when to do it.

BOEING 727 AIRCRAFT, COMPOSITE ELEVATOR STRUCTURAL INSPECTION DOCUMENT (SID)

The 727 SID is comprised of several sections that cover such items as elevator dimensions and station diagrams; general servicing requirements; related illustrations; zone diagrams; access doors and panels; recommended lubrication criteria; scheduled maintenance checks; and structural inspection recommendations.

For each type of maintenance check recommended, a basic package of specific maintenance recommendations is provided. These checks contain maintenance tasks considered appropriate choices to permit maintenance planners to develop airline maintenance programs. The maintenance tasks specified in the lower check(s) must be accomplished together with those of the next higher check(s); i.e., the "C" check also requires the accomplishment of a "preflight/transit," and "A" and "B" checks.

EXPLANATION OF TERMS

Check

A "check," as used in this document, means a maintenance action requiring thorough examination of an item for general condition, as applicable, with special emphasis directed to the following areas: proper attachment, safety wiring, cotter pins and fasteners, linkages, bearings, alignment, clearance tolerances, lubrication, obvious damage, cracks, blistering, delamination, fraying, excessive wear or play, corrosion, rubbing, aging, preservative coating or finish, cleanliness, and general appearance.

Corrosion Prevention

For metallic parts, Boeing Corrosion Prevention Manual D6-41910 provides general information on inspection, detection, corrosion removal, and preventive maintenance measures. The 727 corrosion-prevention tasks outlined in the reference manual are to be completed when called for in section 0-4 of this document. Also, it is imperative that aluminum parts located within 4 in of graphite/epoxy parts be repainted locally, if paint is found to have been removed.

For graphite/epoxy parts, all external surfaces and any surfaces within 4 in of aluminum parts are to be repainted as required when paint is found to have been removed. Also see Structural Repair Manual D6-48756 for additional corrosion prevention measures.

On-Condition (O/C)

"On-condition" maintenance is applicable to components on which a determination of continued airworthiness may be made by visual inspection, measurements, tests, or other means, without a teardown inspection or overhaul. On-condition checks are to be performed within time limitations and intervals prescribed for each check or inspection. Performance tolerances and wear or deterioration limits shall be contained in the air carriers' maintenance manuals. The periodic scheduled O/C checks must constitute meaningful determination of suitability for continued operation for another scheduled interval. If the check discloses enough evidence about the condition and failure resistance of the item to give assurance of reasonable probability of its continued airworthiness during the next check interval, the item is properly categorized as on-condition.

Wear/deterioration curves for components in the O/C category must be progressive, and not of a catastrophic nature. Otherwise, the determination of suitability for continued operation during another check interval cannot be made.

MAINTENANCE MAN-HOUR ESTIMATES

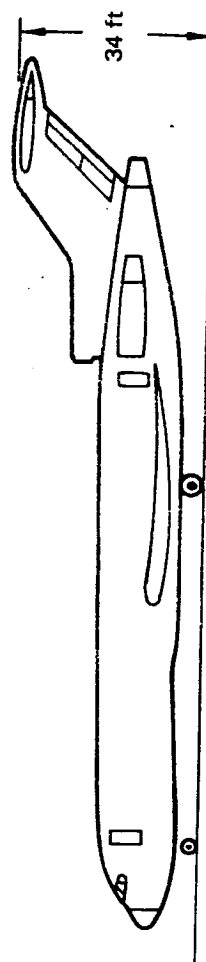
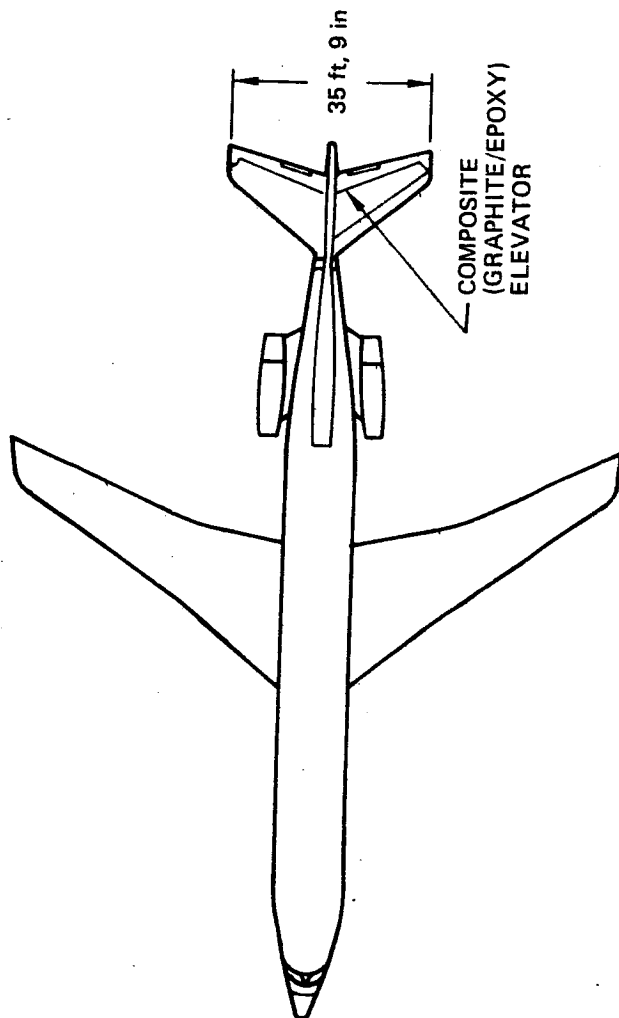
The maintenance task requirements contained herein show estimated time standards required to perform scheduled-type maintenance. Estimated work times are for the performance of listed tasks, and do not include removal or replacement of access doors and panels. Time standards shown in the "elapsed" columns take into consideration optimum use of manpower and equipment. Time estimates as shown in these chapters are based on best judgment factors, use of skilled personnel, and ready availability of required tools and equipment.

MAINTENANCE INSPECTION TIME INTERVALS

Manufacturers' recommendations for aircraft inspection check requirements for domestic operators are contained within this document, and are applicable for initial check intervals.

**SECTION 1-0
GENERAL INFORMATION**

	Page
Zone Diagram	3
Access Doors and Panels--Exterior	5
Recommended Lubrication Intervals	8



Dimensions and Areas, Ground-
Clearance Data, Selected Points,
727-200 Series

ZONE DIAGRAM

General

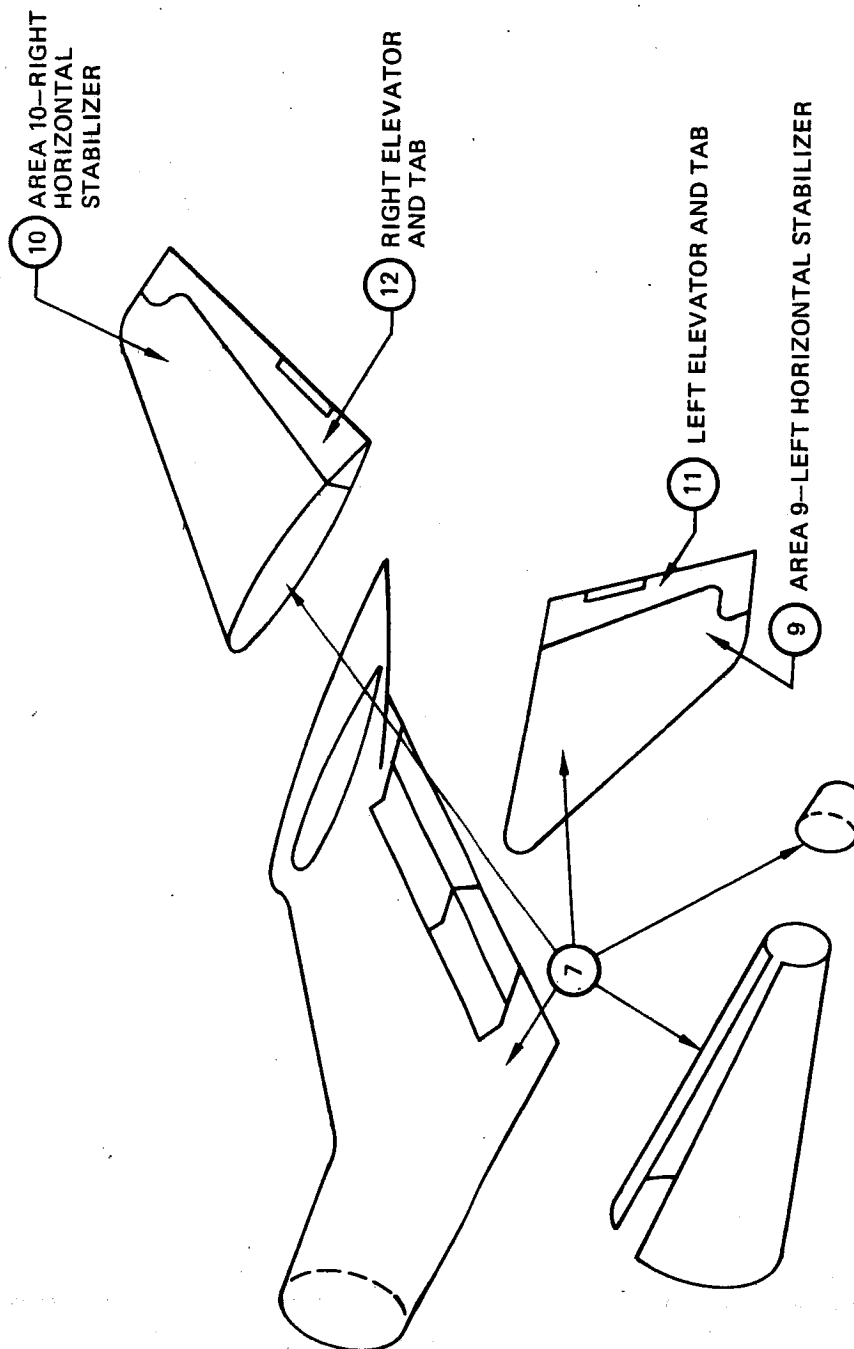
The 727 zone diagram is comprised of seven major zones covering the fuselage, wings, nacelles, and empennage. Further identification breakdown is achieved by use of areas, which denote specific compartments, equipment bays, doors, engines, etc., in conjunction with major zones.

Zone and Area Identification

The zone and area are identified by a number consisting of a first digit, indicating the zone, followed by a dash and a number of one or two digits, indicating the area. Thus, 7-11 is read zone 7, area 11, which identifies the empennage and the left side elevator and tab.

Zone Locations

- Zone 1 --upper half of fuselage (reference)
- Zone 2--lower half of fuselage (reference)
- Zone 3--left wing (reference)
- Zone 4--right wing (reference)
- Zone 5--left nacelle (reference)
- Zone 6--right nacelle (reference)
- Zone 7--empennage



Zone 7--Empennage

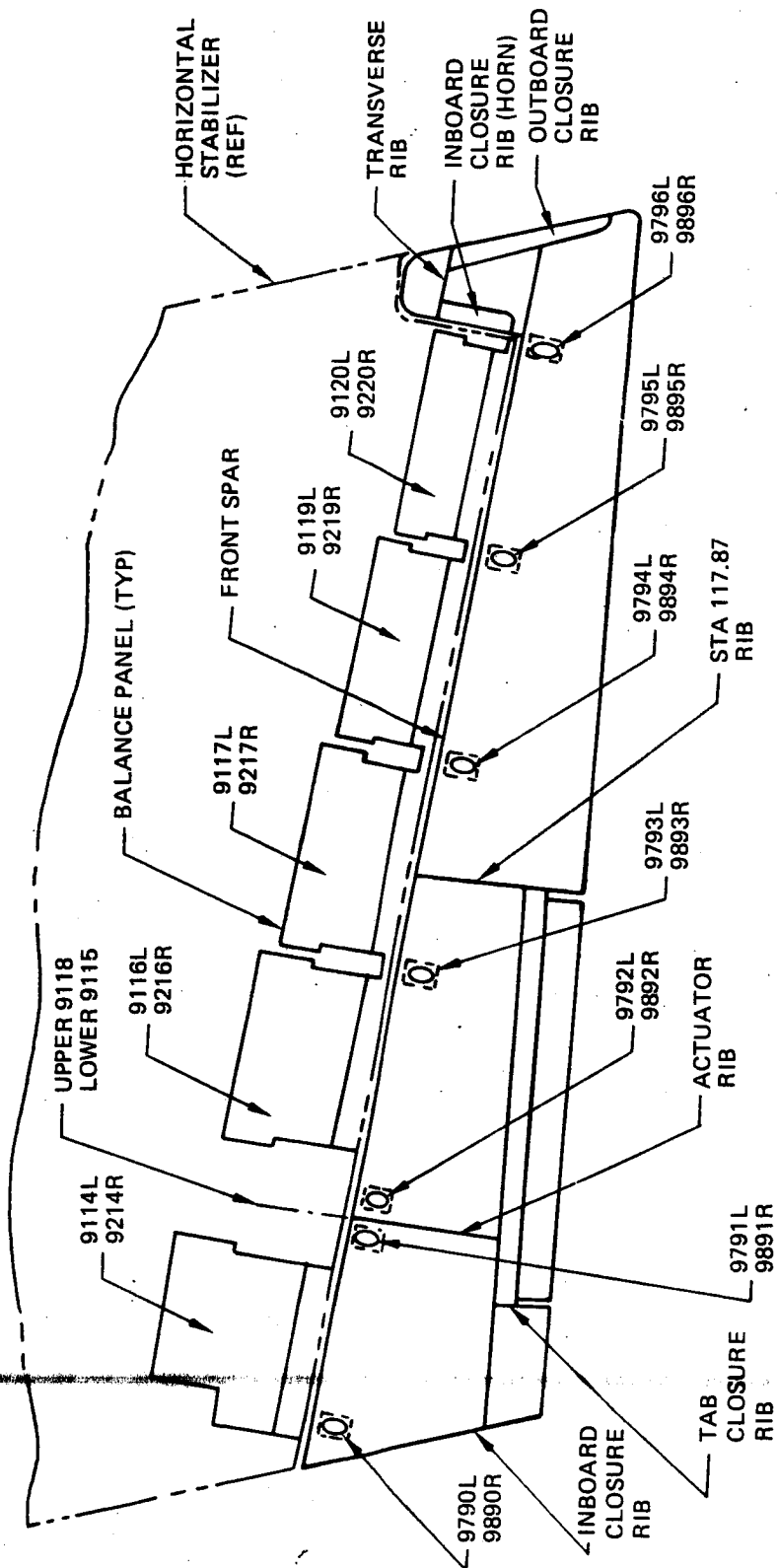
ACCESS DOORS AND PANELS—EXTERIOR

General

Access doors and panels have been assigned a four-digit number, in accordance with a procedure formerly used for identification and location. However, with the introduction of the zone and area diagrams for designating the location of aircraft components and work areas on maintenance work requirement cards, the zone and area concept is also used to designate the location of access doors and panels.

Implementation

To implement the above procedure in this document, an additional column listing the zone and area will be placed near the column listing access doors and panels. The last column lists the primary items or areas to which the panel provides maintenance access. Listings and illustrations appear in this section as shown in the following table.



Lower Surface, Elevator and Stabilizer—
Left Hand Shown, Right Hand Opposite

Access Doors and Panels

Panel number	Airplane section—elevator and horizontal stabilizer	Zone and area	Provides access to:
9114L	Trailing-edge access panel	7-9	Elevator balance panels and hinges
9214R	Trailing-edge access panel	7-10	Elevator balance panels and hinges
9115L	Trailing-edge access panel	7-9	Actuator fitting (lower)
9215R	Trailing-edge access panel	7-10	Actuator fitting (lower)
9116L	Trailing-edge access panel	7-9	Elevator balance panels and hinges
9216R	Trailing-edge access panel	7-10	Elevator balance panels and hinges
9117L	Trailing-edge access panel	7-9	Elevator balance panels and hinges
9217R	Trailing-edge access panel	7-10	Elevator balance panels and hinges
9118L	Trailing-edge access panel	7-9	Actuator fitting (upper)
9218R	Trailing-edge access panel	7-10	Actuator fitting (upper)
9119L	Trailing-edge access panel	7-9	Elevator balance panels and hinges
9219R	Trailing-edge access panel	7-10	Elevator balance panels and hinges
9120L	Trailing-edge access panel	7-9	Elevator balance panels and hinges
9220R	Trailing-edge access panel	7-10	Elevator balance panels and hinges
9790L	Access door	7-11	Thrust backup fitting
9890R	Access door	7-12	Thrust backup fitting
9791L	Access door	7-11	Actuator rib
9891R	Access door	7-12	Actuator rib
9792L	Access door	7-11	Actuator rib
9892R	Access door	7-12	Actuator rib
9793L	Access door	7-11	Hinge number 4 attachment fastener
9893R	Access door	7-12	Hinge number 4 attachment fastener
9794L	Access door	7-11	Hinge number 5 attachment fastener
9894R	Access door	7-12	Hinge number 5 attachment fastener
9795L	Access door	7-11	Hinge number 6 attachment fastener
9895R	Access door	7-12	Hinge number 6 attachment fastener
9796L	Access door	7-11	Hinge number 7 attachment fastener
9896R	Access door	7-12	Hinge number 7 attachment fastener

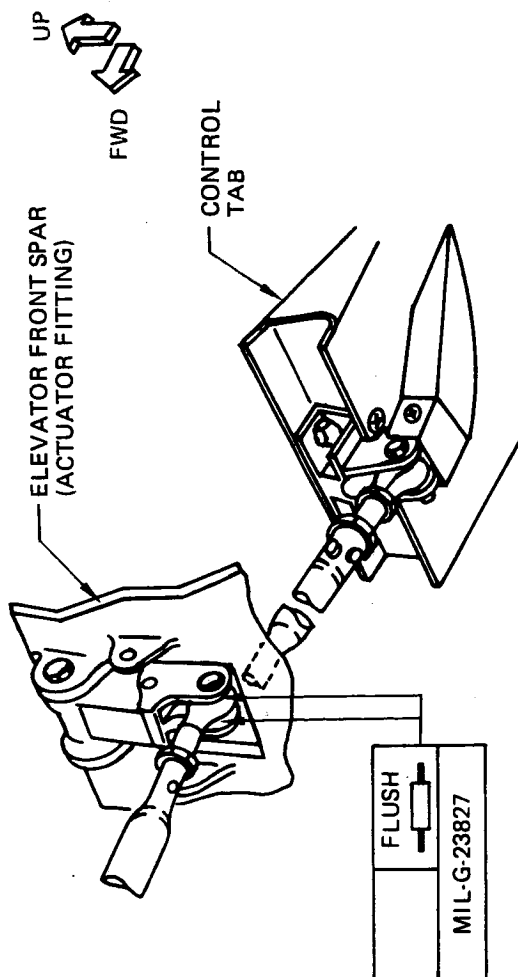
RECOMMENDED LUBRICATION INTERVALS

1. Lubrication intervals recommended in this document are primarily based on operating experience and manufacturers' recommendations.
2. Since the lubrication of certain items is critical, caution should be observed by individual airlines when considering escalation of lubrication intervals along with periodic escalation of maintenance-inspection intervals. Climatic conditions experienced in various parts of the world and specific airline maintenance schedules govern, to a large extent, the frequency of lubrication. Therefore, after sufficient operating experience is attained, each individual airline should determine the most efficient lubrication period.
3. The lubrication intervals associated with aircraft checks (A, B, C, etc.) are shown beside each lubrication block, which also provides the item to be lubricated, method of application, and type lubricant recommended.
4. Lubrication of sealed ball and roller bearings having lubrication provisions requires care to prevent seal blowout during lubrication. A restrictor type nozzle used on the grease gun will aid in preventing seal blowout by limiting the rate of grease flow. A Shafer N-2 nozzle, or equivalent, is recommended for flush-type fittings. The flow of grease should be discontinued at the first evidence of seal deformation or grease seeping from the bearing.

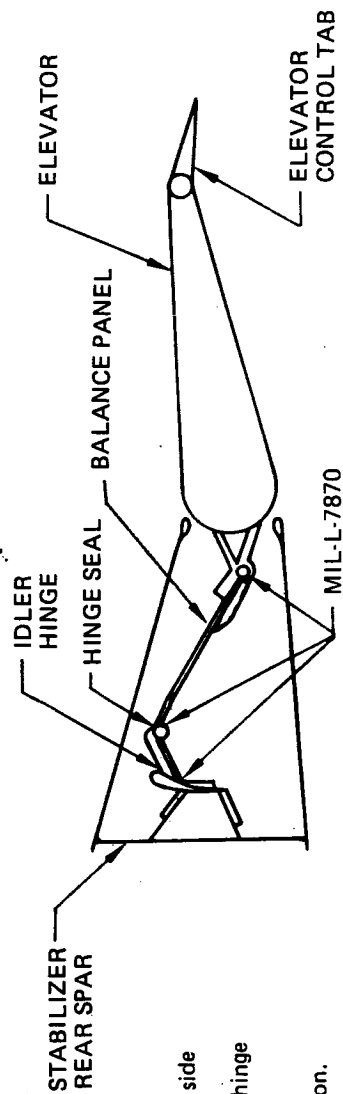
The use of a hand-operated grease gun is recommended.

5. Each 727 operator should refer to Chapter 12 of the Maintenance Manual for additional information on lubrication, and Chapter 20 for bearings and lubricants. In some cases, further information may be found in the related ATA system chapter of the Maintenance Manual.

Actuator Control Rod Lubrication



Elevator Balance Panel Lubrication



Note: Remove access cover and bolts on lower side of balance panel for access to all hinges. Following lubrication, install bolts and hinge seal. Install access cover. Exercise control surface during lubrication.

Elevator Lubrication
(Identical to Production Maintenance Document D6-8766)

SECTION 2-0
PREFLIGHT, TRANSIT, AND "A" CHECKS

	Page
Maintenance Checks	2
Preflight/Transit Check	3
"A" Check	4

MAINTENANCE CHECKS

The airline industry has categorized airplane "minor" maintenance tasks, using terminology such as preflight, transit, through service, overnight service, turnaround, station check, line check, daily inspection, etc. Boeing has elected to use the terms "preflight" and "transit" in this document to designate those minor maintenance checks performed at time intervals less than the "A" check.

Preflight Check

The preflight check, more comprehensive than the transit check, is intended for use at a route terminus, and includes all inspection items in the lesser transit check. A preflight check should be performed before the first flight of the day, or when an aircraft remains on the ground for 4 hr or more.

Transit Check

The transit check requires minor maintenance/servicing, and is intended to ensure continuous serviceability of a transiting aircraft. This check is planned for use at an en route stop, and is basically a walk-around inspection that requires a check of the aircraft interior and exterior for obvious damage, leaks, proper operating equipment, security of attachment, required servicing, etc.

"A" Check

The "A" check is considered a primary inspection and is intended to disclose the general condition of the aircraft. The "A" check is done in conjunction with the above mentioned lesser maintenance inspections. (Preflight and transit checks.)

The "A" check may be done at specified hourly or calendar time intervals.

Definitions of check, operational check, man-hour estimate criteria, etc., are provided in section 0-4 of this manual.

The preflight, transit, and "A" checks as shown herein are recommended minimum maintenance requirements, and may be augmented or revised accordingly by the operator.

Preflight/Transit Check

Model 727-200	Task			Reference	Location		Time		
	Check	Lubricate	Other		Zone and area		Hours and tenths		
							Elapsed	Man-hours	
From ground level, visually inspect elevator (walkaround check)	x						0.10	0.10	

"A" Check

Model 727-200	Task			Reference	Location		Time	
	Check	Lubricate	Other		Zone and area	Access panel number	Hours and tenths Elapsed	Man-hours
<p>Visually inspect the following items for delamination, missing fasteners, and security of installation:</p> <p>Elevator, control tab</p>	x			<p>See Structural Repair Manual D6-48756</p>	<p>7-11 7-12</p>		0.20	0.20

SECTION 3-0
"B" CHECK

Page

2

"B" Check

"B" CHECK

The "B" check is considered to be an intermediate check, and requires an examination of an aircraft to determine its general condition for assuring sustained airworthiness. This check includes selected operational checks, filter servicing, limited lubrication tasks, etc., and requires the opening of specific access doors and panels. The "B" check also requires accomplishment of all items contained in the "A" and preflight checks.

Refer to section 0-4 of this document for a definition of specific terms such as check and operational check, and general information concerning escalation of maintenance inspection intervals, warranty policy, etc. Entries that incorporate a "2" in the check column indicate that the item is to be checked at a "2B" inspection interval. Items designated "2B" are completed during every other "B" check.

The approximate number of man-hours required to open and close or remove and install access doors and panels for the "B" and "2B" check are 1.5 and 2.0 man-hours, respectively.

"B" Check

Model 727-200	Task			Reference	Location		Time	
	Check	Lubricate	Other		Zone and area	Access panel number	Hours and tenths	Man-hours
<ul style="list-style-type: none"> Inspect per D6-8766 								

SECTION 4-0
"C" CHECK

Page

2

"C" Check

"C" CHECK

General

1. The "C" check (periodic) requires a greater depth of inspection throughout the airplane to ensure continued airworthiness. This task involves selected operational/functional checks, and requires removal of access doors and panels, etc., to facilitate the inspection. Performance of the "C" check also requires accomplishment of all items included in the lesser checks.
2. Abbreviations appearing in this section include:

OP/C --operational check
F/C --functional check
3. For an explanation of terms such as check, corrosion prevention, etc., refer to section 0-4 of this document.
4. Zone locations shown in the following maintenance requirements sheets pinpoint specific work areas, and are further identified in the master zone diagram contained in section 1-0 of this document.

Thus, 2-19 in the "zone" location column means:
Zone 2--lower half of the fuselage
Area 19--aft cargo door
5. Entries listed under the "task" column in the ensuing maintenance requirements sheets indicate a requirement for visual operational/functional checks, lubrication, or other special maintenance such as servicing, filter replacement, corrosion prevention, etc.

Some entries under the "check" column may indicate 2, 3, through 13, etc. This type entry means that the specific maintenance requirement should be accomplished at the multiple "C" check interval indicated. Thus, a "6" in the check column means that the item is to be checked at each "6C" inspection interval, or every 6th "C" check.
6. Some task items require lubrication at recommended intervals and are so marked under the "lubricate" column. Appropriate system sketches, lubrication fittings, locations and types of lubricants required are shown in section 1-0 of this document.

7. The estimated work times are for performance of individual "C" check items and do not include the time to position work stands and equipment, or remove and replace access doors and panels. The estimated time standards shown in the "elapsed" columns take into consideration optimum use of manpower and equipment. These standards are based on best judgment factors, use of skilled personnel, and ready availability of tools and equipment.

The following estimated man-hours are required to open and close or remove and replace doors or access panels in the accomplishment of "C" and multiple "C" checks:

Check	Man-hours
C	4
2C	4

"C" Check

Model 727-200	Task			Reference	Location		Time	
	Check	Lubricate	Other		Zone and area	Access panel number	Elapsed	Hours and tenths
<ul style="list-style-type: none"> Left-hand and right-hand elevator (internal) visual inspection <ul style="list-style-type: none"> Inspect front spar, particularly around the actuator fitting, for obvious damage, delamination, loose or missing fasteners, and corrosion. Similarly inspect the rear spar Inspect all inspar ribs for missing paint, blisters, and condition Horn balance weight Balance panels. Check seals for signs of wear. Examine balance panels for deterioration of finish and evidence of corrosion Elevator hinge fittings. Check for corrosion, and teflon sliding bushings. Check fillet seals and any loose fasteners Check balance panel aft hinges and elevator hinge fittings for conditions that would inhibit free spanwise movement between elevator and stabilizer. Reinstall access panels 	x			See Structural Repair Manual D6-48756	7-11 7-12	9114 9214 9116 9216 9117 9217 9119 9219 9120 9220 9790 9890 9791 9891 9792 9892 9793 9893 9794 9894 9795 9895 9796 9896	4	8
	2	2	Corrosion prevention	1 See section 0-4				

1 For metallic parts only, see Corrosion Prevention Manual D6-41910 (sec. 55-00-37)

"C" Check

Model 727-200	Task			Reference		Location		Time	
	Check	Lubricate	Other			Zone and area	Access panel number	Elapsed	Hours and tenths Man-hours
<p>● Left-hand and right-hand elevator (external) visual inspection</p> <p>a. Inspect elevator for missing paint, impact damage (indentations or small cracks), delamination or blistering of skin, particularly in areas adjacent to the hinge fittings and actuator fitting, and along the trailing edge</p> <p>b. Inspect the aluminum lightning strip on the upper skin panel outboard of station 190 for indications of lightning strike or corrosion. Check condition of fillet seal.</p>				See Structural Repair Manual D6-48756				1	2
				See Structural Repair Manual D6-48756				1	2
<p>● Left-hand and right-hand elevator control tab visual inspection</p> <p>a. Inspect tab for missing paint, blistering, impact damage (indentations or small cracks), or delamination of skin, particularly in areas of tab hinge fittings and tab control rod</p> <p>b. Inspect tab hinge fittings</p> <p>Note: Missing paint, blistering, etc., will allow water to collect, freeze, and cause damage to the elevators and tabs. Therefore, if any honeycomb structure shows signs of these discrepancies it is recommended that NDT methods be used. Contact Boeing for these methods.</p>									

APPENDIX

Enclosed is a method of examining the internal elevator structure, without resorting to a teardown inspection or overhaul.

This method has been developed by Boeing Quality Control Research and Development. It has been tried, and has been found to give satisfactory results. This method, therefore, is enclosed with the intention that it will be used primarily as a guideline example of inspection.

RADIOGRAPHIC INSPECTION

The radiographic inspection technique for inspection of honeycomb inspar ribs in graphite/epoxy elevator is as follows:

Purpose: To inspect graphite/epoxy elevators for moisture in the honeycomb vertical inspar ribs.

Equipment: Any X-ray machine that is capable of operating in the range of 20 kV to 30 kV.
Any film that is Kodak Type M or equivalent.

Preparation: Use MEK or acetone to remove contaminants from exterior elevator surface. WIPE SURFACE CLEAN.

Inspection: Make radiographic exposures following the recommendations given in Table 1 and Details 2 through 5. See the appendix for examples showing typical conditions and indications.

If moisture is indicated, further investigation is required to determine location. Radiograph the rib area at a 90-deg angle to the skin surface per Table 2 and Detail 6. Indications present in the vertical shot would imply that the moisture is in the upper or lower skin. Absence of indications in the vertical shot implies that the moisture is in the rib.

Table 1. Radiographic Exposure Recommendations for Skin Panels

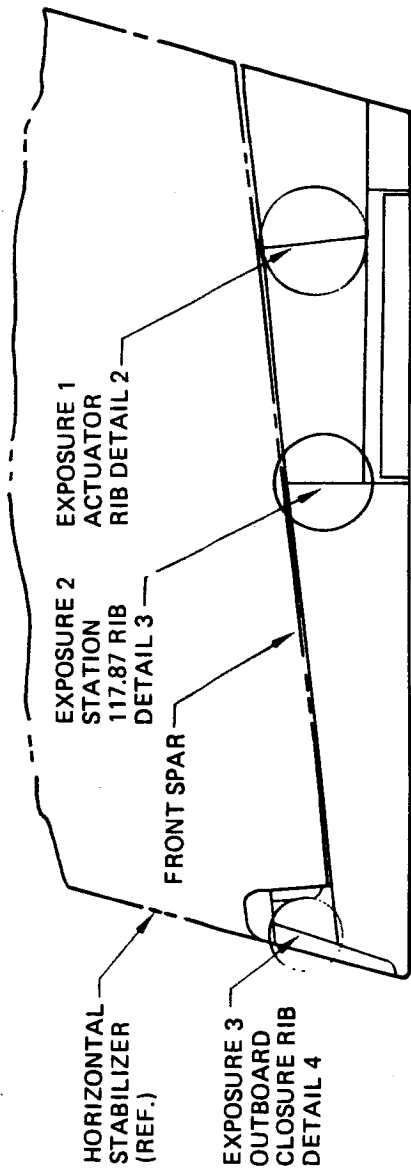
Exposure number	Film			SFD* (in)	Generator settings	
	Number	ASTM class	Size (in)		kV	mAs
1	1 and 2	I	14 x 17	40	28-30	1,108
2	1 and 2	I	10 x 12	40	28-30	1,008
3	1 and 2	I	10 x 12	40	28-30	1,108
4	1 and 2	I	10 x 12	40	28-30	1,108
5	1 and 2	I	10 x 12	40	28-30	1,008
6	1 and 2	I	14 x 17	40	28-30	1,108
7	1, 2, and 3	I	10 x 12	40	28-30	900

*Source-to-film distance

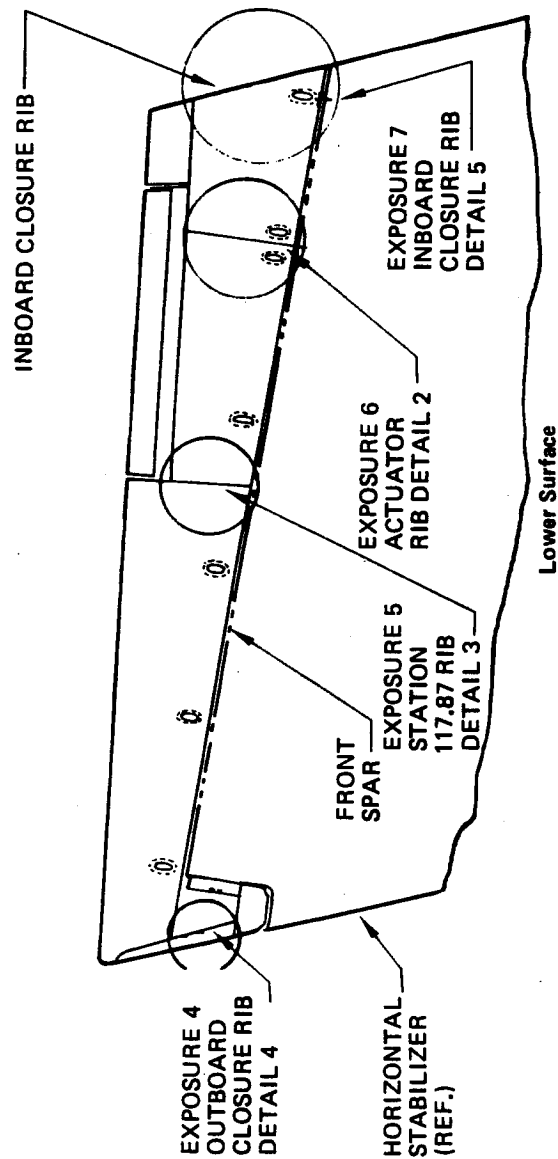
Table 2. Radiographic Exposure Recommendations for Ribs

Exposure number	Film			SFD* (in)	Generator settings	
	Number	ASTM class	Size (in)		kV	mAs
8	1 and 2	I	14 x 17	40	28-30	900

*Source-to-film distance

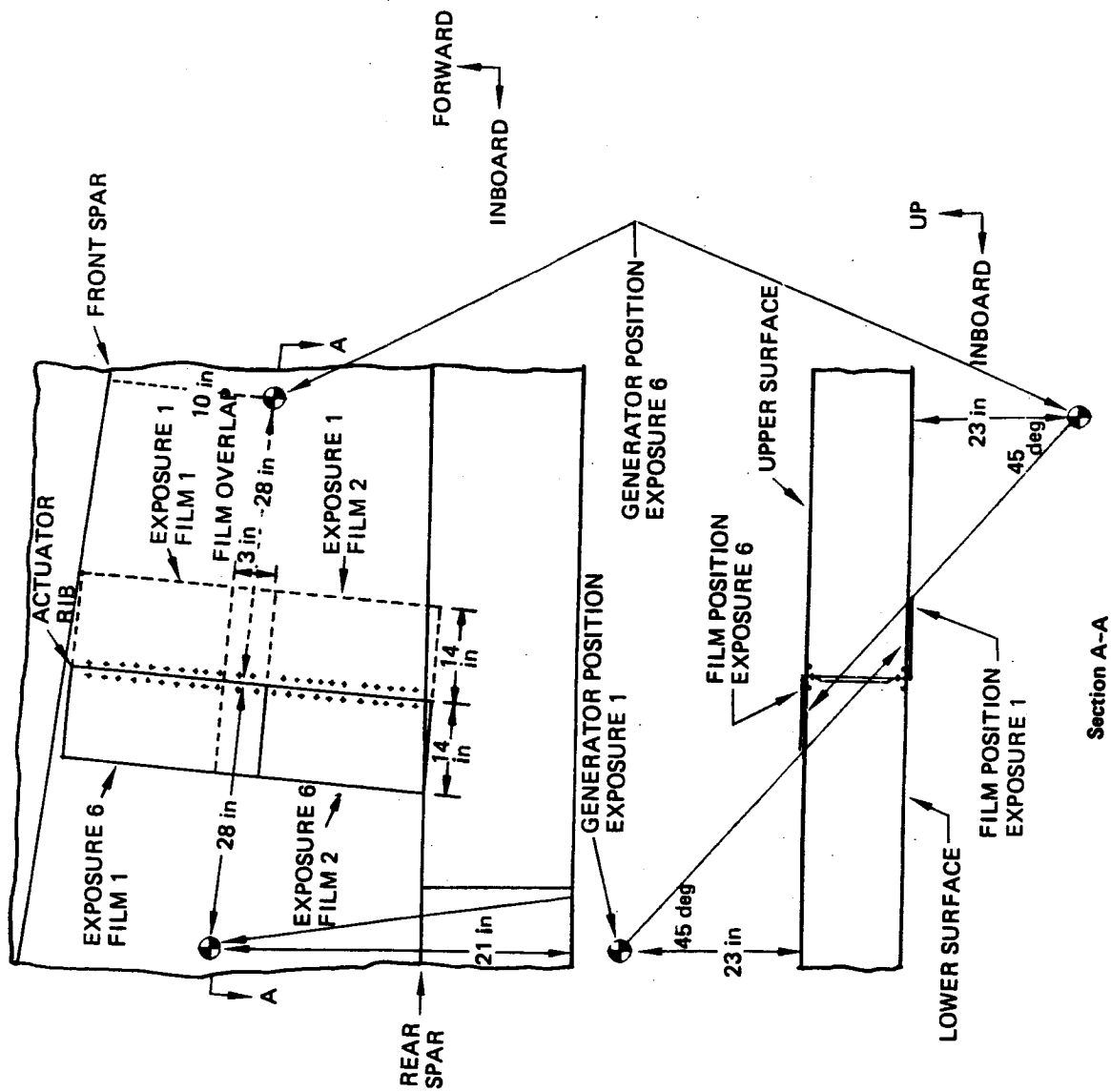


Upper Surface

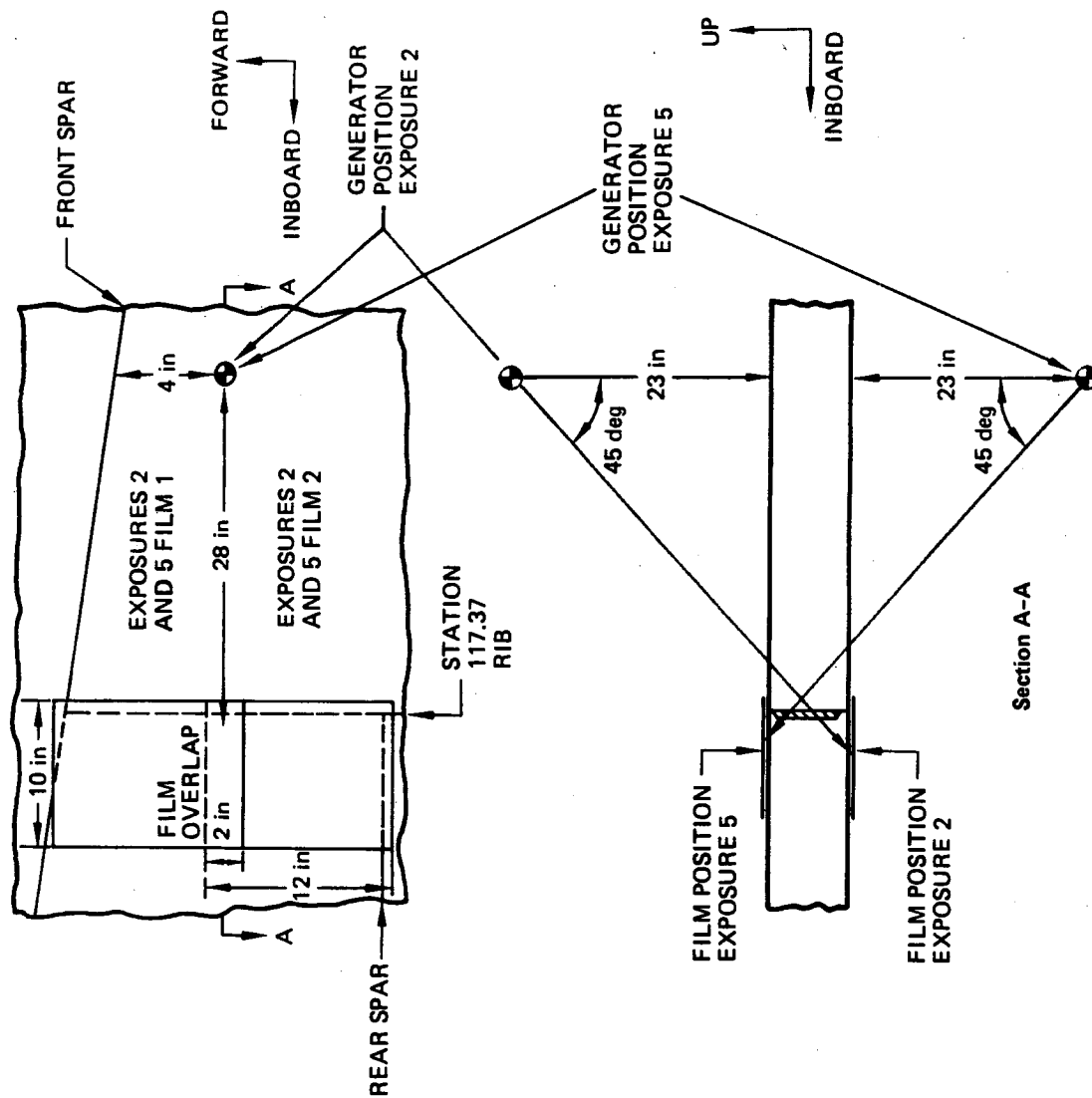


Lower Surface

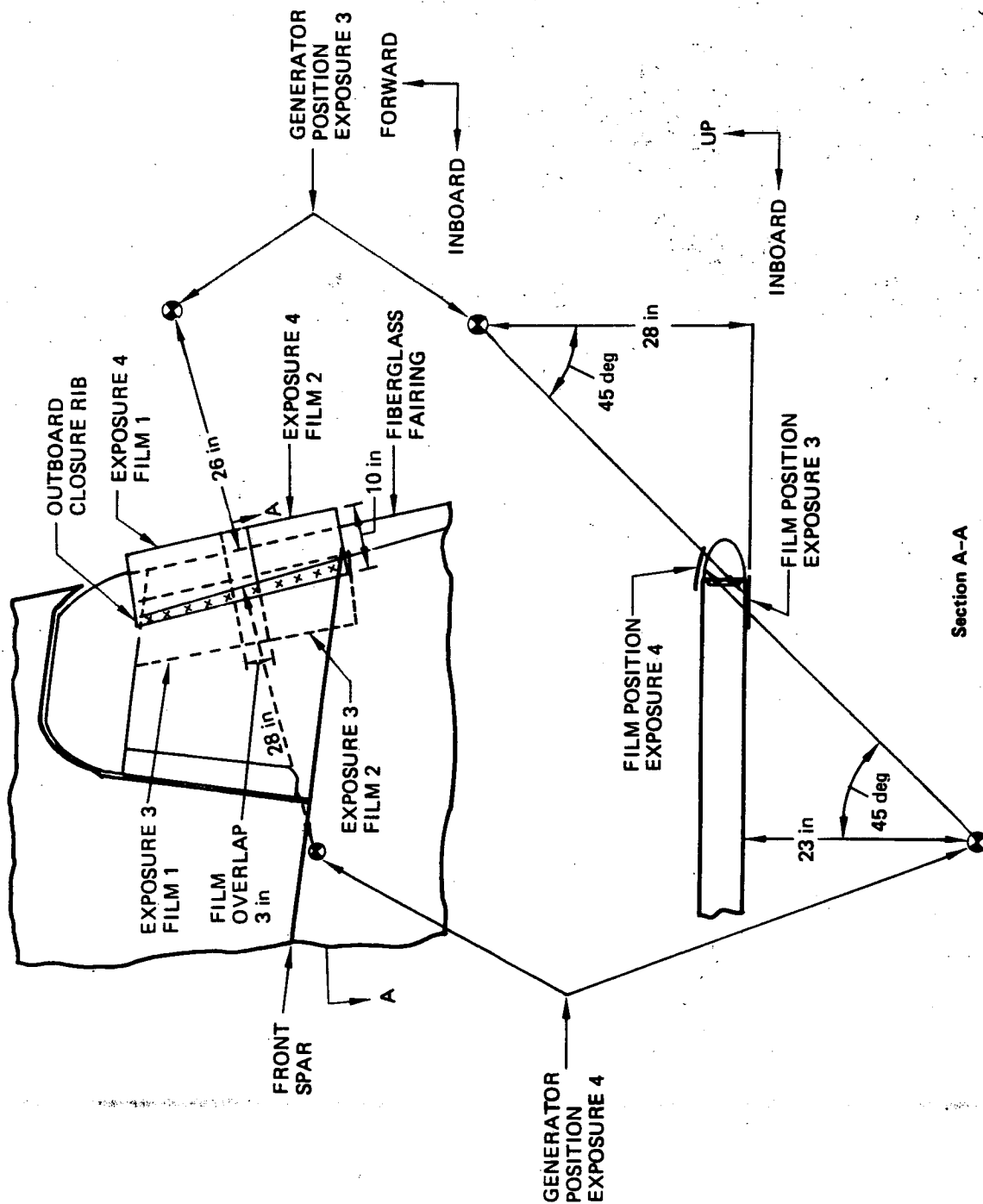
Detail 1. Graphite/Epoxy Elevator Exposure Positions (Left Hand Shown, Right Hand Similar)



Detail 2. Graphite/Epoxy Elevator Rib, Station 58.57, X-Ray Generator and Film Positions, Exposures 1 and 6 (Right Hand Shown, Left Hand Similar)

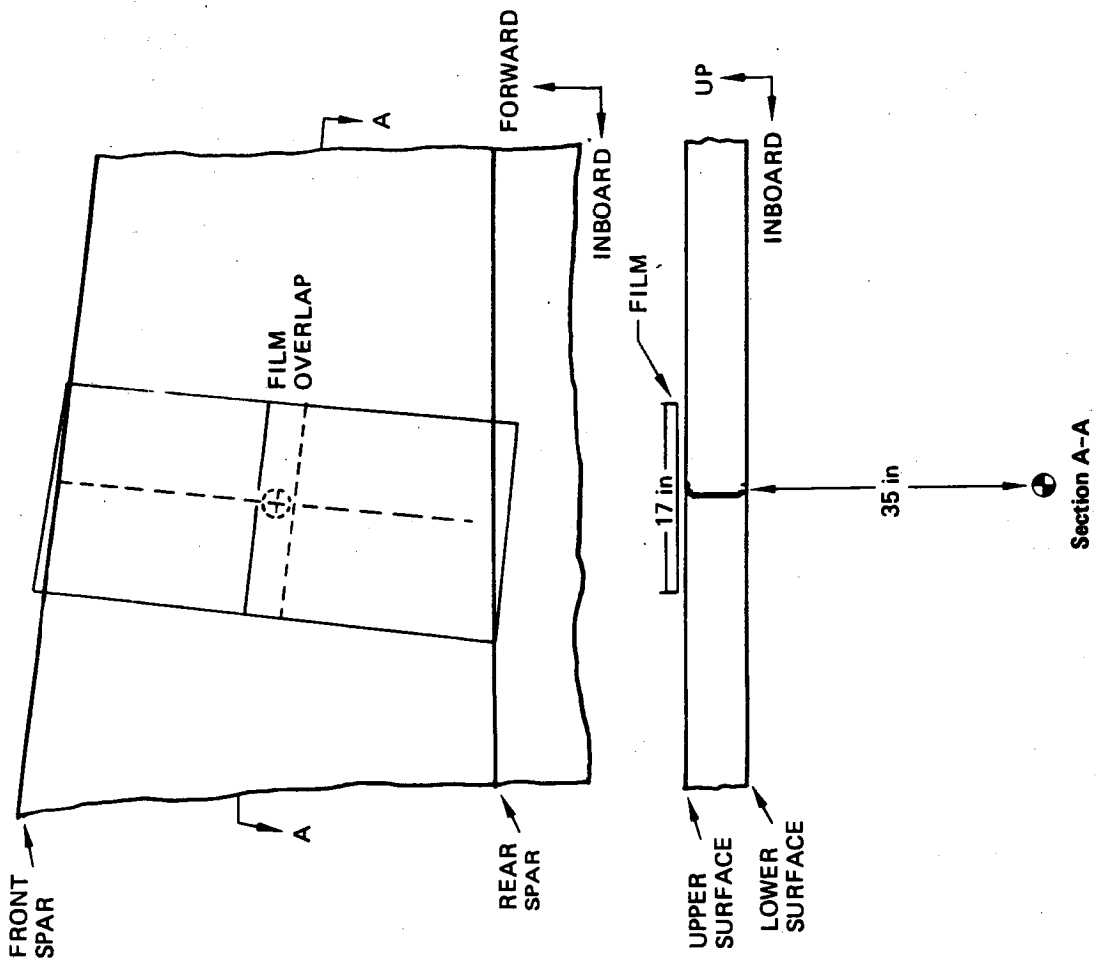


Detail 3. Graphite/Epoxy Elevator Rib, Station 117.37, X-Ray Generator and Film Positions, Exposures 2 and 5 (Right Hand Shown, Left Hand Similar)



Detail 4. Graphite/Epoxy Elevator Rib, Stabilizer BL 210.18, X-Ray Generator and Film Positions, Exposures 3 and 4 (Right Hand Shown, Left Hand Similar)





Detail 6. Vertical Shot as Required for Additional Investigation (Typical)

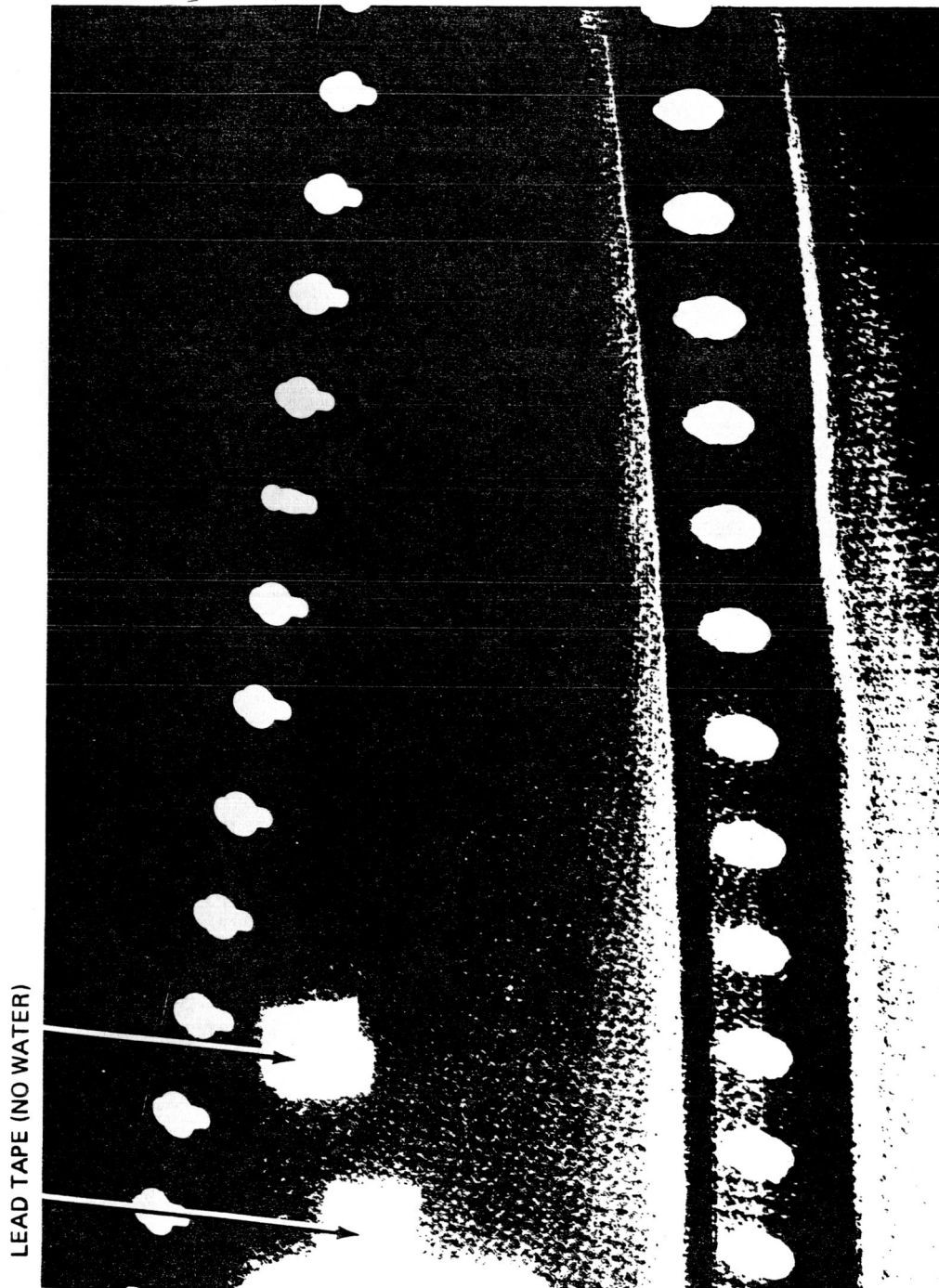


Figure 1. Moisture-Free Inboard Closure. Radiograph Taken per Detail 5

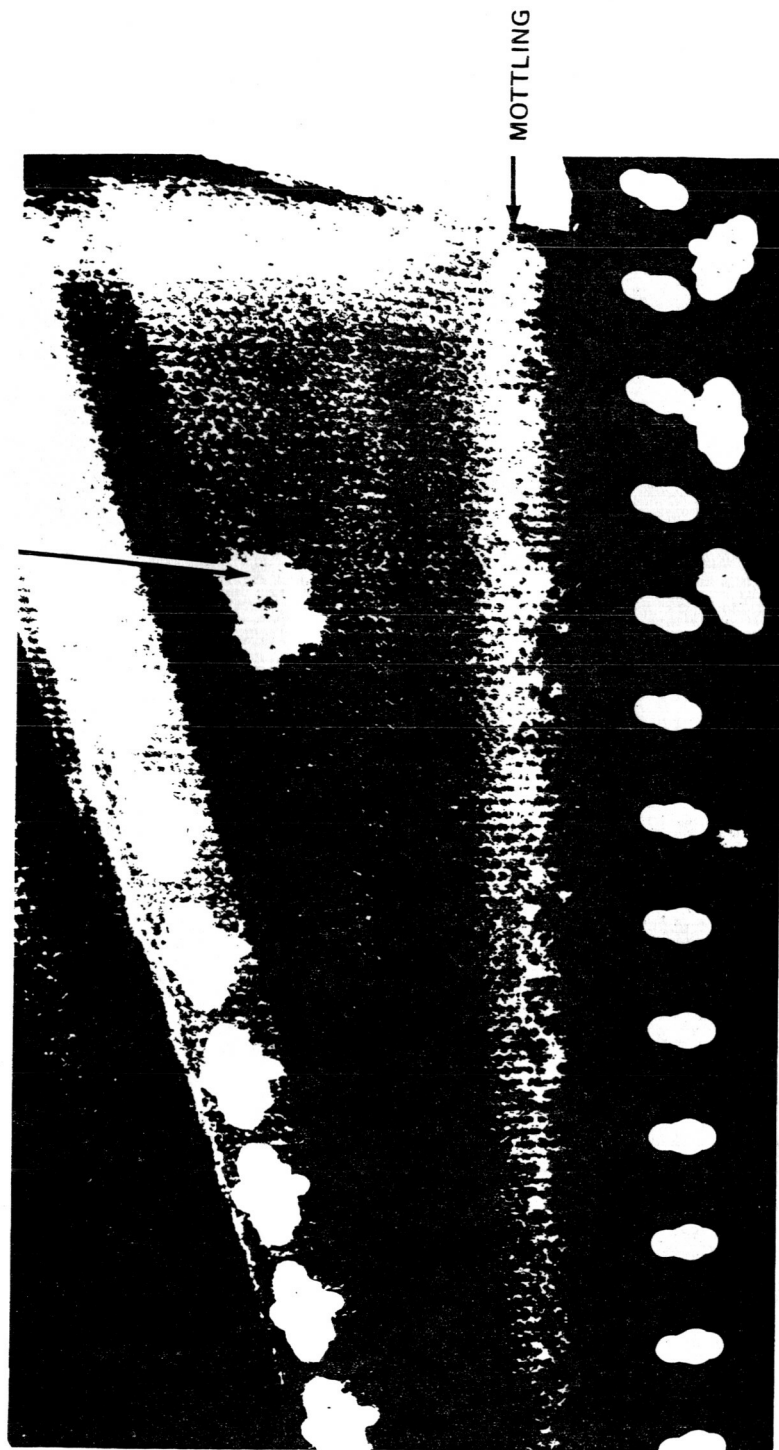
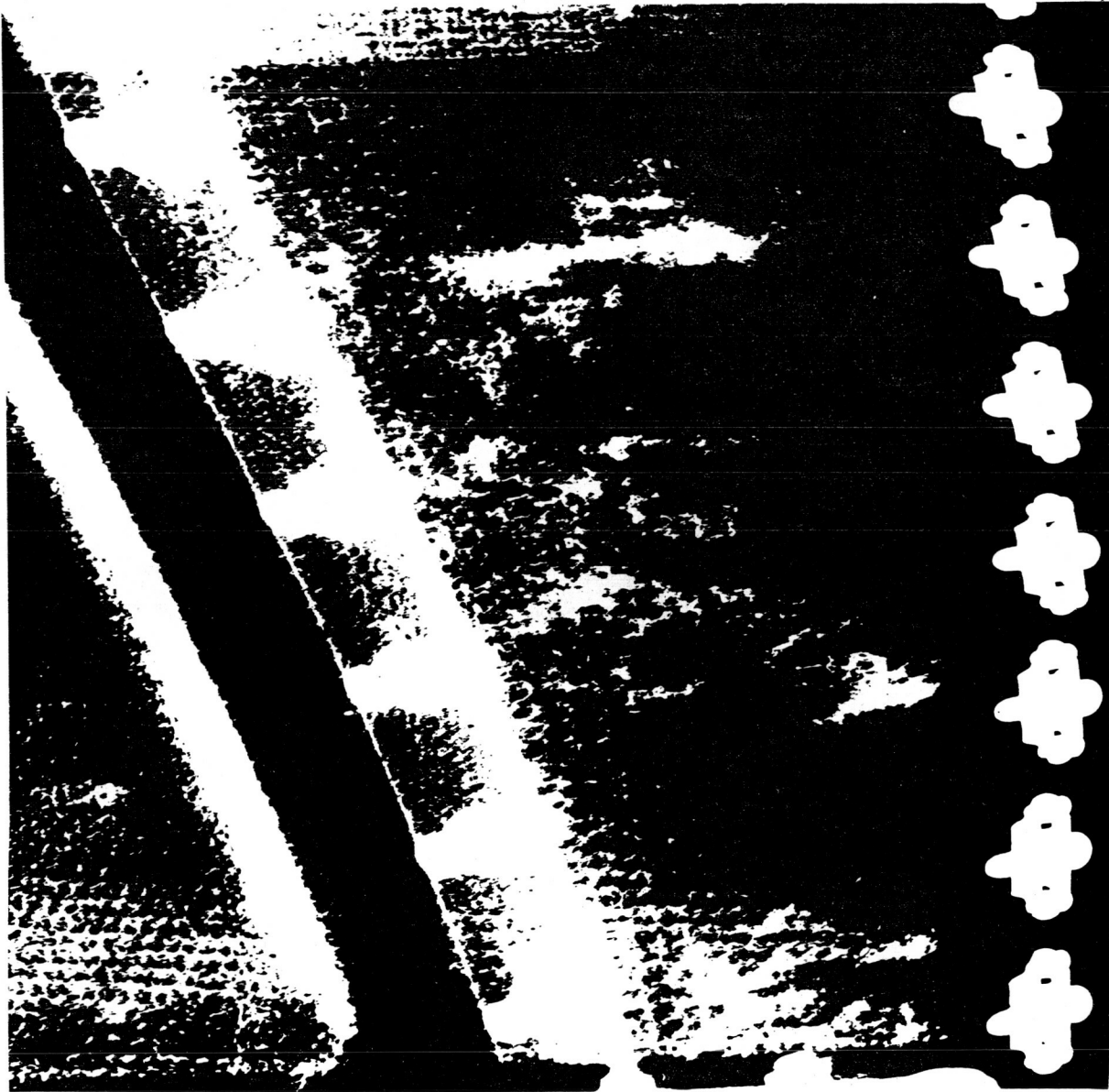


Figure 2. Moisture-Filled Area Indication (Top) and Mottling Due to Variables in Part.
Radiograph Taken per Details 2 Through 4



*Figure 3. Mottling Due to Variations in Elevator or Contamination on Interior Skin Surfaces—No Water.
Radiograph Taken per Details 2 Through 4*

APPENDIX B

D6-48756

**STRUCTURAL REPAIR MANUAL—
727 GRAPHITE/EPOXY ELEVATOR**

BOEING COMMERCIAL AIRPLANE COMPANY
A DIVISION OF THE BOEING COMPANY
SEATTLE, WASHINGTON

DOCUMENT NO. D6-48756

TITLE: STRUCTURAL REPAIR MANUAL - 727 GRAPHITE/EPOXY ELEVATOR

MODEL 727

ISSUE NO. _____ TO: _____ (DATE) _____

J18-047

PREPARED BY	<u>G. N. Roe / J. T. Parsons</u>	<u>8-2-79</u>
SUPERVISED BY	<u>H. Syder / R. Baum</u>	<u>8/15/79</u>
APPROVED BY	<u>J. E. McCarty</u>	<u>8/28/79</u>
APPROVED BY	<u>S. T. Harvey</u>	<u>8/28/79</u>
	_____	_____
	_____	_____ (DATE)

DI 4100 7880 REV. 9/79

REV SYM

DI 4100-00 ORIG. 3/71

LIST OF ACTIVE PAGES															
SECTION	PAGE NUMBER	REV SYM	ADDED PAGES					SECTION	PAGE NUMBER	REV SYM	ADDED PAGES				
			PAGE NUMBER	REV SYM	PAGE NUMBER	REV SYM	PAGE NUMBER				REV SYM	PAGE NUMBER	REV SYM	PAGE NUMBER	REV SYM
1	1.1	A													
	1.2														
	1.3	A													
	1.4														
	1.5														
2	2.1														
	2.2														
	2.3														
	2.4														
	2.5														
	2.6	B													
	2.7														
	2.8	B													
	2.9														
	2.10	B													
3	3.1														
	3.2														
	3.3														
4	4.1														
	4.2														
	4.3														
	4.4														
	4.5														
	4.6														
	4.7														
	4.8														
	4.9														
	4.10														
	4.11														
	4.12														
	4.13														
	4.14	C													
	4.15	C													
	4.16														
	4.17														
	4.18														
	4.19	C													
	4.20	C													
	4.21														
	4.22														
	4.23														
	4.24	C													
	4.25	C													
	4.26														
			5.0												
			5.1	A											

REV SYM C

LIST OF ACTIVE PAGES																		
SECTION	PAGE NUMBER	REV SYM	ADDED PAGES						SECTION	PAGE NUMBER	REV SYM	ADDED PAGES						
			PAGE NUMBER	REV SYM	PAGE NUMBER	REV SYM	PAGE NUMBER	REV SYM				PAGE NUMBER	REV SYM	PAGE NUMBER	REV SYM			
A	A1.1																	
	A1.2																	
	A1.3																	
	A1.4																	
	A1.5																	
	A1.6																	
	A1.7																	
	A1.8																	
	A1.9																	
	A1.10																	
	A1.11																	
	A1.12																	

D1 4100 7700 ORIG. 3/71

REV SYM

J18-047

REVISIONS			
REV SYM	DESCRIPTION	DATE	APPROVAL
A	1. Added information for replacement of loose or missing fasteners. 2. Added allowable damage criteria.	11-1-9	Prepared by: <i>21 R. e.</i> Approved by: <i>G. L. M. 11/1/79</i> Approved by: <i>11/1/79</i>
B	1. Indicated thermocouple requirement is a minimum requirement. 2. Added tolerance to cure temperature.	11-19-9	Prepared by: <i>Donald R. Lee 11/26/79</i> Approved by: <i>11/26/79</i> Approved by: <i>11/26/79</i>
C	1. Revised weight limitations for Control Tabs. 2. Revised the elevator surface required moment to accept heavier Control Tabs.	11-14-9	Prepared by: <i>John J. S. 11/14/79</i> Approved by: <i>11/14/79</i>

D1 4100 7720 ORIG. 3/71

REV SYM C

TABLE OF CONTENTS

<u>SECTION</u>	<u>TITLE</u>	<u>PAGE</u>
1	GENERAL	1.0
2	REPAIR PROCEDURES	2.0
3	REPAINT CLEANING, PRETREATMENT AND PAINTING OF SURFACES	3.0
4	REBALANCE PROCEDURES AFTER REPAIR	4.0
5	FASTENERS	5.0
APPENDIX 1	EXAMPLES OF REPAIRS MADE TO GRAPHITE/ EPOXY COMPONENTS	A1.1

1. GENERAL

- A. This document contains repair procedures for the 727 graphite/epoxy elevator. The major components (ribs, skins, and spars) of this elevator are fabricated of several layers of graphite tape or graphite woven fabric using an epoxy resin matrix. Solid laminates and sandwich panels stiffened with a non-metallic (Nomex) core are used in the elevator. The location of the principal components of the elevator are shown in Figure 1.1.

The limitations of damage which may be repaired using techniques in this document are shown in Figure 1.2. Repair of damage to the elevator exceeding the criteria of Figure 1.2 or repair of solid laminate is considered a special condition and requires coordination with the Boeing Engineering Department.

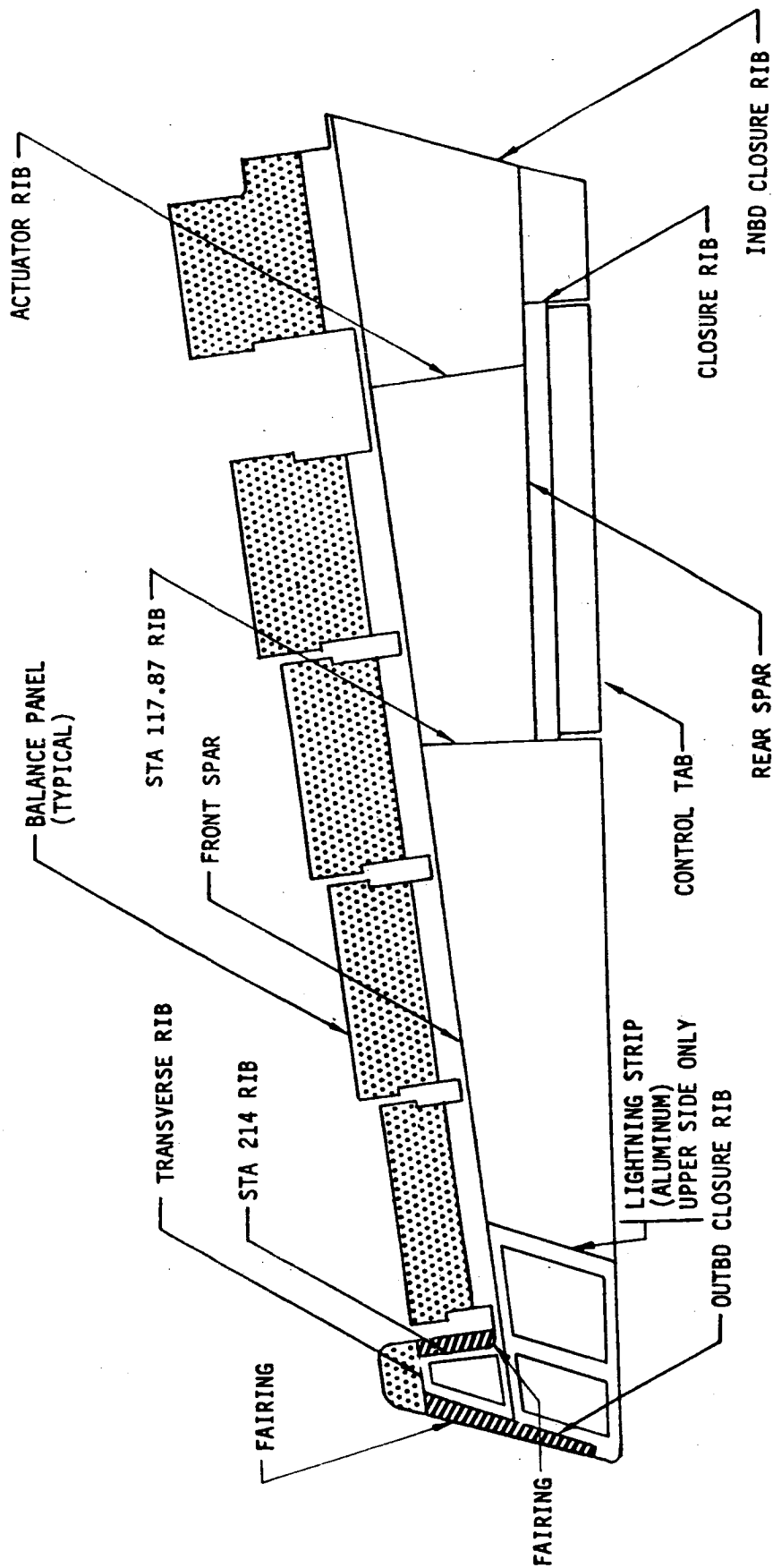
Damage to the face sheets of honeycomb panels may be repaired by bonding a precured graphite/epoxy fabric patch over the damaged area using a 250°F cure with 20 inches of mercury vacuum pressure. See Section 2 for repair procedures and materials.

Replace loose or missing fasteners per Section 5 herein.

To repair the metal components of the elevator use the instructions of D6-4062, "727 Structural Repair Manual" except there are different repair limitations due to different weight and balance requirements. See Section 4 herein.

- B. See Section 3 for elevator refinishing procedures, materials, and limitations.

WARNING: FLIGHT SAFETY DEMANDS THAT THE ELEVATOR AND ELEVATOR TAB SYSTEMS CONTROL SURFACES BE PROPERLY BALANCED AT ALL TIMES.



MATERIAL

GRAPHITE/EPOXY

METAL

FIBERGLASS

NOTE: ALL RIBS AND SPARS ARE GRAPHITE/EPOXY

FIGURE 1.1 - 727 GRAPHITE/EPOXY ELEVATOR

<u>COMPONENT</u>	<u>CONSTRUCTION</u>	<u>ALLOWABLE² DAMAGE</u>	<u>REPAIRABLE DAMAGE</u>	
			<u>MAXIMUM SIZE</u>	<u>MINIMUM SPACING (EDGE TO EDGE)</u>
¹ Skin, Control Tab, Inboard and Outboard Closure Ribs	Graphite/Epoxy Face Sheet, Nomex Honey- comb	Single Face Sheet Damaged 1 Square Inch Damage or 3 Inch Maximum Dimension Allowed For One Flight Only Provided The Damage Is Sealed From Moisture And Sunlight By Use Of No. 850 Scotchcal Tape	Longest Dimension 3 Inches	10 Inches

NOTE 1 - Repair of damage adjacent to lightning strip is permitted as long as edge of patch does not interfere with the lightning strip. Repair of damage under aluminum lightning strip on upper surface requires coordination with the Boeing Engineering Department.

NOTE 2 - Damage includes paint abrasion, delamination, erosion, dents, gouges, scratches and punctures.

FIGURE 1.2 - REPAIR INDEX FOR GRAPHITE REINFORCED
EPOXY ELEVATOR COMPONENTS

- C. Repairs made to the elevator or elevator control tab or repainting of either component will require a check of the elevator or tab balance according to Section 4.

CAUTION: REPAIRS MADE TO CONTROL SURFACES AND/OR ADJACENT STRUCTURE MUST NOT INTERFERE WITH THE DESIGNED OPERATION OF THE CONTROL SURFACE. DAMAGE TO THE AIRPLANE MAY OCCUR.

- D. Check all repairs for interference with operation of control surfaces.

CAUTION: REPAIRS MUST NOT COVER ANY DRAIN HOLES IN PANELS. A CORROSIVE ENVIRONMENT OR POSSIBLE OUT OF BALANCE CONDITION MAY OCCUR IF DRAIN HOLES ARE COVERED.

- E. If repair covers drain hole, drill through repair at existing location.

NOTE: Drain holes are .375 inch in diameter. Refer to Figure 1.3 for location.

- F. Refer to D6-4062, 51-70 for aerodynamic smoothness requirements.

CAUTION: EPOXY RESIN IN GRAPHITE/EPOXY MATERIAL EXPOSED DIRECTLY TO ULTRAVIOLET RADIATION, E.G., SUNLIGHT, BREAKS DOWN LOSING STRUCTURAL STRENGTH.

- G. Repaint all repairs made to the elevators per Section 3 herein.

REV SYM

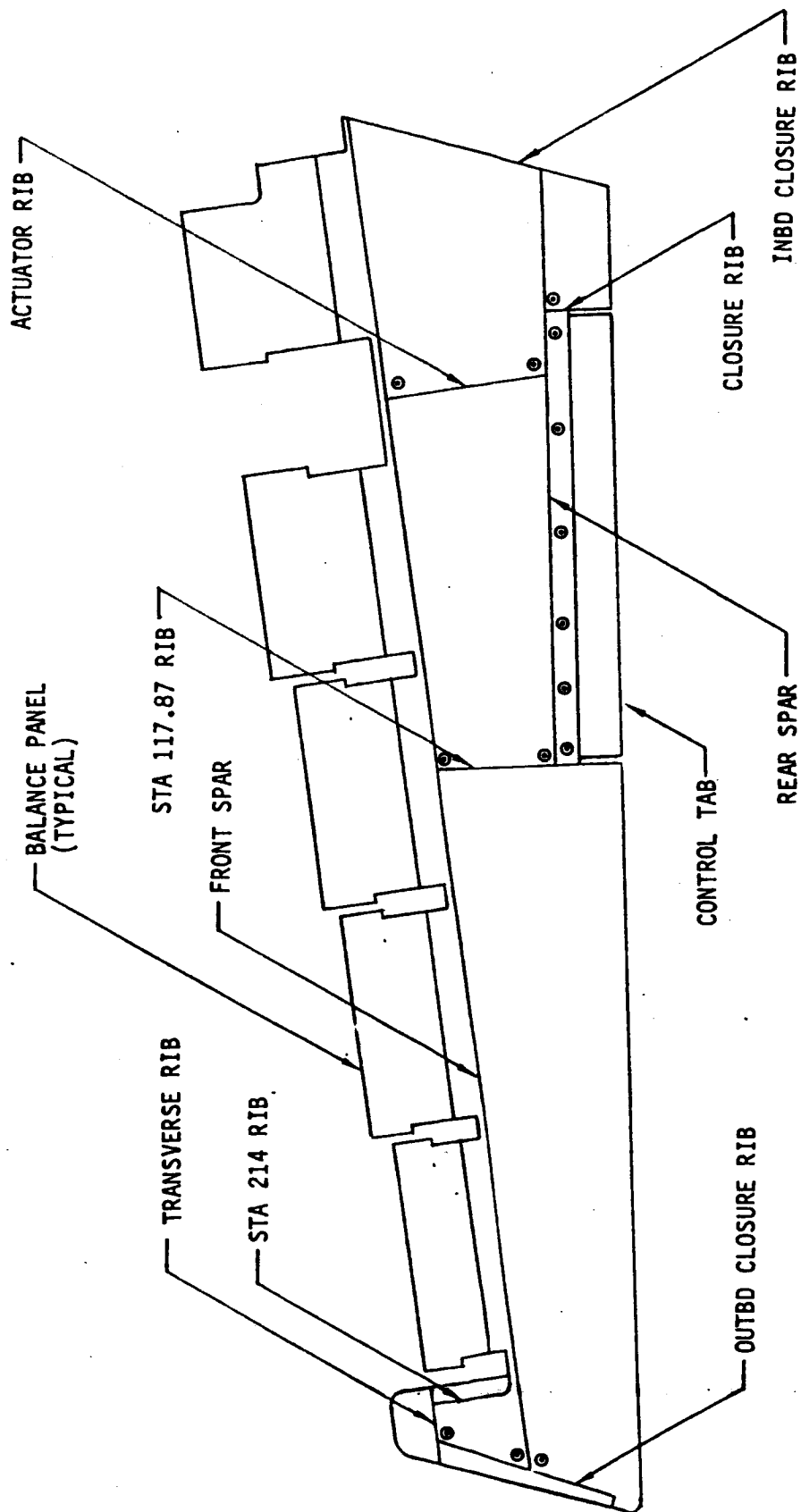


FIGURE 1.3 - DRAIN HOLE LOCATIONS IN THE 727 GRAPHITE/EPOXY ELEVATOR

- INDICATES A .375 INCH DIAMETER DRAIN HOLE LOCATION IN LOWER SURFACE

2. REPAIR PROCEDURES

A. Materials

Only preimpregnated graphic fabric shown in Figure 2.1 may be used to replace damaged graphite plies. The film adhesive shown in Figure 2.1 shall be used to bond core to face sheets or precured patches to face sheets when repairing honeycomb sandwich structure.

Precured patches shall be fabricated using two plies of epoxy resin impregnated woven fabric per BMS 8-212 (plus one ply of Style 120 preimpregnated fiberglass per BMS 8-139 if any portion of the patch will be within four inches of the aluminum lightning strip.) In between the plies of graphite/epoxy fabric place one layer of BMS 8-245 Grade 08 adhesive film. See Figure 2.2 for configuration of precured patches. Vacuum bag the layup and autoclave cure per Figure 2.3.

In addition the materials including supporting equipment (except fabrics and laminating resins) shown in D6-4062, 51-40-09 may be used in repair of graphite/epoxy components.

B. Full Depth Honeycomb Repair - Single Face Sheet Repair (Figure 2.4 and Figure 2.5)

- (1) Determine the extent of damage in accordance with D6-4062, 51-40-09.
 - (a) Check panel in vicinity of damage for entry of water, oil, fuel, dirt or other foreign matter.
 - (b) Check for delamination around the damage.
- (2) Mask over damaged area to prevent tape fibers on surface from delaminating when face sheet damage is removed. Mask off area for a distance of 1.50 inches minimum from edge of damage.
- (3) Removal of Damage.
 - (a) Cut the damaged face sheet to a smooth outline using a sharp knife or rotary carbide cutting disk. Remove

<u>MATERIAL</u>	<u>BOEING MATERIAL SPECIFICATION (BMS)</u>	<u>APPROVED SOURCE</u>	<u>SUPPLIER'S PRODUCT DESIGNATION</u>
Graphite Fabric Pre-impregnated With Epoxy Resin	BMS 8-212, Type II, Class 2, Style 3K-70-P	Narmco Materials, Inc. 600 Victoria Street Costa Mesa, Ca. 92627	Rigidite 5208 Woven T-300 Style 3K-70-P -35 Percent
Filling Adhesive	BMS 8-245, Grade 08	American Cyanamid Co. Bloomingtondale Department Havre deGrace, Md 21078	FM300K.08 PSF Adhesive Film
	BMS 5-80, Type 2 Grade 10 or 15	American Cyanamid Co. Bloomingtondale Department Havre deGrace, Md 21078	FM-123-5
Foaming Adhesive	BMS 5-90, Type 2, Class 250, Grade 50	Hysol Division Dexter Corporation 2850 Willow Rd Pittsburg, Ca. 94565	Thermofoam 3050 Grade 50
		3M Company 3M Center St. Paul, Minn. 55101	AF-3015 Grade 50
Honeycomb (Nomex)	BMS 8-124, Class IV Type V, Grade 3	Hexcel Corporation Casa Grande, Arizona	HRH-10-1/8-3.0
		Ciba-Geigy Corporation Orbitex Products Dept. 3550 N.W. 49th Street Miami, Florida 33142	HMX-7-1/8-3.0

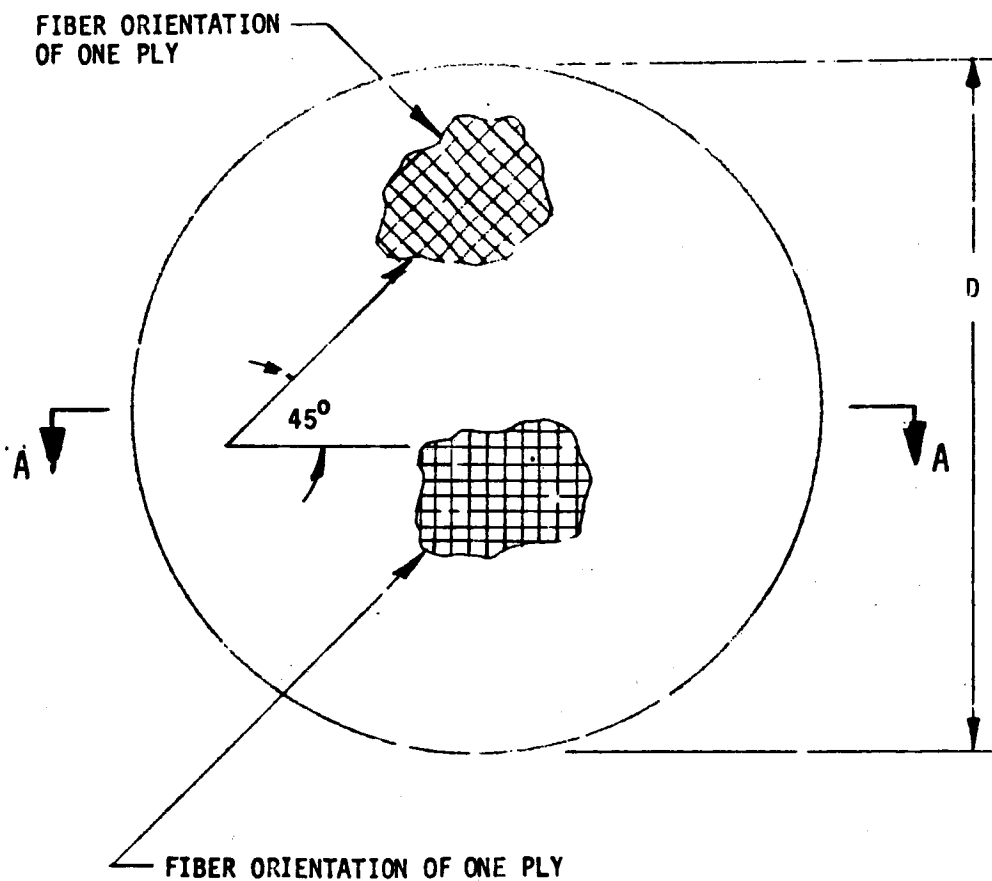
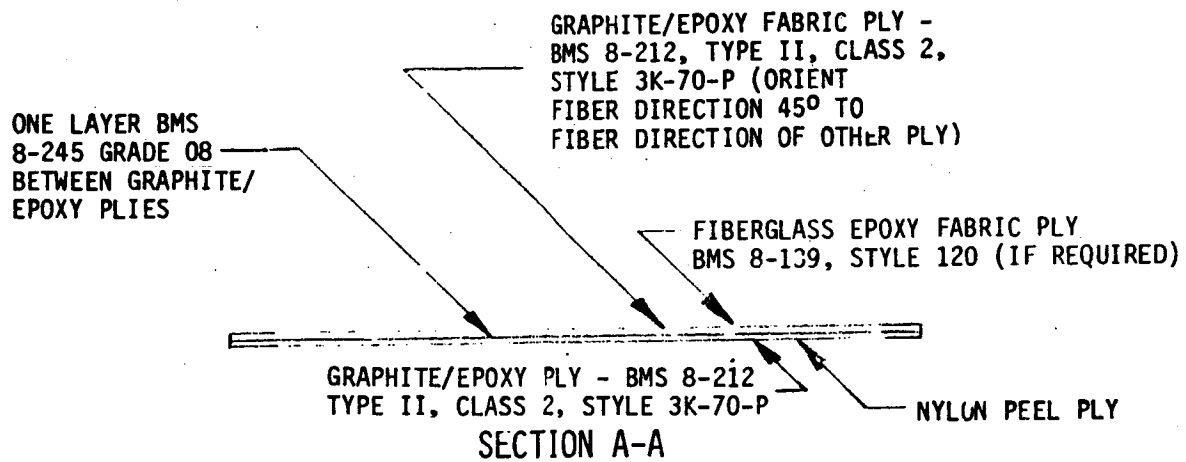
APPROVED MATERIALS FOR USE IN REPAIRING
GRAPHITE REINFORCED ELEVATOR COMPONENTS

FIGURE 2.1 (Sheet 1)

<u>MATERIAL</u>	<u>BOEING MATERIAL SPECIFICATION (BMS)</u>	<u>APPROVED SOURCE</u>	<u>SUPPLIER'S PRODUCT DESIGNATION</u>
Nylon Peel Ply	BMS 15-3, Type I, Class 3	Fiberite West Coast Corp. P.O. Box 738 Orange, Ca. 72699	MXM 7634/52006/60
Fiberglass Preimpregnated with Epoxy Resin	BMS 8-139, Style 120	Hexcel Corporation 11711 Dublin Blvd Dublin, Ca. 94566	120-F161-108 F50
		Celanese Corporation Narmco Materials Div. 600 Victoria Street Costa Mesa, Ca. 92626	Narmco 588-120 Volan A

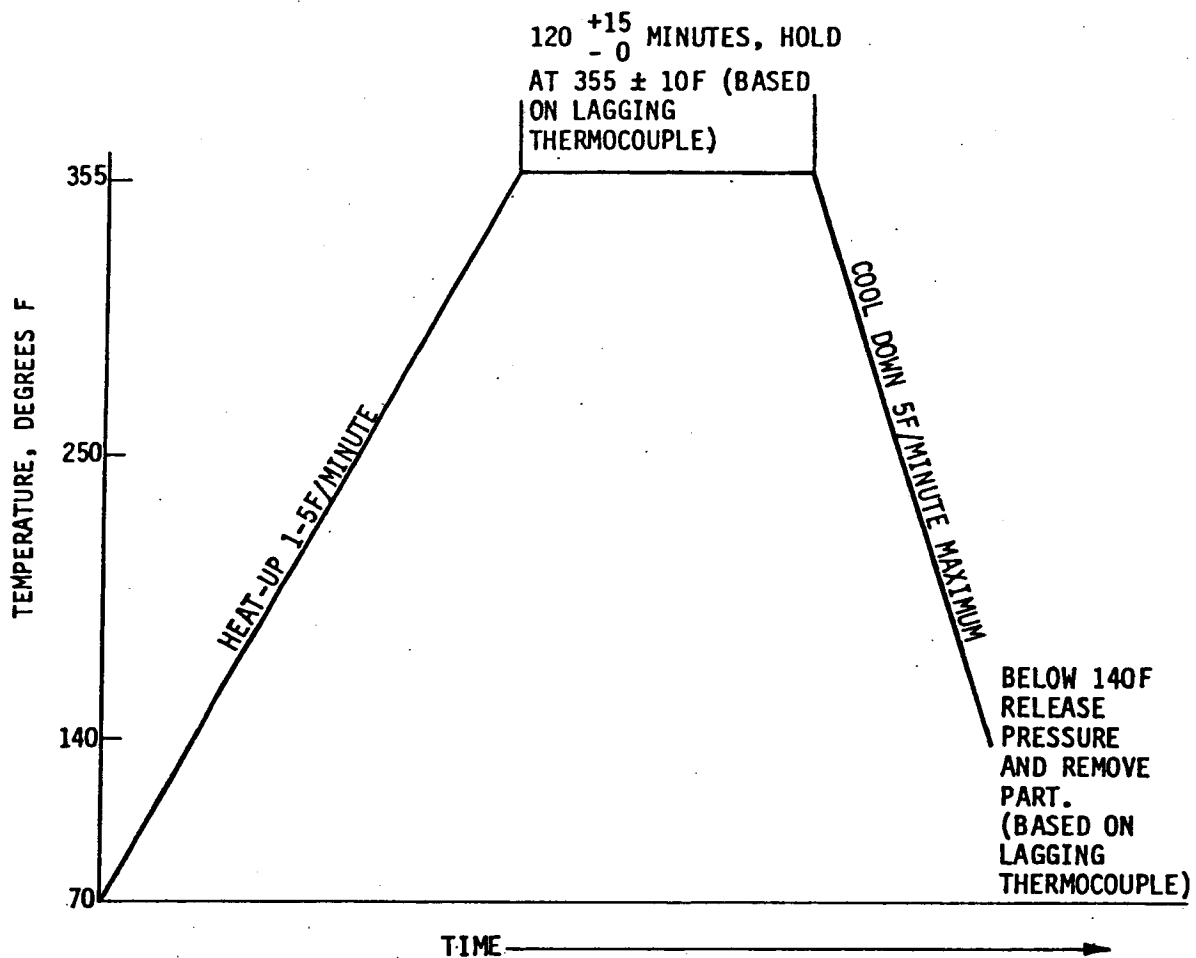
APPROVED MATERIALS FOR USE IN REPAIRING
GRAPHITE REINFORCED ELEVATOR COMPONENTS

FIGURE 2.1 (Sheet 2)



$$D = (\text{DIAMETER OF REPAIR CUTOUT PLUS 2.00 INCH}) \pm .05 \text{ INCH}$$

FIGURE 2.2 - PRECURED PATCH



● APPLY 22 INCHES HG VACUUM MINIMUM TO VACUUM BAG.

● APPLY 85 ⁺¹⁵
- 0 PSIG PRESSURE TO AUTOCLAVE.

NOTE - VENT VACUUM BAG TO ATMOSPHERE WHEN
PRESSURE REACHES 20 PSIG.

FIGURE 2.3 - CURE CYCLE FOR PRECURED REPAIR PATCHES

the damaged face sheet material. Remove the core to the edge of the face sheet hole, unless a potted core repair using techniques in D6-4062, 51-40-09 will be made in which case core removal is not required.

- (4) Lightly sand surface of face sheets on damage side for a distance of 1.50 inch from edge of hole. Use No. 180 sandpaper or equivalent. Avoid abrasion of graphite fibers.
- (5) Sand the far side face sheets lightly on the inner surface in area where replacement core will be bonded. Use No. 180 sandpaper or equivalent. Avoid abrasion of graphite fibers.
- (6) Clean out the repair area with oil free air. Wipe the surfaces with a clean cloth moistened with methyl ethyl ketone.
- (7) Apply one layer BMS 5-80, Type 2, Grade 10 or 15 as shown in Figure 2.4.
- (8) Replace core using BMS 8-124, Class IV, Type V, Grade 3 (1/8 inch cell) Nomex core. Orient ribbon direction in the direction of the original core. The surface of the replacement core should extend slightly above the face sheet surface. Splice core replacement to adjacent core using BMS 5-90, Type 2, Class 250, Grade 50.
- (9) Surround the core replacement with Osnaburg Breather cloth and cover the core replacement with a layer of PVA parting film.
- (10) Tape two thermocouples (minimum) to the panel adjacent to the repair.
- (11) Setup a PVA, nylon or mylar vacuum bag over the repair area.
- (12) Seal the vacuum bag and insulate the panel adjacent to the vacuum bag with 8 or 10 layers of fiberglass fabric.
- (13) Apply heat pad.
- (14) Cover the heat pad with 3 or 4 inches of fiberglass fabric or other insulation.

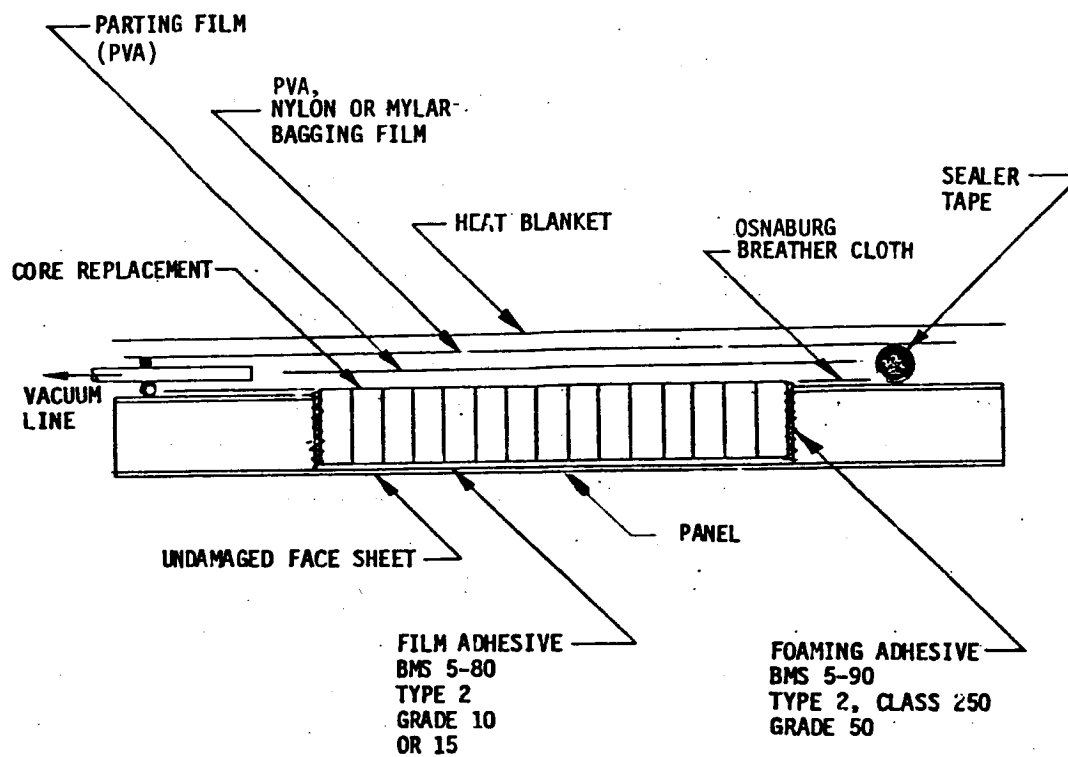


FIGURE 2.4 - LAY-UP ASSEMBLY FOR CORE REPLACEMENT

119-14

- (15) Evacuate the vacuum bag by maintaining a minimum vacuum of 20 inches of mercury gage pressure. Check the vacuum bag for leaks which may prevent minimum vacuum pressure. Correct any leaks in the system.
- (16) Apply heat and maintain $260^{\circ}\text{F} \pm 10^{\circ}\text{F}$ for $60 \begin{smallmatrix} +15 \\ -0 \end{smallmatrix}$ minutes. Do not heat faster than 50°F per minute. Continuously record the temperature.
- (17) After the adhesive has cured cool slowly, remove vacuum bag and wipe surfaces with a clean cloth moistened with MEK (methyl ethyl ketone) or acetone.
- (18) Sand core flush with surface of panel. Caution: Avoid abrasion of the adjacent skin plies.
- (19) Cut precured patch and BMS 5-80, Type 2, Grade 10 or 15 to shape and size to give overlap dimension shown in Figure 2.5.
- (20) Apply one layer BMS 5-80, Type 2, Grade 10 or 15 as shown in Figure 2.5.
- (21) Remove peel ply from bonding surface of precured patch and locate the precured patch over repair area (Figure 2.5).
- (22) Directly above the patch apply a layer of PVA with 4 layers of fiberglass to ensure proper air removal.
- (23) Tape two thermocouples (minimum) to the panel adjacent to the repair patch and surround patch with Osnaburg breather cloth.
- (24) Setup a PVA, nylon, or mylar vacuum bag over the repair area.
- (25) Seal the vacuum bag and insulate the panel adjacent to the vacuum bag with 8 to 10 layers of fiberglass fabric.
- (26) Apply heat pad.
- (27) Cover the heat pad with 3 or 4 inches of fiberglass fabric or other insulation.
- (28) Evacuate the vacuum bag by maintaining a minimum vacuum of 20 inches of mercury gage pressure. Check the vacuum bag for leaks which may prevent minimum vacuum pressure. Correct any leaks in the system.

DL 4100 7740 OR 18.2/71

REV SYM B

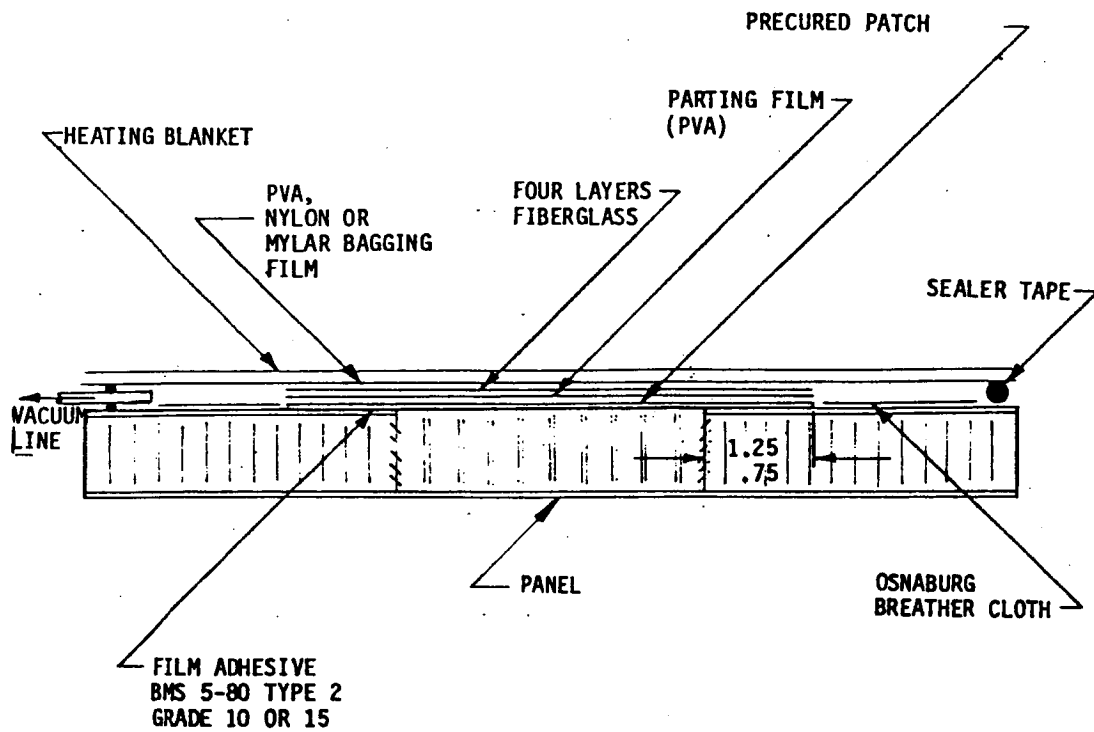


FIGURE 2.5 - LAY-UP ASSEMBLY FOR REPAIRING A FACE SHEET
USING A PRECURED GRAPHITE/EPOXY PATCH

J18-947

- (29) Apply heat and maintain 225^{+35}_{-0} °F for 90^{+15}_{-0} minutes. Do not heat faster than 5°F per minute. Continuously record the temperature.
- (30) After the adhesive has cured cool slowly, remove vacuum bag and wipe surfaces with a clean cloth moistened with MEK (methyl ethyl ketone) or acetone.
- (31) Refinish surface to original condition in accordance with Section 3 herein.

01 4 188 7740 ORIG. 8/71

REV SYM B

3. PREPAINT CLEANING, PRETREATMENT AND PAINTING OF SURFACES

A. General

The graphite/epoxy components of the 727 elevator are protected by the finishes shown in Figure 3.1. Prepaint cleaning, pretreatment and painting of graphite/epoxy elevator components shall be accomplished in accordance with the sections of the "727 Maintenance Manual" listed in Figure 3.2 except no chemical paint strippers may be used to remove paint and the elevator or control tab must be rebalanced after painting in accordance with Section 4 herein.

CAUTION: CHEMICAL PAINT STRIPPERS MAY ATTACK RESIN SYSTEMS, THEREFORE SHOULD NOT BE USED TO REMOVE PAINT.

The only acceptable method for removing paint is hand-sanding using 240 grit or finer abrasive paper. In sanding do not abrade the graphite fibers of the surface. Remove sanding dust by wiping the surface with a tack rag.

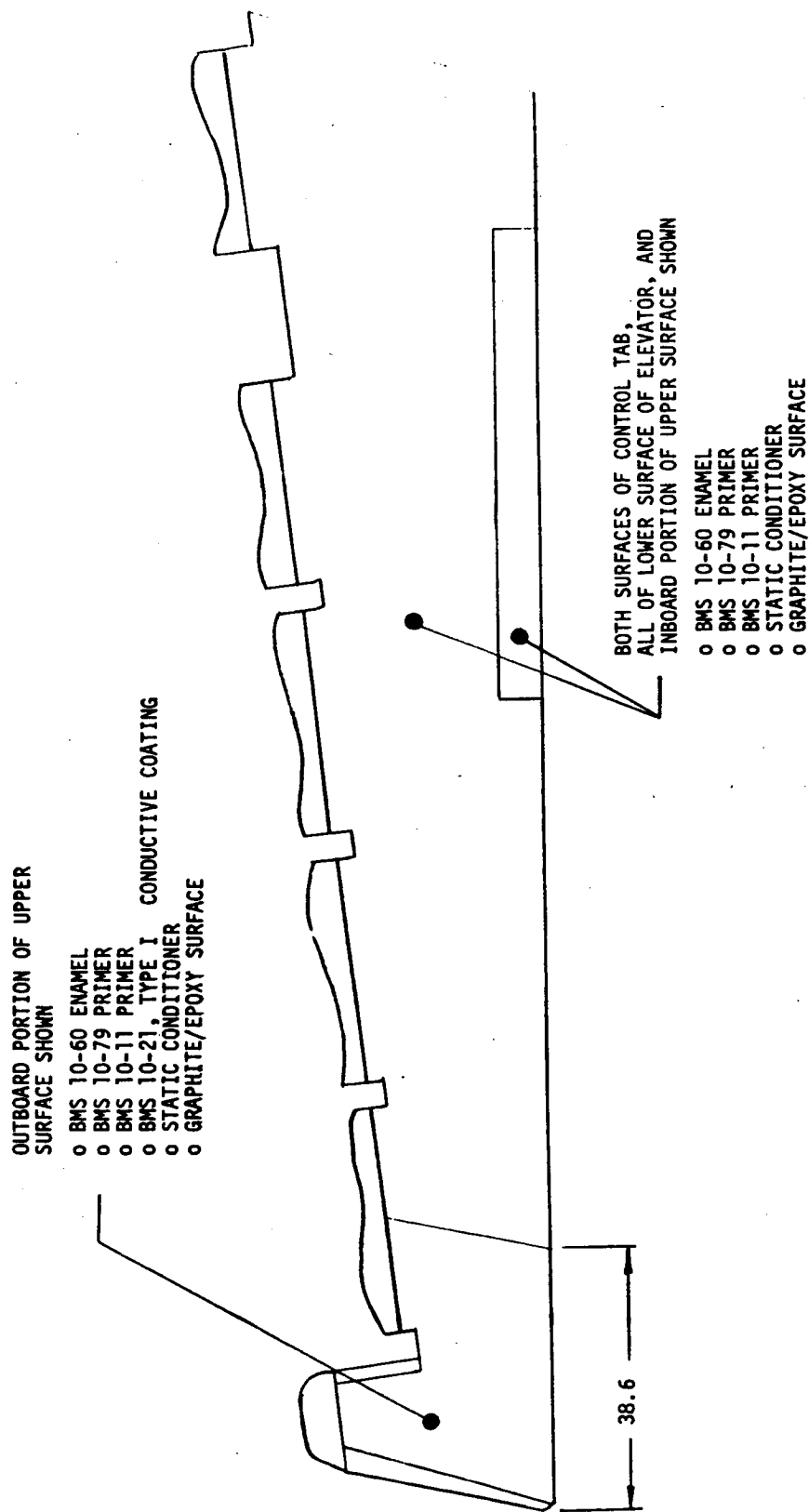


FIGURE 3.1 - FINISHES USED ON GRAPHITE/EPOXY ELEVATOR SURFACES

<u>FINISH TO BE APPLIED</u>	<u>BOEING 727 MAINTENANCE MANUAL SECTION TITLE</u>	<u>SECTION NUMBER</u>
Static Conditioner (Boeing Finish Code F14.67)	Detailed Instructions for Prepaint Cleaning and Pretreatment of Plastic Surfaces	51-20-2 Sections 5.A.(1), 5.A.(2) through 5.A.(4).(a).(2)
BMS 10-11, Type I Primer (Boeing Finish Code F20.02)	Chemical and Solvent Resistant Finish	51-20-31
BMS 10-79, Type II Primer and BMS 10-60, Type II Enamel (Boeing Finish Code F19.41-XXXX)	Decorative Paint System Cleaning/ Painting	51-20-151
BMS 10-21, Type I Conductive Coating (Boeing Finish Code SRF 14.68)	Conductive Coating System for Reinforced Plastic Surfaces - Cleaning/Painting	51-20-51



FIGURE 3-2 - PROCEDURES FOR PREPAINT CLEANING, PRETREATMENT AND
PAINTING GRAPHITE/EPOXY ELEVATOR SURFACES


4. REBALANCE PROCEDURE AFTER REPAIR

A. General

- (1) This section provides static rebalancing procedures for the graphite/epoxy elevator system after repair. The elevator system includes the elevator surface with its balance panels and tab.
- (2) Balance requirements for the graphite/epoxy elevator surface, its balance panels and tab are presented in Table 4.1.
- (3) **WARNING:** ANY COMPONENT OF THE ELEVATOR SYSTEM THAT DOES NOT MEET THE BALANCE LIMITS PRESENTED IN TABLE 4.1 CAN PRODUCE UNDESIRABLE FLUTTER AND DYNAMIC INSTABILITY WHICH COULD AFFECT FLIGHT SAFETY. ANY REPLACED, REPAIRED OR REPAINTED SURFACE MUST BE REBALANCED OR THE QUANTITY OF UNBALANCED MOMENT MUST BE ACCOUNTED FOR BY CALCULATION AND SUBSEQUENT BALANCE ADJUSTMENT.
- (4) Sign convention used in this section is as follows.
 - (a) Distances are considered positive (+) if measured aft from the surface hinge line and negative (-) if measured forward from the surface hinge line.
 - (b) Weight reactions are considered positive (+) if the surface exerts a downward load at the trailing edge and negative (-) if the surface exerts an upward load at the trailing edge.

TABLE 4.1
ELEVATOR SYSTEM COMPONENT BALANCE REQUIREMENT

COMPONENT	MANUFACTURING			OPERATIONAL		
	WEIGHT (POUNDS)	MOMENT (POUND - INCHES)	C.G. LOCATION FWD OF \bar{M} (IN.)	MAXIMUM WEIGHT (POUNDS)	AVAILABLE REPAIR MOMENT	C.G. LOCATION FWD OF \bar{M} (IN.)
ELEVATOR SURFACE	NO REQUIREMENT	-61 ± 3	NO REQUIREMENT	NO REQUIREMENT	$+ 3.0$ POUND - INCHES 	NO REQUIREMENT
BALANCE PANEL BAY 1	$7.06 \pm .15$	NO REQUIREMENT	NO REQUIREMENT	7.36	NO REQUIREMENT	NO REQUIREMENT
BALANCE PANEL BAY 2	$7.68 \pm .15$	NO REQUIREMENT	NO REQUIREMENT	7.98	NO REQUIREMENT	NO REQUIREMENT
BALANCE PANEL BAY 3	$5.20 \pm .10$	NO REQUIREMENT	NO REQUIREMENT	5.40	NO REQUIREMENT	NO REQUIREMENT
BALANCE PANEL BAY 4	$4.51 \pm .10$	NO REQUIREMENT	NO REQUIREMENT	5.11	NO REQUIREMENT	NO REQUIREMENT
BALANCE PANEL BAY 5	$4.63 \pm .10$	NO REQUIREMENT	NO REQUIREMENT	4.83	NO REQUIREMENT	NO REQUIREMENT
CONTROL TAB	$7.85 \pm .25$	NO REQUIREMENT	0.14 TO 0.26	8.60 	(TAB WT.) X (0.04)	0.10 TO 0.26

 FOR REPAIR MOMENTS IN EXCESS OF AVAILABLE REPAIR MOMENT SHOWN, SEE PARAGRAPHS 4.D.(5) AND 4.D.(6)

 FOR INSTRUCTIONS PERTAINING TO CONTROL TABS WEIGHING IN EXCESS OF THE MANUFACTURING MAXIMUM WEIGHT OF 8.10 POUND, SEE PARAGRAPH 4.I

B. Special Tools and Equipment

See Model 727 Structure Repair Manual, Chapter 51-80, Figure 3 for a tabulated listing. For the control tab balance check sliding weight use the weight detailed in Figure 4.7a of this document.

C. Definition of Allowable Repairs**(1) Elevator Surface**

- (a) Repairs to the metal nose structure is restricted to the repair or replacement (with new equivalent parts) of fittings, nose skins and aluminum/bronze hinges and repairs that require the installation of new structural members not previously used in the original assembly.
- (b) Repairs to the graphite/epoxy structure are limited to those described in Section 2 of this document.
- (c) Total or partial repainting of the surface per Section 3 of this document.

(2) Balance Panels

Repairs to the balance panels, include the repair or replacement (with new equivalent parts) of aluminum/bronze hinges, seals or hinge pins, and repairs that require the installation of new structural members not previously used in the original assembly.

(3) Control Tabs

Repairs to the control tab are limited to the repair or replacement (with new equivalent parts) of fittings and fairings, repairs to the graphite/epoxy structure permitted by Section 2 of this document and repainting of the surface per Section 3 of this document.

D. Elevator Surface Rebalancing Procedure - Non-Removal

Note: It is not necessary to remove the elevator surface from the airplane during a rebalance operation after making repairs. However before making a repair determine by calculation if any balance adjust weights (69-69700-1) are required to be added or removed. If balance weights are to be added it should be ascertained if balance adjust weight locations are available. In the event that all locations have been filled the elevator surface must be removed from the airplane and rebalanced to the limits published in Table 4.1, after completion of repairs. It will also be necessary to remove the elevator surface from the airplane when the repair records indicate that a total of more than six (6) balance adjust weights have been either added or removed or when the elevator surface has been repainted.

- (1) Using approved material unit weights detailed in paragraph 4.J.(1), determine the repair weight by subtracting the weight of the removed material from the weight of the material used for the repair. Determine the repair weight to the nearest 0.01 pound. (See paragraph 4.K for a calculation example).

J18-047

- (2) Measure distance Y from the C.G. (center of gravity) of the repair area to the nearest skin edge as shown in Figure 4.1.
- (3) Calculate the repair moment M by multiplying the repair weight in pounds by the distance Y in inches.
- (4) If M does not exceed ± 3.0 pound-inches, the available repair moment (see Table 4.1), no balance adjust weights need to be added or removed. However the unbalanced repair moment M must be recorded in the repair log described in 4.D.(10). When the accumulated total of unbalanced repair moment exceeds ± 3.0 pound-inches, one (1) balance adjust weight must be added or removed.
- (5) If M is between +3.1 and +9.0 pound-inches, one (1) balance adjust weight should be installed in the next highest number location on the elevator nose structure in Bay No. 1. If all positions in Bay No. 1 are occupied the next highest number location in Bay No. 2 should be utilized. See Figures 4.2 and 4.3 for balance adjust weight locations.
- (6) If M is between -3.1 and -9.0 pound-inches, one (1) balance adjust weight must be removed from the highest number location occupied on the elevator nose structure in Bay No. 2. If no balance adjust weights are installed in Bay No. 2 locations, one (1) balance adjust weight must be removed from the highest number location occupied in Bay No. 1. See Figures 4.2 and 4.3 for balance adjust weight locations.
- (7) Subsequent repair moment increments of ± 6.0 pound-inches (or part increments) will require the addition or removal, respectively of one (1) balance adjust weight.

DI 4100 7740 ORIG. 3/71

REV SYM

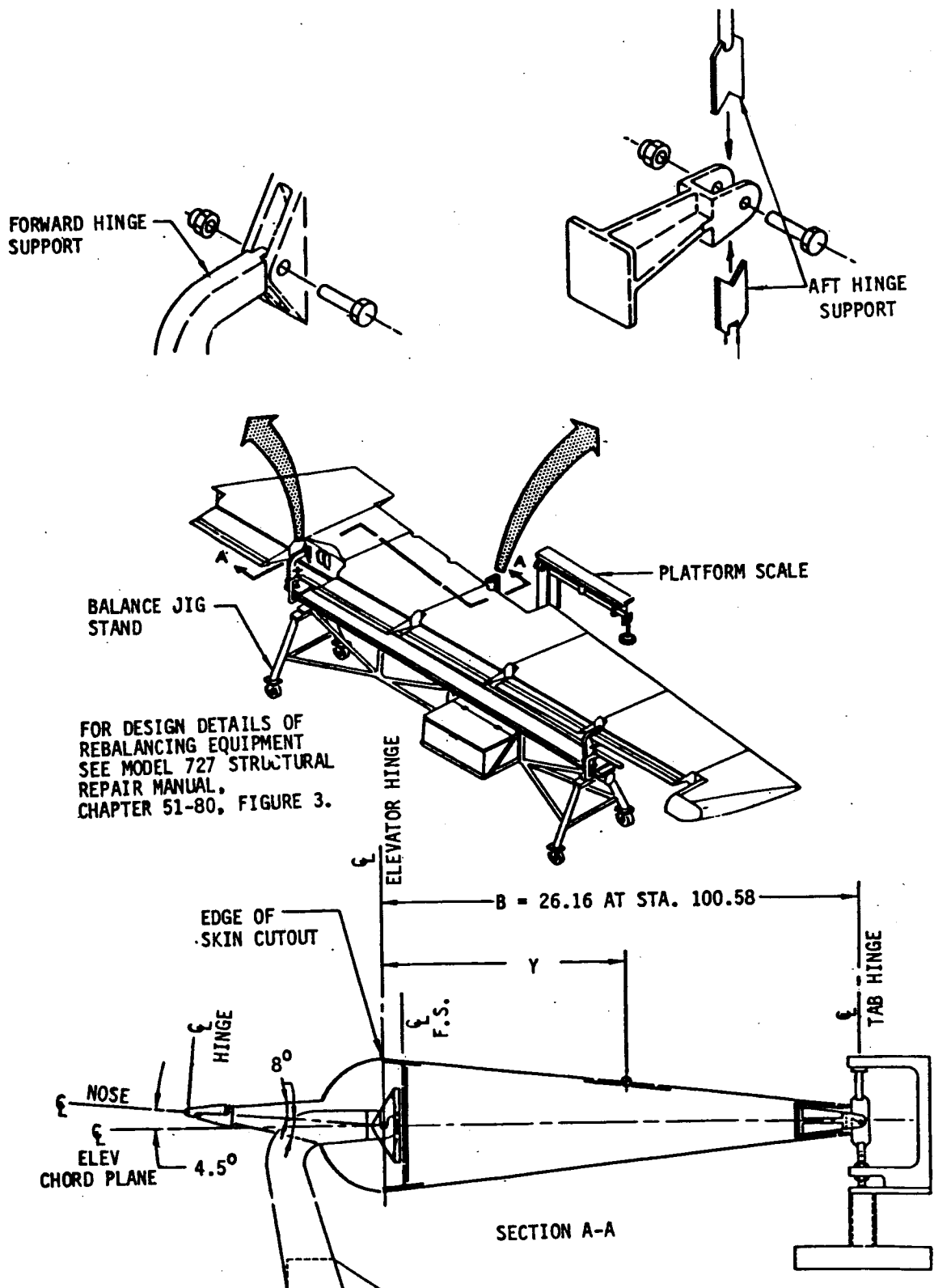


FIGURE 4.1 - ELEVATOR SURFACE REBALANCING

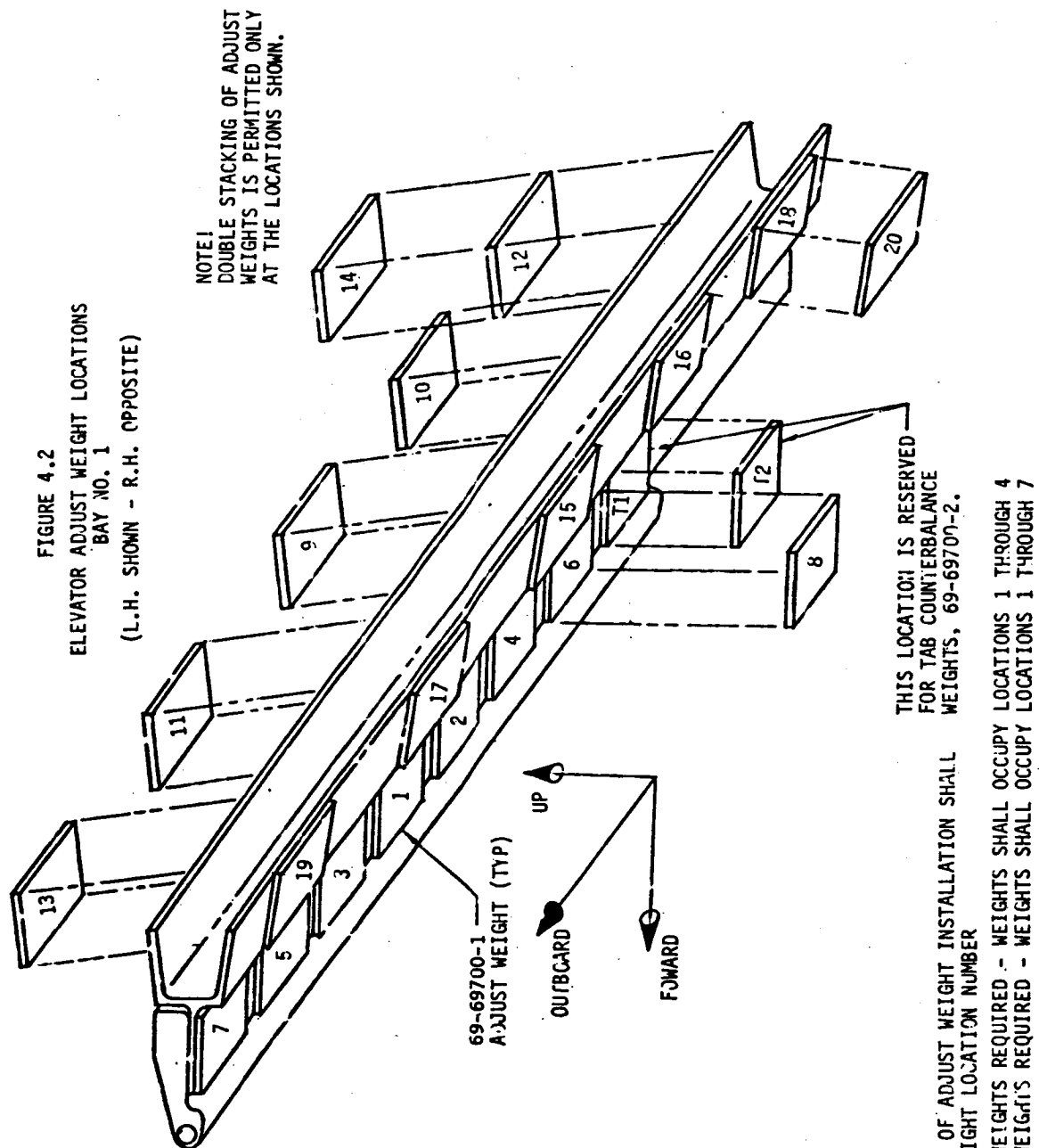
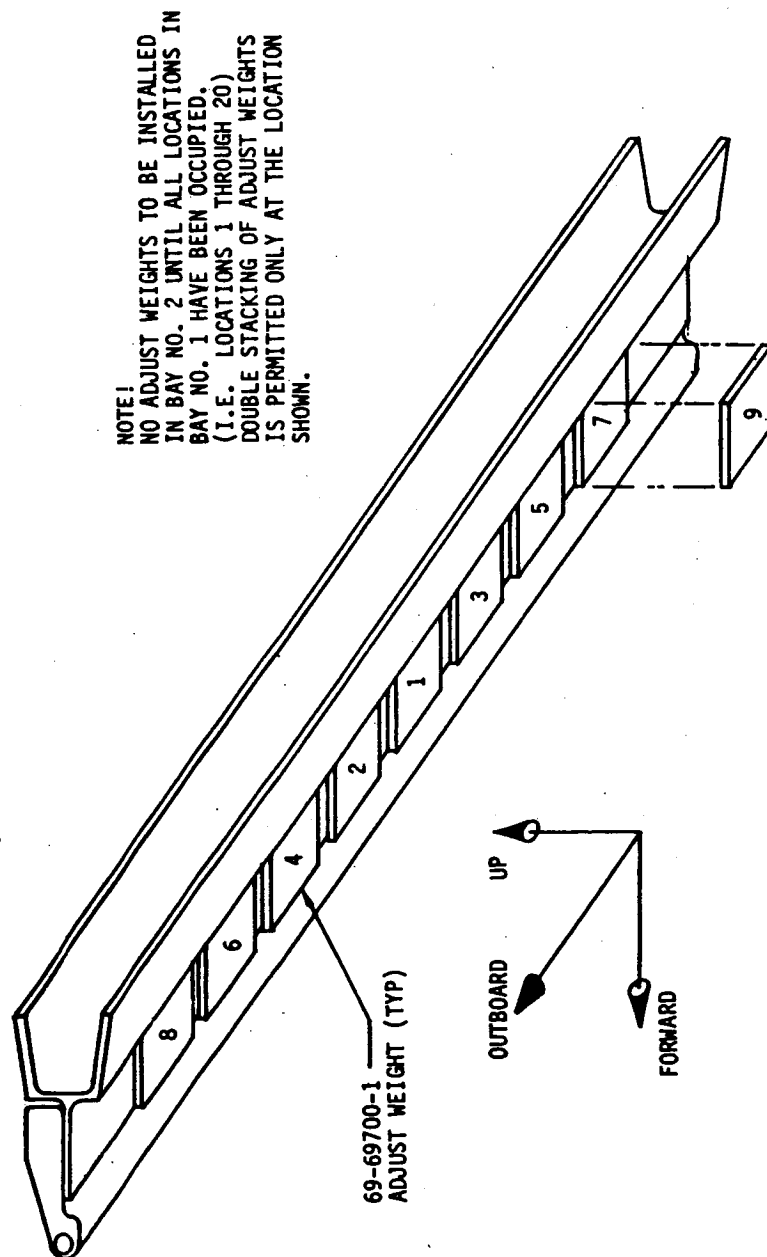


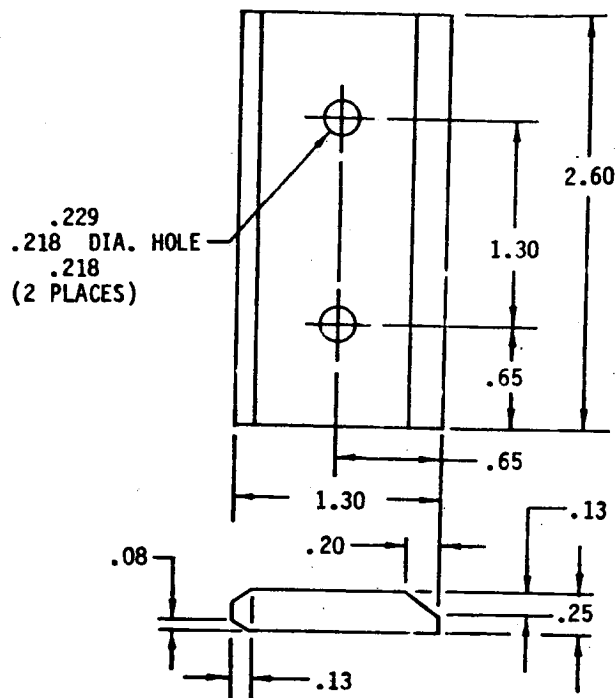
FIGURE 4.3
ELEVATOR ADJUST WEIGHT LOCATIONS
BAY NO. 2
(L.H. SHOWN - R.H. OPPOSITE)



SEQUENCE OF ADJUST WEIGHT INSTALLATION
SHALL BE BY WEIGHT LOCATION NUMBER, AS
IN BAY NO. 1

- (8) When installing or removing balance adjust weights, strict adherence shall be observed to the location number system illustrated in Figures 4.2 and 4.3. Balance adjust weights are not to be installed in the space reserved in Bay No. 1 for tab counterbalance weights (69-69700-2), locations T_1 and T_2 . Balance adjust weights to be installed per Figure 4.4b.
- (9) If Boeing balance adjust weights are not available, similar parts may be fabricated using the dimensions and material as shown in Figure 4.4a.
- (10) An accurate and detailed repair log shall be kept in which each repair must be recorded. It shall contain the repair weight, the repair Y dimension, the repair moment M, the number of balance adjust weights added or removed, the balance adjust weight(s) location number(s) and bay number.
- (11) Repair Weight Example Calculation
- (a) Assume the following values:
- o Weight of material removed = 0.22 pound.
 - o Weight of repair material = 0.73 pound.
 - o Repair weight - $0.73 - 0.22 = 0.51$ pound.
 - o Distance Y = +10 inches (aft of hinge centerline)
See Figure 4.1.
 - o Repair moment M = $0.51 \times +10.0 = +5.1$ pound-inches.
 - o Repair moment M exceeds the available repair moment of +3.0 pound-inches, and is between +3.1 and +9.0 pound-inches. Therefore one (1) balance adjust weight must be installed per paragraph 4.D.(5).
- (b) If the above had been performed on the nose structure, distance Y would be -10.0 inches and moment M would be -5.1 pound-inches. This moment would require the removal of one (1) balance adjust weight per paragraph 4.D.(6).

FIGURE 4.4a - ELEVATOR BALANCE ADJUST WEIGHT 69-69700-1
AND TAB COUNTERBALANCE WEIGHT 69-69700-2
NOMINAL WEIGHT 0.5 POUND

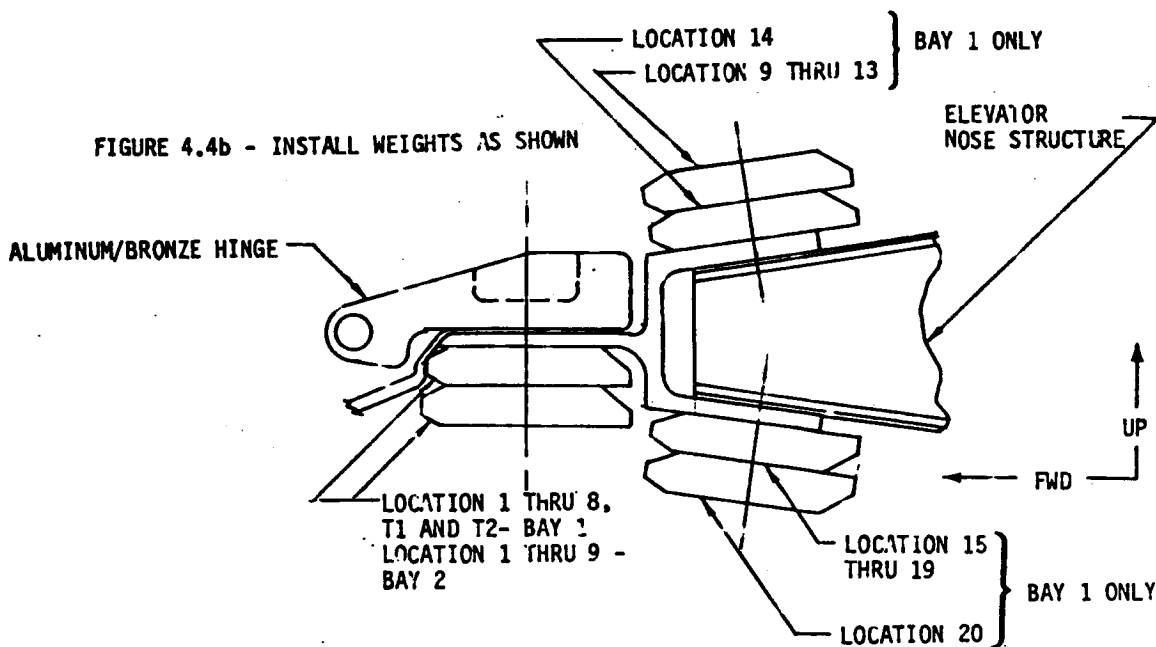


MATERIAL
TUNGSTEN POWDER COMPACT BAR
PER MIL-T-21014 TYPE II CLASS I
(DENSITY: 16.85 - 17.25 GRMS/CU.CM.)

FINISH
-1 F-20.03
-2 F-20.03 PLUS SRF 14.9815-201
(COLOR - GRANGE)

SCALE 1/1

NOTE! -2 IDENTICAL TO -1 EXCEPT
FOR FINISH.



E. Elevator Surface Rebalancing Procedure - Removal

(1) It is necessary to remove the elevator surface from the airplane for rebalancing when one of the following conditions occur: (Remove per maintenance manual, Chapter 27-30-1).

- (a) When all the available balance adjust weight locations are occupied and a repair moment cannot be balanced.
- (b) When the repair records indicate that a total of more than six (6) balance adjust weights have been either removed, added or a combination of both removals and additions.
- (c) When the elevator surface has been repainted.

Note: Total elevator surface repainting, per instructions in Section 3, is estimated to require the addition of approximately six (6) balance adjust weights. A check of available balance adjust weights locations is advisable before repainting is performed.

(2) The condition of the elevator surface for weighing and balancing is as follows: (See Figure 4.6).

- (a) Items that must be installed in their correct locations to ensure proper balancing:
 - o Tab hinge bolts, nuts and washers.
 - o Aft portions of the five (5) aluminum bronze elevator surface/balance panel hinges.
 - o All protective and decorative finish.
 - o All balance adjust weights installed on the nose structure at the time of elevator removal.
 - o All elevator surface nose seals.

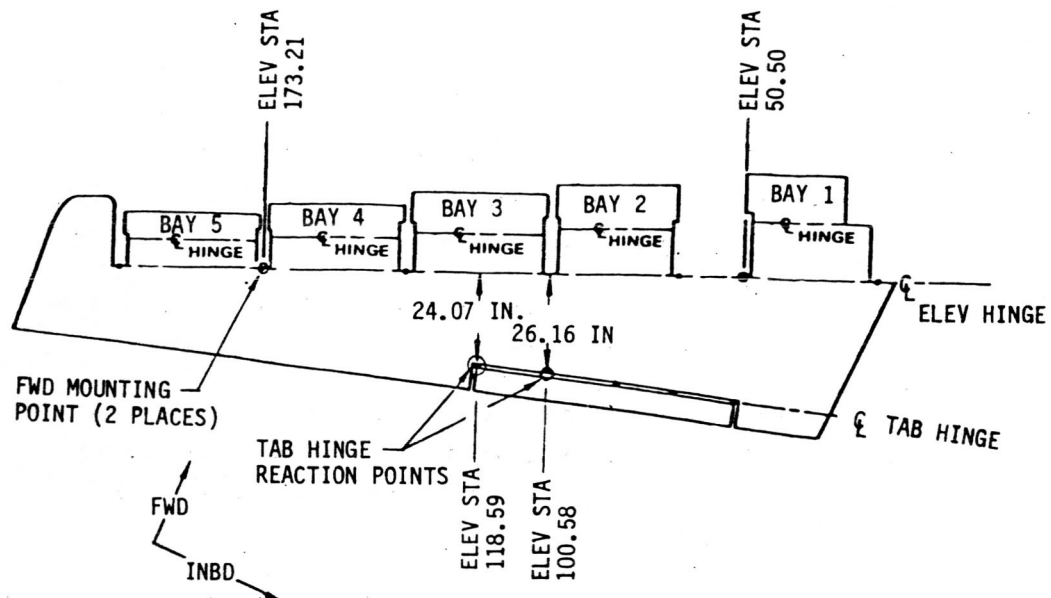


FIGURE 4.5 - ELEVATOR MOUNTING AND REACTION POINTS

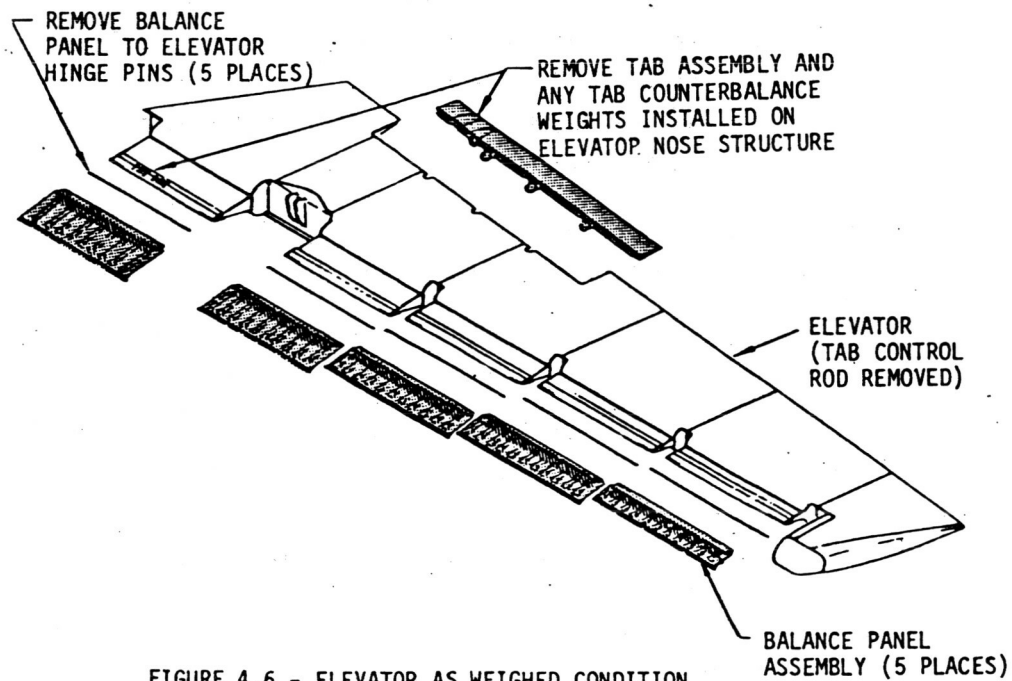


FIGURE 4.6 - ELEVATOR AS WEIGHED CONDITION

(b) Items that must be removed are as follows.

- The control tab and its counterbalance weights (69-69700-2 color orange) from the nose structure, when fitted.
- The five (5) elevator balance panels complete with the forward portions of the five (5) aluminum bronze elevator surface/balance panel hinges and hinge pins.
- Tab control rod part number 69-20193.

- (3) Mount the elevator (top surface up) on a balance jig stand as illustrated in Figure 4.1. See Figure 4.5 for mounting locations. When mounted as shown in Figure 4.2 the surface must be free to rotate a few degrees about the balance fitting without binding.
- (4) With the chord plane horizontal, obtain the weight reaction (W_R) at dimension (B) taken at the centerline of one of the tab hinges as shown in Figure 4.5. Use rear mounting point at either elevator station 100.58 or 118.59.


Note: The weight reaction, W_R , will be a negative value, i.e., upward load at the tab hinge reaction point.


- (5) Obtain a trial moment by multiplying the weight reaction (W_R) (measured in pounds) by the moment arm (B) (measured in inches).

(a) Trial Moment - (W_R) (B)

- (6) Having determined the trial moment, refer to elevator balance table, Table 4.2, and read off the number of weights required.
- (7) If additional balance adjust weights are required they should be installed in the next highest location numbers unoccupied. See Figure 4.2 for Bay No. 1 and Figure 4.3 for Bay No. 2.

TABLE 4.2
ELEVATOR BALANCE TABLE

TRIAL MOMENT (POUND INCHES)	NUMBER OF ADJUST WEIGHTS (69-69700-1) REQ'D	
	BAY NO. 1	BAY NO. 2
- 67.0 to - 64.0		0
- 63.9 to - 58.0	0	0
- 57.9 to - 51.0	1	0
- 50.9 to - 44.0	2	0
- 43.9 to - 38.0	3	0
- 37.9 to - 31.0	4	0
- 30.9 to - 24.0	5	0
- 23.9 to - 17.0	6	0
- 16.9 to - 10.0	7	0
- 9.9 to - 3.0	8	0
- 2.9 to + 3.0	9	0
+ 3.1 to + 9.0	10	0
+ 9.1 to + 15.0	11	0
+ 15.1 to + 21.0	12	0
+ 21.1 to + 27.0	13	0
+ 27.1 to + 34.0	14	0
+ 34.1 to + 40.0	15	0
+ 40.1 to + 46.0	16	0
+ 46.1 to + 52.0	17	0
+ 52.1 to + 58.0	18	0
+ 58.1 to + 64.0	19	0
+ 64.1 to + 70.0	20	0
+ 70.1 to + 76.0	20	1
+ 76.1 to + 81.0	20	2
+ 81.1 to + 87.0	20	3
+ 87.1 to + 92.0	20	4
+ 92.1 to + 98.0	20	5
+ 98.1 to +103.0	20	6
+103.1 to +109.0	20	7
+109.1 to +114.0	20	8
+114.1 to +120.0	20	9

 Elevator negative trial moments larger than -67 pound-inches, requires that balance adjust weights be removed.
(See paragraph 4.E.(8).

- (8) If the trial moment is larger than -67.0 lb-ins, one (1) balance adjust weight should be removed for each -6.0 lb-ins increment or part increment in excess of -67.0 lb-ins.
- (9) After ensuring that the correct number of balance adjust weights are installed, obtain a second trial moment (W_R) by repeating steps 3 thru 5. The moment should lie between -58.0 lb-ins and -64.0 lb-ins. If the moment is not within the specified limits, change the number of weights until a satisfactory balance is obtained.
- (10) Record the changes that were made to the balance adjust weights, the number of weights installed and the moment of the elevator. This moment will now become the base to which additional repair moments can be added.

F. BALANCE PANEL REBALANCE

- (1) Balance panels have a weight requirement only. The balance panel should be examined to determine the extent of the required repair and the weight of the repair should be calculated.
- (2) Repair calculation example.
 - (a) Calculate the weight of the repair by subtracting the weight of the material to be removed (if any) from the weight of the added repair material. For material unit weights refer to Boeing 727 Structural Repair Manual, D6-4062, Chapter 51-80, Figure 4, Sheet 2.
 - (b) The calculated repair weight should be added to the original weight of the panel. If the original weight is not known, the panel must be removed from the airplane as described in Boeing 727 Maintenance Manual, Chapter 27 and weighed.
 - (c) The configuration of the panel at the time of weighing shall include the aluminum/bronze hinge half, the hinge pin for the aluminum/bronze hinge, the forward hinge pin and all seals.
 - (d) The weight of the panel, plus the calculated repair weight, shall not exceed the operational maximum weight for the appropriate bay number panel.
 - (e) If the repaired panel weight does not exceed the operational maximum weight, the panel should be repaired. After repair the panel should be weighed to confirm the calculated repair weight.
 - (f) If the repaired panel weight exceeds the operational maximum weight the panel must be replaced with a panel of the correct weight.

J18-047

(g) All repairs to balance panels must be recorded. The repaired panel weight must be included in this record.

DI 4100 2740 ORIG. 8/71

REV SYM

G. CONTROL TAB REBALANCING - NON-REMOVAL

- (1) Control tabs do not have any provisions for balance adjustment to retain the control tab c.g. location within limits shown in Table 4.2.
- (2) Repairs to control tabs which do not exceed the control tab available repair moment may be performed without removing the tab from the airplane.
- (3) Using the approved material unit weights detailed in paragraph 4.J.(1), determine the control tab repair weight by subtracting the weight of removed material from the weight of material to be used in the repair. Repair weight should be determined to the nearest 0.01 pound. (See paragraph 4.G.(12) for a calculation example).
- (4) Measure distance Z from the c.g. (center of gravity) of the repair to the control tab trailing edge. See Figure 4.7b
- (5) Multiply repair weight W by 6.50 - distance Z to obtain the repair moment M.
- (6) Compare the repair moment M to the available repair moment. Available repair moment is determined by multiplying the tab weight by 0.04 inches.
- (7) Add repair weight W to the tab weight and compare this new control tab weight to the maximum operational weight shown in Table 4.1.
- (8) If repair moment M and the new control tab weight are within the allowable limits, the repair can be performed without removal of the tab from the airplane.

- (9) If repair moment M exceeds the allowable repair moment, the tab should be removed from the airplane and the balance check procedure described in paragraph 4.H should be performed.
- (10) If the new control tab weight exceeds the manufacturing maximum weight of 8.10 pounds and does not exceed the operational maximum weight of 8.60 pound, tab counterbalance weight(s), 69-69700-2, must be added as described in paragraph 4.I.
- (11) All repairs to control tabs must be recorded. The records should include the tab weight before repair, the repair weight, the distance Z , the repair moment and if a balance check, per paragraph 4.H was performed.
- (12) Repair weight example calculation.

(a) Assume the following values.

- The weight of the control tab = 7.92 pounds.
- Available repair moment = $7.92 \times 0.04 = 0.317$ pound inches.
- Weight of removed material = 0.16 pound.
- Weight of repair material = 0.38 pound.
- Repair weight = $0.38 - 0.16 = 0.22$ pound.
- Distance Z (trailing edge to repair c.g.) = 2.50 inches.
- Repair moment $M = 0.22 \times (6.50 - 2.50) = 0.880$ pound inches.

- (b) The repair moment exceeds available repair moment of 0.317 pound-inches and must therefore be removed from the airplane and a balance check described in paragraph 4.H.
- (c) The original control tab weight 7.92 pounds plus the repair weight 0.22 pound totals 8.14 pounds. The new control tab weight exceeds the manufacturing maximum weight, 8.10 pounds and one (1) control tab counterbalance weight is required per paragraph 4.I.2.
- (d) If the repair weight in 4.G.(12).(a) had amounted to 0.13 pound and the Z distance been 4.70 inches the repair moment M would be $0.13 \times (6.50 - 4.70) = 0.234$ pound inches. This repair moment is within the available repair moment and the repair can be performed without a balance check being required.
- (e) The original control tab weight 7.92 pounds plus the repair weight 0.13 pound totals 8.05 pounds. The new control tab weight is below the manufacturing maximum weight, 8.10 pounds, and therefore no further action is necessary.

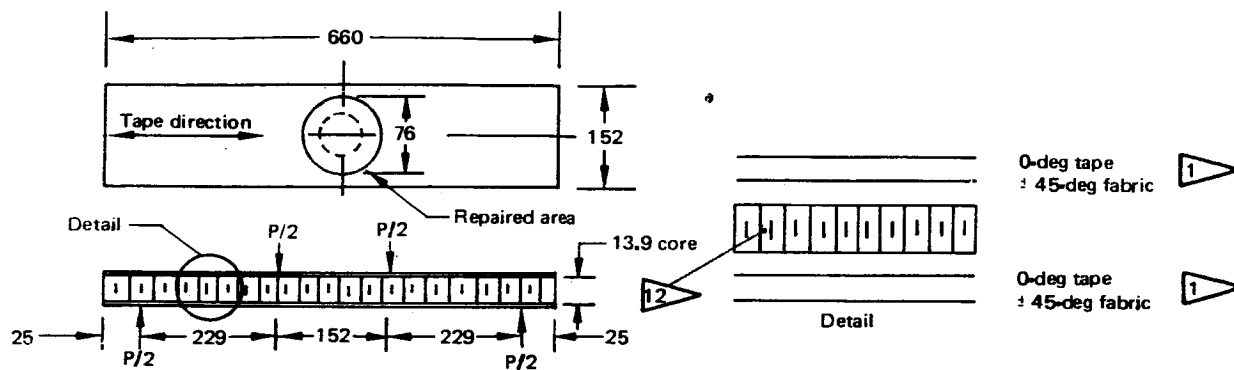
H. CONTROL TAB REBALANCING - REMOVAL

- (1) Control tab repairs which exceed the available repair moment and control tabs which have been repainted must be removed from the airplane and a balance check performed using the following procedure.
- (2) Remove the control tab from the airplane per Maintenance Manual, Chapter 27.
- (3) Remove tab counterbalance weights, 69-69700-2 (color orange) from the elevator nose structure, if fitted. See Figure 4.2, locations T_1 and T_2 .

CAUTION: THE REMOVAL OF A CONTROL TAB FROM AN ELEVATOR SURFACE REQUIRES THAT CONTROL TAB COUNTERBALANCE WEIGHT(S), 69-69700-2 (COLOR ORANGE) WHEN FITTED SHOULD BE REMOVED FROM THE ELEVATOR SURFACE NOSE STRUCTURE. THE COUNTERBALANCE WEIGHT(S) ARE DEEMED A PART OF THE CONTROL TAB ASSEMBLY AND SHOULD ACCOMPANY THE CONTROL TAB AT ALL TIMES. RE-INSTALLATION OF A CONTROL TAB ACCOMPANIED BY CONTROL TAB COUNTERBALANCE WEIGHT(S) REQUIRE THAT THE COUNTERBALANCE WEIGHT(S) BE INSTALLED IN THE LOCATIONS ON THE ELEVATOR SURFACE NOSE STRUCTURE RESERVED FOR THIS PURPOSE (T_1 AND T_2) SEE FIGURE 4.2.

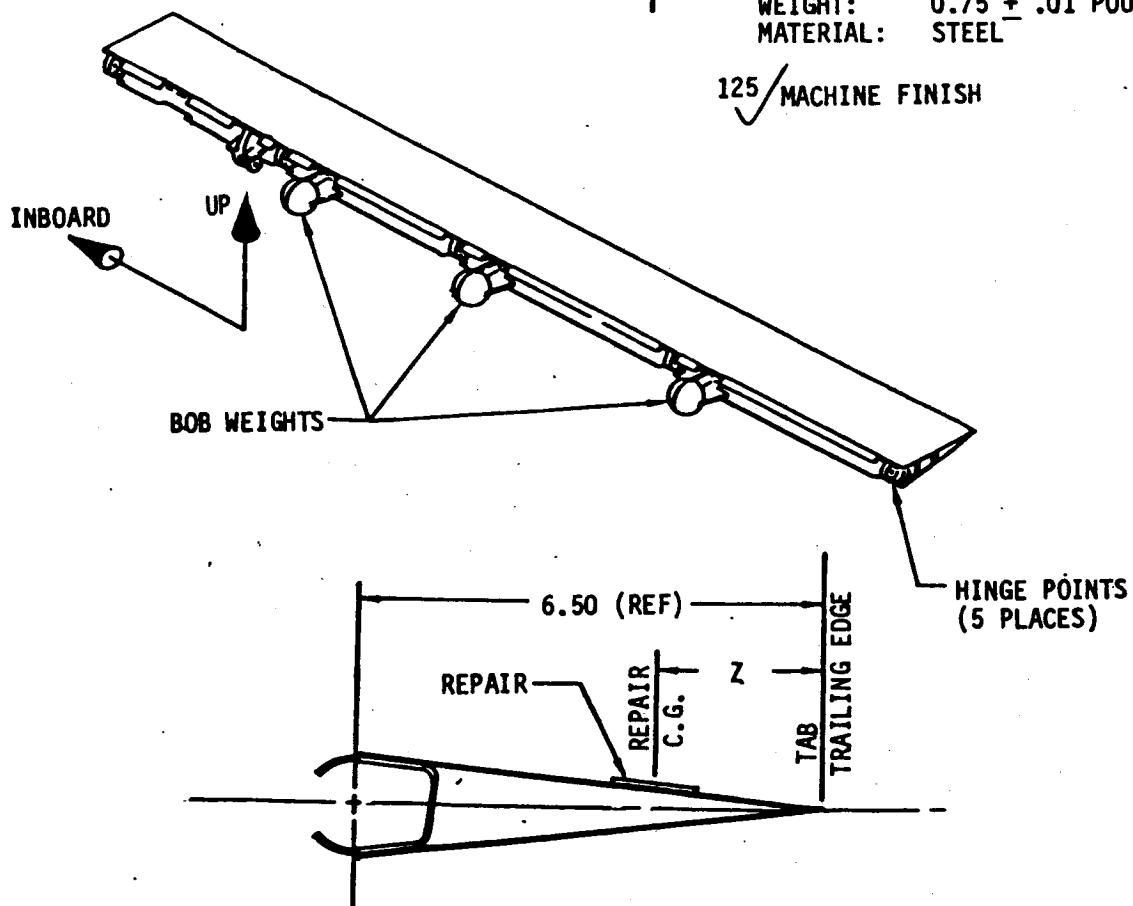
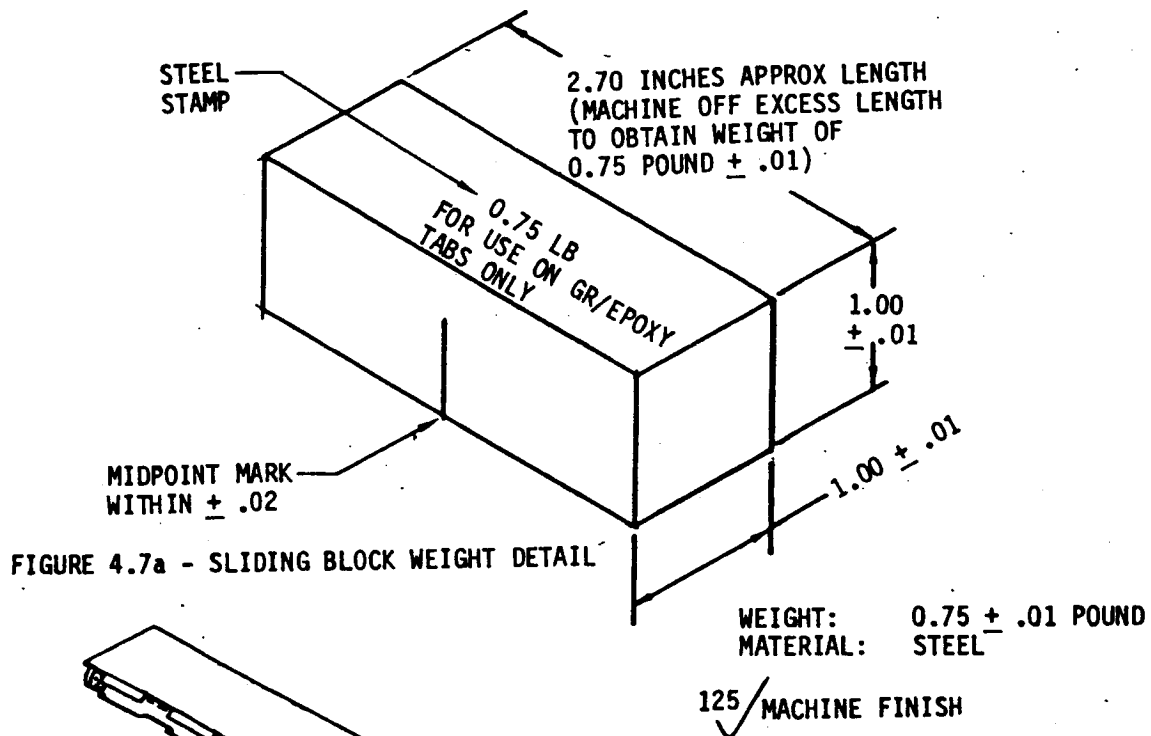
- (4) Complete all repairs, rework or repainting as required.
- (5) Weigh the tab. See Figure 4.7b for the as weighed configuration. All installation bolts, nuts and washers are to be removed.
- (6) Attach ruled paper on the control tab surface with the ruled lines parallel to the control tab hinge line as shown in Figure 4.8.

HONEYCOMB PANEL REPAIR TESTS

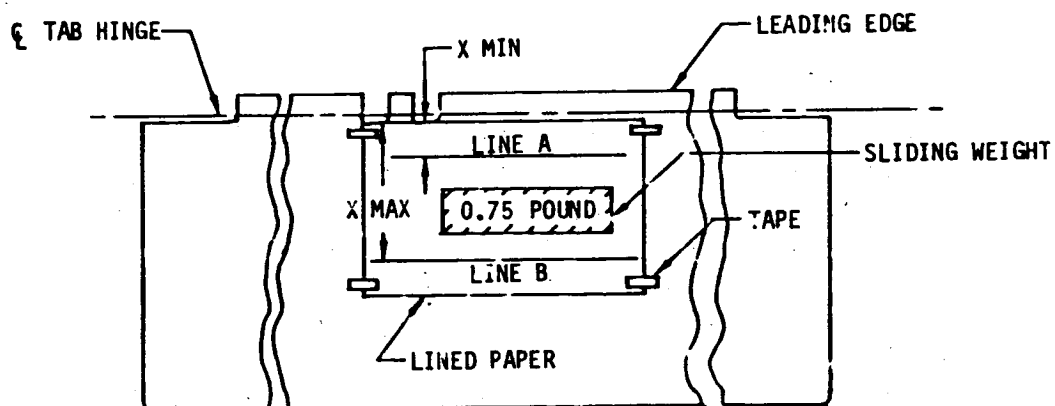
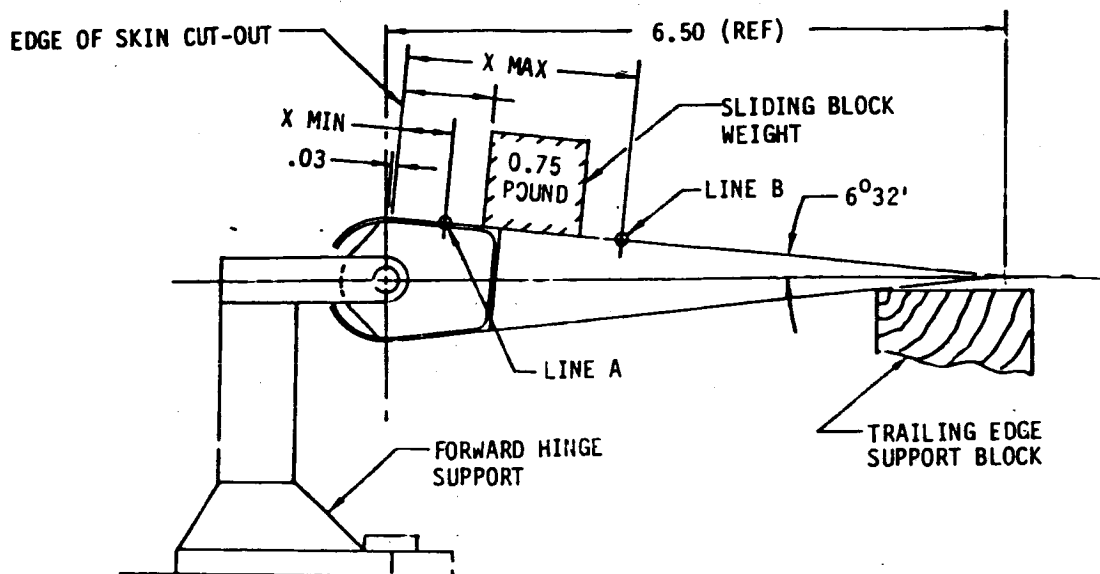


• Dimensions in mm

Drawing and assembly no. 2	Test temperature, °C	Environment condition 4		Failure load, kN 5	Failure stress, MPa 6	E, MPa 7	Strain, ϵ , mm/mm 8	Comments
		Wet	Dry					
65C17721-4	21.1		✓	1.721	324.19	5.45×10^4	0.00595	Baseline specimen
			✓	1.632	307.43		0.00565	
			✓	1.779	335.12		0.00615	
		✓		1.655	311.76		0.00572	
		✓		1.650	310.82		0.00571	
		✓		1.686	317.60		0.00583	Baseline specimen
			✓	1.530	288.21		0.00529	Specimen impacted with 1.13 N-m damage
			✓	1.512	284.82		0.00523	
			✓	1.437	270.70		0.00497	
		✓		1.374	258.83		0.00475	
		✓		1.374	258.83		0.00475	Specimen impacted with 1.13 N-m damage
65C17721-4	21.1	✓		1.508	284.07		0.00522	
65C17721-2	53.9		✓	2.509	472.64		0.00868	Repaired specimen
			✓	2.437	459.07		0.00843	
	53.9		✓	2.798	527.07		0.00968	
	21.1		✓	1.868	351.89		0.00646	
			✓	2.028	382.03		0.00702	
	21.1		✓	1.952	367.71		0.00675	
	71.1		✓	1.477	278.23		0.00511	
			✓	1.597	300.84		0.00552	
	71.1		✓	1.730	325.89		0.00598	
	53.9	✓		2.566	483.37		0.00888	
		✓		1.664	313.46		0.00575	
	53.9	✓		1.681	316.66		0.00582	
	21.1	✓		1.908	359.42		0.00660	
		✓		1.517	285.77		0.00525	
	21.1	✓		1.499	282.38		0.00518	
	71.1	✓		1.397	263.16		0.00483	
		✓		1.285	242.06		0.00445	
65C17721-2	71.1	✓		1.486	279.93	5.45×10^4	0.00514	Repaired specimen



- (7) Refer to Figure 4.8 and using X minimum and X maximum dimensions draw pencil lines A and B parallel to the control tab hinge centerline as shown in Figure 4.8.
- (8) Mount the control tab on the rebalance fixture as shown in Figure 4.8 (see Model 727 Structure Repair Manual, Chapter 51-80 Figure 4.3 for a tabulated listing of rebalance equipment).
- (9) Check that the surface is free to rotate without binding. Rotate the surface such that the chord plane is horizontal using a protractor level set at $6^{\circ}32'$ and block the trailing edge of the surface in the horizontal position while the protractor level is retained on the surface.
- (10) Place the sliding block weight (detailed in Figure 4.7a) on the ruled paper aft of line A as shown in Figure 4.8. Remove protractor level from the surface. Slowly move the block forward towards the control tab leading edge until the trailing edge just begins to rise away from the supporting blocks. Ensure that the sliding block weight is positioned parallel to the control tab hinge centerline. Use the parallel lines on the ruled paper attached to the tab skin for alignment.
- (11) Note the position of the midpoint mark on the forward edge of the sliding block weight.
- (12) If the front edge of the sliding block weight is between line A and line B the control tab is within the operational c.g. limits and can be reused.
- (13) If the front edge of the sliding block weight is forward of line A or aft of line B the control tab is not within the operational c.g. limits and must be replaced.



ATTACHMENT OF LINED PAPER TO UPPER CONTROL TAB SURFACE
 X MIN = 0.50 INCHES X MAX = 2.07 INCHES
 NOTE: X DIMENSIONS MEASURED AFT FROM CUT-OUT
 IN CONTROL TAB LEADING EDGE

FIGURE 4.8 - CONTROL TAB SET-UP FOR BALANCE CHECK

REV SYM C

I. CONTROL TAB COUNTERBALANCE PROVISIONS

- (1) Control tabs which after repair exceed the manufacturing maximum weight of 8.10 pounds can be accommodated in an elevator system by means of the control tab counterbalance provisions.
- (2) A control tab weighing after repair between 8.11 pounds and 8.35 pounds will require one (1) tab counterbalance weight, 69-69700-2 (color orange) to be installed at location T_1 in Bay No. 1 on the elevator nose structure. (See Figure 4.2)
- (3) A control tab weighing after repair between 8.36 pounds and 8.60 pounds will require two (2) tab counterbalance weights, 69-69700-2 (color orange) to be installed at locations T_1 and T_2 in Bay No. 1 on the elevator nose structure. (See Figure 4.2)
- (4) Control tabs that require tab counterbalance weights must also satisfy the C.G. limits as noted in Table 4.1.
- (5) When control tabs requiring tab counterbalance weights are removed from an elevator system, the counterbalance weights must be removed at the same time and accompany the tab at all times.
- (6) When control tabs accompanied by tab counterbalance weights are installed on an elevator system, the tab counterbalance weights must be installed at the locations T_1 or T_1 and T_2 reserved for this purpose on the elevator nose structure.

ATTENTION IS DRAWN TO CAUTION PARAGRAPH 4.H.(3).

NOTE !! A control tab exceeding the maximum allowable weight of 8.60 lb. is not acceptable.

J. MATERIAL WEIGHTS

- (1) The following approved material unit weights should be used when predicting graphite/epoxy repair weights.




BMS 8-212, Type II, Class 2, Style 3K-70-P Graphite Fabric Preimpregnated with Epoxy Resin	= 0.00042 pound/sq.inch
BMS 8-245, Grade 08, Film Adhesive	= 0.00056 pound/sq.inch
BMS 5-80, Type 2, Grade 10 Film Adhesive	= 0.00042 pound/sq.inch
BMS 5-80, Type 2, Grade 15 Film Adhesive	= 0.00059 pound/sq.inch
BMS 5-90, Type 2, Class 250, Grade 50 Foaming Adhesive	= 0.00274 pound/sq.inch
Honeycomb Core Potting Resin, Epocast 1835 + Epocast 9816 Phenoic Microballoons	= 0.0312 pound/cu.inch

Material unit weights for metal structure repairs are detailed in Boeing 727 Structural Repair Manual, D6-4062, Chapter 51-80, Figure 4, Sheet 2.

5. FASTENERS

- A. The fasteners commonly used in graphite epoxy to graphite epoxy joints are passivated titanium or passivated stainless steel bolts, blind fasteners, or Hi-Lok fasteners, passivated stainless steel nuts, nutplates, or collars.
- B. The fasteners commonly used in graphite epoxy to aluminum joints are the same as in 5.A except these fasteners are installed wet using BMS 5-79 or BMS 5-26 sealant.
- C. The fasteners joining aluminum components together are conventional fasteners noted in D6-4062.
- D. Loose or missing fasteners must be replaced.
- E. Install all replacement fasteners with proper grip lengths and hole sizes to preclude looseness. Where the hole size exceeds the requirements of 5F for nominal sized replacement fasteners, use oversize shank fasteners. Oversize fasteners with shank sizes up to 1/32 inch over the nominal size may be installed.
- F. Hole size for replacement fasteners is to be determined as follows:
 - Min Hole Size = Maximum shank diameter of fastener
 - Max Hole Size = Maximum shank diameter of fastener + .003 in.
- G. Use torque values specified in D6-4062, 51-30-4.
- H. Replace a missing fastener with the originally specified fastener or an alternate fastener from Figure 5.1. Fasteners and alternates not shown in Figure 5.1 may be selected from D6-4062.

J18-047

REPAIR FASTENER				
ORIGINAL OR SPECIFIED			EQUIVALENT	ALTERNATIVE
CODE	PART NUMBER	DESCRIPTION		
	BAC B30NN()R()	6A1-4V Titanium Passivated,Phillips Recess,Long Thread 95 KSI		BAC B30NN()K()
	BAC B30MR()R()	6A1-4V Titanium, Passivated, 12 Pt Head,Long Thread 95 KSI		BAC B30MR()K() BAC B30LE()K()
	BAC B30NT()R()	6A1-4V Titanium, Passivated,Phillips Recess,Short Thread 95 KSI		BAC B30NT()K() BAC B30LE()K()
	BAC B30MY()R()	6A1-4V Titanium, Passivated, Protruding Head, 95 KSI		BAC B30MY()K() JLY 1235-()-() 
	PLT 1058S()-() 	Flush Blind Fastener		JLY 1237-()-() 
	BAC B30NU()R()	6A1-4V Titanium, Passivated,Hi-Torque Recess,Flush Head 95 KSI		
	BAC B30NW()R()	6A1-4V Titanium Passivated,Flush Head, 95 KSI		
	AIC 1689-()-()	Titanium, Passivated,Torque Set Recess,Flush Head, 95 KSI		

 Monogram Industries; Los Angeles, California 90040.

FIGURE 5.1 - REPLACEMENT FASTENER SUBSTITUTION TABLE

D14100 7740 ORI 6.3/71

REV SYM A

APPENDIX 1 - EXAMPLES OF REPAIRS MADE TO GRAPHITE/EPOXY COMPONENTS

This appendix provides photographs of some repairs that have been made to graphite/epoxy components by the Boeing Company. The types of repairs include repair of a puncture in a sandwich panel skin, replacement of a large area honeycomb core and repair of a crack in solid graphite/epoxy laminate.

CAUTION: REPAIRS SHOWN IN THIS SECTION MAY EXCEED THE REPAIRABLE DAMAGE CRITERIA SHOWN IN SECTION 1 HEREIN AND ARE CONSIDERED SPECIAL CONDITIONS WHICH REQUIRE COORDINATION WITH THE BOEING COMPANY ENGINEERING DEPARTMENT.

The photographs in Figures A1.1 through A1.12 show some of the major steps of repairing a puncture to a face sheet of a graphite/epoxy sandwich panel.

Figures A1.13 through A1.20 show some of the major steps of repairing core which was mislocated during fabrication of a graphite/epoxy sandwich panel. The graphite plies used in the repair were impregnated with epoxy resin and the repair was cured in an autoclave.

The graphite/epoxy component shown in Figures A1.21 and A1.22 was cracked in a solid laminate area during fabrication. These two figures depict the crack before and after repair.

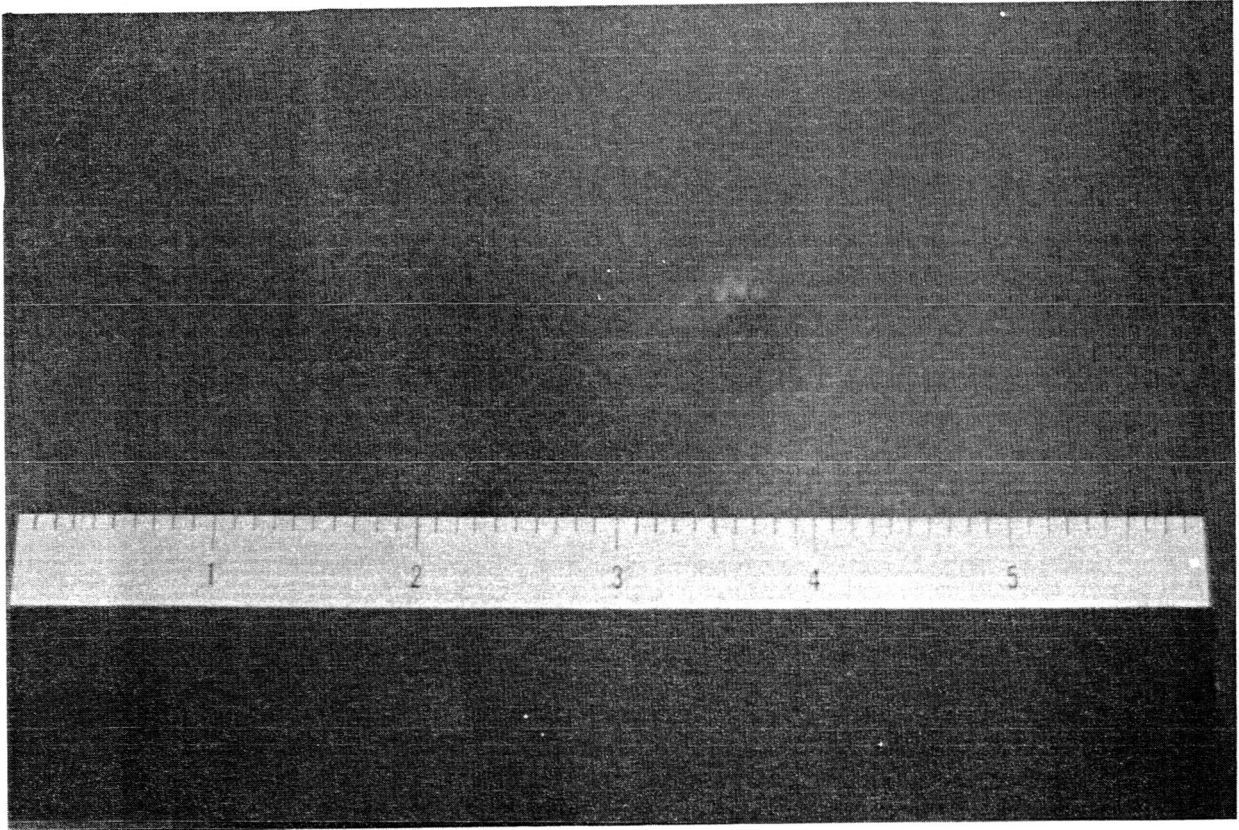


Figure A1.1. Damage to a Sandwich Panel Face Sheet

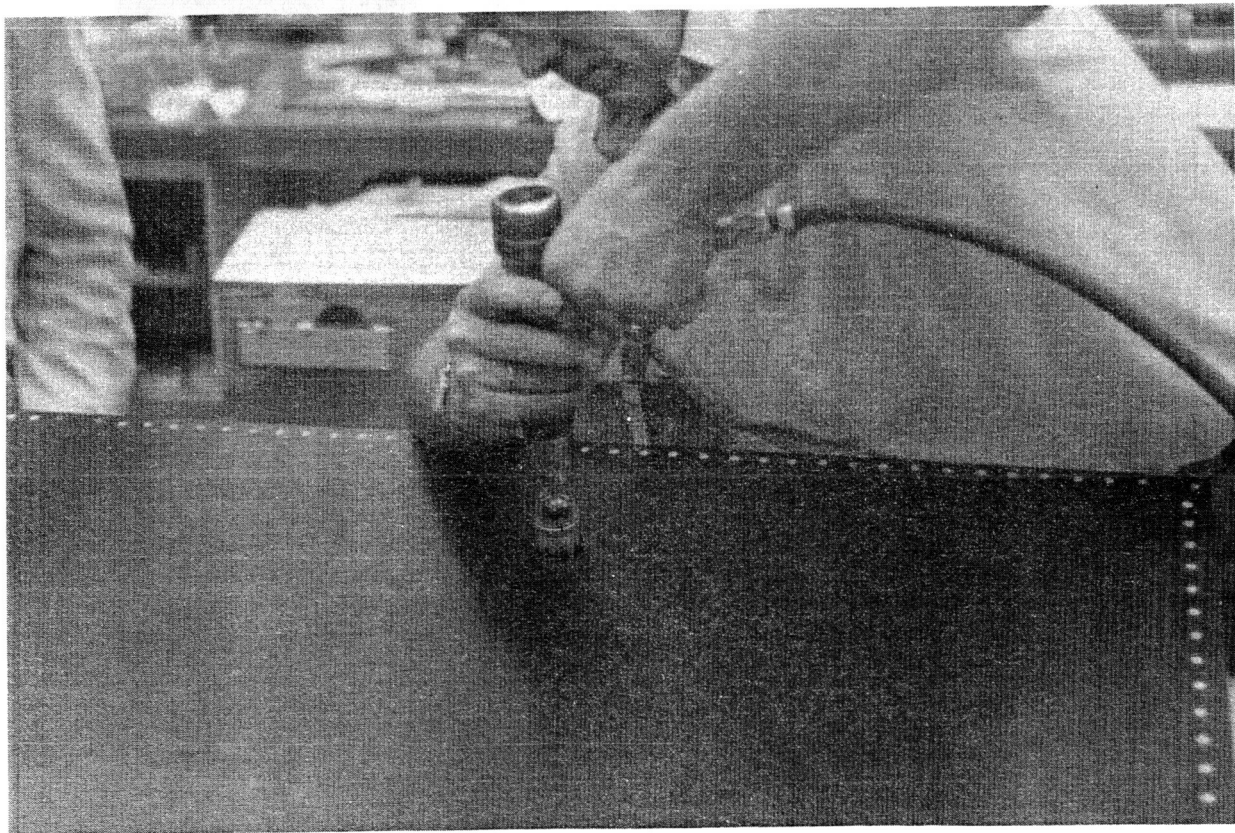


Figure A1.2. Removal of Damaged Face Sheet

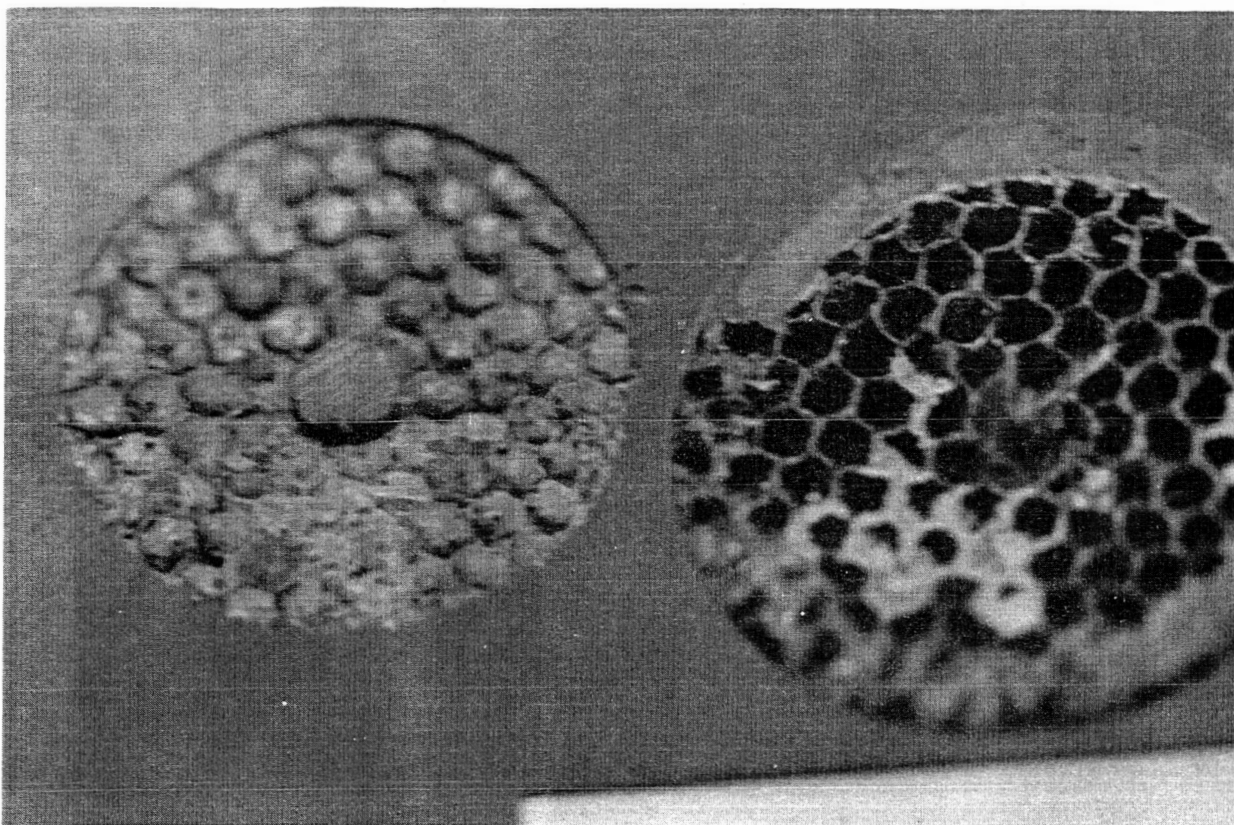


Figure A1.3. Damage Area in Skin Removed

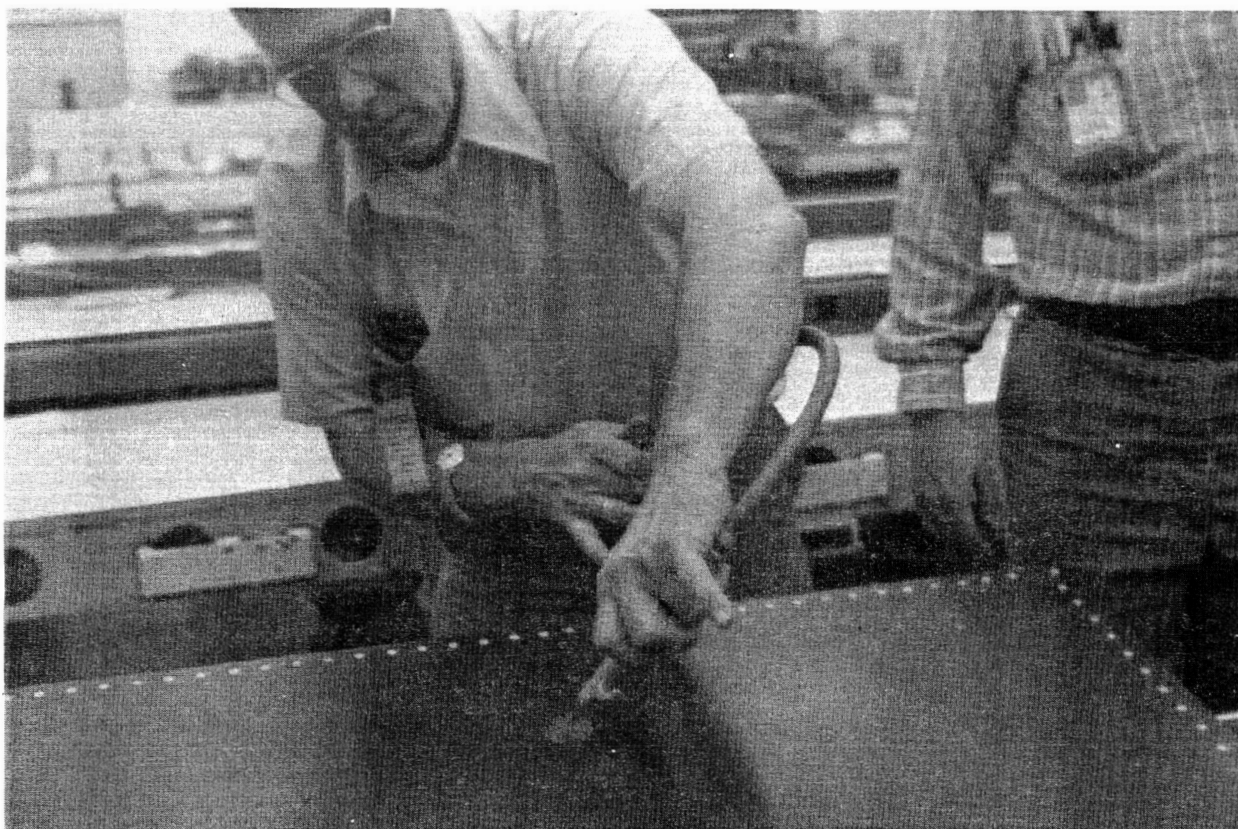


Figure A1.4. Removal of Damaged Core

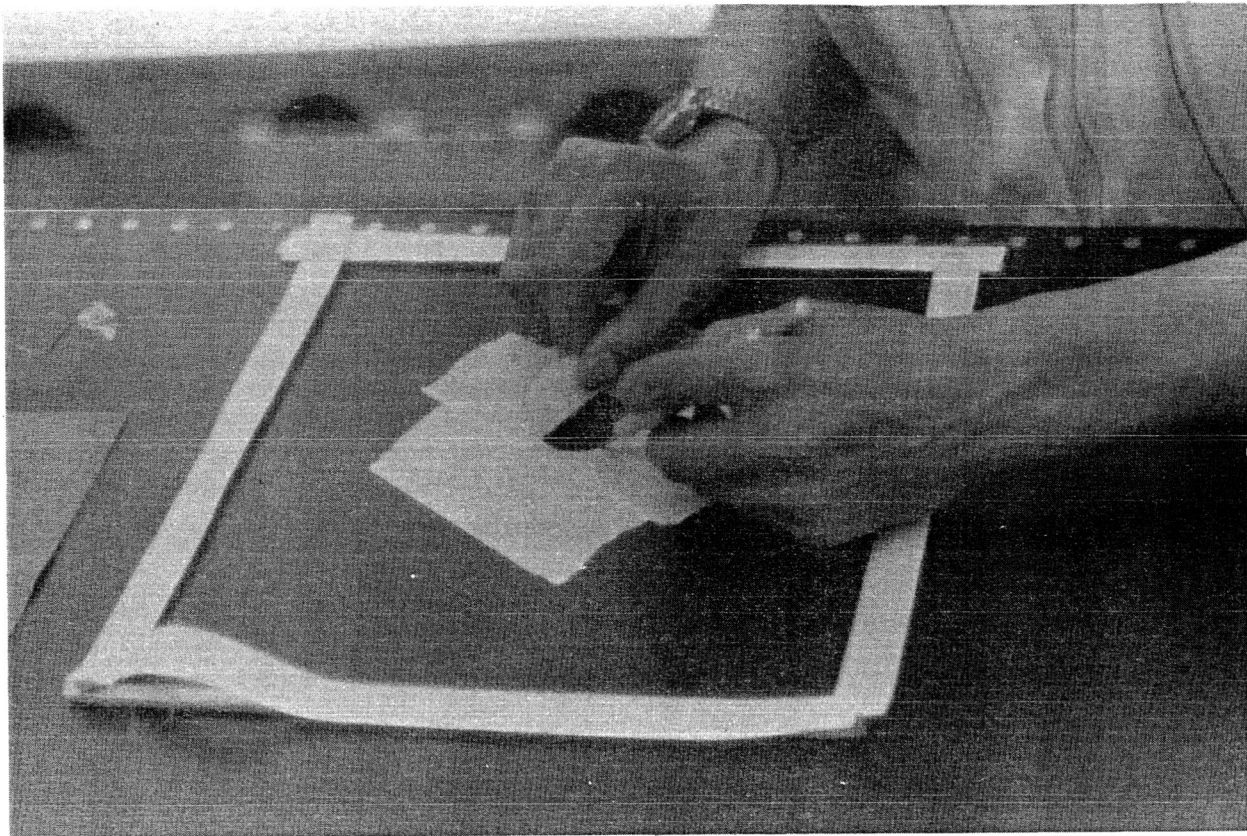


Figure A1.5. Masking of Repair Area

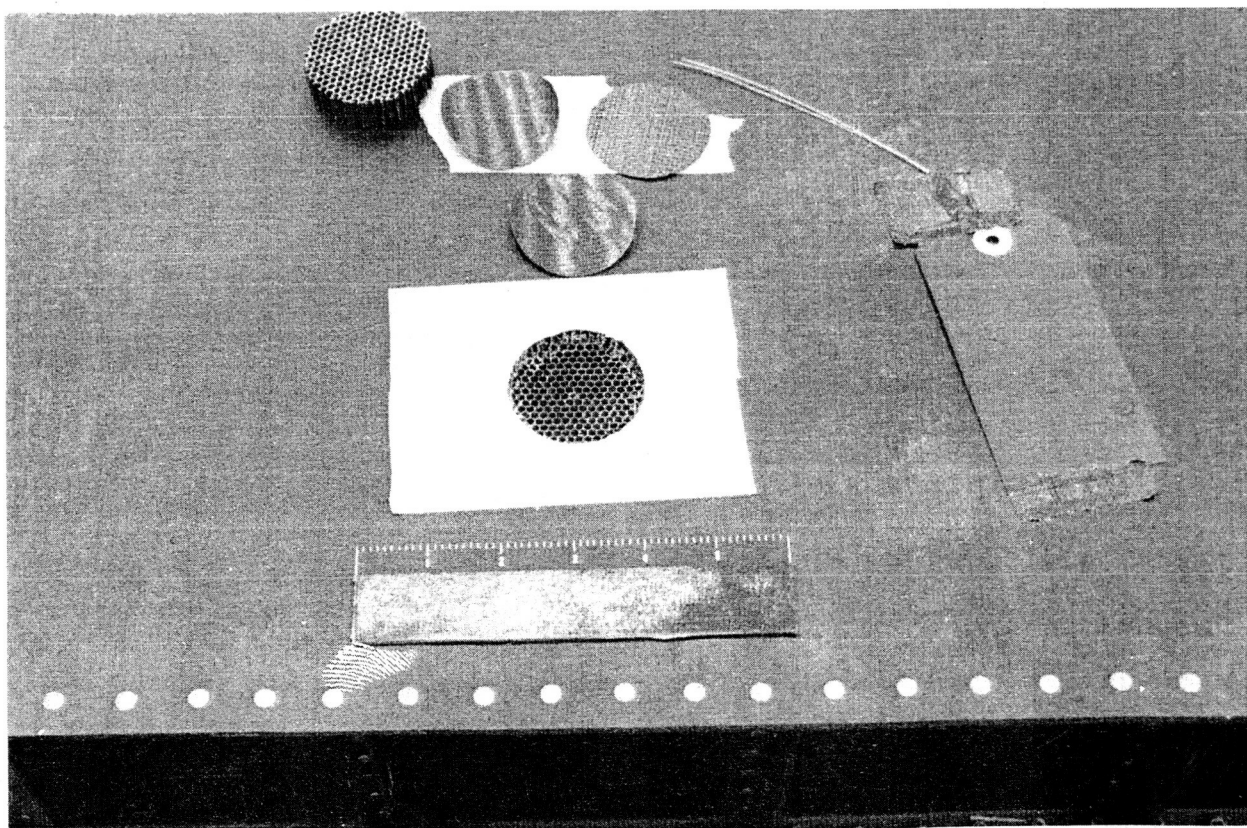


Figure A1.6. Core Replacement and Adhesive Ready for Installation

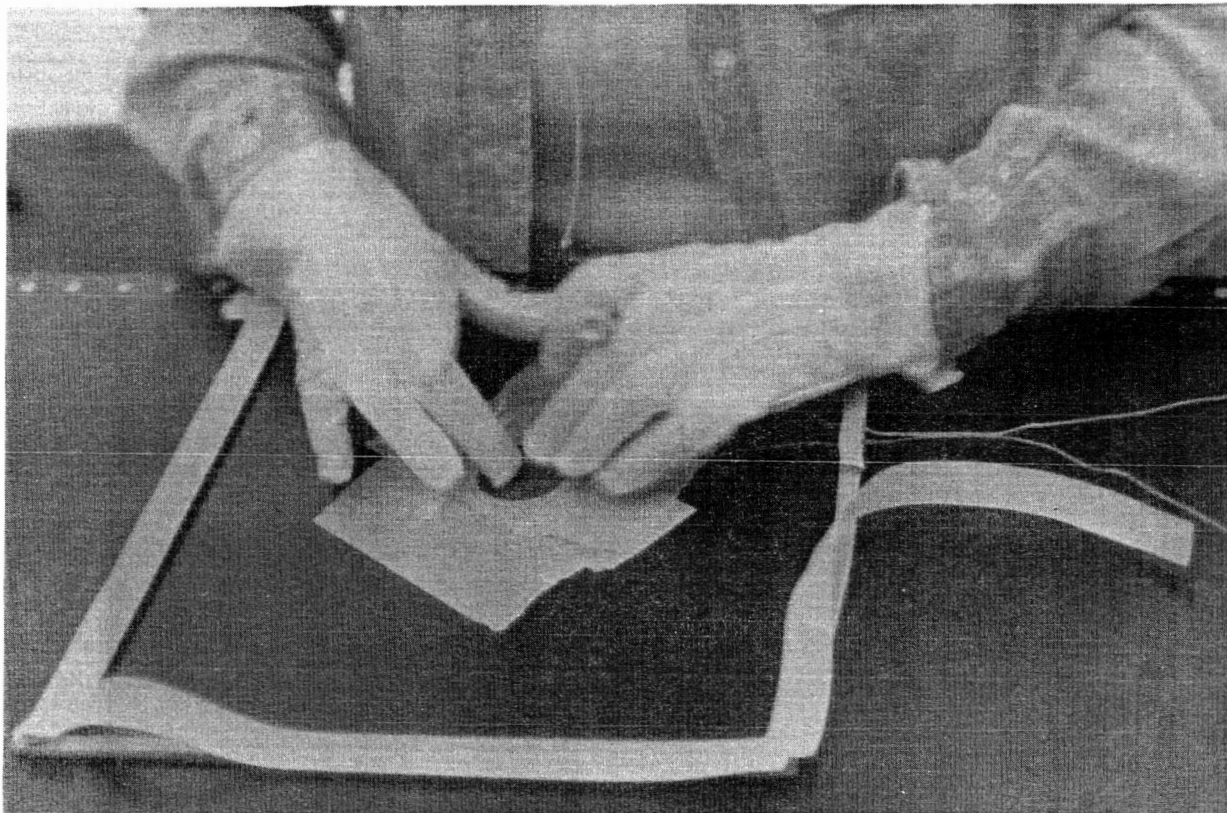


Figure A1.7. Installation of Adhesive

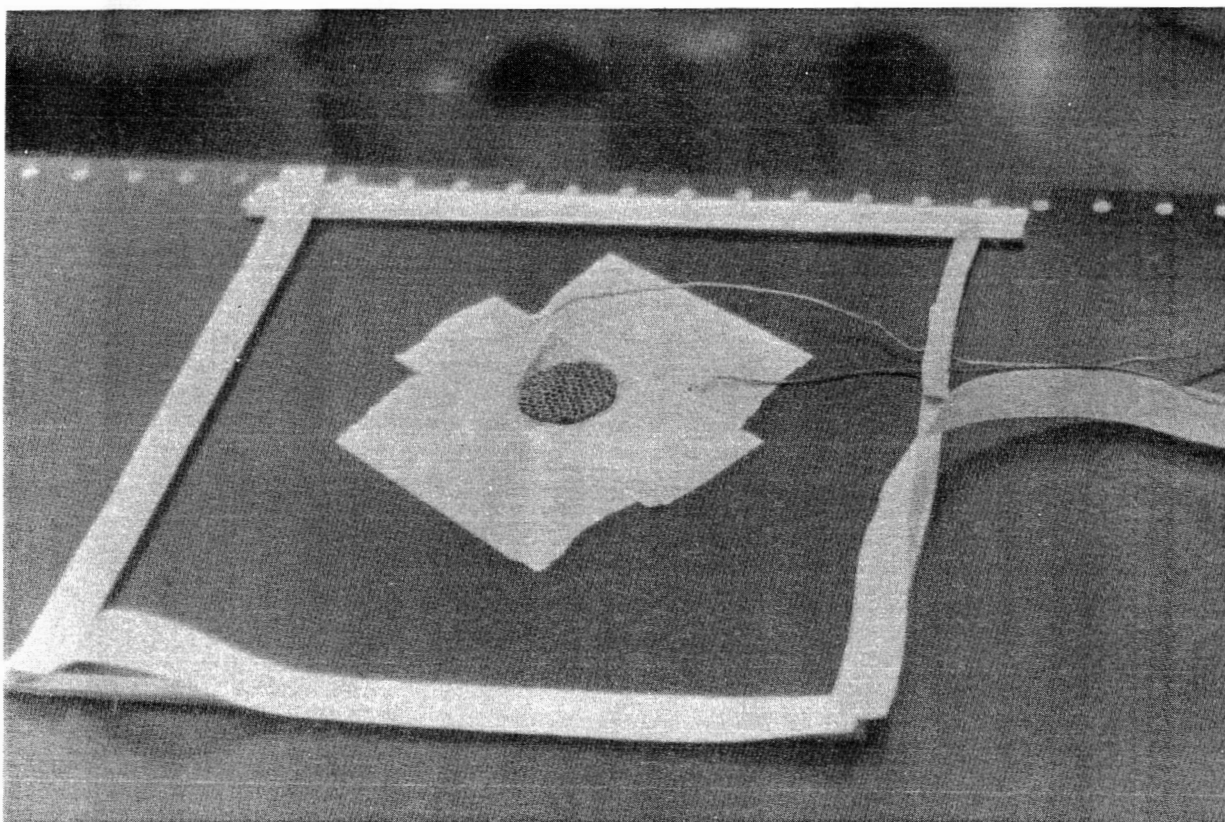


Figure A1.8. Core Replacement in Place

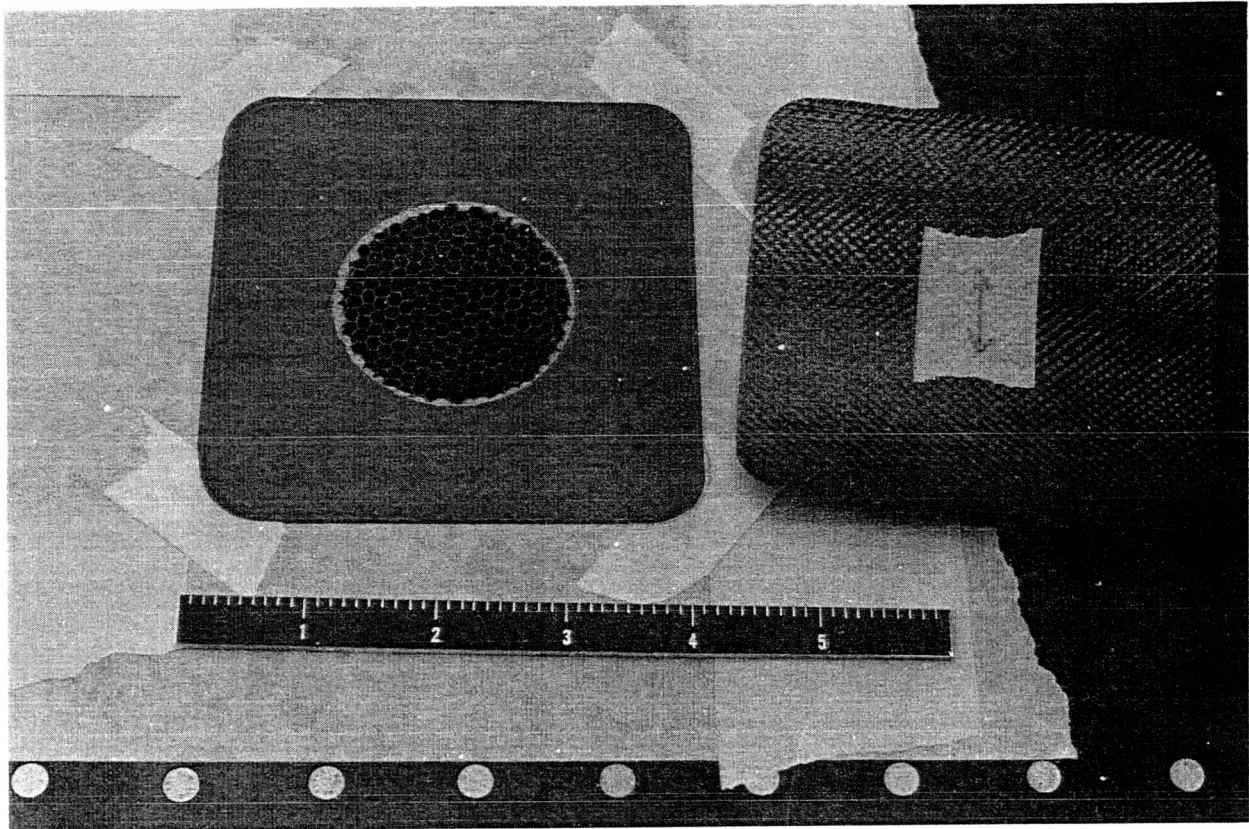


Figure A1.9. Core Replacement after Installation With Precured Patch Ready for Installation

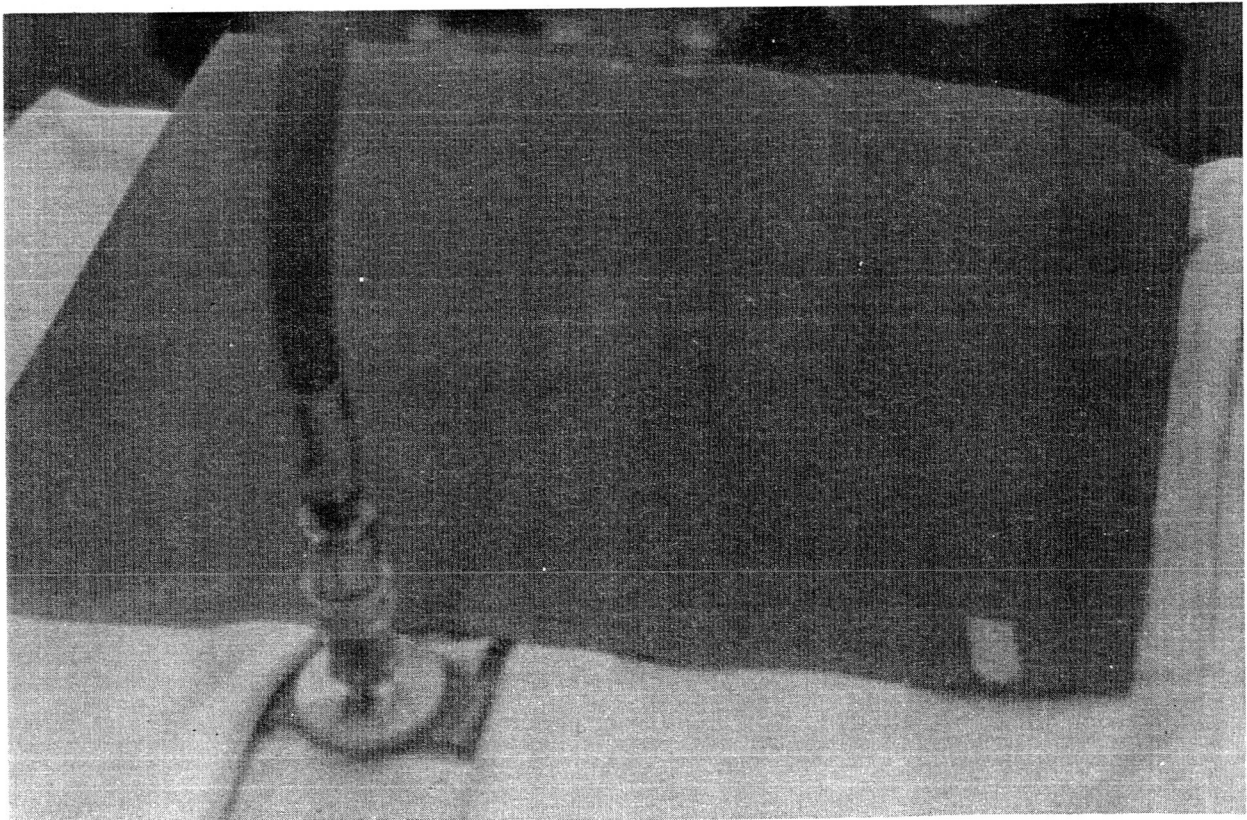


Figure A1.10. Heating Pad in Place

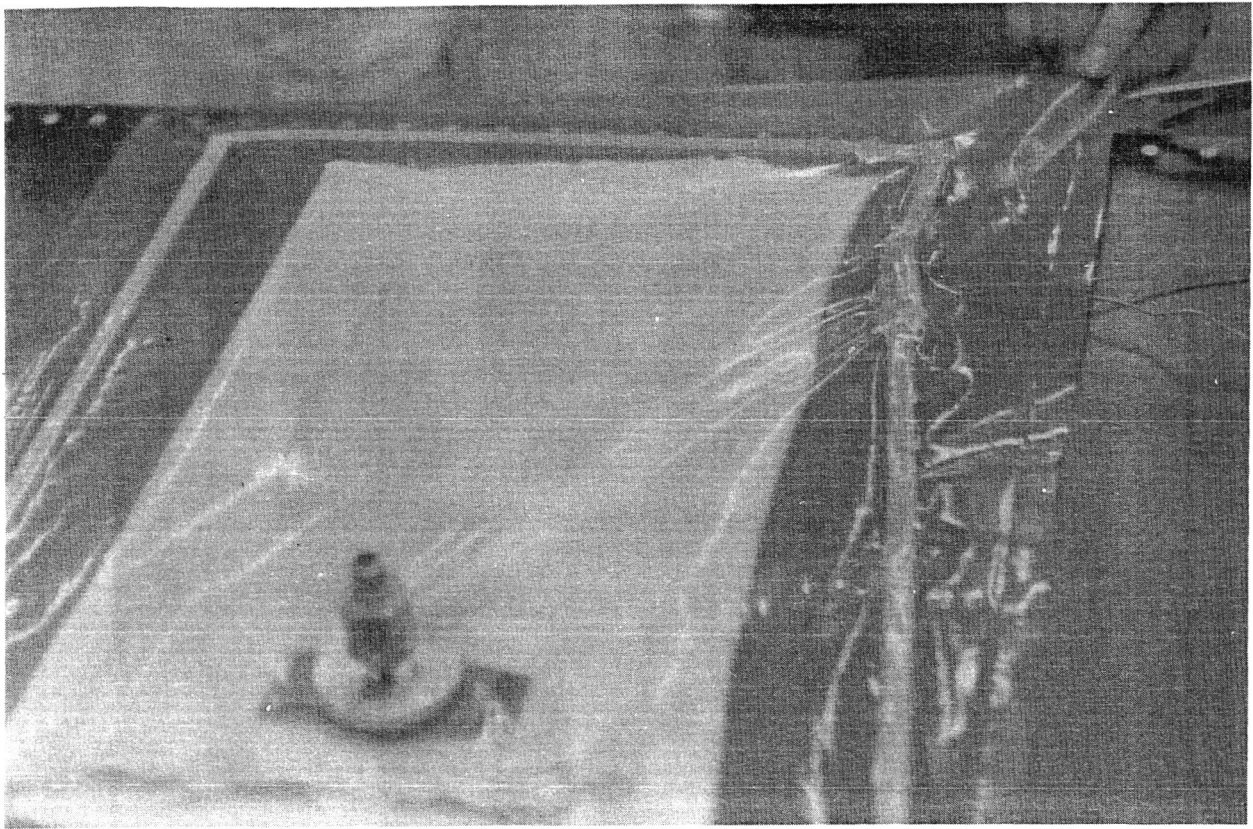


Figure A1.11. Vacuum Bag in Place

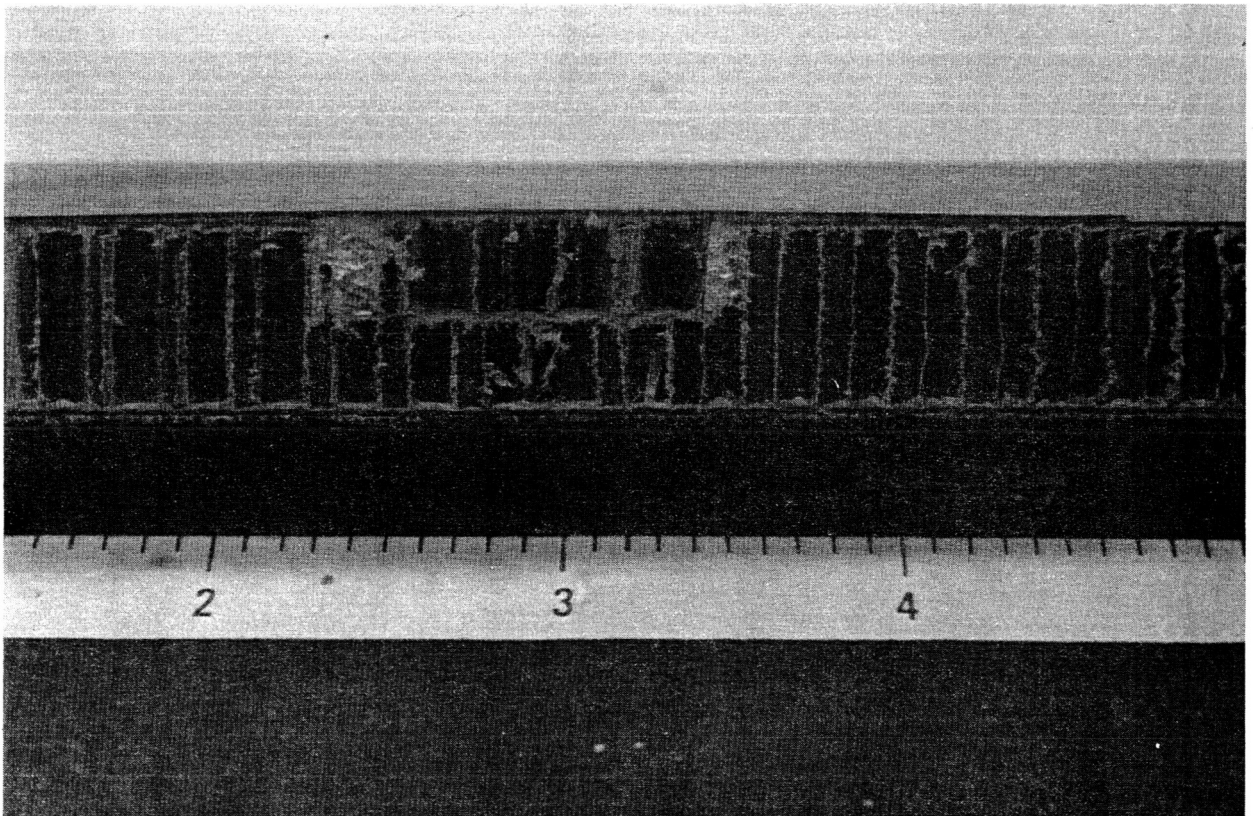


Figure A1.12. Cross-Section Through Repaired Panel

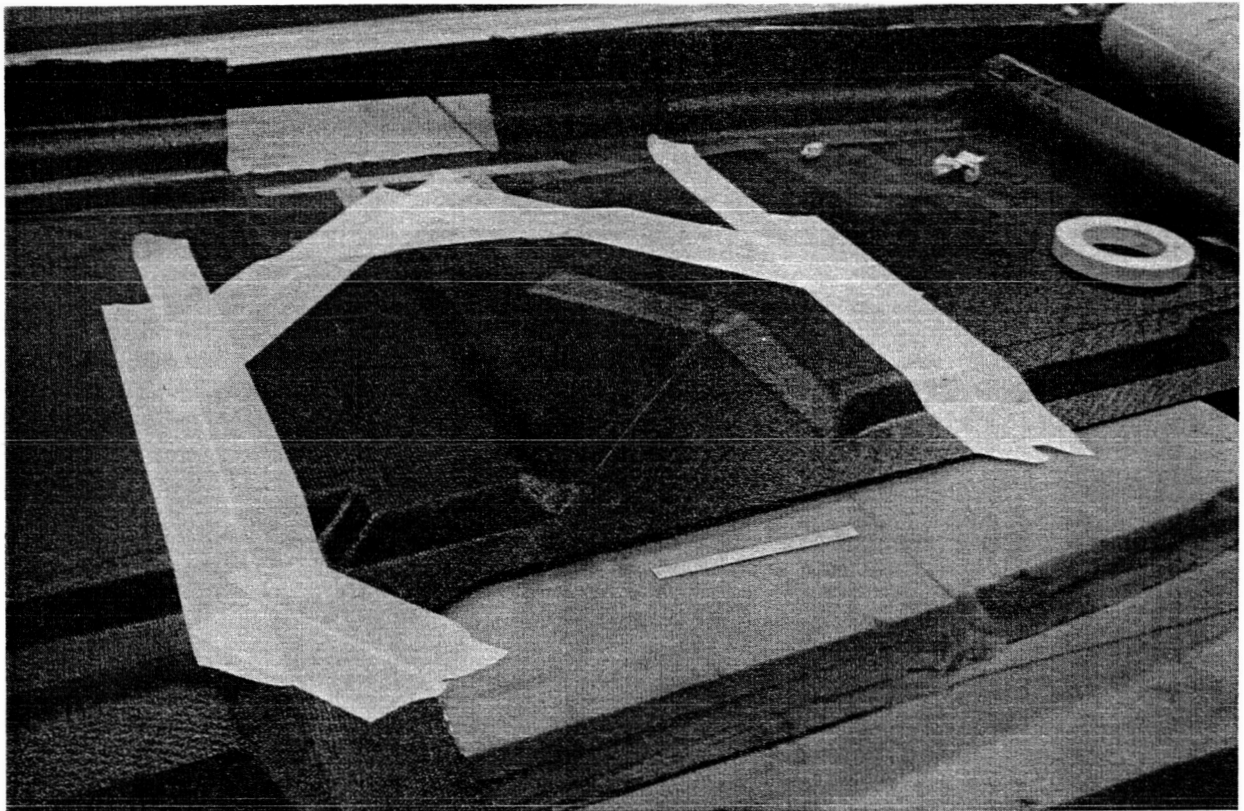


Figure A1.13. Graphite/Epoxy Sandwich Panel Core Repair—Repair Area Masked

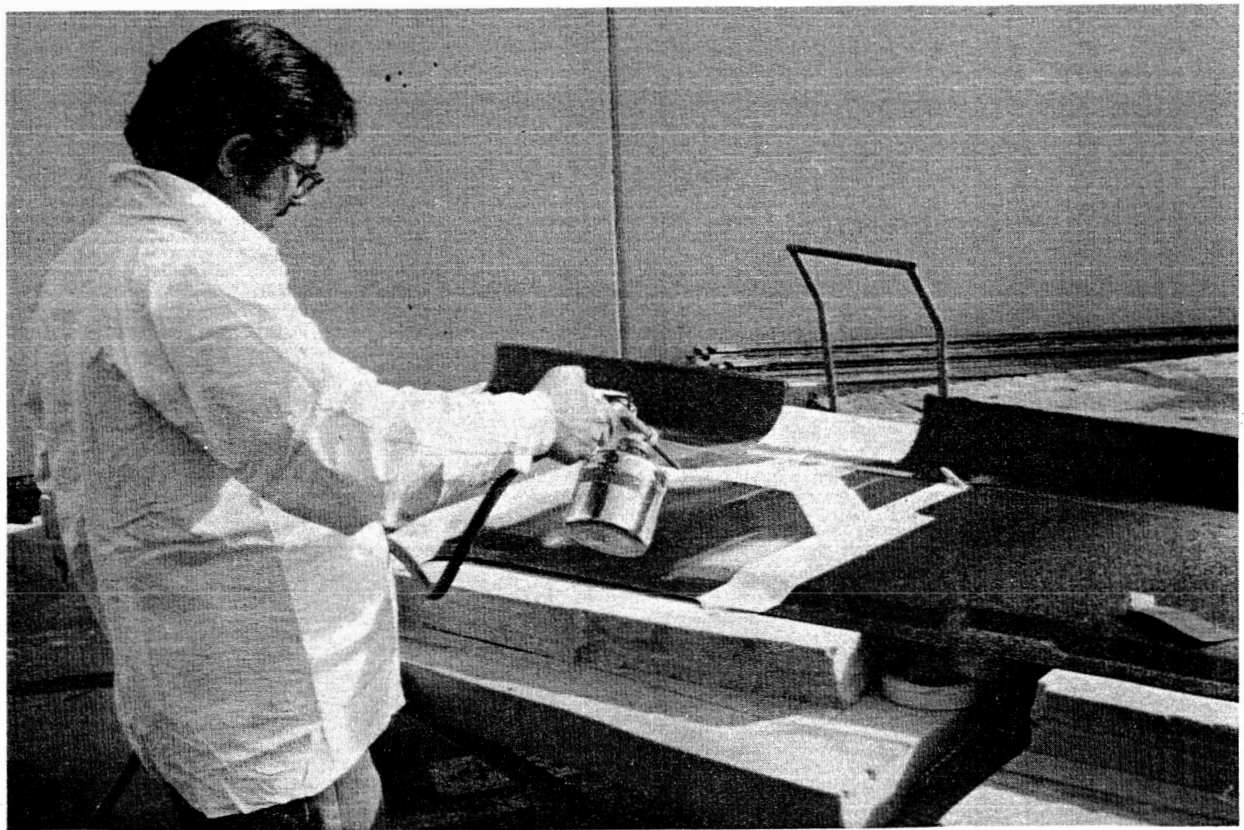


Figure A1.14. Graphite/Epoxy Sandwich Panel Core Repair—Grit Blasting of Tedlar Surface

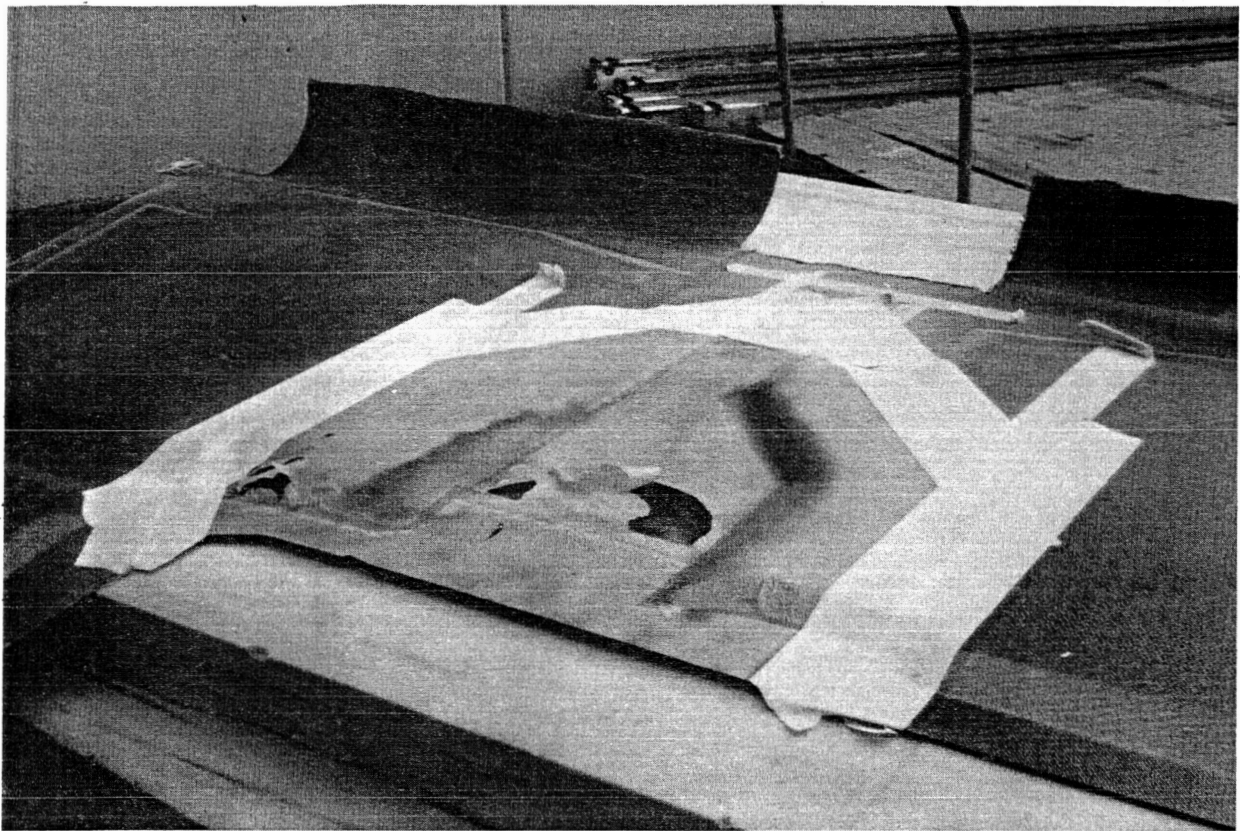


Figure A1.15. Graphite/Epoxy Sandwich Panel Core Repair—Tedlar After Grit Blasting

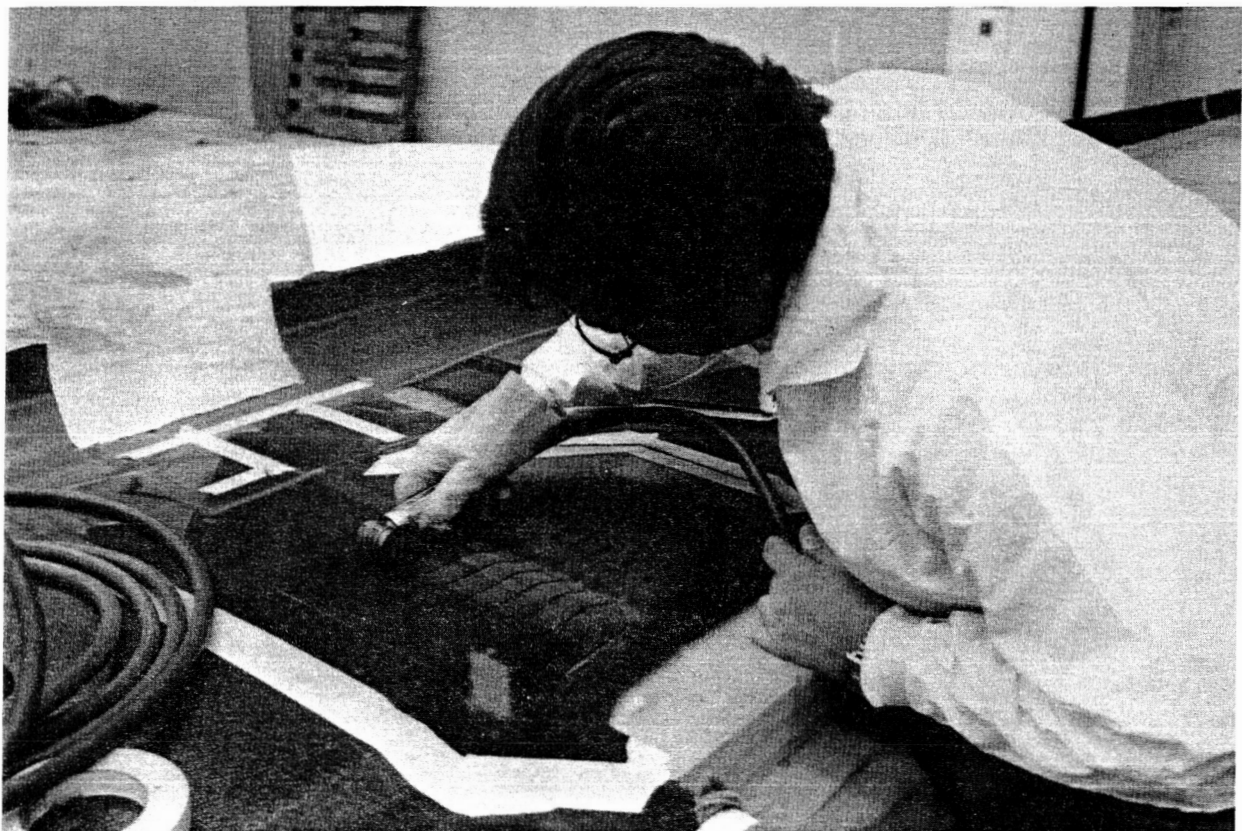


Figure A1.16. Graphite/Epoxy Sandwich Panel Core Repair—Removal of B-61

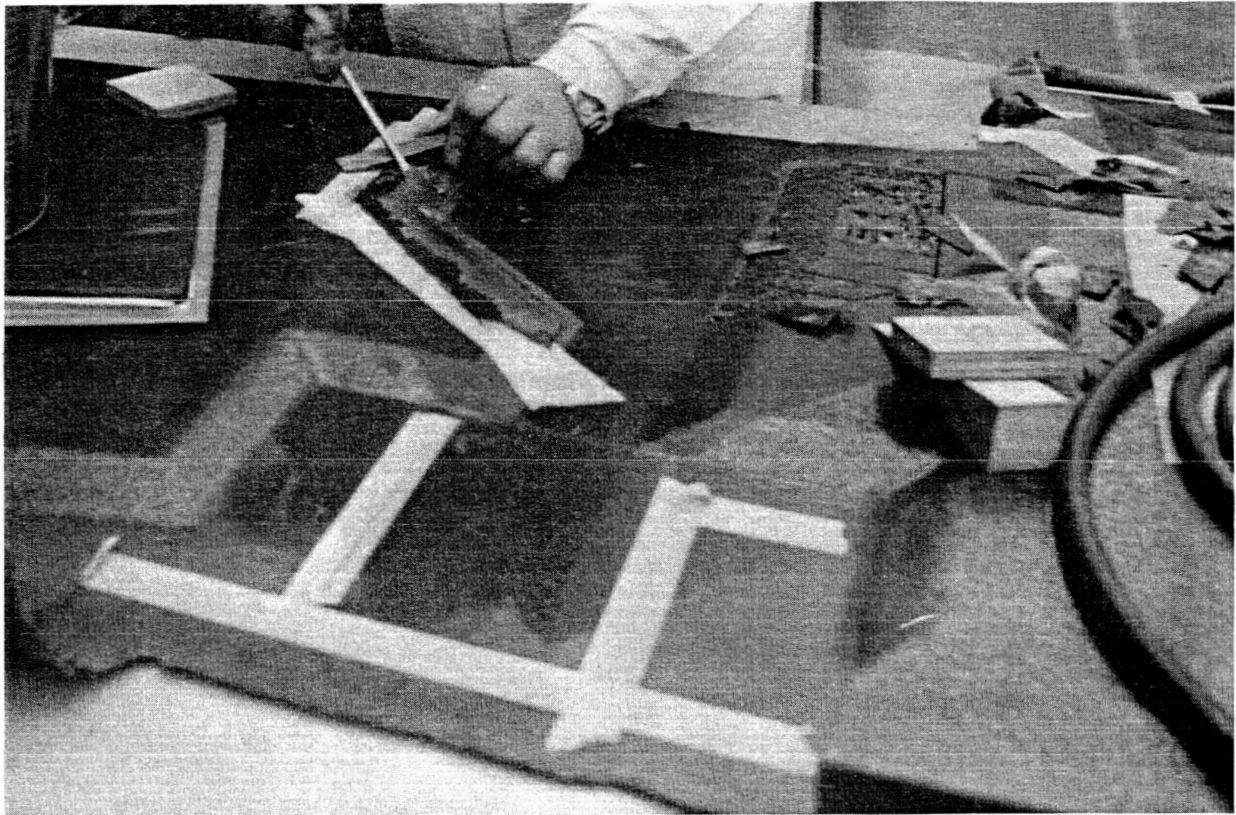


Figure A1.17. Graphite/Epoxy Sandwich Panel Core Repair—Removal of Damaged Core

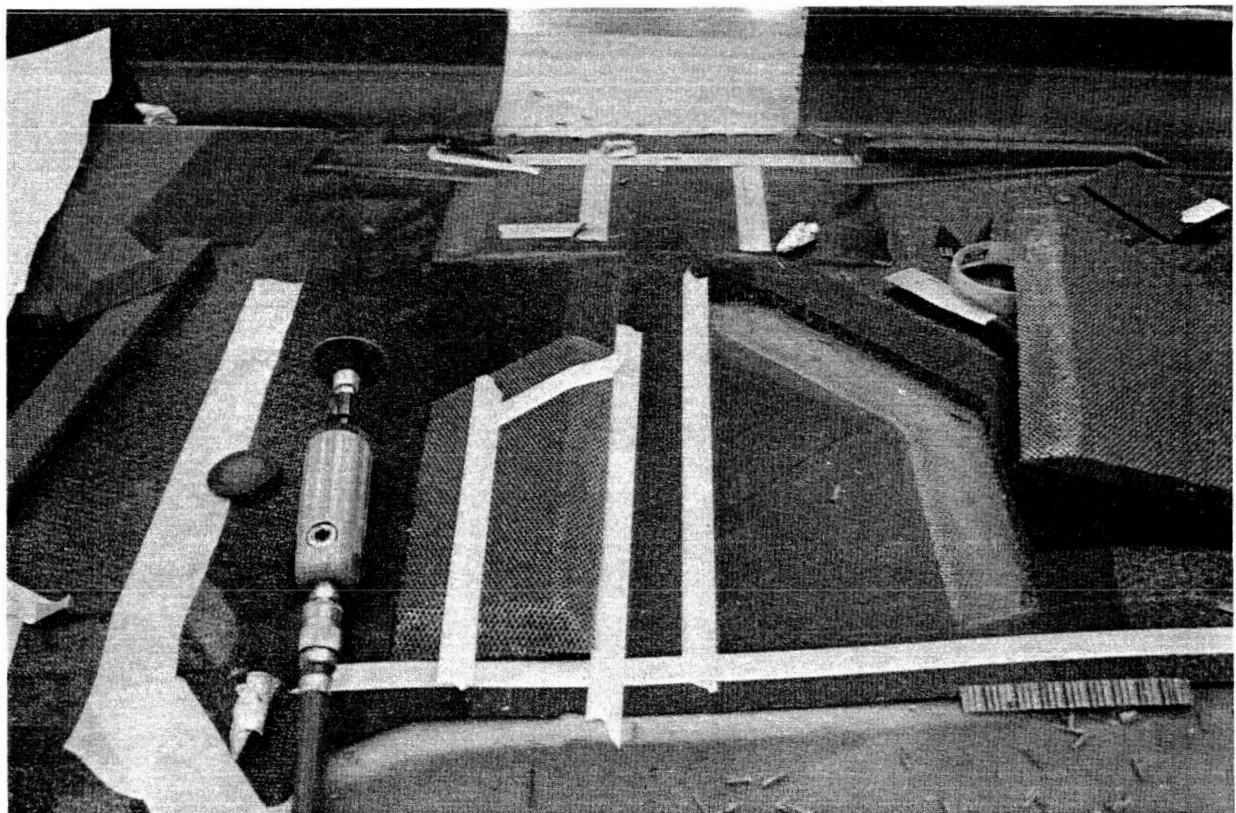


Figure A1.18. Graphite/Epoxy Sandwich Panel Core Repair—Replacement Core in Position (Left) and Core Ready for Installation (Right)

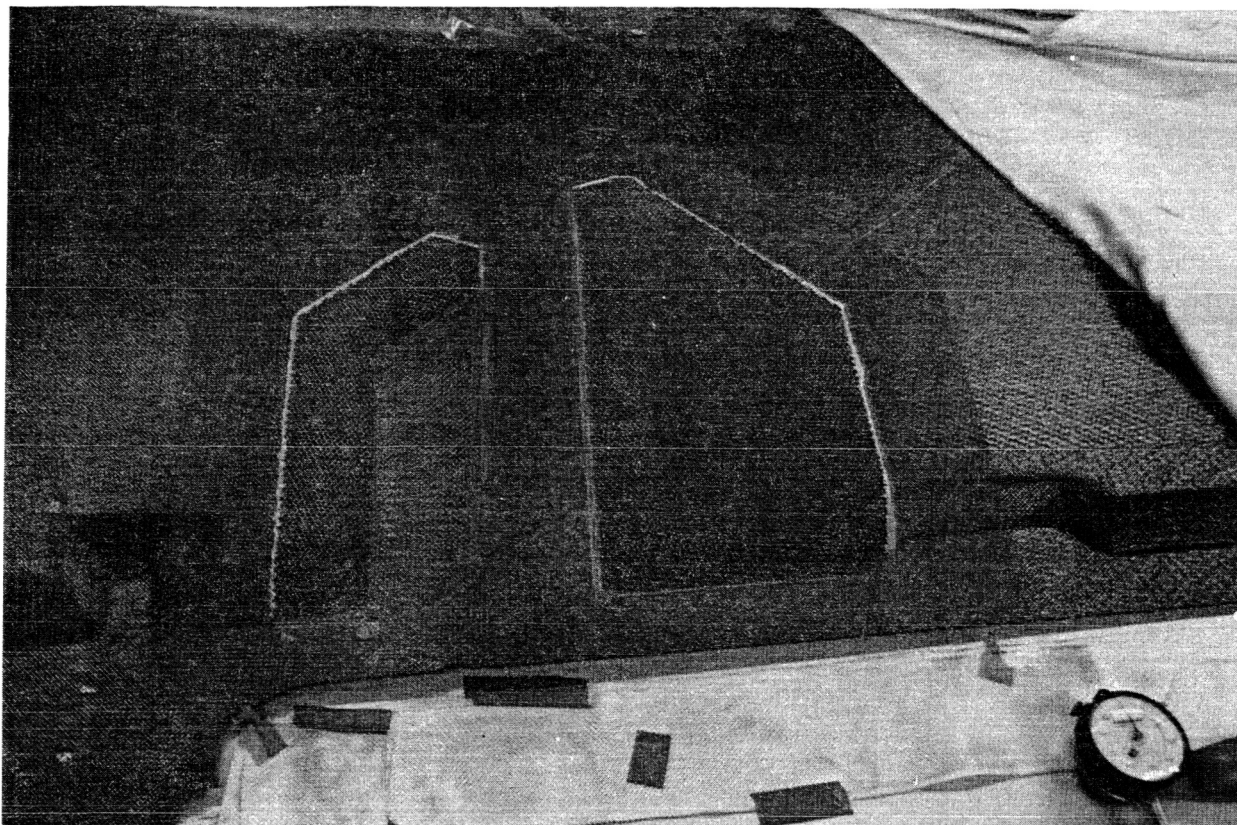


Figure A1.19. Graphite/Epoxy Sandwich Panel Core Repair—Replacement Core Bonded to Panel

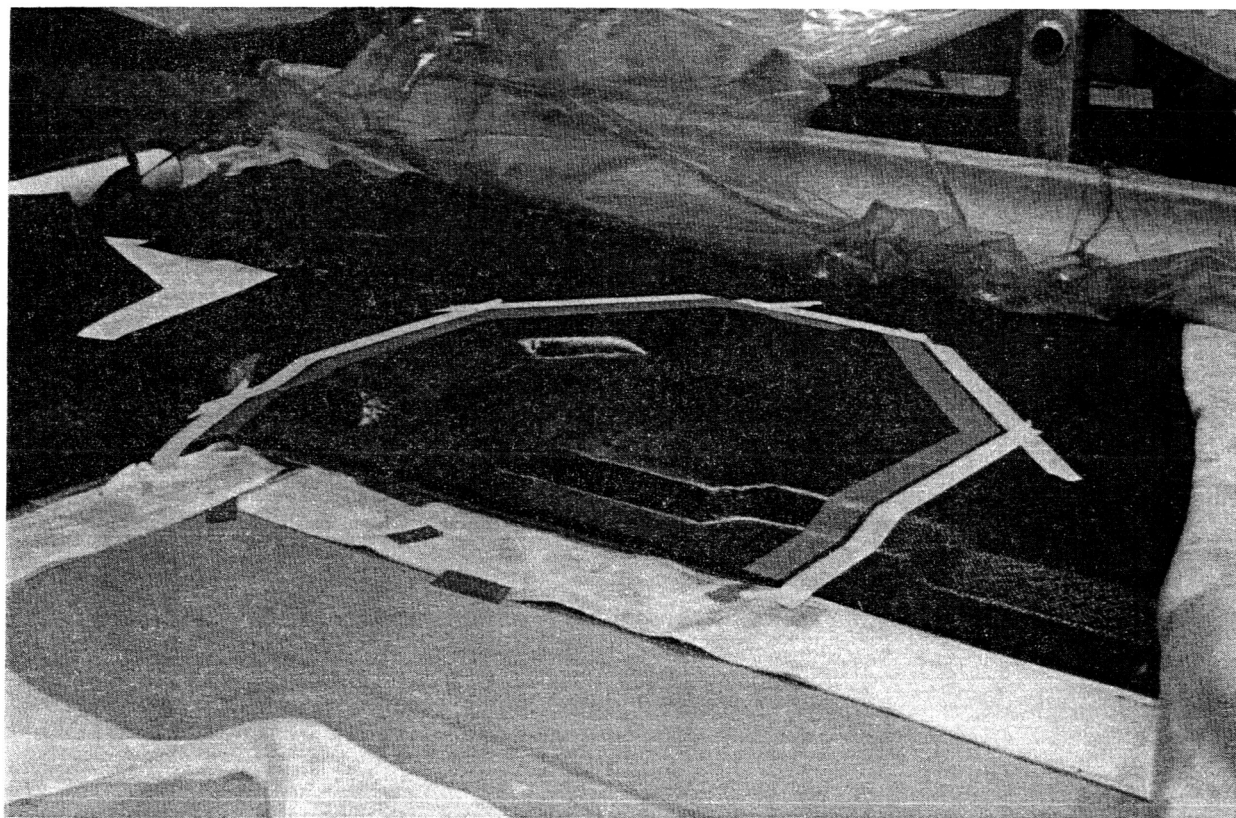


Figure A1.20. Graphite/Epoxy Sandwich Panel Core Repair—Replacement Graphite Plies After Curing

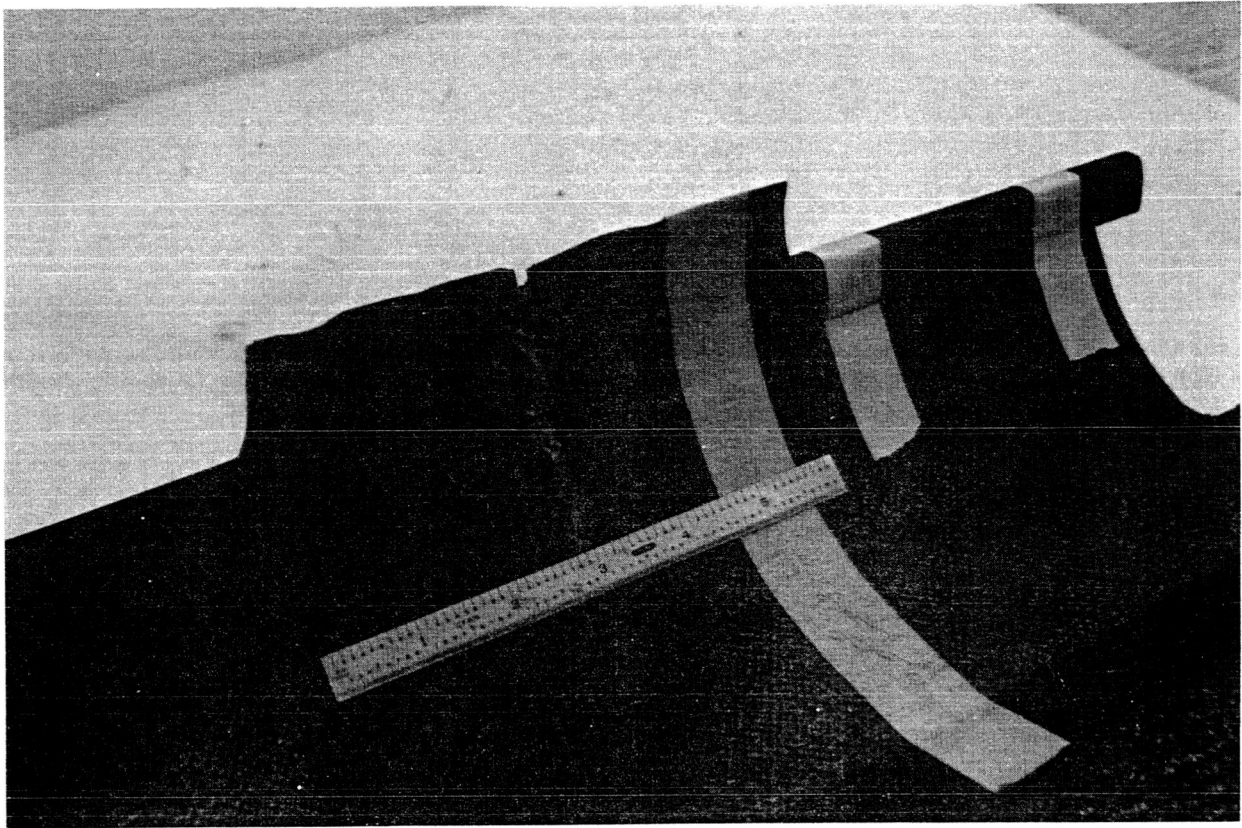


Figure A1.21. Crack in Solid Graphite/Epoxy Laminate Before Repair

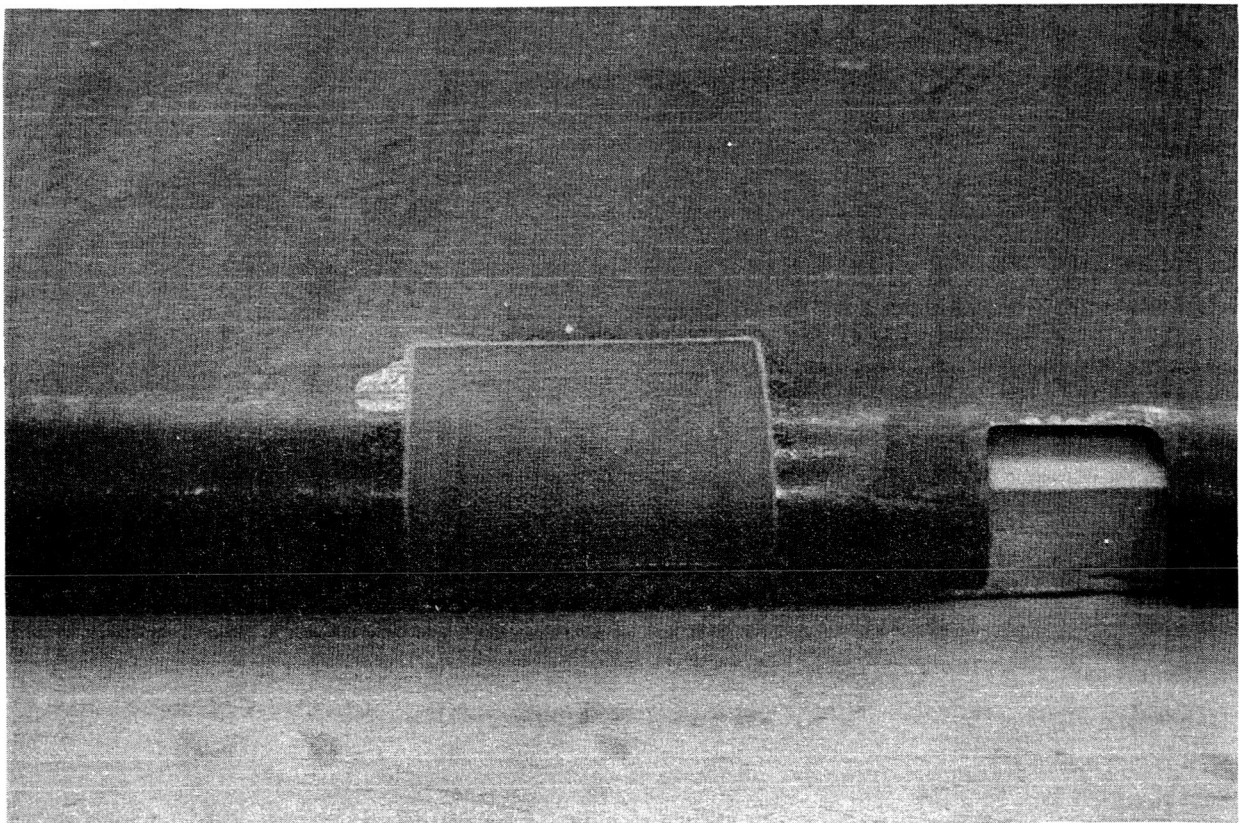


Figure A1.22. Repaired Crack in Graphite/Epoxy Solid Laminate

APPENDIX C
ANCILLARY TEST PROGRAM COUPON TEST DATA

CONTENTS

	Page
Notes and Abbreviations	C-3
Static Tension with Holes (NASA Test 1)	C-5
Static Compression with Holes (NASA Test 1)	C-9
Static Tension (Boeing 7313-16)	C-13
Static Compression (Boeing 7313-16)	C-15
Rail Shear with Holes (NASA Test 1)	C-17
Static Tension with Impact (NASA Test 1)	C-21
Static Compression with Impact (NASA Test 1)	C-23
Static Compression with Delamination (NASA Test 1)	C-25
Four-Point Beam Bending (Boeing 7313-36)	C-27
Mechanical Fastened Joint (NASA Test 4)	C-31
Static Tension, Hard Point (NASA Test 4)	C-37
Static Tension, Filled Holes (NASA Test 4)	C-38
Static Tension, Panel to Rib (NASA Test 8)	C-41
Honeycomb Panel Repair Tests	C-43
Environmental Exposure, Tension, Laminate Coupon (NASA Test 3)	C-45
Environmental Exposure, Compression, Honeycomb Coupon (NASA Test 3)	C-47

NOTES AND ABBREVIATIONS

NOTES

The SI values shown throughout Appendix C have been converted from the corresponding values in English units.

1 Material and specification.

- Fabric—Epoxy impregnated graphite fabric per BMS 8-212 Type II, Class 2, Style 3K-70-P. Fabricate per BAC 5562, nominal thickness—0.19 mm (0.0075 in).
- Tape—Epoxy preimpregnated graphite unidirectional tape per BMS 8-212 Type II, Class 1, Grade 95. Fabricate per BAC 5562, nominal thickness—0.089 mm (0.0035 in).

2 Drawing and assembly number

3 Orientation of fibers with respect to 0-deg reference.

4 Environmental conditioning.

- Dry—Normal laboratory environment.
- Wet—Laminate and honeycomb specimens conditioned according to procedure defined in Section 4.1.6 of this document.

5 Maximum load during test.

6 Failure stress based on failure load, measured specimen width, and nominal ply thickness.

7 Boeing nominal extensional modulus.

8 Calculated strain based on failure load, area, and modulus.

9 Boeing nominal shear modulus.

10 Specimen supported on 38.1 mm (1.50 in) diameter ring and impacted with a 16 mm (0.625 in) diameter spherical impactor.

11 Nonbondable Teflon 0.076 mm (0.0030 in) thick.

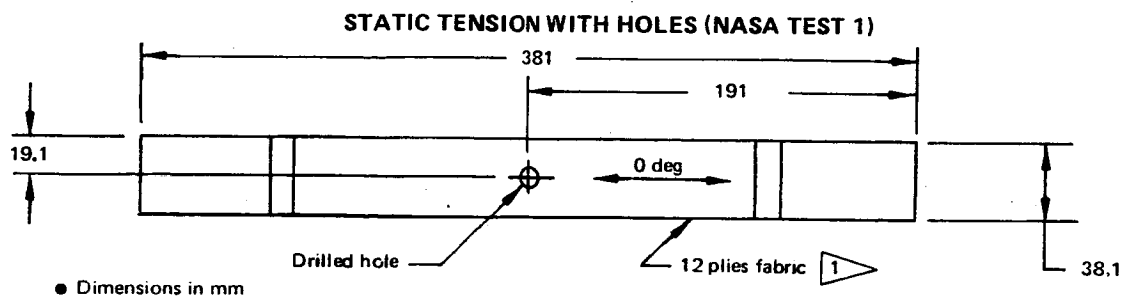
12 Boeing specification 3.18-mm (1/8-in) cell Nomex honeycomb core.

13 Compression strain surface direction.

14 Stress based on fastener nominal diameter and splice plate nominal thickness.

ABBREVIATIONS

mm	measured dimension, millimeters
in	measured dimension, inches
kN	load, kilonewtons
kip	load, kilopounds force
MPa	stress or modulus, megapascals
psi	stress or modulus, pounds force per square inch
RT	room temperature

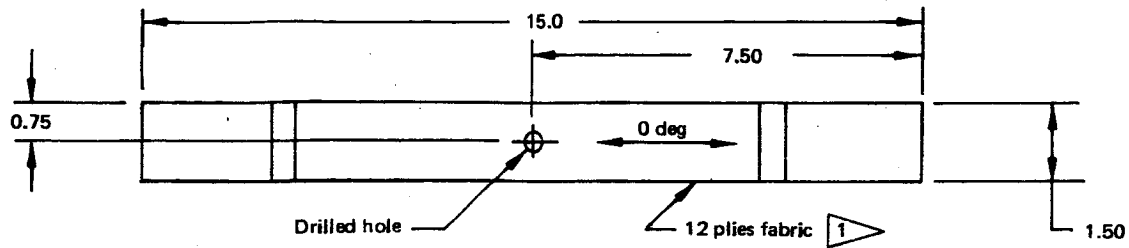


Drawing and assembly no. 2	Cloth warp orien- tation, deg 3	Test tem- per- ature °C	Environment condition 4		Actual hole dia- meter, mm	Speci- men width, mm	Speci- men nominal thick- ness, mm	Failure load, kN 5	Failure stress, MPa 6	E, MPa 7	Strain, ϵ , mm/mm 8
			Wet	Dry							
65C17702-1	±45	21.1		✓	7.95	38.28	2.286	12.944	147.93	2.069 × 10 ⁴	0.00715
				✓	7.98	38.15		13.255	152.00		0.00735
		21.1		✓	7.98	38.28		13.322	152.26		0.00736
		-53.9		✓	8.00	38.15		15.083	172.94		0.00836
				✓	7.98	38.53		14.772	167.71		0.00811
		-53.9		✓	7.98	38.20		14.029	160.66		0.00777
		71.1		✓	7.95	38.25		11.796	134.91		0.00652
				✓	7.98	38.13		11.720	134.49		0.00650
		71.1		✓		38.30		11.796	134.73		0.00651
		21.1	✓			38.35		12.855	146.63		0.00709
			✓		7.98	38.46		12.899	146.75		0.00709
		21.1	✓		7.95	38.30		13.077	149.36		0.00722
		-53.9	✓		7.98	38.28		15.346	175.39		0.00848
			✓		7.92	38.35		15.879	181.12		0.00876
		-53.9	✓		7.98	38.28		16.013	183.01		0.00885
		71.1	✓			38.23		10.786	123.44		0.00597
			✓			38.25		10.497	120.06		0.00580
65C17702-1		71.1	✓		7.98	38.15		10.431	119.61		0.00578
65C17702-2		21.1		✓	2.41	38.56		15.879	180.17		0.00871
				✓		38.35		15.968	182.14		0.00881
65C17702-2				✓	2.41			15.390	175.55		0.00849
65C17702-3				✓	12.70	38.35		10.675	121.77		0.00589
				✓		38.51		10.586	120.28		0.00581
65C17702-3	±45			✓	12.70	38.15		10.586	121.39	2.069 × 10 ⁴	0.00587
65C17702-4	±45/0/90			✓	7.92	38.13		20.018	229.68	4.620 × 10 ⁴	0.00497
				✓		38.10		19.260	221.15		0.00479
		21.1		✓		37.97		18.628	214.61		0.00465
		-53.9		✓		38.05		16.600	190.86		0.00413
				✓		38.07		16.733	192.27		0.00416
		-53.9		✓		38.05		17.748	204.06		0.00442
		71.1		✓				18.544	213.21		0.00462
65C17702-4	±45/0/90	71.1		✓	7.92	38.05	2.286	18.828	216.48	4.620 × 10 ⁴	0.00469

STATIC TENSION WITH HOLES (NASA TEST 1) (CONTINUED)

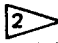
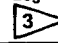





Drawing and assembly no. 2	Cloth warp orientation, deg 3	Test temper- ature, °C	Environment condition 4		Actual hole dia- meter, mm	Speci- men width, mm	Speci- men nominal thick- ness mm	Failure load, kN 5	Failure stress, MPa 6	E, MPa 7	Strain, ϵ , mm/mm 8
			Wet	Dry							
65C17702-4	+ 45/0/90	71.1		✓	7.92	38.05	2.286	19.469	223.85	4.620×10^4	0.00485
↑	↑	21.1	✓		↑	38.10	↑	18.895	216.96	↑	0.00470
↑	↑	↑	✓		↑	38.13	↑	19.429	222.94	↑	0.00483
↑	↑	21.1	✓		↑	38.13	↑	19.055	218.65	↑	0.00473
↑	↑	-53.9	✓		↑	38.15	↑	18.201	208.72	↑	0.00452
↑	↑	↑	✓		↑	38.33	↑	17.454	199.22	↑	0.00431
↑	↑	-53.9	✓		↑	38.13	↑	16.867	193.54	↑	0.00419
↑	↑	71.1	✓		↑	38.05	↑	19.420	223.29	↑	0.00483
↓	↓	↑	✓		↓	38.10	↓	17.925	205.83	↓	0.00446
65C17702-4		71.1	✓		7.92	38.18		19.954	228.66		0.00495
65C17702-5		21.1		✓	2.46	38.02		28.823	331.62		0.00718
↑	↑	↑		✓	↑	37.97		25.354	292.09		0.00632
65C17702-5				✓	2.46	37.97		26.065	300.30		0.00650
65C17702-6				✓	12.70	38.02		14.234	163.76		0.00354
↑	↓	↓		✓	↑	38.10	↓	14.456	165.99	↓	0.00359
65C17702-6	± 45/0/90	21.1		✓	12.70	38.02	2.286	14.901	171.44	4.620×10^4	0.00371

STATIC TENSION WITH HOLES (NASA TEST 1) (CONTINUED)

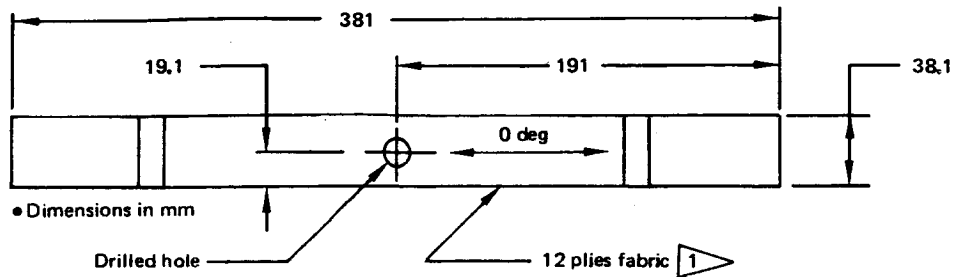


Drawing and assembly no. 2	Cloth warp orientation, deg 3	Test temperature °F	Environment condition 4		Actual hole diameter, in	Specimen width, in	Specimen nominal thickness, in	Failure load, kips 5	Failure stress, lbf/in ² 6	E, lbf/in ² 7	Strain, ε, in/in 8
			Wet	Dry							
65C17702-1	±45	RT		✓	0.313	1.507	0.090	2.910	21,455	3.0 x 10 ⁶	0.00715
				✓	0.314	1.502		2.980	22,045		0.00735
		RT		✓	0.314	1.507		2.995	22,082		0.00736
		-65		✓	0.315	1.502		3.391	25,082		0.00836
				✓	0.314	1.517		3.321	24,324		0.00811
		-65		✓	0.314	1.504		3.154	23,301		0.00777
		160		✓	0.313	1.506		2.652	19,566		0.00652
				✓	0.314	1.501		2.635	19,506		0.00650
		160		✓		1.508		2.652	19,540		0.00651
		RT	✓			1.510		2.890	21,266		0.00709
			✓		0.314	1.514		2.900	21,283		0.00709
		RT	✓		0.313	1.508		2.940	21,662		0.00722
		-65	✓		0.314	1.507		3.450	25,437		0.00848
			✓		0.312	1.510		3.570	26,269		0.00876
		-65	✓		0.314	1.507		3.600	26,542		0.00885
		160	✓			1.505		2.425	17,903		0.00597
			✓			1.506		2.360	17,412		0.00580
65C17702-1		160	✓		0.314	1.502		2.345	17,347		0.00578
65C17702-2		RT		✓	0.095	1.518		3.570	26,131		0.00871
				✓		1.510		2.590	26,416		0.00881
65C17702-2				✓	0.095			3.460	25,460		0.00849
65C17702-3				✓	0.500	1.510		2.400	17,660		0.00589
				✓		1.516		2.380	17,444		0.00581
65C17702-3	±45			✓	0.500	1.502		2.380	17,606	3.0 x 10 ⁶	0.00587
65C17702-4	±45/0/90			✓	0.312	1.501		4.50	33,311	6.7 x 10 ⁶	0.00497
				✓		1.500		4.33	32,074		0.00479
		RT		✓		1.495		4.188	31,126		0.00465
		-65		✓		1.498		3.732	27,881		0.00413
				✓		1.499		3.762	17,885		0.00416
		-65		✓		1.498		3.990	29,595		0.00442
		160		✓				4.169	30,923		0.00462
65C17702-4	±45/0/90	160		✓	0.312	1.498	0.090	4.233	31,397	6.7 x 10 ⁶	0.00469

STATIC TENSION WITH HOLES (NASA TEST 1) (CONTINUED)








Drawing and assembly no. 	Cloth warp orien- tation, deg 	Test temp- erature, °F	Environ- ment condition 		Actual hole diameter, in	Speci- men width, in	Speci- men nominal thickness, in	Failure, load, kips 	Failure stress, lbf/in ² 	E, lbf/in ² 	Strain, ε, in/in 
			Wet	Dry							
65C17702-4	+ 45/0/90	160		✓	0.312	1.498	0.090	4.377	32,466	6.7 x 10 ⁶	0.00485
↑	↑	RT	✓		↑	1.500	↑	4.248	31,467	↑	0.00470
↑	↑	↑	✓		↑	1.501	↑	4.368	32,334	↑	0.00483
↑	↑	RT	✓		↑	1.501	↑	4.284	31,712	↑	0.00473
↑	↑	-65	✓		↑	1.502	↑	4.092	30,271	↑	0.00452
↑	↑	↑	✓		↑	1.509	↑	3.924	28,893	↑	0.00431
↑	↑	-65	✓		↑	1.501	↑	3.792	28,070	↑	0.00419
↑	↑	160	✓		↑	1.498	↑	4.366	32,384	↑	0.00483
↑	↑	↑	✓		↑	1.500	↑	4.030	29,852	↑	0.00446
65C17702-4		160	✓		0.312	1.503		4.486	33,163		0.00495
65C17702-5		RT		✓	0.097	1.497		6.480	48,096		0.00718
↑	↑	↑		✓	↑	1.495	↑	5.700	42,363	↑	0.00632
65C17702-5				✓	0.097	1.495		5.860	43,553		0.00650
65C17702-6				✓	0.500	1.497		3.200	23,751		0.00354
↑	↑	↑		✓	↑	1.500	↑	3.250	24,074	↑	0.00359
65C17702-6	± 45/0/90	RT		✓	0.500	1.497	0.090	3.350	24,865	6.7 x 10 ⁶	0.00371

STATIC COMPRESSION WITH HOLES (NASA TEST 1)

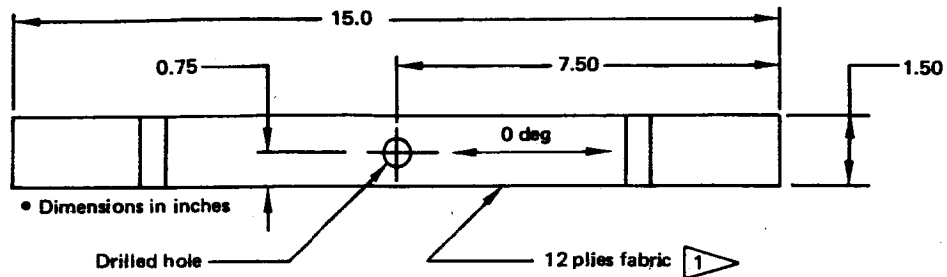


Drawing and assembly no. 2	Cloth warp orientation, deg 3	Test temperature, °C	Environment condition 4		Actual hole diameter, mm	Specimen width, mm	Specimen nominal thickness, mm	Failure load, kN 5	Failure stress, MPa 6	E, MPa 7	Strain, ϵ , mm/mm 8
			Wet	Dry							
65C17702-9	±45	21.1		✓	7.92	38.20	2.286	13.633	156.12	2.069×10^4	0.00755
↑	↑	↑		✓	7.92	38.15	↑	14.323	164.24	↑	0.00794
		21.1		✓	7.90	38.20	↑	14.745	168.86		0.00816
		-53.9		✓	7.92	38.20		16.947	194.07		0.00938
		↑		✓	7.90	38.20		18.348	210.12		0.01016
		-53.9		✓	7.90	38.18		18.370	210.52		0.01018
		71.1		✓	7.92	38.20		11.898	136.26		0.00659
		↑		✓	↑	↑		13.477	154.34		0.00746
		71.1		✓				12.188	139.57		0.00675
		21.1	✓					12.921	147.97		0.00715
		↑	✓					12.201	139.72		0.00675
		21.1	✓					12.757	146.09		0.00706
		-53.9	✓					20.461	234.31		0.01133
		↑	✓		7.92	38.20		18.771	214.96		0.01039
		-53.9	✓		7.87	38.07		19.238	221.04		0.01069
		71.1	✓		7.92	38.18		10.075	115.45		0.00558
↓		↑	✓		7.95	38.15		10.542	120.88		0.00584
65C17702-9		71.1	✓		7.92	38.18		10.542	120.81		0.00584
65C17702-10		21.1		✓	2.54	38.56		19.349	219.54		0.01061
↑		↑		✓	2.54	38.30		19.349	220.99		0.01068
65C17702-10				✓	2.49	38.13		18.504	212.32		0.01026
65C17702-11				✓	12.70	38.07		11.253	129.30		0.00625
↑	↓			✓	↑	38.15		12.054	138.22	↓	0.00668
65C17702-11	±45			✓	12.70	37.95		10.542	121.53	2.069×10^4	0.00588
65C17702-12	±45/0/90			✓	7.95	38.18		23.930	274.23	4.620×10^4	0.00594
↑	↑	↓		✓	↑	↑		21.662	248.23	↑	0.00537
		21.1		✓		38.18		24.642	282.38		0.00611
↓	↓	-53.9		✓		38.13		28.289	324.62	↓	0.00703
65C17702-12	±45/0/90	-53.9		✓	7.95	38.13	2.286	23.663	271.53	4.620×10^4	0.00588

STATIC COMPRESSION WITH HOLES (NASA TEST 1) (CONTINUED)

Drawing and assembly no. 	Cloth warp orien- tation, deg 	Test temp- erature, °C	Environment condition 		Actual hole diameter, mm	Speci- men width, mm	Speci- men nomi- nal thick- ness, mm	Failure load, kN 	Failure stress, MPa 	E, MPa 	Strain, ϵ , mm/mm 
			Wet	Dry							
65C17702-12	±45/0/90	-53.9		✓	7.95	38.15	2.286	23.841	273.39	4.620×10^4	0.00592
↑	↑	71.1	✓		↑	38.23	↑	16.413	187.84	↑	0.00407
		↓	✓			38.20		18.459	211.39		0.00458
		71.1	✓			↑		19.749	226.16		0.00490
		21.1	✓			↓		21.350	244.50		0.00529
		↓	✓			38.20		20.461	234.31		0.00507
		21.1	✓			38.23		21.172	242.30		0.00525
		-53.9	✓			38.13		25.576	293.48		0.00635
		↓	✓			38.10		26.466	303.89		0.00658
		-53.9	✓			38.18		25.398	291.05		0.00630
		71.1		✓		38.15		21.528	246.87		0.00534
		↓		✓		38.15		21.617	247.89		0.00537
65C17702-12		71.1		✓	7.95	38.13		22.729	260.82		0.00565
65C17702-13		21.1		✓	2.49	38.20		28.779	329.57		0.00713
↑		↑		✓	2.46	38.13		31.136	357.28		0.00773
65C17702-13				✓	2.41	38.13		30.736	352.69		0.00763
65C17702-14				✓	12.78	38.23		17.481	200.05		0.00433
↓	↓	↓		✓	12.70	38.23	↓	16.813	192.41	↓	0.00417
65C17702-14	±45/0/90	21.1		✓	12.70	38.25	2.286	16.813	192.29	4.620×10^4	0.00416

STATIC COMPRESSION WITH HOLES (NASA TEST 1) (CONTINUED)

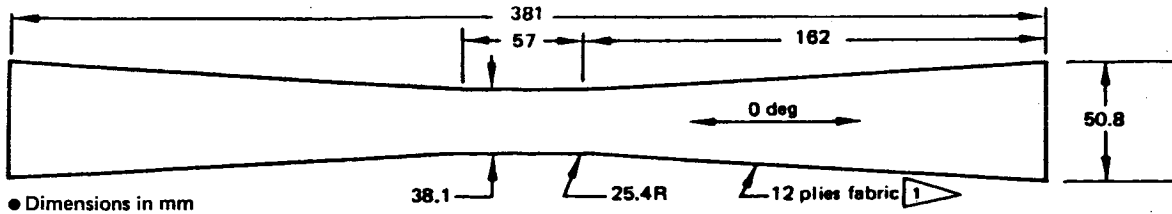


Drawing and assembly no. 2	Cloth warp orientation, deg 3	Test temperature, °F	Environment condition 4		Actual hole diameter, in	Specimen width, in	Specimen nominal thickness, in	Failure load, kips 5	Failure stress, lbf/in ² 6	E, lbf/in ² 7	Strain, ε, in/in 8
			Wet	Dry							
65C17702-9	+45	RT		✓	0.312	1.504	0.090	3.065	22,643	3.0 x 10 ⁶	0.00755
	↑	↑		✓	0.312	1.502	↑	3.220	23,820	↑	0.00794
		RT		✓	0.311	1.504		3.315	24,490		0.00816
		-65		✓	0.312	1.504		3.810	28,147		0.00938
		↑		✓	0.311	1.504		4.125	30,474		0.01016
		-65		✓	0.311	1.503		4.130	30,532		0.01018
		160		✓	0.312	1.504		2.675	19,762		0.00659
		↑		✓	↑	↑		3.030	22,385		0.00746
		160		✓				2.740	20,242		0.00675
		RT	✓					2.905	21,461		0.00715
		↑	✓					2.743	20,264		0.00675
		RT	✓					2.868	21,188		0.00706
		-65	✓					4.600	33,983		0.01133
		↑	✓		0.312	1.504		4.220	31,176		0.01039
		-65	✓		0.310	1.499		4.325	32,058		0.01069
		160	✓		0.312	1.503		2.265	16,744		0.00558
		↑	✓		0.313	1.502		2.370	17,532		0.00584
65C17702-9		160	✓		0.312	1.503		2.370	17,521		0.00584
65C17702-10		RT		✓	0.100	1.518		4.350	31,840		0.01061
↑		↑		✓	0.100	1.508		4.350	32,051		0.01068
65C17702-10				✓	0.098	1.501		4.160	30,794		0.01026
65C17702-11				✓	0.500	1.499		2.530	18,753		0.00625
↑				✓	0.500	1.502		2.710	20,047		0.00668
65C17702-11	+45			✓	0.500	1.494		2.370	17,626	3.0 x 10 ⁶	0.00588
65C17702-12	+45/0/90			✓	0.313	1.503		5.380	39,772	6.7 x 10 ⁶	0.00594
↑	↑	↓		✓	↑	↑		4.870	36,002	↑	0.00537
		RT		✓		1.503		5.540	40,955		0.00611
		-65		✓		1.501		6.360	47,080		0.00703
65C17702-12	+45/0/90	-65		✓	0.313	1.501	0.090	5.320	39,381	6.7 x 10 ⁶	0.00588

STATIC COMPRESSION WITH HOLES (NASA TEST 1) (CONTINUED)

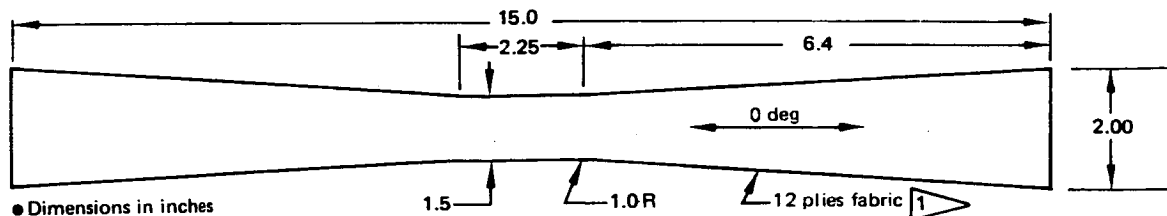
Drawing and assembly no. 2	Cloth warp orientation, deg 3	Test temperature, °F	Environment condition 4		Actual hole diameter, in	Specimen width, in	Specimen nominal thickness, in	Failure load, kips 5	Failure stress, lbf/in ² 6	E, lbf/in ² 7	Strain, ε, in/in 8
			Wet	Dry							
65C17702-12	±45/0/90	-65		✓	0.313	1.502	0.090	5.360	39,651	6.7 × 10 ⁶	0.00592
↑	↑	160	✓		↑	1.505	↑	3.690	27,243	↑	0.00407
		↓	✓			1.504		4.150	30,659		0.00458
		160	✓			↑		4.440	32,801		0.00490
		RT	✓			↓		4.800	35,461		0.00529
		↓	✓			1.504		4.600	33,983		0.00507
		RT	✓			1.505		4.760	35,142		0.00525
		-65	✓			1.501		5.750	42,564		0.00635
		↓	✓			1.500		5.950	44,074		0.00658
		-65	✓			1.503		5.710	42,212		0.00630
		160		✓		1.502		4.840	35,804		0.00534
↓		↓		✓	↓	1.502		4.860	35,952		0.00537
65C17702-12		160		✓	0.313	1.501		5.110	37,827		0.00565
65C17702-13		RT		✓	0.098	1.504		6.470	47,798		0.00713
↑		↑		✓	0.097	1.501		7.000	51,817		0.00773
65C17702-13				✓	0.095	1.501		6.910	51,151		0.00763
65C17702-14				✓	0.503	1.505		3.930	29,014		0.00433
↓	↓	↓		✓	0.500	1.505	↓	3.780	27,906	↓	0.00417
65C17702-14	±45/0/90	RT		✓	0.500	1.506	0.090	3.780	27,888	6.7 × 10 ⁶	0.00416

STATIC TENSION (BOEING 7313-16)



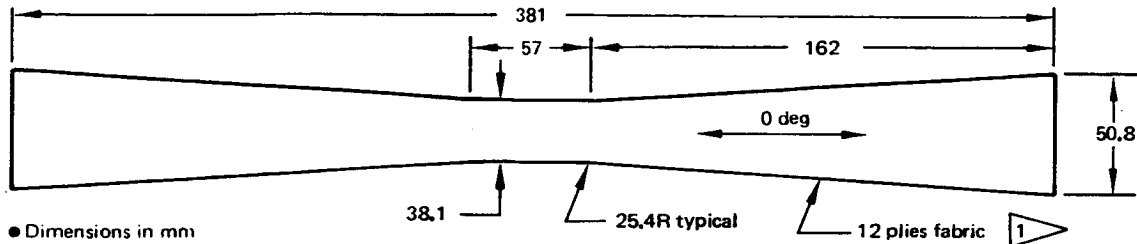
Drawing and assembly no. 2	Cloth warp orientation, deg 3	Test tem- perature °C	Environment condition 4		Specimen width, mm	Specimen nominal thickness, in	Failure load, kN 5	Failure stress, MPa 6	E, MPa 7	Strain, ε, mm/mm 8
			Wet	Dry						
65C19913-3	±45	21.1		✓	38.28	2.286	25.349	289.72	2.069 × 10 ⁴	0.01401
↑	↑	↑		↑	38.25	↑	23.686	270.88	↑	0.01310
					38.23		21.973	251.47		0.01216
					↑		24.620	281.76		0.01362
		21.1			38.23		23.299	266.64		0.01289
		-59.4			38.20		28.396	325.19		0.01572
		↑			38.23		23.485	268.77		0.01299
		↑			38.15		24.420	280.03		0.01354
		↓			38.25		26.154	299.12		0.01446
		-59.4			38.18		26.777	306.86		0.01483
		82.2			38.28		21.092	241.07		0.01165
		↑			38.25		21.190	242.35		0.01172
		↓			38.23		17.645	201.94		0.00976
		82.2			38.28		19.006	217.23		0.01050
		93.3			38.35		16.934	193.15		0.00934
		↑			38.33		15.982	182.41		0.00882
		↑			38.30		15.964	182.33		0.00881
↓	↓	↓			38.25		18.006	205.93	↓	0.00996
65C19913-3	±45	93.3			38.23		16.578	189.72	2.069 × 10 ⁴	0.00917
65C19913-4	±45/0/90	21.1			38.20		35.406	405.47	4.620 × 10 ⁴	0.00878
↑	↑	↑			38.20		36.296	415.66	↑	0.00900
					38.10		36.340	417.28		0.00903
					38.18		37.986	435.30		0.00942
		21.1			38.23		37.630	430.65		0.00932
		-59.4			38.28		34.250	391.44		0.00847
		↑			38.25		33.316	381.02		0.00825
		↑			38.30		33.449	382.04		0.00827
		↓			38.35		33.938	387.11		0.00838
		-59.4			38.20		33.627	385.09		0.00834
		82.2			38.23		37.719	431.67		0.00934
		↑			38.23		38.964	445.92		0.00965
		↑			38.20		38.964	446.22		0.00966
		↓			38.28		38.075	435.16		0.00942
		82.2			38.15		38.742	444.27		0.00962
		93.3			38.25		38.075	435.45		0.00943
		↑			38.23		37.897	433.70		0.00939
		↑			38.15		39.765	455.99		0.00987
↓	↓	↓			38.23		38.520	440.83	↓	0.00954
65C19913-4	±45/0/90	93.3		✓	38.25	2.286	39.721	454.28	4.620 × 10 ⁴	0.00983

STATIC TENSION (BOEING 7313-16) (CONTINUED)



Drawing and assembly no. 2	Cloth warp orientation, deg 3	Test temperature °F	Environment condition 4		Specimen width, in	Specimen nominal thickness, in	Failure load, kips 5	Failure stress, lbf/in ² 6	E, lbf/in ² 7	Strain, ε, in/in 8
			Wet	Dry						
65C19913-3	±45	RT		✓	1.507	0.090	5.699	42,019	3.0 × 10 ⁶	0.01401
↑	↑	↑		↑	1.506	↑	5.325	39,287	↑	0.01310
↑	↑	↑		↑	1.505	↑	4.940	36,471	↑	0.01216
↑	↑	↓		↑	↑	↑	5.535	40,864	↑	0.01362
↑	↑	RT		↑	1.505	↑	5.238	38,671	↑	0.01289
↑	↑	-75		↑	1.504	↑	6.384	47,163	↑	0.01572
↑	↑	↑		↑	1.505	↑	5.280	38,981	↑	0.01299
↑	↑	↑		↑	1.502	↑	5.490	40,613	↑	0.01354
↑	↑	↓		↑	1.506	↑	5.880	43,382	↑	0.01446
↑	↑	-75		↑	1.503	↑	6.020	44,504	↑	0.01483
↑	↑	180		↑	1.507	↑	4.742	34,963	↑	0.01165
↑	↑	↑		↑	1.506	↑	4.764	35,148	↑	0.01172
↑	↑	↓		↑	1.505	↑	3.967	29,288	↑	0.00976
↑	↑	180		↑	1.507	↑	4.273	31,505	↑	0.01050
↑	↑	200		↑	1.510	↑	3.807	28,013	↑	0.00934
↑	↑	↑		↑	1.509	↑	3.593	26,456	↑	0.00882
↑	↑	↑		↑	1.508	↑	3.589	26,444	↑	0.00881
↓	↓	↓		↑	1.506	↑	4.048	29,866	↓	0.00996
65C19913-3	±45	200		↑	1.505	↑	3.727	27,516	3.0 × 10 ⁶	0.00917
65C19913-4	±45/0/90	RT		↑	1.504	↑	7.960	58,806	6.7 × 10 ⁶	0.00878
↑	↑	↑		↑	1.504	↑	8.160	60,284	↑	0.00900
↑	↑	↑		↑	1.500	↑	8.170	60,519	↑	0.00903
↑	↑	↓		↑	1.503	↑	8.540	63,133	↑	0.00942
↑	↑	RT		↑	1.505	↑	8.460	62,458	↑	0.00932
↑	↑	-75		↑	1.507	↑	7.700	56,772	↑	0.00847
↑	↑	↑		↑	1.506	↑	7.490	55,260	↑	0.00825
↑	↑	↑		↑	1.508	↑	7.520	55,408	↑	0.00827
↑	↑	↓		↑	1.510	↑	7.630	56,144	↑	0.00838
↑	↑	-75		↑	1.504	↑	7.560	55,851	↑	0.00834
↑	↑	180		↑	1.505	↑	8.480	62,606	↑	0.00934
↑	↑	↑		↑	1.505	↑	8.760	64,673	↑	0.00965
↑	↑	↓		↑	1.504	↑	8.760	64,716	↑	0.00966
↑	↑	↑		↑	1.507	↑	8.560	63,113	↑	0.00942
↑	↑	180		↑	1.502	↑	8.710	64,433	↑	0.00962
↑	↑	200		↑	1.506	↑	8.560	63,155	↑	0.00943
↑	↑	↑		↑	1.505	↑	8.520	62,901	↑	0.00939
↑	↑	↓		↑	1.502	↑	8.940	66,134	↑	0.00987
↓	↓	↓		↑	1.505	↓	8.660	63,935	↓	0.00954
65C19913-4	±45/0/90	200		✓	1.506	0.090	8.930	65,885	6.7 × 10 ⁶	0.00983

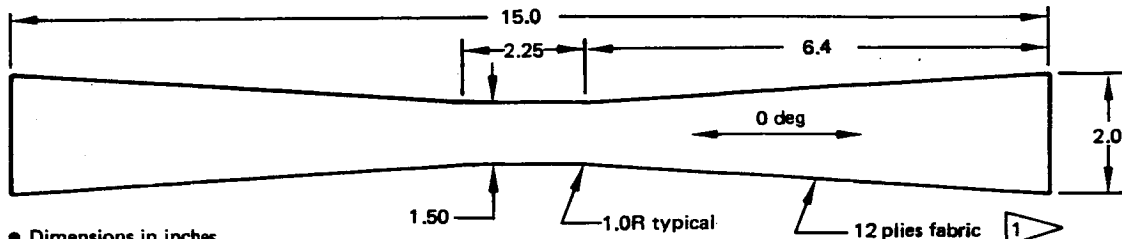
STATIC COMPRESSION (BOEING 7313-16)



● Dimensions in mm

Drawing and assembly no. 2	Cloth warp orientation, deg 3	Test temperature, °C	Environment condition 4		Specimen width, mm	Specimen nominal thickness, mm	Failure load, kN 5	Failure stress, MPa 6	E, MPa 7	Strain, ϵ , mm/mm 8
			Wet	Dry						
65C19913-3	±45	21.1		✓	38.15	2.286	17.836	204.53	2.069 × 10 ⁴	0.00989
					38.25		19.024	217.57		0.01052
					38.13		17.917	205.59		0.00994
					38.13		21.537	247.14		0.01195
		21.1			38.10		19.380	222.53		0.01076
		-59.4					24.175	277.59		0.01342
							25.460	292.35		0.01413
					38.10		22.836	262.22		0.01268
					38.30		25.709	293.64		0.01420
		-59.4			38.20		26.746	306.29		0.01481
		82.2			38.15		13.473	154.50		0.00747
					38.15		16.302	186.94		0.00904
					38.25		13.322	152.36		0.00737
					38.10		16.031	184.07		0.00890
		82.2			38.15		13.531	155.16		0.00750
		93.3			38.20		12.414	142.17		0.00687
					38.18		13.206	151.34		0.00732
					38.35		13.460	153.52		0.00742
					38.30		14.794	168.97		0.00817
65C19913-3	±45	93.3			38.25		12.081	138.16	2.069 × 10 ⁴	0.00668
65C19913-4	±45/0/90	21.1			38.10		33.849	388.67	4.620 × 10 ⁴	0.00841
					38.13		34.872	400.15		0.00866
					38.05		34.783	399.93		0.00866
					38.13		36.607	420.06		0.00909
		21.1			38.20		35.228	403.43		0.00873
		-59.4			38.28		41.144	470.24		0.01018
					38.28		42.612	487.01		0.01054
					38.30		43.501	496.85		0.01026
					38.28		34.783	397.55		0.00861
		-59.4			38.15		37.408	428.96		0.00929
		82.2			38.10		29.535	339.13		0.00734
							32.960	378.46		0.00819
							32.737	375.91		0.00814
					38.10		30.024	344.75		0.00746
		82.2			38.13		32.381	371.57		0.00804
		93.3			38.20		31.937	365.74		0.00792
					38.13		28.512	327.17		0.00708
					38.10		30.780	353.43		0.00765
65C19913-4	±45/0/90	93.3		✓	38.10	2.286	30.469	349.86	4.620 × 10 ⁴	0.00757

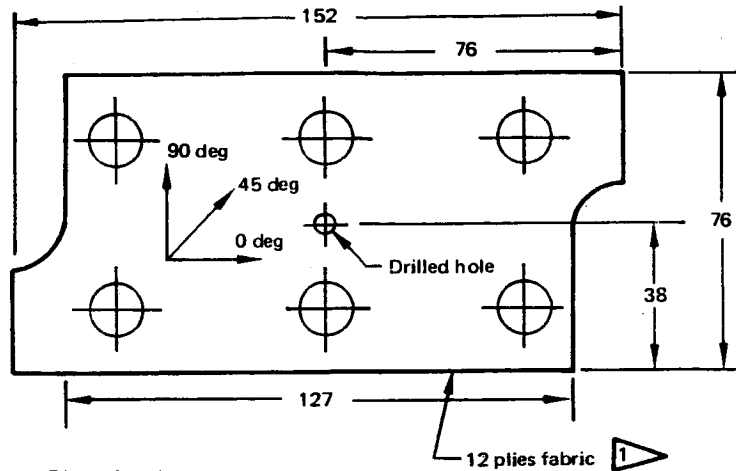
STATIC COMPRESSION (BOEING 7313-16) (CONTINUED)



• Dimensions in inches

Drawing and assembly no. 2	Cloth warp orientation, deg 3	Test temperature, °F	Environment condition 4		Specimen width, in	Specimen nominal thickness, in	Failure load, kips 5	Failure stress, lbf/in ² 6	E, psi lbf/in ² 7	Strain, ε, in/in 8
			Wet	Dry						
65C19913-3	±45	RT		✓	1.502	0.090	4.010	29,664	3.0 x 10 ⁶	0.00989
					1.506		4.277	31,555		0.01052
					1.501		4.028	29,817		0.00994
					1.501		4.842	35,843		0.01195
		RT			1.500		4.357	32,274		0.01076
							5.435	40,259		0.01342
							5.724	42,400		0.01413
					1.500		5.134	38,030		0.01268
		-75			1.508		5.780	42,588		0.01420
					1.504		6.013	44,422		0.01481
					1.502		3.029	22,407		0.00747
					1.502		3.665	27,112		0.00904
		180			1.506		2.995	22,097		0.00737
					1.500		3.604	26,696		0.00890
					1.502		3.042	22,503		0.00750
					1.504		2.791	20,619		0.00687
65C19913-3	±45	200			1.503		2.969	21,949		0.00732
					1.510		3.026	22,266		0.00742
					1.508		3.326	24,506		0.00817
					1.506		2.716	20,038	3.0 x 10 ⁶	0.00668
	±45/0/90	RT			1.500		7.610	56,370	6.7 x 10 ⁶	0.00841
					1.501		7.840	58,035		0.00866
					1.498		7.820	58,003		0.00866
					1.501		8.230	60,922		0.00909
		RT			1.504		7.920	58,511		0.00873
					1.507		9.250	68,200		0.01018
					1.507		9.580	70,633		0.01054
					1.508		9.780	72,060		0.01026
		-75			1.507		7.820	57,657		0.00861
					1.502		8.410	62,213		0.00929
					1.500		6.640	49,185		0.00734
							7.410	54,889		0.00819
		180					7.360	54,519		0.00814
					1.500		6.750	50,000		0.00746
					1.501		7.280	53,890		0.00804
					1.504		7.180	53,044		0.00792
65C19913-4	±45/0/90	200			1.501		6.410	47,450		0.00708
					1.500		6.920	51,259		0.00765
				✓	1.500	0.090	6.850	50,741	6.7 x 10 ⁶	0.00757

RAIL SHEAR WITH HOLES (NASA TEST 1)



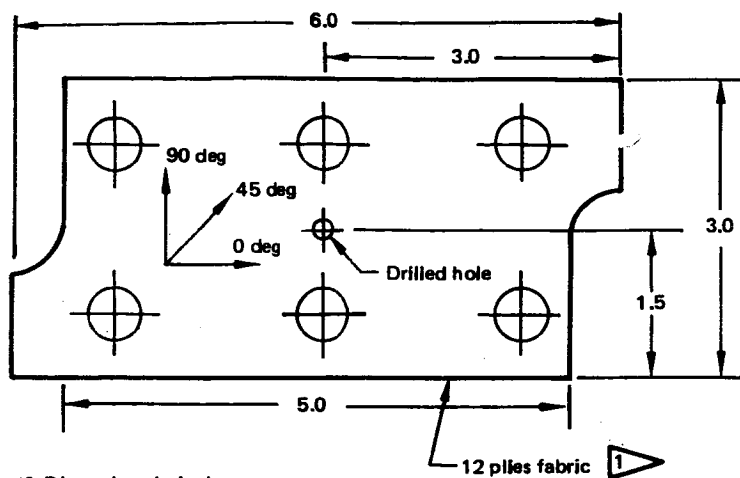
● Dimensions in mm

Drawing and assembly no. 2	Cloth warp orientation, deg 3	Test temperature, °C	Environment condition 4		Open hole size, mm	Specimen width, mm	Specimen nominal thickness, mm	Failure load, kN 5	Failure stress, MPa 6	G, MPa 9	Shear strain, γ, mm/mm 8
			Wet	Dry							
65C17702-41	±45	21.1		✓	2.54	127.0	2.286	69.567	239.64	2.930 x 10 ⁴	0.00818
				✓				61.471	211.75		0.00723
		21.1		✓				74.460	256.49		0.00875
		-53.9		✓				67.699	233.20		0.00796
				✓				72.769	250.67		0.00855
		-53.9		✓				75.705	260.78		0.00890
		71.1		✓				75.260	259.25		0.00885
				✓				72.058	248.22		0.00847
		71.1		✓	2.54			69.567	239.64		0.00818
		21.1	✓		2.38			75.171	258.9F		0.00884
			✓					73.659	253.74		0.00866
		21.1	✓					69.300	238.72		0.00815
		-53.9	✓					69.834	240.56		0.00821
			✓					68.499	235.96		0.00805
		-53.9	✓					71.791	247.30		0.00844
		71.1	✓					68.499	235.96		0.00805
			✓					76.861	264.77		0.00904
65C17702-41	±45	71.1	✓		2.38	127.0	2.286	75.438	259.87	2.930 x 10 ⁴	0.00887
65C17702-44	±45/0/90	21.1	✓		2.54	127.0	2.286	53.910	185.70	1.793 x 10 ⁴	0.01036








RAIL SHEAR WITH HOLES (NASA TEST 1) (CONTINUED)

Drawing and assembly no. 2	Cloth warp orientation, deg 3	Test temperature, °C	Environment condition 4		Open hole size, mm	Specimen width, mm	Specimen nominal thickness, mm	Failure load, kN 5	Failure stress, MPa 6	G, MPa 9	Shear strain, γ , mm/mm 8
			Wet	Dry							
65C17702-44	±45/0/90	21.1		✓	2.54	127.0	2.286	60.760	209.30	1.793 x 10 ⁴	0.01168
↑	↑	21.1		✓	↑	↑	↑	65.386	225.24	↑	0.01256
		-53.9		✓	↑	↑	↑	69.211	238.42	↑	0.01330
		↑		✓	↑	↑	↑	66.809	230.14		0.01284
		-53.9		✓	↑	↑	↑	69.923	240.86		0.01344
		71.1		✓	↑	↑	↑	60.493	208.38		0.01162
		↑		✓	↓	↑	↑	61.382	211.45		0.01180
		71.1		✓	2.54			66.275	228.30		0.01274
		21.1	✓		2.38			66.097	227.69		0.01270
		↑	✓		↑			65.119	224.32		0.01251
		21.1	✓		↑			65.741	226.46		0.01263
		-53.9	✓		↑			62.895	216.65		0.01209
		↑	✓		↑			65.475	225.54		0.01258
		-53.9	✓		↑			70.545	243.01		0.01356
		71.1	✓		↑	↑	↑	59.336	204.40		0.01140
		↑	✓		↓	↓	↓	66.275	228.30	↓	0.01274
65C17702-44	±45/0/90	71.1	✓		2.38	127.0	2.286	63.606	219.11	1.793 x 10 ⁴	0.01222

RAIL SHEAR WITH HOLES (NASA TEST 1) (CONTINUED)



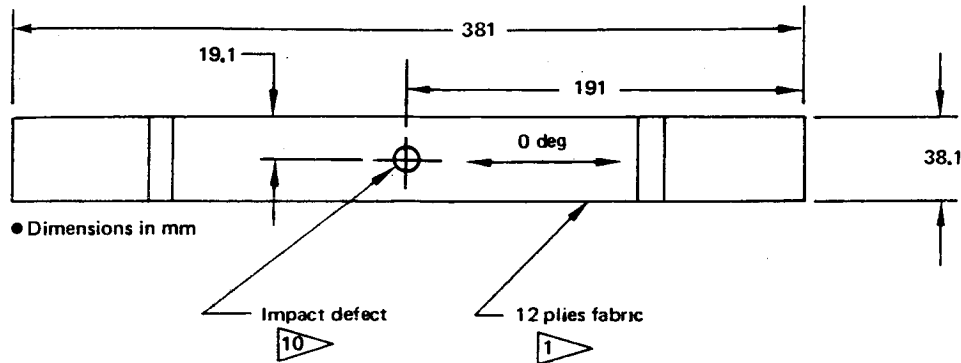
• Dimensions in inches

Drawing and assembly no. 	Cloth warp orientation, deg 	Test temperature, °F	Environment condition 		Open hole size, in	Specimen width, in	Specimen nominal thickness, in	Failure load, kips 	Failure stress, lbf/in ² 	G, lbf/in ² 	Shear strain, γ, in/in 
			Wet	Dry							
65C17702-41	±45	RT		✓	0.10	5.0	0.090	15.64	34,756	4.25 × 10 ⁶	0.00818
↑	↑	↕		✓	↑	↑	↑	13.82	30,711	↑	0.00723
		RT		✓				16.74	37,200		0.00875
		-65		✓				15.22	33,822		0.00796
		↕		✓				16.36	36,356		0.00855
		-65		✓				17.02	37,822		0.00890
		160		✓				16.92	37,600		0.00885
		↕		✓	↓			16.20	36,000		0.00847
		160		✓	0.10			15.64	34,756		0.00818
		RT	✓		0.094			16.90	37,556		0.00884
		↕	✓		↑			16.56	36,800		0.00866
		RT	✓					15.58	34,622		0.00815
		-65	✓					15.70	34,889		0.00821
		↕	✓					15.40	34,222		0.00805
		-65	✓					16.14	35,867		0.00844
		160	✓					15.40	34,222		0.00805
↓	↓	↕	✓		↓			17.28	38,400	↓	0.00904
65C17702-41	±45	160	✓		0.094	↓	↓	16.96	37,689	4.25 × 10 ⁶	0.00887
65C17702-44	±45/0/90	RT	✓		0.10	5.0	0.090	12.12	26,933	2.60 × 10 ⁶	0.01036

RAIL SHEAR WITH HOLES (NASA TEST) (CONTINUED)

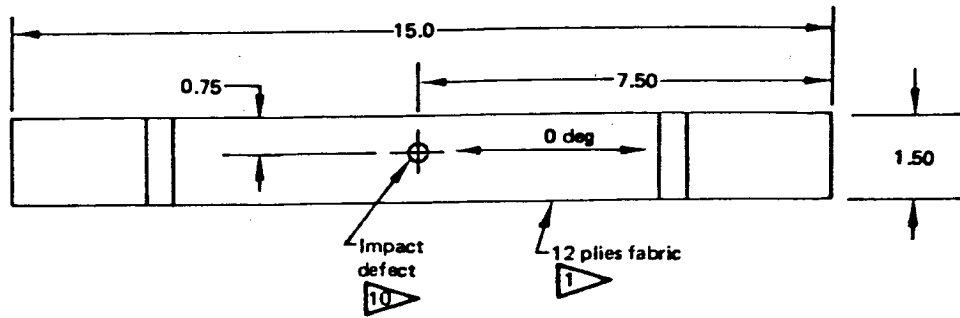
Drawing and assembly no. 2	Cloth warp orien- tation, deg 3	Test temp- erature, °F	Environment condition 4		Open hole size, in	Speci- men width, in	Specimen nominal thickness, in	Failure load, kips 5	Failure stress, lbf/in ² 6	G, lbf/in ² 9	Shear strain, %, in/in 8
			Wet	Dry							
65C17702-44	±45/0/90	RT		✓	0.10	5.0	0.090	13.66	30,356	2.6 x 10 ⁶	0.01168
↑	↑	RT		✓	↑	↑	↑	14.70	32,667	↑	0.01256
		-65		✓				15.56	34,578		0.01330
		↕		✓				15.02	33,378		0.01284
		-65		✓				15.72	34,933		0.01344
		160		✓				13.60	30,222		0.01162
		↕		✓	↓			13.80	30,667		0.01180
		160		✓	0.10			14.90	33,111		0.01274
		RT	✓		0.0937			14.86	33,022		0.01270
		↕	✓		↑			14.64	32,533		0.01251
		RT	✓					14.78	32,844		0.01263
		-65	✓					14.14	31,422		0.01209
		↕	✓					14.72	32,711		0.01258
		-65	✓					15.86	35,244		0.01356
		160	✓					13.34	29,644		0.01140
		↕	✓					14.90	33,111	↓	0.01274
65C17702-44	±45/0/90	160	✓		0.0937	5.0	0.090	14.30	31,778	2.6 x 10 ⁶	0.01222

STATIC TENSION WITH IMPACT (NASA TEST 1)



Drawing and assembly no. 2	Cloth warp orientation, deg 3	Test temperature, °C	Environment condition 4		Impact energy, N-m	Specimen width, mm	Specimen nominal thickness, mm	Failure load, kN 5	Failure stress, MPa 6	E, MPa 7	Strain, ε, mm/mm 8
			Wet	Dry							
65C17702-121	+45	21.1	✓		3.39	38.15	2.286	13.477	154.55	2.069 × 10 ⁴	0.00747
↑	↑	↑	✓		↑	38.18	↑	14.171	162.40	↑	0.00785
↑	↑	↑	✓		3.39	38.20	↑	14.412	165.04	↑	0.00798
↑	↑	↑		✓	1.13	38.18	↑	16.591	190.12	↑	0.00919
↑	↑	↑		✓	↑	38.13	↑	16.324	187.32	↑	0.00906
↑	↑	↑		✓	1.13	38.13	↑	16.947	194.46	↑	0.00940
↑	↑	↑		✓	2.26	38.20	↑	15.657	179.30	↑	0.00867
↑	↑	↑		✓	↑	38.10	↑	15.568	178.74	↑	0.00864
↑	↑	↑		✓	2.26	38.23	↑	15.790	180.71	↑	0.00874
↑	↑	↑		✓	3.39	38.20	↑	14.367	164.53	↑	0.00795
↓	↓	↓		✓	↑	38.15	↑	14.856	170.36	↓	0.00824
65C17702-121	±45			✓	↑	38.20	↑	14.856	170.13	2.069 × 10 ⁴	0.00822
65C17702-124	±45/0/90		✓			38.10	↑	17.014	195.36	4.620 × 10 ⁴	0.00423
↑	↑	↑	✓		↓	38.13	↑	18.370	210.79	↑	0.00456
↑	↑	↑	✓		3.39	38.13	↑	17.570	201.61	↑	0.00436
↑	↑	↑		✓	1.13	38.10	↑	37.630	432.09	↑	0.00935
↑	↑	↑		✓	↑	↑	↑	35.228	404.51	↑	0.00876
↑	↑	↑		✓	1.13	↑	↑	37.675	432.60	↑	0.00936
↑	↑	↑		✓	2.26	↑	↑	28.400	326.11	↑	0.00706
↑	↑	↑		✓	↑	↑	↑	28.022	321.77	↑	0.00697
↑	↑	↑		✓	2.26	↑	↑	33.040	379.38	↑	0.00821
↑	↑	↑		✓	3.39	↑	↑	21.884	251.28	↑	0.00544
↓	↓	↓		✓	↑	↓	↓	23.530	270.18	↓	0.00585
65C17702-124	±45/0/90		✓		3.39	38.10	2.286	25.932	297.76	4.620 × 10 ⁴	0.00845
65C17702-127	±45			✓	1.70	37.97	1.524	9.919	171.42	2.069 × 10 ⁴	0.00829
↑	↑	↑		✓	↑	37.85	↑	10.186	176.62	↑	0.00854
65C17702-127	±45			✓	1.70	37.97	↑	10.230	160.72	2.069 × 10 ⁴	0.00777
65C17702-128	±45/0/90		✓		6.22	38.23	↑	15.479	265.72	4.620 × 10 ⁴	0.00575
↑	↑	↑		✓	↑	38.20	↓	16.280	279.65	↑	0.00605
65C17702-128	±45/0/90	21.1		✓	6.22	38.18	1.524	16.191	278.30	4.620 × 10 ⁴	0.00602

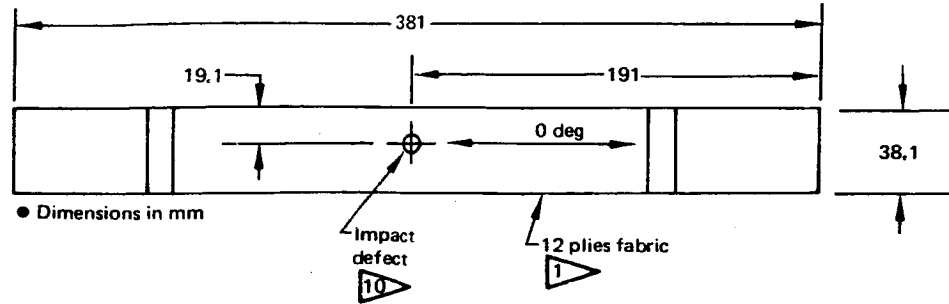
STATIC COMPRESSION WITH IMPACT (NASA TEST 1) (CONTINUED)



• Dimensions in inches

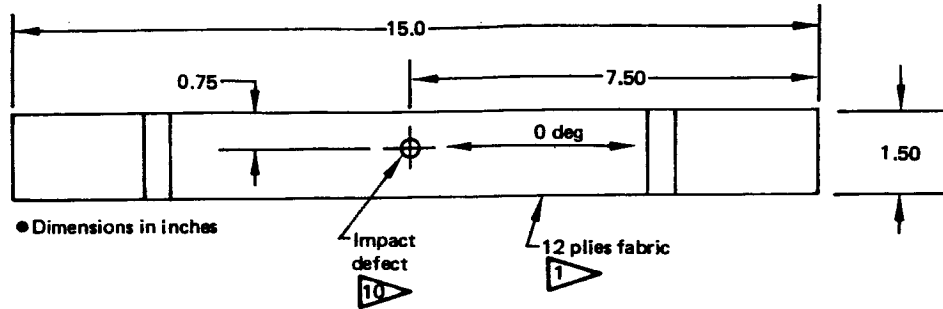
Drawing and assembly no. 2	Cloth warp orientation, deg 3	Test temperature, °F	Environment condition 4		Impact energy, in-lbf	Specimen width, in	Specimen nominal thickness, in	Failure load, kips 5	Failure stress, lbf/in ² 6	E, lbf/in ² 7	Strain, ε, in/in 8
			Wet	Dry							
65C17702-23	±45	RT	✓		30	1.496	0.09	3.040	22,579	3.0 × 10 ⁶	0.00753
↑	↑	↑	✓		↑	1.496	↑	3.060	22,727	↑	0.00758
			✓		30	1.498		2.930	21,733		0.00724
				✓	10	1.499		4.373	32,414		0.01080
				✓	↑	1.499		4.230	31,354		0.01045
				✓	10	1.496		4.173	30,994		0.01033
				✓	20	1.498		3.748	27,800		0.00927
				✓	↑	↑		3.611	26,784		0.00893
				✓	20	1.498		3.547	26,309		0.00877
				✓	30	1.496		3.453	25,646		0.00855
↓	↓			✓	↑	↑		3.394	25,208	↓	0.00840
65C17702-23	±45			✓	↑	1.496		3.440	25,550	3.0 × 10 ⁶	0.00852
65C17702-26	±45/0/90		✓			1.500		4.053	30,022	6.7 × 10 ⁶	0.00448
↑	↑		✓		↓	1.499		4.013	29,746	↑	0.00444
			✓		30	1.501		3.825	28,314		0.00423
				✓	10	1.497		5.450	40,451		0.00604
				✓	↑	1.498		5.610	41,611		0.00621
				✓	10	1.502		5.590	41,352		0.00617
				✓	20	1.499		4.210	31,206		0.00466
				✓	↑	↑		4.410	32,688		0.00488
				✓	20	1.499		4.460	33,059		0.00493
				✓	30	1.497		3.800	28,205		0.00421
↓	↓			✓	↑	1.499	↓	3.980	29,501	↓	0.00440
65C17702-26	±45/0/90			✓	30	1.498	0.09	4.050	30,040	6.7 × 10 ⁶	0.00448
65C17702-29	±45			✓	15	1.502	0.06	2.360	26,187	3.0 × 10 ⁶	0.00873
↑	↑			✓	↑	1.501	↑	2.190	24,317	↑	0.00811
65C17702-29	±45			✓		1.500		2.040	22,667	3.0 × 10 ⁶	0.00756
65C17702-30	±45/0/90			✓	↑	↑		2.540	28,222	6.7 × 10 ⁶	0.00421
↑	↑			✓	↓	↓	↓	2.780	30,889	↑	0.00461
65C17702-30	±45/0/90	RT		✓	15	1.500	0.06	2.750	30,556	6.7 × 10 ⁶	0.00456

STATIC COMPRESSION WITH IMPACT (NASA TEST 1)



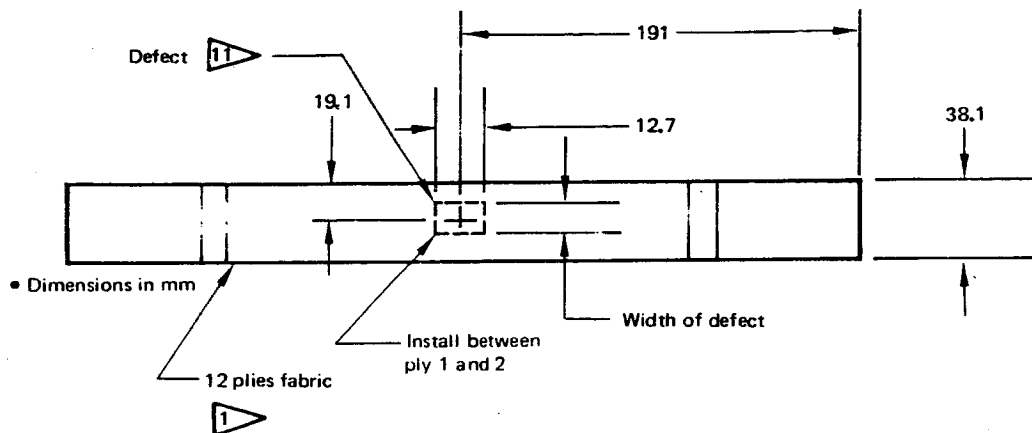
Drawing and assembly no. 2	Cloth warp orientation, deg 3	Test temperature, °C	Environment condition 4		Impact energy, N-m	Specimen width, mm	Specimen nominal thickness, mm	Failure load, kN 5	Failure stress, MPa 6	E, MPa 7	Strain, ε, mm/mm 8
			Wet	Dry							
65C17702-23	±45	21.1	✓		3.39	38.00	2.286	13.522	155.68	2.069×10 ⁴	0.00753
			✓			38.00		13.611	156.70		0.00753
			✓		3.39	38.05		13.033	149.85		0.00724
				✓	1.13	38.07		19.451	223.49		0.01080
				✓		38.07		18.815	216.19		0.01045
				✓	1.13	38.00		18.562	213.70		0.01033
				✓	2.26	38.05		16.671	191.68		0.00927
				✓				16.062	184.68		0.00893
				✓	2.26	38.05		15.777	181.40		0.00877
				✓	3.39	38.00		15.359	176.83		0.00855
				✓				15.097	173.81		0.00840
65C17702-23	±45			✓		38.00		15.301	176.17	2.069×10 ⁴	0.00852
65C17702-26	±45/0/90		✓			38.10		18.028	207.00	4.620×10 ⁴	0.00448
			✓			38.67		17.850	205.10		0.00444
			✓		3.39	38.13		17.014	195.23		0.00423
				✓	1.13	38.02		24.242	278.91		0.00604
				✓		38.05		24.953	286.91		0.00621
				✓	1.13	38.15		24.864	285.12		0.00617
				✓	2.26	38.07		18.726	215.17		0.00466
				✓				19.616	225.38		0.00488
				✓	2.26	38.07		19.838	227.94		0.00493
				✓	3.39	38.02		16.902	194.47		0.00421
				✓		38.07		17.703	203.41		0.00440
65C17702-28	±45/0/90		✓		3.39	38.05	2.286	18.014	207.13	4.620×10⁴	0.00448
65C17702-29	±45			✓	1.70	38.15	1.524	10.497	180.56	2.069×10 ⁴	0.00873
				✓		38.13		9.741	167.67		0.00811
65C17702-29	±45			✓		38.10		9.074	156.29	2.069×10 ⁴	0.00756
65C17702-30	±45/0/90			✓				11.298	194.59	4.620×10 ⁴	0.00421
				✓				12.365	212.98		0.00461
65C17702-30	±45/0/90	21.1		✓	1.70	38.10	1.524	12.232	210.68	4.620×10 ⁴	0.00456

STATIC COMPRESSION WITH IMPACT (NASA TEST 1) (CONTINUED)



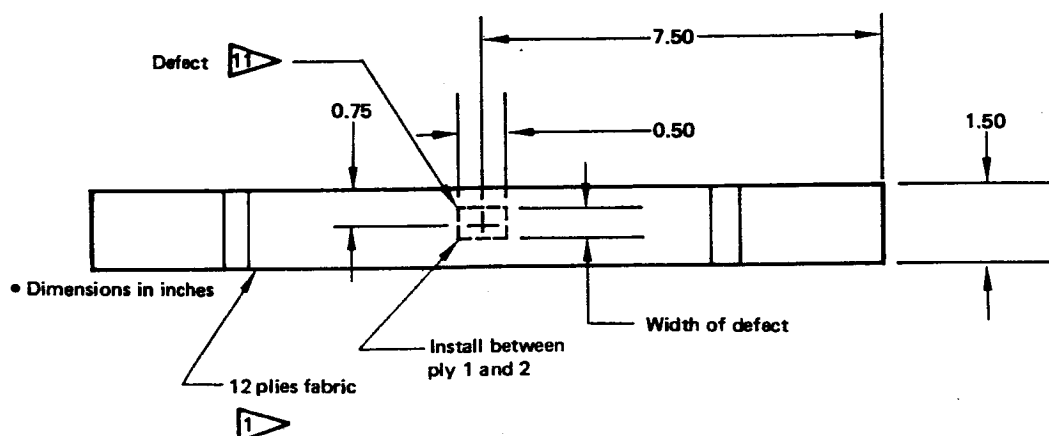
Drawing and assembly no. 2	Cloth warp orientation, deg 3	Test temperature, °F	Environment condition 4		Impact energy, in-lbf	Specimen width, in	Specimen nominal thickness, in	Failure load, kips 5	Failure stress, lbf/in ² 6	E, lbf/in ² 7	Strain, ε, in/in 8
			Wet	Dry							
65C17702-23	±45	RT	✓		30	1.496	0.09	3.040	22,579	3.0 x 10 ⁶	0.00753
			✓			1.496		3.060	22,727		0.00758
			✓		30	1.498		2.930	21,733		0.00724
				✓	10	1.499		4.373	32,414		0.01080
				✓		1.499		4.230	31,354		0.01045
				✓	10	1.496		4.173	30,994		0.01033
				✓	20	1.498		3.748	27,800		0.00927
				✓				3.611	26,784		0.00893
				✓	20	1.498		3.547	26,309		0.00877
				✓	30	1.496		3.453	25,646		0.00855
				✓				3.394	25,208		0.00840
65C17702-23	±45			✓		1.496		3.440	25,550	3.0 x 10 ⁶	0.00852
65C17702-26	±45/0/90		✓			1.500		4.053	30,022	6.7 x 10 ⁶	0.00448
			✓			1.499		4.013	29,746		0.00444
			✓		30	1.501		3.825	28,314		0.00423
				✓	10	1.497		5.450	40,451		0.00604
				✓		1.498		5.610	41,611		0.00621
				✓	10	1.502		5.590	41,352		0.00617
				✓	20	1.499		4.210	31,206		0.00466
				✓				4.410	32,688		0.00488
				✓	20	1.499		4.460	33,059		0.00493
				✓	30	1.497		3.800	28,205		0.00421
				✓		1.499		3.980	29,501		0.00440
65C17702-26	±45/0/90		✓		30	1.498	0.09	4.050	30,040	6.7 x 10 ⁶	0.00448
65C17702-29	±45		✓		15	1.502	0.06	2.360	26,187	3.0 x 10 ⁶	0.00873
			✓			1.501		2.190	24,317		0.00811
65C17702-29	±45		✓			1.500		2.040	22,667	3.0 x 10 ⁶	0.00756
65C17702-30	±45/0/90		✓					2.540	28,222	6.7 x 10 ⁶	0.00421
			✓					2.780	30,889		0.00461
65C17702-30	±45/0/90	RT	✓		15	1.500	0.06	2.750	30,556	6.7 x 10 ⁶	0.00456

STATIC COMPRESSION WITH DELAMINATION (NASA TEST 1)



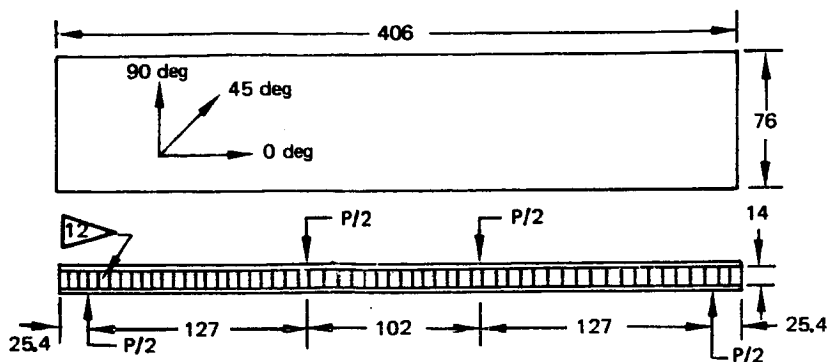
Drawing and assembly no. 2	Cloth warp orientation, deg 3	Test temperature, °C	Environment condition 4		Width of defect, mm	Specimen width, mm	Specimen nominal thickness, mm	Failure load, kN 5	Failure stress MPa 6	E, MPa 7	Strain, ϵ , mm/mm 8
			Wet	Dry							
65C17702-17	±45	21.1		✓	2.54	38.10	2.286	18.904	217.06	2.069×10^4	0.01049
↑	↑	↑		✓	↑	↑	↑	19.126	219.62	↑	0.01062
65C17702-17	↑	↑		✓	2.54	38.10	↑	19.215	220.64	↑	0.01067
65C17702-18	↑	↑		✓	7.62	38.15	↑	15.390	176.48	↑	0.00853
↑	↑	↑		✓	↑	38.13	↑	19.349	222.03	↑	0.01073
↑	↑	↑		✓	↑	38.10	↑	18.948	217.58	↑	0.01052
↑	↑	↑	✓		↑	38.10	↑	18.250	209.56	↑	0.01013
↑	↑	↑	✓		↑	38.13	↑	19.464	223.35	↑	0.01080
65C17702-18	↑	↑	✓		7.62	38.13	↑	20.301	232.95	↑	0.01126
65C17702-19	↑	↑		✓	12.70	38.10	↑	18.459	211.96	↑	0.01025
↑	↑	↑		✓	↑	38.15	↑	18.948	217.29	↑	0.01050
65C17702-19	±45	↑		✓	12.70	38.15	↑	19.438	222.89	2.069×10^4	0.01078
65C17702-20	±45/0/90	↑		✓	2.54	38.20	↑	33.449	383.06	4.620×10^4	0.00829
↑	↑	↑		✓	↑	38.18	↑	34.250	392.48	↑	0.00850
65C17702-20	↑	↑		✓	2.54	38.20	↑	32.826	375.92	↑	0.00814
65C17702-21	↑	↑		✓	7.62	38.20	↑	32.470	371.85	↑	0.00805
↑	↑	↑		✓	↑	38.18	↑	34.027	389.94	↑	0.00844
↑	↑	↑		✓	↑	38.10	↑	34.605	397.36	↑	0.00860
↑	↑	↑	✓		↑	38.13	↑	35.050	402.19	↑	0.00871
↑	↑	↑	✓		↑	↑	↑	31.403	360.34	↑	0.00780
65C17702-21	↑	↑	✓		7.62	↑	↑	32.248	370.04	↑	0.00801
65C17702-22	↑	↑		✓	12.70	↑	↑	30.914	354.73	↑	0.00768
↑	↑	↑		✓	↑	38.13	↑	35.895	411.89	↑	0.00892
65C17702-22	±45/0/90	21.1		✓	12.70	38.10	2.286	34.250	393.27	4.620×10^4	0.00851

STATIC COMPRESSION WITH DELAMINATION (NASA TEST 1) (CONTINUED)

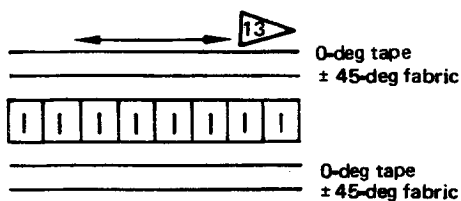


Drawing and assembly no. 2	Cloth warp orientation, deg 3	Test temperature, °F	Environment condition 4		Width of defect, in	Specimen width, in	Specimen nominal thickness, in	Failure load, kips 5	Failure stress, lbf/in ² 6	E, lbf/in ² 7	Strain, ε, in/in 8
			Wet	Dry							
65C17702-17	±45	RT		✓	0.1	1.500	0.090	4.250	31,481	3.0 x 10 ⁶	0.01049
↕	↕	↕		✓	↕	↕	↕	4.300	31,852	↕	0.01062
65C17702-17	↕	↕		✓	0.1	1.500	↕	4.320	32,000	↕	0.01067
65C17702-18	↕	↕		✓	0.3	1.502	↕	3.460	25,596	↕	0.00853
↕	↕	↕		✓	↕	1.501	↕	4.350	32,201	↕	0.01073
↕	↕	↕		✓	↕	1.500	↕	4.260	31,556	↕	0.01052
↕	↕	↕	✓		↕	1.500	↕	4.103	30,393	↕	0.01013
↕	↕	↕	✓		↕	1.501	↕	4.376	32,393	↕	0.01080
65C17702-18	↕	↕	✓		0.3	1.501	↕	4.564	33,785	↕	0.01126
65C17702-19	↕	↕		✓	0.5	1.500	↕	4.150	30,741	↕	0.01025
↕	↕	↕		✓	↕	1.502	↕	4.260	31,514	↕	0.01050
65C17702-19	±45	↕		✓	0.5	1.502	↕	4.370	32,327	3.0 x 10 ⁶	0.01078
65C17702-20	±45/0/90	↕		✓	0.1	1.504	↕	7.520	55,556	6.7 x 10 ⁶	0.00829
↕	↕	↕		✓	↕	1.503	↕	7.700	56,923	↕	0.00850
65C17702-20	↕	↕		✓	0.1	1.504	↕	7.380	54,521	↕	0.00814
65C17702-21	↕	↕		✓	0.3	1.504	↕	7.300	53,930	↕	0.00805
↕	↕	↕		✓	↕	1.503	↕	7.650	56,554	↕	0.00844
↕	↕	↕		✓	↕	1.500	↕	7.780	57,630	↕	0.00860
↕	↕	↕	✓		↕	1.501	↕	7.880	58,331	↕	0.00871
↕	↕	↕	✓		↕	↕	↕	7.060	52,261	↕	0.00780
65C17702-21	↕	↕	✓		0.3	↕	↕	7.250	53,668	↕	0.00801
65C17702-22	↕	↕		✓	0.5	↕	↕	6.950	51,447	↕	0.00768
↕	↕	↕		✓	↕	1.501	↕	8.070	59,738	↕	0.00892
65C17702-22	±45/0/90	RT		✓	0.5	1.500	0.090	7.700	57,037	6.7 x 10 ⁶	0.00851

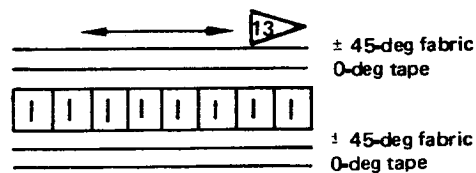
FOUR-POINT BEAM BENDING (BOEING 7313-36)



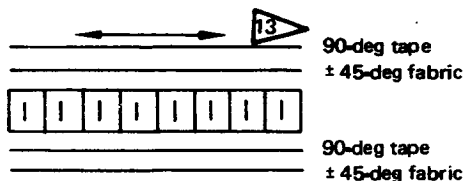
• Dimensions in mm



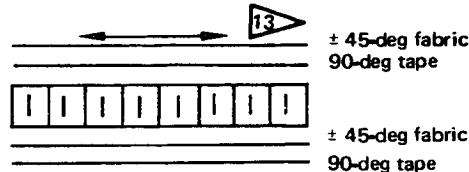
Test configuration 1



Test configuration 3



Test configuration 2



Test configuration 4

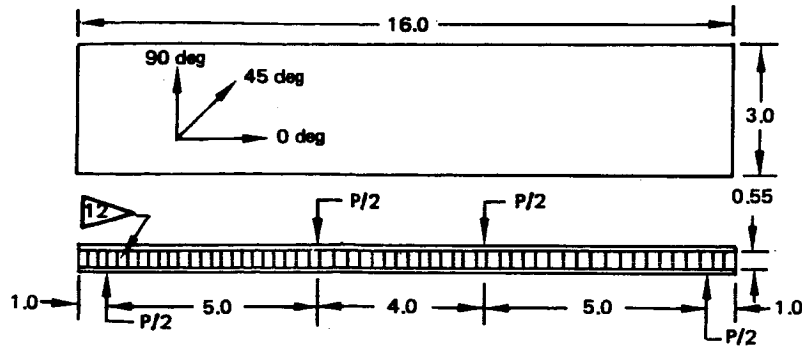
• Fabric and tape

Drawing and assembly no. 2	Test configuration	Test temperature, °C	Environment condition 4		Actual specimen size, mm		Failure load, kN 5	Failure stress, MPa 6	E, MPa 7	Strain, ε, mm/mm 8
			Wet	Dry	Width	Thickness				
65C17727-1	1	21.1		✓	76.53	14.224	1.766	376.09	5.447x10 ⁴	0.00690
		21.1		✓	76.66	14.249	1.630	345.88		0.00635
		21.1		✓	76.58	14.224	1.657	352.65		0.00647
		-59.4	✓		75.95	14.402	1.948	412.87		0.00758
		-59.4	✓		76.35	14.453	2.039	428.35		0.00786
		82.2	✓		76.33	14.351	1.263	267.33		0.00491
		82.2	✓		76.38	14.427	1.250	262.91		0.00483
		21.1		✓	76.71	14.199	1.753	373.07		0.00685
	3	21.1		✓	76.58	14.224	1.824	388.15	5.447x10 ⁴	0.00713
		21.1		✓	76.68	14.224	1.861	395.68		0.00726
		-59.4	✓		76.48	14.529	2.260	471.27		0.00865
		-59.4	✓		76.45	14.478	1.808	378.58		0.00695
		82.2	✓		76.38	14.427	1.108	232.97		0.00428
		82.2	✓		76.48	14.453	1.143	239.70		0.00440

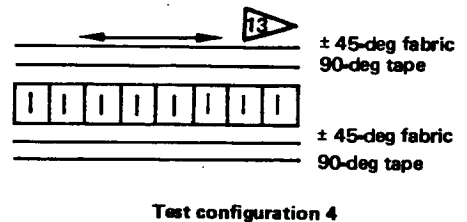
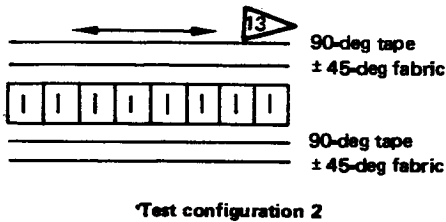
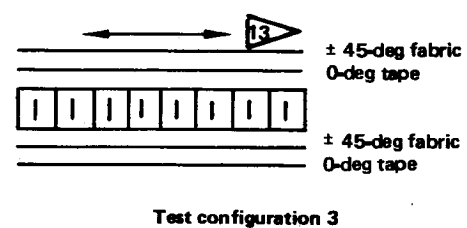
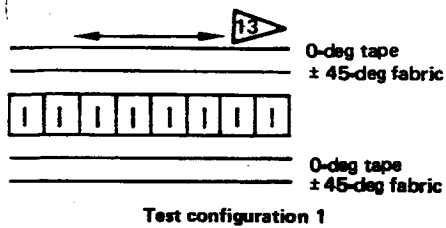
FOUR-POINT BEAM BENDING (BOEING 7313-36) (CONTINUED)

Drawing and assembly no. <div>2</div>	Test configuration	Test temperature, °C	Environment condition <div>4</div>		Actual specimen size, mm		Failure load, kN <div>5</div>	Failure stress, MPa <div>6</div>	E, MPa <div>7</div>	Strain, ε, mm/mm <div>8</div>
			Wet	Dry	Width	Thickness				
65C17727-2	2	21.1		✓	76.45	14.199	1.016	217.08	2.620×10 ⁴	0.00829
	↑	↑		✓	76.56	14.351	0.967	204.12	↑	0.00779
		21.1		✓	76.68	14.478	1.025	214.03		0.00817
		-59.4	✓		76.33	14.427	1.366	287.42		0.01097
		-59.4	✓		76.12	14.529	1.328	278.21		0.01062
	↓	82.2	✓		76.63	14.580	0.707	146.69		0.00560
	2	82.2	✓		76.40	14.529	0.674	140.69		0.00537
	4	21.1		✓	76.58	14.376	0.999	210.24		0.00802
	↑	↑		✓	76.71	14.402	1.030	216.05		0.00825
		21.1		✓	76.56	14.376	0.996	209.84		0.00801
		-59.4	✓		76.12	14.453	1.105	232.86		0.00889
	↓	-59.4	✓		76.00	14.580	1.526	319.09	↓	0.01218
	65C17727-2	4	82.2	✓		76.45	14.580	0.678	141.02	2.620×10 ⁴

FOUR-POINT BEAM BENDING (BOEING 7313-36) (CONTINUED)



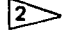




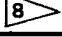
• Dimensions in inches



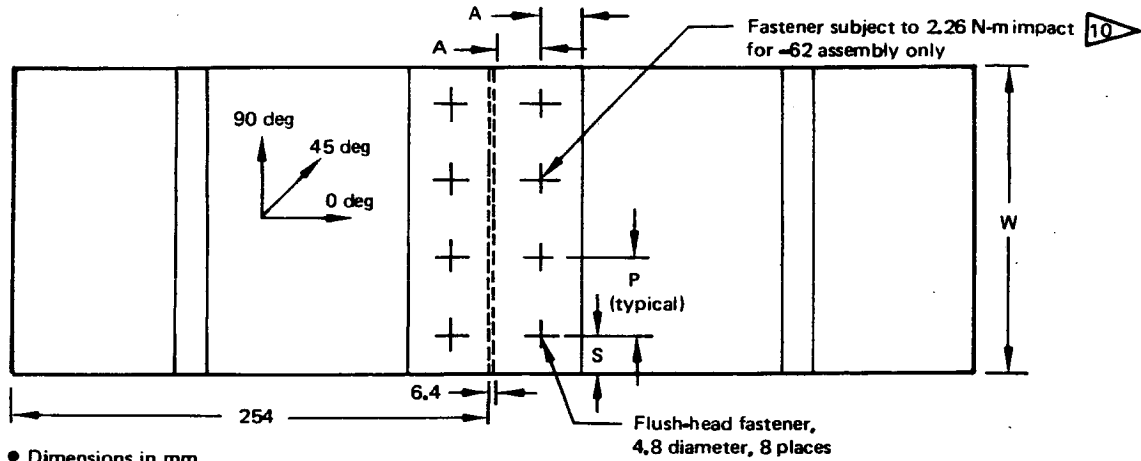
• Fabric and tape

Drawing and assembly no. 2	Test configuration	Test temperature, °F	Environment condition 4		Actual specimen size, in		Failure load, lbf 5	Failure stress, lbf/in ² 6	E, lbf/in ² 7	Strain, ε, in/in 8
			Wet	Dry	Width	Thickness				
65C17727-1	1	RT		✓	3.013	0.560	397.0	54,546	7.9 × 10 ⁶	0.00690
				✓	3.019	0.561	366.5	50,164		0.00635
		RT		✓	3.015	0.560	372.5	51,146		0.00647
		-75	✓		2.990	0.567	438.0	59,879		0.00758
		-75	✓		3.006	0.569	458.5	62,125		0.00786
		180	✓		3.005	0.565	284.0	38,771		0.00491
		180	✓		3.007	0.568	281.0	38,130		0.00483
		RT		✓	3.020	0.555	394.0	54,107		0.00685
		RT		✓	3.015	0.560	410.0	56,295		0.00713
		RT		✓	3.019	0.560	418.5	57,386		0.00726
65C17727-1	3	-75	✓		3.011	0.572	508.0	68,350		0.00865
		-75	✓		3.010	0.570	406.5	54,907		0.00695
		180	✓		3.007	0.568	249.0	33,788		0.00428
		180	✓		3.011	0.569	257.0	34,764	7.9 × 10 ⁶	0.00440

FOUR-POINT BEAM BENDING (BOEING 7313-36) (CONTINUED)

Drawing and assembly no. 	Test config- uration	Test temp- erature, °F	Environment condition 		Actual specimen size, in		Failure load, lbf 	Failure stress, lbf/in ² 	E, lbf/in ² 	Strain, ϵ , in/in 
			Wet	Dry	Width	Thickness				
65C17727-2	2	RT		✓	3.010	0.559	228.5	31,484	3.8×10^6	0.00829
↑	↑	↑		✓	3.014	0.565	217.5	29,604	↑	0.00779
		RT		✓	3.019	0.570	230.5	31,042		0.00817
		-75	✓		3.005	0.568	307.0	41,686		0.01097
		-75	✓		2.997	0.572	298.5	40,350		0.01062
	↓	180	✓		3.017	0.574	159.0	21,275		0.00560
	2	180	✓		3.008	0.572	151.5	20,404		0.00537
	4	RT		✓	3.015	0.566	224.5	30,492		0.00802
	↑	↑		✓	3.020	0.567	231.5	31,334		0.00825
		RT		✓	3.014	0.566	224.0	30,434		0.00801
		-75	✓		2.997	0.569	248.5	33,772		0.00889
	↓	-75	✓		2.992	0.574	343.0	46,278	↓	0.01218
65C17727-2	4	180	✓		3.010	0.574	125.5	20,452	3.8×10^6	0.00538

MECHANICAL FASTENED JOINT (NASA TEST 4)



• Dimensions in mm

• Splice plate thickness

• -58-8 plies fabric

• -49 through -57, -61, and -62-12 plies fabric

• -60-16 plies fabric

Drawing and assembly no. 2	Cloth warp orientation, deg 3	Test temperature, °C	Environment condition 4		A, mm	S, mm	P, mm	Specimen width, mm	Specimen nominal thickness, mm	Failure load, kN 5	Bearing failure stress, MPa 14	E, MPa 7	Comments
			Wet	Dry									
65C17702-49	±45/0/90	21.1		✓	7.4	7.4	14.5	57.9	2.286	40.210	461.71	4.62 x 10 ⁴	Net tension failure
				✓						38.964	447.41		
65C17702-49				✓		7.4	14.5	57.9		42.879	492.35		Net tension failure
65C17702-50				✓		12.2	24.1	96.5		39.498	453.54		Shear out failure
				✓				96.6		42.923	492.86		
				✓				96.6		41.277	473.99		
			✓					96.8		42.256	485.20		
			✓							45.014	516.87		
65C17702-50			✓			12.2	24.1	96.8		40.210	461.71		
65C17702-51				✓		17.0	33.8	135.0		40.121	460.69		
				✓				135.4		38.431	441.28		
65C17702-51				✓	7.4	17.0	33.8	135.1		38.342	440.26		Shear out failure
65C17702-52				✓	12.2	7.4	14.5	58.0		42.523	488.27		Net tension failure
				✓				57.9		46.081	529.13		
65C17702-52				✓		7.4	14.5	57.9		50.262	577.14		Net tension failure
65C17702-53				✓		12.2	24.1	95.8		60.493	694.61		Bearing failure
				✓				96.5		62.984	723.21		
		21.1		✓				96.5		61.516	706.35		
		-53.9		✓				96.7		61.293	703.80		
				✓				96.6		57.957	665.50		
65C17702-53	±45/0/90	-53.9		✓	12.2	12.2	24.1	96.6	2.286	62.939	722.70	4.62 x 10 ⁴	Bearing failure

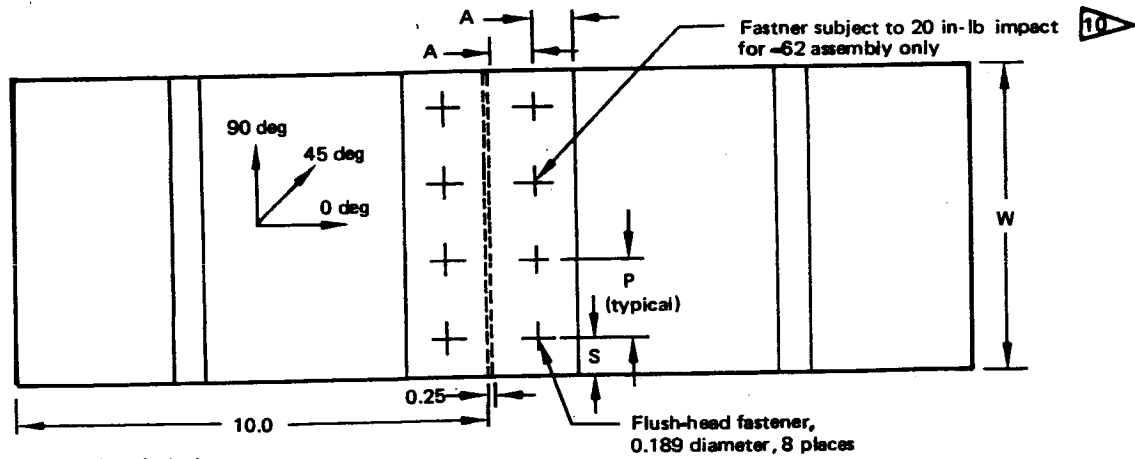
MECHANICAL FASTENED JOINT (NASA TEST 4) (CONTINUED)

Drawing and assembly no. 2	Cloth warp orientation, deg 3	Test temperature, °C	Environment condition 4		A, mm	S, mm	P, mm	Specimen width, mm	Specimen nominal thickness, mm	Failure load, kN 5	Bearing failure stress, MPa 14	E, MPa 7	Comments
			Wet	Dry									
65C17702-53	±45/0/90	71.1		✓	12.2	12.2	24.1	96.6	2.286	52.264	600.12	4.62 x 10 ⁴	Bearing failure
↑	↑	↑		✓	↑	↑	↑	96.6	↑	51.196	587.86	↑	↑
		71.1		✓				96.4		49.195	564.88		
		21.1	✓					96.9		63.918	733.93		
		↑	✓					96.9		64.096	735.98		
		21.1	✓					97.1		63.740	731.89		
		-53.9	✓					96.4		62.272	715.04		
		↑	✓					96.6		66.364	762.03		
		-53.9	✓					95.9		59.870	687.46		
		71.1	✓					96.4		53.954	619.53		
↓		↑	✓			↓	↓	96.4		51.775	594.50		
65C17702-53		71.1	✓			12.2	24.1	96.2		57.735	662.94		
65C17702-54		21.1		✓		17.0	33.8	135.2		59.870	687.46		
↑		↑		✓	↓	↑	↑	135.1		63.162	725.25		↓
65C17702-54				✓	12.2	17.0	33.8	135.2		60.404	693.59		Bearing failure
65C17702-55				✓	17.0	7.4	14.5	57.8		48.038	551.60		Net tension failure
↑				✓	↑	↑	↑	57.9		46.348	532.19		↑
65C17702-55				✓		7.4	14.5	57.9		46.437	533.21		Net tension failure
65C17702-56				✓		12.2	24.1	96.6		59.158	679.29		Bearing failure
↑				✓		↑	↑	96.5		62.272	715.04		↑
				✓				96.6		57.646	661.92		
				✓				96.5		59.114	678.77		
↓				✓				96.6		59.425	682.35		
65C17702-56				✓		12.2	24.1	96.6		61.516	706.35		
65C17702-57				✓		17.0	33.8	134.5		63.162	725.25		
↑				✓	↓	↑	↑	134.5	↓	61.116	701.76		
65C17702-57				✓	17.0	17.0	33.8	134.9	2.286	66.587	764.58		
65C17702-58				✓	12.2	12.2	24.1	96.5	1.524	38.275	659.24		
↑				✓	↑	↑	↑	↑	↑	40.299	694.10		
				✓				96.5		38.119	656.56		
				✓				96.3		36.829	634.34		
↓				✓				96.4	↓	33.760	581.48		
65C17702-58				✓				96.4	1.524	34.828	599.87		
65C17702-60				✓				96.5	3.048	79.441	684.14		
↑				✓				96.6	↑	81.132	698.69		
				✓				96.4		81.132	698.69		
				✓				96.6		80.731	695.24		
↓				✓				96.6	↓	80.731	695.24		
65C17702-60				✓				96.3	3.048	82.332	709.03		Bearing failure
65C17702-61	± 45/0/90	21.1		✓	12.2	12.2	24.1	96.6	2.286	63.918	733.93	4.62 x 10 ⁴	Teflon defect bearing failure

MECHANICAL FASTENED JOINT (NASA TEST 4) (CONTINUED)

Drawing and assembly no. 2	Cloth wrap orientation, deg 3	Test temperature, °C	Environment condition 4		A, mm	S, mm	P, mm	Specimen width, mm	Specimen nominal thickness, mm	Failure load, kN 5	Bearing failure stress, MPa 14	E, MPa 7	Comments
			Wet	Dry									
65C17702-61	±45/0/90	21.1		✓	12.2	12.2	24.1	96.5	2.286	63.918	733.93	4.62 x 10 ⁴	Teflon defect bearing failure
↑	↑	↑		✓	↑	↑	↑	96.6	↑	64.674	742.62	↑	Teflon defect bearing failure
↓			✓					96.5		63.251	691.03		Bearing failure
			✓					96.5		60.181	687.97		Bearing—net tension failure
65C17702-61			✓					96.6		59.915	687.97		Net tension failure
65C17702-62				✓				96.6		51.108	586.84		Bearing failure
↑				✓				96.7		48.572	557.73		↑
				✓				96.6		53.376	612.89		
			✓					96.7		50.752	582.76		
↓	↓	↓	✓		↓	↓	↓	96.7	↓	52.397	601.65	↓	↓
65C17702-62	±45/0/90	21.1	✓		12.2	12.2	24.1	96.8	2.286	55.022	631.79	4.62 x 10 ⁴	Bearing failure

MECHANICAL FASTENED JOINT (NASA TEST 4) (CONTINUED)



• Dimensions in inches

• Splice plate thickness

• -58-8 plies fabric

• -49 through -57, -61, and -62-12 plies fabric

• -60-16 plies fabric

Drawing and assembly no. 2	Cloth warp orientation, deg 3	Test temperature, °F	Environment condition 4		A, in	S, in	P, in	Specimen width, in	Specimen nominal thickness, in	Failure load, kips 5	Bearing failure stress, lbf/in ² 14	E, lbf/in ² 7	Comments
			Wet	Dry									
65C17702-49	±45/0/90	RT		✓	0.29	0.29	0.57	2.280	.090	9.040	66,963	6.7 X 10 ⁶	Net tension failure
↑	↑	↑		✓	↑	↑	↑	2.278	↑	8.760	64,889	↑	↑
65C17702-49				✓		0.29	0.57	2.280		9.640	71,407		Net tension failure
65C17702-50				✓		0.48	0.95	3.800		8.880	65,778		Shear out failure
↑				✓		↑	↑	3.802		9.650	71,481		↑
				✓				3.803		9.280	68,741		
			✓					3.810		9.500	70,370		
↓			✓					3.810		10.120	74,963		
65C17702-50			✓			0.48	0.95	3.810		9.040	66,963		
65C17702-51				✓		0.67	1.33	5.314		9.020	66,815		
↑				✓		↑	↑	5.329		8.640	64,000		↓
65C17702-51				✓	0.29	0.67	1.33	5.318		8.620	63,852		Shear out failure
65C17702-52				✓	0.48	0.29	0.57	2.283		9.560	70,815		Net tension failure
↑				✓	↑	↑	↑	2.280		10.360	76,741		↑
65C17702-52				✓		0.29	0.57	2.281		11.300	83,704		Net tension failure
65C17702-53				✓		0.48	0.95	3.771		13.600	100,741		Bearing failure
↑				✓		↑	↑	3.800		14.160	104,889		↑
		RT		✓				3.800		13.830	102,444		
		-65		✓				3.806		13.780	102,074		
↓		↑		✓		↓	↓	3.804		13.030	96,519		↓
65C17702-53	±45/0/90	-65		✓	0.48	0.48	0.95	3.803	0.090	14.150	104,815	6.7 X 10 ⁶	Bearing failure

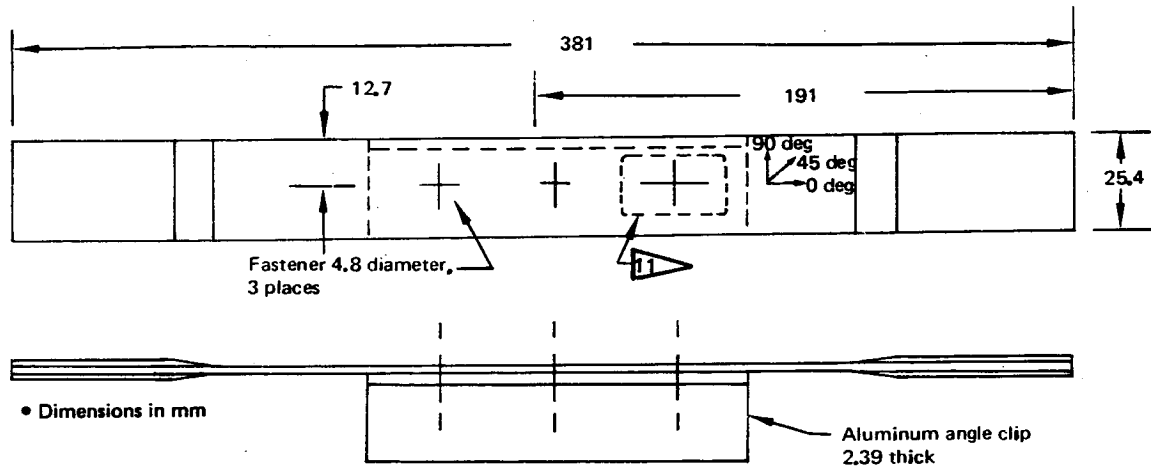
MECHANICAL FASTENED JOINT (NASA TEST 4) (CONTINUED)

Drawing and assembly no. 2	Cloth warp orientation, deg 3	Test temperature, °F	Environment condition 4		A, in	S, in	P, in	Specimen width, in	Specimen nominal thickness, in	Failure load, kips 5	Bearing failure stress, lbf/in ² 14	E, lbf/in ² 7	Comments
			Wet	Dry									
65C17702-53	±45/0/90	160		✓	0.48	0.48	0.95	3.803	0.090	11.750	87,037	6.7 x 10 ⁶	Bearing failure
↑	↑	↑		✓	↑	↑	↑	3.803	↑	11.510	85,259	↑	↑
		160		✓				3.795		11.060	81,926		
		RT	✓					3.814		14.370	106,444		
		↑	✓					3.814		14.410	106,741		
		RT	✓					3.824		14.330	106,148		
		-65	✓					3.795		14.000	103,704		
		↑	✓					3.802		14.920	110,519		
		-65	✓					3.774		13.460	99,704		
		160	✓					3.795		12.130	89,852		
↓		↑	✓					3.795		11.640	86,222		
65C17702-53		160	✓			0.48	0.95	3.789		12.980	96,148		
65C17702-54		RT		✓		0.67	1.33	5.324		13.460	99,704		
↑		↑		✓	↓	↑	↑	5.318		14.200	105,185		↓
65C17702-54			✓		0.48	0.67	1.33	5.322		13.580	100,593		Bearing failure
65C17702-55			✓		0.67	0.29	0.57	2.275		10.800	80,000		Net tension failure
↑			✓		↑	↑	↑	2.279		10.420	77,185		↑
65C17702-55			✓			0.29	0.57	2.279		10.440	77,333		Net tension failure
65C17702-56			✓			0.48	0.95	3.803		13.300	98,519		Bearing failure
↑			✓			↑	↑	3.800		14.000	103,704		↑
			✓					3.803		12.960	96,000		
			✓					3.800		13.290	98,444		
↓			✓					3.803		13.360	98,963		
65C17702-56			✓			0.48	0.95	3.802		13.830	102,444		
65C17702-57				✓		0.67	1.33	5.297		14.200	105,185		
↑			✓		↓	↑	↑	5.297	↓	13.740	101,778		
65C17702-57			✓		0.67	0.67	1.33	5.311	0.090	14.970	110,889		
65C17702-58			✓		0.48	0.48	0.95	3.801	0.060	8.605	95,611		
↑			✓		↑	↑	↑	3.801	↑	9.060	100,667		
			✓					3.801		8.570	95,222		
			✓					3.790		8.280	92,000		
↓			✓					3.795	↓	75.590	84,333		
65C17702-58			✓					3.795	0.060	7.830	87,000		
65C17702-60				✓				3.799	0.120	17.860	99,222		
↑			✓					3.803	↑	18.240	101,333		
			✓					3.795		18.240	101,333		
			✓					3.802		18.150	100,833		
↓			✓					3.802	↓	18.150	100,833		↓
65C17702-60			✓					3.793	0.120	18.510	102,833		Bearing failure
65C17702-61	±45/0/90	RT		✓	0.48	0.48	0.95	3.802	0.090	14.370	106,444	6.7 x 10 ⁶	Teflon defect bearing failure

MECHANICAL FASTENED JOINT (NASA TEST 4) (CONTINUED)

Drawing and assembly no. 2	Cloth wrap orientation, deg 3	Test temperature, °F	Environment condition 4		A, in	S, in	P, in	Specimen width, in	Specimen nominal thickness, in	Failure load, kips 5	Bearing failure stress, lbf/in ² 14	E, lbf/in ² 7	Comments
			Wet	Dry									
65C17702-61	±45/0/90	RT		✓	0.48	0.48	0.95	3.801	0.090	14.370	106,444	6.7x10 ⁶	Teflon defect bearing failure
↑	↑	↑		✓	↑	↑	↑	3.802	↑	14.540	107,704	↑	Teflon defect bearing failure
↓	↓	↓	✓		↑	↑	↑	3.798		14.220	100,222		Bearing failure
↓	↓	↓	✓		↑	↑	↑	3.798		13.530	99,778		Bearing—net tension failure
65C17702-61			✓		↑	↑	↑	3.802		13.470	99,778		Net tension failure
65C17702-62				✓	↑	↑	↑	3.805		11.490	85,111		Bearing failure
↑	↑	↑		✓	↑	↑	↑	3.807		10.920	80,889		↑
↓	↓	↓		✓	↑	↑	↑	3.802		12.000	88,889		
↓	↓	↓	✓		↑	↑	↑	3.809		11.410	84,519		
↓	↓	↓	✓		↑	↑	↑	3.808		11.780	87,259		
65C17702-62	±45/0/90	RT	✓		0.48	0.48	0.95	3.812	0.090	12.370	91,630	6.7x10 ⁶	Bearing failure

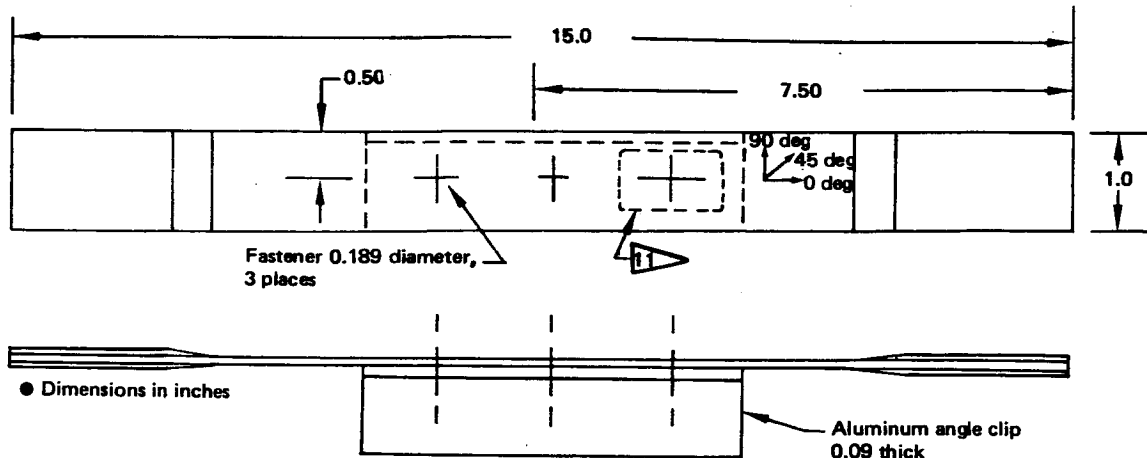
STATIC TENSION, HARD POINT (NASA TEST 4)



- Laminate thickness
 - -15-8 plies fabric 1
 - -16 through -19-12 plies fabric 1
- Flush-head fastener - -15, -16, and -18
- Protruding-head fastener - -17 and -19
- Teflon 11 7.6 x 12.7 mm - -18 and -19

Drawing and assembly no. 2	Cloth warp orientation, deg 3	Test temperature, °C	Environment condition 4		Specimen width, mm	Specimen nominal thickness, mm	Failure load, kN 5	Failure stress, MPa 6	E, MPa 7	Strain, ε, mm/mm 8
			Wet	Dry						
65C17706-15	±45/0/90	21.1		✓	25.6	1.524	8.785	224.44	4,620 × 10 ⁴	0.00487
↑	↑	↑		↑	25.6	↑	8.896	228.01	↑	0.00494
65C17706-15	↑	↑		↑	25.7	1.524	8.807	225.28	↑	0.00488
65C17706-16	↑	↑		↑	25.4	2.286	12.032	207.44	↑	0.00449
↑	↑	↑		↑	25.3	↑	11.921	205.73	↑	0.00445
65C17706-16	↑	↑		↑	25.4	↑	12.365	213.19	↑	0.00461
65C17706-17	↑	↑		↑	25.3	↑	13.188	227.60	↑	0.00493
↑	↑	↑		↑	↑	↑	12.276	212.08	↑	0.00459
65C17706-17	↑	↑		↑	↑	↑	13.033	225.15	↑	0.00487
65C17706-18	↑	↑		↑	25.3	↑	12.864	222.01	↑	0.00481
↑	↑	↑		↑	25.4	↑	12.303	212.12	↑	0.00459
65C17706-18	↑	↑		↑	↑	↑	12.810	220.86	↑	0.00478
65C17706-19	↑	↑		↑	25.4	↑	14.652	252.36	↑	0.00546
↑	↑	↑		↑	25.3	↑	13.077	225.69	↑	0.00489
65C17706-19	±45/0/90	21.1		✓	25.3	2.286	14.145	244.11	4,620 × 10 ⁴	0.00528

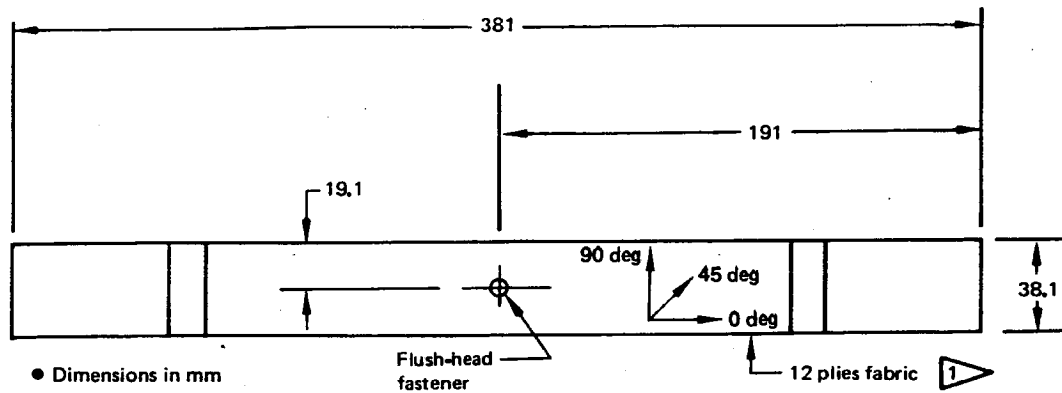
STATIC TENSION, HARD POINT (NASA TEST 4) (CONTINUED)



- Laminate thickness
 - -15-8 plies fabric
 - -16 through -19-12 plies fabric
- Flush-head fastener-- -15, -16, and -18
- Protruding-head fastener-- -17 and -19
- Teflon 0.30 x 0.50 in-- -18 and -19

Drawing and assembly no. 2	Cloth warp orientation, deg 3	Test temperature, °F	Environment condition 4		Specimen width, in	Specimen nominal thickness, in	Failure load, kips 5	Failure stress, lbf/in ² 6	E, lbf/in ² 7	Strain, ε, in/in 8
			Wet	Dry						
65C17706-15	±45/0/90	RT		✓	1.009	0.060	1.975	32,623	6.7 x 10 ⁶	0.00487
65C17706-15					1.008		2.000	33,069		0.00494
65C17706-15					1.010	0.060	1.980	32,673		0.00488
65C17706-16					0.999	0.090	2.705	30,086		0.00449
65C17706-16					0.998		2.680	29,837		0.00445
65C17706-16					0.999		2.780	30,920		0.00461
65C17706-17					0.998		2.965	33,010		0.00493
65C17706-17					0.997		2.760	30,759		0.00459
65C17706-17					0.997		2.930	32,654		0.00487
65C17706-18					0.998		2.892	32,198		0.00481
65C17706-18					0.999		2.766	30,764		0.00459
65C17706-18					0.999		2.880	32,032		0.00478
65C17706-19					1.000		3.294	36,600		0.00546
65C17706-19					0.998		2.940	32,732		0.00489
65C17706-19	±45/0/90	RT		✓	0.998	0.090	3.180	35,404	6.7 x 10 ⁶	0.00528

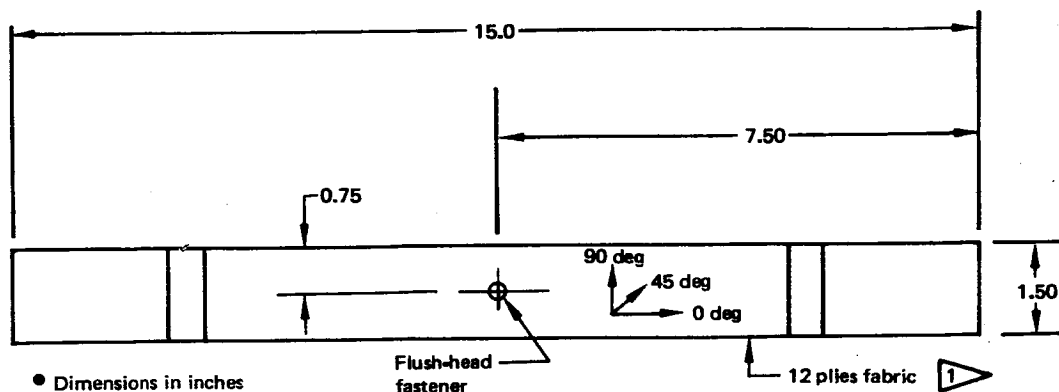
STATIC TENSION, FILLED HOLE (NASA TEST 4)



- Dimensions in mm
- Fasteners
 - 4.8 diameter— -20
 - 6.35 diameter— -21
 - 7.9 diameter— -22

Drawing and assembly no. 2	Cloth warp orientation, deg 3	Test temperature, °C 4	Environment condition 4		Specimen width, mm	Specimen nominal thickness, mm	Failure load, kN 5	Failure stress, MPa 6	E, MPa 7	Strain, ϵ , mm/mm 8
			Wet	Dry						
65C17706-20	±45/0/90	21.1		✓	38.23	2.286	21 199	242.61	4.620×10^4	0.00525
↑	↑	↑		✓	38.20	↑	21.110	241.75	↑	0.00523
65C17706-20				✓	38.18		22.093	253.18		0.00548
65C17706-21				✓	38.15		19.473	223.30		0.00483
↑				✓	38.05		18.690	214.90		0.00465
↑				✓	38.10		20.550	235.96		0.00511
↓			✓		38.13		20.995	240.91		0.00521
↓			✓		38.15		21.840	250.44		0.00542
65C17706-21			✓		38.23		21.128	241.79		0.00523
65C17706-22				✓	38.13		17.516	201.00		0.00435
↑				✓	38.20	↓	18.659	213.68	↓	0.00463
65C17706-22	±45/0/90	21.1		✓	38.07	2.286	19.749	226.92	4.620×10^4	0.00491

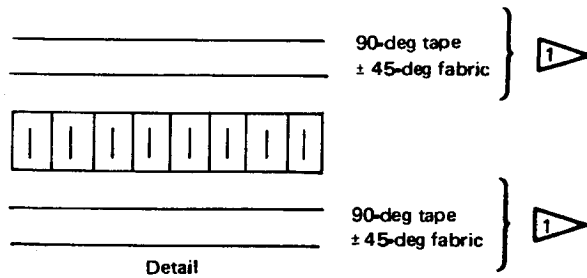
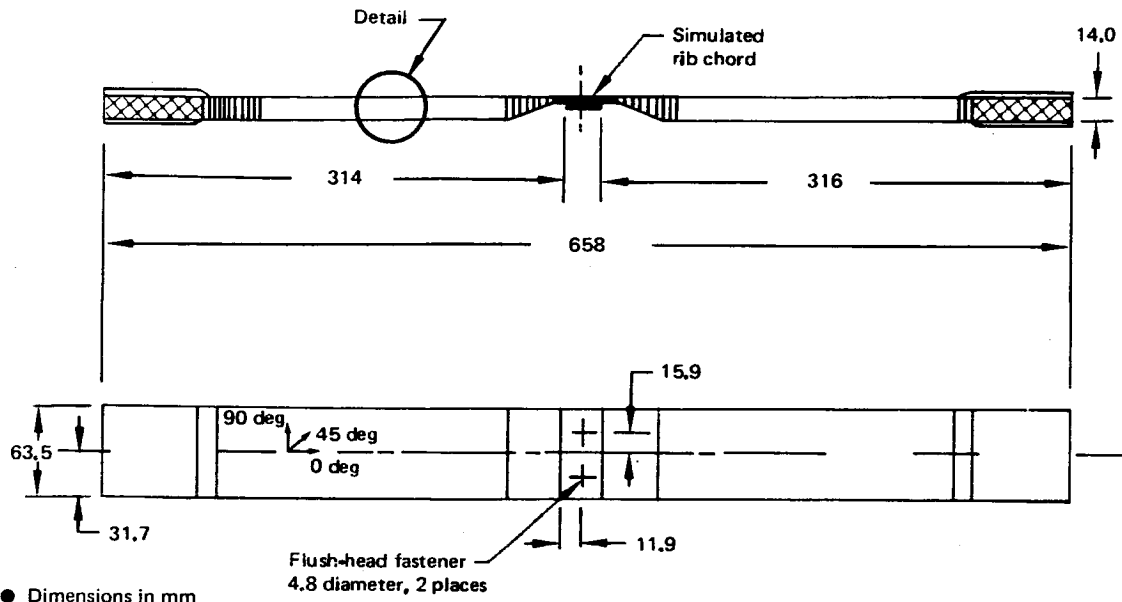
STATIC TENSION, FILLED HOLE (NASA TEST 4) (CONTINUED)



- Dimensions in inches
- Fasteners
 - 0.189 diameter— -20
 - 0.25 diameter— -21
 - 0.313 diameter— -22

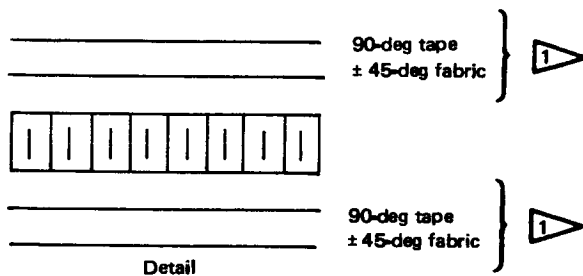
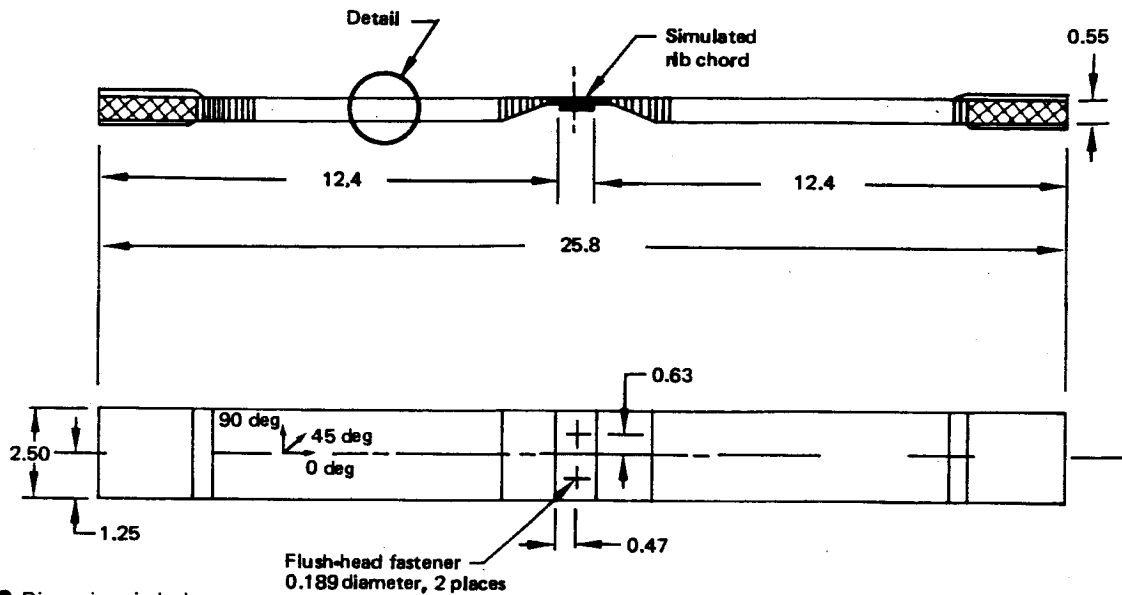
Drawing and assembly no. 2	Cloth warp orientation, deg 3	Test temperature, °F	Environment condition 4		Specimen width, in	Specimen nominal thickness, in	Failure load, kips 5	Failure stress, lbf/in ² 6	E, lbf/in ² 7	Strain, ϵ , in/in 8
			Wet	Dry						
65C17706-20	±45/0/90	RT		✓	1.505	0.090	4.766	35,186	6.7×10^6	0.00525
↑	↑	↑		✓	1.504	↑	4.746	35,062	↑	0.00523
65C17706-20				✓	1.503		4.967	36,719		0.00548
65C17706-21				✓	1.502		4.378	32,386		0.00483
↑				✓	1.498		4.202	31,167		0.00465
				✓	1.500		4.620	34,222		0.00511
			✓		1.501		4.720	34,940		0.00521
↓			✓		1.502		4.910	36,322		0.00542
65C17706-21			✓		1.505		4.750	35,068		0.00523
65C17706-22				✓	1.501		3.938	29,151		0.00435
↑	↓	↓		✓	1.504	↓	4.195	30,991	↓	0.00463
65C17706-22	±45/0/90	RT		✓	1.499	0.090	4.440	32,911	6.7×10^6	0.00491

STATIC TENSION, PANEL TO RIB (NASA TEST 8)



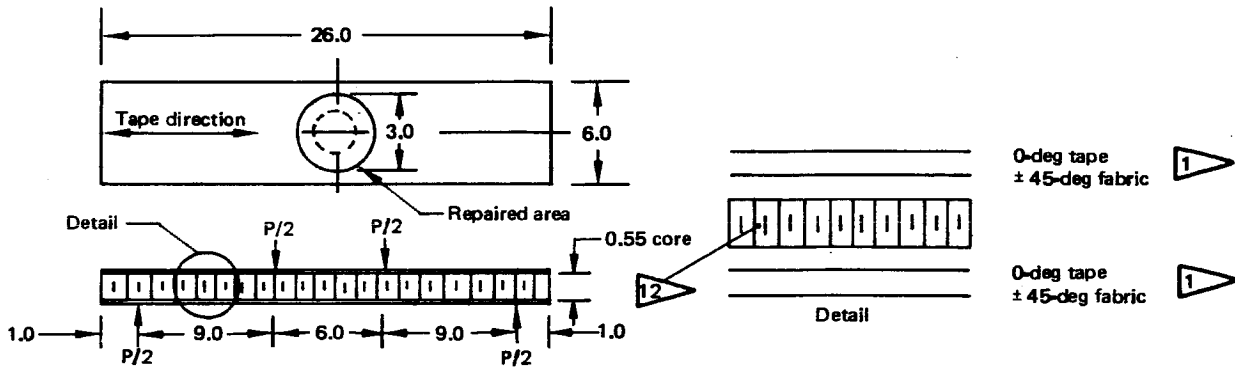
Drawing and assembly no. 2	Test temperature, °C	Environment condition 4		Specimen width, mm	Specimen nominal thickness, mm	Failure load, kN 5	Failure stress, MPa 6	E, MPa 7	Strain, ε, mm/mm 8
		Wet	Dry						
65C17708-1	21.1		✓	63.50	0.559	5.249	147.93	2.620 × 10 ⁴	0.00565
↑	↑		✓	↑	↑	5.471	154.20	↑	0.00589
↑	↑		✓	↑	↑	7.784	219.39	↑	0.00837
↑	↑		✓	↑	↑	6.672	188.05	↑	0.00718
↑	↑		✓	↑	↑	6.850	193.06	↑	0.00737
↓	↓	✓		↓	↓	8.273	233.18	↓	0.00890
↓	↓	✓		↓	↓	7.828	220.64	↓	0.00842
65C17708-1	21.1	✓		63.50	0.559	6.850	193.06	2.620 × 10 ⁴	0.00737

STATIC TENSION, PANEL TO RIB (NASA TEST 8) (CONTINUED)



Drawing and assembly no. 2	Test temperature, °F	Environment condition 4		Specimen width, in	Specimen nominal thickness, in	Failure load, kips 5	Failure stress, lbf/in ² 6	E, lbf/in ² 7	Strain, ε, in/in 8
		Wet	Dry						
65C17708-1	RT		✓	2.500	0.022	1.18	21,455	3.8 × 10 ⁶	0.00565
↑	↑		✓	↑	↑	1.23	22,364	↑	0.00589
↑	↑		✓	↑	↑	1.75	31,818	↑	0.00837
↑	↑		✓	↑	↑	1.50	27,273	↑	0.00718
↑	↑		✓	↑	↑	1.54	28,000	↑	0.00737
↓	↓	✓		↓	↓	1.86	33,818	↓	0.00890
↓	↓	✓		↓	↓	1.76	32,000	↓	0.00842
65C17708-1	RT	✓		2.500	0.022	1.54	28,000	3.8 × 10 ⁶	0.00737

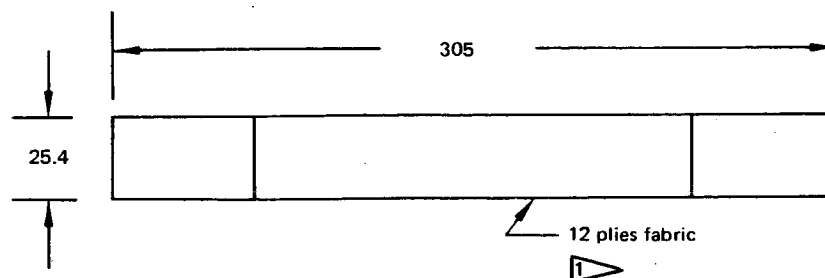
HONEYCOMB PANEL REPAIR TESTS (CONTINUED)



• Dimensions in inches

Drawing and assembly no. 2	Test temperature, °F	Environment condition 4		Failure load, lb 5	Failure stress, lb/in ² 6	E, lbf/in ² 7	Strain, ε, in/in 8	Comments
		Wet	Dry					
65C17721-4	70		✓	387	47034	7.9 x 10 ⁶	0.00595	Baseline specimen
			✓	367	44604		0.00565	
			✓	400	48614		0.00615	
		✓		372	45211		0.00572	
		✓		371	45090		0.00571	
		✓		379	46062		0.00583	Baseline specimen
			✓	344	41808		0.00529	Specimen impacted with 10 in-lb damage
			✓	340	41322		0.00523	
			✓	323	39256		0.00497	
		✓		309	37555		0.00475	
		✓		309	37555		0.00475	Specimen impacted with 10 in-lb damage
65C17721-4	70	✓		339	41201		0.00522	
65C17721-2	-65		✓	564	68546		0.00868	Repaired specimen
			✓	548	66802		0.00843	
	-65		✓	629	76446		0.00968	
	70		✓	420	51045		0.00646	
			✓	456	55420		0.00702	
	70		✓	439	53354		0.00675	
	160		✓	332	40350		0.00511	
			✓	359	43631		0.00552	
	160		✓	389	47278		0.00598	
	-65	✓		577	70126		0.00888	
		✓		374	45454		0.00575	
	-65	✓		378	46941		0.00582	
	70	✓		429	52139		0.00660	
		✓		341	41444		0.00525	
	70	✓		337	40958		0.00518	
	160	✓		314	38162		0.00483	
		✓		289	35124		0.00445	
65C17721-2	160	✓		334	40593	7.9 x 10 ⁶	0.00514	Repaired specimen

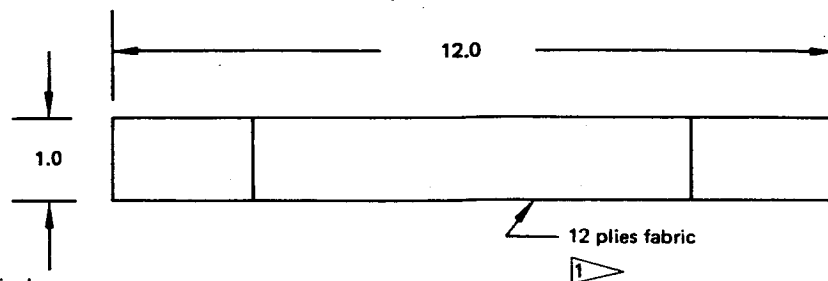
ENVIRONMENTAL EXPOSURE, TENSION, LAMINATE COUPON (NASA TEST 3)



• Dimensions in mm

Drawing and assembly no. 2	Cloth warp orientation, deg 3	Exposure condition	Test temper- ature, °C	Actual specimen size, mm		Effective area, mm ²	Failure load, kN 5	Failure stress, MPa 6	E, MPa 7	Strain, ε, mm/mm 8
				Width	Thickness					
65C17703-1	± 45	Zero time	21	25.50	2.29	58.29	10.898	186.96	2.07 x 10 ⁴	0.00903
				25.50		58.29	10.831	185.81		0.00898
				25.53		58.35	11.476	196.67		0.00950
				25.50		58.29	10.742	184.28		0.00891
							11.298	193.82		0.00937
		12 months					11.351	194.73		0.00941
		laboratory		25.50		58.29	12.214	209.54		0.01013
		shelf		25.53		58.46	11.284	193.58		0.00934
				25.50		58.29	10.786	185.04		0.00894
65C17703-1				25.50		58.29	12.970	222.51		0.01075
65C17703-17		12 months		25.91		59.33	11.463	193.21		0.00933
		outdoor		26.01		59.56	11.427	191.86		0.00929
		rack		25.91		59.33	11.342	191.17		0.00924
				26.11		59.79	12.979	217.08		0.01052
65C17703-17	± 45		21	25.86	2.29	59.22	12.530	211.58	2.07 x 10 ⁴	0.01025

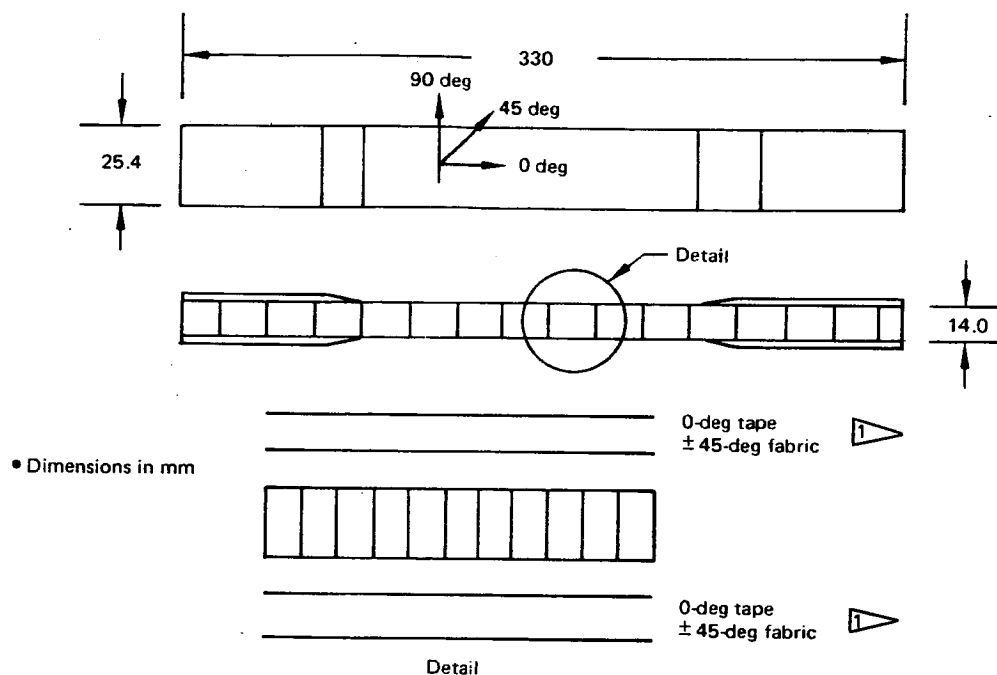
ENVIRONMENTAL EXPOSURE, TENSION, LAMINATE COUPON (NASA TEST 3) (CONTINUED)



● Dimensions in inches

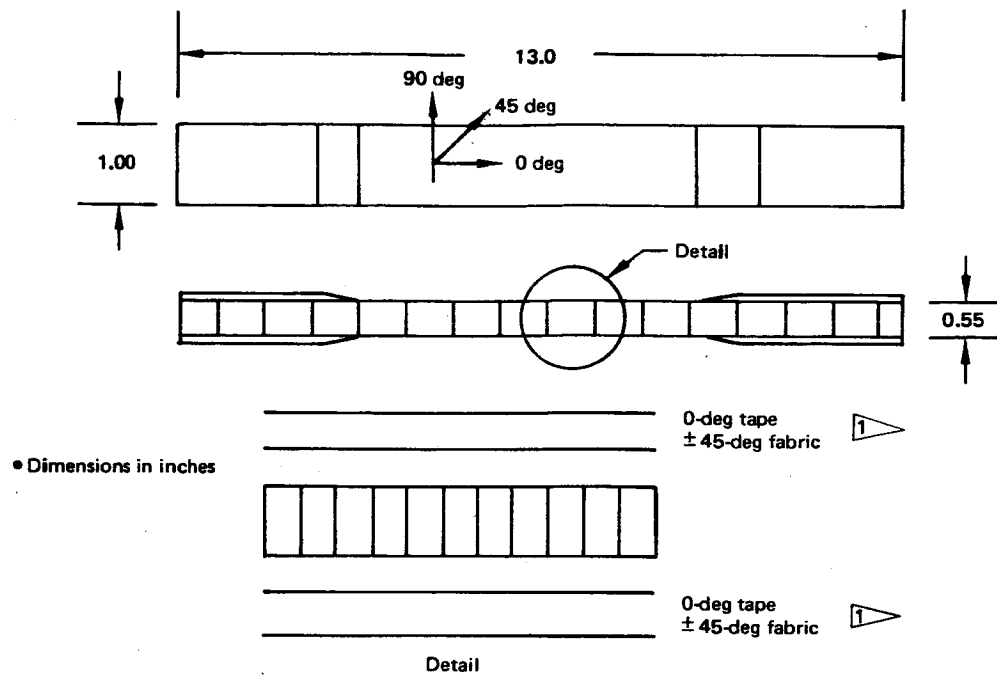
Drawing and assembly no. 2	Cloth warp orientation, deg 3	Exposure condition	Test temperature, °F	Actual specimen size, in		Effective area, in ²	Failure load, lbf 5	Failure stress, lbf/in ² 6	E, lbf/in ² 7	Strain, ε, in/in 8
				Width	Thickness					
65C17703-1	± 45	Zero time	70	1.004	0.090	0.0904	2450	27,102	3.0 x 10 ⁶	0.00903
				1.004		0.0904	2435	26,936		0.00898
				1.005		0.0905	2580	28,508		0.00950
				1.004		0.0904	2415	26,715		0.00891
							2540	28,097		0.00937
		12 months					2552	28,230		0.00941
		laboratory		1.004		0.0904	2746	30,376		0.01013
		shelf		1.005		0.0905	2537	28,033		0.00934
				1.004		0.0904	2425	26,825		0.00894
65C17703-1				1.004		0.0904	2916	32,257		0.01075
65C17703-17		12 months		1.022		0.0920	2575	27,989		0.00933
		outdoor		1.024		0.0922	2569	27,863		0.00929
		rack		1.022		0.0920	2550	27,717		0.00924
				1.028		0.0925	2918	31,546		0.01052
65C17703-17	± 45		70	1.018	0.090	0.0916	2817	30,753	3.0 x 10 ⁶	0.01025

ENVIRONMENTAL EXPOSURE, COMPRESSION, HONEYCOMB COUPON (NASA TEST 3)



Drawing and assembly no. 2	Exposure condition	Test temperature, °C	Actual specimen size, mm		Effective area, mm ²	Failure load, kN 5	Failure stress, MPa 6	E, MPa 7	Strain, ε, mm/mm 8
			Width	Thickness					
65C17703-4	Zero time	21	27.03	0.559	15.10	3.047	201.78	2.62 × 10 ⁴	0.00770
			27.28		15.24	3.238	212.47		0.00811
			26.92		15.04	3.581	238.10		0.00908
			27.48		15.35	3.696	240.78		0.00919
65C17703-4			26.92		15.04	3.029	201.40		0.00768
65C17703-20	12 months		27.15		15.18	3.460	227.93		0.00870
	outdoor		27.03		15.11	3.981	263.47		0.01006
	rack		27.03		15.11	3.874	256.39		0.00979
65C17703-20		21	26.80	0.559	14.98	3.821	255.06	2.62 × 10 ⁴	0.00974

ENVIRONMENTAL EXPOSURE, COMPRESSION, HONEYCOMB COUPON (NASA TEST 3) (CONTINUED)



Drawing and assembly no. 2	Exposure condition	Test temperature, °F	Actual specimen size, in		Effective area, in ²	Failure load, lbf 5	Failure stress, lbf/in ² 6	E, lbf/in ² 7	Strain, ε, in/in 8
			Width	Thickness					
65C17703-4	Zero time	70	1.064	0.022	0.02341	685.0	29,261	3.8 × 10 ⁶	0.00770
			1.074		0.02363	728.0	30,808		0.00811
			1.060		0.02332	805.0	34,520		0.00908
			1.082		0.02380	831.0	34,916		0.00919
65C17703-4			1.060		0.02332	681.0	29,202		0.00768
65C17703-20	12 months		1.069		0.02352	778.0	33,078		0.00870
	outdoor		1.064		0.02341	895.0	38,232		0.01006
	rack		1.064		0.02341	871.0	37,206		0.00979
65C17703-20		70	1.055	0.022	0.02321	859.0	37,010	3.8 × 10 ⁶	0.00974

1. Report No. NASA CR-159258		2. Government Accession No.		3. Recipient's Catalog No.	
4. Title and Subtitle ADVANCE COMPOSITE ELEVATOR FOR BOEING 727 AIRCRAFT				5. Report Date November 1980	
				6. Performing Organization Code	
7. Author(s) D. V. Chovil, W. D. Grant, E. S. Jamison, H. Syder O. E. Desper, S. T. Harvey, J. E. McCarty				8. Performing Organization Report No.	
				10. Work Unit No.	
9. Performing Organization Name and Address Boeing Commercial Airplane Company P.O. Box 3707 Seattle, Washington 98124				11. Contract or Grant No. NAS1-14952	
				13. Type of Report and Period Covered Contractor Report	
12. Sponsoring Agency Name and Address National Aeronautics and Space Administration Washington, D.C. 20546				14. Sponsoring Agency Code	
15. Supplementary Notes Langley Technical Monitor: Dr. Herbert A. Leybold Final Report					
16. Abstract This report defines and discusses the design, development, analyses, testing, production activities, and associated costs that were required to produce five and one-half advanced-composite elevator shipsets for Boeing 727 aircraft.					
17. Key Words (Suggested by Author(s)) advanced composites Energy Efficient Transport Program long-term durability structural integrity weight savings			18. Distribution Statement FEDD distribution		
19. Security Classif. (of this report) Unclassified	20. Security Classif. (of this page) Unclassified	21. No. of Pages 405	22. Price		